655001

# Aberfoyle Resources Limited

EXPLORATION DIVISION

OPEN FILE

TCR 93-3441

## EXPLORATION LICENCE 106/87

## LAKE MACKINTOSH

## TASMANIA

MINES
FILE REF. EL 106/87
15 JUN 1993
DOC. REF.
OFFICER | FOR ACTION | FOR INFO.
See Folios 94-97
RESUBMIT TO | DATE

MICROFILMED
FICHE No. 012721-29B

**Progress Report for the Period**

**April 1992 - April 1993**

**Volume 1 of 3**

**Text and Appendices I - II**

Prepared by:

S. Richardson

S Richardson

Issued by:

David Wallace

D B Wallace
Regional Exploration
Manager

Internal Report No: Mackintosh 52

Distribution

| | |
|---|---|
| Aberfoyle - Burnie | (1/3) |
| Aberfoyle - Hawthorn | (2/3) |
| **Division of Mines** | **(3/3)** |

# CONTENTS


| | | Page No: |
|---|---|---|
| 1.0 | SUMMARY | 1 |
| 2.0 | INTRODUCTION | 2 |
| 3.0 | RESEARCH | 3 |
| 3.1 | Volcanology | 3 |
| 3.2 | Structural Project | 3 |
| 4.0 | DATA COMPILATION | 5 |
| 4.1 | Introduction | 5 |
| 4.2 | Geological Mapping | 5 |
| 5.0 | SOUTH QUE RIVER | 6 |
| 5.1 | Introduction | 6 |
| 5.2 | DDH MAC 30 | 6 |
| 5.2.1 | Geophysics | 6 |
| 6.0 | MOUNT CHARTER AREA | 8 |
| 6.1 | Introduction | 8 |
| 6.2 | DDH MAC 32 | 10 |
| 6.2.1 | Introduction | 10 |
| 6.2.2 | Geology | 10 |
| 6.2.3 | Geochemistry | 12 |
| 6.2.4 | Geophysics | 13 |
| 6.3 | DDH MAC 33 | 13 |
| 6.3.1 | Introduction | 13 |
| 6.3.2 | Geology | 13 |
| 6.3.3 | Geochemistry | 17 |
| 6.3.4 | Geophysics | 18 |
| 7.0 | MURCHISON HIGHWAY ZONE | 19 |
| 7.1 | Introduction | 19 |
| 7.2 | DDH MAC 34 | 20 |
| 7.3 | DDH MAC 35 | 20 |

655003

7.3.1 Introduction 20
7.3.2 Geology 21
7.3.3 Geochemistry 23
7.3.4 Geophysics 24

8.0 AEROMAGNETIC AND RADIOMETRIC SURVEY 25

8.1 Introduction 25
8.2 Survey Results 25

9.0 CONCLUSIONS 26

10.0 REFERENCES 27

## APPENDICES

I Research, Que Hellyer Volcanics, volcanology project progress report.

II Research, Que Hellyer Volcanics, structural project final report.

III DDH MAC 30, DHEM survey results.

IV DDH MAC 32, detailed log.

V DDH MAC 32, core grind geochemsitry.

VI DDH MAC 33, detailed log, petrographic report.

VII DDH MAC 33, core grind geochemistry.

VIII DDH MAC 34, detailed log.

IX DDH MAC 35, detailed log, petrographic report.

X DDH MAC 35, core grind geochemistry.

XI Heliborne magnetic and radiometric survey logistics report.

## PLATES (VOLUME 3)

| Plate | Scale | Title |
|---|---|---|
| MAC 360 | 1:10,000 | Inferred Cambrian Structures |
| MAC 365 | 1:1,000 | MAC 32-33 Cross Section |
| MAC 365A | 1:1,000 | MAC 33, Geochemical Profiles |
| MAC 365B | 1:1,000 | MAC 33, Geochemical Profiles |
| MAC 366 | 1:1,000 | MAC 35 Cross Section |
| MAC 366A | 1:1,500 | MAC 35, Geochemical Profiles |
| MAC 366B | 1:1,500 | MAC 35, Geochemical Profiles |
| MAC 378A | 1:1,000 | MAC 32, Geochemical Profiles |
| MAC 378B | 1:1,000 | MAC 32, Geochemical Profiles |
| MAC 380 | 1:10,000 | Hellyer - Mount Charter, Interpretive Geology |

## FIGURES

1. Mackintosh District - Tenure Summary
2. Mount Charter Area - Summary Geology
3. Murchison Highway Zone - Summary Geology

## 1.0 SUMMARY

Work on EL 106/87 during the first half of the reporting period focussed on delineation of the Cambrian syn-volcanic fault network of the Que-Hellyer Volcanic Basin. Areas of prospective stratigraphy at depth, adjacent to syn-volcanic fault intersections, are seen as conceptual targets for Volcanic Hosted Massive Sulphides (VHMS).

During the latter half of the reporting period two such geological targets were drill tested. At Mount Charter and the Murchison Highway Zone two holes were abandoned and two holes completed for a total of 2408.7 m.

A helicopter borne, close spaced, magnetic and radiometric survey of EL 106/87 was completed.

## 2.0 INTRODUCTION

The Lake Mackintosh Exploration Licence (EL 106/87) was granted to Aberfoyle Resources Limited on 5 February, 1988, subject to the Hellyer Mine Agreement Ratification Act 1987. The licence comprised 135 sq km previously covered by EL's 2/70 (Mackintosh) and 15/73 (Hatfield) and encloses the 20.2 $km^2$ of CML's 68M/84 and 103M/87 (encompassing the Que River and Hellyer mines and facilities).

Under the terms of this Act the licence was issued for ten years with partial relinquishments required on the second and fifth anniversaries. The first partial relinquishment was effected in February, 1990 when the licence was reduced from 135 to 95 sq km. The second partial relinquishment from 95 to 54 sq km was effected on 5 February,1992. Current tenure is shown on Fig. 1.

This report summarises exploration completed in the Mackintosh district on EL 106/87 for the period April 1992 to April 1993.

655008

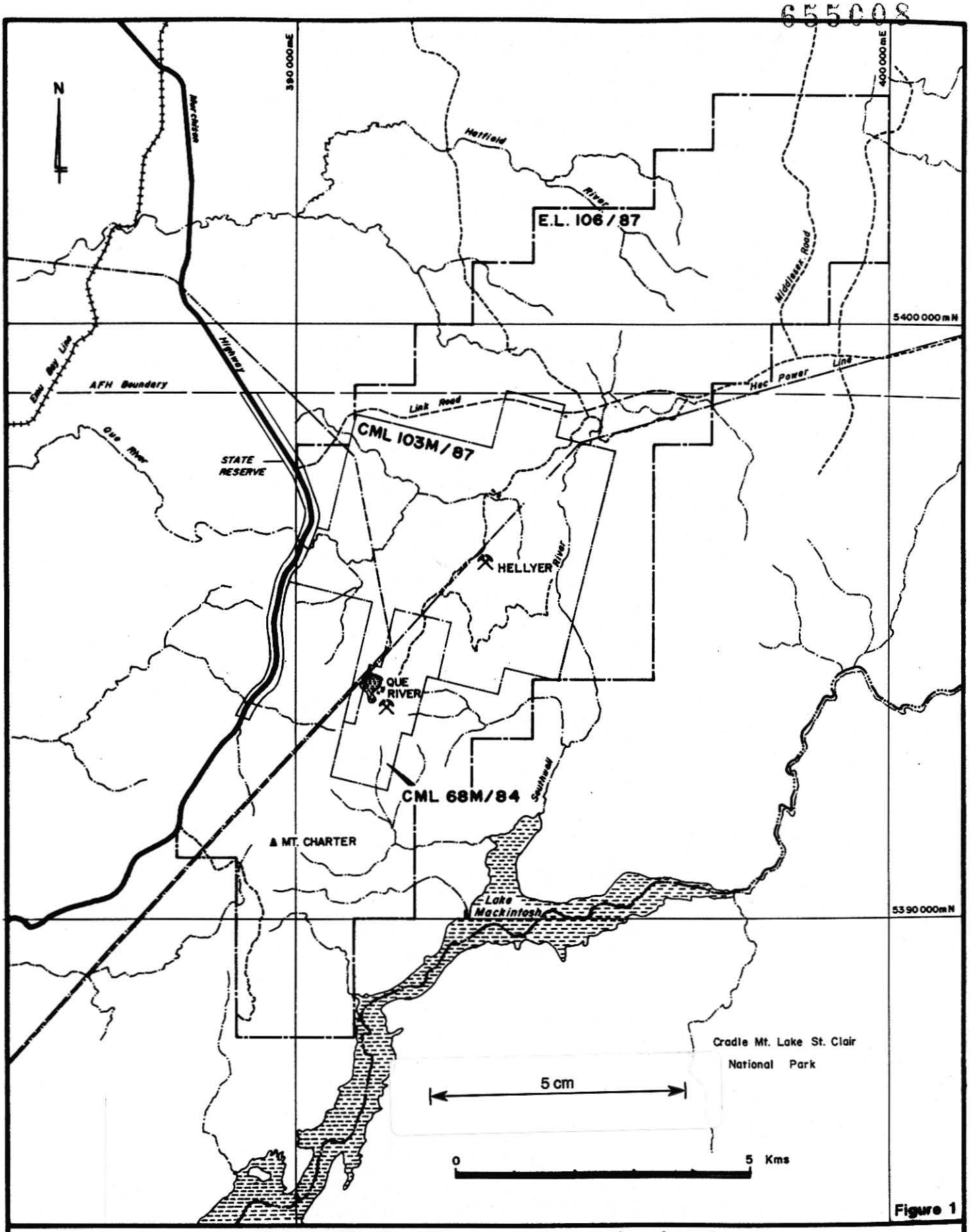



Figure 1

# Aberfoyle Resources Limited

EXPLORATION DIVISION

| REVISIONS | | | |
|---|---|---|---|
| Init. | Date | Init. | Date |
| RJE | May 90 | | |
| JMS | Feb 93 | | |
| | | | |
| | | | |
| | | | |

Location Code : K55/6/44

NORTH WEST TASMANIA

MACKINTOSH DISTRICT

TENURE SUMMARY

Scale : As shown

Date : May, 1990

Compiled : AMcN

Drawn :

Traced :

Checked :

Plate No. : MAC 181

1511

# 3.0 RESEARCH

## 3.1 Volcanology

A PhD project on the volcanology and sedimentology of the Que-Hellyer Volcanics was initiated in 1988. This project is undertaken by J. Waters under the supervision of Dr. R. Cas, Monash University.

One progress report was issued during this reporting period (Appendix I). Work concentrated on description of dacitic volcanics within the Mixed Sequence.

## 3.2 Structural Project

It has long been recognised that base metal mineralisation in the Que-Hellyer Volcanics is associated with Cambrian syn-depositional structures that bounded and localised the narrow trench like basins with which the footwall epiclastics, hydrothermal alteration and mineralisation are associated.

In a more regional sense, syn-volcanic faults have been suspected of controlling the thickness and distribution of stratigraphic units within the Que Hellyer Volcanics. For example, thinning of the volcanic pile to the NW was inferred to occur across a series of growth faults and some dramatic thickness and compositional changes in the Mixed Sequence were attributed to growth faults.

Such structures are seen as potential focci for venting hydrothermal fluids and localisation of massive sulphide deposition.

At the beginning of 1992 a structural study of the Que Hellyer Volcanics was undertaken by Etheridge and Henley Pty Ltd. Their aim was to develop an integrated structural framework for basin development, mineralisation and subsequent deformation. This study would form the basis for future work leading to drilling of deep conceptual targets below surface EM penetration range.

The results of this study are presented in Appendix II.

The structure of the Que-Hellyer Volcanics is interpreted to reflect the effects of two compressional deformation events, superimposed on a complex array of syn-depositional extensional and strike slip faults. The syn-depositional fault network is inferred to comprise north east trending normal faults linked by north west trending transfer faults. A subtle change in the stress regime during Mixed Sequence time is inferred to localise dilation, extension and subsidence at or near the intersection of normal and transfer faults. Highly channelised fluid flow through these dilatent areas led to orebody formation.

# 4.0 DATA COMPILATION

## 4.1 Introduction

The Etheridge and Henley Pty Ltd structural project was seen as a starting point from which Aberfoyle could develop, in more detail, its own inferred syn-depositional fault network for the Que Hellyer Volcanic basin.

Inferred Cambrian fault intersections are potential sites of dilation and subsidence resulting in focussed hydrothermal fluid flow; possibly leading to massive sulphide accumulation. Where prospective stratigraphy is preserved at depth in these areas, conceptual drill targets would be proposed.

## 4.2 Geological Mapping

A programme of re-interpretation of existing 1:2500 scale fact mapping was undertaken, from Hellyer to the Mount Charter Fault. Emphasis was on the recognition of faults as these could reflect reactivated Cambrian structures.

The resulting interpretive geological map is attached as Plate MAC 380. A map showing the location of inferred Cambrian structures is attached as Plate MAC 360.

# 5.0 SOUTH QUE RIVER

## 5.1 Introduction

The South Que River area lies between Que River Mine and Mount Charter. Diamond drilling on the southern-most section at Que River Mine (6700N) failed to close off the Que River alteration zone. This zone was interpreted on the basis of IP data and mapping to daylight around 6200N and plunge to the north. However, lineament studies and a review of the geophysical data suggested it to be equally plausible that the alteration zone plunged south.

A diamond drill hole, MAC 28, was proposed to test for the southern extension of this alteration zone. The geology and geochemistry of MAC 28 were discussed in McNeil, 1991. Footwall style alteration was intersected and a DHEM survey indicated the presence of a conductor centred around 650 m downhole.

MAC 29 and MAC 30 were subsequently drilled at the inferred conductor but failed to intersect the source. The results of these holes were described in the last annual report. As a DHEM survey of MAC 30 was not complete at that time, the results are presented below.

## 5.2 DDH MAC 30

### 5.2.1 Geophysics

A two loop down hole EM (DHEM) survey was undertaken in MAC 30. Loop locations and survey results are attached as Appendix III.

A conductive response is still evident. Work is currently in progress to investigate the source of this response and will be reported in the next annual report.

# 6.0 MOUNT CHARTER AREA

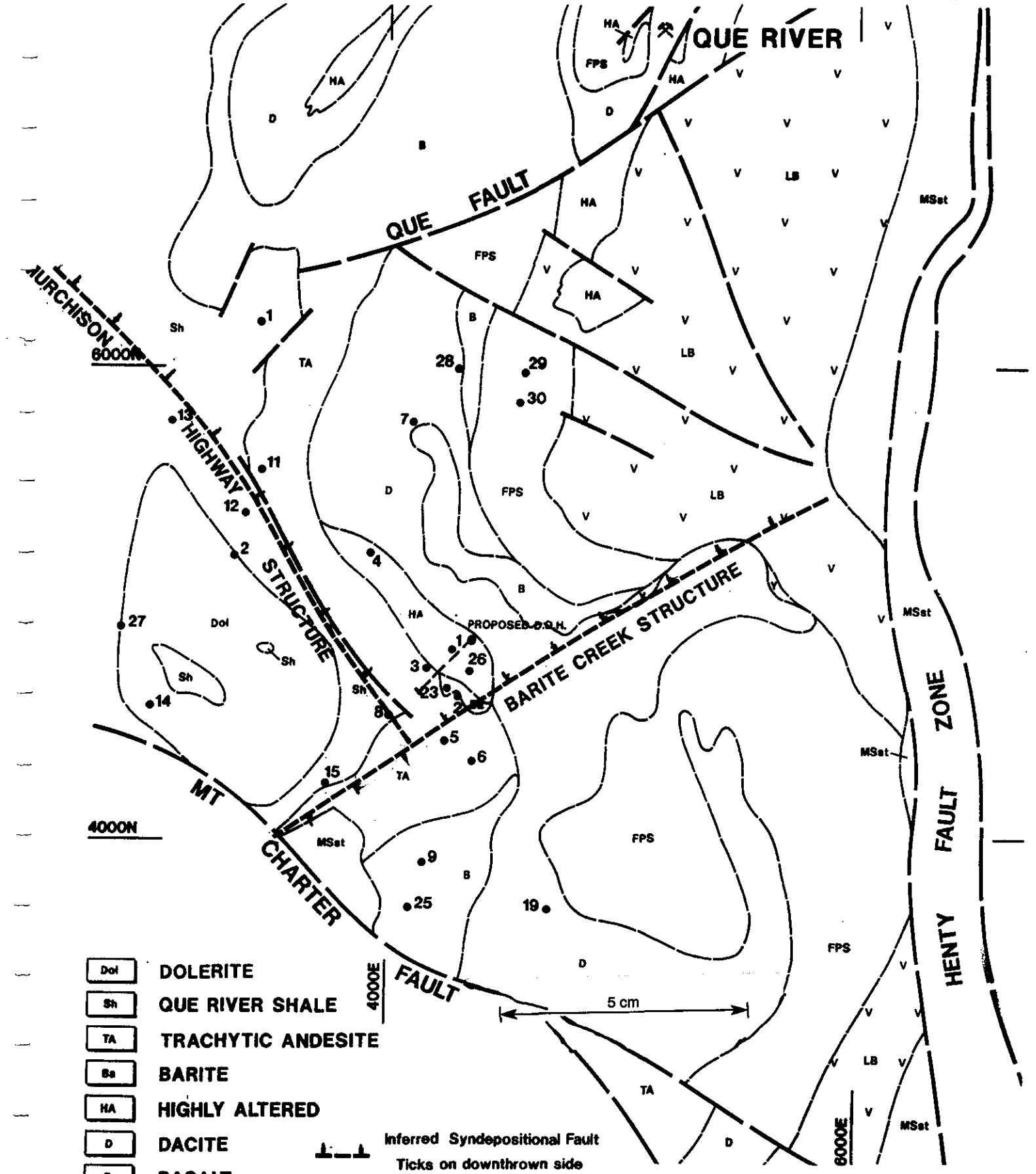
## 6.1 Introduction

A re-interpretation of the Mount Charter area was carried out with an emphasis on recognition of syn-volcanic faults. Re-interpreted mapping is summarised on Fig. 2.

A prominent feature of the Mount Charter area is the elongate orientation of the Mount Charter alteration zone parallel to the basin bounding Mount Charter Fault. The boundary between the Que River Shale and andesite is mapped as a normal fault dipping steeply south west, parallel to both the alteration zone and Mount Charter Fault.

A major Cambrian fault (a basin sidewall fault) with north east side down, parallel to the Mount Charter Fault and dipping to the north east at an unknown angle, is inferred to exist west of the Mount Charter alteration zone. The faulted shale-andesite boundary is inferred to represent a normal fault propagated from the unseen syn-volcanic fault during later reactivation.

This major intra-basinal structure, known as the Murchison Highway Structure, is inferred to continue to the north west through EL 37/89 (Sock Creek) and EL 39/85 (Bulgobac) until it joins with the Mount Charter Fault four kilometres from Mount Charter. Leaman (1988) regarded the north west end of this structure, in EL 39/85, as a growth fault. Although striking north west its orientation is oblique to the true transfer fault orientation of Windh and Etheridge (1992). Hence a component of normal fault movement is evident.




# MT CHARTER AREA
# SUMMARY GEOLOGY

0 500m 1000m
SCALE

FIG. 2

SR/lms 20-10-1992

The other major Cambrian structure inferred in the Mount Charter area is the Barite Creek Structure, Fig. 2. Apparently not reactivated this feature appears to exhibit control over thickness and distribution of lithological units. For example, the rapid apparent increase in thickness of Lower Basalt north of the structure and the anomalous north east trend of the dacite body running along it. Striking around 055° G it has a similar orientation to the 045° G trend of 2B feeder veins, dykes and alignment of feeders at Hellyer; Gemmel (1992).

The Mount Charter barite occurs at the intersection of these two inferred Cambrian structures; on the interpreted most downthrown block. Stratigraphically the mineralisation occurs at the top of the Mixed Sequence, unlike Hellyer and Que River that are hosted lower in the sequence.

Rand (1988) favoured a replacement model for the massive barite, with low temperature seawater rich fluids circulating through dacitic volcanics, precipitating barite at the overlying impermeable contact with the andesite. Such a model could be analogous to the hangingwall plume over Hellyer where hydrothermal activity continued after burial of the sulphide mound.

This allows the possibility of VHMS mineralisation stratigraphically lower than the barite. Only one hole (MAC 26) had tested the base of the Mixed Sequence at Mount Charter but was at least 350-400 m from the target area near the intersection of the above two structures. Therefore a significant sulphide body would probably have been missed by DHEM.

A drill target was proposed for the base of the Mixed Sequence near the junction of the two inferred Cambrian structures. The hole would be targetted at the most downthrown block hosting the barite, alteration and thickest dacite.

## 6.2 DDH MAC 32

### 6.2.1 Introduction

DDH MAC 32 was planned to drill south west, perpendicular to the strike of the Mount Charter alteration zone as north west was considered the most likely long dimension of any mineralisation.

However, this required drilling across strike of cleavage at about 45°. Azimuth deviation, in cleaved rocks of the Mount Charter alteration zone, could not be controlled and MAC 32 was abandoned at 278.4 m.

### 6.2.2 Geology

A detailed log is attached as Appendix IV, whilst a cross section is included as Plate MAC 365. A summary log is as follows:

| | | | |
|---|---|---|---|
| 0 | - | 29.9m | Silica (Si) + Sericite (Se) + Pyrite (Py) altered volcaniclastic - Mount Charter alteration zone. |

| | | |
|---|---|---|
| 29.9 - | 35.1m | Si + Se + Py altered polymict epiclastic - Mount Charter Alteration Zone. |
| 35.1 - | 56.6m | Si + Se + Py altered dacite lava and breccia - Mount Charter Alteration Zone. |
| 56.6 - | 62.8m | Polymict epiclastic - Mixed Sequence. |
| 62.8 - | 104.5m | Dacitic volcaniclastic - Mixed Sequence. |
| 104.5 - | 229.1m | Si + Se + Py altered dacite lava - Mount Charter Alteration Zone. |
| 229.1 - | 264.3m | Si + Se + Py altered dacitic volcaniclastics - Mount Charter Alteration Zone. |
| 264.3 - | 278.4m | Si + Se + Py altered dacite lava - Mount Charter Alteration Zone. |

MAC 32 was collared on the north east edge of the Mount Charter Alteration Zone. The hole intersected variably altered dacite lava and less common volcaniclastics over its entire length.

Alteration is pervasively silica + sericite + pyrite and is most intense from surface to 33.5 m. From 56.6 to 97.5 m alteration is weak sericite + chlorite but rapidly increases again below 97.5 m to be strongly pervasive Si + Se + Py to hole end. Strongly altered rocks host pyritic veins, stockworks and disseminations averaging 5-10% pyrite. Also sporadically developed within the alteration zone are barite + carbonate $\pm$ galena $\pm$ sphalerite veins to about 30 cm thick.

### 6.2.3 Geochemistry

Thirty two core grind samples covering the length of MAC 32 were submitted for whole rock and Zr, Cr, Ba, As, S, Cu, Pb, Zn, Ag and Au assay. Sample intervals up to ten metres were chosen to coincide with lithological boundaries. Results are presented on Plates MAC 378 A and B and in Appendix V.

Gold and silver values from sericite and silica altered rocks are elevated; in particular from the most intensely altered rocks above 33.5 m where a peak value of 1.2 ppm Au and 64 ppm Ag over 1.7 m above 25.2 m is recorded. Best interval is 32.2 m at 0.4 g/t Au above 32.2 m.

Zinc and lead are sporadically elevated throughout the pyritic alteration reflecting the presence of minor thin sphalerite + galena + pyrite veins. Peak values of 0.43% Zn and 155 ppm Pb (different samples) were recorded. Copper is only weakly elevated with up to 536 ppm but in general there is good correlation with gold grade. Arsenic values up to 858 ppm correlate well with S and hence pyrite content. Barium assays up to 15% reflect the common barite veins.

Alteration indices [100 x $K_2O$ + MgO)/CaO + $Na_2O$ + $K_2O$ + MgO] are uniformlly high (>90) throughout the hole suggesting very strong alteration. This includes the apparently relatively unaltered interval between 56.6 m and 104.5 m which is depleted in Na and Ca. An increased Mg content in this interval reflects the presence of chlorite.

Ti/Zr values (around 15) and $P_2O_5$ values (around 0.2%) were higher than expected for typical Mixed Sequence dacites. Cr is generally less than 50 ppm as expected.

### 6.2.4 Geophysics

No DHEM survey was undertaken in MAC 32 as the DHEM survey of the upper part of MAC 26 and have surface UTEM surveys tested this area.

## 6.3 DDH MAC 33

### 6.3.1 Introduction

MAC 33 was drilled to test the same target as MAC 32. The hole was collared on the opposite side of the Mount Charter Alteration Zone to MAC 32 and drilled toward the north east (i.e. 180° to MAC 32) to remain perpendicular to the strike of the Murchison Highway Structure. Most of the drilling would be outside cleaved rocks of the alteration zone and therefore not deviate in azimuth as MAC 32 had done.

### 6.3.2 Geology

A detailed log and petrographic descriptions are attached as Appendix VI, whilst a cross section is included as Plate MAC 365. A summary log is as follows:

| | | | |
|---|---|---|---|
| 0 | - | 73.6m | Cambrian (?) dolerite. |
| 73.6 | - | 155.5m | Que River Shale. |
| 155.5 | - | 170.5m | Cambrian (?) dolerite. |
| 170.5 | - | 216.1m | Que River Shale. |
| 216.1 | - | 510.3m | Basaltic to dacitic locally feldspar phyric lava and volcaniclastic - Upper Basalt correlate ? |
| 510.3 | - | 519.4m | Polymict lapilli to breccia volcaniclastic - Mixed Sequence ? |
| 519.4 | - | 613.4m | Feldspar phyric dacite lava and volcaniclastic. |
| 613.4 | - | 621.1m | Basalt lava. |
| 621.1 | - | 631.1m | Feldspar phyric dacite lava and volcaniclastic. |
| 631.1 | - | 672.0m | Basalt lava. |
| 672.0 | - | 750.5m | Feldspar phyric dacite lava and volcaniclastic. |
| 750.5 | - | 805.7m | Feldspar phyric silicic andesite lava and volcaniclastic. |
| 805.7 | - | 823.4m | Ash volcaniclastic with minor basalt lava interbeds. |
| 823.4 | - | 910.7m | Mica Sandstone. |

MAC 33 was collared in the Mount Charter dolerite sill. A faulted chilled margin at 73.6 m marked the boundary with black carbonaceous Que River Shale. Five bands to 90 cm thick of felsic fine lapilli volcaniclastic were intersected within the shale down to 103.7 m. Dolerite was intersected again between 155.5 m and 170.5 m. This intrusive has a vesicular top as is seen in the Hellyer Tailings Dam dolerite (HL 541) until an interval of basaltic peperite marked the top of the Que Hellyer Volcanics at 216.1 m.

Amygdaloidal polymict basaltic lapilli volcaniclastics to 254.4 m contain common silica + sericite + sphalerite + galena altered fragments indicative of hydrothermal alteration before emplacement. Below this depth mineralised fragments are rare and amygdaloidal fragments become less common.

The bulk of the interval between 254.4 m and 510.3 m is composed of variably feldspar phyric volcaniclastics of andesitic to dacitic composition. Fragments are dominantly chlorite altered within a more siliceous often ashy matrix. Massive lavas are less common than volcaniclastics.

Below a thin interval of polymict epiclastic (?) (510.3-519.4 m) lavas and volcaniclastics become coarsely feldspar phyric and dacitic in composition. This sequence persists effectively to 805.7 m although geochemistry suggests the basal 55 m is probably siliceous andesite.

Conformably underlying the siliceous andesite but in faulted contact with Mica Sandstone is a basal sequence 17. 7 m thick of ash volcaniclastic containing two basalt lava lenses to 1.3 m thick. These basalt lenses may be thin correlates of the Lower Basalt Sequence.

It is uncertain whether the feldspar phyric dacite sequence (510.3-805.7 m) is a correlate of the Mixed Sequence dacites and therefore there are effectively no footwall andesites/basalts in the area. Alternatively these dacites are a more felsic equivalent of the footwall feldspar phyric andesites.

The stratigraphic sequence in MAC 33, with a thick sequence of dacite resting on thin andesite or Mica Sandstone, is consistent with that intersected by other holes in the SW corner of the Que Hellyer Volcanic basin e.g. BRD 01, BRD 05 (Placer) and BHD 3 (Pasminco).

Disseminated sphalerite mineralisation (1-2% Sp), associated with patchy and vein silica alteration, is a feature of the basalts underlying the Que River Shale. Alteration and mineralisation decrease with depth but occur sporadically in all volcanics in MAC 33. This style of mineralisation, over very broad intervals, principally in the Upper Basalt Sequence, is a feature of holes in the High Point - Mount Charter area.

MAC 33 did not cross the Murchison Highway Structure and is inferred to have remained in the less prospective footwall block. However, the thickness of Que Hellyer Volcanics in MAC 33 is around 600 m whilst MAC 26 only 500 m away indicates the volcanics are well in excess of 850 m. This major thickness change occurs across the inferred Murchison Highway Structure and appears to confirm its existance and support the exploration concept.

MAC 33 failed to intersect the targetted inferred prospective downthrown block but a DHEM survey of MAC 33 combined with the DHEM survey of MAC 26 will effectively test the original target.

### 6.3.3 Geochemistry

Eighty one core grind samples covering the length of MAC 33 were submitted for assay. Sample intervals up to 15 m were chosen to coincide with lithological boundaries. The Que River Shale was assayed for Cu, Pb, Zn, Ag and Au only whilst other samples were submitted for whole rock and Zr, Cr, Ba, As, S, Cu, Pb, Zn, Ag and Au. Results are included as Plates MAC 365 A and B and Appendix VII.

Zinc and lead values are highest in the dominantly andesitic sequence underlying the Que River Shale and correlated with the Upper Basalt Sequence. Peak values of 4238 ppm Zn and 1130 ppm Pb were recorded from different samples. An interval averaging 2000 ppm Zn and 500 ppm Pb is evident between 234.4 m and 359.0 m.

These values reflect disseminated sphalerite and galena found in altered basaltic clasts or associated with overprinting siliceous alteration. Zinc and lead are only locally elevated elsewhere in the hole whilst copper is always less than 300 ppm.

Gold and silver assays are all below detection limits of 0.008 ppm and 2 ppm respectively. Arsenic values are only locally weakly elevated within the broad zone of sphalerite mineralisation but show no direct correlation with zinc or lead.

Alteration associated with the disseminated sphalerite and galena mineralisation is not reflected by significant major element mobility.

The dominantly andesitic sequence correlated with the Upper Basalt Sequence is elevated in $P_2O_5$ (> 0.25%) but low in Cr (generally < 20 ppm). This is typical of andesites equivalent to the Hellyer Mine Pillow Lava Sequence south east of the orebody. Basalts within the feldspar phyric dacitic to andesitic sequence and at the base of the volcanics,are high in Cr (> 400 ppm). The dolerite sills and detrital chromite bearing Mica Sandstone are also high in Cr returning > 700 ppm and > 350 ppm respectively.

Ti/Zr ratios reflect volcanic composition. Dacite-basalt equated with the Upper Basalt Sequence range from 17 to 27 and indicate two major units separated by an epiclastic horizon. An upper unit from 216.1 m to 389.1 m has Ti/Zr of 23-27 whilst the lower unit from 392.1 - 510.3 m is characterised by Ti/Zr of 14-19.

The underlying feldspar phyric sequence has a Ti/Zr ratio that decreases up hole through several units. Basal silicic andesite ranges from 20-24, the bulk of the sequence from 12-19 and an upper unit is typified by Ti/Zr of 9-11.

### 6.3.4 Geophysics

At the time of writing the planned DHEM survey of MAC 33 is incomplete. Results of this survey will be presented in the next annual report.

# 7.0 MURCHISON HIGHWAY ZONE

## 7.1 Introduction

During Aberfoyle's study of the Que Hellyer Volcanic basin syn-volcanic fault network, one area surpassed all others for the number of Cambrian faults that were present. Four well defined syn-volcanic structures were inferred to converge in the area south east of the Que River Mine access road and Murchison Highway junction. This area is referred to as the Murchison Highway Zone, Fig. 3.

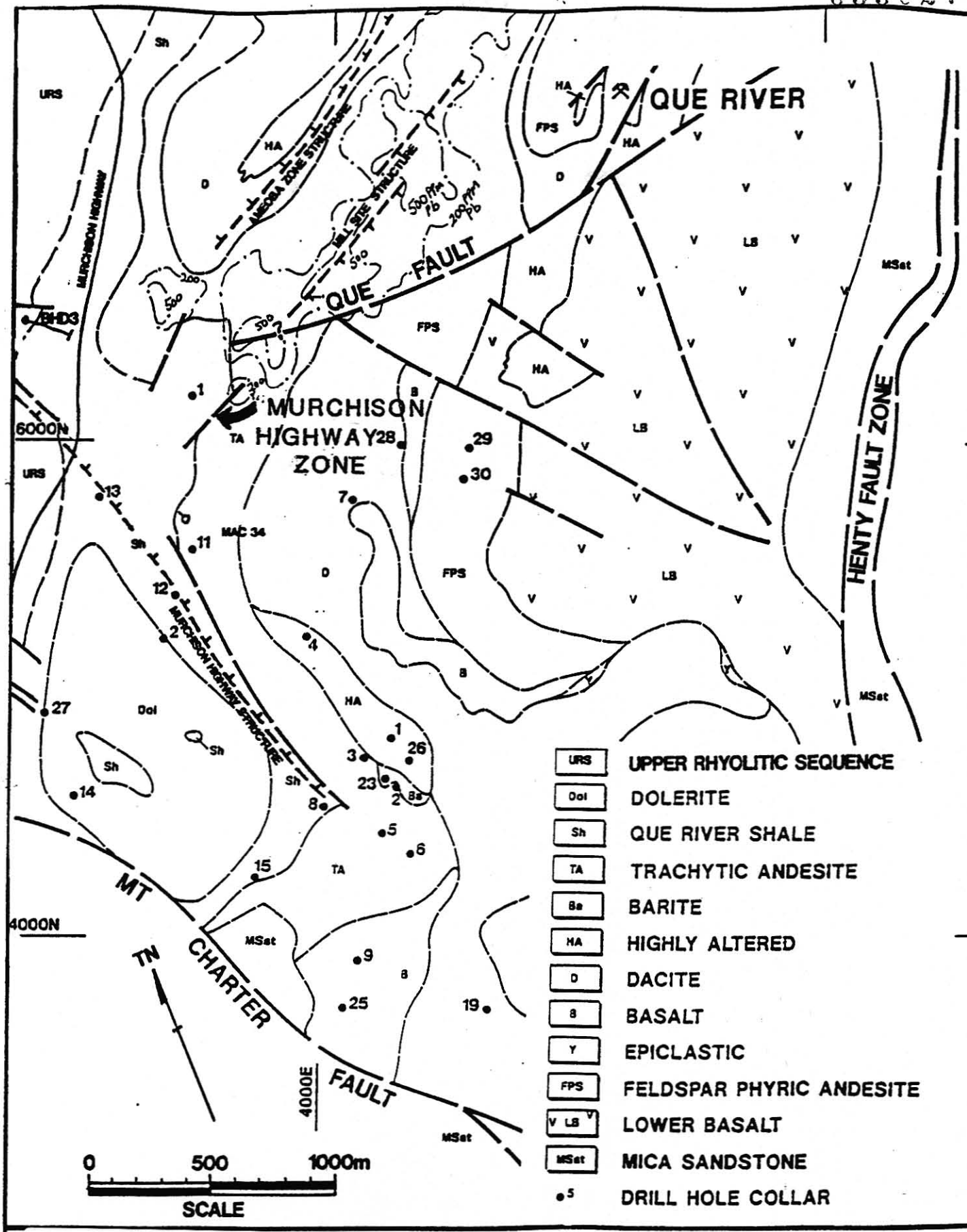
The four structures that converge are:

1) *Que Fault* - Upper Basalt sequence changes from basalt dominant north of the fault to low Cr andesite south of the fault.

2) *Mill Site Structure* - A line of base metal soil anomalies reflects the presence of a north east trending syn-volcanic structure that controls the thickness of Mixed Sequence dacite within the Old Mill Site syncline. Dacite is thickest on the eastern side.

3) *Amoeba Zone Structure* - Sub parallel to the above structure and defined by a zone of silica + sericite + pyrite alteration about 100 m across. Potentially downthrown on the western side during the Cambrian.

4) *Murchison Highway Structure* - A basin sidewall fault along which the Mount Charter alteration zone is developed, parallelling the Mount Charter Fault.




5 cm

Aberfoyle Resources Limited
EXPLORATION DIVISION

Figure 3

| REVISIONS | | | |
|---|---|---|---|
| Init. | Date | Init. | Date |
| | | | |
| | | | |
| | | | |
| | | | |
| | | | |

NORTH WEST TASMANIA
EL 106/87 MACKINTOSH
**MURCHISON HIGHWAY ZONE**
**SUMMARY GEOLOGY**

Compiled : SR
Drawn :
Traced :
Checked : SR

Location Code :
Scale : AS SHOWN
Date : 28-12-92
Plate No. :

1511

The Murchison Highway Zone was considered prospective for VHMS on the basis that the intersection of so many structures presented good potential for dilatant areas to have developed; especially during Mixed Sequence time.

A target was proposed in the core of the small syncline along strike from the Old Mill Site base metal soil geochemical trend, interpreted to reflect the underlying Old Mill Site Structure. The target was the base of the Mixed Sequence on section 5950N at -100 RL.

## 7.2 DDH MAC 34

DDH MAC 34 was designed to drill perpendicular to the syncline axial trace. Collared on the edge of the Que River Shale the hole azimuth immediately deviated to the south due to cleavage strike crossing the hole path at about 45°.

The hole was abandoned at 30 m and re-collared as DDH MAC 35.

A detailed log is attached as Appendix VIII.

## 7.3 DDH MAC 35

### 7.3.1 Introduction

DDH MAC 35 was drilled due grid west to intersect the same target as MAC 34.

### 7.3.2 Geology

A detailed log and petrographic descriptions are attached as Appendix IX, whilst a cross section is included as Plate MAC 366. A summary log is as follows:

| | | | |
|---|---|---|---|
| 0 | - | 262.45m | Feldspar phyric andesite lava and volcaniclastic - Upper Basalt Sequence. |
| 262.45- | | 746.7m | Amygdaloidal (feldspar phyric) basalt lava and volcaniclastic - Upper Basalt Sequence. |
| 746.7 - | | 778.1m | Feldspar phyric dacite lava and volcaniclastic. |
| 778.1 - | | 897.3m | Polymict dacitic lapilli volcaniclastic, local interbedded basalt lava - Mixed Sequence. |
| 897.3 - | | 1189.6m | Feldspar phyric dacite lava and volcaniclastic. |

The hole was collared in feldspar phyric andesites that underlie the Que River Shale south of the Que Fault. These were locally silica + albite altered with minor disseminated sphalerite + galena $\pm$ pyrite. A 7.5 m interval of locally strongly fuchsite altered andesitic and basaltic lapilli volcaniclastic (epiclastic ?) marks the boundary with the underlying basaltic sequence.

With a true thickness of nearly 400 m the basalt sequence was thicker than expected. It comprised an upper unit of pillow lava overlying a sequence of amygdaloidal to locally feldspar phyric lava and volcaniclastic. The pillow lava contained up to 10% interpillow pyrite and was locally fuchsite altered.

A poorly defined contact marked the transition to feldspar phyric dacite lava and volcaniclastic at around 750 m but this soon passes at around 778 m to a thick interval of polymict epiclastic; an inferred correlate of the Mixed Sequence. These epiclastics are weakly sericite + silica + carbonate altered and dominated by lapilli to breccia sized feldspar phyric dacite to andesite lava clasts in an originally ashy matrix. A true thickness of around 80 m is inferred.

From 897 m to hole end at 1189.6 m feldspar phyric dacite lavas and subordinate volcaniclastics, similar to those overlying the epiclastics, were intersected. This sequence correlates with the thick dacite sequence in MAC 33 and other holes in the south west corner of the Que Hellyer Volcanic basin. It is uncertain whether they are correlates of the Mixed Sequence or a felsic equivalent of the feldspar phyric andesites.

MAC 35 does not appear to have crossed any major syn-volcanic fault but is interpreted to be adjacent to the Murchison Highway Structure on its downthrown side. Thick epiclastics correlated with the Mixed Sequence may reflect thick deposits built up against this structure.

### 7.3.3 Geochemistry

One hundred and fourteen core grind samples covering the length of MAC 35 were submitted for whole rock and Zr, Cr, Ba, As, S, Cu, Pb, Zn, Ag and Au assay. Sample intervals were chosen coinciding with lithological boundaries or ten metres in areas of uniform lithology. Results are presented on Plates MAC 366A and B and in Appendix X.

Base metals are elevated in several areas but most consistently in the upper andesitic sequence and in particular the silica + albite altered intervals. Between 140 m and 211 m an average of 2000 ppm Zn and 900 ppm Pb was returned. Highest Zn value of 0.49% (1.75 m) was recorded from the volcaniclastics between the andesite and basalt sequences.

This unit also hosts the maximum gold assay of 0.09 ppm Au whilst gold and silver assays in other areas are uniformly low. A peak arsenic value of 505 ppm is also related to this volcaniclastic but elevated values occur in the underlying basalt, decreasing to background with depth.

The andesitic sequence is characterised by low Cr (<50 ppm) and elevated $P_2O_5$ (> 0.24%). MgO is generally less than 4% consistent with its evolved character noted in petrology.

At least four geochemically distinct "units" are evident within the basaltic sequence. There is a progression toward increased $P_2O_5$ and Cr upward through the pile. The pillow lavas at the top of the sequence are marked by high Cr (> 500 ppm), high $P_2O_5$ (> 0.4%) and high CaO (up to 25%). CaO values this high are unusual and reflect intense clacite veining of this unit.

Dacites above and below the Mixed Sequence (?) epiclastics are geochemically similar. They have a relatively low Ti/Zr of around 10-14 and low $P_2O_5$ (< 0.11%) and low Cr (< 100 ppm).

### 7.3.4 Geophysics

At the time of writing the planned DHEM survey of MAC 35 is incomplete. Results of this survey will be presented in the next annual report.

# 8.0 AEROMAGNETIC AND RADIOMETRIC SURVEY

## 8.1 Introduction

Prior to March, 1993 the magnetic data available for EL 106/87 was a compilation of several generations of ground surveys that could not be integrated without producing severe striping in a N-S and E-W direction. These prominent features masked any subtle structural trends that may otherwise be evident in the data.

Although the Que-Hellyer Volcanics are relatively magnetically quiet, the ground data did show some prominent geological features. Sufficient magnetic susceptibility contrast appeared to exist for geological features to be clearly defined if a high quality survey were to be undertaken. The proposed new survey would be used to confirm geological trends and more accurately locate structures inferred from geological and geochemical data.

## 8.2 Survey Results

During March, 1993 Geoterrex Pty Ltd conducted a 1087 line km helicopter borne aeromagnetic and radiometric survey over EL 106/87. Line spacing was 100 m with flight line direction chosen to cross inferred Cambrian fault orientations at as high an angle as possible.

Survey specifications and a logistics report are attached as Appendix XI. At the time of writing interpretation of the survey is incomplete. Results will be discussed in the next annual report.

Survey data in digital format on magnetic tape is provided with this report.

## 9.0 CONCLUSIONS

Several major syn-volcanic faults have been identified on EL 106/87. These are inferred to control the distribution and thickness of volcanics within the Que-Hellyer Volcanics. Intersections of syn-volcanic faults are potential focci for venting hydrothermal fluids that may have lead to orebody formation.

Deep geological drill targets are indicated where prospective stratigraphy occurs adjacent to these structures, below surface EM penetration. Drill testing of two targets to date has not intersected mineralisation but has provided support for the exploration concept.

Interpretation of the recently completed aeromagnetic survey will lead to the refinement of existing and possible identification of new syn-volcanic structures. Further drill targets will be generated and tested during the coming year.

655035



## 10.0 REFERENCES

Gemmel, J. B., Large, R. R., 1992. Stringer System and Alteration Zones Underlying the Hellyer Volcanic Hosted Massive Sulphide Deposit, Tasmania, Australia: Economic Geology, Vol. 87, pp 620-649.

Leaman, D., 1988. Que Road Gravity Survey. EL 39/85 Unpub. Report for CSR Ltd.

McNeil, A. W., 1991. Exploration Licence 106/87. Progress Report for the Period May 1990 to April 1991. Aberfoyle Resources Ltd. Unpub. Report.

Rand, S. W., 1988. The Geology and Mineralisation of the Mount Charter Prospect. Upub. Hons. Thesis, University of Tasmania.

Richardson, S. M., 1992. Exploration Licence 106/87. Progress Report for the Period April 1991 to April 1992. Aberfoyle Resources Ltd. Unpub. Report.

# APPENDIX I

655037

# ERUPTIVE ACTIVITY, PRODUCTS AND DEPOSITIONAL SETTING OF THE CAMBRIAN VOLCANIC-SEDIMENTARY SUCCESSION HOSTING MASSIVE SULPHIDE MINERALISATION (VMS) AT HELLYER AND QUE RIVER MINES, MT. READ VOLCANIC BELT, WESTERN TASMANIA.

PROGRESS REPORT NO.13

by
John Waters, Ph.D. Student,
Department of Earth Sciences, Monash University.

JANUARY 1992 - JUNE 1992

*Introduction*

This report is the thirteenth in a series of progress reports to Aberfoyle Resources on the Ph.D study of the Hellyer - Que River Volcano - Sedimentary succession. The report concentrates on the modification and redescription of the dacitic to rhyodacitic volcanics within the succession, looking at the association between facies and suggesting eruption and emplacement mechanisms for these units.

Volcanics of dacitic to rhyodacitic composition occur as relatively small, generally elongate bodies within the Mixed Sequence or host horizon to mineralisation. These have been identified from north of the Hellyer deposit, south through Que River to Mt. Charter and have correlates in the Sock Creek area to the south west (Corbett and Komyshan, 1989). Most of these bodies are composed of both coherent and fragmental zones, with some of the fragmental debris being resedimented and incorporated into the Mixed Sequence volcaniclastics. Intrusive, as well as extrusive, forms have been identified with most of the mineralisation associated with bodies which are partly or wholly extrusive in character. It is therefore critical to recognise the products of various eruption types and mechanisms, and distinguish the shallow intrusive sill like bodies from the extrusives. This is also important from a stratigraphic view point as well as working out the relative timing of events which led to the formation of the Que - Hellyer succession.

Work on the project to date has identified two major associations of facies which are still being refined. The first is a "basalt-andesite-mudstone" association which consists of facies which represents lithologies emplacement as shallow intrusive sill / laccolith like bodies which may have become extrusive locally (e.g. Lower Andesites and Basalts and the Hellyer Basalt). The second association is a "dacite-rhyodacite-volcaniclastic-sulphide" association which represents a dominantly extrusive/surface process dominated association which has some associated intrusives. This association is approximately equivalent to the Mixed Sequence units of the Que - Hellyer Volcanics and is important in that this association is more likely to host syngenetic exhalative sulphide mineralisation than the shallow intrusive dominated association.

This report will deal with the three felsic to intermediate volcanic facies within the second association interpreting their formation and proposing a possible model for their emplacement. The volcaniclastic facies within this association, which include the polymict volcaniclastic breccias and sandstones of the Mixed Sequence, which have been discussed briefly in previous reports, and the sulphide facies will not be discussed here, but form a major part of this association.

*Field Work*

Two field trips to the Que River - Hellyer area were conducted during the period covered by this report. The first of these trips focused on the final two sections to be covered by this study at the Que River deposit (7712.5 N and 7900 N). A combined total of 24 drill holes were logged from these sections to complete the six sections to be used to investigate the nature of the Mixed Sequence at the Que River deposit. The aim of the second trip was to complete the northern end of the regional north - south section. This involved the logging of 5 surface hole (Hat-3, Mac-12, Mac-18, HL-345 and HL-469, a, b and c).

## Facies of the Dacite-Rhyodacite-Volcaniclastic-Sulphide Association in the Que - Hellyer Volcanics

The Mixed Sequence horizon within the QHV consists of a complex association of volcanic, volcaniclastic and sulphide facies which together represent deposition in a moderate to deep water environment. Facies within this association are best formed in areas immediately adjacent to mineralisation. These facies primarily involve units emplaced or deposited on the sea floor by surface processes. Such facies therefore are controlled in part by the existing structure and topography of the seafloor and in turn modify the seafloor therefore affecting the characteristics of subsequent facies. Such controls may explain rapid lateral facies transitions and thickness variations within the volcanics and especially the volcaniclastics.

The three facies discussed below represent the products of felsic volcanism within the Que - Hellyer Volcanics. Terminology with regards to the composition of these volcanics is based on a combination of geochemistry and modal mineralogy of the volcanics. For example, volcanics containing greater than a few percent modal quartz phenocrysts are termed rhyodacites, dacites are those feldspar bearing intermediate to felsic volcanics with less than 1 - 2% modal quartz and Zr over $TiO_2$ ratios in the dacite field of Winchester and Floyd, (1977). Selected geochemistry for these felsic volcanics, along with felsic volcanics from the Southwell subgroup and intrusive in the area are shown in Figure 1.

### Rhyodacite

A NE-SW trending body of rhyodacite at occurs to the west of the Hellyer deposit stratigraphically below the Hellyer Basalt (Figs. 2 and 3). The unit is not known to crop out east of the Murchison highway, being found to date only in drill holes. This rhyodacite unit is composed of coherent and fragmental intervals, with the fragmental zones consisting of autoclastic debris, both insitu and resedimented. The body has a true thickness up to roughly 80-90 metres in the vicinity of Hat-009 and HL-469. The lower and upper contacts of this facies contain variable quantities of fine

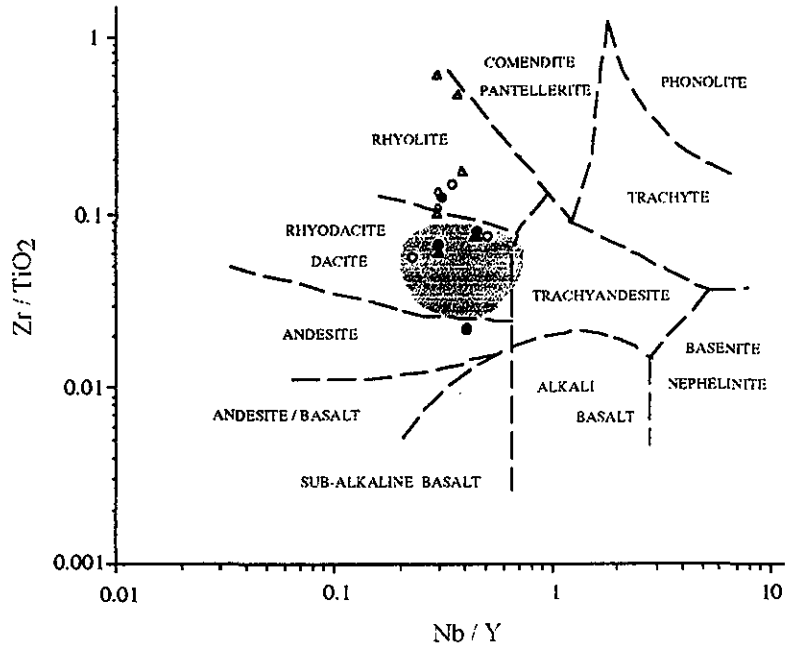



Figure 1: Plot of Nb/Y vs Zr/TiO2 for selected felsic rocks from the Que - Hellyer and Sock Creek areas (fields after Winchester and Floyd, 1977). The shaded area shows the field where Que - Hellyer 'dacites' plot; solid circles = Sock Creek felsic volcanics; open circles = Southwell Subgroup; solid triangles = quartz-feldspar porphyries of Corbett and Komyshan, 1989; and open triangles = felsic intrusives of Corbett and Komyshan, 1989. Note the quartz-feldspar porphyries of Corbett and Komyshan, 1989 (Rhyodacite facies of this report) plot within the Que - Hellyer field. All the felsic volcanics in the area show roughly the same alkalinity (Nb/Y ratio), varying only in their degree of differentiation ($Zr/TiO_2$ ratio).

grained sediments as inclusions within the coherent lava and as a matrix to the fragmental zones.

The zones of coherent lava are moderately porphyritic with up to 25% total phenocrysts of dominantly quartz and plagioclase. These phenocrysts range up to 2mm in diameter and are generally euhedral to subhedral. Rare (≤1%) pseudomorphs after biotite and orthopyroxene or amphibole(?) are present in samples from Hat-9, Hat-5 and Mac-10. Some intersections of the rhyodacite lava appear slightly more porphyritic toward the top. The groundmass is weakly spherulitic and altered to a mosaic of quartz and feldspar. Patches of sericite or chlorite rich groundmass give handspecimens a mottled dark green-grey to cream coloured pseudobrecciated appearance. Intervals of coherent lava reach up to 70 metres in core thickness within Hat-9 (Fig. 3).

Fragmental zones within this facies are represented by massive to very weakly graded clast supported to matrix supported breccias. Closed framework, clast supported breccias occasionally exhibit weak to moderate jigsaw fit of fragments and are often

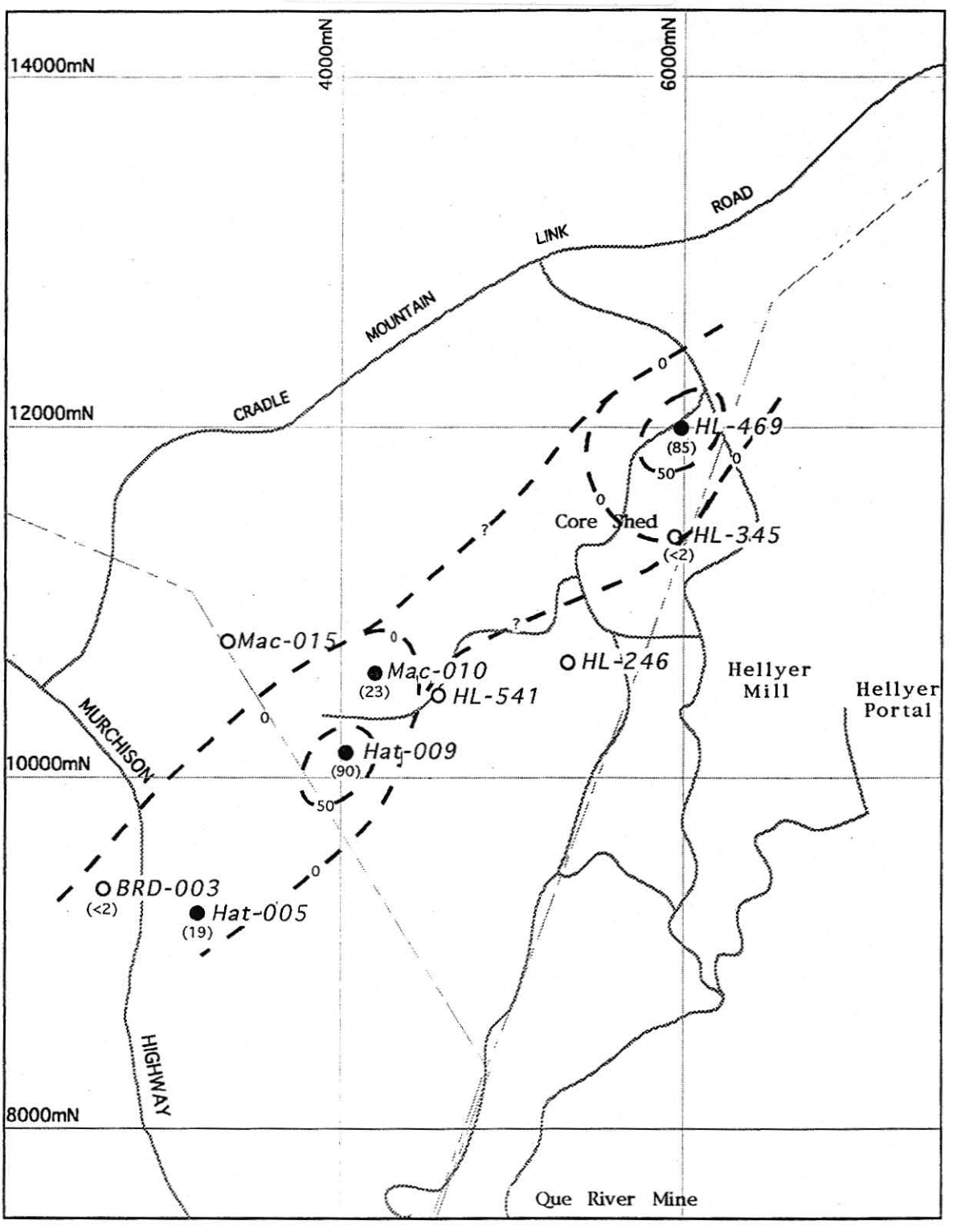



Figure 2: Subsurface distribution of the Rhyodacite facies east of the Murchison Highway. Filled circles represent holes containing this facies, with approximate thickness in brackets. Shaded circles represent drill holes with intervals of fragmentals / volcaniclastics which probably represent the distal margins of this facies. Open circles represent adjacent holes not containing this facies. HL-345 possibly contains resedimented debris from the lava identified in HL-469 (see Figure 3). Approximate isopacs of this facies are shown with thickness in metres. The distribution of this facies may either be interpreted as representing a single north-east trending body or several (2-3), dome like bodies.

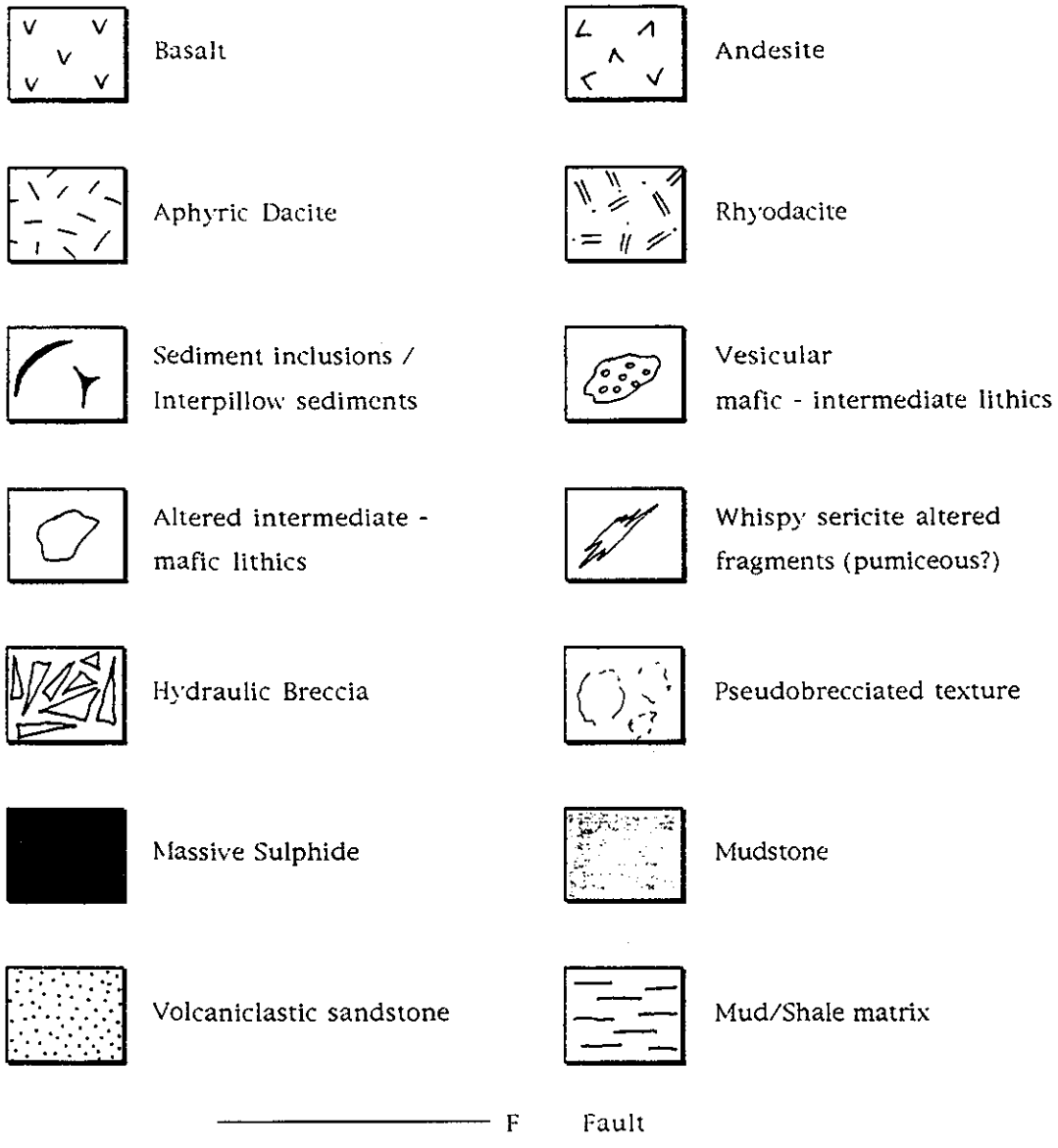
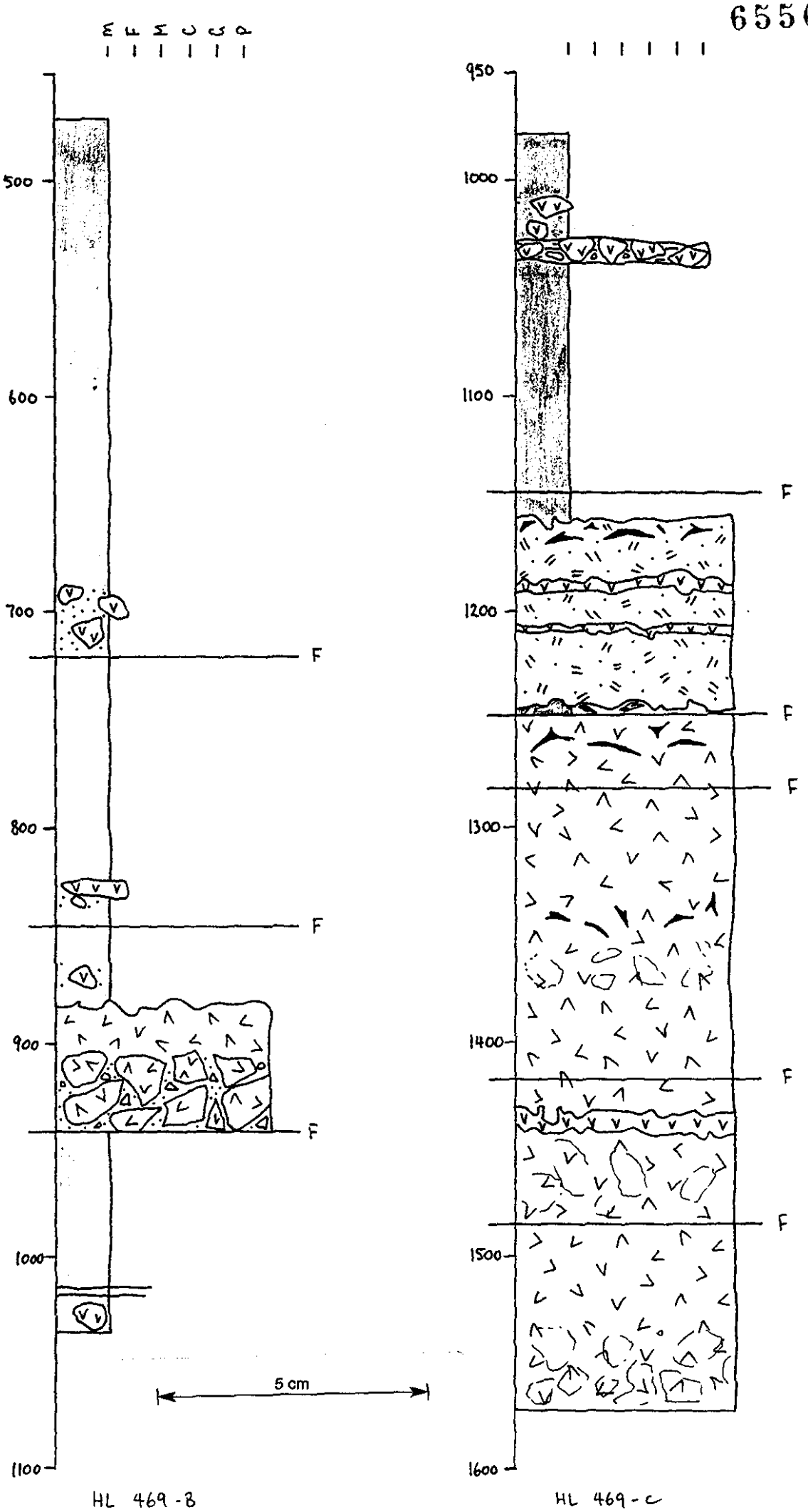


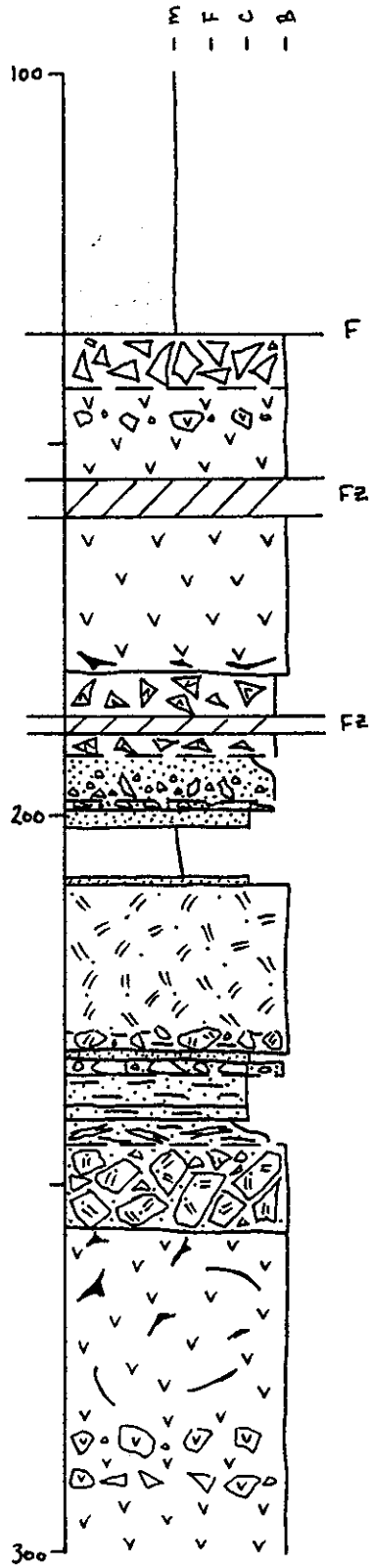

Figure 3 (following pages): Distribution of Rhyodacite facies within selected intervals of drill holes shown in Figure 2. Coherent and autoclastic lithotypes of this facies have been found in drill holes HL-469, Hat-5, Hat-9 and Mac-10, while HL-345 appears to contain 2 narrow horizons rich in resedimented debris very similar to that found within the Rhyodacite facies. (*)

655043

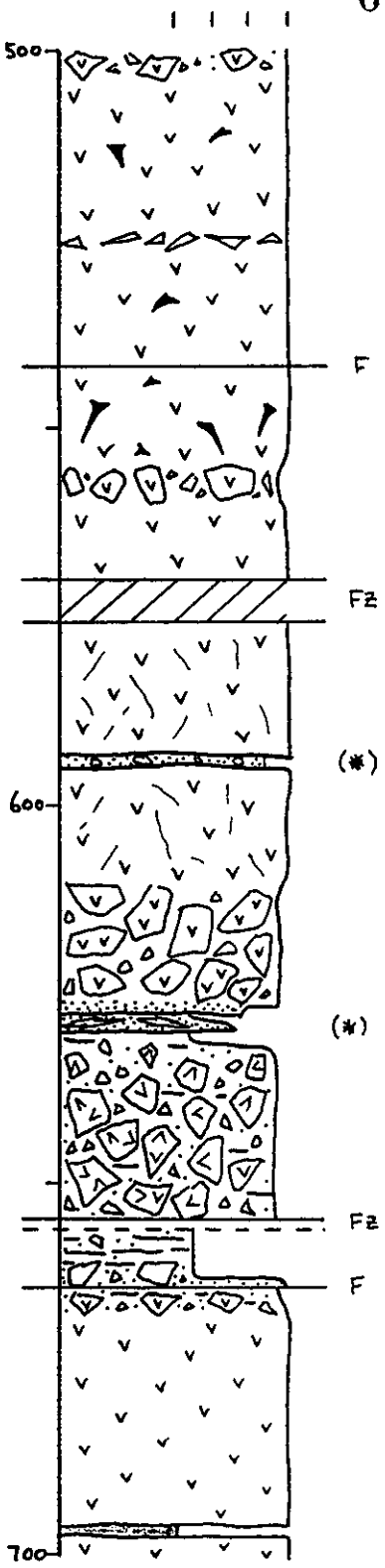



HL 469-B

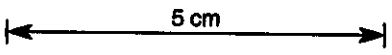
HL 469-C



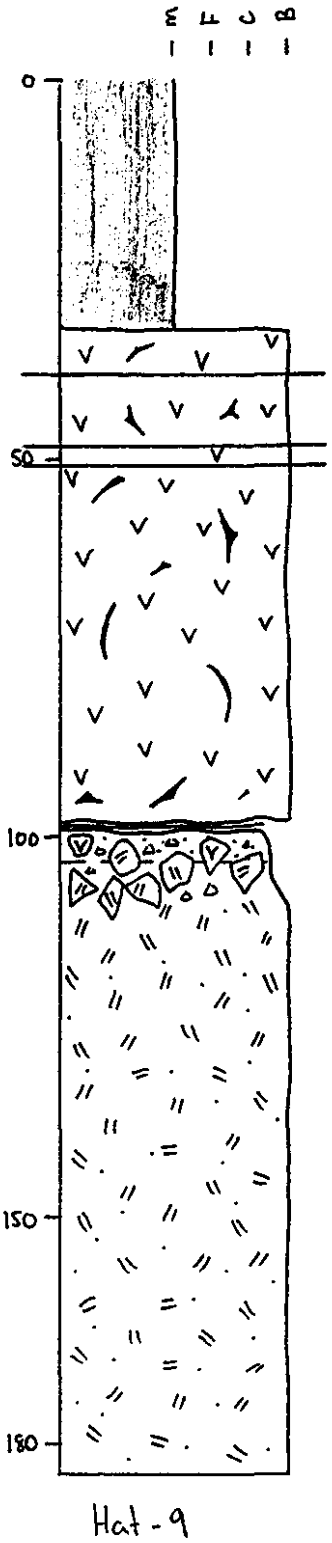

Hat-5



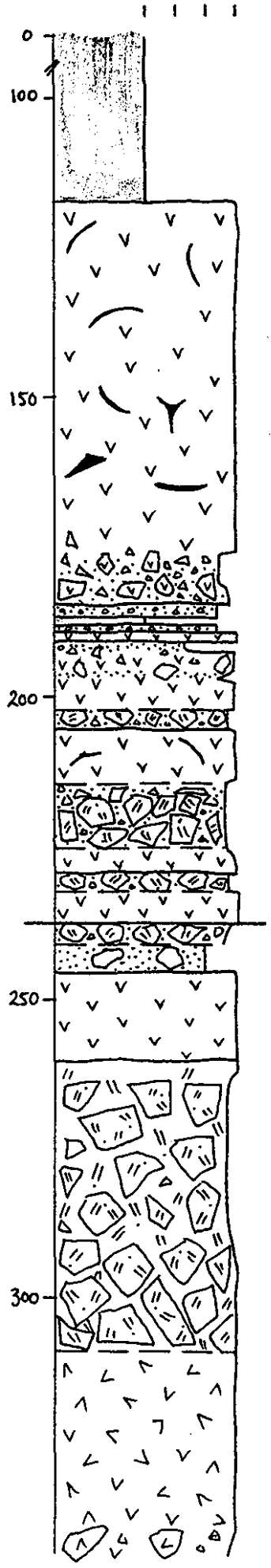

HL - 345



655045




Hat-9




Mac-10



in gradational contact with zones of coherent lava in core. Closed to open framework breccias, not related to coherent zones in core, generally lack jigsaw fit of fragments. Fragments within these breccias are angular and irregular to blocky in shape. Sorting within the breccias is poor. Fragments range in size from sand to in excess of cobble size, with some showing a diffuse flow banding. Compositionally these fragments are identical to the coherent intervals. The matrix comprises up to 20% of the breccias and is dominated by muds which appear very similar in character to the overlying sediments. Areas of relatively high matrix within these breccias give this zone a peperitic texture. Occasionally found within the matrix is sand sized dacite fragments and very minor crystals. Rare fossils including brachiopods, sponge spicules and a currently unidentified organism have been found within the mud matrix to these breccias within Hat-5.

*Interpretation*

Figure 2 indicates that this facies could be comprised of either a single northeast trending body approximately 2.5 by 0.4 kilometres, or up to 3 smaller dome like bodies of rhyodacite composition, up to several hundred metres in diameter. These are interpreted as representing high level rhyodacitic cryptodomes /sills and flows with associated quench fragmented to autobrecciated margins. Breccias not related to the coherent zones in core, and lacking signs of insitu fragmentation (i.e. jig saw fit), most likely represent areas of resedimented autoclastic debris. The massive, poorly sorted nature of these zones is not in consistent with emplacement of resedimented autoclastic debris as mass flows associated with the emplacement of the felsic bodies. If this is a single felsic body the high length to width ratio suggests that its distribution was controlled either by topography or by eruption related processes (e.g. fed by a elongate fissure, or multiple point sources rather than a single point source).

Due to the presence of moderate volumes of mud matrix within some the autoclastics of this facies, especially to the west of Hellyer, the unit is thought to have locally intruded wet, unconsolidated sediments. This wet unconsolidated sediment was deposited in a marine environment as suggested by the occurrence of marine fossils within it. Locally however these bodies must have become extrusive to enable the resedimentation of the autoclastic debris.

Aphyric Dacite

Several bodies of aphyric to weakly porphyritic dacite occur within the Mixed Sequence throughout the Que - Hellyer Volcanics. These bodies are best developed in the vicinity of mineralisation at both Que River and Mount Charter. A smaller body have also been located at the switchback, between the Hellyer and Que River deposits.

655047

These dacitic bodies occur predominantly as dome or wedge shaped bodies, often elongate in roughly a north north-east direction (Fig. 4). Most of these dacites fall along a trend from Mount Charter to Hellyer, which parallels the trend of mineralisation within the volcanics. These domes are comprised of both coherent and fragmental zones. In the vicinity of Que River these bodies reach a thickness of approximately 100 metres and are occasionally located on top of dykes with sheet like morphologies which are interpreted as their feeders.

The coherent zones within this facies are non-vesicular to very weakly vesicular with areas of diffuse flow banding. Flows are generally aphyric with occasional porphyritic zones containing up to a maximium of 10% plagioclase to 1 mm in length. Most feldspar phenocrysts are euhedral to subhedral and are replaced by carbonate and sericite. The least altered of these phenocrysts appear to be moderately to strongly zoned and rich in inclusions. The groundmass consists of a mosaic of quartz and feldspar, which probably represents the recrystallisation of an original devitrification texture. Preserved locally within this groundmass are spherulties. Variable and patch alteration often gives the coherent zones a pseudobrecciated texture.

Breccias within this facies are often in rapid gradational contact with coherent zones (Fig. 5). These consist of closed framework, blocky, angular metre to millimetre sized fragments. Contacts between fragments in these closed framework breccias occasionally show jig saw fit. Breccias enveloping the switchback dacite quickly grade from blocky with jigsaw fit textures to poorly sorted chaotic units which lack jigsaw fit. The composition of the fragments is identical to the coherent zones, with some more juvenile fragments with whispy appearances occurring in the open framework peperitic breccias. Rare accessory fragments including massive sulphide clasts and mud rafts have been found in the more chaotic zones furthest.from the coherent lavas (e.g. switchback dacite).

The matrix to the breccias varies from a few percent up to 25% in the case of the peperitic breccias (e.g. QR-699; 42-47m). The matrix generally consists of pale grey, strongly indurated muds (e.g. QR-90;~90-100m).

Hydraulic breccias also occur within this facies. These consist of angular blocky fragments, generally moderately to highly altered, with a carbonate and quartz cement between the fragments. This cement makes up to 20% in some breccias. Most fragments show jigsaw fit, with some fragments showing rotation and transport after fracturing.

655048

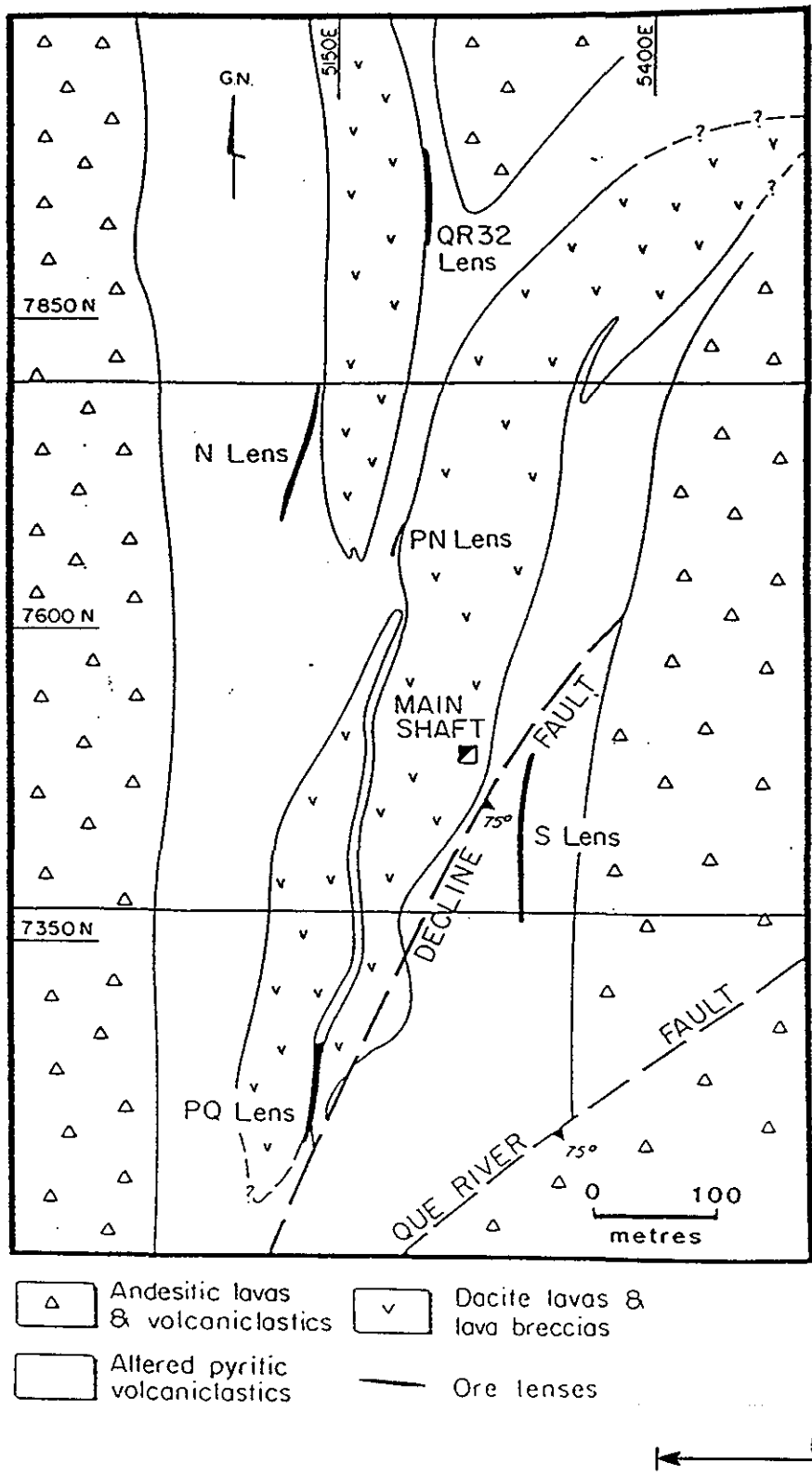
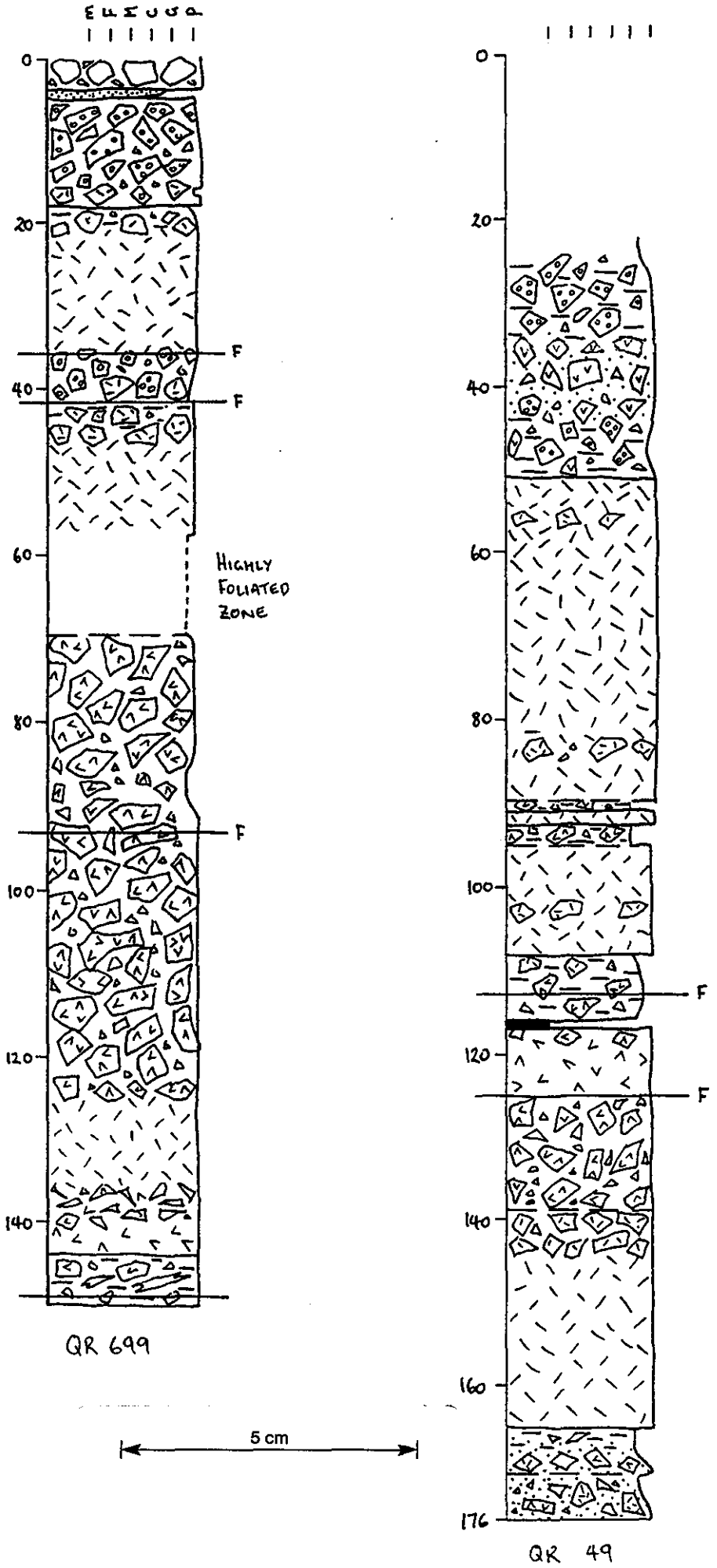



Figure 4: Plan view of the distribution of the aphyric to weakly porphyrictic dacites around Que River showing the elongate nature of the bodies. The underlying feeder parallels this trend (from Mc Arthur and Dronseika, 1990).

655049

Figure 5: Distribution of the aphyric to weakly porphyrictic dacite facies in drill holes at the northern end of Que River (7900 N.). Shows the relationship of many of the coherent zones with autoclastic margins. (see figure 3 for explanation to the symbols used.)

655050


0
20
40
60
80
100
120
140
F
F
F
HIGHLY FOLIATED ZONE
QR 699
5 cm
0
20
40
60
80
100
120
140
160
176
F
F
QR 49

655051

*Interpretation*

These dacites were emplaced mainly as flows or very shallow intrusive cryptodomes. The flows were small volume and relatively confined, spatially, close to their eruption points. The elongate wedge shape morphology of the flows is most likely a function of the morphology of the feeder system. The direction of elongation of the dacites is parallel to the sheet like dyke which feeds the flows. The orientation of this feeder may however, be controlled by pre-existing structural elements in the area.

Due to the relatively low phenocryst content and abundance of textures which indicate an initially glassy groundmass these flows are interpreted to have been emplaced at or near there liquidus temperatures. As they were emplaced the margins of the flows fragmented due to a combination of quench fragmentation and autobrecciation. Growth of theses flows or cryptodomes, or possibly later movement of these bodies, led to the over steepening and instability of the autoclastic margins. This produced mass flows of dacitic debris forming aprons around the coherent bodies like that found around the switchback dacite. During the resedimentation of this debris a small volume of externally derived, non dacitic, fragments were incorporated. The presence of resedimented debris associated with these bodies suggests that they had to be partly if not wholly extrusive in character. The presence of open framework peperitic tops to some flows, however, suggests that at least some were emplaced locally into wet, unconsolidated sediments (e.g. Kokelaar et al., 1985).

Dacite pumice breccia

At Que River a dacite pumice breccia is present closely associated with the aphyric to weakly porphyritic dacite facies. These dacite pumice breccias reach an in core thickness of around 10 metres on 7800 N (mine Grid) (see Fig. 3 Report-12), but more commonly are only a few metres thick. These breccias are commonly found within 10 metres of a coherent body of dacite lava.

These breccias consist of a closed framework of tube pumice fragments which are characteristically blocky with ragged edges. Fragments average 1 to 3 centimetres in size and have a diffuse banding, which in thin section is very fine tube vesicles. Pumice fragments are aphyric to very weakly porphyritic with rare carbonate pseudomorphs after plagioclase phenocrysts reaching 1 mm in length. The bulk of the tube pumice fragments contain a groundmass of subrounded to subangular quartz and feldspar crystals (< 0.2 mm diameter), which appear to be recrystallisation of original devitrification textures. Rare aphyric to weakly porphyritic dacite lithic fragments occur within these breccias.

655052

*Interpretation*

Due to the blocky coarse grained nature of the pumiceous fragments, and their close relationship with coherent lavas, these breccias are interpreted to represent the quench fragmented vesicular carapace of lavas or lava domes of the aphyric to weakly porphyritic dacite facies. Due to their restricted distribution and association with coherent bodies of dacite is is unlikely that these breccias represent subaerially erupted, phreatomagmatic generated, pumice settling through water. The compositional similarity of the pumice and the associated lavas and autoclastics of the aphyric to weakly porphyritic dacite facies also suggests that they are genetically related, therefore implying the pumice is not from an external source. Some of the breccias which are slightly removed from the coherent units are interpreted as being resedimented equivalents of the insitu breccias. Similar association between non-pyroclastic pumiceous debris and the coherent bodies they were sourced from have been described from subaerial environments (e.g. Fink, 1986).

Generation of this tube pumice is most likely due to a shear stress acting on a finely vesiculated lava. This shear stress could have been imposed in the vent associated with the eruption of the lava or within the margins of the lava while it was flowing.

The breccias observed may also have been generated via small scale subaqueous eruptions where the pumice generated by the eruption cools rapidly, becomes water logged and settles near the vent (e.g. Kato, 1987, 1988). Such pumice was termed woody pumice by Kato, (1987) . Kato, (1987,1988) did not specify the mode of eruption of this pumice, although the discussion regarding their impact onto the seafloor suggests that the eruption mechanism involves the generation of pumice as ejecta and is therefore implied to be partly explosive.

Discussion

The dacitic to rhyodacitic facies within the Que - Hellyer Volcanics represent multiple, small volume, non-explosive volcanic events. These are are relatively restricted to the position of the Mixed Sequence, although due to the shallow intrusive nature of some of these bodies they are probably best treated as a separate unit(s) which occur dominantly within, and adjacent to the Mixed Sequence Volcaniclastics. Corbett and Komyshan, 1989 have located similar bodies in the Sock Creek area within the Que River Shale and to the north in the overlying 'felsic tuff sequence' (Southwell subgroup ?). This relationship suggests that the emplacement of these small volume felsic bodies continued into at least the early stages of Southwell subgroup deposition. None of these moderately porphyritic felsic bodies are known to have associated base metal mineralisation.

To date economic mineralisation is only associated with the aphyric to weakly porphyritic bodies within the Que Hellyer Volcanics. The timing of the emplacement of these bodies relative to mineralisation varies from immediately pre- to post-mineralisation. These dacites are dominantly extrusive and have associated autoclastics, both insitu and resedimented. Unlike these dacites, the rhyodacitic volcanics at about the same stratigraphic position to the west of the Que River and Hellyer deposits appear to have a considerable intrusive component.

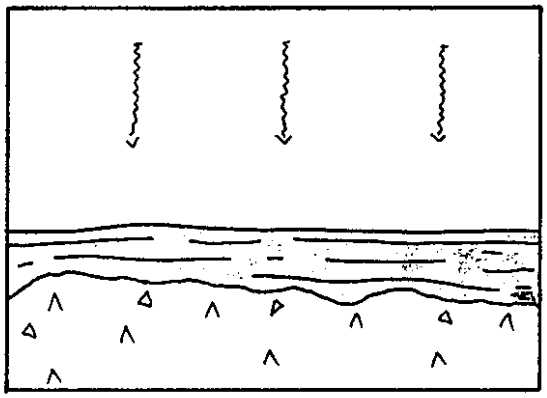
The body of rhyodacite to the west and north of the Hellyer deposit represents a single or multiple small shallow intrusive cryptodomes. These domes were emplaced into wet unconsolidated sediments (Fig. 6). Continued doming of these bodies led to the destabilisation of the overlying autoclastic debris and mudstones. Sheding of this debris from the tops of the domes led to there exposure enabling further resedimentation of rhyodacitic debris. No mineralisation has yet been discovered associated with these bodies, nor has any debris from these porphyritic bodies been found in the volcaniclastics associated with mineralisation. Due to they relatively close proximity to areas of mineralisation it is inferred that they were isolated from these areas by some structural or topographic feature, they remained largely intrusive or they pre- or post-date the mineralising event.

The aphyric to weakly porphyritic dacites however, are temporally and spatially associated with mineralisation. As mentioned before these dacites appear to consist of domes and flows strongly controlled by the geometry of the underlying feeder system. Dykes located beneath the dacites have a sheet like morphology and probably represent intrusion along a pre-existing structural feature (i.e. fault). The occurrence of minor sediments within the autoclastics associated with these dacites suggests that the initial phases of the eruption was at least partly into unconsolidated fine grained sediments. However, the association of the lavas both with probable resedimented autoclastic debris and the identification of dacitic debris within mass flow volcaniclastics of the Mixed Sequence suggests that these lavas were dominantly extrusive.

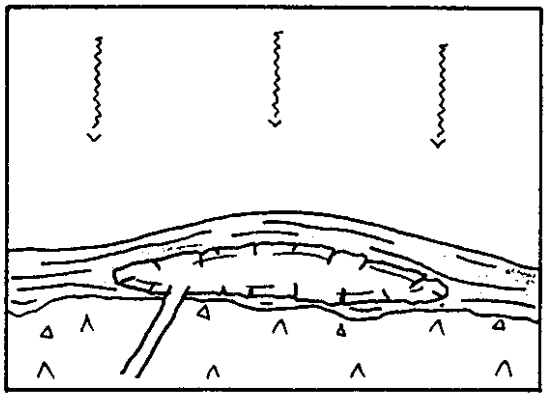
The occurrence of the pumiceous breccia, spatially restricted to areas containing coherent dacitic volcanics at Que River, and its locally gradational contact with these volcanics suggest that they are genetically related. Pumice in these breccias is thought to be non-explosive in origin and represents a moderately vesiculated quench fragmented carapace to the lava, which has in places been resedimented. The generation of this pumiceous debris from an extrabasinal source via explosive eruption is unlikely due to its limited distribution and relationship with the dacites.

655054

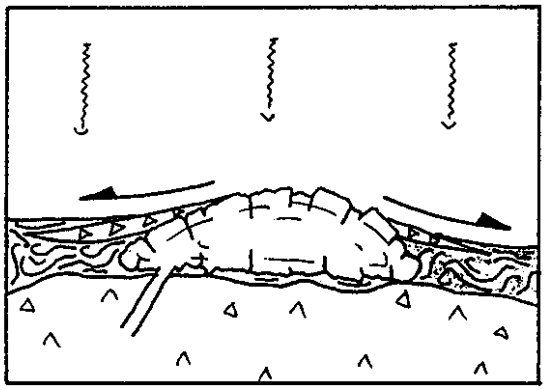
Figure 6: Model for the emplacement of the shallow intrusive to extrusive felsic volcanics in the Hellyer - Que River area. Stage 1: Prior to the eruption of the felsic magmas fine grained sediments of pelagic and hemipelagic origin accumulated upon the Lower Andesites and Basalts. Stage 2: Initial eruption and emplacement of the felsic bodies as shallow intrusions into wet unconsolidated sediments. Stage 3: Continued emplacement of shallow intrusive causing doming and slumping of overlying sediments. Removal of overlying sediments by slumping results in lava breaking through to the surface. Resedimentation of some of the exposed autoclastic debris. Stage 4: Continued emplacement of magma followed by burial by fine grained sediments. Stage 5: Cessation of magma emplacement, exposed part of dome buried by background sedimentation and/or emplacement of overlying volcanics.



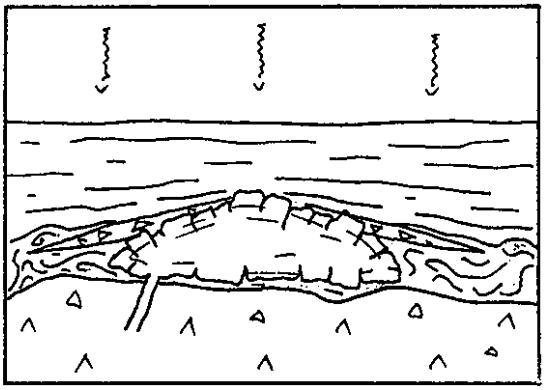
I



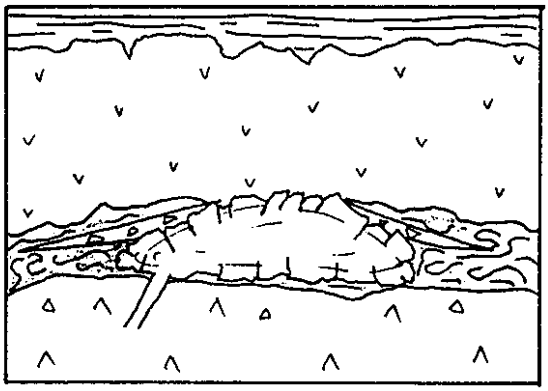
II



III



IV



V

Generation of this debris via very small scale explosive activity associated with the emplacement of the dacite by a method similar to that described by Kato, (1988, 1987) may be possible although an autoclastic origin is favoured at present.

Within this association the aphyric to weakly porphyrictic bodies show a close relationship to monomict and polymict volcaniclastics of mass flow origin. The generation of mass flows of debris wholly or partly sourced from these dacites is a surface process requiring the exposure of these volcanics. The distribution of these volcaniclastics suggests deposition within a local depression which was also the site for mineralisation.

*Future Work:*

Future work on this project will focus on the compilation of the data collected and writing of draft copies of thesis chapters. One final trip will have to be undertaken in order to log one of QR-1169 or QR-1216 to complete an east west traverse from the Bulgobac area through the Que River Deposit. This trip will also be used to log some of the holes at the far southern end of the Hellyer deposit (i.e. 10100 N. / 10200 N. ) to aid in the investigation of the host sequence to mineralisation within the volcanics.

***References:***

Corbett, K. D. and Komyshan, P. 1989: Geology of the Hellyer - Mt. Charter area. Department of Mines, Tasmania, 48 p.

Fink, J. H. 1986: Origin of pumiceous and glassy textures in rhyolite flows and domes. Geol. Soc. Am. Spec. Paper, v. 212, p. 77-88.

Kato, Y. 1987: Woody pumice generated with submarine eruptions. Jour. Geol. Soc. Japan, v. 93, p. 11-20.

Kato, Y. 1988: Woody pumice - and indicator of submarine eruption. Kagoshima International Conference on Volcanoes, Kagoshima, Japan, Abstracts volume. p. 143-146.

Kokelaar, B. P., Bevins, R. E. and Roach, R. A. 1985: Submarine silicic volcanism and associated sedimentary and tectonic process, Ramsey Island, SW Wales. J. Geol. Soc. Lond., v. 142, p. 591-613.

Mc Arthur, G. J. and Dronseika, E. V. 1990: Que River and Hellyer zinc-lead-silver deposits., *In* Hughes, F.E., Geology of the Mineral Deposits of Australia and Papua New Guinea, Monograph No.14, Australasian Institute of Mining and Metallurgy, Melbourne, p.1229-1239.

Winchester, J. A. and Floyd, P. A. 1977: Geochemical discrimination of different magma series and their differentiation products using immobile elements. Chem. Geol., v. 20, p. 325-343.

# APPENDIX II

655058

Etheridge & Henley - Geoscience Consultants

for

Aberfoyle Resources Ltd.

# Structural Setting of the Mackintosh Block and its Mineralisation

by

Jacqueline Windh

Mike Etheridge

with important contributions from

Andrew McNeill

Jocelyn McPhie

655059

## Table of Contents

**Executive Summary** ..... 1
**Introduction to Mackintosh Structural Study** ..... 3
Background ..... 3
Aims of Project ..... 4
Methodology ..... 4
**Geometry: Structural shapes/patterns in the Que-Hellyer Basin** ..... 5
Map Patterns ..... 6
Mt. Charter Fault ..... 6
Henty Fault Zone ..... 6
Que Fault-Mt. Cripps Fault ..... 7
Cross-sectional Patterns ..... 8
Hellyer Area ..... 8
Que River Area ..... 9
South of Que Fault ..... 9
Section parallel to strike ..... 9
Integrating Map and Sections ..... 10
**Structure and stratigraphy** ..... 11
Volcanic and sedimentary facies ..... 12
Fault fabrics ..... 13
Mt. Charter Fault ..... 13
Henty Fault Zone ..... 13
Ductile Fault Zones north of Hellyer ..... 14
Que Fault ..... 14
Mt. Cripps Fault ..... 14
Smaller faults ..... 14
Folds and cleavage ..... 15
Alteration patterns ..... 16
Mine-scale structures ..... 16
Hellyer ..... 16
Que River ..... 18
**Synthesis of geological information** ..... 18
Relative timing of structures ..... 18
Early (syn-depositional) structures ..... 18
Ductile compressional structures ..... 18
Late brittle structures ..... 19

655060

**Geologic history of the Mackintosh area** ..... 19
Formation of the Que-Hellyer Basin ..... 19
Early deformation ..... 20
Late deformation ..... 20
Discussion ..... 21
Integration with regional geologic history ..... 21
Mt. Read Volcanic Belt. ..... 21
Southeastern Australia. ..... 22
Problems with the Model ..... 22
**Structural Controls on Mineralization** ..... 23
General Statement on Structural Control ..... 23
Structural Control and Basin Evolution in the Mackintosh Block ..... 24
**Implications for exploration** ..... 27
Recommendations for collecting structural data ..... 29
**References** ..... 31
**Appendix** ..... 33

655061

## List of Figures


| | | | |
|---|---|---|---|
| Figure 1 | Summary structural map of Mackintosh Block area. | after | 7 |
| Figure 2 | 1:25,000 geological map of Mackintosh Block and immediate environs. | after | 7 |
| Figure 3 | 1:25,000 scale cross-sections and long-sections from this study. | after | 8 |
| Figure 4 | 1:25,000 structural framework map of Mackintosh Block showing both basin-forming extensional and younger compressional structures. | after | 10 |
| Figure 5 | 3D schematic view of the shape of the base of the Que River Shale. | after | 10 |
| Figure 6 | 3D schematic diagrams showing relationship between facies development and active structures in a mixed strike-slip extensional basin. | after | 10 |
| Figure 7 | 1:25,000 structural framework map of the Mackintosh Block . | after | 16 |
| Figure 8 | Schematic plan views of the principal structural elements of the Mackintosh Block. | after | 19 |
| Figure 9 | Schematic block diagrams. | after | 19 |
| Figure 10 | Map of Tasmania with inferred major Cambrian, NW-trending transfer faults and extended regions that evolved into volcano-sedimentary sub-basins. | after | 21 |
| Figure 11 | Cambrian structural/tectonic reconstruction of Australia after Shaw et al (1991). | after | 22 |
| Figure 12 | Block diagram showing the relationship between the Rosebery Fault and syndepositional normal faults at a high angle to it (from Berry, 1991). | after | 25 |
| Figure 13 | 1:25,000 structural framework map of the Mackintosh Block (see Figure 4). | after | 29 |

655062

## Executive Summary

A structural study of the Mackintosh Block was carried out between February and May 1992. The principal objectives of this study were to develop a structural framework for basin development, mineralisation and subsequent deformation in the Block, and thereby to provide a structural conceptual model for the localisation of and exploration for stratiform mineralisation.

The study involved the examination of maps, key surface and underground exposures and drillcore. The structural framework was principally based on the construction of 10 cross and long sections to build a complete 3D picture of the present structure. This picture of the shape or pattern of the structure was then integrated with stratigraphic information to construct a basin history, and to place mineralisation in this basin structural framework.

The principal outcomes of the study are as follows:

- The present structure of the Mackintosh Block has been considerably refined, and is presented as a series of cross-sections, revisions of the 1:10 000 Aberfoyle maps and summary maps and a block diagram.

- The present structure of the Mackintosh Block largely reflects the effects of probably two, relatively low-strain compressional deformation events (?one late Cambrian, one mid-Devonian?), superimposed on a complex array of syn-depositional extensional and strike-slip faults. Most of the compressional structures formed in response to reactivation of the earlier faults. There is no evidence of the large-strain thrusting with consequent structural repetition and/or overturning of units that has recently been recognised at the Buchans massive sulphide deposit.

- The syndepositional fault pattern has been broadly determined to include the following elements:
  - A few, probably older major faults that form a regional linked network throughout the Mt Read volcanic belt (e.g, Henty, Mt Charter and ?Mt Cripps faults); a probably subtle change in the stress field and resultant movement pattern on these faults produced localised extension in the vicinity of their intersection, and thereby controlled the location of the Mackintosh (Que-Hellyer) Basin.
  - A linked array of NE-trending, dip-slip normal faults and NW-trending, steeply dipping transfer (accommodation) faults that actually accomplished the extension and subsidence in the Mackintosh basin.

- A change in the stress regime caused a relatively subtle, but critical change in the movement patterns on all of these faults, but particularly on the intrabasinal normal and transfer faults. This change appeared to localise dilation, extension and subsidence at or near the intersections between the principal NE and NW-trending faults. This event coincided with the cessation of andesitic vulcanism through most of the basin, with the formation of highly localised depocentre filled with 'Mixed Sequence', with the intrusion/extrusion of felsic magmas and most importantly with massive, highly channelised fluid flow through the dilatent areas to give rise to the major sites of mineralisation. It also heralded a major change in basin configuration, depth and sediment supply at Que River Shale (QRS) time. However, we consider that there is more than one dacitic or 'mixed sequence' horizon in the stratigraphy, and that the lower ones do not appear to be as prospective.

- A preliminary outline of the regional tectonic setting of the Mackintosh Basin is presented, although development of regional setting and correlations will be carried further in the next phase of the project.

- The structural and basin-formation framework presented here has much in common with previous and present ideas within and outside Aberfoyle. However, this is probably the first time that a coherent structural framework has placed the mineralisation firmly within such a framework. The framework has some important implications for exploration of the Mackintosh Block:
  - The principal stratiform mineralisation in the Mackintosh Block is considered to be limited to a specific time and therefore stratigraphic interval, because it is associated with a specific and probably short-lived structural event. Such short lived 'stress-pulses' and minor reactivation of basin-forming structures are being increasingly recognised in petroleum exploration. This has the implication that only areas where that interval is preserved sub-surface are prospective for this style of mineralisation. Unfortunately, our reconstruction of the cross-sections strongly suggests that much of the eastern and southern portion of the Mackintosh Block is therefore unprospective.
  - The preservation consideration is particularly important and not wholly resolved at Mt Charter. Our preferred interpretation has much, if not all of the Mt Charter alteration zone stratigraphically below the key mineralised horizon, and therefore probably footwall to an eroded ore position. However, our reinterpretation of the Que river Mine section, which places a local graben filled with dacite and mixed sequence structurally within the footwall andesites, does permit further evaluation of the Mt Charter area.

- The prospective stratigraphic interval is clearly sub-surface in the western part of the Mackintosh Block, and we recommend that detailed structural investigations be concentrated there to attempt to identify reactivated basin-forming faults which may provide prospective structural sites. We recommend several specific areas in the report, most of them along the interpreted NW-trending transfer zones.

- Some recommendations as to future mapping and logging practices are provided to enable the structural framework developed here to be built upon, tested and refined to the point where it can be integrated with other techniques to target further drilling.

## Introduction to Mackintosh Structural Study

### Background

The Mt. Read Volcanic Belt has been explored for volcanogenic massive sulphide deposits for over 20 years. For the latter part of this period, exploration strategies have been dominated by geophysical methods. In the Que-Hellyer area, geophysical surveys played an important part in the discovery of the Hellyer orebody in 1983. Since that time, drilling on the Mackintosh EL has been aimed dominantly at geophysical targets, and has led to the discovery of several pyritic alteration zones. No new base metal deposits have been discovered, however, and the area of the El within reach of ground-based geophysical (EM) surveys (top 200 - 300 m) has been essentially sterilized.

So far, exploration strategy has not relied heavily on concepts based on structural geology. It is clear that the base metal sulphide deposits within the Mt. Read Volcanics are broadly syngenetic. However, regardless of their timing relative to deposition of their host rocks, their presence requires that large volumes of fluids were channeled through relatively small volumes of rock, i.e. that structures active at the time of and/or soon after vulcanism and sedimentation were responsible for focussing fluid flows. Such structures would have been syn-depositional faults and/or fractures. The orientation of these structures would have been controlled by the general stress régime responsible for formation of the basin. Therefore, understanding the general tectonic environment in which the Que-Hellyer Basin formed, and identifying early, syn-depositional faults, might form a powerful concept for further exploration oriented towards deeper targets on the Mackintosh EL.

The Que River and Hellyer deposits appear to be hosted by the same stratigraphic horizon. In targeting drilling programs it is important to determine whether there is only one "favourable" horizon that may host ore, or whether there is more than one ore position. In addition, it is important to understand the effects of later, compressive deformation on the ore horizon(s).

For example, recent work on the Ordovician Buchan's VMS deposits in Newfoundland has shown that low-angle thrusting has duplicated stratigraphy, and has resulted in significant revision of stratigraphic interpretations. The possibilities of multiple ore horizons, or thrust duplications of ore horizons, also have bearing on targeting of exploration drillholes.

The Mackintosh Structural Study was proposed by Dick Henley on the above basis and accepted by Aberfoyle Resources Ltd. The project was principally carried out by Jackie Windh and overseen by Mike Etheridge of Etheridge and Henley - Geoscience Consultants. Andrew McNeill and Jocelyn McPhie were contracted to provide expert assistance with the local Que-Hellyer geology and the regional volcanic stratigraphy respectively. The field work was carried out during February/March 1992 and the final report submitted in May 1992.

## Aims of Project

The aims of this project are to provide Aberfoyle with a reliable structural framework for the Mackintosh area which will form the basis for future exploration strategy. The specific objectives include:

- geometrical analysis, in order to first identify the shapes of stratigraphic contacts and structures, and then to identify general structural patterns and zones of anomalous deformation style;
- integration of stratigraphic, structural, and alteration data in order to identify syn-depositional faults;
- working out the relationships between early faults, late faults, fold patterns, and zones of alteration and mineralization;
- developing a syn-depositional structural framework for the Que-Hellyer volcanic basin and its mineralisation;
- assessing the predictive capacity of the structural framework for base metal exploration in the Mackintosh area, and developing programs of future structural work that can be undertaken by Aberfoyle geologists.

## Methodology

The methodology to achieve the aims outlined above has been as follows:

- spending two weeks working with Andrew McNeill, in order to gain familiarity with the area and stages of work so far completed, and to target areas that are complex and/or poorly understood;

- compiling of all surface structural data from Aberfoyle 1:2500 maps and costean plans, and from Hellyer and Que River mine plans and sections, on to 1:10,000 maps to overlay on to lithological maps (data maps submitted separately to Aberfoyle for drafting);
- interpreting the structural compilation maps *out of context of the lithological maps*, then comparing the structural-based interpretation with the lithological-based interpretation;
- identifying "problem areas", where either the structural and lithological interpretations do not agree with one another, or there is a lack of structural data, in which to undertake surface structural work *aimed at solving the specific problem* (i.e. not general structural mapping, but targeted structural analysis);
- choosing areas of good exposures of sedimentary rocks (mostly roadcuts) for surface structural work aimed at identifying fold patterns and understanding the relationship of cleavage to the folds, then relating these discrete areas both with each other and with the larger-scale structural patterns;
- using surface lithological data and structural data to start to compile a new set of 1:10,000 sections, including both cross-sections and long-sections to help tie the cross-sections together;
- using drillhole logs and sections to help complete 1:10,000 sections at depth, and examining core where necessary to determine the nature of contacts (e.g. ductile shear zone, brittle fault, conformable...) and bedding-core axis angles;
- tying sections and maps together, ensuring that sections are compatible with *all of* the following: map patterns, adjacent sections, tie-in long-sections, surface structural measurements, and drillcore data, e.g. bedding-core axis measurements;
- using the maps and sections to develop a three-dimensional model for the *shape* of stratigraphic units and structures, and then a tectonic model for the Que-Hellyer basin that is compatible with both mine-scale and regional structural relationships; (mention temporal);
- relating zones of alteration and mineralization to the structural history of the area, and developing proposals for further exploration.

## Geometry: Structural shapes/patterns in the Que-Hellyer Basin

To start to understand the *genesis* of a geological domain, it is first necessary to understand the *geometry* of structures within that area. This is accomplished by working out the *shapes and orientations* of lithological or stratigraphic units and of structures such as shear zones and faults, and identifying *patterns* that are characteristic of particular structural environments.

Because the Mackintosh area has been subject to one and probably two compressional deformation events after deposition and mineralisation (Cooke, 1991), we began by attempting to understand present shapes so that we could 'see through' the effects of the compressional deformation(s) and reconstruct the syn-depositional structural framework.

It is important to note whether general structural patterns are common throughout an area, or whether there are discrete zones, or *domains*, of different structural style. In analysing the compressional structures of the Mackintosh area it has proven useful to identify a "typical" structural style (in this case, gentle folding), and "anomalous" structures (in this case, steep bedding dips and zones of relatively intense foliation).

In this section we look at the map patterns and cross-sectional patterns with the aims of understanding the *three-dimensional* compressional structural patterns, and identifying regions of "typical" and "anomalous" deformation style. References to directions in this report will be with respect to *true north*, which is 22° west of grid north and 12° west of magnetic north.

## Map Patterns

This analysis of the map patterns is based on the 1:10,000 mapping by McNeill, which is summarized in Figure 1 and 2. Patterns on the map are dominated by several discrete structural breaks, which separate domains of distinct structural and stratigraphic style. The most important of these breaks are:

- *Mt. Charter Fault* - a generally NNW-trending structure with a sinuous surface trace, that consists of a more northerly trend and a more northwesterly trend. The fault separates the Que-Hellyer volcanics to the northeast, from a domain to the southwest where the strata that both underlie and overlie the Que-Hellyer volcanics are present and apparently conformable, but the volcanics themselves are missing. The Mt. Charter Fault merges to the south with the more N-trending boundary that separates the Mt. Read Volcanics to the west from the Precambrian Tyennan Block to the east.
- *Henty Fault Zone* - another sinuous or discontinuous fault zone that is generally NNE-trending, and disappears in the vicinity of the Shark's Fin. The Henty Fault Zone is shown on the 1:100,000 map to cross the Mt. Charter Fault in the vicinity of Lake Mackintosh, but may also merge with the major N-trending eastern boundary structure of the Mt. Read Volcanics to the south. In the Mackintosh area, the Henty Fault Zone separates generally west-younging Que-Hellyer Volcanics to the west, from younger, east-younging sedimentary (Owen Conglomerate and younger Siluro-Devonian) rocks to the east.

- *Que Fault-Mt. Cripps Fault* - two fairly straight faults approximately along strike with one another. The Que Fault separates folded Que-Hellyer volcanics to the north, with gently west-dipping and west-younging volcanics to the south, and appears to die out to the west, i.e. it does not affect the contact of the QRS with the overlying URS. It appears to represent a change in the volcanics immediately underlying the QRS, however, from dominantly basalt in this stratigraphic position to the north, to dominantly andesite to the south. The step from the Que Fault to the Mt. Cripps Fault coincides with the disappearance of the Henty Fault, as well as with a zone of more anomalous fold patterns and east-west stratigraphic trends north of the faults, in the vicinity of the Hellyer portal road. The Mt. Cripps Fault separates a thick succession of east-younging Tyndall Group volcanic and volcaniclastic rocks to the north, from younger, folded sedimentary rocks to the south.

These major structures divide the Mackintosh area into domains of quite different structural trend and style. Some, and perhaps all, of these major structures represent discontinuities in thickness and/or facies of major stratigraphic units. **These relationships indicate that many of the faults originated as early structures *during* basin formation, and were reactivated during later compressive deformation. This is a key conclusion, because it enables us to use the present, largely compressional, structural patterns to directly infer the location and styles of some of the syn-depositional structures.**

Folds are obvious from the map pattern only north of the Que Fault, and are generally NE-trending, with the exception of the area of convergence of the Henty, Que, and Mt. Cripps faults. The eastern limb of the main Hellyer anticline is anomalous in map pattern in that stratigraphy along it appears to be attenuated, and the strike of the limb is sub-parallel to the axial trace of the anticline. Cook (1991) has noted that the Portal Syncline is anomalous in its more northeasterly trend, and much steeper plunge, than the adjacent folds. The orientation and significance of this structure is discussed in the following sections.

655069

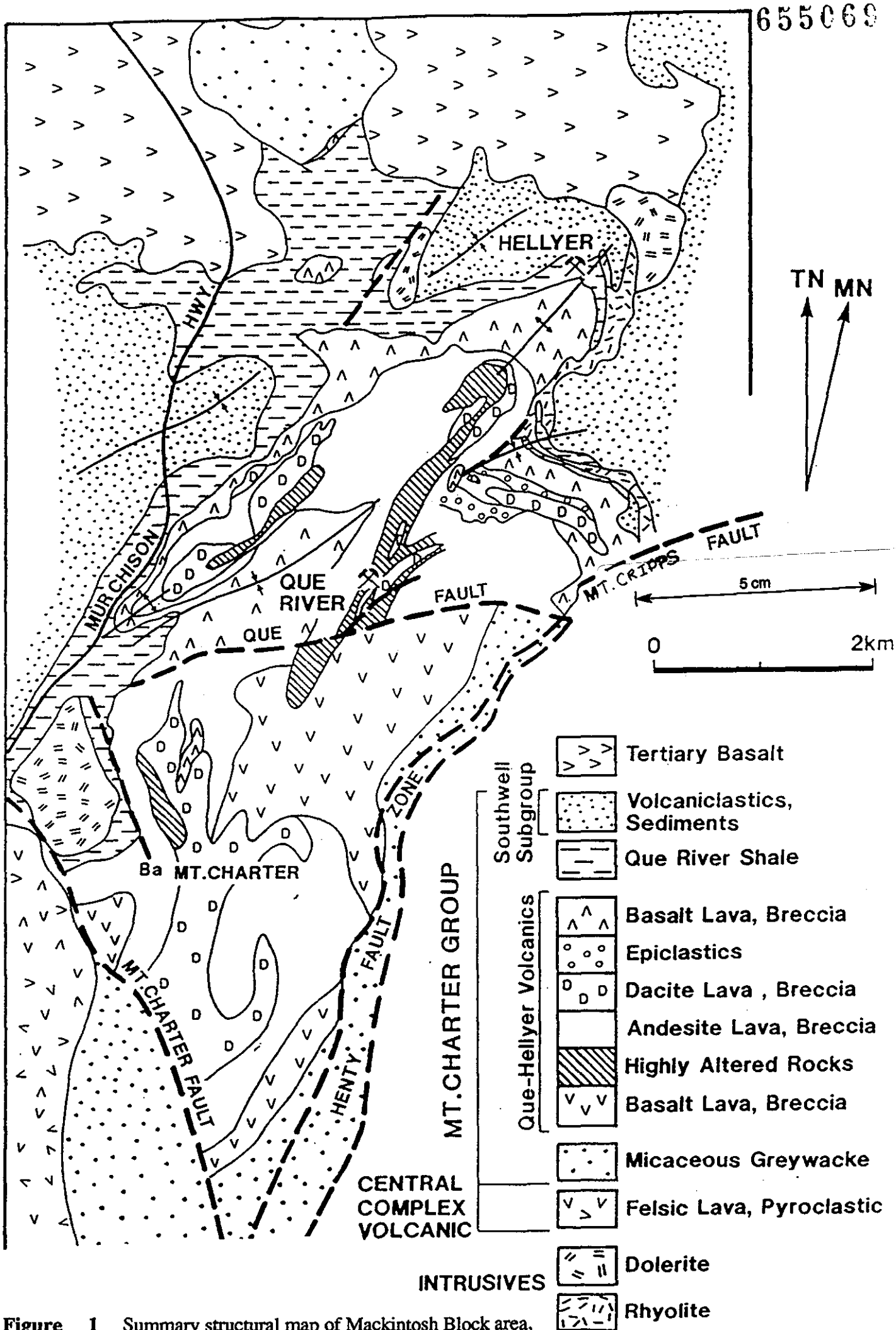
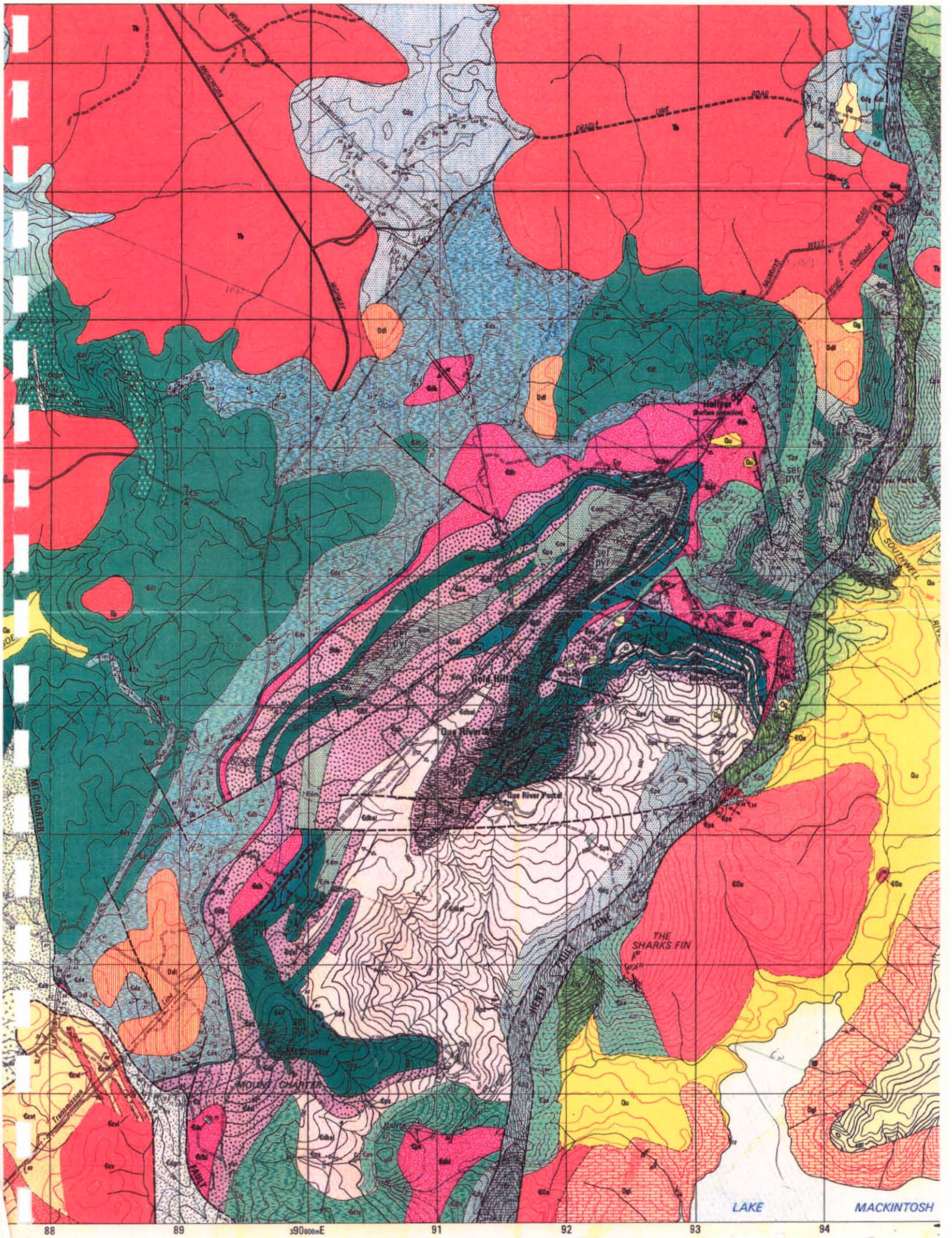



**Figure 1** Summary structural map of Mackintosh Block area, from Waters and Wallace (in press).

655070

**Figure 2** 1:25,000 geological map of Mackintosh Block and immediate environs, from Tasmanian Mines Department map by Komyshan (1986)

655071


Hollyer
Hole Hill
Que River Camp
Que River Portal
MT CHARTER
MOUNT CHARTER
THE SHARKS FIN
LAKE
MACKINTOSH
88
89
390000mE
91
92
93
94

5 cm

## Cross-sectional Patterns

This discussion of cross-sectional geometry is based upon 1:10,000 cross-sections and long-sections constructed as part of this study, enclosed in the back of this report, and summarized in Fig. 3.

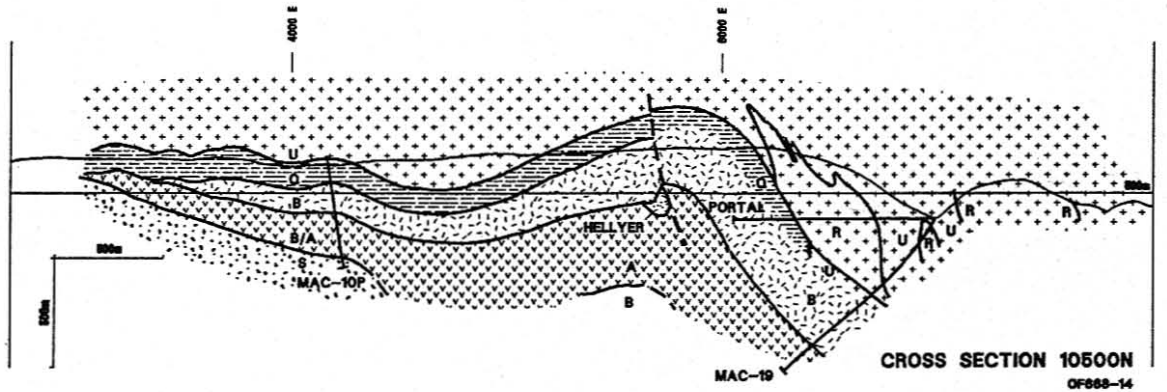
*Hellyer Area.*
Cross-sections north of the Que Fault show a general pattern of gentle folding. (Cross-sections have been constructed parallel to east-west grid lines, which is somewhat oblique to the trend of the Hellyer anticline. Fold limbs on the sections are thus *apparent dips*, and are shallower than the true dips, but generally only by a few degrees).

Sections in the north, e.g. 10500 N, show that the east limb of the Hellyer anticline has anomalously steep dips relative to the gentle style of folding further west, and show a general westward thinning of the Que-Hellyer volcanics, from a thickness in excess of 1 km at Hellyer, to only a few tens of metres 3 km to the west, in MAC-15. The top of the Mica Sandstone dips gently eastward between MAC-15 and MAC-10, compatible with surface fold patterns of the QRS and eastward thickening of the volcanics, but has not been intersected in deep drillholes under Hellyer, e.g. HL-306 and MAC-19, indicating that the volcanics must thicken very abruptly to the east at about 4500 E.

Successive sections south of 10500 N, towards the Que Fault, show westward disposition of the crest of the Hellyer anticline, reflecting its trend to the east of grid north. Southward, the steep eastern limb of the anticline evolves into a shallower limb cut by a steep, east-side-down fault (8600 N and 7800 N). In the 8600N and 7800N sections, another anticline appears to the east of the Hellyer anticline. The crest of this Eastern anticline migrates from 5100 E in section 7800 N, to 6200 E in section 8600 N, indicating an ENE trend of its axial trace relative to grid north, or a nearly easterly trend relative to true north.

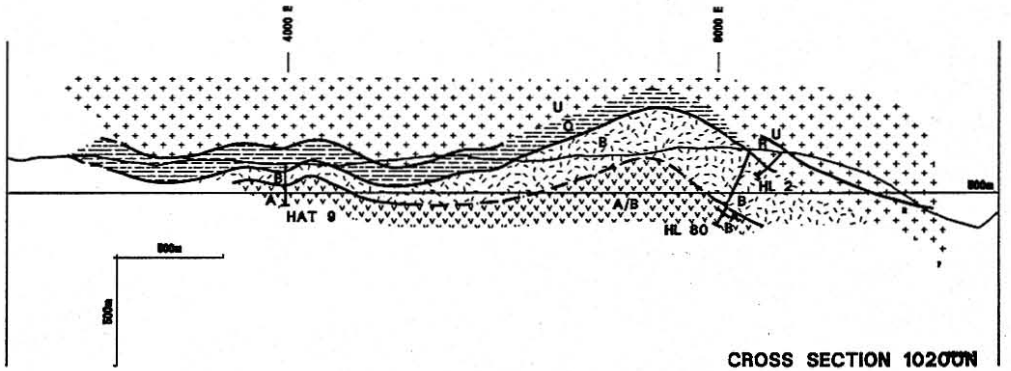
The long-section through this area, at 6200 E, shows this eastern fold crest at 8600 N, with a relatively shallowly dipping south limb, and a moderately to steeply dipping north limb. The interpretation of this anticline is aided by bedding-core axis angles in Mica Sandstone at the base of MAC-12. An alternative interpretation would connect stratigraphic units through MAC-14 and MAC-12 so that they are parallel with the north-dipping stratigraphy further north (Fig. 3). This interpretation would have bedding oriented perpendicular to the core axis at the base of MAC-12. However, bedding is oriented at 10° to 30° to the core axis, and supports the fold interpretation. The long-section has been continued northward by putting stratigraphic contacts at depth from cross-sections 9300, 9900, 10200, and 10500 N, and reveals a smaller anticline of similar attitude with a crest at about 10200 N, where surface exposures consist only of

**Figure 3** 1:25,000 scale cross-sections and long-sections from this study. 6 cross-sections from the Que-Hellyer segment and 2 cross-sections from the Que-Mt. Charter area. An oblique long-section along the hinge region of the Hellyer Anticline ties all of the cross-sections. A shorter long-section through the complex NE part of the area provides an additional tie there. 1:10,000 scale cross sections are provided separately.




CROSS SECTION 10500N

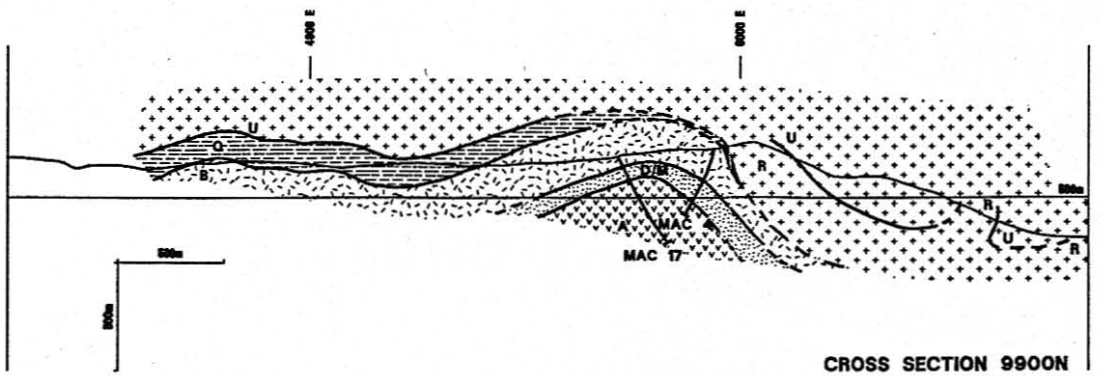
OF668-14




CROSS SECTION 10200N

OF668-7

2000m

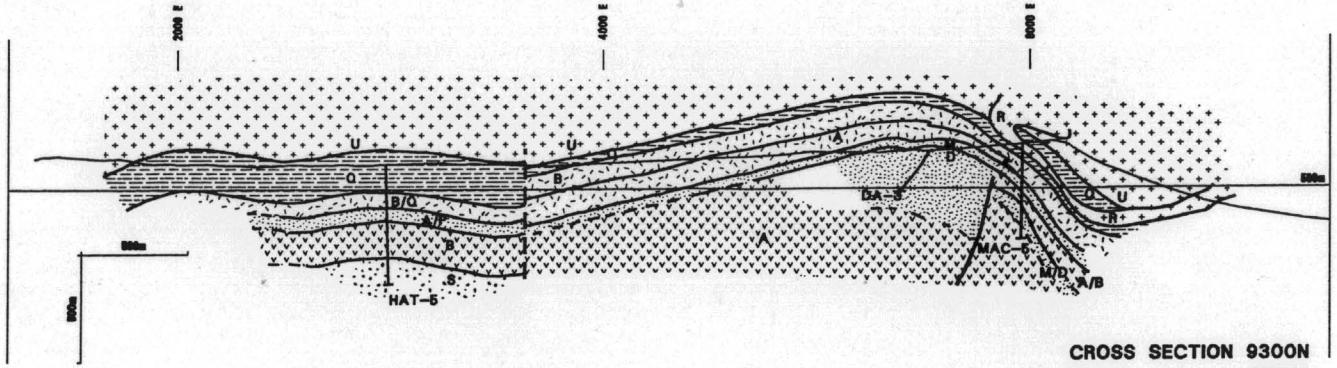


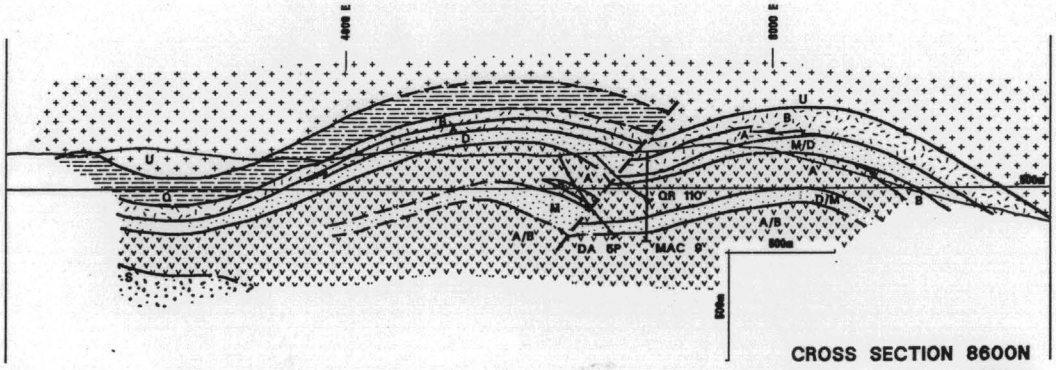

CROSS SECTION 9900N

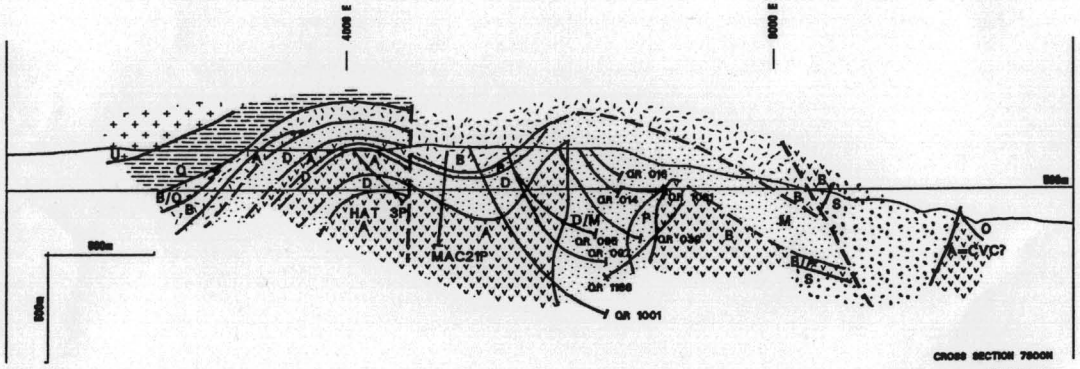
OF668-15

5 cm

6550574




1000m = 113mm

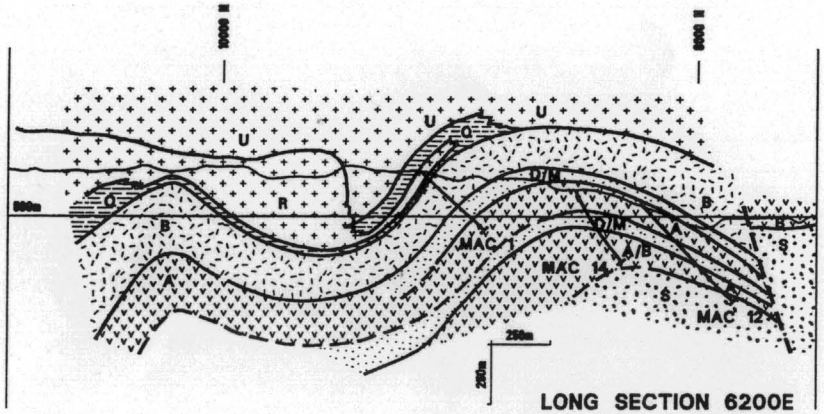
1:35,400 Scale.

* 1.42 will give

1:25000

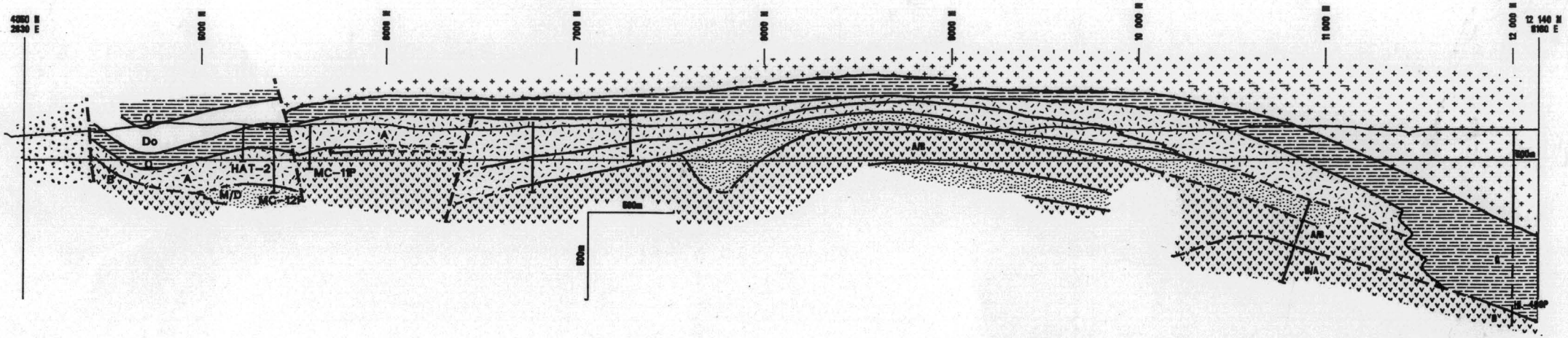
5 cm

65502/5




LONG SECTION 6200E

OF668–6

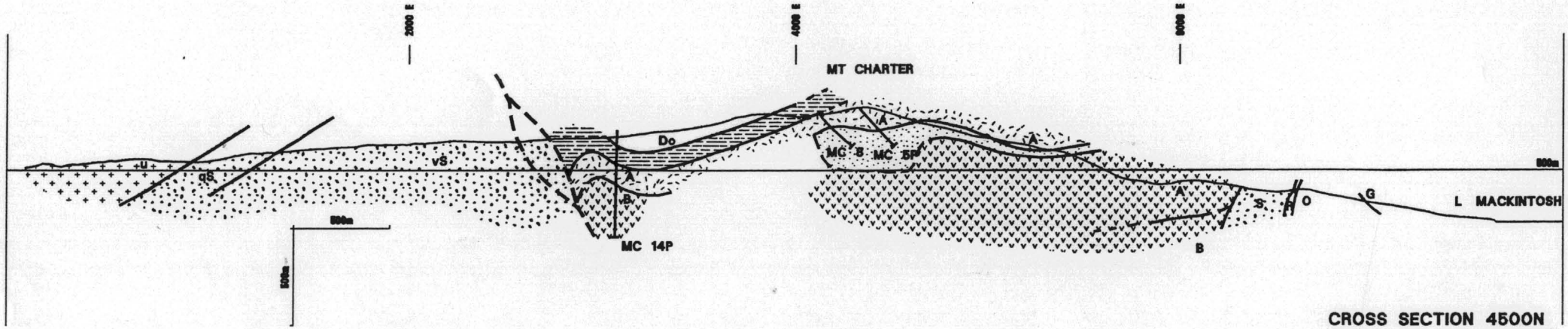



OBLIQUE LONG SECTION ALONG CREST OF HELLYER ANTICLINE

OF668–13

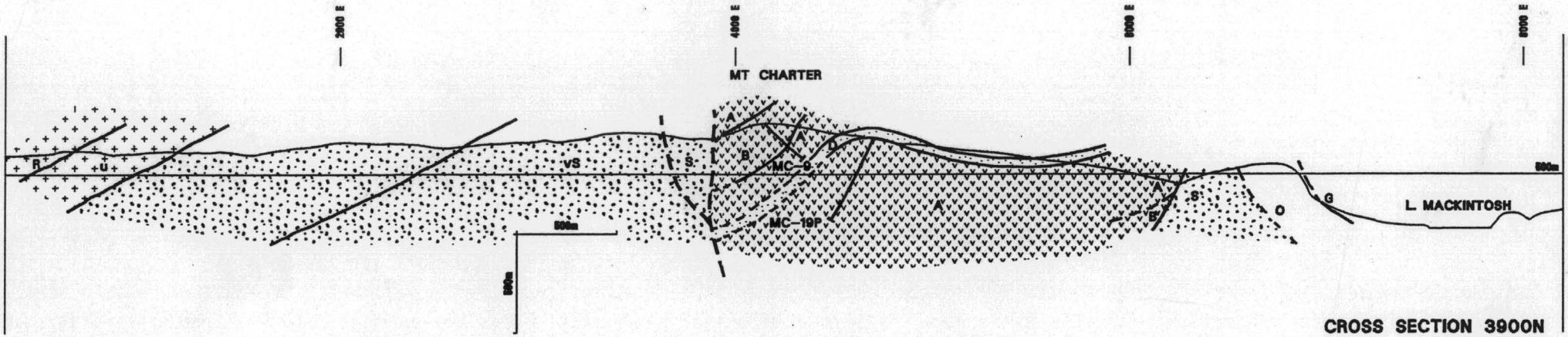
5 cm

65506




CROSS SECTION 4500N

OF668-11




CROSS SECTION 3900N

OF668-10

5 cm

65507

intrusive rhyolite. This section also shows a relatively thin volcanic succession around 8000 N, and indicates a relatively rapid northward thickening of stratigraphy at about 8200 N.

*Que River Area.*

The Que River area (7800 N) is a domain of structural complexity and strong alteration, in which stratigraphic marker horizons are very difficult to trace or even recognise. However, west of Que River there is a gentle syncline which is compatible with map relationships and the next cross-section to the north, and east of Que River stratigraphy dips gently to the east, as constrained by map relationships and the long-section 6200 E. These relationships indicate that the Que River structure is an *anticline*, rather than a syncline. The abundance of Mixed Sequence and highly altered material at the core of this anticline indicates rapid thickening of Mixed Sequence rocks, rather than a synclinal structure, and suggests that the Que River orebodies were bounded on one, or probably both, sides by syn-depositional faults.

*South of Que Fault.*

South of the Que Fault, cross-sectional geometry changes abruptly. There are less surface structural data, and fewer stratigraphic markers to constrain dips of volcanic units, but stratigraphy appears to be generally gently west-dipping and west-younging, with minor, very gentle, folding. The Henty Fault Zone is a steeply west-dipping structure in the east of each section, in contact on its west side with steeply west-dipping Mica Sandstone that youngs consistently upward into Footwall Basalt. Dips of the volcanic rocks, based on drillhole correlations and surface mapping, are distinctly shallower. The nature of this transition, from steep dips in Mica Sandstone, to shallow dips in the volcanics, is uncertain. Volcanic stratigraphy thins gradually westward, with local abrupt thickenings of dacitic and Mixed Sequence-type material, e.g. at Mt. Charter (Fig. 3, section 4500 N, around 4400 E), that probably reflect west-side-down syn-depositional faults and/or the preservation of volcanic palaeotopography. There is no obvious thickening of stratigraphy toward the Mt. Charter Fault.

*Section parallel to strike.*

A long diagonal section (section LD, Fig. 3) has been constructed along the crest of the Hellyer anticline, in order to help tie the cross-sections together, to look for any structural or stratigraphic trends oriented *perpendicular* to the general fold trend, i.e. parallel to the cross-sections, and to attempt to relate the dominantly andesitic volcanic stratigraphy south of the Que Fault to the more basaltic stratigraphy north of the fault.

The section shows very clearly the doubly plunging character of the Hellyer anticline, and it shows several abrupt facies or thickness variations in the volcanic rocks. The most marked of these is the abrupt transition from about 100 to 150 m of QRS above Hellyer, to over 400 m of QRS only 1 km north, in HL-469. The simplest correlation of stratigraphic units, keeping

bedding orientations relatively constant, suggests that the volcanics in HL-469 correlate with the *Footwall Basalt*, i.e. stratigraphy well below the Hellyer ore position, and that the Footwall Andesite, Mixed Sequence, and Pillow Basalt Sequence, are all missing in this region.

The QRS in HL-469 contains significant detrital basaltic material, indicating that it was deposited close to a site of volcanic activity. This rapid facies variation suggests the presence of a significant syn-depositional structure at about 11,550 N, but does not give a clear indication of which side was downthrown. Other syn-depositional structures are suggested by northward thickening of volcanic units at about 9000 N and 7500 N.

Facies variations in the vicinity of the Mt. Charter Fault are very rapid (including in numerous adjacent drillholes not shown on this section), suggesting syn-depositional fault activity, but there is no obvious thickening of volcanic units towards the Mt. Charter Fault.

## Integrating Map and Sections

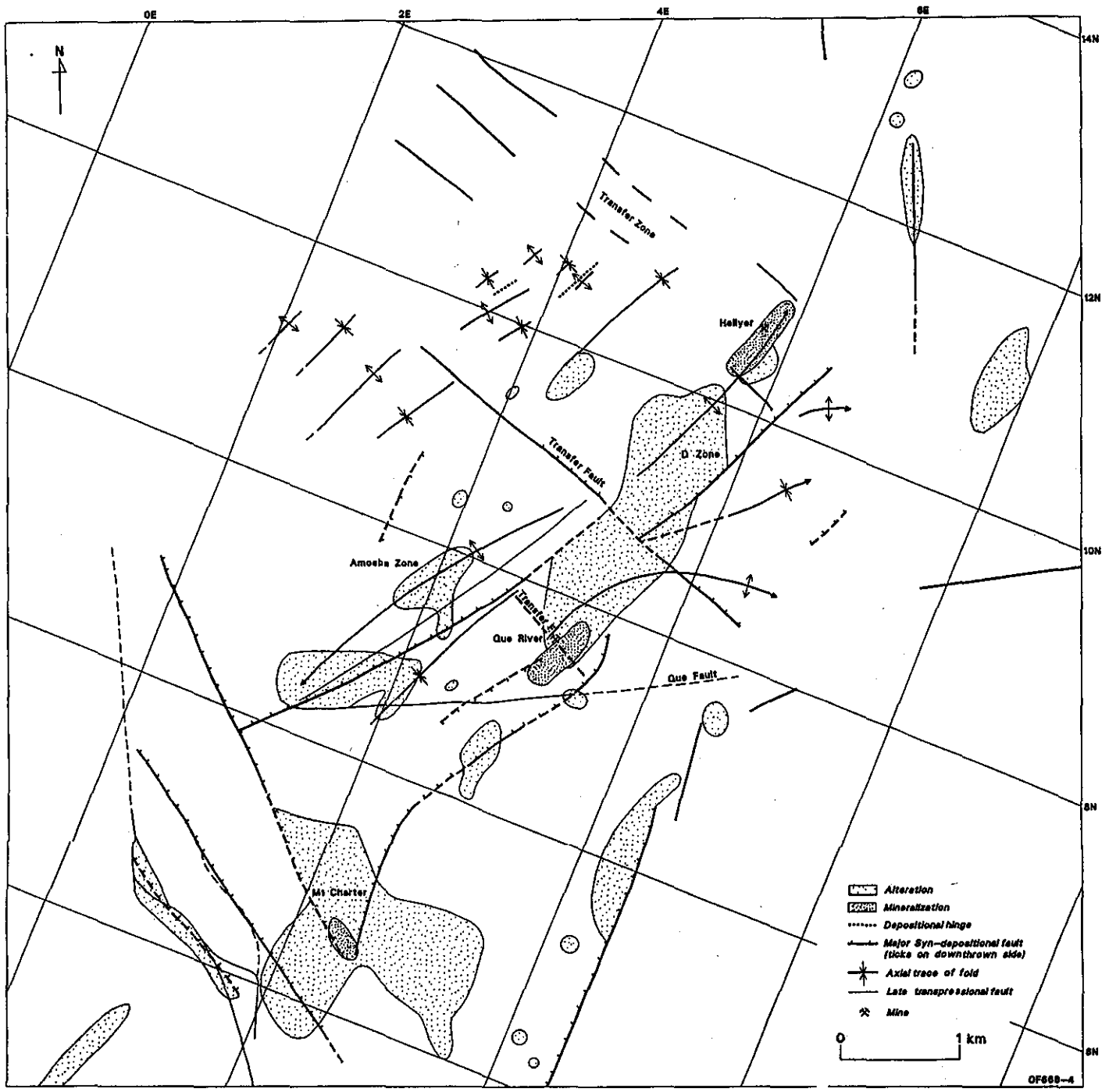
Comparing and inter-relating the geometry of structures apparent on the map with those apparent on sections provides a clearer picture of the orientation and shape of the structures in three dimensions. Map data are used to construct the sections, but then structures identified on sections that are not so obvious from surface mapping, e.g. the folds evident in long-section 6200 E, may be put on the map.

Figure 4 compiles structures identified from both maps and sections, and Figure 5 is a three-dimensional diagram depicting the shape of the surface represented by the base of the QRS. Syn-depositional faults are shown in Figure 4 with ticks on the side with the thicker stratigraphy; *this does not require that these faults were simple, dip-slip normal faults.* As noted in the Appendix, in tectonic environments that involve a component of strike-slip faulting, strike-slip and transfer faults can control deposition of relatively thick volcanic or sedimentary successions. In particular, in the Mackintosh area there are several discrete orientations of syn-depositional faults, which itself suggests that not all of these faults were normal.

Several early structures that represent stratigraphic breaks do not have clear thickening relationships that demonstrate which was the down-thrown side (e.g. fault at 3600 E in section 9300 N). These faults are generally NW-trending, and may represent transfer faults, oriented at high angles to the more NE-trending faults that have clear thickening relationships and probably represent normal faults (see references in Appendix, Figure 6). The Mt. Charter Fault must have a large component of northeast-side-down displacement, based on the absence of Que-Hellyer volcanics to its southwest and on stratigraphic correlations by Jocelyn McPhie

**Figure 4** 1:25,000 structural framework map of Mackintosh Block showing both basin-forming extensional and younger compressional structures.

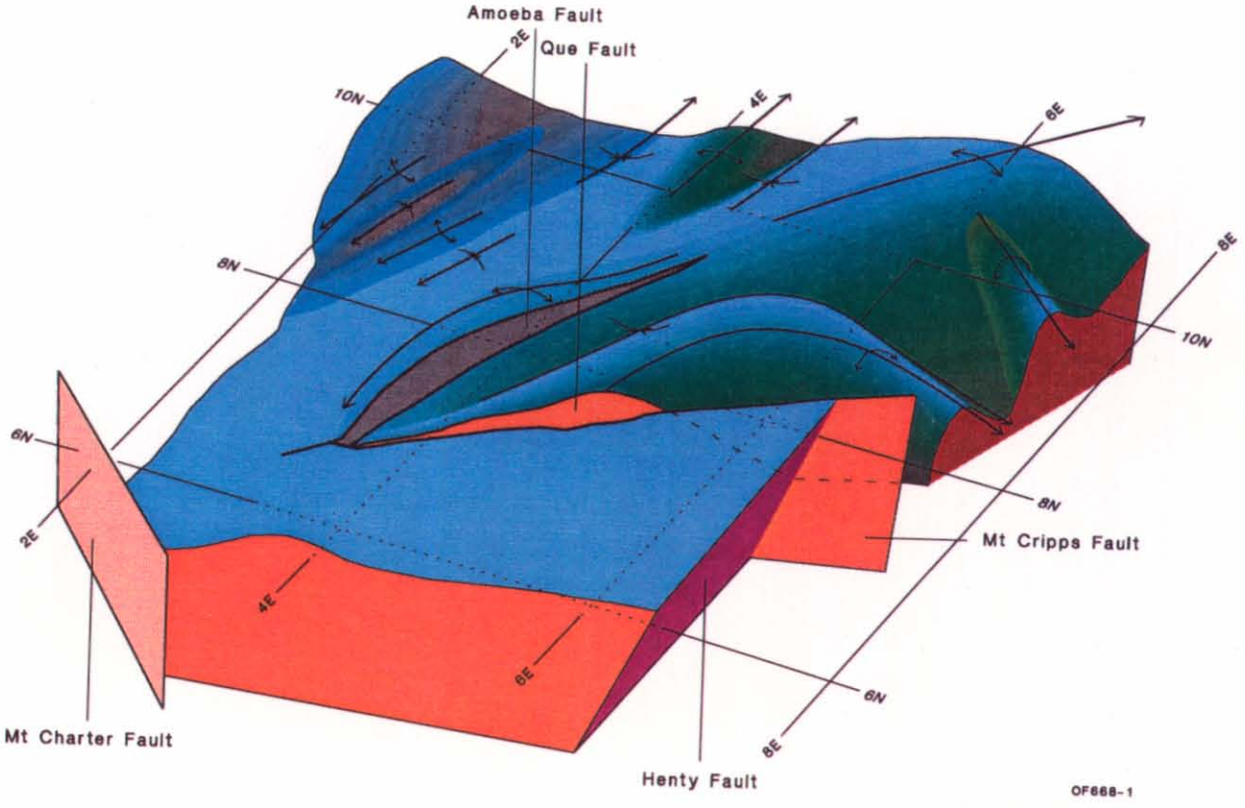
655081


0E
2E
4E
6E
14N
12N
10N
8N
8N
N
Transfer Zone
Hellyer
Transfer Fault
D Zone
Amoeba Zone
Transfer
Que River
Que Fault
Mt Charter
Alteration
Mineralization
Depositional hinge
Major Syn-depositional fault (ticks on downthrown side)
Axial trace of fold
Late transpressional fault
Mine
0
1 km
OF668-4

5 cm

**Figure 5** 3D schematic view of the shape of the base of the Que River Shale. Compare with Figures 3 and 4.

655083


Amoeba Fault
2E
Que Fault
10N
4E
6E
8N
6E
10N
6N
2E
8N
Mt Cripps Fault
4E
6E
6N
8E
Mt Charter Fault
Henty Fault
OF668-1

5 cm

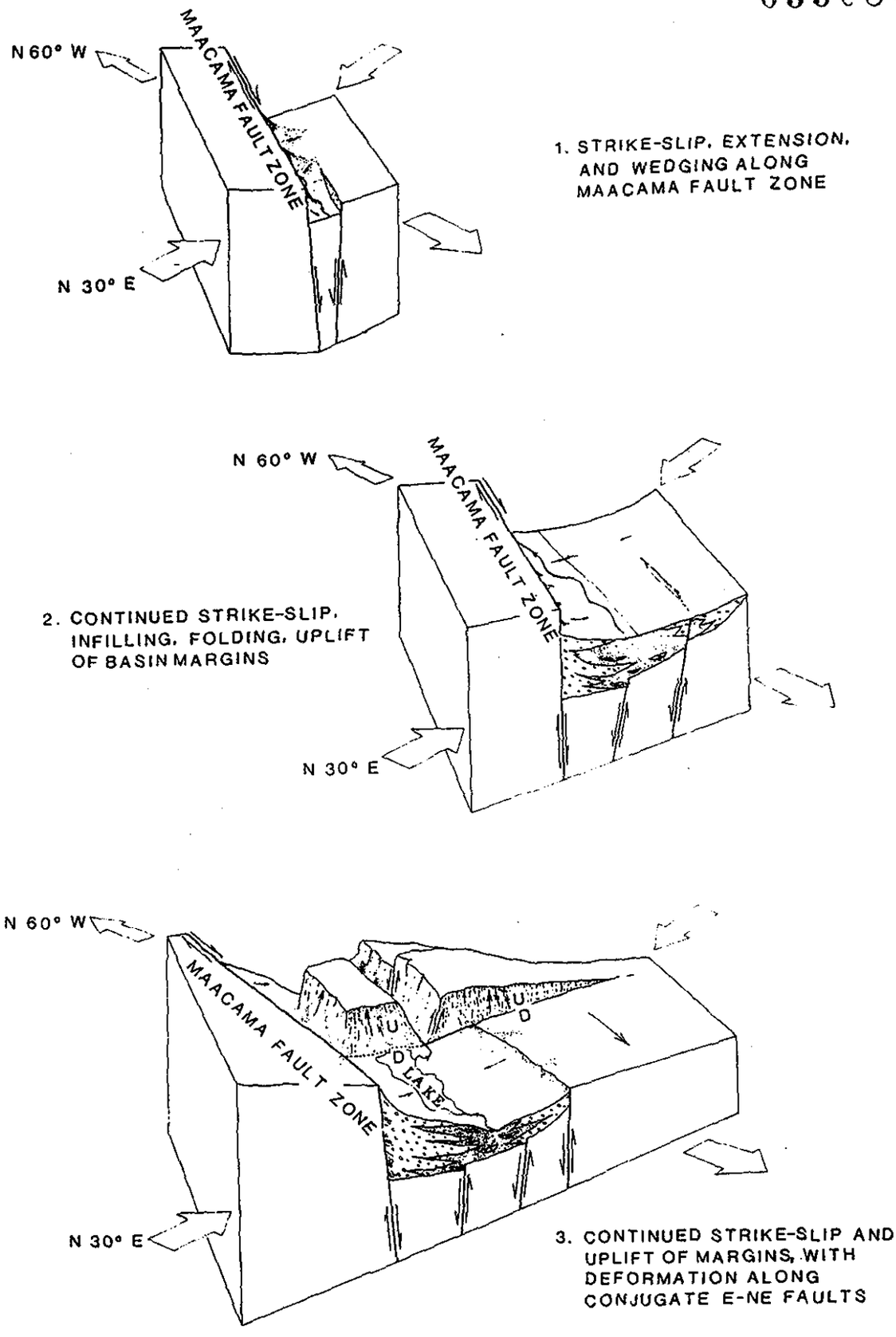



**Figure 6** 3D schematic diagrams showing relationship between facies development and active structures in a mixed strike-slip extensional basin. See other diagrams in references in Appendix for further illustration (from McLaughlin and Nilsen, 1985 p. 98.)

5 cm

(discussed below), but in the long diagonal section there is no obvious thickening of volcanic units towards it. These relationships suggest that it is a transfer fault rather than a normal fault.

**There is a clear spatial association of compressional structures with earlier syn-depositional faults.** The Hellyer anticline occurs immediately west of a large, syn-depositional fault, and its steep eastern limb overlies the early fault, suggesting that reactivation of early faults played a part in creating folds (Cooke, 1991). There is a distinct step in both the Hellyer anticline and the adjacent early fault across the NW-trending syn-depositional structure between Que River and Hellyer, consistent with its identification as an early transfer fault. There is also a marked change in fold style across this structure, manifested east of Hellyer by the appearance of the steeply plunging Portal Syncline and east-plunging Eastern anticline, and west of Hellyer by a break in fold trends, so that across it anticlines are along strike with synclines.

These observations collectively suggest that the inferred early transfer fault was not reactivated significantly during later deformation, but did reactivate to the extent that it allowed domains on either side of it to deform differently. The Henty Fault Zone and Mt. Charter Fault both represent significant shear zone reactivation of major, early faults, with the Mt. Charter Fault representing an early transfer fault with a component of normal (east-side down) movement, and the Henty Fault Zone representing a major basin-bounding fault with a large component of west-side-down movement.

The timing of *initiation* of the Que/Mt Cripps Faults is more difficult to determine. They separate domains of different structural style, and so were active during compressive deformation. There is insufficient detailed stratigraphic information to document offset marker horizons and thickness variations. The greater abundance of andesite relative to basalt south of the Que Fault suggests that it was active early in basin formation, but there is not enough stratigraphic information available in the areas south and west of Que River to determine where this andesite sits relative to the Hellyer stratigraphy . Section 4500 N suggests that it may represent Footwall Andesite, and that the Pillow Basalt Sequence is absent. **Note that this implies that much or all of the Mt Charter area is occupied at the surface by stratigraphic levels below the mineralised interval, and that any "Mt.Charter deposit" is likely to have been eroded.**

## Structure and stratigraphy

This section reviews and discusses data and observations relevant to the structural geology of the Mackintosh area that have not been addressed in the geometrical analysis above.

**Volcanic and sedimentary facies**

This discussion of facies variations and their significance is based dominantly on the work of Jocelyn McPhie and John Waters, and a number of Aberfoyle geologists. Much further work on the volcanology, sedimentology, and stratigraphy of the Mt. Read Volcanics is required in order to understand the processes of basin development, and this discussion is restricted to a relatively random set of observations that have implications for the tectonic environment.

McPhie's stratigraphic correlations have identified a pumiceous breccia unit that overlies the QRS and represents the base of the URS, which can be traced from the Sock Creek South area to at least 11 km north to HL-469, north of Hellyer. It is absent, however, from the area of the Hellyer portal (MAC-19), less than 2 km southeast of HL-469, on the east side of the syn-depositional fault east of Hellyer. The pumiceous breccia is overlain at Sock Creek South by massive rhyolite with distinctive, very coarse-grained quartz eyes. In all of the other areas where McPhie has identified the pumiceous breccia (HP, BRD, HL-541. HL-469), it is overlain by volcaniclastic sediments which contain very coarse-grained detrital quartz eyes. She believes that these distinctive sediments were shed from the rhyolites at Sock Creek; the boundary between the rhyolitic source area and the volcaniclastic sediments occurs at the Mt. Charter Fault. Although the pumiceous breccia is absent from MAC-19, the quartz eye volcanic sediments are abundant, suggesting that the Hellyer syn-depositional fault was less active or inactive by the time of URS deposition.

Detailed mapping of the Mica Sandstone in the area of the Hellyer Tailings Dam and the Cradle Mountain Link Road indicate that it dips and youngs to the southeast, and thus stratigraphically underlies the QRS, and from drillcore relationships (section 10,500 N) also underlies the Que-Hellyer volcanics. Along the Link Road it consists of dominantly feldspathic, volcaniclastic sediments, that are stratigraphically overlain in the Tailings Dam area by more quartzose and micaceous, cross-bedded and graded sandstones and shale. All of these relationships support correlation of this unit with the Animal Creek Greywacke southwest of the Mt. Charter Fault, and along the Henty Fault Zone, and are consistent with the identification of volcanics to the north on McNeill's map, as Central Volcanic Complex. Cross-beds noted in several locations in the Animal Creek Greywacke, and particularly near the Henty Fault Zone, are indicative of current flow from the north, and may indicate that the basin was elongate in a north-south direction; much further sedimentological work is required to determine whether these observations are representative of the area as a whole.

The general stratigraphy of the Que-Hellyer volcanics can be divided into four main stages:

- a stage of extensive volcanism and rapid rates of deposition, represented by the Footwall Basalt and Footwall Andesite, and the lack of significant clastic input;

- a transition period, represented by dacitic volcanics and/or shallow intrusives, volcaniclastic rocks of the Mixed Sequence and ore deposition;
- a period of relative quiescence, coinciding with deposition of the QRS, and with volcanic activity apparently restricted to the Pillow Basalt Sequence;
- a period of extensive volcaniclastic deposition (URS-Southwell Sub-group), indicating rapid filling of the Que-Hellyer Basin, and probably signifying the end of its existence as a distinct depocentre. The URS was probably sourced in the south from the southern Sock Creek area, and in the north possibly from the northeast, based upon the identification by McPhie of biotite porphyry clasts in volcaniclastic sediments on the Link Road, probably sourced from the Bond Range Porphyry.

These features suggest that the general tectonic régime changed at about the time of ore deposition, and that after QRS deposition the Que-Hellyer basin ceased to be very active and simply filled up.

**Fault fabrics**

The general position and orientation of faults, discussed above, gives some indication of their relative timing. In addition, textural fabrics can give indications of relative timing of structures. In the Mackintosh area, most of the faults are not well exposed at surface, and it is often difficult to unequivocally relate faults intersected in drillcore with major structures mapped at surface. This section discusses structures and textures observed at surface and in drillcore for some of the major and minor faults:-

- *Mt. Charter Fault* - Surface exposures were examined along the road and in the trenches in the vicinity of the transmission line, west of Mt. Charter; along the Murchison Highway; and along the road to Sock Creek, just west of the Murchison Highway. In all cases, the fault is poorly exposed, and is evident as a zone of intense foliation, with only local development of a steeply plunging stretching lineation. A faulted contact in MAC-25 at 458 m has been correlated with the Mt. Charter Fault. It consists of massive and relatively undeformed volcanic rock in contact with kinked, foliated sedimentary rocks. This style of faulting suggests that the fault in core is a relatively minor, late, brittle fault, and not the main Mt. Charter Fault.

- *Henty Fault Zone* - The Henty Fault Zone was visited where it is well exposed around the spillway to the Lake Mackintosh dam. In the spillway it consists of steeply dipping, isoclinally folded sedimentary rocks that probably correlate with the Animal Creek Greywacke. A strong cleavage is axial planar to the folds, and fold axes plunge steeply to the north. Local zones of intense foliation development dip to the west and contain a moderately south-pitching stretching lineation and S-C fabrics

indicative of reverse-dextral movement. Later sinistral movement along the fault zone is indicated by fault zones parallel to the main fault fabrics, which contain sub-horizontal striations, and which kink the main cleavage. Fault exposures in the hills south of the spillway contain asymmetrical quartz fibres which are indicative a dominantly dextral, and lesser reverse, sense of movement. This analysis of fabric orientations and movement directions is consistent with the detailed analysis of the Henty Fault Zone by Berry (1989). The character of the Henty Fault was also examined in oriented samples collected by Andrew McNeill from the southwest flank of the Shark's Fin. Here it consists of a well developed shear foliation with a sub-vertical stretching lineation, and S-C fabrics and asymmetrical shadows around feldspar porphyroclasts indicative of steep reverse (west-side-up) movement.

- *Ductile Fault Zones north of Hellyer* - A N-trending zone of shearing is poorly exposed on the north side of the Link Road, 250 m east of the Hellyer access road. It is covered to the north and south by Tertiary basalt, but appears to represent a major deformation zone similar in style, orientation, and movement sense, to the Henty Fault Zone. It is more intensely deformed than the moderately E-dipping volcaniclastic sediments of the Southwell Sub-group to the east, and consists of tightly folded, quartzose sedimentary rocks with locally preserved cross-beds, that almost certainly correlate with the Mica Sandstone (Animal Creek Greywacke). This deformation zone thus juxtaposes strata from below the Que-Hellyer succession with strata from above it, and probably represents a major shear zone.

- *Que Fault* - The Que Fault was examined in QR-1169 at 242 m. It consists of 2.5 m of broken core separating relatively massive basalt from dacite with patchily developed foliation. If this intersection is typical of the Que Fault, it suggests that the Que Fault is a brittle, and relatively late fault.

- *Mt. Cripps Fault* - The Mt. Cripps fault was examined in an exposure along the logging road south of Mt. Cripps. It consists of a >100 m wide zone of sheared siliciclastic rocks of the Eldon Group, juxtaposed against relatively massive quartz-phyric volcaniclastic rocks to the northwest. The shear foliation dips steeply, and is NE-trending, distinctly oblique to the more east-west mapped trace of the fault. No lineation or fabric asymmetries that indicate sense of movement were observed. Stratigraphic juxtaposition of the Eldon Group to the south indicates a component of south-side-down displacement.

- *Smaller faults* - Numerous smaller faults were observed in the field. The largest ones are the NW-trending faults northwest of the Hellyer Tailings Dam. The most southerly of these faults has been mapped by McNeill, and juxtaposes southeast-

dipping Mica Sandstone to the north, with younger, southeast-dipping QRS to the south. This relationship, coupled with horizontal quartz fibres, indicate dextral displacement. The basalt exposed in the canal north of the Tailings Dam is NW-trending and subvertical, and separated southeast-dipping Mica Sandstone to the north from southeast-dipping QRS to the south. These relationships indicate that the basalt occurs along a discordant fault plane, with the same orientation and dextral displacement as the fault mapped by McNeill. The lack of fault-related fabric development in the basalt, its vesicular nature, and its proximity (<100 m) to Tertiary basalt outcrops and to a clearly discordant mafic dike, all suggest that this basalt is a Tertiary feeder dike intruded along an older fault plane, rather than a distal correlate of the Que-Hellyer volcanics. Similarly oriented faults occur in Passing Bay 6 on the portal road, where W- to NW-trending brittle faults contain sub-horizontal striations and local quartz fibres indicative of dextral displacement, and are associated with N-trending brittle faults with sinistral displacement. These fault orientations also occur in the cleared QRS exposure west of the spillway at the Hellyer tailings dam. Minor NE-dipping faults with steeply plunging quartz fibres are common in roadcuts on the Link Road, and appear to have a normal sense of movement. A single, discordant, NW-dipping reverse fault with well developed asymmetrical quartz fibres indicative of reverse movement is exposed on the south side of the Link Road, 500 m north of the transmission road. All of these brittle structures are indicative of NW-directed compression, and probably developed contemporaneously.

## Folds and cleavage

Cooke (1991) noted two phases of folding in the QRS in the Hellyer tailings dam area, an earlier NW-trending phase and a later NE-trending phase. Mapping of fold patterns in the Mica Sandstone to the north of this area has confirmed these same fold orientations, and the same relative timing of the fold phases is inferred, based upon a weak, unfolded, NE-trending cleavage in this area which is probably associated with the later phase of folding. Gentle NW-trending folds occur in the QRS southwest of Mt. Charter, in outcrops on the north side of the MC-15 collar, where they are cross-cut by a NE-trending cleavage, indicating that although this early phase of folding was gentle, it is of regional significance.

As noted above, folds show a strong spatial association with what we interpret to have been early growth faults, indicating that they represent zones of deformation associated with fault reactivation, rather than a regional fold belt. This is also obvious when attempting to relate cleavage to the folds. Although cleavage is generally N- to NE-trending, approximately parallel to the later phase of folding, in detail it is not axial planar to the folds. This is especially

apparent at the southern end of the Hellyer anticline, where the Amoeba Fault (Figs 4 and 5) has replaced the east-dipping fold limb. In map view, cleavage is oriented anticlockwise to the apparent fold trend, and in sectional view, the fold proves to have no east-dipping limb, and appears as a monoclinal structure.

## Alteration patterns

Areas of alteration noted on Aberfoyle 1:2500 maps have been outlined and transferred on to the 1:25,000 structural compilation map (Fig. 7). There is a clear association between large areas of alteration and the interpreted early faults, and in particular, areas of early fault intersections. Little alteration appears to be associated with later faults, except where they represent reactivated early faults. Areas of most intense alteration and/or economic mineralization are concentrated at early fault intersections as follows:

- Mt. Charter occurs at the intersection of a major NW-trending early fault and a smaller ~NE-trending fault, in the down-dropped side of both faults;
- Que River Mine occurs within an extremely thick sequence of altered Mixed Sequence-type rocks that appear to have been deposited in a local graben between two NE-trending faults;
- The Amoeba Zone alteration occurs on the downthrown side of a major early fault, along strike with a probable early fault identified about 1 km to the north;
- Extensive alteration around the D-Zone occurs at the intersection of two major NE-trending (normal faults) with a NW-trending transfer fault;
- Hellyer occurs to the west of a major normal fault, and probably along a smaller-scale parallel fault, on the south side of a facies change that probably represents a NW-trending transfer fault.

## Mine-scale structures

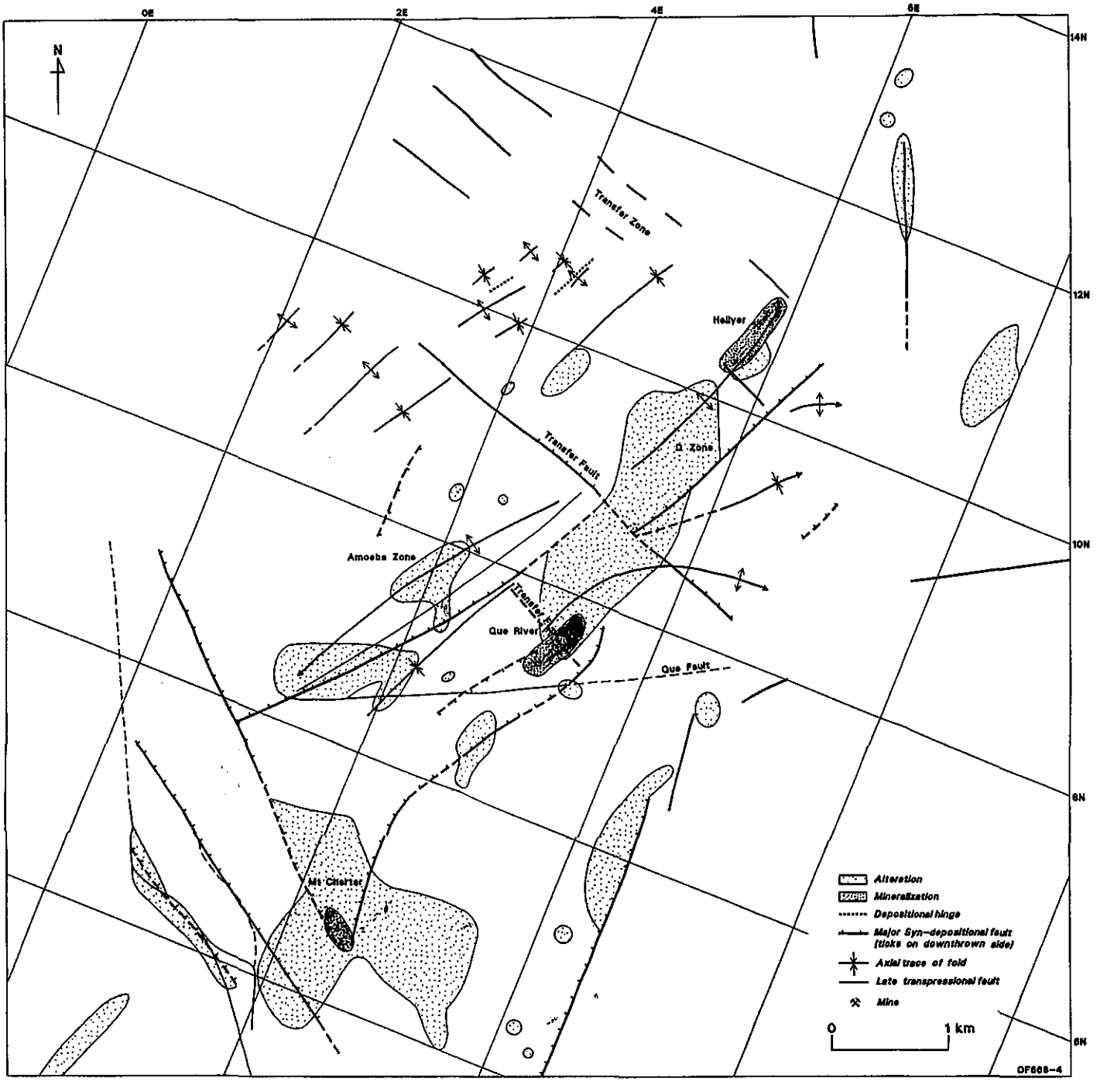
This section describes some of the significant mine-scale structures that have been identified by Aberfoyle mine and exploration geologists, and by Bruce Gemmell.

*Hellyer*

Important early structures identified at Hellyer are sulphide feeder veins to the orebody, and feeder dikes to the PLS, with a main grid 045° trend and a less important grid 090° trend (e.g. MacArthur, pers comm; Gemmell, pers comm; Downs, 1990; Drown 1990). This main trend is nearly parallel to the main syn-depositional normal fault trend identified in the Hellyer area, but the lesser trend has no clear relation to major early faults so far identified. The grid 045°

**Figure 7** 1:25,000 structural framework map of the Mackintosh Block (see Figure 4), with areas of moderate (green) and intense (pink) alteration marked to show the common spatial association between interpreted syn-depositional structures and alteration.

655092


0E
2E
4E
6E
14N
12N
10N
8N
6N
N
Transfer Zone
Hellyer
Transfer Fault
D Zone
Amoeba Zone
Transfer Fault
Que River
Que Fault
Mt Charter
Alteration
Mineralization
Depositional hinge
Major Syn-depositional fault (ticks on downthrown side)
Axial trace of fold
Late transpressional fault
Mine
0
1 km
OF565-4

5 cm

trend is important because it is derived from extensional features, and thus probably reflects the pure extensional plane in the basin during ore deposition and volcanism. There are indications that one or both sides of the orebody are bounded by syn-depositional faults, but numerous late faults which cut and offset the orebody make the exact location(s) of these faults difficult to identify.

Ductile structures noted at Hellyer include the main N- to NE-trending foliation that is prominent in phyllosilicate-rich parts of the footwall alteration, and banding in the sulphide ore. The foliation in footwall alteration is associated with flattening of altered clasts. Banding within the orebody, observed underground at its eastern contact (360 level, 92 pillar) is interpreted to be very largely tectonic. The banding indicates at least local west-side-up movement by asymmetrical strain shadows around a large, pyritic porphyroclast. Banding in a sub-horizontal drillhole, HL-643, just below the sub-horizontal crest of the orebody, is perpendicular to the core axis, and hence must be vertical, i.e. strongly discordant to the orebody contact. These features all indicate a significant amount of shortening within the orebody and within the alteration zone below it, both of which were less competent than the surrounding unaltered volcanic host rocks. Shortening could not have been accomplished in these rocks without some compensatory deformation in the more brittle, hangingwall rocks. Thrust faults such as the M Fault described by Downs (1990), and numerous smaller brittle faults in the PLS, probably account for this shortening in the hangingwall. The M Fault, as described by Downs (internal report), "has a shallow easterly dip and appears to follow the HVS horizon east of the orebody. When it encounters the orebody the dip steepens to near vertical and it passes out of the HVS into the overlying basalt (PLS)". Smaller-scale E- and W-dipping conjugate thrusts have also been noted by Downs in the less altered footwall andesite and in the siliceous core to the alteration zone, and likely also compensate for the more homogeneous shortening in the phyllosilicate-rich rocks.

Numerous late faults disrupt the orebody, the most obvious of which is the sinistral Jack Fault. The fact that the shape of the orebody is restorable along the fault *along the observed lineation direction* indicates that the Jack Fault itself is a *late* fault, not a reactivated early fault (although its presence might be controlled by some nearby early fault). Work in progress by Henry Kurth has identified a WNW-trending dextral fault which is offset by the Jack Fault, and which has reactivated and offset the Jack Fault by about 80 m. This evidence for contemporaneous N-trending sinistral faulting and W- to NW-trending dextral faulting is entirely compatible with the late fault patterns noted in areas such as Passing Bay 6 and the Hellyer Tailings Dam.

*Que River*

Que River structural data on maps and sections were examined, but were difficult to relate to the faults described above because they lacked textural descriptions indicative of whether faults were brittle or ductile in character. The main structural features of Que River appear to be zones of extensive alteration with a N-trending foliation and steep stretching lineation, as exposed at surface at S Lens, and steep N-trending faults linked by numerous smaller faults of variable strike and dip. Mine plans show that at least some of these smaller faults contain horizontal striations; much of the complexity of the fault patterns here appears to relate to fault movements that relate to the late NW-directed compressional event, but that are strongly influenced by the location and orientations of pre-existing faults.

## Synthesis of geological information

### Relative timing of structures

*Early (syn-depositional) structures*

Structures in the Mackintosh area that can be identified as early include faults with significant thickness or facies changes across them, and mine-scale structures that are demonstrably syn-mineralization or syn-volcanic, i.e. feeder veins and dikes. These structures indicate an early structural geometry that consisted of:

- Sub-vertical ENE-trending extensional veins and dikes (grid 045°);
- NE-trending faults associated with abrupt thickness changes of volcanic units, suggesting a significant component of normal displacement;
- NW-trending faults with associated facies changes but no significant or consistent thickness changes, supporting their identification as transfer faults.

Faults such as the Mt. Charter Fault and its adjacent early faults are of intermediate orientation to the normal and transfer faults, and show thickening of some stratigraphic units. These NNW-oriented faults probably represent sidewall faults to the basin with a moderate component of normal displacement across them; their orientation may have been controlled by the structure of the underlying basement..

*Ductile compressional structures*

Ductile compressional structures consist of the early, gentle, NW-trending folds; later, gentle, NE-trending folds; a steep N- to NE-trending cleavage present in most sedimentary rocks; and local, generally N-trending, zones of intense foliation and shearing with locally developed steep lineations (including Mt. Charter and Henty Fault Zones). All of these structures, except for

the early NW-trending folds which are cross-cut by the cleavage, can be related to a ~ENE-directed compressional direction, and probably developed contemporaneously. The early NW-trending transfer faults show little evidence for ductile deformation, save for representing a break in fold trends west of Hellyer, and were probably unfavourably oriented for reactivation during this event.

*Late brittle structures*

Brittle faults include N-trending sinistral faults and NW- to W-trending dextral faults that appear to be common wherever outcrop is well exposed, i.e. underground and numerous roadcuts. Good exposures at surface and underground demonstrate that the faults developed contemporaneously, i.e. that they represent a conjugate set. Known displacements associated with individual faults do not appear to exceed several hundred m. Their orientations are indicative of NW-directed compression. Less common NE-dipping normal faults and NW-dipping reverse faults are compatible with this compression direction and probably developed at the same time.

## Geologic history of the Mackintosh area

This section integrates all of the evidence described above for relative orientation, movement sense, and timing of structures into a model for formation and deformation of the Mackintosh area. The progressive structural evolution is summarised in Figures 8 and 9.

### Formation of the Que-Hellyer Basin

The Que-Hellyer Basin occurs at the northern termination of a regional, N-trending, basin-bounding fault, where it splays into the N- to NNW-trending (Mt. Charter) segment, which forms a major bounding fault to the Que-Hellyer Basin, but appears to die out northward, and NNE-trending (Henty) segment. The deformation zone exposed on the Link Road appears to correlate with the Henty Fault Zone, indicating that the Henty Fault Zone has stepped to the right. Extensional features such as normal faults and feeder veins and dikes indicate a NNW-trending extension direction during basin formation. These features together suggest that the Que-Hellyer Basin formed in a dilational jog (right step) within a larger, N-trending, dextral strike-slip system (Figs. 8a, 9a). Dilational jogs in strike-slip sytems are the most feasible environments in which rapid subsidence and basin infill can be localized in very small areas, and the vertical nature of the major bounding faults and fault intersections can create vertical conduits that allow significant migration of magma to surface. As an order-of magnitude calculation, if extension across the Que-Hellyer Basin, measured in the direction *parallel to the N-trending strike-slip faults*. is on the order of 2 to 3 km (the approximate north-south minimum distance between sub-surface drill intersections of Animal Creek Greywacke), then

**Figure 8** Schematic plan views of the principal structural elements of the Mackintosh Block, depicting the 3-stage evolution of the area. See text for explanation.

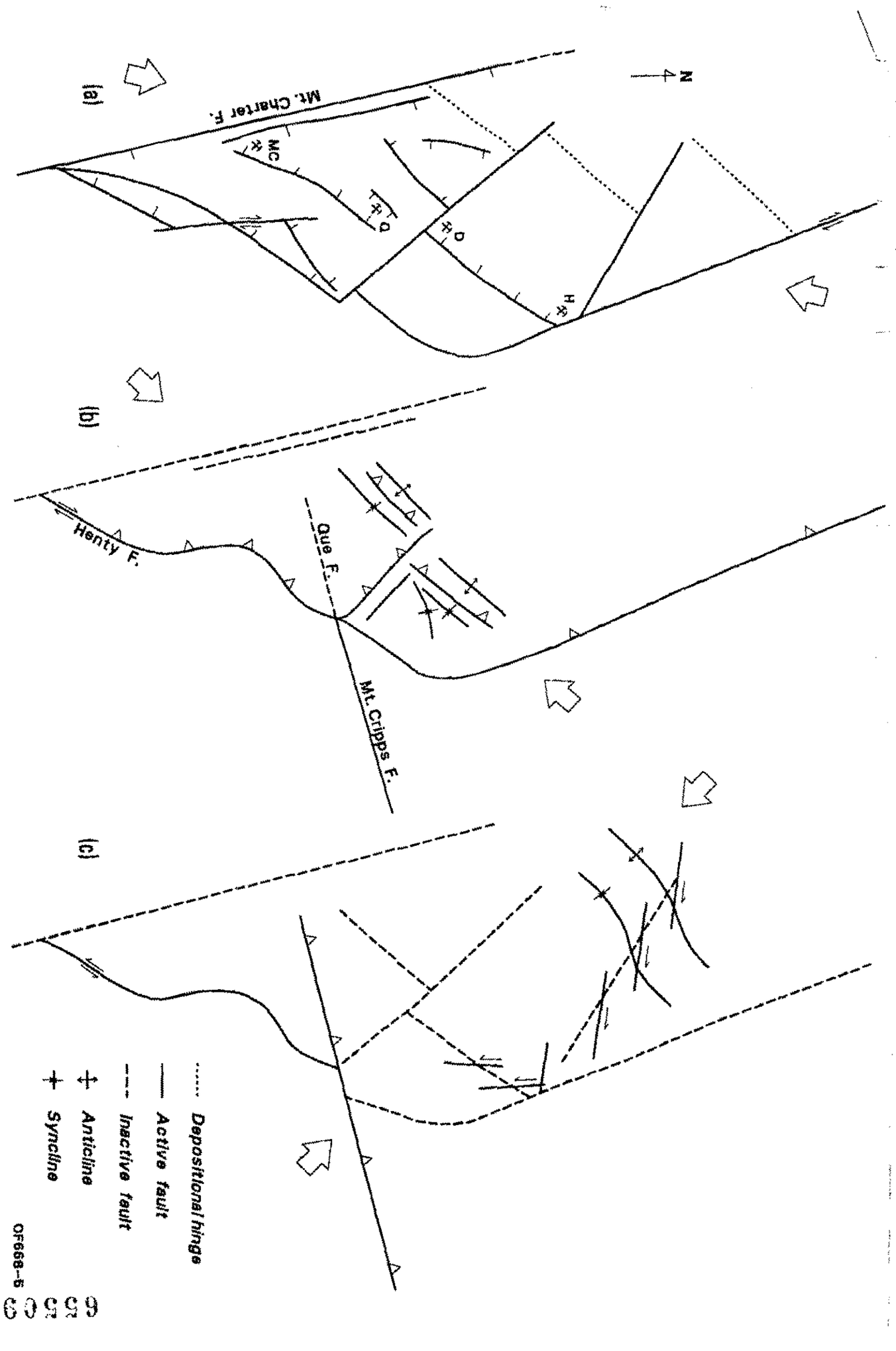
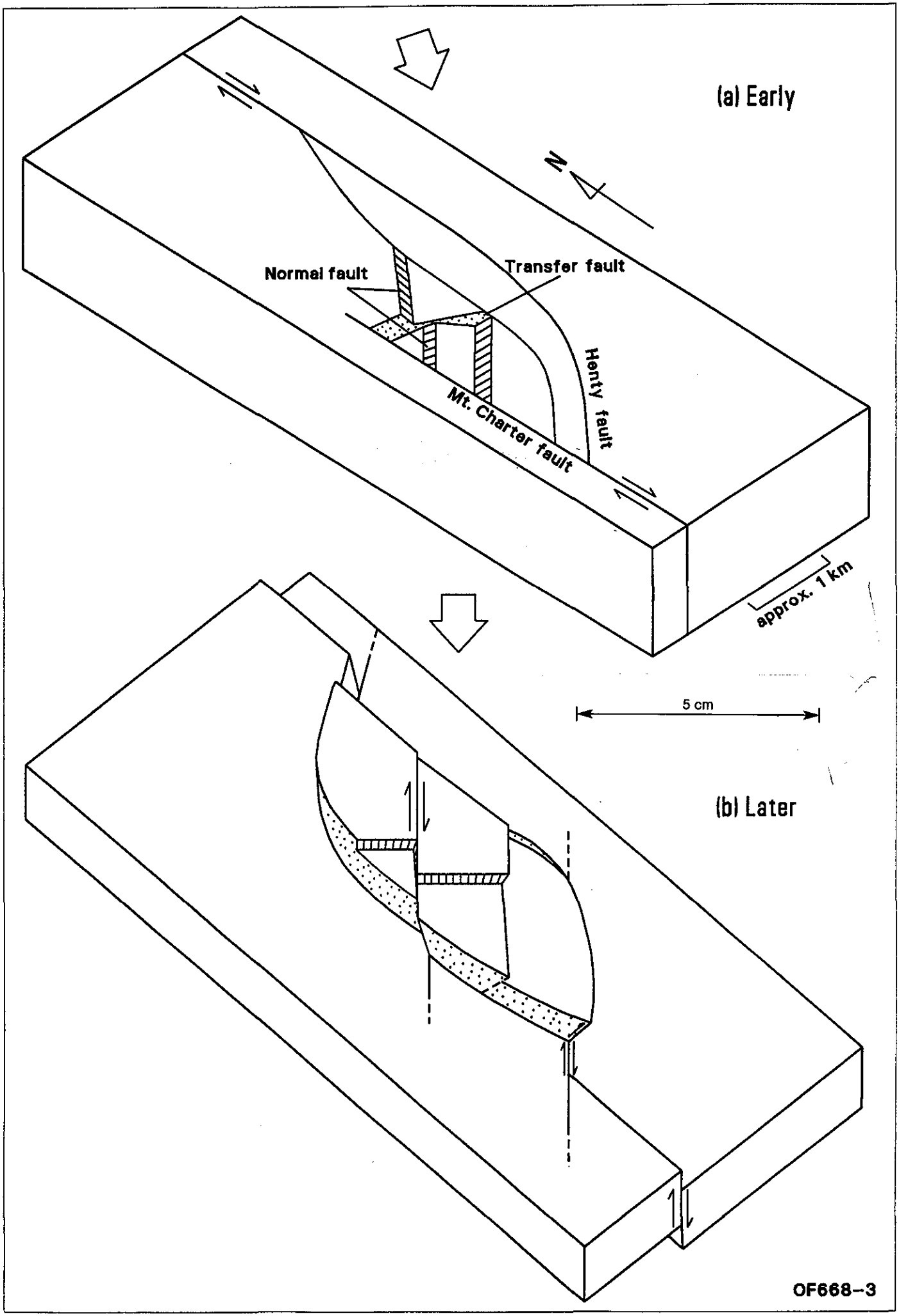

(a)
Mt. Charter F.
MC
Q
D
H
N
(b)
Henty F.
Que F.
Mt.Cripps F.
(c)
Depositional hinge
Active fault
Inactive fault
Anticline
Syncline
OF668-5

**Figure 9** Schematic block diagrams generalising the switch from oblique extension followed by oblique compression (transpression) in response to a relatively small rotation of the principal stresses. (a), (b) correspond to Figure 8a, b.


(a) Early
N
Normal fault
Transfer fault
Henty fault
Mt. Charter fault
approx. 1 km
5 cm
(b) Later
OF668-3

assuming moderate fault slip rates of 2 to 3 cm/a, it appears reasonable that time required to form the Que-Hellyer Basin is in the order of *100,000 years*. The early, NW-trending fold orientation is compatible with such a dextral strike-slip system (Fig. 8a, 9a).

### Early deformation

Ductile deformation appears to be associated dominantly with reactivation of the early N-trending faults as dextral-reverse faults. This reactivation requires only a small clockwise re-orientation of the stress régime responsible for the earlier dextral strike-slip system, and may represent a later stage of the same tectonic event, rather than a distinct, later event. During this event, folds evolved over early normal faults that reactivated as dextral-reverse faults (e.g. the Amoeba Fault, the equivalent of which probably occurs at depth, below the steep limb of the Hellyer anticline). The Henty Fault, which formerly had been an oblique dextral-normal fault, reactivated as a dextral-reverse fault. The present wavy surface trace of the Henty Fault suggests that during reactivation, more N-trending strike-slip fault segments linked with more NE-trending normal or dextral-normal fault segments, thereby accounting for its present sinuous trace. This may also apply to the Mt. Charter Fault, which trends almost due north, except for a local flexure to a trend more parallel to the early transfer faults.Where the Henty Fault terminates, at its intersection with the D-zone transfer fault, northward movement along its western side was taken up by the transfer fault, which controlled the formation of the anomalous Eastern anticline and Portal Syncline (Fig. 8b). The reverse component of movement along the Henty Fault appears to have been taken up by a component of sinistral movement on the Mt. Cripps Fault, which propagated westwards to form the apparently late Que Fault. Continued sinistral movement along the Mt. Cripps-Que Faults accounted for folding of the volcanic sequence north of the Que Fault, which behaved essentially as a tear fault (Fig. 8b). This relative minor stress re-orientation caused the Que-Hellyer Basin (Fig. 9a) to invert into an anticlinal structure (Fig. 9b).

### Late deformation

Late, brittle deformation consists of brittle faults indicative of NW-directed compression. The faults do not appear to have displacements in excess of several hundreds of metres, but are very important on the mine scale, where they may cause significant displacements to the orebodies, e.g. the Jack Fault, and probably many of the faults at Que River. The dextral faults may have been localized around the NW-trending transfer faults, perhaps occurring as *en echelon* arrays over the basement faults, e.g. the apparent corridor of such faults that occurs from the Hellyer Tailings Dam area towards Hellyer. Much of the complexity of fault patterns evident from the Que River mine plans probably results from the superimposition of these faults upon faults associated with earlier deformation.

## Discussion

The absolute timing of the three main deformation events has not so far been addressed here. The main deformation event has traditionally been considered to be Devonian, but if it indeed represents a later phase of the same event responsible for formation of the Que-Hellyer Basin, it must have shortly followed volcanism, and hence have occurred in Late Cambrian or Ordovician time. The occurrence of dolerite sills on fold noses in the QRS suggests that mafic magmatic activity was on-going during folding, and if these sills are co-magmatic with Que-Hellyer volcanics, may support this earlier timing for folding. The later, brittle faulting event cross-cuts, and hence post-dates, the folds. This event has traditionally been considered to be Mesozoic or Tertiary. Dikes of Devonian granite near Renison, shown on the 1:100,000 Mt. Read Volcanic compilation map, trend NW and suggest that the principle compressive stress direction in Devonian time was NW-directed. These relationships lead to the suggestion that the main deformation in the Que-Hellyer Basin was Cambro-Ordovician, and that the later, brittle structures formed during NW-directed compression represent the Devonian event. Future geochronological work may help resolve the timing of these events, but Ar-Ar ages of alteration assemblages at Hellyer of 480 and 440 Ma are not consistent with either deformation shortly following Que-Hellyer Basin formation at ca. 500 Ma (based upon Perkin's U-Pb zircon dating) or with Devonian deformation. Field relationships and textural details of samples for dating by isotopic systems subject to resetting will have to be carefully constrained in order to understand the significance of the dates obtained.

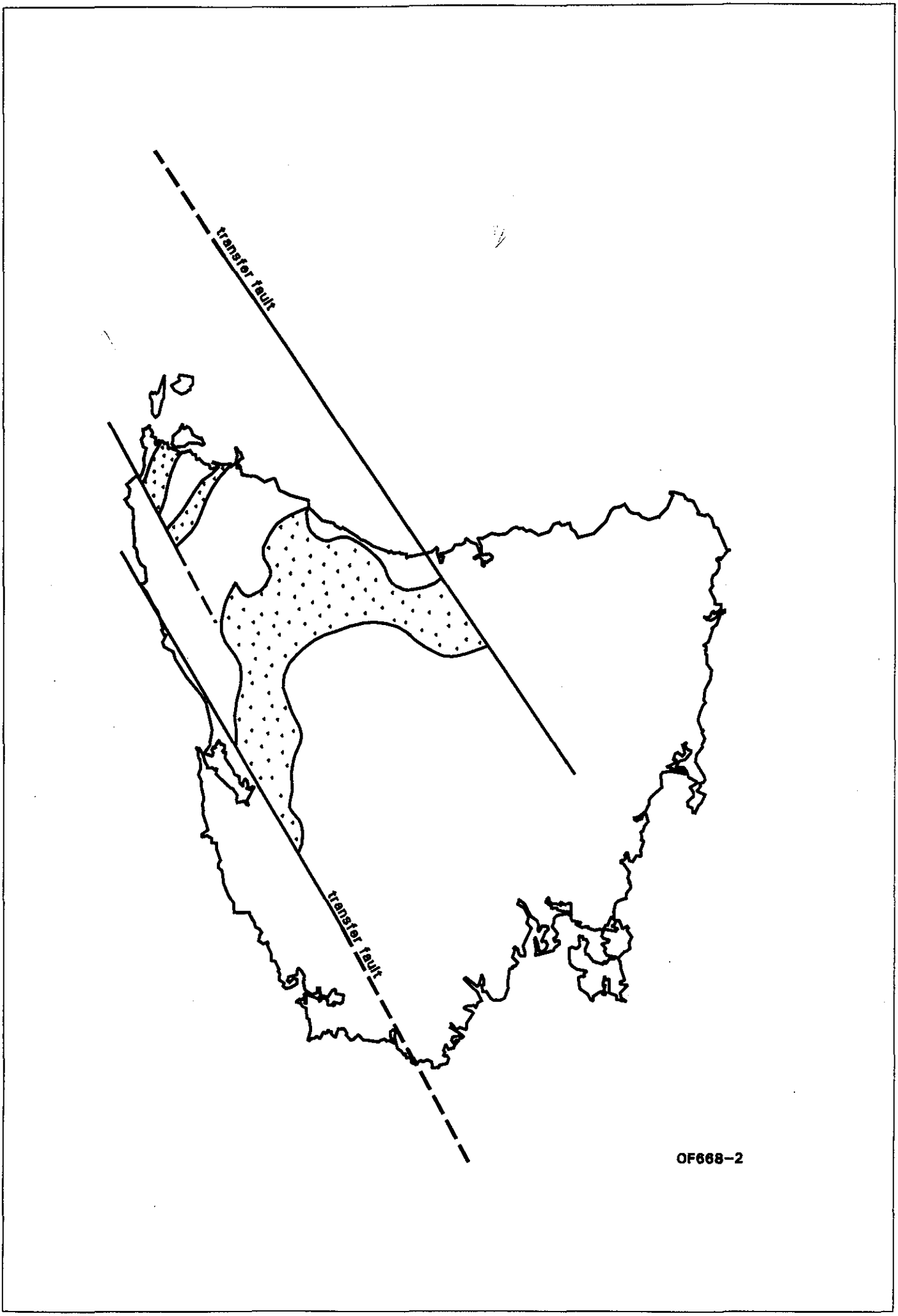
## Integration with regional geologic history

This section briefly discusses the geological history of the Que-Hellyer Basin in light of regional geological relationships, first on the scale of the Mt. Read Volcanic Belt, then on the scale of Tasmania in context with eastern Australia.

*Mt. Read Volcanic Belt.* The following comments are based mainly upon observations about the 1:100,000 Mt. Read Volcanic compilation map, and on reports on regional structural work by Berry, Rattenbury and Keele in reports from the University of Tasmania AMIRA project on the structure of the Mt. Read Volcanics. These aspects will be developed in the regional airmag. project, and are only summarised here to provide a context.

The dominant map trends of the Mt. Read Belt are oriented N and NNE (Fig. 10), similar to the main trends within the Que-Hellyer Basin. The most prominent of these is the N-trending eastern boundary of the belt, which separates Mt. Read Volcanics from the Precambrian Tyennan Block. The Precambrian rocks are unconformably overlain by Owen Conglomerate, which to the west overlies Mt. Read Volcanics, indicating that the volcanic rocks were probably never deposited east of this boundary. Surface traces of major faults (the Henty Fault and its

**Figure 10** Map of Tasmania with inferred major Cambrian, N-W trending transfer faults and extended regions that evolved into volcano-sedimentary sub-basins. The Mt. Read Volcanic Belt is interpreted to have developed along a Pre-Cambrian N-S, crustal-scale fault zone that was reactivated in transtension to the south of its intersection with the major transfer zone.




m:/marine/mstation/of668/of668-2.d May. 11, 1992 09:50:30

splays, and the Rosebery Fault) are wavy and irregular, suggesting that they represent linked networks of earlier faults. A Proterozoic inlier 20 km west of Hellyer and Que River, and a smaller inlier along strike to the south near Mt. Dundas, have eastern boundaries conformable with the curved northwestern boundary of the Tyennan Block, and would appear to fit back together with the Tyennan Block along a NW trajectory, parallel to the extension direction determined for the Que-Hellyer Basin. Orientations such as the NW trend of the Rosebery Fault near Rosebery, and the NW-trending boundary of volcanics with Precambrian rocks on the north side of Macquarie Harbour, may reflect transfer fault orientations, parallel to the NW-directed extensional direction. The major N-trending boundary of the basin may be controlled by reactivated Precambrian basement structure . These structures suggest that, although the Que-Hellyer Basin is certainly younger than the CVC and the bulk of the Mt. Read Volcanics, all of the Mt. Read Volcanics may have formed during an approximately NW-directed oblique extensional event.

*Southeastern Australia.* The Mt. Read Volcanic Belt curves from its general northerly trend, around the north end of the Tyennan Block, to a more easterly trend. The belt is in general not highly deformed, which suggests that the curvature is primary and depositional, rather than a result of post-depositional deformation. The curvature of the belt is parallel to the Precambrian structural grain of the Rocky Cape Block, suggesting that Cambrian extension and volcanism were localized along pre-existing zones of weakness in basement rocks.
If the NW-oriented extensional direction determined for the Que-Hellyer area, and inferred for the rest of the Mt. Read Belt to the south, is also applicable to this northern continuation, it suggests that extension northeast of the Mackintosh area was more orthogonal than oblique, and that further east, where the boundary is E-trending, extension may have been *sinistral-oblique* . The eastern boundary of volcanic rocks with Precambrian rocks, in north-central Tasmania, is parallel to the western boundary at Macquarie Harbour, and to the extension direction suggested for the Mt. Read Volcanic Belt, suggesting that these structures may represent (reactivated) crustal-scale, Cambrian transform faults. Normal faults juxtaposing Cambrian and Precambrian rocks are mapped south of Macquarie Harbour, and are supportive of NW-directed Cambrian extension. This orientation is in good agreement with the extension directions and transfer fault orientations that have been determined for Cambrian time for eastern Australia (Fig. 11).

## Problems with the Model

The tectonic analysis outlined above is consistent with most structural, stratigraphic, and textural relationships observed on the mine scale, basin scale, and continental scale. Some relationships that are not yet well understood include:

655105

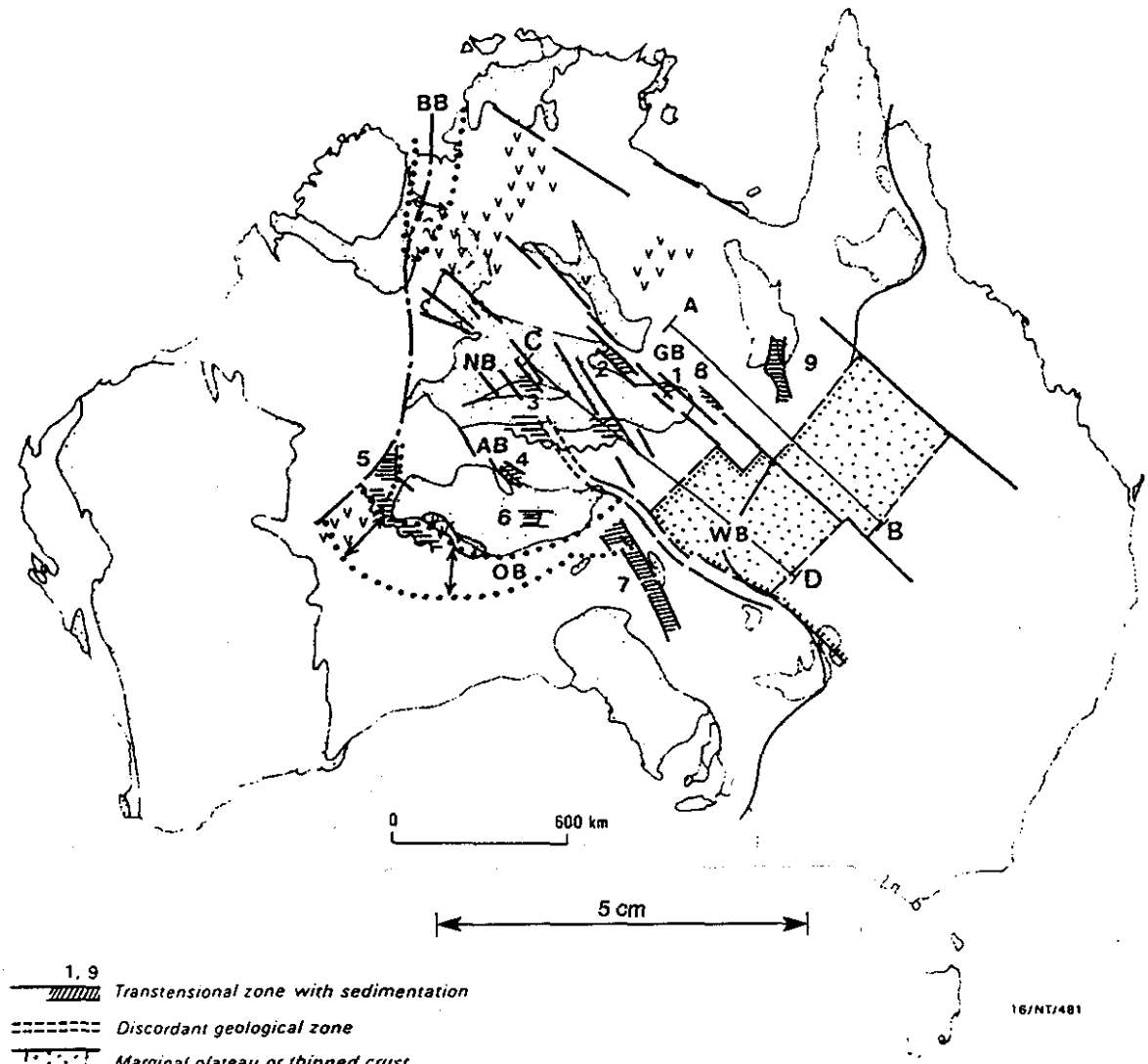



Fig. 17. Map showing structures inferred to have been active during widespread continental extension in the Early Cambrian (see Figure 20 and text for further discussion). Discordant geological, gravity and aeromagnetic features are also shown. Early Cambrian accommodation and transtensional basins, including half-grabens, are occupied by the following units: 1, Mount Baldwin Formation; 2, Central Mount Stuart beds; 3, Yuendumu Sandstone; 4, possibly the Mount Currie Conglomerate; 5, beds in Clutterbuck Graben (northwesternmost Officer Basin); 6, beds in Levenger Trough (central Musgrave Block); 7, sediments west of the Peake and Denison Ranges; 8, Sylvester Sandstone (southwestern Georgina Basin); and 9, Mount Burnie beds (Burke River Belt, eastern Georgina Basin). Basins of preservation are AB, Amadeus Basin; BB, Bonaparte Gulf Basin; GB, Georgina Basin; NB, Ngalia Basin; WB. Warburton Basin; and OB, Officer Basin.

**Figure 11** Cambrian structural/tectonic reconstruction of Australia after Shaw et al (1991), showing the array of NW-SE transfer faults that are interpreted to have segmented the Tasman extensional province throughout eastern Australia.

- The timing of *initiation* of the Que and Mt. Cripps Faults. It is clear that they are associated with late movement, both from textural relationships and from strata and structures they displace. There is presently insufficient stratigraphic information to determine whether there are thickness changes indicative of syn-depositional movement along the Mt. Cripps Fault. It is, however, appropriately oriented to have been a conjugate sinistral fault to the main dextral fault system. The Que Fault appears to represent a late fault that propagated from the Mt. Cripps Fault. The abundance of andesite south of it, relative to the more basaltic sequence north of it, is suggestive that it had some primary control on deposition. If the andesite south of the fault does indeed represent footwall andesite, the stratigraphic variation across the fault may be erosional or may reflect a stratigraphic pinch-out, and does not *require* a syn-depositional fault in this area. More detailed correlation of stratigraphic units in existing diamond drillholes in this area may help to understand the nature of the stratigraphic variation here.

- Why the Animal Creek Greywacke is so continuous adjacent to the Henty Fault Zone, and why it dips and youngs so consistently westward. This orientation is not consistent with listric normal fault movement, which predicts strata to dip and young toward the fault, or with reverse movement, which predicts strata to be dragged into steeper dips than the fault, and to young towards the fault.

- The nature of the Mt. Charter Fault flexure. The general Mt. Charter Fault trend is parallel to, and along strike with, the main basin-bounding fault to the south. The flexure represents a distance of about 1.5 km where the fault is NW-trending. This trend is parallel to the Que-Hellyer Basin transfer fault orientation, and may reflect local reactivation of a transfer fault, although the exact geometry of such a system is difficult to picture. Alternatively, it is along strike with the main syn-depositional normal faults in the Que-River Basin, and the flexure may have evolved from some strike-slip movement along these faults. However, this would require sinistral movement along these faults, which is not compatible with any of the tectonic events so far recognized for the Que-Hellyer Basin.

## Structural Controls on Mineralization

### General Statement on Structural Control

A simple mass-balance calculation based on the metal content of the Hellyer orebody and the solubility of the metals in a typical mineralising fluid demonstrates that the volume of fluid

required to have passed through the feeder system at Hellyer must have been about $10^{12}$ to $10^{13}$ litres, or 1 to 10 times the volume of Sydney Harbour!! In addition, the stratigraphic and sedimentological evidence (J. Waters, pers comm) suggests that ore formation was likely to have occupied a relatively short time - probably thousands to a hundred thousand years. These constraints demand very large fluid fluxes through the Hellyer feeder zone, and therefore **require the maintenance of unusually large permeabilities throughout the ore-forming process.**

Even though the ore-forming environment at Que-Hellyer was at or very close to the sea-floor, it is very unlikely that a static, previously formed structure could have maintained sufficiently high permeabilities to permit the fluid flux required. In particular, any relic permeability from an earlier period of faulting would have been rapidly destroyed as the rapidly cooling fluids altered the rocks and clogged porosity in the feeder zone. **The only way to maintain high permeability in the face of the rapid precipitation from the mineralising fluid is to continue the deformation on the fault / feeder zone. Only active structures can maintain effective permeabilities to channel the large fluid volumes required to form an ore deposit.**

In addition to requiring an active structure at and immediately below the site of deposition, both the fluid volumes and metal contents require an efficient, long-range structural channel system. In other words, it is not sufficient to identify the immediate feeder structure and demonstrate syn-depositional activity on that structure. **Ore formation almost certainly demands that the syn-depositional deformation is contemporaneously activating (or reactivating) a linked, throughgoing network of faults that traverse a sufficient rock volume to provide a source for both fluid and metals.**

In summary, ore formation in the Mackintosh block is likely to have been very tightly structurally controlled in both time and space. In time, because quite specific stress conditions would have been required to synchronously activate the linked network of structures and provide the continuous channelways required. In space, again because specific stress conditions were required to activate the structures such that the fluid flow through the linked fault network was very efficiently channelled into a few particularly dilatent structures which could access the sea-floor.

### Structural Control and Basin Evolution in the Mackintosh Block

As detailed above, our study has concluded that the Mackintosh Block is part of a complex array of linked basins formed by a combination of extension and strike-slip. The best modern analogue for such a basin array occurs at the southern end of the San Andreas Fault System in

California. In fact, the infamous Death Valley is an active basin with many of the structural / depositional characteristics of the Mackintosh Block, although without the vulcanism. Other analogues include Lakes Tanganyika and Malawi in the East African Rift System and the Devonian to Carboniferous basins of northern Britain and Scandinavia. We have included copies of several papers outlining the general and specific geometries of these mixed extension / strike-slip basins in the Appendix.

We have provided above some preliminary conclusions as to how the Mackintosh Block fits into the whole Mt Read Volcanic Belt and indeed into the Cambrian evolution of eastern Australia to indicate the importance and extent of the linked fault systems required to generate such features. The next phase of the project, involving regional interpretation of the geology and airborne magnetic imagery of the whole of the Cambrian Volcanic Belt of western Tasmania, will develop these ideas further. The more regional ideas should not be taken as more than preliminary at this stage. However, it is interesting that Berry's (1991) recent reconstruction of the syndepositional structure at Rosebery has much in common with the structural environment outlined here. In particular, Berry interpreted the Rosebery Fault as a 'sidewall' (i.e., essentially strike-slip) fault with the extensional, normal faults at a high angle to it localising the mineralisation (Figure 12).

The key conclusions of this study concerning the structural setting and controls on mineralisation in the Mackintosh Block are as follows:

- The Mackintosh Block/Basin is small, short-lived basin formed by a specific combination of extension and strike-slip on a complex array of faults. The principal faults that controlled the location and style of the Mackintosh Basin were the Henty and Mt Charter Faults, although there may have been another fault to the north of the presently exposed block.
- The Mackintosh Basin overlies the Central Volcanic Complex and is in turn overlain by another felsic volcanic/volcaniclastic sequence (Tyndall Group). Both of these volcanic/sedimentary sequences have quite different distributions to the Que-Hellyer Volcanics. **We therefore conclude that the Mackintosh Basin formed at a particular site in the regional fault framework in response to a transient change in the regional stress field and therefore the displacement directions on the principal regional faults.** This does not mean that there are no analogues of the Mackintosh Basin, just that they are likely to be similarly restricted and to show similar spatial and geometric relationships to the regional fault array. Indeed, the Queenstown and Rosebery areas may well be equivalents of the Mackintosh Basin (Berry, 1991; Figure 12).
- **The Mackintosh Basin formed as a result of approximately NW-SE extension,** which itself was a local response to specific motions on the Henty, Mt

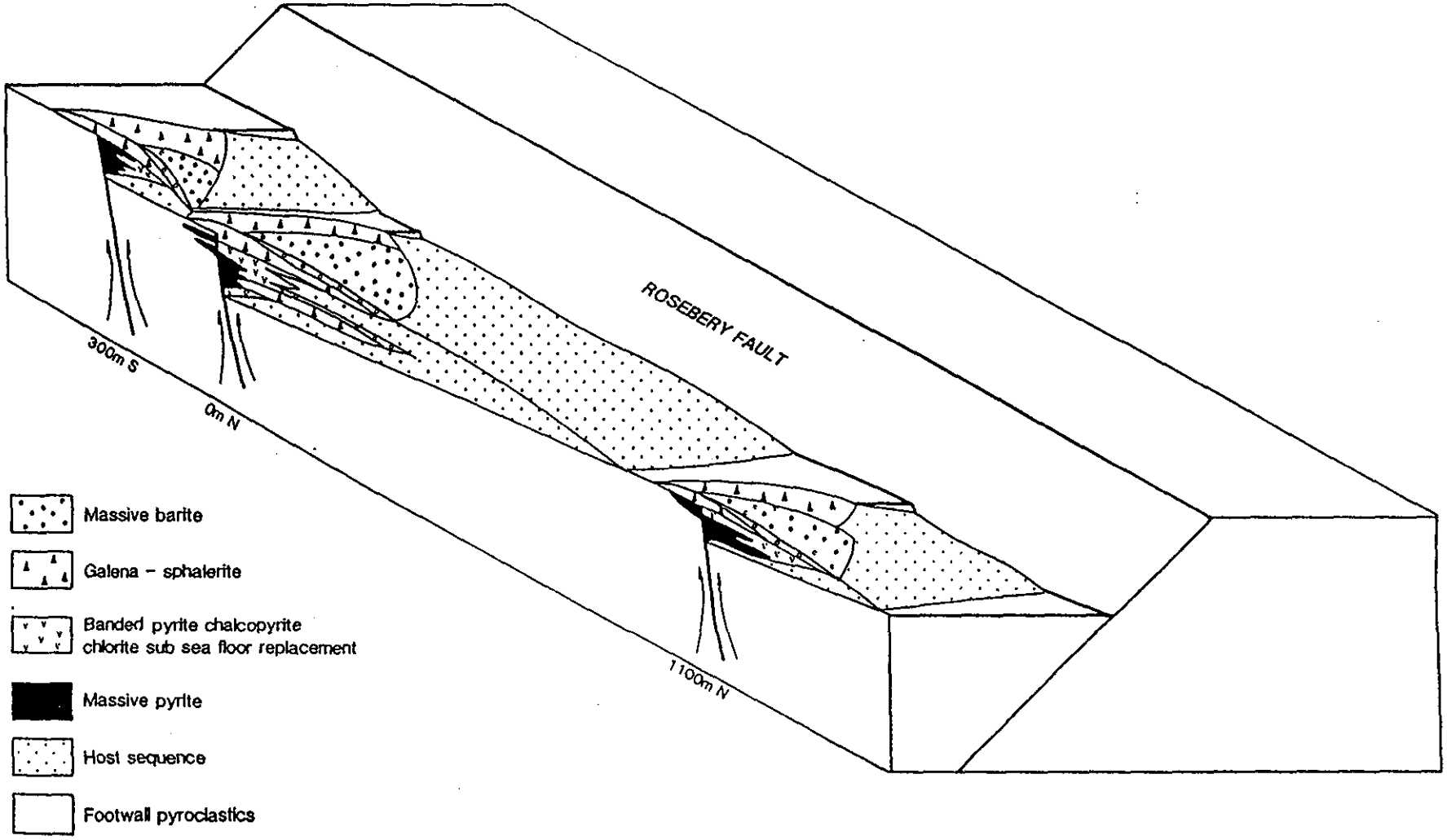



**Figure 12** Block diagram showing the relationship between the Rosebery Fault and syndepositional normal faults at a high angle to it (from Berry, 1991) to have been localised at or near the fault intersections. This relationship is analogous to but different in detailed geometry from the setting of mineralisation in the Mackintosh Block.

5 cm

69353

Charter and possibly other faults (e.g., ?Mt Cripps). Away from the bounding faults, a typical extensional fault array, comprising NE-trending normal faults and NW-trending transfer faults, underlies the main part of the basin. The extensional fault array controlled the internal distribution of facies and thicknesses throughout the development of the basin.

- **The mineralisation in the Mackintosh Basin appears to have formed at one specific time during basin development.** The lower part of the basin fill is dominated by basalt, andesite and related volcaniclastics which are interpreted to represent the principal period of extension. There was then a change from volcanic-dominated to more sediment-dominated and from andesite + basalt to dacite in the igneous component. This change was also accompanied by a subtle but locally significant change in basin geometry. Specifically
  - local depocentres developed near fault intersections (e.g., Que River mine, ?Hellyer mine); these depocentres filled with thick 'Mixed Sequence' volcaniclastics and were the sites of preferential dacite intrusion/extrusion;
  - apart from the Hanging Wall Basalt, there was a remarkably sharp cessation of both vulcanism and clastic input into the basin, corresponding to the base of the Que River Shale; the basin must have undergone very rapid subsidence to prevent erosion of any remaining topography;
  - the Que River Shale thickens towards the NW, in the opposite direction to the underlying volcaniclastic sequence.

  Together, these features are interpreted to indicate that the Mackintosh Basin underwent a significant change in stress regime and resulting fault activity at a time corresponding to the deposition of the principal Mixed Sequence unit, leading directly to the flooding and starvation of the basin at Que River Shale time. **In our view, the Que River and Hellyer deposits, and probably all other significant mineralisation and intense alteration, were formed at this time, directly as a result of the change in stress regime and fault activity.**
- The details of the fault geometry at the specific time of mineralisation are not well understood, but the basis for doing so by means of a detailed re-appraisal of the Que River and Hellyer geology is provided in this report. **However, we can say that the principal structural control on the localisation of mineralisation appears to be the intersection between NE trending intra-basinal normal faults and NW-trending transfer zones.** The change in stress regime is interpreted to have led to oblique reactivation of these faults that localised dilation at the intersections. The dilation is evidenced both by the local increase in thickness of Mixed Sequence in the vicinity of the deposits, and by the highly localised fluid flow that was required to produce the deposits themselves.

The structural framework for basin evolution and mineralisation in the Mackintosh Block that we have presented here is just that - a framework. It remains to be tested, refined and modified by ongoing exploration and related more detailed investigations. However, it does have some immediate implications for exploration of the Mackintosh Block.

## Implications for exploration

The following implications for future exploration of the Mackintosh Block follow directly or indirectly from this study. A number of these conclusions simply provide support for opinions already held within Aberfoyle, but others (e.g., the locations of particularly prospective structures) have largely been generated from this study.

- A principal outcome of this study has been the demonstration that **the known mineralisation and related alteration are localised at or near the intersections between syn-depositional normal and transfer faults.** While these syn-depositional faults are difficult to precisely define, a linked network of them has been interpreted (Figure MAP). It is concluded that significant mineralisation is unlikely to occur within the Mackintosh Block away from these faults, and that they therefore represent primary targets for exploration. In particular, the NW-trending transfer fault zones, which were not previously well defined, appear to exert a strong control on the location of the known mineralisation.

- Another important constraint on prospectivity is provided by the very tight temporal control on mineralisation that has come from the basin structural and stratigraphic framework detailed above. The recognition of a specific period of fault reactivation that localised dilation, subsidence, fluid flow, magma migration and mineralisation at or near normal fault / transfer fault intersections can explain the following:
  - The spatial and temporal association between erosion, deposition, facies and thickness changes and felsic intrusion/extrusion that go to make up the so-called 'Mixed Sequence'.
  - The decrease in both volcanic activity and clastic input into the basin (Que River Shale) immediately following the Mixed Sequence and coinciding with a change in overall basin slope.
  - The formation of small and relatively deep depocentres at Que River and Hellyer which host the mineralisation.

- The implication of these conclusions / observations for exploration is that mineralisation is only likely to be found within a relatively narrow stratigraphic

interval that is just below the base of the Que River Shale ± Hangingwall Basalt. This stratigraphic level is typified by the so-called Mixed Sequence, although our experience is that the Mixed Sequence is difficult to define stratigraphically as there are other levels in the stratigraphy where dacites and epiclastics occur. Overall, we conclude that large parts of the southern and eastern portions of the Mackintosh Block have low prospectivity because the stratigraphic level at the surface is below the prospective interval. In particular, we tentatively conclude that the Mt Charter area is probably just too deeply eroded to be prospective, and that the strong alteration and sporadic mineralisation encountered there was footwall to any mineralisation. However, more intensive effort should be made in the Mt Charter area to define the time-stratigraphic level.

- Given the intensive exploration history and inappropriate stratigraphic level along much of the Hellyer / Que River / Mt Charter trend, we suggest that the exploration focus be shifted to the western part of the Block where we know that the prospective stratigraphic interval is sub-surface, and where there are some indications of the prospective structural features. Again, we emphasise the need for more intensive follow up of our structural framework as a prelude to detailed exploration, but we tentatively recommend the following areas as moderately prospective for deep exploration
  - Along the W to NW projections of the main transfer faults/zones shown on Figure MAP. Since we have concluded that the intersections between transfers and normal faults might be particularly prospective, detailed mapping should be carried out in the Que River Shale (esp detailed shape/pattern analysis from bedding and bedding/cleavage observations) to document anomalous, NE-trending structural zones.
  - The projected intersection between the principal normal fault through Hellyer and west of Que River and Mt Charter and the complex Mt Charter fault zone is an obviously favourable structural site which is also a zone of highly anomalous alteration and geochemistry. The area where the Bulgobac River crosses the Murchison Highway and immediately to the south has many of the appropriate structural characteristics.
  - The area between Hellyer mine and the Murchison Highway, largely occupied in outcrop by QRS warrants further detailed structural work to look for complexities that may be due to reactivated normal / transfer faults. The NW projection of the inferred transfer zone through Hellyer looks particularly interesting structurally, even though it does pass beneath the edge of the Tertiary basalt.

- The NW extension of the major interpreted transfer fault between Hellyer and Que River mines (through 'D' Zone). Dips/strikes in the QRS suggest somewhat more complex (?reactivation) structure along this trend.

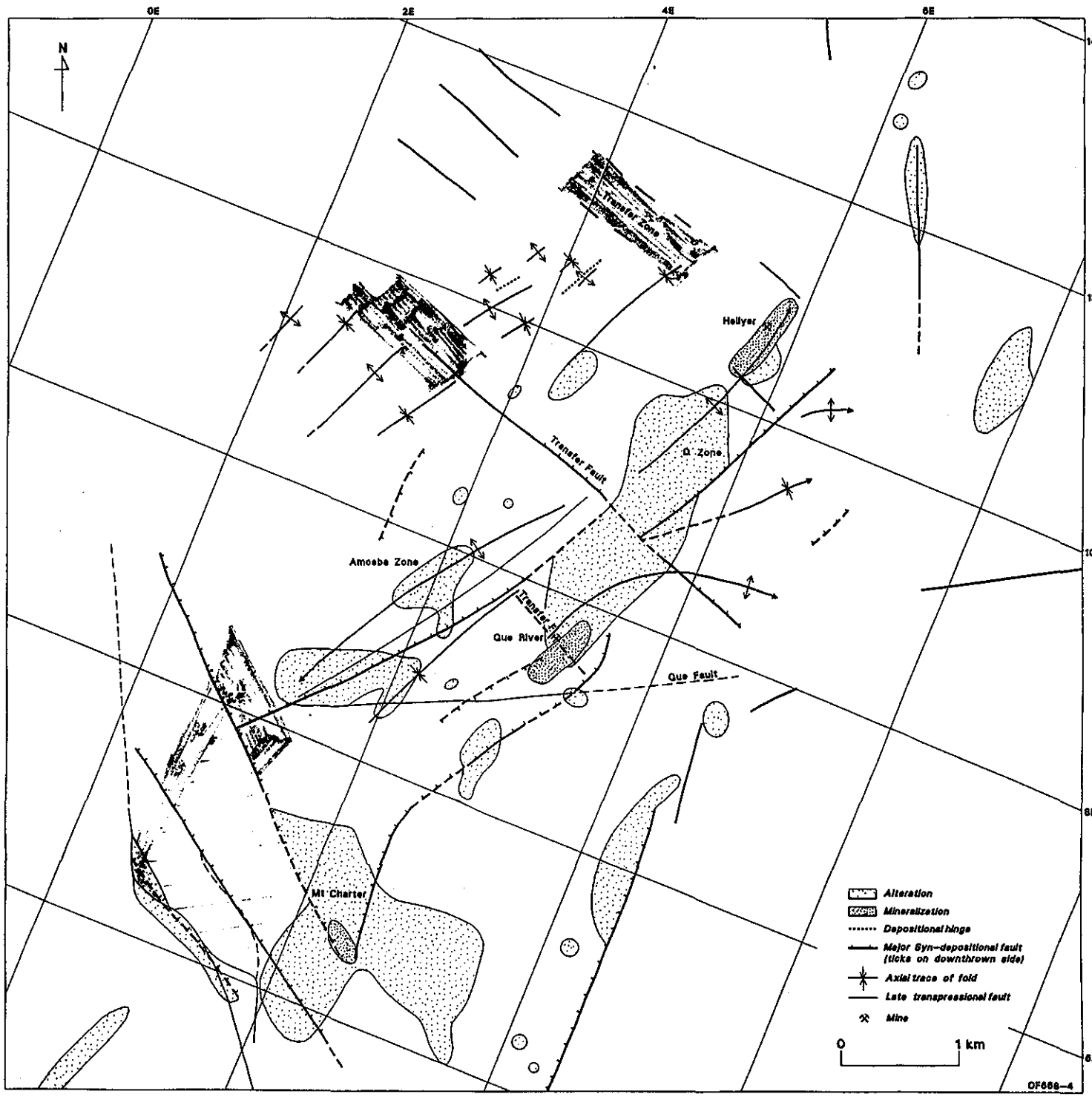
- From the viewpoint of designing a systematic deep drilling program, we suggest that much of the Mackintosh Block is effectively sterilised either because the prospective stratigraphic interval has been eroded, or because there are no indications of the presence of the prospective syn-depositional structures. Figure 13 provides a tentative guide to prospectivity on the 1:25 000 structural base map.
- The next phase of this study, although more regional in scope, may identify structures or trends in the airborne magnetics that have not been recognised during this project. We strongly recommend that the ongoing exploration program continues to test and refine the model of basin-formation and structural / stratigraphic controls on mineralisation presented here. It is also important to integrate the structural work commenced here with other exploration methods, because it is unlikely that the structural framework will have the spatial precision to directly target drilling.

**Recommendations for collecting structural data**

In addition to the specific recommendations concerning prospectivity, there a number of suggestions as to what might broadly be called 'work practices' to optimise any follow-up of this study by the exploration and mine geologists.

- In sediments, try to get bedding and cleavage at the same location to work out problems of cleavage superimposed on older folds versus folded cleavage and folds; also collect bedding orientations with the specific purpose of building a 3D 'shape' or 'pattern', rather than to fill in the map; use fan lines parallel to strike between dip/strike readings to present the pattern information on the map.
- Although there is no evidence for overturned stratigraphy, try to get way-up direction in sedimentary rocks, esp. in areas of steep bedding dips or anomalous deformation style.
- Measure bedding-core angles from drill core wherever possible, and always use them when plotting sections.
- Where holes of different orientations intersect the same structure use both to constrain orientation of structure in 3D.
- When orienting core, as soon as its out of the ground, piece together as many fragments together as possible and trace top-of-core orientation line on them, to maximize amount of orientation information. This appears to be routine practice in the mine but not necessarily in exploration.
- When projecting DDH onto lines of section, project them along geology, i.e. along strike, or along plunge if possible, rather than along the closest straight line (that's

**Figure 13** 1:25,000 structural framework map of the Mackintosh Block (see Figure 4), with the more prospective areas proposed in this report coloured. See text for explanation.


0E
2E
4E
6E
14N
12N
10N
8N
6N
N
Transfer Zone
Hellyer
Transfer Fault
D Zone
Amoeba Zone
Transfer Fault
Que River
Que Fault
Mt Charter
Alteration
Mineralization
Depositional hinge
Major Syn-depositional fault (ticks on downthrown side)
Axial trace of fold
Late transpressional fault
Mine
0
1 km
OF668-4

5 cm

why some of the DDH on the sections accompanying this report are apparently collared in the air!)

- The style of work being undertaken largely by Henry Kurth at Hellyer is particularly important for testing and refining the structural / stratigraphic controls on localisation of mineralisation. This work includes 1:500 scale detailed correlation of DDH, depth-to-horizon contours which help to constrain late faults and distinguish them from syn-depositional faults, and isopachs of selected units (e.g. HVS), which further constrain the position and displacement of syn-depositional faults.
- Double-check drafted copies - many maps we tried to compile from had strike symbols different from azimuth written beside them, or azimuth not recorded separately from the symbol. This causes loss of data, and in some cases, incorrect data, which can make subsequent interpretation difficult. We suggest always writing azimuth next to the symbol on the map.
- Use mapped structure and lithological / stratigraphic data to create sections and vice versa, i.e. develop iterative procedures to refine both maps and sections to build a genuinely 3D interpretation. Make sure cross-sections are compatible with adjacent ones, use long sections to tie them together and to look for along-strike variations. Exploration of the Mackintosh Block has reached the stage where it has in some respects more in common with petroleum exploration than with conventional mineral exploration. Depth-to-horizon and isopach maps should be constructed to enable drilling to be targeted in the absence of a surface geochemical or geophysical anomaly.

## References

Berry, R. F., 1990, Structure of the Rosebery Deposit, in Structure and Mineralisation of Western Tasmania, AMIRA Project P.291, Report No. 1, Sept. 1990, p. 17-26.

Berry, R. F., 1989, The history of movement of the Henty Fault Zone, Western Tasmania: An analysis of fault striations, AJES, 36 p. 189-205.

Christie-Blick, N., & Biddle, K. T., 1985, Deformation and basin formation along strike-slip faults, in Biddle & Christie-Blick (eds.), Strike-slip deformation, basin formation and sedimentation, Soc. Econ. Paleontologists & Mineralogists, Spec. Pub. No. 37, p. 1-34.

Cooke, A., 1991, Structural study of the Hellyer-Que River area, private Aberfoyle Report.

Downs, 1990, Hellyer Faulting Study.

Etheridge, M. A., Symonds, P. A., Powell, T. G. & Lister, G. S., 1988, Application of the detachment model for continental extension to hydrocarbon exploration in extensional basins, APEA J., 28, p. 167-187.

Harding, T. P. & Vierbuchen, R. C., 1985, Structural styles, plate-tectonic settings, and hydrocarbon traps of divergent (transtensional) wrench faults, in Biddle & Christie-Blick (eds.), Strike-slip deformation, basin formation and sedimentation, Soc. Econ. Paleontologists & Mineralogists, Spec. Pub. No. 37, p. 51-77.

Large, R. R., McGoldrick, P. J., Berry, R. F. & Young, C. H., 1988, A tightly folded, gold-rich, massive sulfide deposit: Que River Mine, Tasmania, Econ. Geol. 83 p. 681-693.

McArthur, G. J., 1986, The Hellyer massive sulphide deposit, in Large, R. R. (ed.), The Mt. Read Volcanics and associated ore deposits, GSA Symposium, p.11-20.

Nilsen, Tor H., & McLaughlin, R. J., 1985, Comparison of tectonic framework and depositional patterns of the hornelen strike-slip basin of Norway and the ridge and Little Sulphur Creek strike-slip basins of California, in Biddle & Christie-Blick (eds.), Strike-slip deformation, basin formation and sedimentation, Soc. Econ. Paleontologists & Mineralogists, Spec. Pub. No. 37, p. 79-103.

Perkins, C., 1991, Isotopic dating of precious and base metal deposits and their host rocks in eastern Australia, AMIRA-Project P. 334 Annual Report, June 1991, 100 pp.

Shaw, R. D., Etheridge, M.A. & Lambeck, K, 1991, Development of the late proterozoic to mid-paleozoic, intracratonic Amadeus Basin in Central Australia: A key to understanding tectonic forces in plate interiors, Tectonic, v. 10, No. 4, p.688-721.

Waters, J. C. & Wallace, D. B., Volcanology and sedimentology of the host succession to the Hellyer and Que River VMS deposit, north-western Tasmania, in press.

# Appendix

## Selected references, information & diagrams on

## Extensional & strike-slip structural environments and related basin development

## Extensional Terranes

***Extension or stretching of the continental lithosphere is the most widespread mechanism for the formation of sedimentary basins.*** In particular, it is the driving mechanism for most of the volcano/sedimentary basins that dominate the Precambrian and Palaeozoic mineral provinces of Australia.

***Continental extension is just as much an orogenic process (i.e., accompanied by extensive deformation, metamorphism, intrusive activity and even mountain building) as crustal shortening.***

***Extension is dominated by faulting rather than folding***, but it may produce large areas of strongly foliated rocks.

***Crustal extension thins the crust (and lithosphere), and therefore gives rise to subsidence and basin formation.*** However, extension of the lithosphere also leads to an increase in thermal gradient and heat flow which can induce transient uplift (e.g., Basin and Range province, SW USA). Extensional terranes are typified by high heat flow, extensive hydrothermal activity, igneous extrusion/intrusion (usually of bimodal character) and low pressure metamorphism.

The key structural characteristics of extensional orogens / sedimentary basins are as follows:

- ***Crustal extensions of 50% to 200% are relatively common***, so large strain structures, esp. large displacement faults and shear zones are widespread.
- ***The textbook picture of extensional regions with symmetrical horsts and graben bounded by steeply dipping normal faults is wrong.***
- ***Crustal extension requires large horizontal rather than vertical motions*** and therefore requires movement on shallowly dipping faults.

- ***Extensional fault systems typically comprise imbricate moderately to shallowly dipping, rotational normal faults that sole into sub-horizontal, large area and large displacement detachment faults*** - ∴extensional fault systems are directly analogous to compressional thrust systems with their imbricates, decollements, duplexes, etc.

- ***Extensional fault systems are typically asymmetric in cross-section.*** Extensional or rift basins comprise half-graben bounded by faults which dominantly dip the same way on any cross-section.

- ***Extensional terranes are compartmentalised along strike by sub-vertical transfer faults.*** Transfer faults permit the geometry, position and/or sense of asymmetry of the normal fault arrays and crustal extension to vary along the strike of the terrane.

- ***Crustal extension perpendicular to elongate rifts is transitional through complex oblique extension rifts to pull-apart basins associated with wrench faults.***

Extension and thinning of the crust, especially by large, shallowly dipping normal faults / shear zones, may lead to tectonic erosion of the upper crust and very rapidly expose middle to lower crustal rocks at the surface where they will be covered in volcanics and sediments. In this way, extensional faulting leads to the telescoping or partial omission of metamorphic gradients.

Extensional terranes/basins are commonly overprinted by compressional and/or strike-slip deformation, and the recognition of extensional structures is not easy. However, it is usually worth the effort, because the extensional geometry controls much of basin geometry and the character of the volcano-sedimentary sequences and because the extensional structures are commonly reactivated during later deformation.

655122

## 9.5 Extensional fault systems

It is comparatively common for regions of the crust to exhibit sets of related faults on which the individual displacements produce a net extension in the system as a whole. Such fault systems are characteristic of *extensional* or *divergent tectonic regimes*, which are associated (i) with constructive plate boundaries, at *oceanic* and *continental rift zones*; (ii) with destructive plate boundaries, in regions of *back-arc extension* such as the Basin-and-Range province of the western USA, and in oceanic marginal basins; (iii) with certain continental *intraplate* regions marked by rifts and extensional basins.

Classical views on faulting and on the formation of graben and rifts visualized extension being accommodated by dip-slip movements on steep normal faults (see Figure 9.3*A*) or by the filling of extensional fissures by magma. However, more recently, the importance of *low-angle normal faults* has been emphasized as a method of achieving the much larger extensions (of 100–200%) that have been estimated in certain extensional provinces such as, for example, the Basin-and-Range province.

There appear to be three principal geometric elements in *extensional fault systems*: (i) *low-angle normal faults* acting as detachment planes; (ii) *rotated fault blocks*; and (iii) curved or *listric fault* surfaces (Figure 9.12*A*). The widespread occurrence of such geometries has been confirmed by seismic records obtained in petroleum exploration of marine basins, and is summarized by Gibbs (1984). The listric fault achieves a rotation in the hangingwall as a geometric consequence of the displacement, and may be accompanied by an accommodation anticline, known as a *rollover anticline* (Figure 9.12*B*). The detachment or *sole fault* in extensional systems has the same function as that in thrust fault systems, and may possess a similar *ramp-flat* geometry (Figure 9.12*C*) necessitating complex accommodation strains in the hangingwall. The accommodation may take place by the formation of a set of *antithetic faults* that have the effect of extending and thinning the hangingwall in order to relieve the accommodation strain (Figure 9.12*D*). As extension proceeds, the sole fault may migrate into the footwall producing a set of *synthetic 'horsetail' listric faults*, known as a *listric fan* (Figure 9.12*E*), in an analogous way to the propagation of thrusts into the foreland in piggyback thrust sequences. The fault blocks formed in this process are termed *riders*. The migration of the sole fault into the footwall may create an *extensional duplex* bounded by a *roof fault*. Figure 9.12*F* shows the complex type of geometry that may be produced by a combination of hangingwall and footwall collapse resulting from progressive extension. The rotated blocks formed by these processes form *half-graben* at the surface; these may become filled with sediment. Upper-crustal extension on fault systems of this type may be transferred to mid-crustal levels and below by low-angle shear zones (see section 9.7).

Extensional fault systems also frequently contain steep faults with strike-slip displacements. Such faults are integral to the system and transfer displacement from one dip-slip plane to another. They are therefore termed *transfer faults*, and are smaller-scale counterparts of oceanic transform faults (see section 14.3). Figure 9.12*G* shows how two dip-slip faults may be linked by a transfer fault, each detaching on the same sole fault. Transfer faults may separate imbricate fault-fold packages that are geometrically distinct and uncorrelatable across the fault.

655123



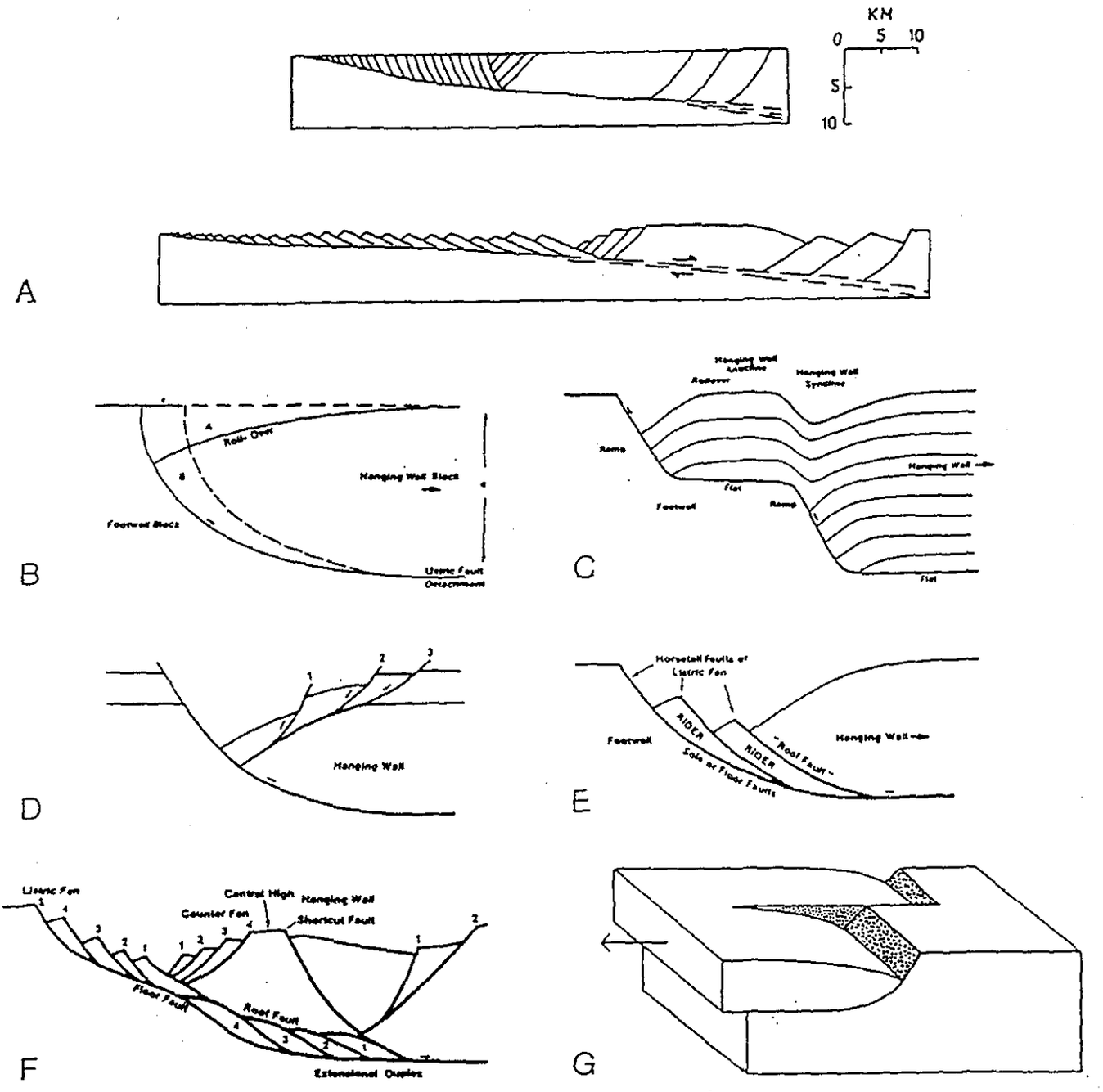



Figure 9.12 Extensional fault systems. *A*. Method of accommodating extension by block rotation above a low-angle extensional fault-shear zone. After Wernicke, B. (1981) *Nature* 291, 645–648. *B*. Listric fault with hangingwall roll-over anticline. Areas A and B are equal. The adjustment in hangingwall shape implies internal strain. *C*. Flat/ramp geometry of fault produces geometrically necessary folding in hangingwall. *D*. Antithetic faults in hangingwall. *E*. Synthetic faults in footwall. *F*. Extensional duplex with associated listric fan, counter fan and elevated central high. *B–F*. from Gibbs, A.D. (1984) *J. geol. Soc. Lond.* 141, 609–620. *G*. Two *listric faults* linked by a *transfer fault*. All three faults detach on a sole thrust.

655124

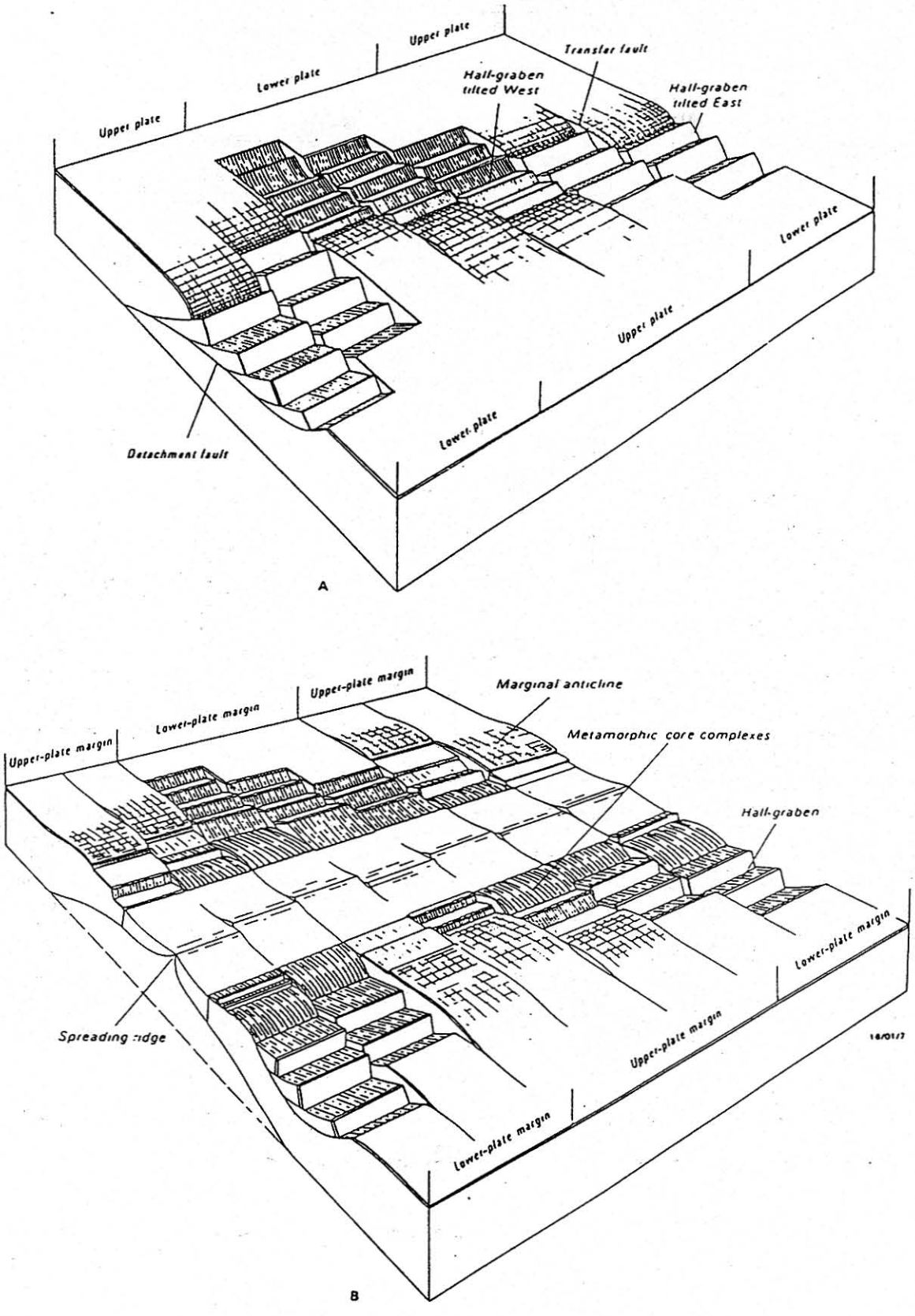



**Figure 4** — Along-strike variations in the geometry of the detachment and/or lower plate stretching are accommodated by transfer faults. This pair of figures illustrates the segmentation of an extended terrane by transfer faults at both (a) continental rift, and (b) passive margin stages. Complete switches in the dip direction of the detachment and, therefore, in the polarity, or asymmetry, of the extended terrane can be accommodated by transfer faults, juxtaposing upper and lower plate margin segments on the same margin (after Lister et al., 1986).

## Wrench or Strike-Slip Systems

Individual wrench faults are relatively easy to map, as they generally have linear traces in plan and have sub-vertical dips. ***However, quite small departures from the linearity of the map traces of strike-slip faults can/must lead to severe, localised structural complexity.***

There are three principal steps in mapping wrench fault systems

- **Determine the sense of shear / displacement**
- **Identify the principal displacement plane and the restraining and releasing bends**
- **Relate kinematics (movement) in the bends and at branches/splays to the geometry of secondary structures.**

The basis for these tasks was outlined in the previous chapter, but the underlying message is that

- **Determining the kinematic and large scale geometric framework is the key to successful mapping in wrench systems.**

***Strike-slip faults rarely, if ever, consist of a single, straight fault that accomplishes solely horizontal motion.*** Rather strike-slip fault systems are generally quite complex fault ± fold arrays that have the following common properties, as shown in the accompanying diagrams:

- ***Even the principal displacement structure(s) in a strike-slip array usually consists of en echelon fault segments***, especially at the higher crustal levels. Particular structural complexity is common at the stepovers between these segments.
- ***Stepovers, jogs or bends in strike-slip faults are the locus of either compression (restraining bends or compressional jogs) or extension (releasing bends or dilatent jogs)*** depending on the direction of the step or bend relative to the displacement direction.

- ***Strike-slip fault arrays generally branch or splay in both strike and dip.*** Splays in strike must have a component of normal to reverse movement.

- Branching upwards geometries are common in strike-slip fault systems. ***These branching upwards structures are known as flower structures.***

- ***Positive (i.e., compressional) flower structures contain oblique reverse faults or even thrusts and give rise to uplift.***

- ***Negative (i.e., extensional) flower structures contain oblique normal faults and produce local subsidence and even basin formation.***

On the tectonic scale, ***releasing bends*** in large scale wrench systems leads to rapid subsidence and the formation of sedimentary basins that are commonly small and deep. These basins - ***pull-apart basins*** - are commonly important sources of both petroleum and minerals, and they also commonly contain compressional structures due either to continuing fault movement or to reversal in the master fault displacement. Large ***restraining bends*** are the locus of uplift and often intense compression, and may broadly resemble compressional fold belts in their structural style.

- **Vertical motions and the necessary compressional and/or extensional structures are a natural consequence of even relatively simple strike-slip fault systems.**

It is very important to understand that ***wrench fault systems generally contain classical extensional and compressional structures at various times and places in their history.*** Some areas along a wrench fault may also undergo a very complex deformational history during what is essentially a single period of movement on the master fault. ***Always be on the lookout for keys to the larger scale movement picture.***

655127

## 9.6 Strike-slip fault systems

Sets of related faults on which the individual displacements produce a *net strike-slip* displacement in the system as a whole are characteristic of tectonic regimes associated with major *conservative plate boundaries* (*transform fault* zones—see section 14.3) and also occur within continental plates such as, for example, the Asian plate north of the current plate boundary with the Indian plate (see Figure 15.5). The main features of a continental strike-slip regime have been analysed by Reading (1980) who pointed out the importance of differential vertical movements, which create uplifted blocks and depressed basins in such a zone.

Major strike-slip zones such as the San Andreas fault zone are of the order of 100 km across, within which quite complex tectonic effects take place. If the zone is considered as a deformable sheet, the deformation may be visualized as a combination of pure shear and simple shear, the pure shear component arising from net extension or compression across the zone, and the simple shear component from the strike-slip displacement of the boundaries of the zone. Considering only the simple shear component, the possible structures are summarized Figure 9.13*A*, which shows the orientation normal faults, reverse faults, and conjugate se strike-slip faults, as well as folds, within the zo The orientation of these subsidiary structu within a strike-slip zone conveys important inf mation as to the sense of strike-slip motion addition of an extensional component across zone produces *transtension* and a compressio component produces *transpression*. Transtens results in clockwise rotation of the extension a (in dextral shear) and transpression in an clockwise rotation (see Figure 9:13*B*). The verse would hold for sinistral shear.

Important geometrical effects result from t irregularity of the fault geometry. Local chang of direction in strike-slip faults create local zon of transtension or transpression. In complex fau networks where branching faults have oppose dips, this process leads to alternate zones raised and depressed blocks resulting from t convergence and divergence of wedge-shape blocks (Figure 9.13*B*). The combinations of fol and faults produced in these local zones a termed *flower structures*. These are *positive* f uplifted blocks and *negative* for depressed bloc (Figure 9.13*D*). *Strike-slip duplexes* (Figure 9.13 may be formed at bends in a strike-slip fault as result of the progressive migration of the acti fault into one wall.

The duplexes may be either transtensional transpressional, and are morphologically equ valent to extensional and thrust duplexes respec tively. Large pieces of crust may become de tached and isolated from one block, transferre to the opposing block, and transported far fron their sites of origin, becoming *displaced terrane* (see section 15.3).

Another cause of complication arises from *fault offsets*, which produce localized strain around the fault terminations that are either compressional or extensional, depending on the sense of movement (see Figure 15.3).

Major strike-slip zones, particularly those tha constitute plate boundaries, are presumed to continue at depth as strike-slip shear zones (see section 9.7). Studies of deeply eroded Precam brian shield regions demonstrate the importance of major strike-slip shear zones at deep crus levels. Other strike-slip zones may detach on su horizontal décollement zones within or at the base of the crust.

655128



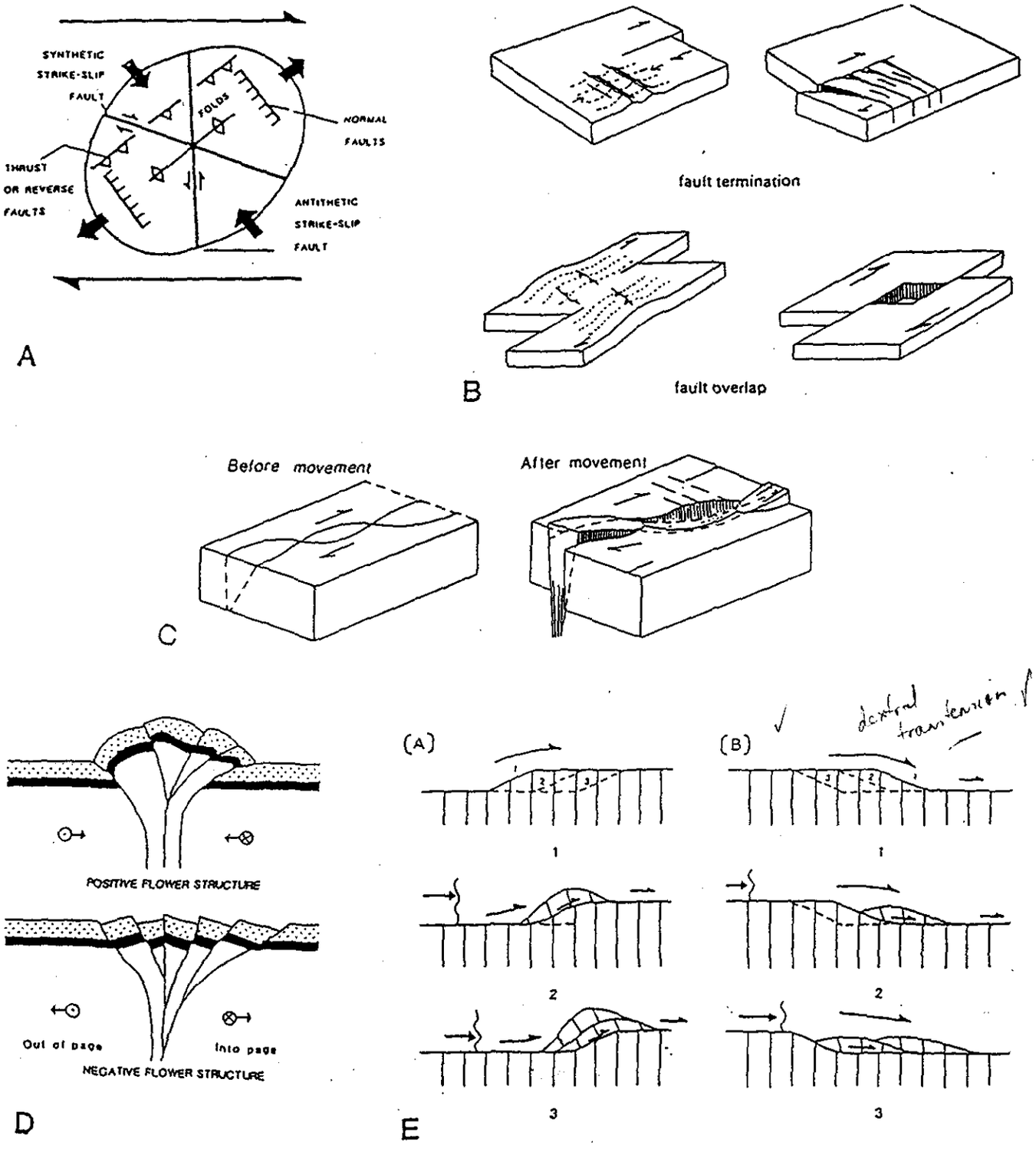
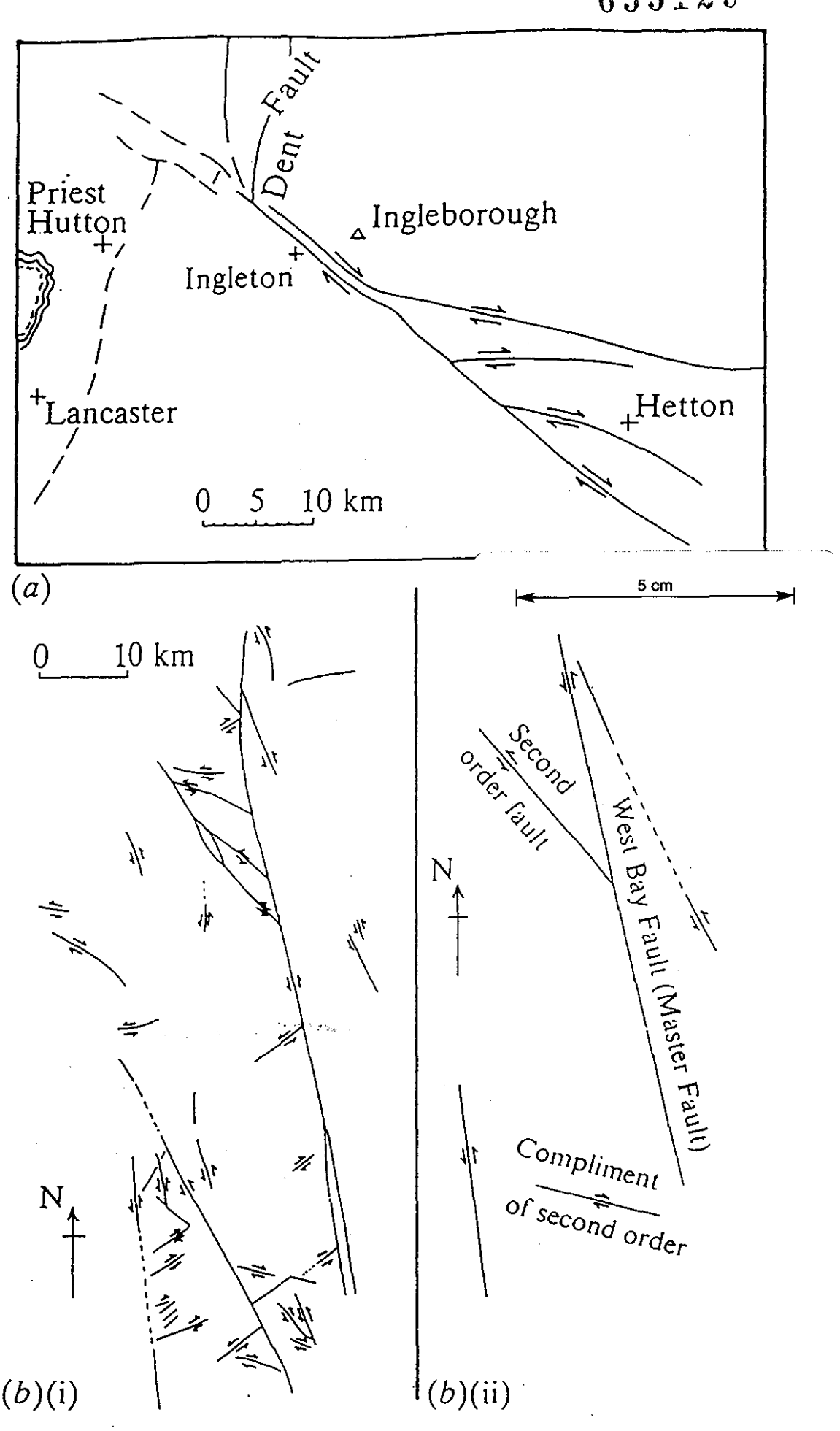



Figure 9.13 Strike-slip fault systems. *A*. Diagrammatic representation of the structural pattern produced by a dextral simple-shear couple, after Harding, T.P. and Lowell, J.D. (1974), *Bull. Am. Assoc. petrol. Geol.* 63, 1016–1058 and Reading, (1980). *B*. Local compressional and extensional structures produced by fault terminations and fault overlaps in strike-slip faulting. *C*. Formation of raised and depressed wedge-shaped blocks by local transpression and transtension on a branching strike-slip system. *B*, *C*. after Reading (1980). *D*. Positive and negative *flower structures* produced by convergence and divergence respectively in strike-slip motion. Dot and cross symbols within circles indicate out-of-page and into-page components of motion respectively. *E*. Diagrams illustrating the formation of strike-slip duplex structure in transpression (A) and transtension (B). Note that the structures are analogous morphologically to compressional and extensional dip-slip fault duplexes respectively. *D*, *E*. from Park, R.G. (1988) *Geological Structures and Moving Plates*, Blackie, Glasgow and London.

655129




**6A: Sketches illustrating the geometry of typical strike-slip systems which comprise branching and en echelon arrays of slip, oblique-slip, normal and reverse faults.**

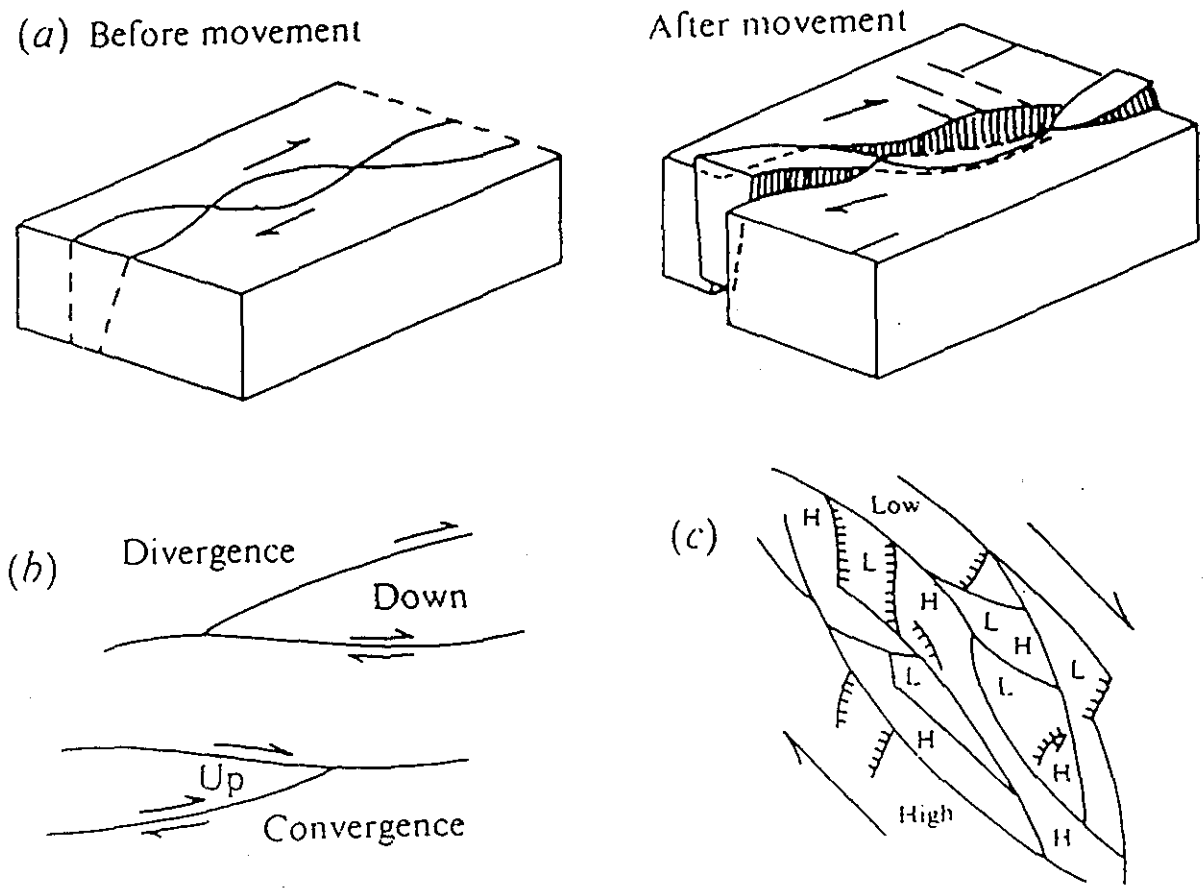



**Figure 6B: Sketches of strike-slip fault systems illustrating how vertical motions are natural consequences of curved and branching (especially in strike) fault geometries.**

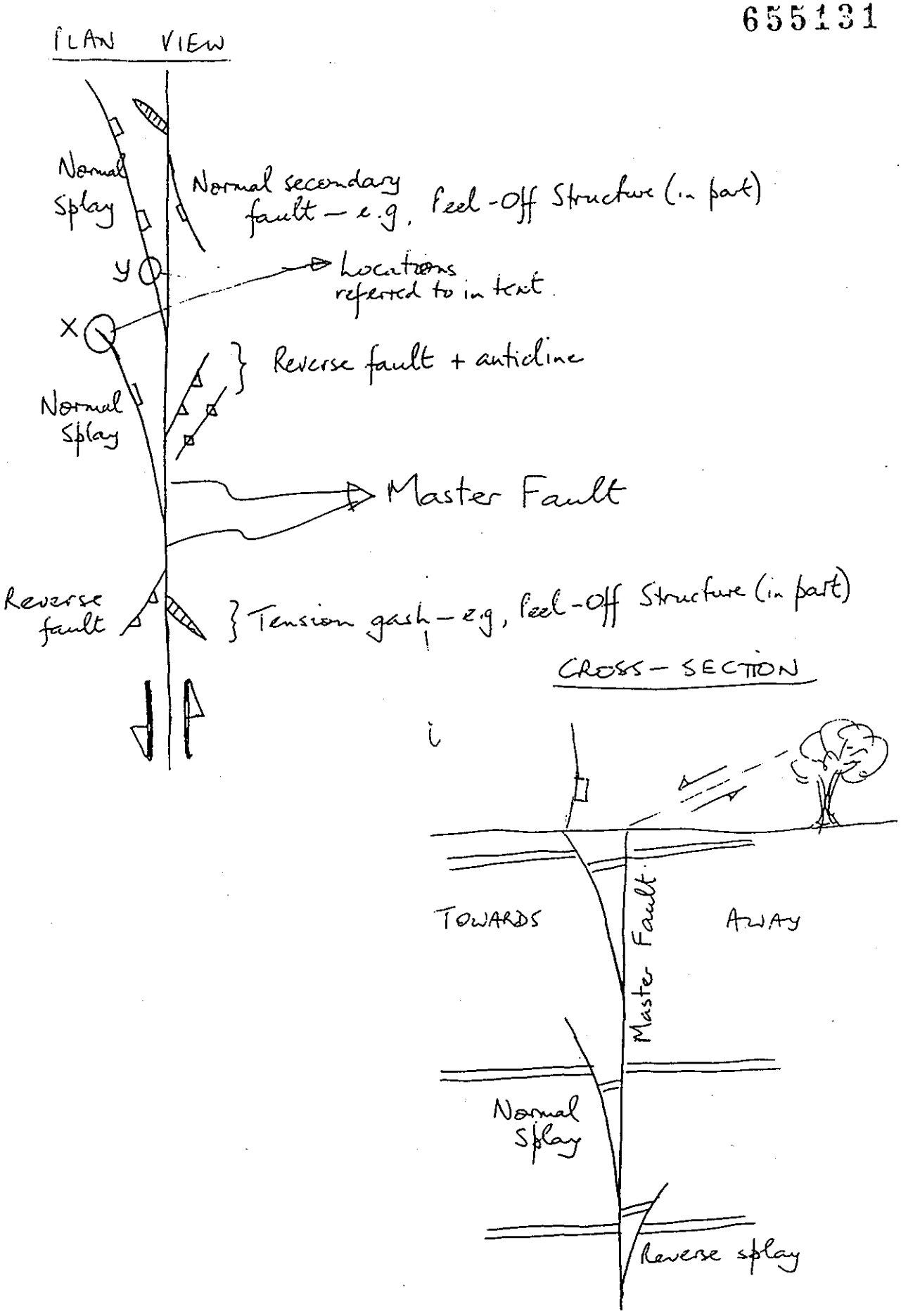



**Figure 6C:** Plan and cross-sectional views of a 'type' left-lateral strike-slip fault system, showing the full assemblage of structures which may be present.

655132

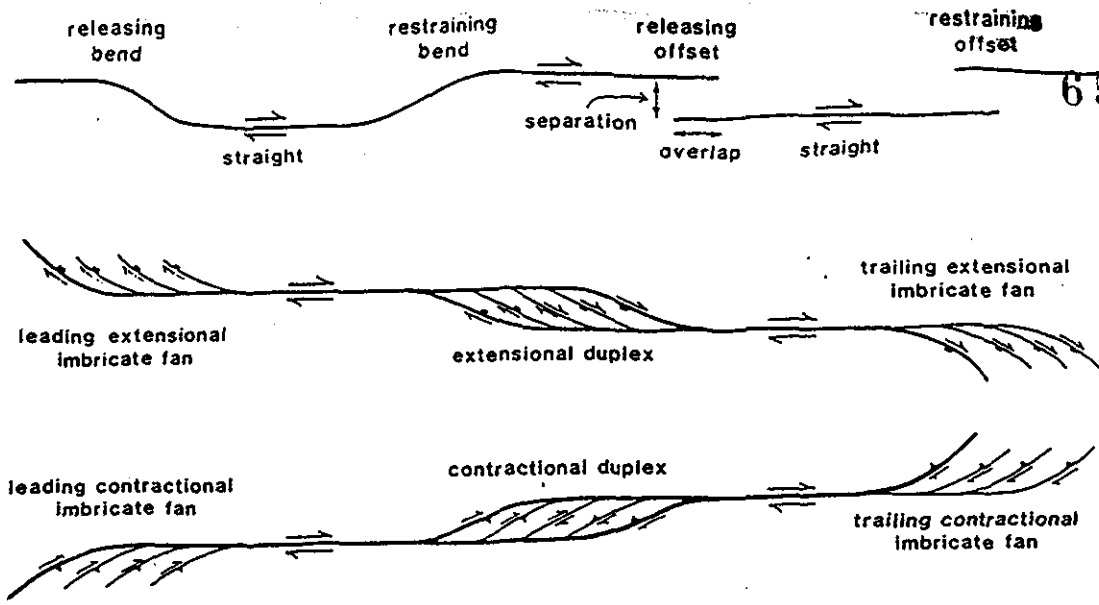



Fig. 1. Map view of an idealized dextral strike-slip system to illustrate terminology.

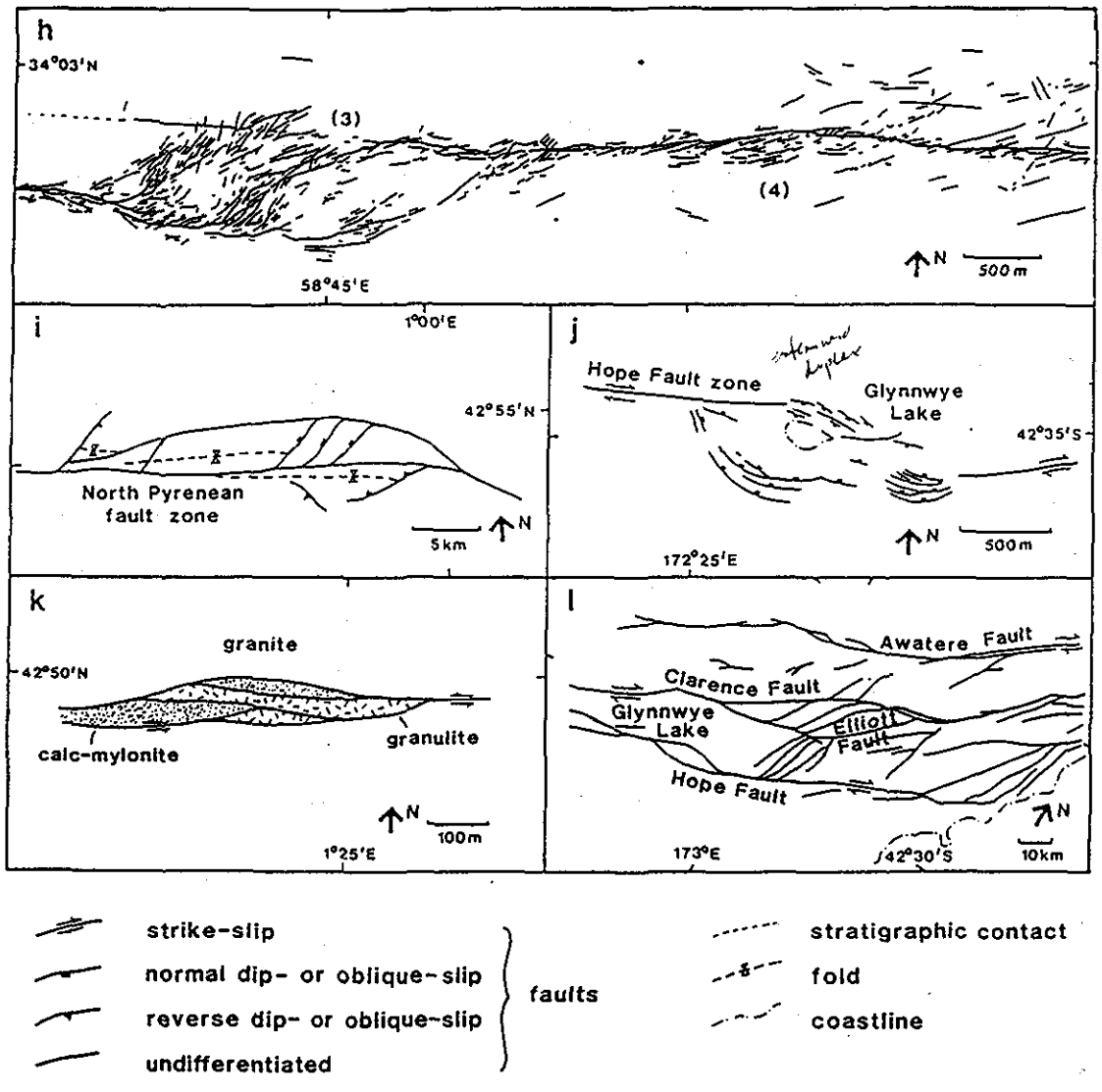
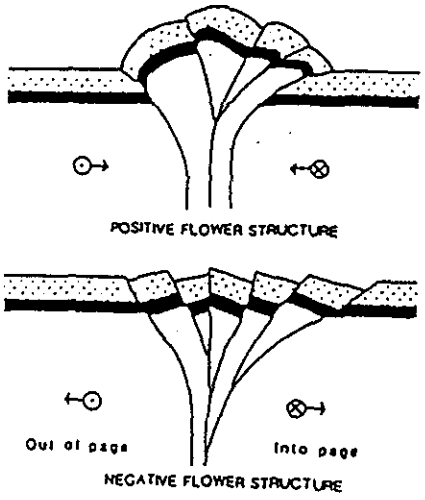



Fig. 2 *continued* (h) Dasht-e-Bayaz fault, Nimbluk Valley, Iran (Tchalenko & Ambraseys 1970); (i & k) North Pyrenean fault zone (Fischer 1984); (j) Glynnwye Lake, New Zealand (Freund 1971) and (l) Marlborough fault system, New Zealand (Freund 1974).

5 cm

**Figure 6D: Even the master fault components of most strike-slip fault systems are typically en echelon or stepping. The sense of stepping, the amount of offset at each step and the angle of the fault segments to the overall fault zone trend are a function of the component of transpression or transtension.**



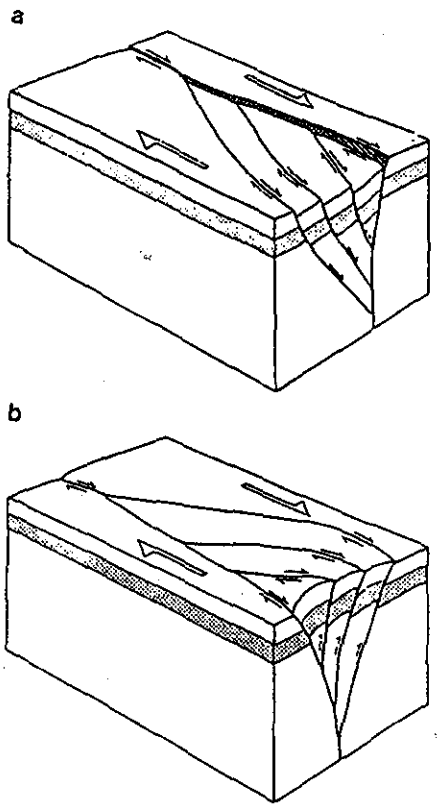
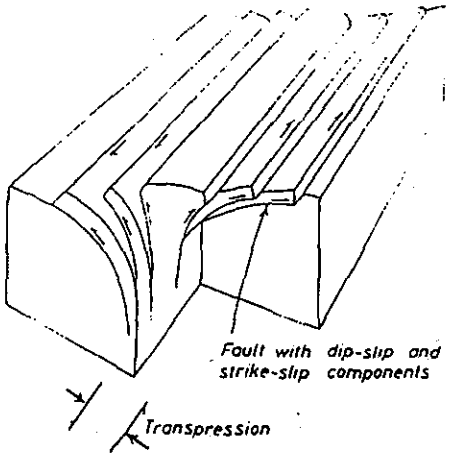
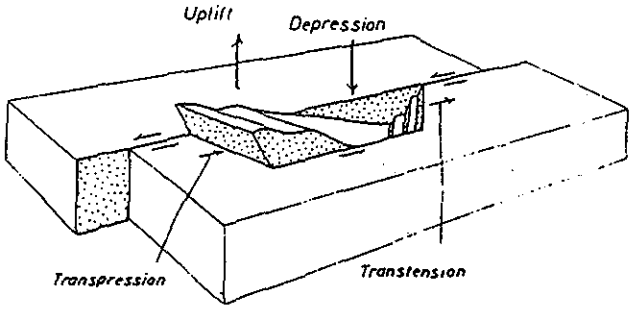




Fig. 12. Postulated three-dimensional form of (a) an extensional duplex (showing negative flower structure) and (b) a contractional duplex (showing positive flower structure).



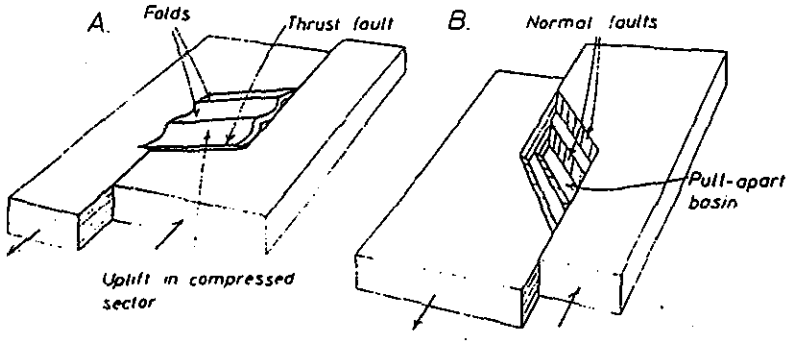




**Figure 1E: Strike-slip faults generally branch in both dip and strike, forming the so-called 'flower structures'. Branches in dip are commonly also oblique in strike and therefore have oblique-slip displacements.**

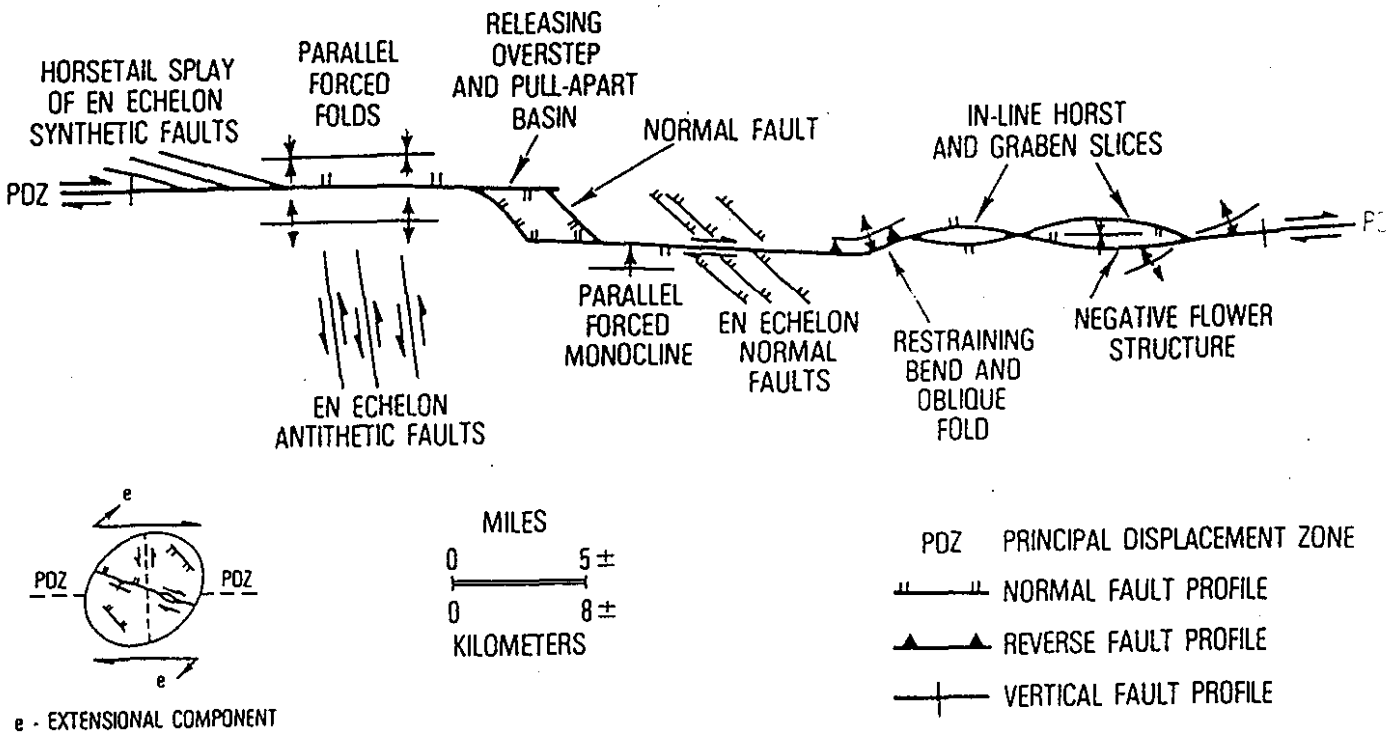
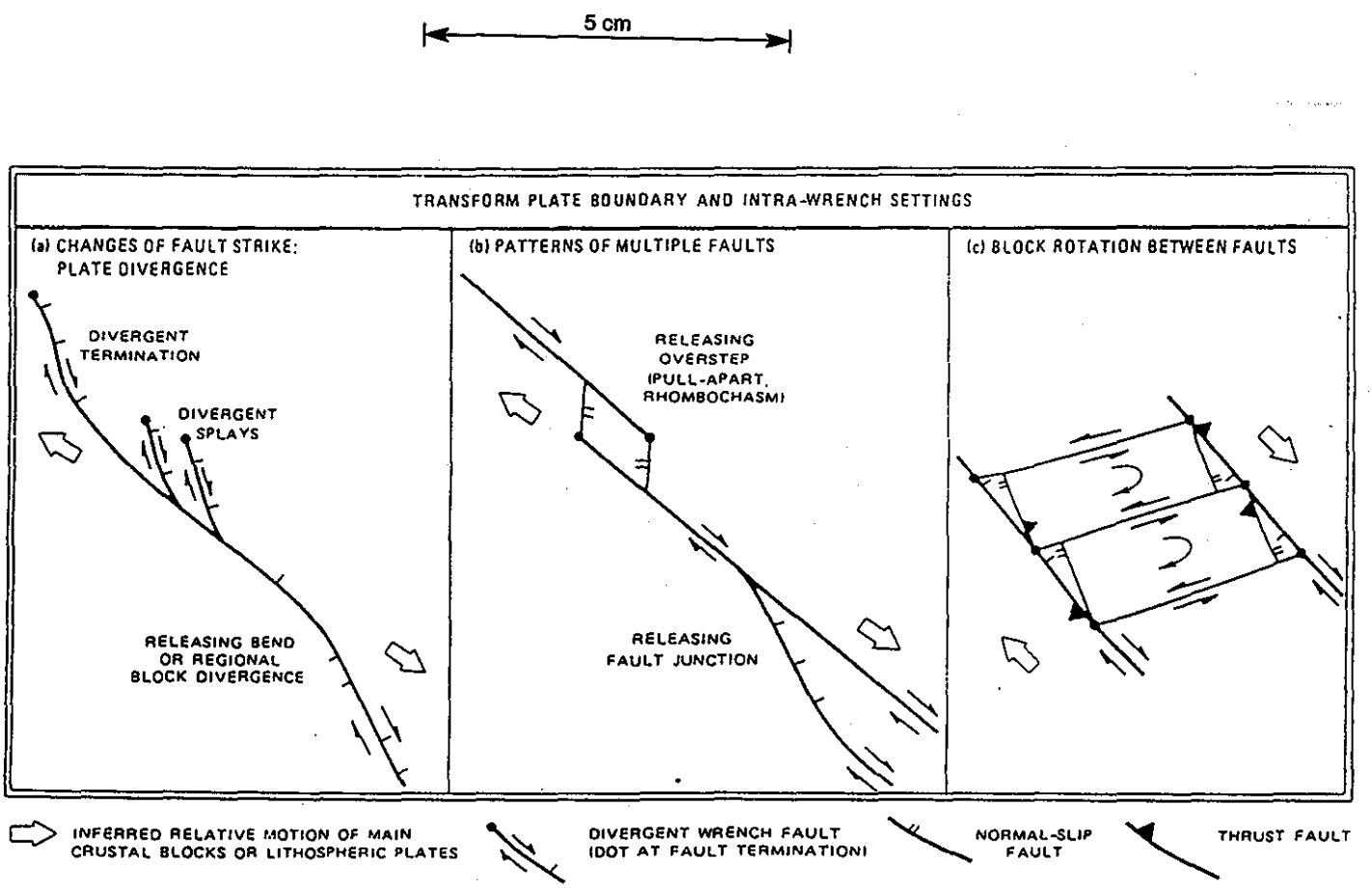



FIG. 1.—Assemblage of structures associated with divergent wrench faults and simplified strain ellipse for right-slip deformation (inset). Not all divergent wrench zones contain every feature and those structures present may be combined in different ways. The assemblage shown here is a composite of examples presented in this paper and others cited in the references.



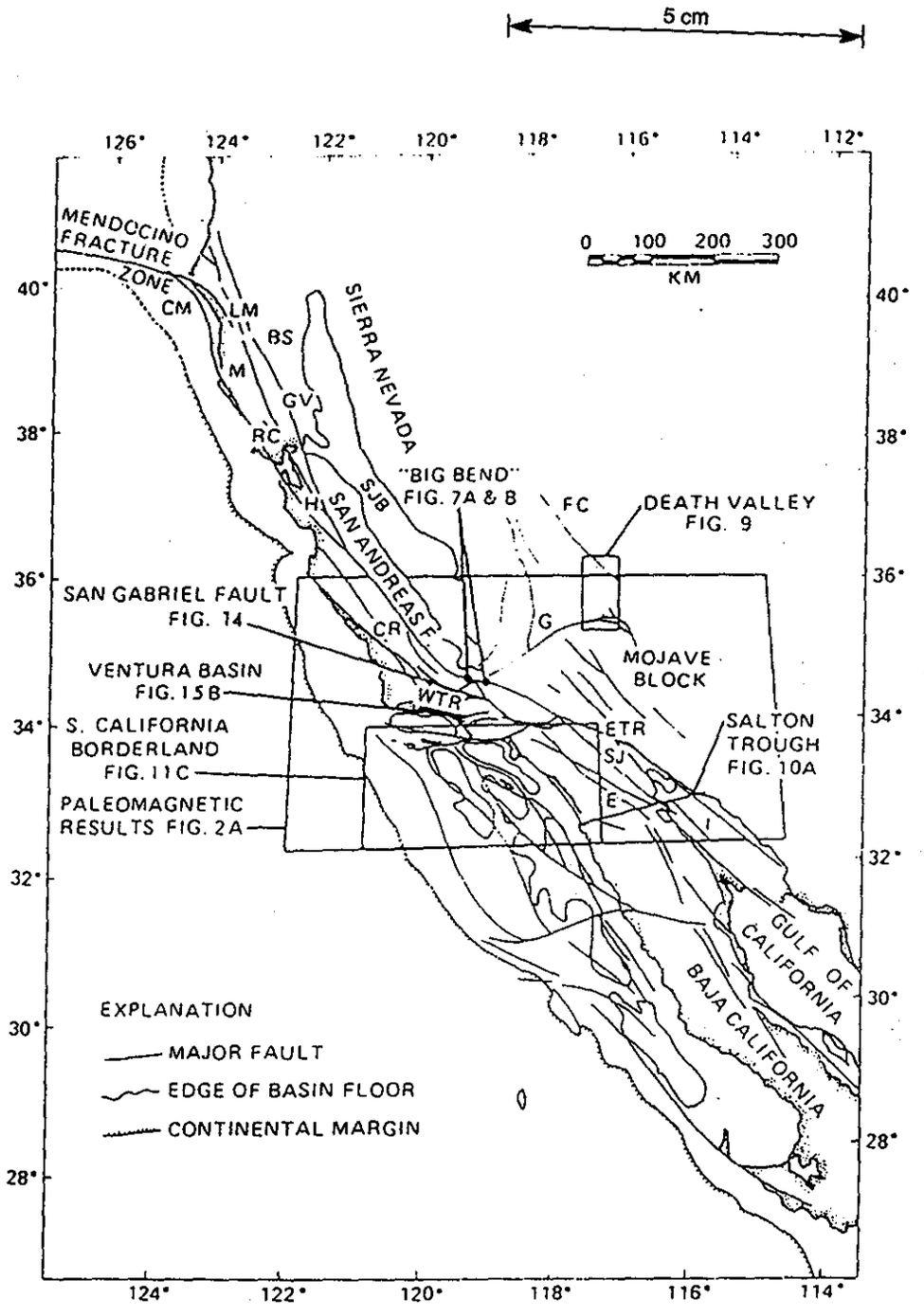



FIG. 1.—Major faults in the diffuse transform plate boundary of California and adjacent parts of Baja California, together with selected basins and elevated blocks mentioned in the text: BS, Bartlett Springs fault zone; CM, Cape Mendocino; CR, Coast Ranges; E, Elsinore fault; ETR, eastern Transverse Ranges; FC, Northern Death Valley-Furnace Creek fault zone; G, Garlock fault; GV, Green Valley fault zone; H, Hayward fault zone; I, Imperial fault; LM, Lake Mountain fault zone; M, Maacama fault zone; RC, Healdsburg-Rodgers Creek fault zone; SJ, San Jacinto fault; SJB, San Joaquin Basin; WTR, western Transverse Ranges (from King, 1969; Crowell, 1974a; Herd, 1978; Nilsen and McLaughlin, 1985 this volume). Map shows locations of areas and cross sections illustrated in Figures 2A, 7, 9, 10A, 11C, 14, 15B.

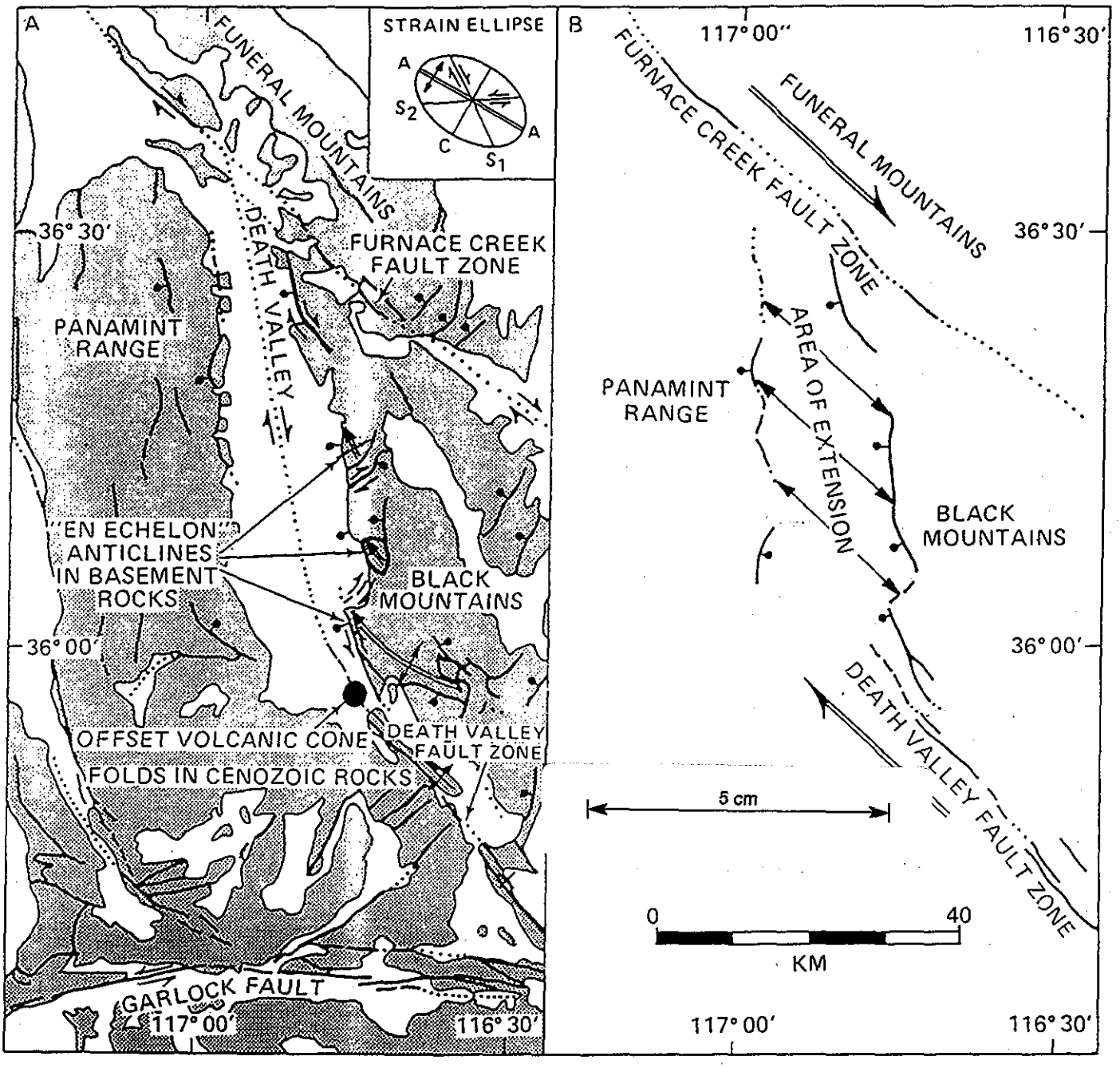



FIG. 9.—Major fault zones in the Death Valley area, California (*modified from Stewart, 1983; see Fig. 1 for location*), showing the interpretations of A) Hill and Troxel (1966), and B) Burchfiel and Stewart (1966). Shading (A) indicates outcrops of Proterozoic to Tertiary sedimentary and volcanic rocks; unshaded area represents Quaternary alluvial deposits. Evidence for strike slip along the northern Death Valley-Furnace Creek and southern Death Valley fault zones includes en echelon folds in Cenozoic rocks and an offset volcanic cone, together with *regional stratigraphic* arguments.

A) A *buried strike-slip fault is inferred in the central north-trending segment* of Death Valley on the basis of oblique striae on fault surfaces in the Black Mountains, and of "en echelon" anticlines in basement rocks (Hill and Troxel, 1966). The insert compares the orientations of observed structures with an idealized strain ellipse for the overall deformation; right slip inferred parallel to direction C is incompatible with orientations summarized in Figure 5.

B) Death Valley interpreted as a pull-apart along an oblique segment of a strike-slip fault system (Burchfiel and Stewart, 1966). Indicators of *crustal stress and regional seismicity* indicate continued extension in an approximately northwest-southeast direction parallel with the Furnace Creek and southern Death Valley fault zones (Sbar, 1982). See text for further explanation.

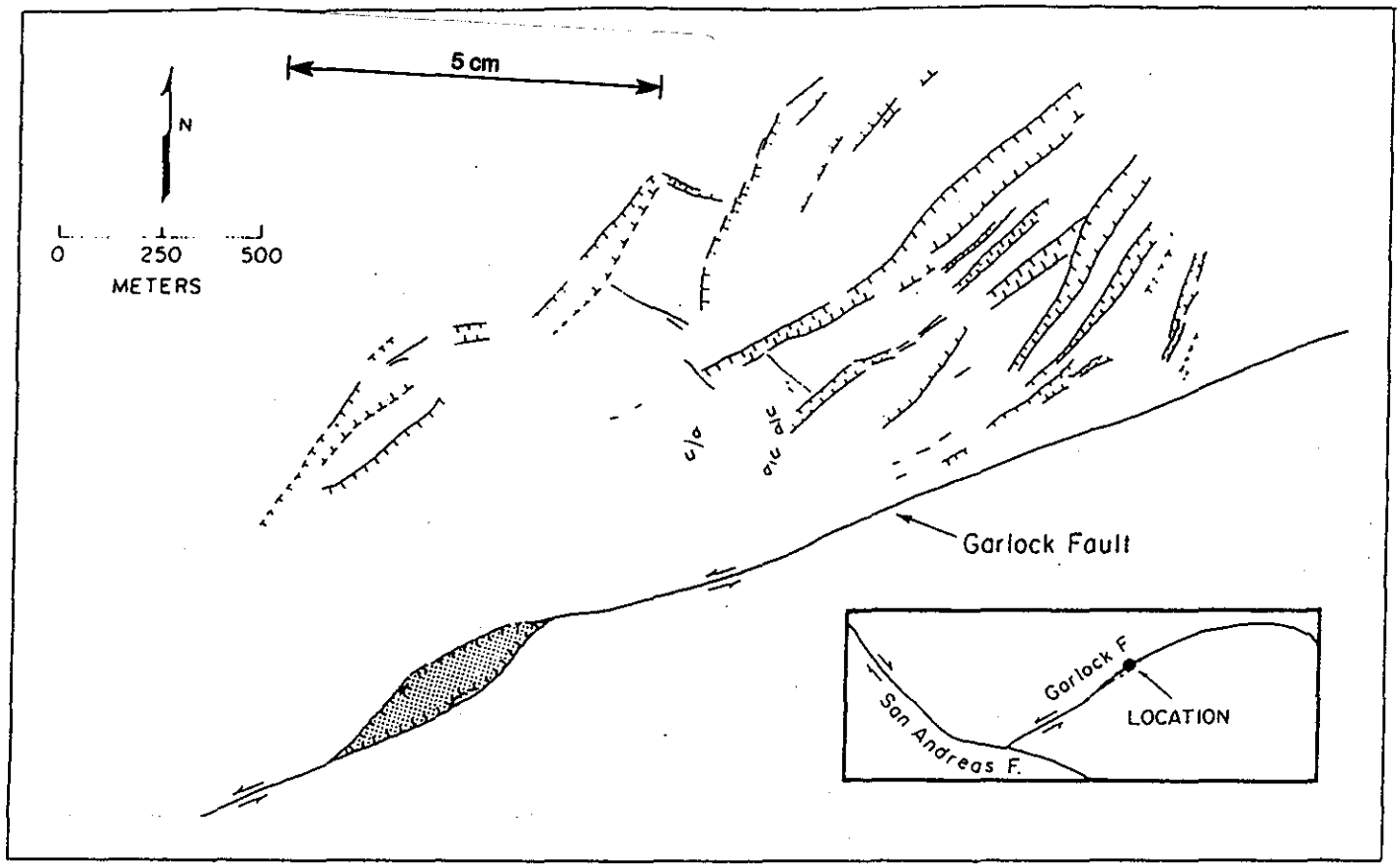



FIG. 4.—A series of horsts and grabens and a small pull-apart (shaded) within the Cantil Valley composite pull-apart basin along the Garlock fault (see inset for location). The orientation of the normal faults within the composite pull-apart basin is about parallel to the bounding diagonal faults of the small pull-apart. The angle between the trend of strike-slip faults and the bounding normal faults of the pull-apart basin is highly oblique (35–45°).

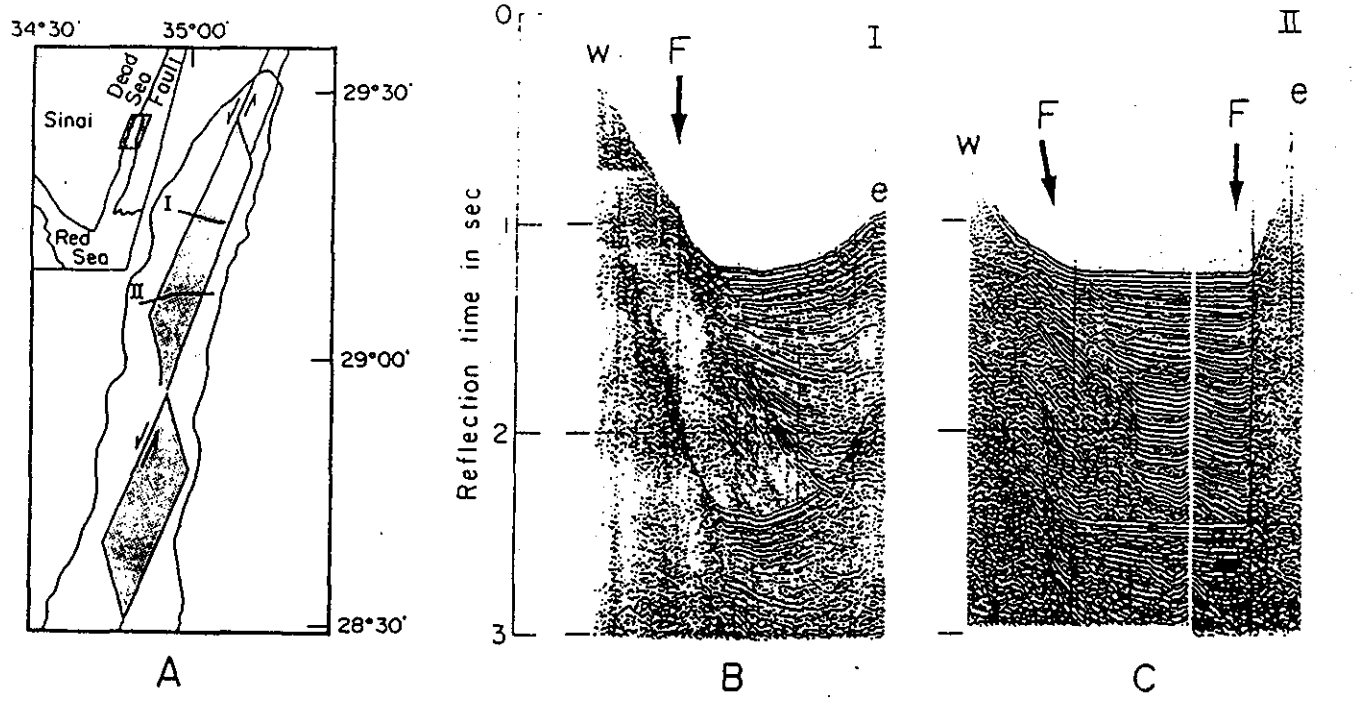



FIG. 5.—Seismic reflection profiles (B and C) across the Elat pull-apart basin (A) in the Gulf of Aqaba (see the location map in A) showing the dip-slip component on the overlapped portions of the strike-slip faults and their approximate dip angles (from Ben-Avraham et al., 1979).

655138

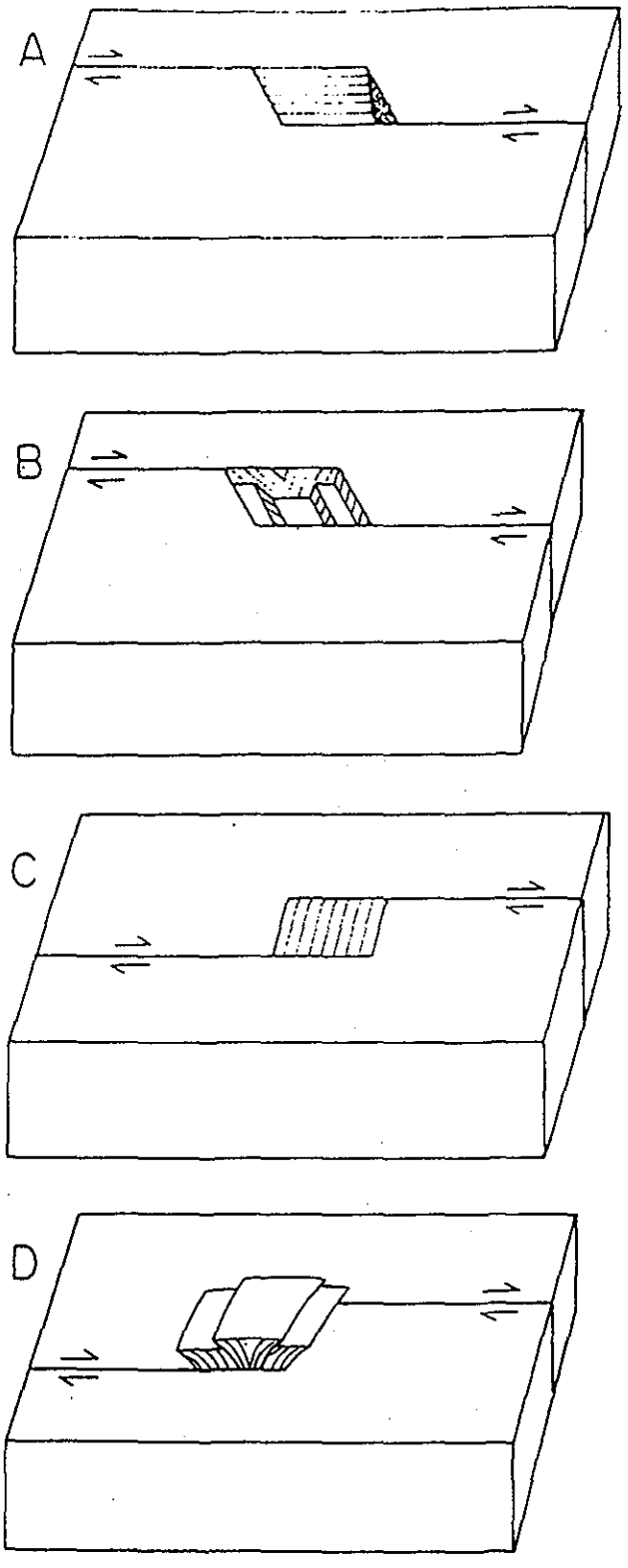



FIG. 3.—Major modes of deformation at extensional (A and B) and compressional (C and D) along-strike stepovers. A) Opening mode (line pattern shows approximate direction of motion on strike-slip fault and dotted pattern indicates extensional fracture surface). B) Shearing mode (lines show approximate direction of slip on oblique and normal faults). C) Cleavage or pressure solution formation (thin lines represent orientation). D) Reverse/thrust faulting (thin lines indicate oblique-slip direction on the bounding fault).

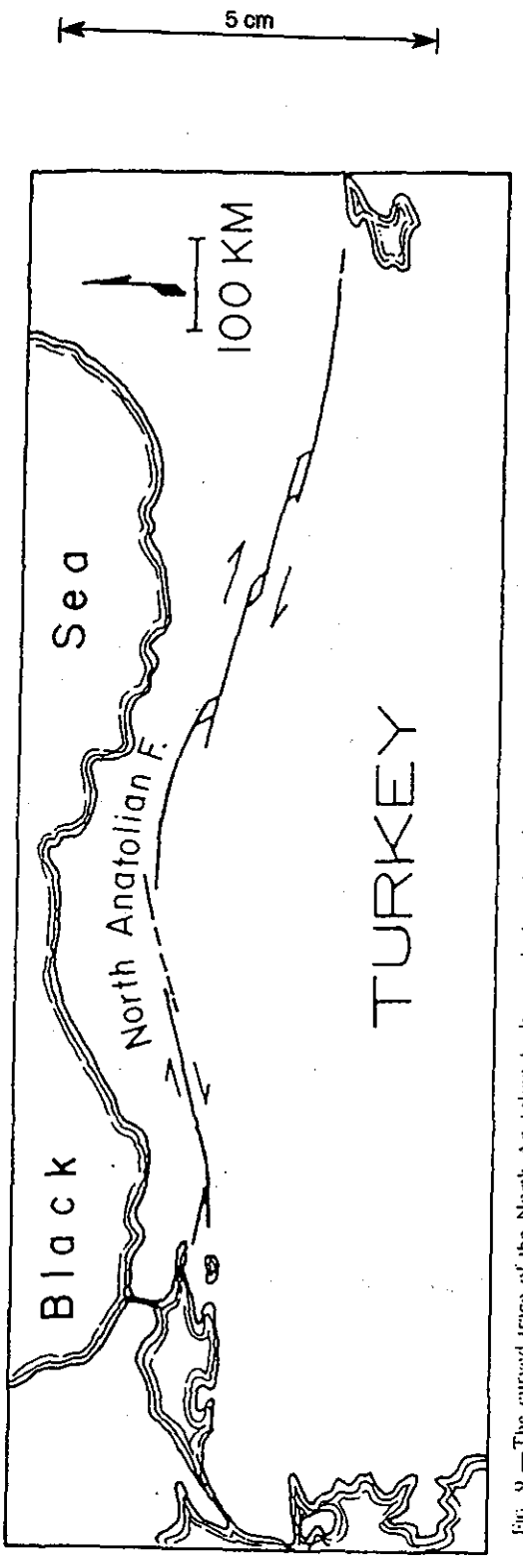



FIG. 9.—The curved trace of the North Anatolian fault, a right-lateral strike-slip fault in Turkey, and right sense of stepovers (simplified from Ketin, 1969).

655139

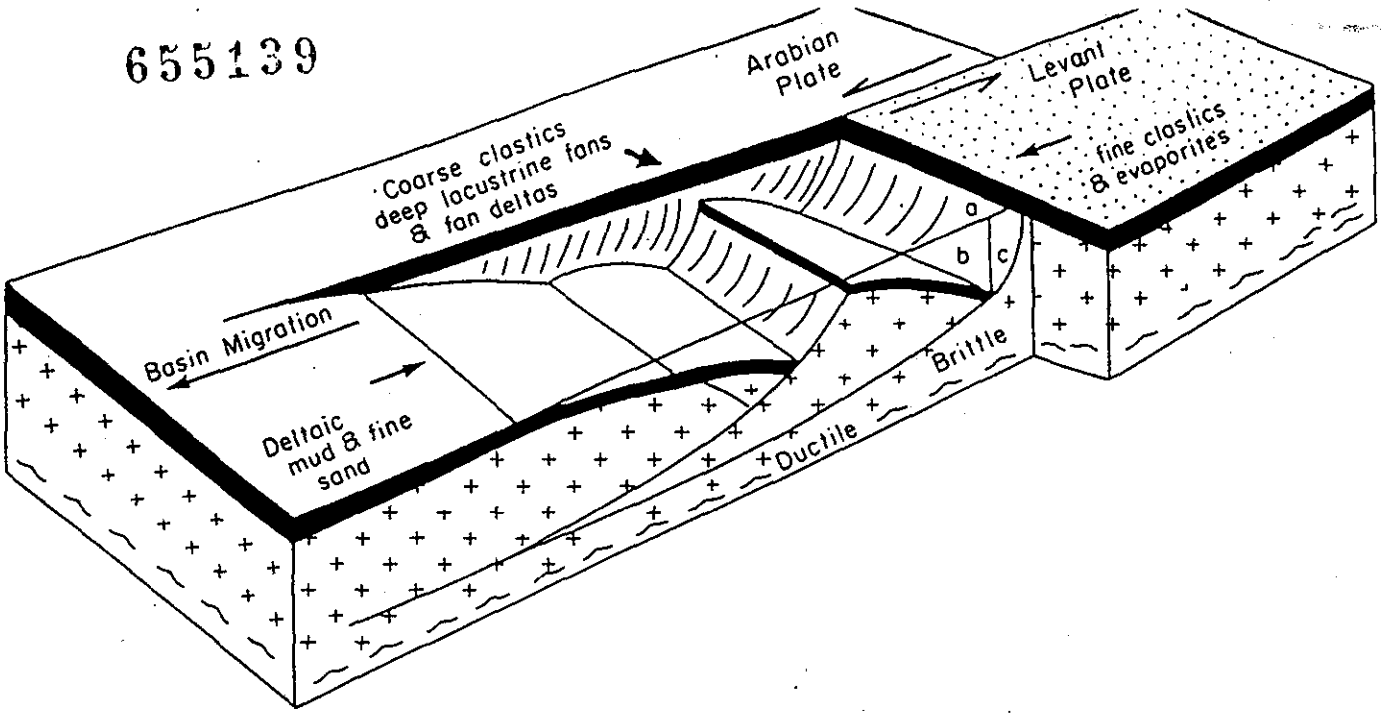



FIG. 13.—Schematic pull-apart model for the Dead Sea Basin, viewed to the southeast, modified from K. Arbenz (written commun., 1984). The nearly vertical walls are characterized by oblique slip (c), involving a component of dip slip (b) that exceeds the component of strike slip (a). Listric normal faults occur at the southern margin (right), and a basement flexure with minor normal faults at the northern one (*left*). The basin migrates to the north. The diagram does not illustrate the rhomb shape of the basin or its lateral asymmetry. The distribution of modern facies is shown around the basin margins.

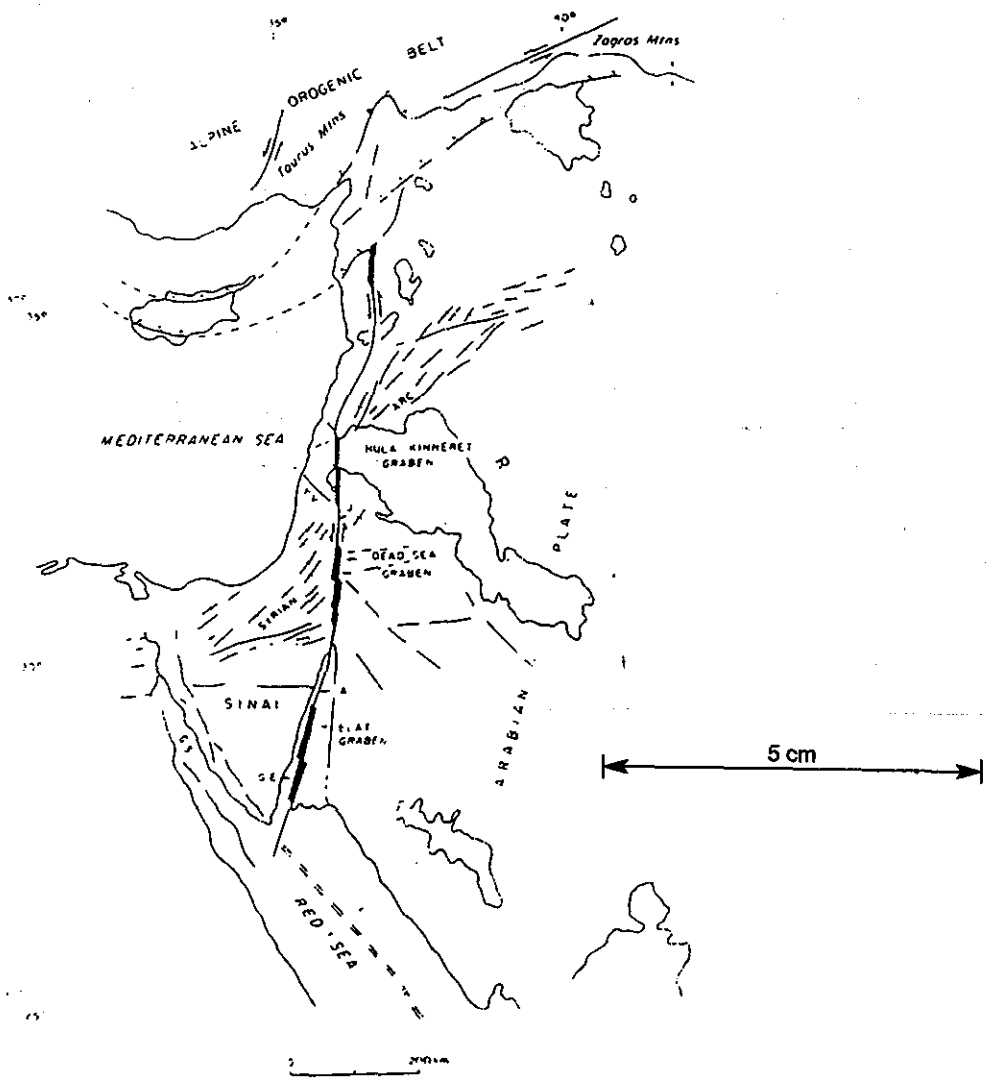



FIG. 1.—Regional tectonic setting of the Dead Sea Transform (after Garfunkel et al., 1981). Abbreviations: YV, Yisreel Valley; J, Jordan Valley; A, Arava Valley; G.S., Gulf of Suez; G.E., Gulf of Elat (Aqaba).

655140

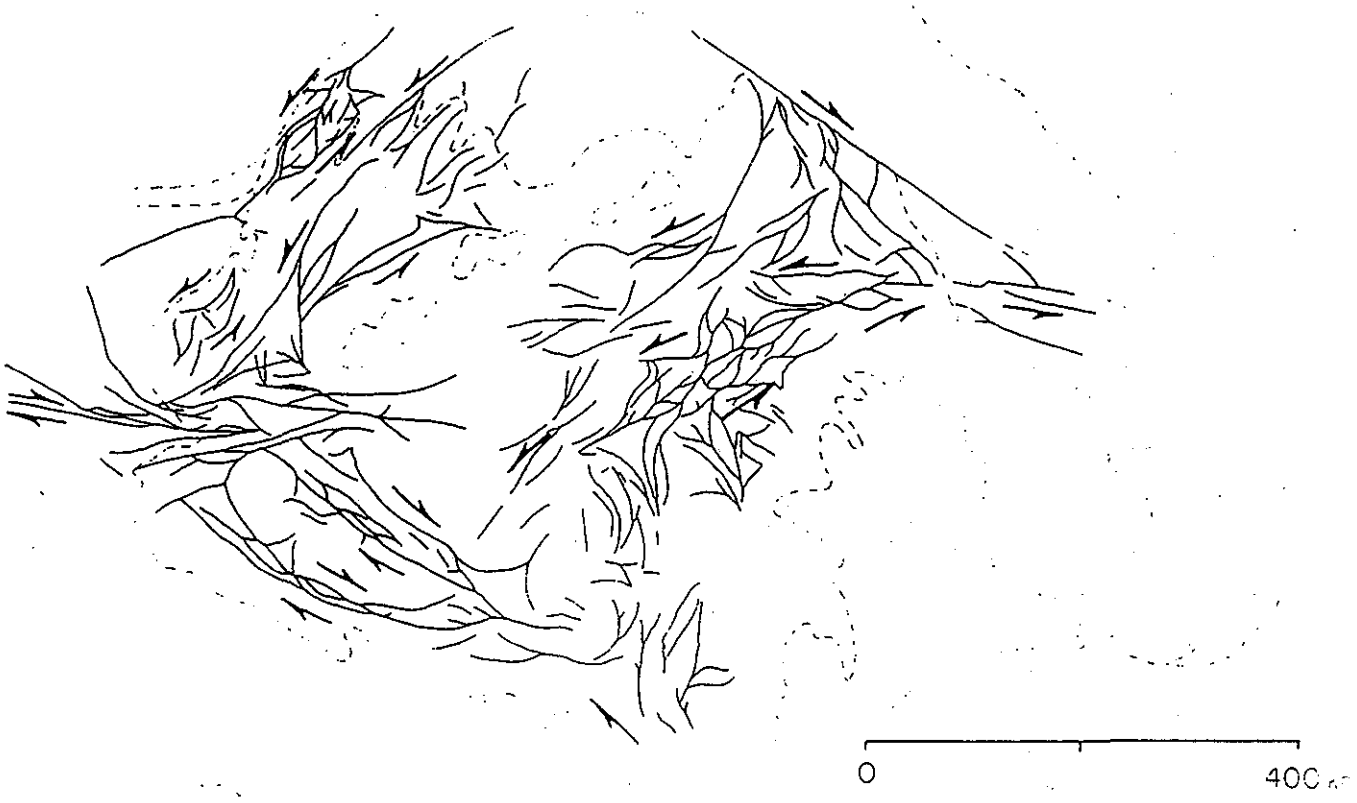



FIG 7.—Generalized map of Neogene faults in the intra-Carpathian region. Arrows indicate sense of shear along strike-slip zones. Some basins are interpreted as pull-apart basins, whereas others are regions of extension bounded by zones of differential shear. From Royden et al. (1982).

5 cm

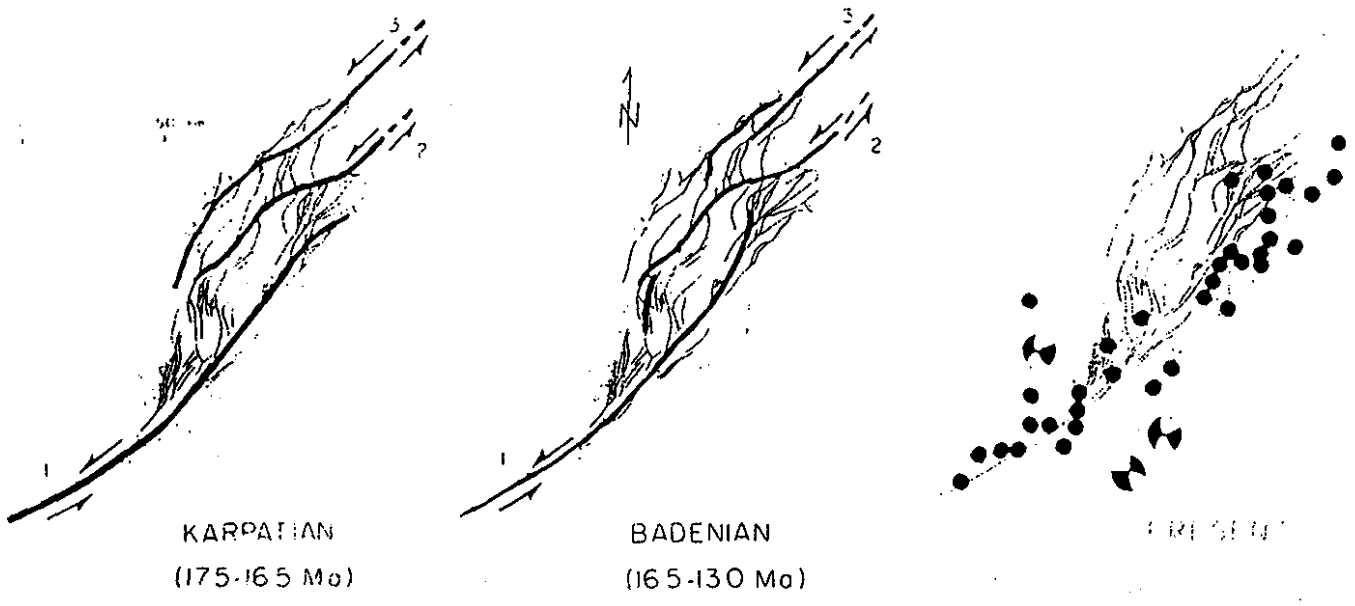



FIG. 10.—Three major fault systems (bold lines) of the Vienna Basin inferred to have been active at three different times during the evolution of the basin. These three fault zones are meant only as a simplified representation of cumulative movements on many faults, some large and some small. Inferred sense of strike-slip displacement is shown by large arrows. Fine lines indicate other prominent faults of Miocene to Quaternary age within the Vienna Basin (after Wessely, in prep.). Small dots indicate areas of rapid subsidence in Karpatian and Badenian time. For the present day, large dots represent epicenters of earthquakes with seismic intensity greater than 5 (after Gutdeutsch and Aric, in prep.). Fault-plane solutions are after Gutdeutsch and Aric (1976).

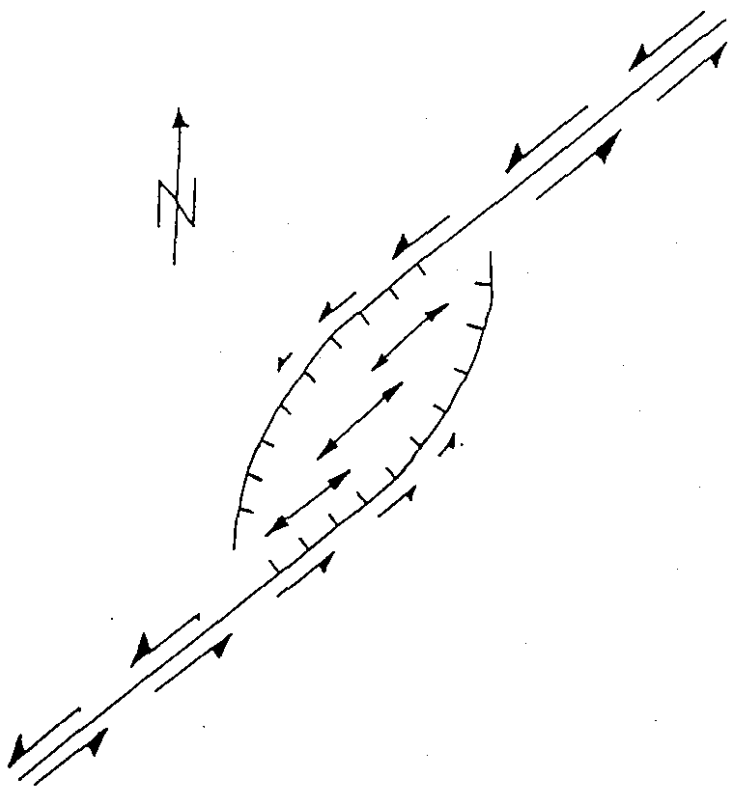


FIG. 12.—Simplified pull-apart interpretation of the Vienna Basin. Displacement on northeast-striking left-slip faults decreases along the faults within the basin, so that near the ends of the faults there is little strike-slip component. Within the basin, the faults have both strike-slip and normal-slip components of displacement. Where the fault segments strike roughly north-south in the basin, displacement is predominantly normal slip. Extension is approximately parallel to the strike-slip faults.

655142

# DEFORMATION AND BASIN FORMATION ALONG STRIKE-SLIP FAULTS[1]

NICHOLAS CHRISTIE-BLICK,
*Department of Geological Sciences and*
*Lamont-Doherty Geological Observatory of Columbia University*
*Palisades, New York 10964;*
AND
KEVIN T. BIDDLE
*Exxon Production Research Company*
*P.O. Box 2189*
*Houston, Texas 77252-2189*

ABSTRACT: Significant advances during the decade 1975 to 1985 in understanding the geology of basins along strike-slip faults include the following: (1) paleomagnetic and other evidence for very large magnitude strike slip in some orogenic belts; (2) abundant paleomagnetic evidence for the pervasive rotation of blocks about vertical axes within broad intracontinental transform boundaries; (3) greater appreciation for the wide range of structural styles along strike-slip faults; (4) new models for the evolution of strike-slip basins; and (5) a body of new geophysical and geological data for specific basins. In the light of this work, and as an introduction to the remainder of the volume, the purpose of this paper is to summarize the major characteristics of and controls on structural patterns along strike-slip faults, the processes and tectonic settings of basin formation, and distinctive stratigraphic characteristics of strike-slip basins.

Strike-slip faults are characterized by a linear or curvilinear principal displacement zone in map view, and in profile, by a subvertical fault zone that ranges from braided to upward-diverging within the sedimentary cover. Many strike-slip faults, even those involving crystalline basement rocks, may be detached within the middle to upper crust. Two prominent characteristics are the occurrence of en echelon faults and folds, within or adjacent to the principal displacement zone, and the co-existence of faults with normal and reverse separation. The main controls on the development of structural patterns along strike-slip faults are (1) the degree to which adjacent blocks either converge or diverge during strike slip; (2) the magnitude of displacement; (3) the material properties of the sediments and rocks being deformed; and (4) the configuration of pre-existing structures. Each of these tends to vary spatially, and, except for the last, to change through time. It is therefore not surprising that structural patterns along strike-slip faults differ in detail from simple predictions based on the instantaneous deformation of homogeneous materials. In the analysis of structural style, it is important to attempt to separate structures of different ages, and especially to distinguish structures due to strike-slip deformation from those predating or post-dating that deformation. Distinctive aspects of structural style for strike-slip deformation on a regional scale include evidence for simultaneous shortening and extension, and for random directions of vergence in associated thrusts and nappes.

Sedimentary basins form along strike-slip faults as a result of localized crustal extension, and, especially in zones of continental convergence, of localized crustal shortening and flexural loading. A given basin may alternately experience both extension and shortening through variations in the motion of adjacent crustal blocks, or extension in one direction (or in one part of the basin) may be accompanied by shortening in another direction (or in another part of the basin). The directions of extension and shortening also tend to vary within a given basin, and to change through time; and the magnitude of extension may be depth-dependent. Theoretical studies and observations from basins where strike-slip deformation has ceased suggest that many strike-slip basins experience very little thermally driven post-rift subsidence. Strike-slip basins are typically narrow (less than about 50 km wide), and they rapidly lose anomalous heat by accentuated lateral as well as vertical conduction. Detached or thin-skinned basins also tend to be cooler after rifting has ended than those resulting from the same amount of extension of the entire lithosphere. In some cases, subsidence may be arrested or its record destroyed as a result of subsequent deformation. Subsidence due to extension, thermal contraction, or crustal loads is amplified by sediment loading.

The location of depositional sites is determined by (1) crustal type and the configuration of pre-existing crustal structures; (2) variations in the motion of lithospheric plates; and (3) the kinematic behavior of crustal blocks. The manner in which overall plate motion is accommodated by discrete slip on major faults, and by the rotation and internal deformation of blocks between those faults is especially important. Subsidence history cannot be determined with confidence from present fault geometry, which therefore provides a poor basis for basin classification. Every basin is unique, and palinspastic reconstructions are useful even if difficult to undertake.

Distinctive aspects of the stratigraphic record along strike-slip faults include (1) geological mismatches within and at the boundaries of basins; (2) a tendency for longitudinal as well as lateral basin asymmetry, owing to the migration of depocenters with time; (3) evidence for episodic rapid subsidence, recorded by thick stratigraphic sections, and in some marine basins by rapid deepening; (4) the occurrence of abrupt lateral facies changes and local unconformities; and (5) marked differences in stratigraphic thickness, facies geometry, and occurrences of unconformities from one basin to another in the same region.

## INTRODUCTION

Strike-slip deformation occurs where one crustal or lithospheric block moves laterally with respect to an adjacent block. In reality, most "strike-slip" faults accommodate oblique displacements along some segments or during part of the time they are active; and most are associated with an assemblage of related structures including both normal and reverse faults. A component of oblique slip is also required for the formation of sedimentary basins. However, the title of this paper and that of the volume were chosen to emphasize tectonics and sedimentation in regions where strike-slip deformation is prominent.

In this paper, we follow Mann et al. (1983) in using the term "strike-slip basin" for any basin in which sedimentation is accompanied by significant strike slip. We acknowledge that at any given time some strike-slip basins are hybrids associated with regional crustal extension or shortening, and most are composite, influenced by varying tectonic controls during their evolution (for various recent perspectives about sedimentary basins in a plate-tectonic framework see Green, 1977; Dickinson, 1978; Bally and Snelson, 1980; Klemme, 1980; Bois et al., 1982; Dewey,

[1]Lamont-Doherty Geological Observatory Contribution No. 3910.

Copyright © 1985, The Society of Economic Paleontologists and Mineralogists

655143

1982; Reading, 1982; Kingston et al., 1983a; Perrodon and Masse, 1984). Strike-slip basins also occur in a wide range of plate-tectonic settings including (1) intracontinental and intraoceanic transform zones; (2) divergent plate boundaries and extensional continental settings; and (3) convergent plate boundaries and contractional continental settings.

Among numerous articles on aspects of strike-slip deformation, basin formation, and sedimentation published in the last decade or so, several have been influential (Wilcox et al., 1973; Crowell, 1974a, b; Freund, 1974; Sylvester and Smith, 1976; Segall and Pollard, 1980; a collection of articles edited by Ballance and Reading, 1980a; Reading, 1980; Aydin and Nur, 1982a; Mann et al., 1983). Sylvester (1984) provides a compilation of classic papers on the mechanics, structural style, and displacement history of strike-slip faults, with emphasis on examples from California. In view of these existing summaries, we draw attention here to significant recent advances in understanding the large-scale characteristics of strike-slip faults and strike-slip basins, including several topics not discussed or only briefly mentioned in Ballance and Reading (1980a) and Sylvester (1984).

The remainder of this summary paper introduces two broad themes, which are elaborated in the articles that follow: (1) the characteristics of and controls on structural patterns along strike-slip faults; and (2) the processes and tectonic settings of basin formation, and distinctive aspects of the stratigraphic record of strike-slip basins.

## PROGRESS DURING THE DECADE 1975–1985

Examples of advances in understanding the geology of strike-slip basins during the decade 1975 to 1985 include the following: (1) paleomagnetic and other evidence suggesting the very large magnitude of strike slip in some orogenic belts; (2) abundant paleomagnetic evidence where continents are intersected by diffuse transform plate boundaries for pervasive rotation of blocks about vertical axes, with implications for processes of deformation, basin formation and palinspastic reconstruction of strike-slip basins; (3) greater appreciation for the range of structural styles along strike-slip faults, both on the continents and in the ocean basins, and for the processes by which those styles arise; (4) new theoretical and empirical models for the evolution of strike-slip basins; and (5) new geophysical and geological data for many strike-slip basins, some of which are reported in this volume.

### *Large-Magnitude Strike Slip in Orogenic Belts*

The role of strike slip in the evolution of orogenic belts and associated sedimentary basins has been recognized for several decades (references in Ballance and Reading, 1980b; and Sylvester, 1984), but the possible magnitude of such deformation may have been underestimated. A combination of paleomagnetic, faunal, and other geological data now indicate that in some complex orogens such as the North American Cordillera, individual elements of the tectonic collage (Helwig, 1974), termed terranes, have moved thousands not merely hundreds of kilometers with respect to each other along the trend of the orogen (Jones et al., 1977; Irving, 1979; Beck, 1980; Coney et al., 1980; Irving et al., 1980; Champion et al., 1984; Eisbacher, 1985 this volume). Although part of this longitudinal displacement in the Cordillera pre-dates accretion, a significant component occurred after the terranes were sutured to North America. The Stikine Terrane, for example, appears to have been displaced northward by 13° to 20° since early Cretaceous time, or on the order of 1,500 km with respect to the North American craton (Jones et al., 1977; Irving et al., 1980; Chamberlain and Lambert, 1985; Eisbacher, 1985 this volume).

Large-scale strike-slip deformation also permits lateral tectonic escape in zones of continental convergence, such as between India and Eurasia (Molnar and Tapponnier, 1975), or on a smaller scale, in Turkey (Şengör et al., 1985 this volume). Molnar and Tapponnier (1975) estimated that about one third to half of the relative plate motion between India and Eurasia since the onset of continental collision in Eocene-Oligocene time (at least 1,500 km) could be accounted for by a comparable amount of strike-slip faulting in China and Mongolia.

We do not imply that such huge displacements characterize all orogenic belts, or that available paleomagnetic results are in every case without ambiguity, but only that the possibility of large-scale strike slip should be seriously entertained unless precluded by firm data. In the Appalachian-Caledonide orogen, for example, paleomagnetic studies initially suggested cumulative sinistral offset of as much as 2,000 km in late Paleozoic time (Kent and Opdyke, 1978, 1979; van der Voo et al., 1979; van der Voo and Scotese, 1981; Kent, 1982; van der Voo, 1982, 1983; Perroud et al., 1984). The timing, magnitude, and sense of displacement have recently been questioned on the basis of (1) new determinations of the Early Carboniferous pole for cratonic North America (Irving and Strong, 1984; Kent and Opdyke, 1985); (2) doubt about the age of the magnetization directions measured in some of the samples from eastern North America and Scotland (Donovan and Meyerhoff, 1982; Roy and Morris, 1983; Cisowski, 1984); and (3) the difficulty of finding appropriate faults on which to distribute the displacement (Ludman, 1981; Bradley, 1982; Donovan and Meyerhoff, 1982; Parnell, 1982; Winchester, 1982; Smith and Watson, 1983; Briden et al., 1984; Haszeldine, 1984). Where large displacements have occurred, however, even relatively young basins may have been dismembered and strung out over huge distances, and some geological mismatches may be resolved only by considering the history of an entire orogenic belt.

### *Rotations About Vertical Axes*

The rotation of blocks about vertical axes and the bending of segments of orogenic belts have long been postulated on structural grounds (Carey, 1955, 1958; Albers, 1967; Freund, 1970; Garfunkel, 1974; Dibblee, 1977). Paleomagnetic data now confirm that such rotations tend to be pervasive in strike-slip regimes over a wide range of scales, especially where continents are intersected by diffuse transform plate boundaries (Figs. 1, 2), and the data suggest additional constraints on the timing of rotation and on the kinematics of deformation (Beck, 1980; Cox, 1980; Lu-

655144



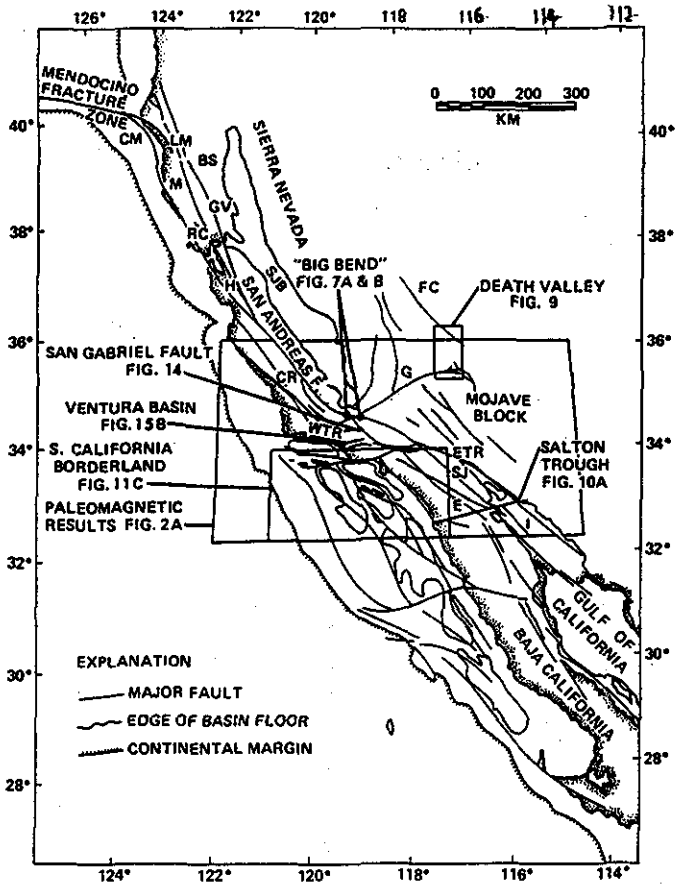



FIG. 1.—Major faults in the diffuse transform plate boundary of California and adjacent parts of Baja California, together with selected basins and elevated blocks mentioned in the text: BS, Bartlett Springs fault zone; CM, Cape Mendocino; CR, Coast Ranges; E, Elsinore fault; ETR, eastern Transverse Ranges; FC, Northern Death Valley-Furnace Creek fault zone; G, Garlock fault; GV, Green Valley fault zone; H, Hayward fault zone; I, Imperial fault; LM, Lake Mountain fault zone; M, Maacama fault zone; RC, Healdsburg-Rodgers Creek fault zone; SJ, San Jacinto fault; SJB, San Joaquin Basin; WTR, western Transverse Ranges (from King, 1969; Crowell, 1974a; Herd, 1978; Nilsen and McLaughlin, 1985 this volume). Map shows locations of areas and cross sections illustrated in Figures 2A, 7, 9, 10A, 11C, 14, 15B.

yendyk et al., 1980, 1985; Ron et al., 1984; Ron and Eyal, 1985).

Paleomagnetic evidence from Neogene rocks of southern California indicates that blocks such as the western Transverse Ranges (WTR in Fig. 1), bounded by east-striking left-slip faults, have experienced net clockwise rotations of between 35° and 90°, with sites near one major right-slip fault being rotated by more than 200° (near DB in Fig. 2A; Luyendyk et al., 1985). In contrast, the Mojave block, located between the San Andreas and Garlock faults, and characterized by northwest-striking right-slip faults, seems to have been rotated counterclockwise by about 15° ± 11° since 6 Ma (c in Fig. 2A; Morton and Hillhouse, 1985), but with large variations in declination over distances of 30 to 120 km from one sub-block to another. In the Cajon Pass region (f in Fig. 2A), there has been no significant rotation since 9.5 Ma (Weldon et al., 1984). These results generally support the tectonic models of Freund (1970), Garfunkel (1974), and Dibblee (1977), in which major crustal blocks deform internally like a set of dominoes. Garfunkel (1974) suggested as much as 30° of rotation for the Mojave block, approximately twice that determined paleomagnetically, but he probably overestimated by a factor of two to three the magnitude of displacement on the strike-slip faults (Dokka, 1983).

The dimensions of the rotating blocks are uncertain for three reasons: (1) As noted above, blocks tend to deform internally, producing dispersion in declination anomalies; (2) In some cases, rotation seems to have occurred during deposition or eruption of the sedimentary and volcanic rocks studied, so that there is a systematic variation in the magnitude of rotation with age (Luyendyk et al., 1985); (3) Similar rotations may characterize blocks that were actually behaving independently. It is also likely that the boundaries of crustal fragments have changed through time, as displacement occurred sequentially along different strike-slip faults. Some blocks may have undergone, at different times, both clockwise and counterclockwise rotation. A possible example is the San Gabriel block between the San Gabriel and San Andreas faults (SB and e in Fig. 2A), although available data are inconclusive (Ensley and Verosub, 1982; Luyendyk et al., 1985). Small blocks can rotate at an alarming speed. Plio-Pleistocene sediments of the Vallecito-Fish Creek Basin in the western Imperial Valley (d in Fig. 2A) have been rotated 35° since 0.9 Ma (Opdyke et al., 1977; Johnson et al., 1983), and there is thus no assurance that rotation accumulates at a uniform rate, any more than does displacement.

Paleomagnetic and structural data from northern Israel indicate that Neogene intraplate deformation was accommodated by block rotation and strike-slip deformation similar to but on a smaller scale than that documented in California (Fig. 2B; Ron et al., 1984; Ron and Eyal, 1985). Domains of left-slip faults (Galilee and Carmel regions) have rotated clockwise by 23° to 35° since the Cretaceous, and domains of right-slip faults (Galilee and Tiberias regions), counterclockwise by 23° to 53° since the Cretaceous and Miocene, respectively. Sites associated with east-striking normal faults in Galilee yield the expected Cretaceous direction. Strike slip on individual faults west of the Dead Sea fault zone (Sea of Galilee, Fig. 2B) is measurable in hundreds of meters, beginning in late Miocene to early Pliocene time (Ron and Eyal, 1985). The normal faults are predominantly of post-middle Pliocene age.

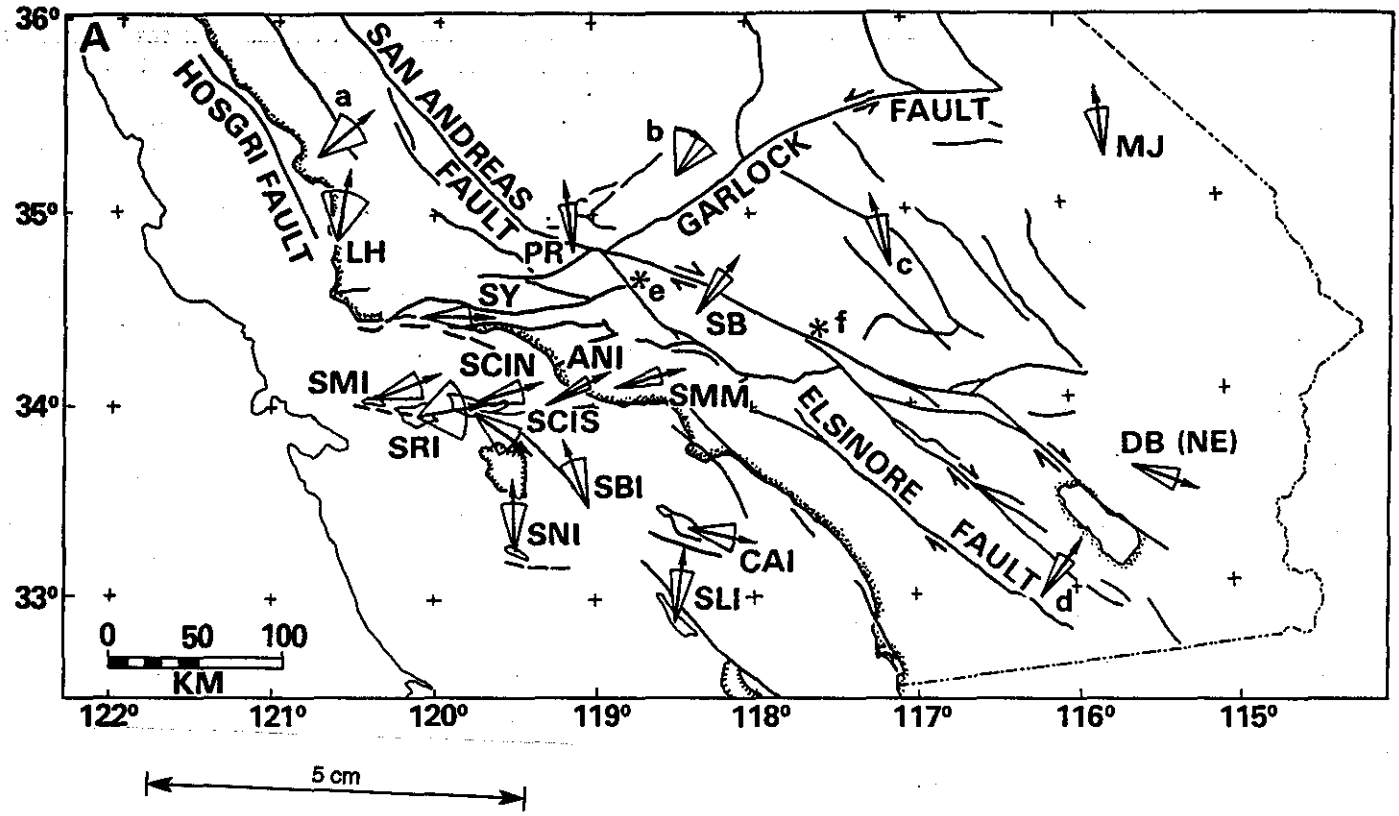
The significance of these paleomagnetic results is that strike-slip basins can no longer be viewed solely in terms of bends, oversteps or junctions along strike-slip faults, to list some popular models; rotations may play an important role in basin formation. In addition, we should expect facies and paleogeographic elements not only to be offset along strike-slip faults, but also to be systematically misaligned. A further implication of block rotations, discussed below, is that the blocks and bounding faults are detached at some level in the crust or upper mantle (Terres and Sylvester, 1981; Dewey and Pindell, 1985).

### *Structural Style of Strike-Slip Faults*

There is growing appreciation for the wide range of structural styles along strike-slip faults, both on the conti-

655145





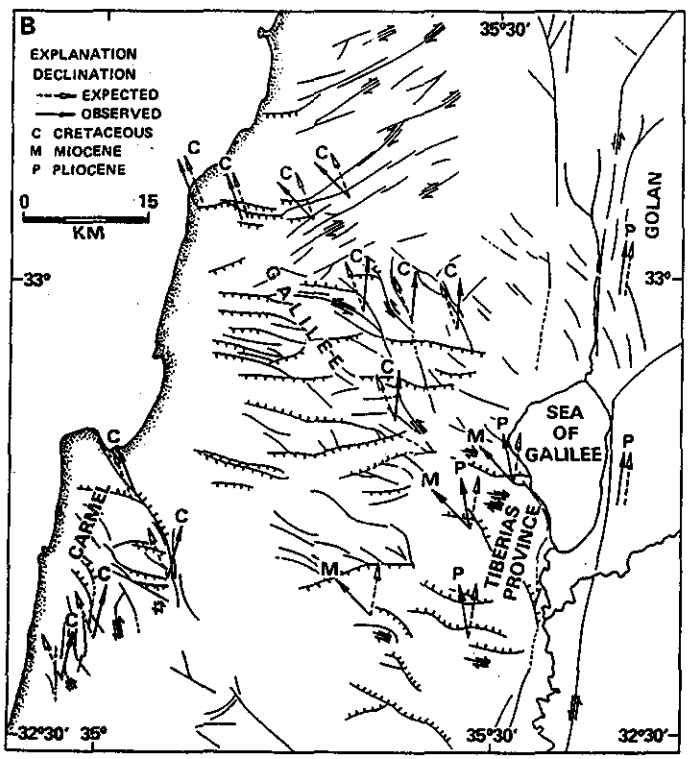




FIG. 2.—A) Paleomagnetic declinations measured in rocks of Neogene age (older than 13 Ma, except where indicated) and Quaternary sediments (site d) in southern California (see Fig. 1 for location). For each site, except e and f, the mean declination is shown along with the 95% confidence limit on the mean. Most of the data and the figure are from Luyendyk et al. (1985). Additional published data: a, Greenhaus and Cox (1979); b, apparent rotation between about 80 and 20 Ma (in comparison with the late Cretaceous pole of Irving, 1979; Kanter and McWilliams, 1981); c, mean counterclockwise rotation of 15° ± 11° since 6 Ma, but with large variations in declination from one sub-block to another (Morton and Hillhouse, 1985); d, 35° clockwise rotation since 0.9 Ma (Opdyke et al., 1977; Johnson et al., 1983); e, no major rotation since 8.5 Ma; the data can be interpreted in terms of clockwise rotation prior to 7.5 Ma, and counterclockwise rotation after that time (Ensley and Verosub, 1982); f, no significant rotation since 9.5 Ma (Weldon et al., 1984). Abbreviations for sites: ANI, Anacapa Island; CAI, Catalina Island; DB (NE) northeastern Diligencia Basin; LH, Lions Head; MJ, Mojave; PR, Plush Ranch Formation, Lockwood Valley; SB, Soledad Basin; SBI, Santa Barbara Island; SCIN, north Santa Cruz Island; SCIS, south Santa Cruz Island; SLI, San Clemente Island; SMI, San Miguel Island; SMM, Santa Monica Mountains; SNI, San Nicolas Island; SRI, Santa Rosa Island; SY, Santa Ynez Range; a, Morro Rock-Islay Hill Complex; b, southern Sierra Nevada; c, Mojave block; d, Vallecito-Fish Creek Basin; e, Ridge Basin; f, Cajon Pass. Faults are from Jennings (1975).

B) Paleomagnetic declinations measured in rocks of Cretaceous, Miocene, and Pliocene age in northern Israel; strike-slip faults, with sense of slip; and normal faults, indicated by hachures on downthrown side (simplified from Ron et al. 1984; Ron and Eyal, 1985). Domains associated with left-slip faults have undergone clockwise rotation, whereas those associated with right-slip faults have experienced counterclockwise rotation; domains associated predominantly with normal faults yield the expected declination.

nents and in the ocean basins, and for the processes by which those styles arise. Wilcox et al. (1973) recognized that one of the main controls on structural style along continental strike-slip faults cutting appreciable thicknesses of sediment is the degree to which adjacent blocks either converge or diverge during deformation. Little attention has been paid subsequently to the structures associated with divergence (see Harding et al., 1985 this volume). In addition, although experimental models, such as those of Wilcox et al. (1973), constitute a useful point of departure for analyzing the development of structures along strike-slip faults, they cannot account adequately for the considerably larger length scale, lower strain rate, greater strength, complex variations in block motion, syn-deformational sedimentation, or material heterogeneity inherent in natural examples (for further discussion, see Hubbert, 1937).

Since transform faults were first recognized in the ocean basins (Wilson, 1965; Sykes, 1967), a wealth of information has accumulated about their physiographic and structural characteristics, particularly from investigations with deep-towed echo-sounding and side-scan sonar instruments such as Deep Tow, GLORIA, Sea Beam, and Sea MARC 1 (Lonsdale, 1978; Macdonald et al., 1979; Searle, 1979, 1983; Bonatti and Crane, 1984; Fox and Gallo, 1984), the deep-towed ANGUS camera (Karson and Dick, 1983), and the deep-sea submersible ALVIN (Choukroune et al., 1978; Karson and Dick, 1983). The gross crustal structure across fracture zones has been determined by a variety of geophysical means, including seismic refraction experiments (e.g., Detrick and Purdy, 1980; Sinha and Louden, 1983), and multichannel seismic reflection profiles (e.g., Mutter and Detrick, 1984). Fossil oceanic fracture zones have also been studied in ophiolites such as the Coastal Complex of Newfoundland (Karson, 1984). Sediment accumulations in oceanic transform zones are generally thinner than about 1 km, except in areas such as the northern Gulf of California, where there is an abundant supply of terrigenous detritus (Crowell, 1981a; Kelts, 1981). The main structural features of the transforms are therefore expressed largely in igneous and metaigneous rocks, and they differ in detail from the styles of many continental strike-slip faults.

The morphology of oceanic transforms is in part a function of the offset and spreading rate of associated ridges (Fox and Gallo, 1984), and of changes in spreading direction (Menard and Atwater, 1969; Macdonald et al., 1979; Bonatti and Crane, 1984). For example, slow-slipping transforms (full rate of 1.5 to 5 cm/yr), such as those of the North Atlantic, are characterized by prominent linear topography and aligned closed basins oriented transverse to offset ridges. The relief increases from about 1,500 m for small-offset (<30 km) transforms to several thousand meters for those with large offset (>100 km), and gradients of valley walls are typically 20° to 30°, with scarps locally near vertical (Fox and Gallo, 1984). Ridge-flank topography tends to deviate in the direction of strike-slip within a few kilometers of the transform. In contrast, many fast-slipping transforms (full rate of 12 to 18 cm/yr), such as those of the eastern Pacific, are characterized by broad zones (7 to 150 km wide), composed of numerous small-offset transform segments, linked by oblique extensional domains. Relief ranges from several hundred to a few thousand meters (Fox and Gallo, 1984). The pronounced topography of some transforms may be an expression of changes in plate motion, and of convergent strike-slip deformation. For example, near its eastern intersection with the mid-Atlantic ridge, the Romanche fracture zone shallows to little more than 1,000 m below sea level, and the presence of reefal limestone shows that it was locally emergent at about 5 Ma (Bonatti and Crane, 1984). About 400 km farther east, there is evidence from a seismic reflection profile for reverse faulting and folding on the north flank of the fracture zone (Lehner and Bakker, 1983).

The investigation of oceanic transform faults is currently a major frontier in the geological and geophysical sciences, but in view of the emphasis of this volume on strike-slip deformation and basin formation in continental settings, in the remainder of this paper we focus primarily on continental examples.

### *Models for Strike-Slip Basins*

Models for strike-slip basins are of two kinds: (1) theoretical models, derived from relatively simple assumptions about the thermal and mechanical properties of the lithosphere, but which can be compared with natural basins (Rodgers, 1980; Segall and Pollard, 1980; and in this volume, Aydin and Nur, 1985; Guiraud and Seguret, 1985; Pitman and Andrews, 1985; Royden, 1985); and (2) empirical models, which represent a distillation of geological and geophysical data from several different basins (Crowell, 1974a, b; Aydin and Nur, 1982a; Mann et al., 1983; and in this volume, Nilsen and McLaughlin, 1985; Şengör et al., 1985).

One theoretical approach for investigating the development of a pull-apart basin (Fig. 11A, B below; Burchfiel and Stewart, 1966; Crowell, 1974a, b), the simplest type of basin along a strike-slip fault, is to model the state of stress, secondary fracturing, and vertical displacements produced by infinitesimal lateral displacements on overstepping discontinuities. It is assumed for the sake of simplicity that the discontinuities are planar, vertical, and parallel, that the crust is composed of an isotropic, homogeneous, linear elastic material, and that the far-field stress is spatially uniform (Rodgers, 1980; Segall and Pollard, 1980; based on earlier studies by Chinnery, 1961, 1963; Weertman, 1965). Although such models reproduce the first-order characteristics of pull-apart basins located between overstepping strike-slip faults, they do not account satisfactorily for protracted deformation, material heterogeneity, inelastic behavior, variations in the state of stress with depth, or changes in fault geometry with depth; and currently available models are not applicable to more complex geometry and kinematic history.

Another approach (e.g., Pitman and Andrews, 1985 this volume; Royden, 1985 this volume) is to consider the subsidence and thermal history of pull-apart basins using models similar to the stretching model of McKenzie (1978), but incorporating such effects as finite rifting times, accentuated lateral heat flow from narrow basins, and depth-dependent extension (Jarvis and McKenzie, 1980; Royden and

655147



Keen, 1980; Steckler, 1981; Steckler and Watts, 1982; Cochran, 1983). In the McKenzie model, subsidence results from instantaneous, uniform extension of the lithosphere (rifting), and from subsequent cooling by vertical conduction of heat. Theoretical studies and observations from basins where strike-slip deformation has ceased suggest that many strike-slip basins experience very little thermally driven post-rift subsidence. Basins along strike-slip faults are typically narrow (less than about 50 km wide; Aydin and Nur, 1982a; and in this volume, Aspler and Donaldson, 1985; Cemen et al., 1985; Guiraud and Seguret, 1985; Johnson, 1985; Link et al., 1985; Manspeizer, 1985; Nilsen and McLaughlin, 1985; Royden, 1985; Şengör et al., 1985), and much of the thermal anomaly decays during the rifting stage (Pitman and Andrews, 1985 this volume). In some cases, the absence of evidence for post-rift thermal subsidence may also be due to subsequent deformation of the basin (Reading, 1980; Mann et al., 1983; Nilsen and McLaughlin, 1985 this volume). An example of a large pull-apart basin that may have experienced some thermal subsidence after extension ceased is the Magdalen Basin (Carboniferous), approximately 100 km by 200 km, and situated in the Gulf of St. Lawrence between Newfoundland and New Brunswick (Bradley, 1982; Mann et al., 1983). From an analysis of subsidence and heat-flow data for the Vienna Basin (Miocene), Royden (1985 this volume) has shown that extension was confined to shallow crustal levels, and that the basin formed as a pull-apart between tear faults of the Carpathian nappes (Fig. 10B below). Detached or thin-skinned basins such as the Vienna Basin, also tend to be cooler during post-rift subsidence than those produced by the same amount of extension of the entire lithosphere.

Theoretical models are useful for analyzing processes of basin formation along strike-slip faults, although they are difficult to evaluate owing to the complexities of the real world. Examples of uncertainties are as follows: (1) lithospheric and crustal thickness prior to strike-slip deformation; (2) for predominantly extensional basins, the magnitude of extension, and the variation of extension with depth and from one part of a basin to another; (3) the relative contributions of lithospheric stretching and igneous intrusion in accommodating extension; (4) the manner in which complex fault geometry evolved, and the possible role in basin subsidence of flexural loading due to crustal shortening; (5) for starved basins, poor paleobathymetry; and for non-marine basins, the lack of a suitable datum from which to measure subsidence; (6) age control, particularly in non-marine basins; (7) the degree to which lithification occurred by physical compaction or by cementation of externally derived minerals; (8) the magnitudes of background heat flow and of heat production within the basin sediments; and (9) the relative contributions of vertical and lateral heat conduction, and of fluid motion in thermal history. In spite of these uncertainties, however, modelling studies have great potential when applied to areas for which there is abundant geological and geophysical data.

Recent empirical models for strike-slip basins (e.g., Aydin and Nur, 1982a; Mann et al., 1983) emphasize the mechanisms by which basins evolve along a single strike-slip fault or at fault oversteps, but no attempt has been made to improve on the qualitative models of Crowell (1974a, b) for more complicated basins involving intersecting strike-slip faults and significant block rotation. In spite of notable improvements in palinspastic reconstructions for orogenic belts, such restorations are commonly difficult to undertake in individual basins, which may have been deformed and dislocated by subsequent strike slip.

### *Geophysical, Stratigraphic, and Sedimentological Data From Strike-Slip Basins*

Seismic-reflection profiles provide an important tool for basin analysis, augmenting seismic refraction, gravity, and magnetic data, which suggest only the broadest features of basin geometry. Where outcrops and wells or boreholes are few, reflection data, calibrated by available information from wells, are indispensible in developing time-stratigraphy and determining the internal geometry of the basin fill (Vail et al., 1977), and they can provide important insights into the large-scale relations between structural evolution and sedimentation. During the past decade, there has been tremendous progress in techniques for the acquisition and processing of multichannel seismic data, considerable amounts of which have been obtained by industry and academic institutions in areas affected by strike-slip deformation. Unfortunately, much of this information remains relatively inaccessible to a large part of the scientific community. One exception is a series of three volumes edited by A. W. Bally (1983) that includes several seismic profiles across strike-slip zones (D'Onfro and Glagola, 1983; Harding, 1983; Harding et al., 1983; Lehner and Bakker, 1983; Roberts, 1983). In the future, data such as these, when coupled with standard field observations, should significantly improve our understanding of the development of strike-slip basins.

Deep seismic-reflection studies, such as those undertaken in a variety of tectonic settings in the United States by COCORP and CALCRUST, in Canada by LITHOPROBE, and in Europe by BIRPS, should also provide important information about the large-scale characteristics of crustal structure associated with strike slip. By running the seismic recorders for longer than in conventional seismic experiments, it is possible to obtain images of geological structure through the crust to the Moho, and into the upper mantle (White, 1985). Direct sampling of the deep crust may also be possible through programs such as Continental Scientific Drilling.

Continued refinement of the correlation between biostratigraphy, magnetostratigraphy and the numerical timescale (e.g., Armstrong, 1978; Harland et al., 1982; Palmer, 1983; Salvador, 1985) permits improved resolution of times, durations, and rates of sedimentation. Of special significance for the analysis of strike-slip basins in complex continental settings is the more precise correlation obtainable between non-marine, marginal marine and marine successions (e.g., Royden, 1985; Şengör et al., 1985, both in this volume).

Modern facies analysis has drawn attention to the numerous factors influencing basin fill, such as basin geometry and subsidence history, climate, sediment source, drainage patterns, transport and depositional mechanisms, depositional setting, and geological age. Examples of facies

655148



analysis in strike-slip basins are numerous papers in the volumes edited by Ballance and Reading (1980a) and by Crowell and Link (1982); and articles in this volume by Aspler and Donaldson (1985), Johnson (1985), Link et al. (1985), and Nilsen and McLaughlin (1985).

## STRUCTURES ALONG STRIKE-SLIP FAULTS

### *Major Characteristics*

Strike-slip faults are characterized by a linear or curvilinear principal displacement zone in map view (Fig. 3), because significant lateral displacement cannot be accommodated where there are discontinuities or abrupt changes in fault orientation without pervasive deformation within one or both of the juxtaposed blocks. For example, angular deviations of as little as 3° between 12 to 13 km-long fault segments along the southern San Andreas fault zone may be responsible for young topographic features, as well as for the spatial distribution of aseismic triggered slip (Bilham and Williams, 1985). As viewed in profile, and in places in outcrop, most prominent strike-slip faults involve igneous and metamorphic basement rocks as well as supracrustal sediments and sedimentary rocks. Such faults are commonly termed "wrench faults," particularly in the literature of petroleum geology (e.g., Kennedy, 1946; Anderson, 1951; Moody and Hill, 1956; Wilcox et al., 1973; Harding et al., 1985 this volume). Typically, they consist of a relatively narrow, sub-vertical principal displacement zone at depth, and within the sedimentary cover, of braided splays that diverge and rejoin both upwards and laterally (Fig. 4). Arrays of upward-diverging fault splays are known as "flower structures" (attributed to R. F. Gregory by Harding and Lowell, 1979), or less commonly, "palm tree structures" (terminology of A. G. Sylvester and R. R. Smith; Sylvester, 1984). Some strike-slip faults terminate at depth (or upward) against low-angle detachments that may be located entirely within the sedimentary section or involve basement rocks as well. Examples are high-angle to low-angle tear faults and lateral ramps of foreland thrust and fold belts (Dahlstrom, 1970; Butler, 1982; Royden et al., 1982; Royden, 1985 this volume), and tear faults associated with pronounced regional extension, as in the Basin and Range Province of the western United States (Wright and Troxel, 1970; Davis and Burchfiel, 1973; Guth, 1981; Wernicke et al., 1982; Stewart, 1983; Cheadle et al., 1985).

The distinction between wrench faults and tear faults according to whether they are "thick-skinned" or "thin-skinned" (e.g., Sylvester, 1984) is somewhat arbitrary. Several authors have suggested that crustal blocks and associated wrench faults in central and southern California are decoupled near the base of the seismogenic crust (10–15 km) from a deeper aseismic shear zone that accommodates mo-

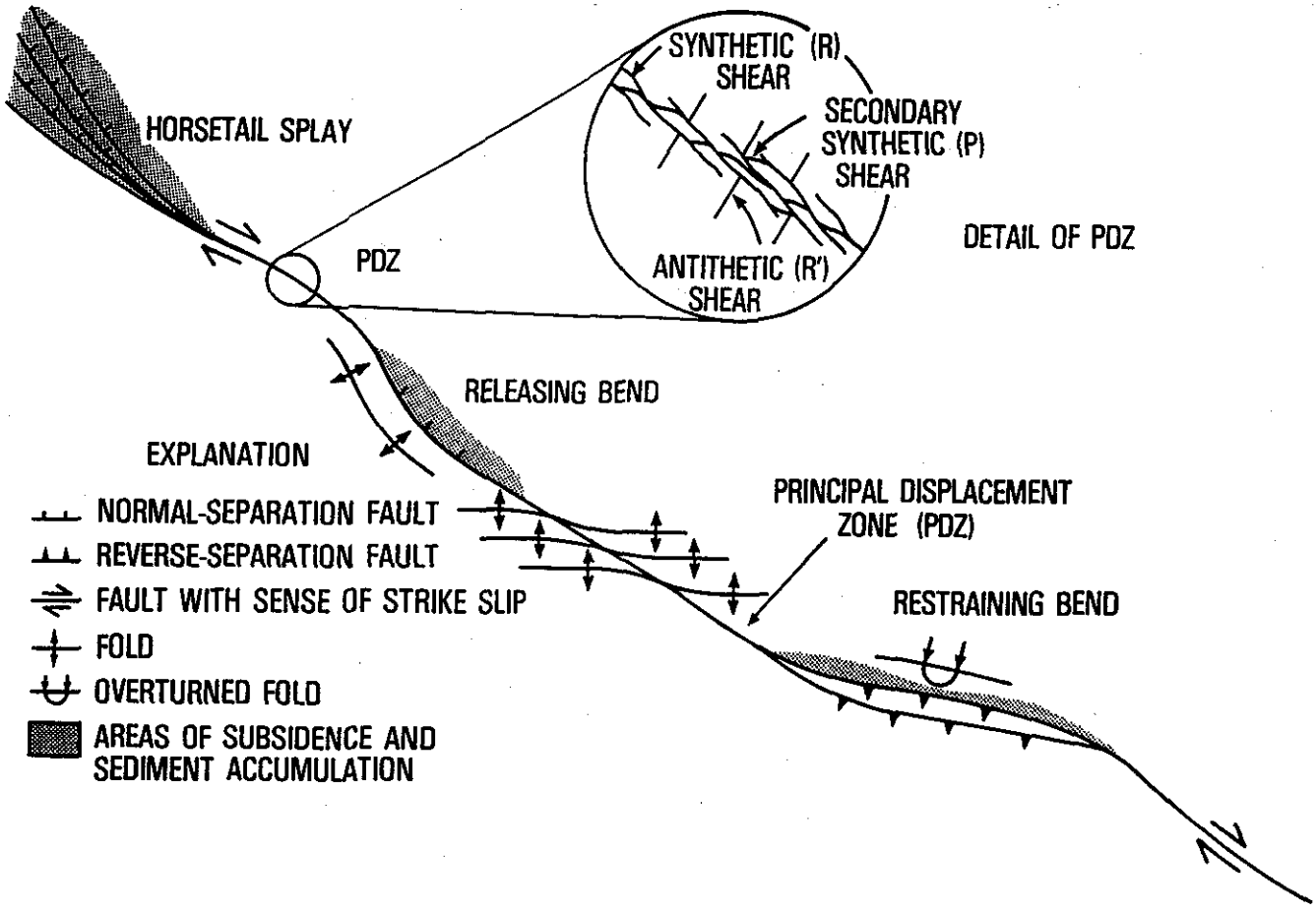
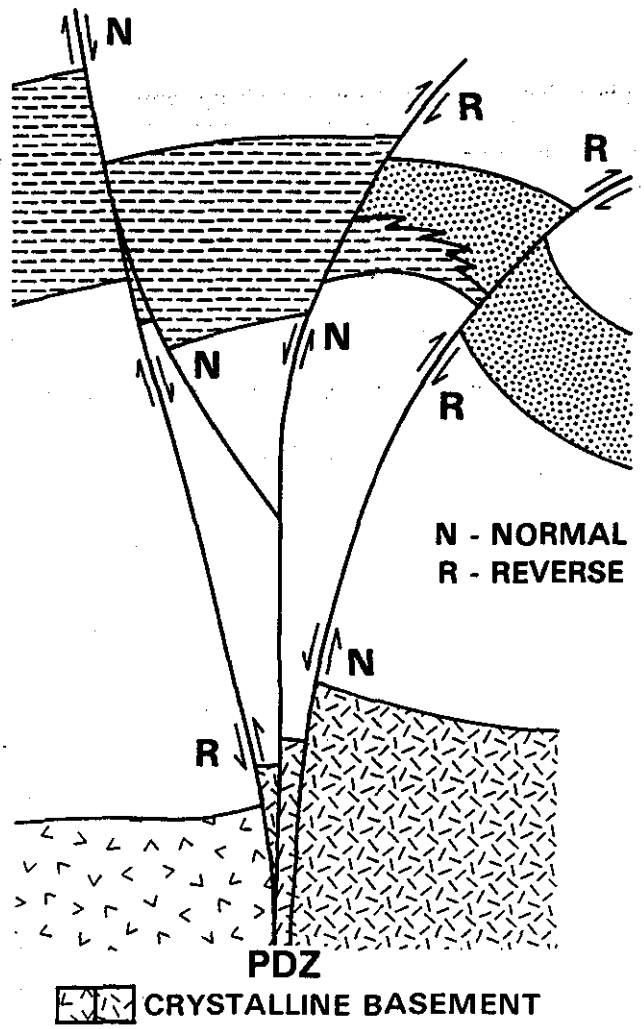



FIG. 3.—The spatial arrangement, in map view, of structures associated with an idealized right-slip fault.

655149






**MAJOR CHARACTERISTICS**

- BASEMENT - INVOLVED
- PDZ SUB-VERTICAL AT DEPTH
- UPWARD DIVERGING & REJOINING SPLAYS

**JUXTAPOSED ROCKS**

- CONTRASTING BASEMENT TYPE
- ABRUPT VARIATIONS IN THICKNESS & FACIES IN A SINGLE STRATIGRAPHIC UNIT

**SEPARATION IN ONE PROFILE**

- NORMAL- & REVERSE-SEPARATION FAULTS IN SAME PROFILE
- VARIABLE MAGNITUDE & SENSE OF SEPARATION FOR DIFFERENT HORIZONS OFFSET BY THE SAME FAULT

**SUCCESSIVE PROFILES**

- INCONSISTENT DIP DIRECTION ON A SINGLE FAULT
- VARIABLE MAGNITUDE & SENSE OF SEPARATION FOR A GIVEN HORIZON ON A SINGLE FAULT
- VARIABLE PROPORTIONS OF NORMAL- & REVERSE-SEPARATION FAULTS

TIME-STRATIGRAPHIC UNIT WITH VARIABLE SEDIMENTARY FACIES

FIG. 4.—The major characteristics, in transverse profile, of an idealized strike-slip fault.

tion between the Pacific and North American plates (e.g., Hadley and Kanamori, 1977; Lachenbruch and Sass, 1980; Yeats, 1981; Hill, 1982; Crouch et al., 1984; Turcotte et al., 1984; Nicholson et al., 1985a, b; Webb and Kanamori, 1985). Recent COCORP seismic reflection profiling in California suggests that the Garlock fault, long recognized as both a major wrench zone (Moody and Hill, 1956) and a tear fault bounding an extensional allochthon (Davis and Burchfiel, 1973; Burchfiel et al., 1983), may terminate downwards against a mid-crustal (9–21 km), low-angle reflecting horizon (Cheadle et al., 1985).

A prominent feature of many strike-slip faults is the occurrence of "en echelon" faults and folds within and adjacent to the principal displacement zone (Figs. 3, 5). The term en echelon refers to a stepped arrangement of relatively short, consistently overlapping or underlapping structural elements that are approximately parallel to each other, but oblique to the linear zone in which they occur (Biddle and Christie-Blick, 1985a this volume; modified from Goguel, 1948, p. 435; Cloos, 1955; Campbell, 1958; Harding and Lowell, 1979). En echelon has also been used for oblique elements extending tens or even hundreds of kilometers from a principal displacement zone (e.g., Wilcox et al., 1973), where it is doubtful that they have much to do with strike-slip deformation (see Harding et al., 1985 this volume), and in several classic papers on thrust and fold belts for inconsistently overlapping elements arranged parallel to a zone of deformation (e.g., Rodgers, 1963; Gwinn, 1964; Armstrong, 1968; Fitzgerald, 1968; Dahlstrom, 1970). We prefer to describe the latter as a "relay" arrangement (Harding and Lowell, 1979), because it is geometrically different and because it characterizes distinctly different tectonic regimes, those associated with regional extension or with regional shortening rather than with strike slip (Harding and Lowell, 1979; Harding, 1984).

In strike-slip regimes, we also distinguish between en echelon arrangements of structures along a given principal displacement zone, and oversteps between different segments of the principal displacement zone ("en relais" of Harris and Cobbold, 1984; Biddle and Christie-Blick, 1985a this volume). Solitary oversteps (Guiraud and Seguret, 1985 this volume) and many multiple oversteps (Biddle and

655150



Christie-Blick, 1985a this volume) do not constitute a linear zone and by our definition are not en echelon. This is not simply a matter of scale or semantics. Oversteps between different segments and en echelon structures (our usage) appear to have different origins (Aydin and Nur, 1985 this volume; see discussion below). We note, however, that there is no general agreement about such distinctions.

Idealized en echelon arrangements, such as those shown in Figure 3, are reproduced most closely in model studies involving clay, unconsolidated sand, sheets of paraffin wax, Plasticine, or wet tissue paper (Riedel, 1929; Cloos, 1955; Pavoni, 1961; Emmons, 1969; Morgenstern and Tchalenko, 1967; Tchalenko, 1970; Wilson, 1970; Lowell, 1972; Wilcox et al., 1973; Courtillot et al., 1974; Freund, 1974; Mandl et al., 1977; Graham, 1978; Groshong and Rodgers, 1978; Rixon, 1978; Gamond, 1983; Odonne and Vialon, 1983; Harris and Cobbold, 1984), in the experimental deformation of homogeneous rock samples under confining pressure (Logan et al., 1979; Bartlett et al., 1981), and in the deformation of alluvium during large earthquakes (Tchalenko, 1970; Tchalenko and Ambraseys, 1970; Clark, 1972, 1973; Sharp, 1976, 1977; Philip and Megard, 1977). Five sets of fractures are commonly observed (Fig. 5): (1) synthetic strike-slip faults or Riedel (R) shears; (2) antithetic strike-slip faults or conjugate Riedel (R′) shears; (3) secondary synthetic faults or P shears; (4) extension or tension fractures (see Biddle and Christie-Blick, 1985a this volume); and (5) faults parallel to the principal displacement zone, or Y shears of Bartlett et al. (1981). In experimental deformation of Indiana limestone, Bartlett et al. (1981) have also described what they call X shears (not shown in Fig. 5). These are symmetrical with R′ in relation to the principal displacement zone. The sense of offset for R and P shears is the same as that of the principal displacement zone, whereas R′ and X shears have the opposite sense of offset. The approximate orientation at which faults and associated folds develop under simple conditions is indicated in Figure 5. For the right-slip system illustrated, folds, P shears and X shears are right-handed (Campbell, 1958; Wilcox et al., 1973; Biddle and Christie-Blick, 1985a this volume), whereas R shears, R′ shears and extension (tension) fractures are left-handed. As discussed below, however, geological examples tend to be more complicated, and even in the case of Holocene deformation (Fig. 7 below), observed arrangements of structures do not necessarily conform to those predicted by models or experiments. This is because rocks are heterogeneous, because structures develop sequentially rather than instantaneously, and because early-formed structures tend to be rotated during protracted deformation. The structural style is also affected by even a small component of extension or shortening across the principal displacement zone (Wilcox et al., 1973; Harding et al., 1985 this volume), a circumstance that favors fault-parallel folds rather than en echelon ones.

In addition to the occurrence of flower structures, strike-slip faults exhibit several characteristics in profile that result in part from the segmentation of wedge-shaped sediment or rock bodies with laterally variable facies, and in part from a component of convergence or divergence across different fault strands (Fig. 4). Examples are (1) the presence in a given profile across the principal displacement zone of both normal- and reverse-separation faults, and of variable proportions of normal and reverse faults in different profiles; (2) the tendency in a single profile for the magnitude and sense of separation of a given fault splay to vary from one horizon to another; and (3) the tendency in successive profiles for a given fault to dip alternately in one direction and then in the opposite direction, and to display variable separation (both magnitude and sense) for a single horizon.

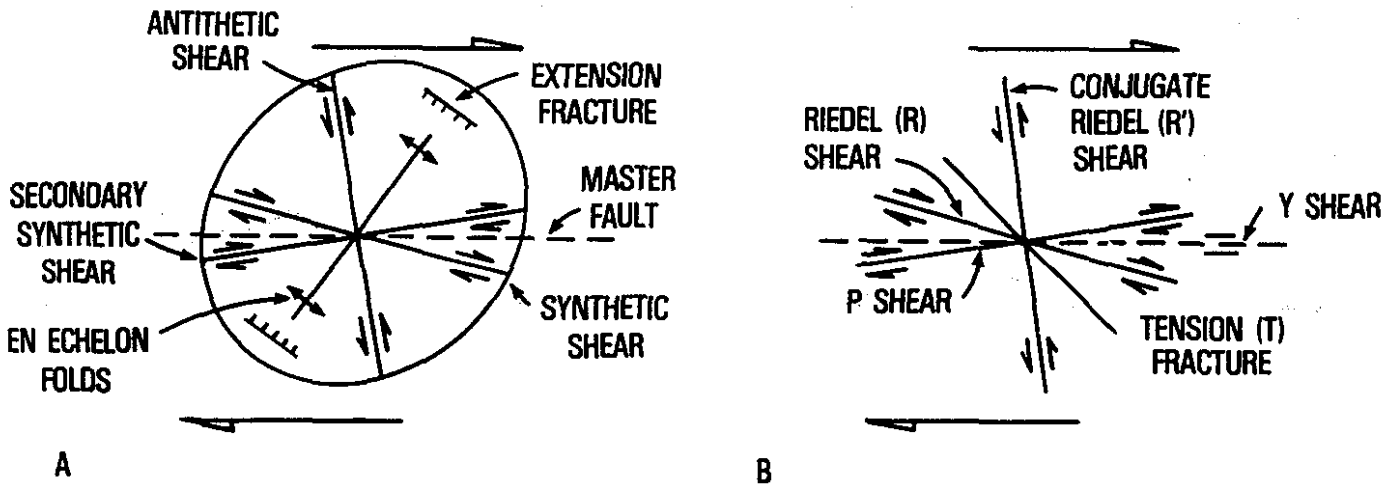



FIG. 5.—*The angular relations between structures that tend to form in right-lateral simple shear under ideal conditions, compiled from clay-cake models and from geological examples. Arrangements of structures along left-slip faults may be determined by viewing the figure in reverse image.* A) Terminology largely from Wilcox et al. (1973), superimposed on a strain ellipse for the overall deformation. B) Reidel shear terminology, modified from Tchalenko and Ambraseys (1970) and Bartlett et al. (1981). Extension fractures form when effective stresses are tensile (i.e., when pore-fluid pressure exceeds lithostatic pressure); tension fractures form when lithostatic loads become negative (J. T. Engelder, personal commun., 1985). In geological examples, faults with normal separation tend to develop parallel to the orientation of the extension and tension fractures in A and B; faults with reverse separation tend to develop parallel to the orientation of the fold in A. See text for further discussion of structures along strike-slip faults.

655151



On a regional scale, distinctive aspects of strike-slip structural style are evidence for simultaneous shortening and extension, and for random directions of vergence in associated thrusts and nappes (e.g., Heward and Reading, 1980; Miall, 1985 this volume).

### *Controls on Structural Patterns*

The main controls on the development of structural patterns along individual continental strike-slip faults are (1) the degree to which adjacent blocks either converge or diverge during strike-slip; (2) the magnitude of displacement; (3) the material properties of the sediments and rocks being deformed; and (4) the configuration of pre-existing structures. Each of these factors tends to vary along any given fault, and, except for the last, to change through time. Individual faults are commonly elements of broader regions of deformation, particularly along major intracontinental transform zones, and different faults may be active episodically at different times as a result of block rotation or the reorganization of block boundaries. Structural style may also be influenced directly by the rotation of small blocks that can produce segments of relative convergence and divergence even along straight strike-slip faults (Fig. 6), where adjacent blocks are for the most part neither converging nor diverging. The material properties of the sediments and rocks being deformed tend to change with time where, for example, strike slip is accompanied by sedimentation, so that sediments formerly near the surface become progressively more deeply buried; or where strike slip is accompanied by uplift, so that once buried strata are brought closer to the surface (as in the familiar mechanism of Karig, 1980, for raising "knockers" from great depths in accretionary prisms). Pre-existing structures can markedly influence the location and orientation of strike-slip faults, or simply complicate the overall structural pattern without being reactivated during strike-slip deformation.

*Convergent, Divergent and Simple Strike-Slip Faults.*—The terms "convergent wrench fault" and "divergent wrench fault" were introduced by Wilcox et al. (1973) to describe basement-involved strike-slip fault zones that, judging from the proportions of reverse-separation and normal-separation faults along and adjacent to the principal displacement zone, are thought to involve a significant component of shortening or extension, respectively. Convergent and divergent thus imply much the same as transpressional and transtensional of Harland (1971), although they refer to kinematics rather than to stress, and are for this reason preferred. We note that the use of these terms in the context of deformational process, rather than for description alone, presupposes that strike slip and transverse shortening or extension occurred simultaneously, not sequentially. In some cases, it may be difficult to make such distinctions. Faults along which there is no evidence for preferential convergence or divergence were described by Wilcox et al. (1973) as "simple parallel wrench faults," by Harding and Lowell (1979) as "side-by-side wrench faults," and by Mann et al. (1983) as "slip-parallel faults." Here, we use the term "simple strike-slip fault" in order to avoid confusion with a geometrical pattern in which a number of faults are actually parallel to each other or arranged side-by-side, and because for any fault, slip is by definition parallel with the fault surface (see Biddle and Christie-Blick, 1985a this volume).

In comparison with simple strike slip, convergent strike slip leads to the development not only of abundant reverse faults, including low-angle thrust faults, but also of folds that are arranged both en echelon and parallel to the principal displacement zone (Fig. 3; Lowell, 1972; Wilcox et al., 1973; Sylvester and Smith, 1976; Lewis, 1980; and in this volume, Anadón et al., 1985; Mann, et al., 1985; Şengör et al., 1985; Steel et al., 1985). In cases of pronounced convergence, as in the western Transverse and Coast Ranges of California (WTR and CR in Fig. 1), the structural style becomes similar to that of a thrust and fold belt (Nardin and Henyey, 1978; Suppe, 1978; Yeats, 1981, 1983; Crouch et al., 1984; Davis and Lagoe, 1984; Wentworth et al., 1984; Namson et al., 1985). In contrast, along divergent strike-slip faults, folds are less well developed, and commonly consist of flexures arranged parallel rather than oblique to the principal displacement zone, although both types are known (Fig. 3; Wilcox et al., 1973; Nelson and Krausse, 1981; Harding et al., 1985 this volume).

Flower structures develop along both convergent strike-slip faults (Allen, 1957, 1965; Wilcox et al., 1973; Sylvester and Smith, 1976; Harding and Lowell, 1979; Harding et al., 1983; Harding, 1985), where they are associated with prominent antiforms and known as positive flower structures, and along divergent faults, where they are associated with synforms and termed negative (D'Onfro and Glagola, 1983; Harding, 1983, 1985; Harding et al., 1985 this volume). The occurrence of upward-diverging fault splays is thus not due essentially to convergence but to the propagation of faults upward through the sedimentary cover toward a free surface (Allen, 1965; Sylvester and Smith, 1976), an interpretation confirmed in experimental studies with unconsolidated sand (Emmons, 1969) and with homogeneous rock samples under confining pressure (Bartlett et al., 1981).

Strike-slip faults may be characterized by convergence or divergence for considerable distances (Namson et al., 1985; Harding et al., 1985 this volume), or only locally at restraining and releasing bends, fault junctions, and oversteps (Crowell, 1974b; Aydin and Nur, 1982b; Mann et al., 1985 this volume). Shortening and extension can occur simultaneously at oversteps associated with block rotation. A small-scale example is provided by a set of left-stepping en echelon R shears formed in a newly seeded carrot field during the Imperial Valley, California, earthquake of 15 October, 1979 (Fig. 6A; Terres and Sylvester, 1981). Elongate blocks of soil separated along furrows, became detached from the less rigid subsoil (a "Riedel flake" of Dewey, 1982), and rotated as much as 70°. The complex pattern of fractures, faults, folds and buckles, and gaps is related to motion on individual blocks. Şengör et al. (1985 this volume) describe an analogous rotated flake more than 70 km long, along the North Anatolian fault. Block rotation may also produce local convergence and divergence along relatively straight fault segments (Fig. 6B; Dibblee, 1977; Nicholson et al., 1985a, b). From an analysis of earthquake hypocentral locations and first-motion studies near the intersection of the San Andreas and San Jacinto faults, California, Ni-

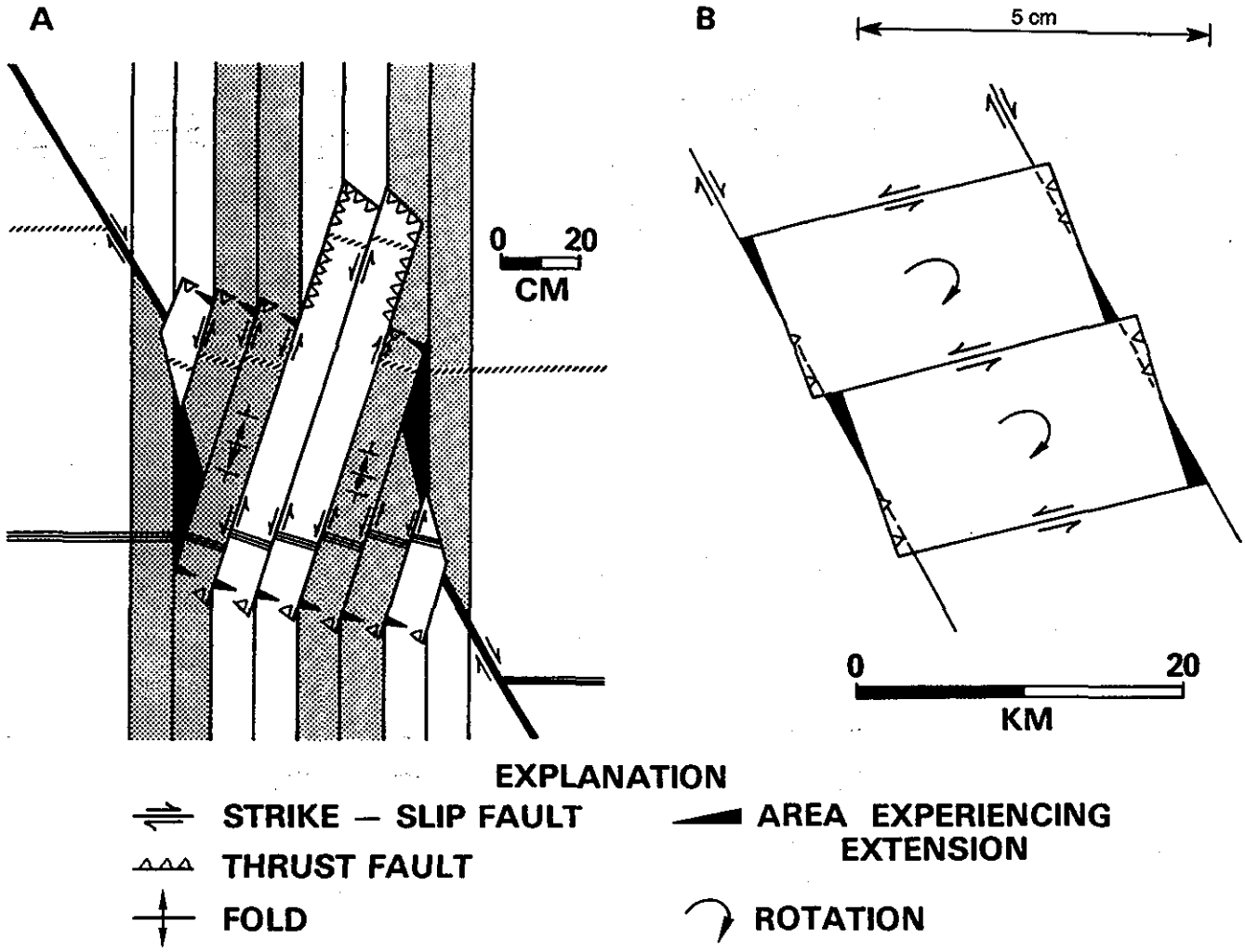



FIG. 6.—A) Geometric model illustrating the development of fractures, faults, folds and buckles, and gaps observed in a surface rupture in the Imperial Valley, California (1 in Fig. 1), following the earthquake of 15 October, 1979 (from Terres and Sylvester, 1981). The spaced parallel ruling represents the furrows in a newly seeded carrot field.

B) A model for the rotation of blocks near the intersection of the San Andreas and San Jacinto faults, California, from earthquake hypocentral locations and first-motion studies (from Nicholson et al., 1985a, b; and similar to a figure of Dibblee, 1977). During a large earthquake, there is right slip on one of the major bounding faults; during the inter-seismic interval, the major faults are locked, and right-lateral motion is taken up by clockwise rotation of small blocks, and by minor left-slip faults. Incompatible motion at the corners of blocks leads to the development of normal and reverse fault segments, which alternate along the major right-slip faults. If such a non-elastic process were to continue on a geological timescale, it would produce complex wedge-shaped basins in areas subject to extension, and crustal flakes detached above thrust faults merging with the right-slip faults.

cholson et al. (1985a, b) have shown that incompatible motion at the corners of blocks leads to the development of normal- and reverse-fault segments, which alternate along the major right-slip faults.

*Displacement Magnitude.*—Experimental work, sub-surface studies and field observations indicate that structural style along strike-slip faults is influenced qualitatively by the magnitude of displacement (Wilcox et al., 1973; Harding, 1974; Harding and Lowell, 1979; Bartlett et al., 1981). In experiments, folds and shear fractures tend to form sequentially, although not in the same abundance or in the same order for all materials under all conditions (Wilcox et al., 1973; Bartlett et al., 1981). In clay models, for example, folds and Riedel shears develop first, followed by P shears, and finally by the development of a relatively narrow through-going principal displacement zone (Morgenstern and Tchalenko, 1967; Tchalenko, 1970; Wilcox et al., 1973). In experiments with rock samples under confining pressure, R and P shears develop concurrently, and R shears tend to propagate toward the orientation of the principal displacement zone with increasing displacement (Bartlett et al., 1981). R′ and X shears form at this latter stage. The simultaneous development of both R and P shears cannot be explained by the Coulomb-Mohr failure criterion. The width of the zone of deformation increases rapidly during the initial development of folds and fractures, but tends to stabilize quickly because weakening of the sheared material leads to the concentration of subsequent deformation (Odonne and Vialon, 1983). Early-formed structures tend to rotate during progressive deformation (Tchalenko, 1970;

655153



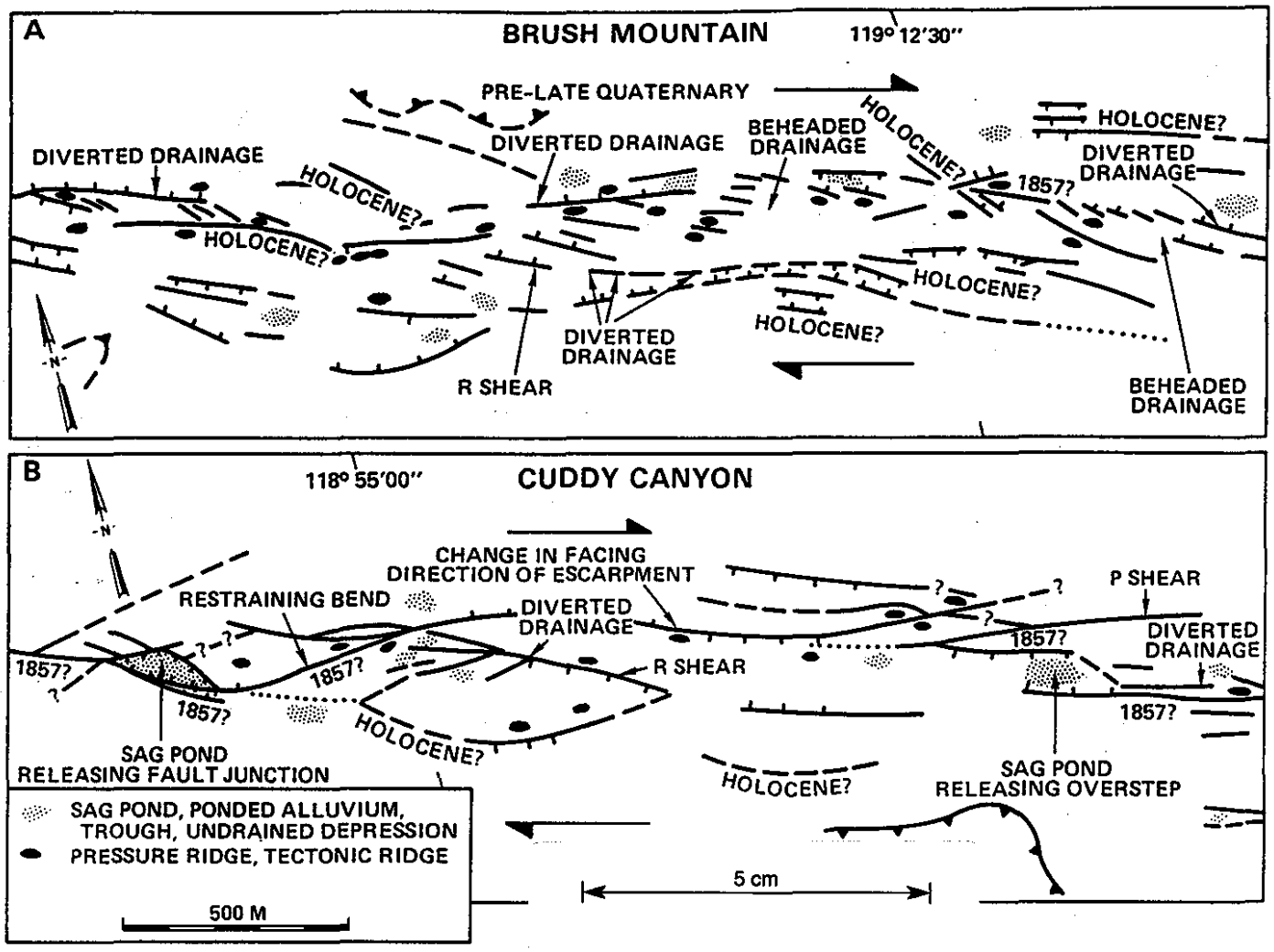



FIG. 7.—Holocene faults and tectonic landforms along the "big bend" of the San Andreas fault, California, A) south of Brush Mountain, and B) in Cuddy Canyon, east of Frazier Park (simplified from T. Davis and E. Duebendorfer, unpublished mapping, 1981, with permission from the authors; see Fig. 1 for location). Hachures on topographically lower side of fault traces; sawteeth on upper plate of thrust faults. The maps indicate the structural complexity that can develop in a few thousand years along a major strike-slip fault. The sediments at the surface are largely of Neogene and Quaternary age (A) and Quaternary age (B). The stipple pattern indicates the sites of basins (sag ponds, ponded alluvium, troughs, undrained depressions); elliptical black dots indicate elevated blocks (pressure ridges, tectonic ridges). Except for a few obvious examples of basins at releasing fault junctions or releasing oversteps, at the scale of these examples, there is no obvious relation between sites of sedimentation and fault geometry.

Wilcox et al., 1973; Rixon, 1978; Odonne and Vialon, 1983), particularly R′ shears, initially oriented at a high angle to the principal displacement zone. Thus the final orientations of folds and faults depend on the magnitude of displacement and on the time at which these structures formed during the deformation history.

Many of these features documented in experiments, can also be observed in geological examples. For instance, strike-slip faults with small lateral displacement in the basement are generally expressed within the sedimentary cover by discontinuous faults and folds (e.g., the Newport-Inglewood fault zone of the Los Angeles Basin with right slip of about 200 to 750 m; Harding, 1974). At the same scale, faults with large displacement (such as the San Andreas) consist of a through-going principal displacement zone (see Fig. 5 of Harding and Lowell, 1979). One difference, however, between experiments and natural examples is that in nature, deformation is commonly accompanied by sedimentation, so that younger sediments record less offset than older ones. Faults within Holocene alluvium along the San Andreas fault zone tend to be discontinuous (Fig. 7; from T. Davis and E. Duebendorfer, unpublished mapping, 1981). Figure 7 also illustrates the rate at which structural complexities can arise. Given an immensely longer geological timescale, and the fact that rocks and sediments are heterogeneous even before deformation, we should not be surprised if the orientation and geometry of observed structures along a given strike-slip fault depart significantly from those predicted by idealized strain ellipse summaries (Fig. 5). This is of considerable importance to the petroleum geologist constructing structure maps for a prospective exploration target from limited data. Idealized models are useful, but they should be applied with caution. That such models commonly "match" geological observations is in part due

655154



to the large number of different fault orientations available (Fig. 5), and interpretations based on such comparisons are not necessarily correct. In addition, the absence of a simple strike-slip structural style does not eliminate the possibility that strike slip played a major role in the deformation.

*Material Properties.*—The character of a given strike-slip fault zone is also a function of the lithology of the juxtaposed rocks, the confining pressure, fluid pressure, and temperature conditions at which deformation occurred, and the rates of strain and recovery (Donath, 1970; Mandl et al., 1977; Sibson, 1977; Logan, 1979; Logan et al., 1979; Ramsay, 1980; Bartlett et al., 1981; Wise et al., 1984). These factors are likely to change during continuing strike-slip deformation as a result of lateral variations in depositional facies, or through sedimentation and burial, uplift and erosion, changes in provenance, or changes in heat flow.

Though difficult to predict, fault-zone characteristics are of significance to petroleum geologists because they influence the tendency of faults to behave as either conduits or barriers to fluid migration. Depending on the conditions of deformation, the accumulation of displacement along a fault may be accompanied by the development of gouge, which can act as a barrier to fluid migration (e.g., Pittman, 1981). However, displacement may also promote fracturing and additional avenues for leakage. As with other faults, strike-slip faults may juxtapose rocks with significantly different permeability, thus forming either seals or conduits for the migration of petroleum across the fault surface (see Downey, 1984, for a general treatment of hydrocarbon seals).

*Pre-existing Structures.*—In regions where strike-slip faults are present, pre-existing structures are of two kinds, "essential" and "incidental." As applied to the analysis of strike-slip deformation, essential structures are defined here as those which significantly influence the location and orientation of faults and folds during strike slip. Incidental structures are inherited and contribute little to that deformation. Both types of structure are elements of the overall structural pattern of the region, but incidental ones should be excluded from the analysis strike-slip structural style.

Essential structures commonly influence patterns of strike-slip deformation on the continents. The process can be observed today in the Upper Rhine graben (Fig. 8), formed by extension in middle Eocene to early Miocene time in response to Alpine deformation (Illies, 1975; Illies and Greiner, 1978; Şengör et al., 1978). In Pliocene to Holocene time, normal faults parallel to the graben were reactivated as strike-slip faults during uplift of the Alps. Earthquake first-motion studies suggest that much of the current deformation is due to left slip (Fig. 8; Ahorner, 1975), and this sense of displacement is consistent with measurements of in-situ stress (Illies and Greiner, 1978). Other examples of essential structures are discussed in this volume by Cemen et al. (1985), Harding et al. (1985), Mann et al. (1985), Royden (1985), Şengör et al. (1985), and Zalan et al. (1985). In the oceans, the location of some major transform faults is controlled by weaknesses within the continents prior to continental separation (e.g., the Atlantic equatorial megashear zone; Bonatti and Crane, 1984; Zalan et al., 1985 this volume).

Some basement-involved folds in the Death Valley area, southeastern California, illustrate the concept of incidental pre-existing structures (Figs. 1, 9). Central Death Valley developed in late Miocene through Holocene time as an east-tilted half graben bounded to the north and south by northwest-striking right-slip faults (the northern Death Valley–Furnace Creek fault zone and the southern Death Valley fault zone; Stewart, 1983). Although the type example of a pull-apart basin (Fig. 9B; Burchfiel and Stewart, 1966; Mann et al., 1983), Death Valley is not a particularly good example, because it is only one of many grabens in the Basin and Range Province that formed in response to late Cenozoic regional extension, not as a result of a bend or an overstep in a strike-slip fault (see reviews of the Basin and Range Province by Stewart, 1978; Eaton, 1982; and Fig. 1 of Cemen et al., 1985 this volume). The strike-slip faults appear to be tear faults within an extensional allochthon separating areas that experienced different amounts of extension (Wright and Troxel, 1970; Wernicke et al., 1982; Stewart, 1983). There is no evidence for strike slip within and parallel to the *central* segment of Death Valley (Wright and Troxel, 1970), although the basin undoubtedly opened obliquely, as shown in Figure 9B, and is at present extending in an approximately northwest-southeast direction (Sbar, 1982). Such a strike-slip fault was shown on an earlier map by Hill and Troxel (1966; trend $S_1$ in the strain ellipse insert of Fig. 9A), and reproduced by Mann et al. (1983). Evidence cited to support that interpretation, in addition to the presence of oblique striae on fault surfaces in the Black Mountains, consists of spectacular northwest-plunging folds within the basement (trend A in Fig. 9A). Hill and Troxel (1966) described the folds as en echelon, but regional arguments, including evidence for the pressure and temperature conditions at the time of folding, suggest that they are probably incidental oblique structures predating strike-slip deformation. Folds with similar orientation are present in metamorphic rocks of both the Panamint Range, west of central Death Valley, and in the Funeral Mountains, north of (and approximately parallel to) the northern Death Valley-Furnace Creek fault zone. Metamorphism in the Funeral Mountains occurred, probably in late Mesozoic time, at a temperature of 600° to 700° C, and at a pressure of 7.2 to 9.6 kb (Labotka, 1980). In the Panamint Range, folding occurred at 70 to 80 Ma during retrograde metamorphism, and at a temperature of about 450° C, following prograde metamorphism at 400° to 700° C (Labotka, 1981; Labotka and Warasila, 1983). These metamorphic conditions and the age of folding inferred in the Panamint Range are incompatible with the Miocene and younger tectonic denudation that accompanied strike-slip deformation in the Death Valley area (see Cemen et al., 1985 this volume). Although low-angle normal faults follow the top of the basement, the folds themselves are incidental structures.

## BASINS ALONG STRIKE-SLIP FAULTS

Some basins along strike-slip faults developed as a direct response to strike-slip deformation. Others owe their origin to a different tectonic regime, in which strike slip played only a subsidiary role in basin development. Examples of

655155



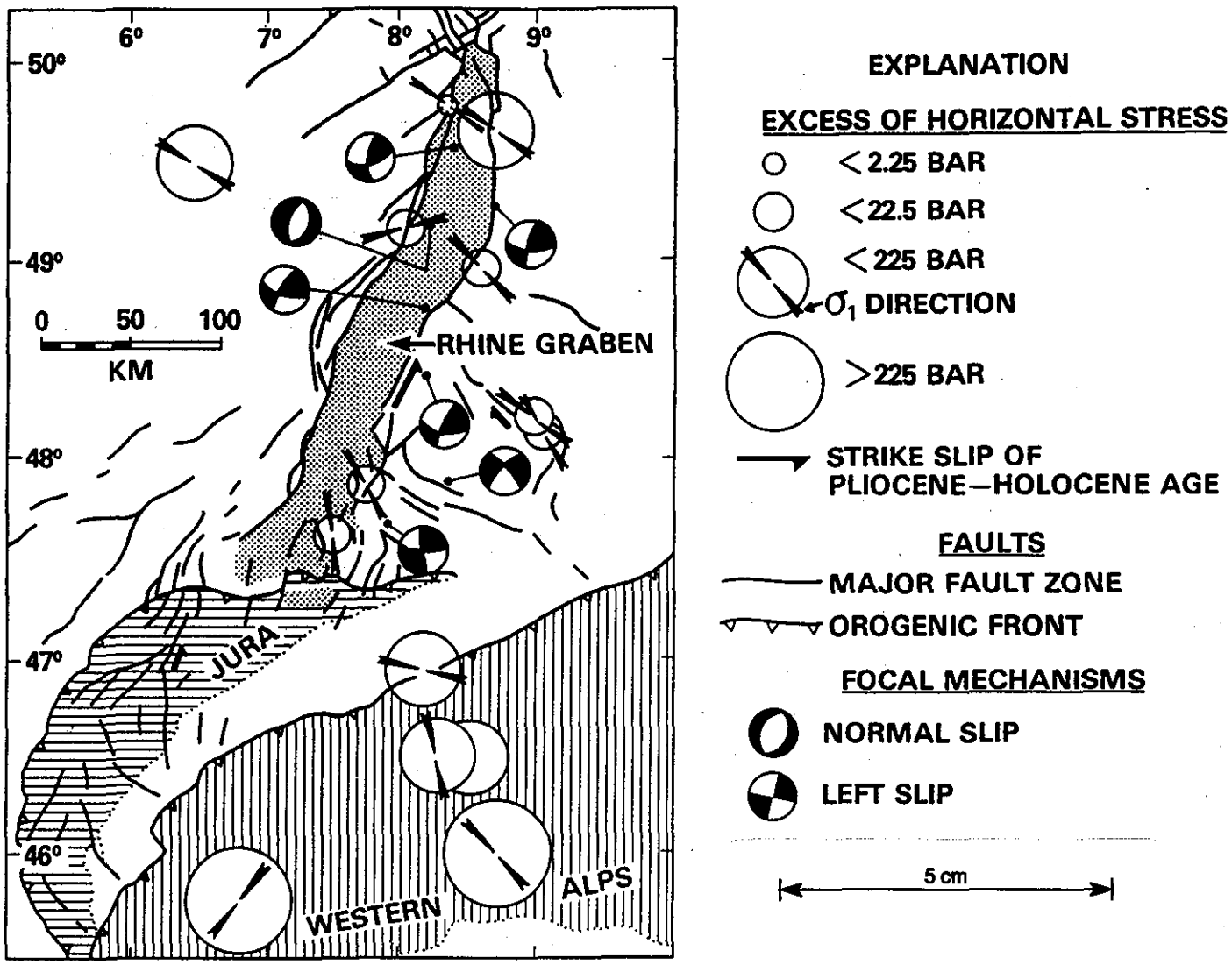



FIG. 8.—The Rhine graben and adjacent segments of the Jura and western Alps; with selected examples of the excess horizontal stress from in situ determinations; and earthquake focal mechanisms (modified from Ahorner, 1975; Illies and Greiner, 1978). Normal faults of Eocene to Miocene age were reactivated as left-slip faults in Pliocene to Holocene time, during uplift of the Alps.

the latter are (1) some intracontinental grabens, foreland basins, and forearc basins associated with strike-slip faults, which though active during sedimentation, had little influence on sedimentation patterns; and (2) various basins that were subsequently reactivated by strike-slip deformation. Basins of these types are considered here only to the extent that the geology is related to strike-slip deformation.

One of the most obvious characteristics of a strike-slip basin is its present geometry in map view, particularly the geometry of any bounding faults, and this has been a useful point of departure for various classification schemes and for most discussions about processes of basin formation (Carey, 1958; Kingma, 1958; Lensen, 1958; Quennell, 1958; Burchfiel and Stewart, 1966; Clayton, 1966; Belt, 1968; Freund, 1971; Crowell, 1974a, b, 1976; Ballance, 1980; Aydin and Nur, 1982a, b; Burke et al., 1982; Crowell and Link, 1982; Fralick, 1982; Mann and Burke, 1982; Mann et al., 1983; Mann and Bradley, 1984; see glossary in Biddle and Christie-Blick, 1985a this volume). However, with the exception of very young sedimentary accumulations, the geometry, location, and perhaps orientation of a given basin have undoubtedly changed with time, and some prominent faults may be younger than much of the sedimentary fill. In many cases, present geometry may thus provide only limited information about either the kinematic history or the ultimate controls on basin evolution, and the utility of some of the classification schemes is questionable.

In this section, we focus on processes of basin formation, on the tectonic setting of depositional sites, and on certain distinctive characteristics of the stratigraphic record along strike-slip faults. We emphasize as others have before (Bally and Snelson, 1980) that every basin has a unique history, and that simple models may provide only a superficial summary of basin development. No strike-slip basin can be considered thoroughly understood unless its history can be reconstructed by a series of well-constrained palinspastic

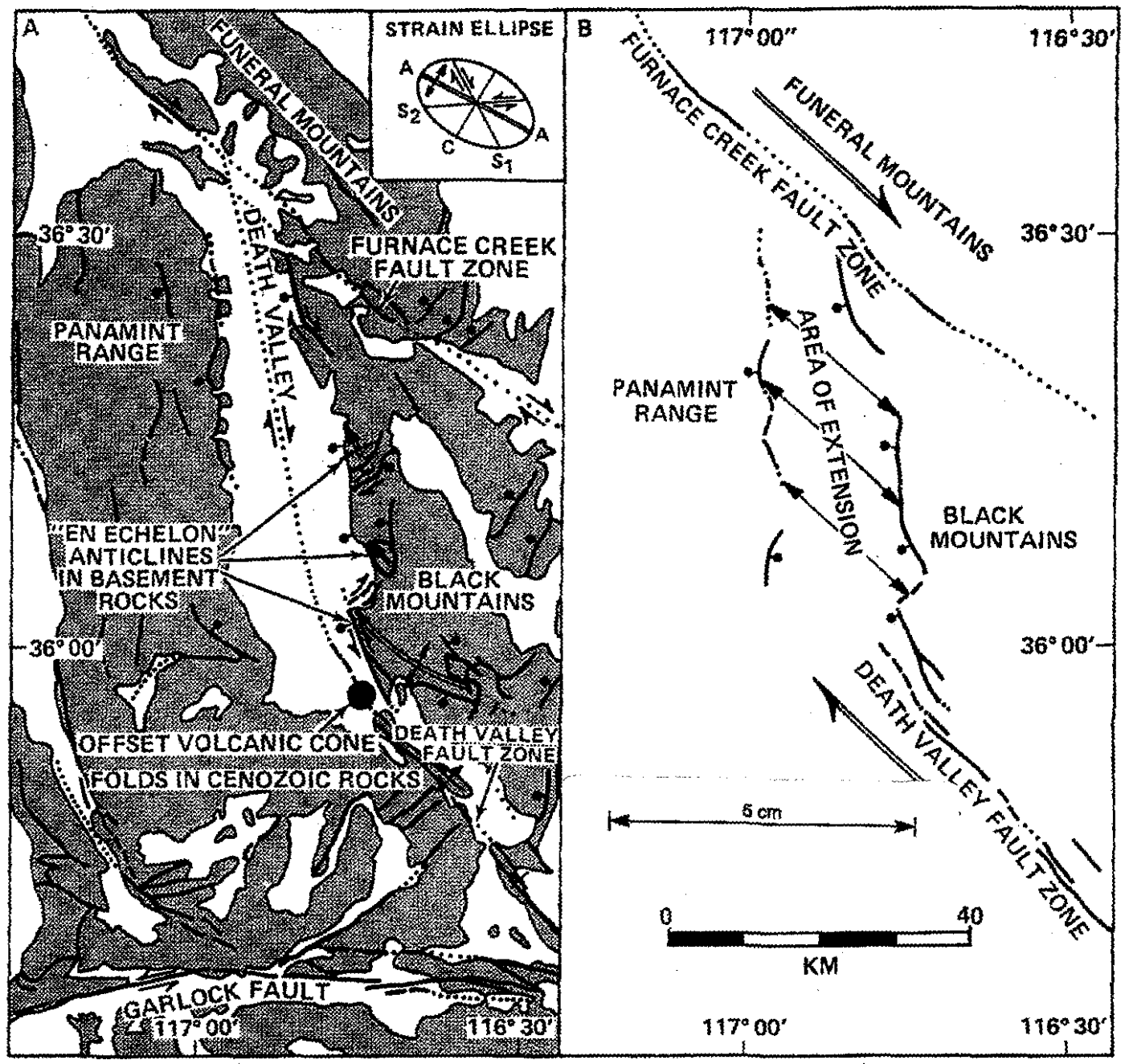



FIG. 9.—Major fault zones in the Death Valley area, California (modified from Stewart, 1983; see Fig. 1 for location), showing the interpretations of A) Hill and Troxel (1966), and B) Burchfiel and Stewart (1966). Shading (A) indicates outcrops of Proterozoic to Tertiary sedimentary and volcanic rocks; unshaded area represents Quaternary alluvial deposits. Evidence for strike slip along the northern Death Valley-Furnace Creek and southern Death Valley fault zones includes en echelon folds in Cenozoic rocks and an offset volcanic cone, together with regional stratigraphic arguments.

A) A buried strike-slip fault is inferred in the central north-trending segment of Death Valley on the basis of oblique striae on fault surfaces in the Black Mountains, and of "en echelon" anticlines in basement rocks (Hill and Troxel, 1966). The insert compares the orientations of observed structures with an idealized strain ellipse for the overall deformation; right slip inferred parallel to direction C is incompatible with orientations summarized in Figure 5.

B) Death Valley interpreted as a pull-apart along an oblique segment of a strike-slip fault system (Burchfiel and Stewart, 1966). Indicators of crustal stress and regional seismicity indicate continued extension in an approximately northwest-southeast direction parallel with the Furnace Creek and southern Death Valley fault zones (Sbar, 1982). See text for further explanation.

[redacted]

655157



maps. Many of the examples discussed are taken from California, a classic region with which we are most familiar, but where appropriate, we draw attention to articles in this volume dealing with strike-slip basins in other parts of the world.

### *Processes of Basin Formation*

Sedimentary basins form along strike-slip faults as a result of localized crustal extension, and especially in zones of continental convergence, of localized crustal shortening. Individual basins vary greatly in size (e.g., Aydin and Nur, 1982a; Mann et al., 1983), but they tend to be smaller than those produced by regional extension (many intracontinental grabens) or regional shortening (foreland and forearc basins). In addition, a given basin may alternately experience both extension and shortening on a timescale of thousands to millions of years, through variations in the motion of adjacent crustal blocks (e.g., the Ventura Basin, California, Fig. 15 below; and in this volume, Miall, 1985; Nilsen and McLaughlin, 1985; Steel et al., 1985); or extension in one direction (or in one part of the basin) may be accompanied by shortening in another direction (or in another part of the basin). A possible example of the latter is the occurrence of positive flower structures in the Mecca Hills on the northeastern side of the Salton Trough, southern California, a basin that can be related to extension in a northwestward direction in the overstep between the San Andreas and Imperial faults (Fig. 1; Sylvester and Smith, 1976; Crowell, 1981b; Fig. 6 of Harding et al., 1985 this volume). The directions of extension and shortening also tend to vary within a given basin and to change through time, especially where crustal blocks rotate (as seen on a small scale in Fig. 6 A), where there are significant differences in the rate of internal strain of adjacent crustal blocks (see Figs. 10, 11, and 12 of Şengör et al., 1985 this volume), or when there are changes in lithospheric plate motion.

In the simplest strike-slip basins (e.g., the "pull-apart hole" and "sharp pull-apart basin" of Crowell, 1974a, b), the bounding blocks are torsionally rigid and deform only at their edges, and subsidence is due to extension only in a direction parallel to the regional strike of the fault(s). Examples include many small pull-apart basins (Aydin and Nur, 1982a; Mann et al., 1983), and some detached or thin-skinned basins such as the Vienna Basin (Fig. 10B; Royden, 1985 this volume). In the vicinity of the Salton Trough, however, the crustal structure inferred from seismic refraction and gravity data (Fuis et al., 1984) suggests that significant crustal thinning has occurred outside the overstep between the San Andreas and Imperial faults (Fig. 10A). The interpretation of the gravity data is not unique, but the relatively flat gravity profile across the Salton Trough requires that the upper surface of the subbasement (lined area) largely mirror the contact between the sedimentary rocks and basement (Fuis et al., 1984). The subbasement was modelled with a density of 3.1 gm/cm$^3$, and refraction data suggest a P-wave velocity of greater than or equal to 7.2 km/s, consistent with significant amounts of mafic igneous rocks intruded into the lower part of the crust. The depth to the top of the subbasement decreases abruptly from 16 km at the Salton Sea to approximately 10 km at the U.S.-Mexico border, about 30 km to the south, indicating that the gross crustal structure is for the most part related to the opening of the Gulf of California, and is not simply inherited from an earlier phase of regional extension.

The profile shown in Figure 10A is probably characteristic of junctures between continental transform systems and divergent plate boundaries, but some strike-slip basins are detached. Examples are known from (1) areas of pronounced regional shortening, such as the Vienna Basin, which formed adjacent to tear faults of the Carpathian nappes (Fig. 10B; Royden, 1985 this volume), and the St. George Basin, located in the forearc of the Bering Sea, Alaska (Marlow and Cooper, 1980); and (2) areas subject to marked regional extension, such as the West Anatolian extensional province of Turkey (Fig. 18 of Şengör et al., 1985 this volume), and the Basin and Range Province of the western United States (Cemen et al., 1985; Link et al., 1985, both in this volume). Detached strike-slip basins may also prove to be relatively common in intracontinental transform zones, particularly those located along former convergent plate boundaries. In central and southern California, for example, the presence of mid-crustal detachments is suggested by (1) earthquakes with low-angle nodal planes, and the alignment of earthquake hypocenters parallel to the gently dipping base of the seismogenic crust (Nicholson et al., 1985a, b; Webb and Kanamori, 1985); (2) a pronounced change, near the junction of the San Andreas and San Jacinto faults (SJ in Fig. 1), in the patterns of seismicity with depth, with shallow seismicity suggesting the rotation of small crustal blocks (Fig. 6B; Nicholson et al., 1985a, b); (3) regional patterns of earthquake travel-time residuals (Hadley and Kanamori, 1977); (4) the distribution of upper crustal seismic velocities (Hearn and Clayton, 1984; Nicholson et al., 1985a); (5) geodetic constraints on the effective elastic thickness of the upper crust (Turcotte et al., 1984); (6) paleomagnetically determined patterns of large-scale block rotation (Fig. 2A; Luyendyk et al., 1985); (7) deep seismic-reflection studies that reveal the presence of low-angle reflecting horizons (Cheadle et al., 1985); and (8) evidence from surface geology and shallow seismic reflection profiles for numerous Neogene and Quaternary low-angle faults (Yeats, 1981, 1983; Crouch et al., 1984; Wentworth et al., 1984; Namson et al., 1985). We note that it is not yet clear how much of the California margin is detached, although the scale probably exceeds that of individual basins. Manspeizer (1985 this volume) interprets the Dead Sea Basin as detached on a smaller scale above listric normal faults bounded by the overstepping strands of the Dead Sea fault zone (his Fig. 13, after a concept of K. Arbenz, and reproduced on the cover of this book).

As discussed above, lithospheric or crustal extension produces a thermal anomaly, and subsequent cooling leads to additional subsidence (McKenzie, 1978; Royden and Keen, 1980; Steckler and Watts, 1982). In narrow basins, and in those for which extension is not "instantaneous," but occurs over an interval of more than about 10 m.y., a significant fraction of the thermal anomaly decays during the rifting stage, increasing the amount of syn-rift subsidence at the expense of the post-rift (Jarvis and McKenzie, 1980;

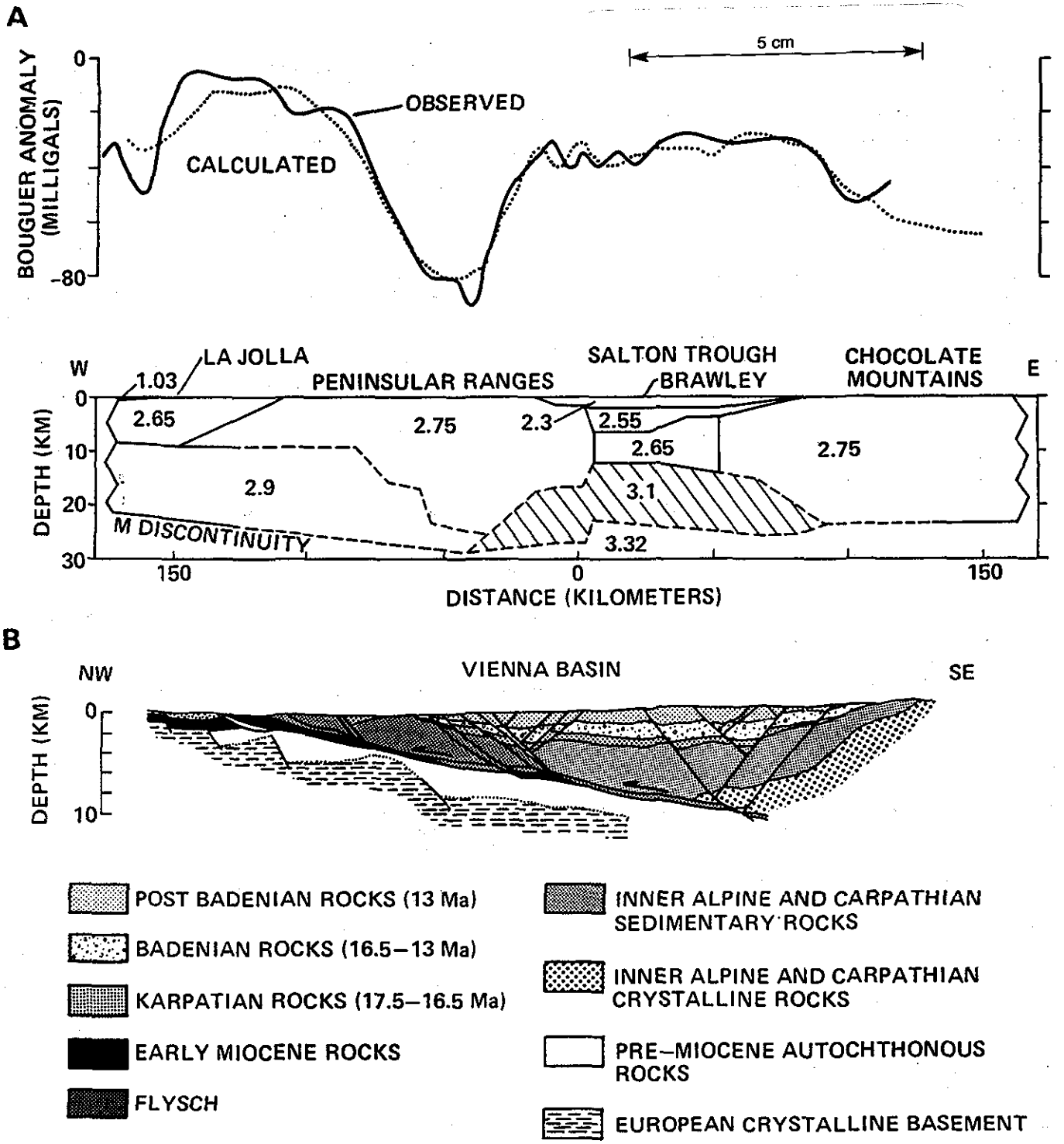



FIG. 10.—A comparison of thick-skinned and thin-skinned pull-apart basins: the Salton Trough, California (A), and the Vienna Basin, Austria and Czechoslovakia (B).

A) Cross section of southern California from La Jolla to the Chocolate Mountains (from Fuis et al., 1984, see Fig. 1 for location). The observed gravity anomaly is compared with the anomaly calculated from the model (densities in gm/cm$^3$). Solid boundaries are those controlled by seismic refraction data; dashed lines indicate boundaries adjusted to fit the gravity data. Sub-basement (lined area, density 3.1 gm/cm$^3$) beneath the Salton Trough provides most of the gravitational compensation for sedimentary rocks (densities 2.3 and 2.55 gm/cm$^3$) and inferred metasedimentary rocks (density 2.65 gm/cm$^3$). The San Andreas and Imperial faults are located near the east and west edges of the block with density of 2.65 gm/cm$^3$.

B) Cross section of the Miocene Vienna Basin, a detached pull-apart basin superimposed partly on nappes of the outer Carpathian flysch belt, and partly on nappes of the inner Carpathians (section 3 from Fig. 6 of Royden, 1985 this volume). Tertiary thrusts are indicated by arrows; Miocene normal faults displace Miocene rocks at the surface; normal faults confined to the autochthon are mainly Jurassic syn-sedimentary faults associated with Mesozoic rifting.

655159



Steckler, 1981; Cochran, 1983; Pitman and Andrews, 1985 this volume). The post-rift thermal anomaly is also less for detached basins than for those produced by an equivalent amount of extension of the entire lithosphere, and detached basins thus experience reduced post-rift subsidence. Extensional strike-slip basins tend to be short-lived, but the rifting stage is preferentially represented in the stratigraphic record because most such basins are small, in some cases detached, and in many cases subject to subsequent uplift and erosion.

Another potentially important mechanism for basin subsidence along strike-slip faults, in addition to crustal extension, is loading due to the local convergence of crustal blocks (e.g., the Ventura Basin of southern California; Fig. 15 below; Burke et al., 1982; Yeats, 1983). Similar basins bounded by major thrust faults are discussed by Şengör et al. (1985 this volume) and by Steel et al. (1985 this volume). As in foreland basins (Beaumont, 1981), patterns of subsidence are likely to be influenced by lithospheric flexure, a mechanism of regional isostatic compensation in which loads are supported by broad deflection of the lithosphere as a result of lithospheric rigidity (Forsyth, 1979; Watts, 1983), but to our knowledge, no attempt has yet been made to model flexure in strike-slip basins. Some strike-slip basins experience both extension and shortening (e.g., a pull-apart basin adjacent to a convergent strike-slip fault). Flexural effects are reduced when the lithosphere is warm and relatively weak, and we presume that in such circumstances subsidence induced by loading would be localized.

Subsidence due to extension, thermal contraction or crustal loads is amplified by sediment loading (Steckler and Watts, 1982). Simple isostatic considerations indicate that for typical crustal and sediment densities, sediment loading accounts for about half the total subsidence. Loading by water is important only to the extent that sea level or lake level varies.

Although it is relatively simple to construct models of the processes outlined above for hypothetical basins, it is clearly difficult to unravel the processes from the geological record of a given strike-slip basin. A fruitful avenue of research will be to use a combination of geological and geophysical data from well studied basins to test these theoretical concepts.

### *Tectonic Setting of Depositional Sites*

The location of depositional sites along strike-slip faults is controlled by several factors operating at a variety of length scales and time scales. Along intracontinental transform zones, such as in California, and the Dead Sea fault zone, these include (1) crustal type and the configuration of pre-existing crustal structures, especially the distribution, orientation and dimensions of zones of weakness, such as faults; (2) variations in the overall motion of adjacent lithospheric plates; and (3) the kinematic behavior of crustal blocks within the transform zone.

*Pre-existing Crustal Structure.*—Pre-existing crustal structure influences the location of major strike-slip faults, and the way in which crustal blocks between those faults move and deform to produce basins. The San Andreas fault, for example, originated in southern California by about 8 Ma, with most of the 320 km of right slip accumulating since about 5.5 Ma during oblique opening of the Gulf of California (Fig. 1; Karig and Jensky, 1972; Crowell, 1981b; Curray and Moore, 1984). Strike-slip faulting is only the latest event in a long geologic history, extending back into Proterozoic time, and including the assembly, amalgamation and accretion of various suspect terranes to North America during Mesozoic time; Mesozoic to Miocene arc magmatism, associated forearc and perhaps back-arc sedimentation; and Oligocene to Miocene Basin and Range extension (Hamilton, 1978; Crowell, 1981a, b; Dokka and Merriam, 1982; Champion et al., 1984). The present Gulf is the result of seafloor spreading beginning in latest Miocene time, but possibly along the line of a somewhat older Miocene tectonic depression that has been termed the proto-Gulf of California (Karig and Jensky, 1972; Terres and Crowell, 1979; Crowell, 1981a, b; but see Curray and Moore, 1984, for a modified interpretation). With local exceptions, such as in the vicinity of the Transverse Ranges (ETR and WTR in Fig. 1), the San Andreas fault and related transform faults to the south in the Gulf of California approximately parallel the boundaries of older tectonic elements, and occupy a position along the eastern edge of the Cretaceous Peninsular Ranges and Baja California Batholith (Hamilton, 1978).

Vink et al. (1984) suggested that the Gulf of California and the associated transform system formed just within the continent because continental lithosphere is weaker than oceanic lithosphere, and that rifting close to a continent-ocean boundary invariably follows a continental pathway. A similar model has been proposed by Steckler and ten Brink (1985) to explain the development in mid-Miocene time of the Dead Sea fault, at the expense of extension in the Gulf of Suez. According to their model, the hinge zone along the Mediterranean margin between thinned and unthinned continental crust acted as a barrier to continued northward propagation of the Red Sea rift.

The distribution of Neogene basins in California is probably influenced to a certain extent by crustal composition and thickness, and by the location of older basins (Blake et al., 1978). For example, the San Joaquin Basin (SJB in Fig. 1), located along the eastern side of the San Andreas Fault in central California, is superimposed on a forearc basin of late Jurassic to mid-Miocene age, which in turn overlies the boundary between Sierran-arc and ophiolitic basement (Blake et al., 1978; Hamilton, 1978; Bartow, 1984; Bartow and McDougall, 1984; Namson et al., 1985).

*Relative Plate Motion.*—Another factor that influences the development of sedimentary basins along a continental transform zone is the overall relative motion of the adjacent lithospheric plates (Crowell, 1974b; Mann et al., 1983). Such motion may be strictly transform, or it may involve a component of either convergence or divergence (Harland, 1971). In practice, however, it is generally difficult to predict the behavior of individual blocks solely on this basis, owing to the complex jostling that takes place in a broad transform plate boundary, even when there is little variation in relative plate movement. The character of the plate boundary is also sensitive to the migration of any unstable

655160



triple junctions, and to changes in the position of the instantaneous relative-motion pole. Either of these eventualities may be associated with the reorganization of plate-boundary geometry, and with the transfer of slices of one plate to another (Crowell, 1979).

Mann et al. (1983) argued that the gross distribution of regions of extension and shortening along the San Andreas and Dead Sea transform systems can be explained by comparing the orientation of the major faults with the interplate slip lines suggested by Minster et al. (1974). According to Mann et al., active strike-slip basins occur preferentially where the principal displacement zone is divergent with respect to overall plate motion (e.g., the Wagner and Delfin Basins of the northern Gulf of California; and the Dead Sea Basin); push-up blocks (the Transverse Ranges, California, and the Lebanon Ranges) occur where the principal displacement zone is convergent. Such statements are probably valid where most of the plate motion is taken up along a single fault (e.g., Dead Sea fault zone), but less certain where the motion is accommodated by a number of major faults, and especially where crustal blocks rotate or deform internally.

Estimates of relative motion between the Pacific and North American plates, and of Quaternary slip rates for strike-slip faults in California suggest that there should be pronounced shortening across the Transverse Ranges of California (ETR and WTR in Fig. 1), an observation qualitatively supported by abundant geological observations (Nardin and Henyey, 1978; Jackson and Yeats, 1982; Yeats, 1983; Crouch et al., 1984). About half to two thirds of the Pacific-North American relative motion (56 mm/yr; Minster et al., 1974; Minster and Jordan, 1978, 1984) occurs on the San Andreas fault (Sieh and Jahns, 1984; Weldon and Humphreys, 1985). Recent estimates of the slip rate are 25 mm/yr during the Quaternary in southern California (Weldon and Sieh, 1985), and 34 mm/yr during the Holocene in central California (Sieh and Jahns, 1984). The remaining displacement is thought to be taken up by the San Jacinto and Elsinore faults (about 10 and 1 mm/yr, respectively, for Quaternary time; Sharp, 1981; Ziony and Yerkes, 1984), and by offshore faults such as the San Gregorio-Hosgri (6 to 13 mm/yr for the late Pleistocene and Holocene; Weber and Lajoie, 1977; fault not shown in Fig. 1), assuming that Quaternary plate motion has been much the same as the average motion for the past 5 to 10 m.y. In assessing these data, Weldon and Humphreys (1985) have concluded that the magnitude of Quaternary shortening across the Transverse Ranges is considerably smaller than expected. They suggest that plate motion may have been taken up not merely by translation on the major faults but in part by counterclockwise rotation about a pole 650 km southwest of the "big bend" of the San Andreas fault (Fig. 1), an interpretation that contrasts with paleomagnetic evidence for predominantly clockwise rotations west of the San Andreas on a longer time scale (Fig. 2A; Luyendyk et al., 1985). The rates of both strike-slip faulting and regional shortening are uncertain (see Bird and Rosenstock, 1984, for a different model), but available data indicate only a qualitative relation between the orientation of interplate slip lines and patterns of uplift and subsidence, even for tectonic features as prominent as the Transverse Ranges. In zones of continental convergence, such as Turkey (Şengör et al., 1985 this volume), patterns of deformation are even more complicated.

The Neogene history of California also provides examples of plate boundary reorganization resulting from the migration of unstable triple junctions and changes in the position of the instantaneous relative-motion pole. The transform plate margin originated in California at about 30 Ma, following the impingement of the Pacific plate against the North American plate (Atwater, 1970; Atwater and Molnar, 1973). The transform system lengthened, probably intermittently, by northward motion of the northern trench-transform-transform triple junction and by generally southward motion of the southern transform-trench-ridge triple junction. At the same time, perhaps because of irregularities along the plate boundary (Crowell, 1979), slices of the North American plate were incorporated within the evolving transform system and offset differentially along the plate margin (Crouch, 1979). By about 5.5 Ma, the southern triple junction reached the mouth of the proto-Gulf of California, and much of the transform motion was taken up by the San Andreas fault, effectively transferring the Peninsular Ranges and Baja California to the Pacific plate (Curray and Moore, 1984). This reorganization of the plate boundary may be related to a small change in the relative plate motion determined by Page and Engebretson (1984). Another consequence of the inferred change in plate motion may be the onset in Pliocene and Pleistocene time of the shortening, described above, across the Transverse Ranges and Coast Ranges of California, and an acceleration in the subsidence rates for several basins (Yeats, 1978). In the Ventura Basin, for example, where considerable geochronological precision is possible, subsidence rates are estimated to have increased from approximately 250 m/m.y. at about 4 Ma to between 2,000 and 4,000 m/m.y. in the past million years. Note that these figures of Yeats (1978) incorporate inferred changes in water depth, but no corrections for compaction, loading or eustatic changes in sea level.

A modern analogue for the geological complexities at a trench-transform-transform triple junction, and a mechanism by which tectonic slices are transferred from one plate to another, has been described by Herd (1978). In the vicinity of the Cape Mendocino triple junction, the San Andreas fault appears to split into two subparallel fault zones, approximately 70 to 100 km apart. The western zone, the San Andreas proper, terminates at Cape Mendocino (CM in Fig. 1). The eastern zone, consisting of the right-stepping Hayward, Healdsburg-Rodgers Creek, Maacama and Lake Mountain fault zones (H, RC, M, and LM in Fig. 1), appears to be very youthful, and extends northward onto the continental shelf about 150 km north of Cape Mendocino.

*Kinematic Behavior of Crustal Blocks.*—The kinematic behavior of fault-bounded crustal blocks within a transform zone has long been considered the principal control on the development of strike-slip basins (Lensen, 1958; Kingma, 1958; Quennell, 1958; Crowell, 1974a, b, 1976; Reading, 1980; Aydin and Nur, 1982a; Mann et al., 1983). The general idea is that subsidence tends to occur where strike slip is accompanied by a component of divergence, as a result,

655161



for example, of a bend or an overstep in the fault trace ("pull-apart basin" of Burchfiel and Stewart, 1966) or through extension near a fault junction ("fault-wedge basin" of Crowell, 1974b). Uplift occurs where there is a component of convergence, although an overridden block may be depressed by the overriding one. Examples of strike-slip basins with different geometry and of different size are illustrated in Figure 11. Crowell (1974b) described bends associated predominantly with stretching and subsidence or with shortening and uplift as "releasing" and "restraining" bends, respectively, and here, we extend the use of the terms "releasing" and "restraining" to kinematically equivalent oversteps and fault junctions. As recognized by Crowell (1974a, b), the kinematic behavior of individual crustal blocks is superimposed on broader patterns of plate interaction, and in complexly braided fault systems, many basins experience episodic subsidence as a result of changes in fault geometry and/or block motion. In some cases, therefore, the stratigraphic record of a strike-slip basin may not be related in a simple way to the present configuration of faults, and it may even be difficult to predict contemporary patterns of subsidence and uplift from fault geometry.

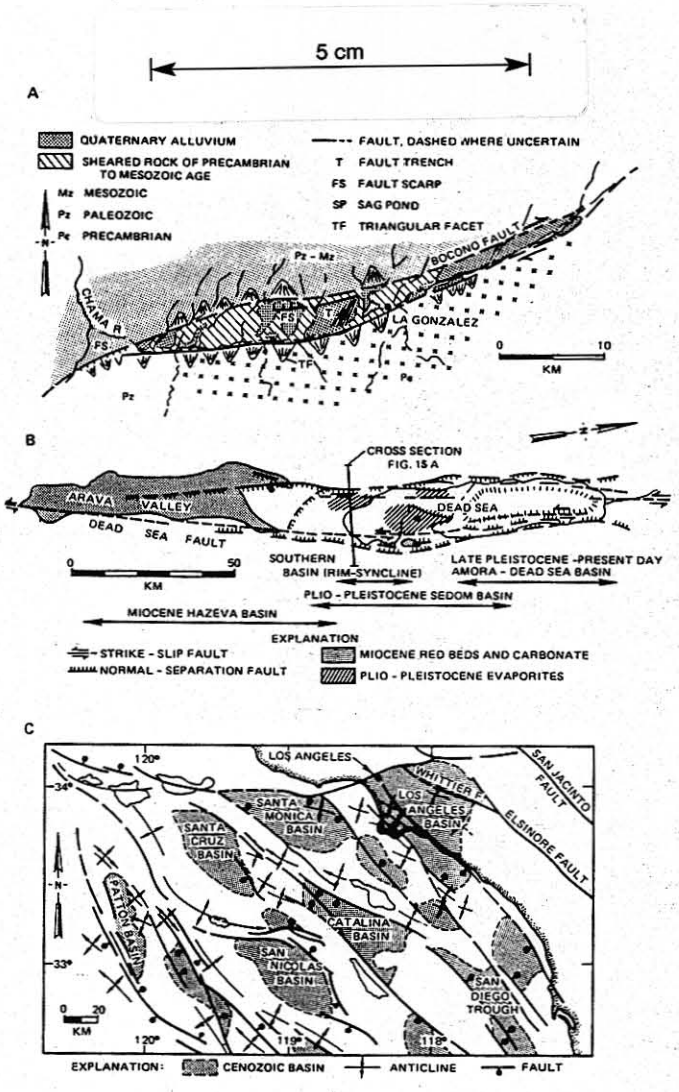



FIG. 11.—A comparison in map view of strike-slip basins of different ages, geometry, and scale.

A) The La González Basin, a lazy Z-shaped pull-apart basin of Pliocene (?) to Quaternary age along the Boconó fault zone, Venezuela (from Schubert, 1980).

B) The Dead Sea Rift, a rhomboidal pull-apart basin of Miocene to Holocene age (from Zak and Freund, 1981). Since Miocene time, the depocenter has migrated northward from the Arava Valley to the site of the present Dead Sea. For cross section, see Figure 15 A.

C) Selected faults, anticlines, and Cenozoic strike-slip basins in the southern California borderland (modified from Moore, 1969; Junger, 1976; Howell et al., 1980; see Figs. 1 and 2A for location). Many of these basins differ from the La González and Dead Sea Basins in being bounded by strike-slip faults of different orientations in a broad transform zone.

Consider, for example, basins and horsts associated with fault junctions. Some of the numerous possible patterns of subsidence and uplift at a simple fault junction are illustrated in Figure 12, modified from Figure 11 of Crowell (1974b). As originally discussed by Crowell, and reproduced in subsequent summary articles (e.g., Bally and Snelson, 1980; Reading, 1980, 1982; Freund, 1982), the wedge between the faults shown in Figure 12A is said to be "compressed and elevated" where the "faults converge," and "extended" where the "faults diverge." It is clear, however, that faults that converge in one direction diverge in the opposite direction. Assuming deformation only along the edges of blocks, and rotation only to the extent required by fault curvature, uplift and subsidence are related to the orientation (dip and strike) of the faults with respect to the overall slip vectors of the blocks (horizontal in Fig. 12B), and to the amount of extension or shortening associated with each fault. Although distinct in cross section, note that similar map-view configurations of basins and horsts can arise at either releasing or restraining junctions. More complicated arrangements can be envisaged at junctions with both releasing and restraining characteristics, and where blocks are internally deformed or rotated (see Fig. 6). Segmentation of the block between the branching faults may produce grabens within a horst or horsts within a graben, as in the Dead Sea fault zone (Garfunkel, 1981). In general, we expect basins and horsts to evolve continuously by a combination of fault slip and rotations about both vertical and horizontal axes, but there are also discontinuous changes due to episodic slip and rotation, and to the propagation of new faults. These are needed from time to time to eliminate tectonic knots, or complexities that inhibit further strike-slip deformation. Thus basins with thick sedimentary accumulations may at times experience uplift, and horsts with little preserved sediment may subside. Many strike-slip basins are actually slices of basins offset along one or more younger strike-slip faults.

An important aspect of strike-slip deformation and basin formation, but one for which documentation is acquired with difficulty, is the manner in which complexities sueh as fault bends, oversteps and junctions arise or are subsequently removed. Some curvature in strike-slip faults is attributable to a near pole of plate rotation (e.g., the Dead Sea fault zone; Garfunkel, 1981), and some bends may result from crustal heterogeneity or from local variations in the distribution of stress influencing the path of fault propagation. In eastern Jamaica, for example, a prominent right-hand restraining bend between the left-lateral east-striking Plan-

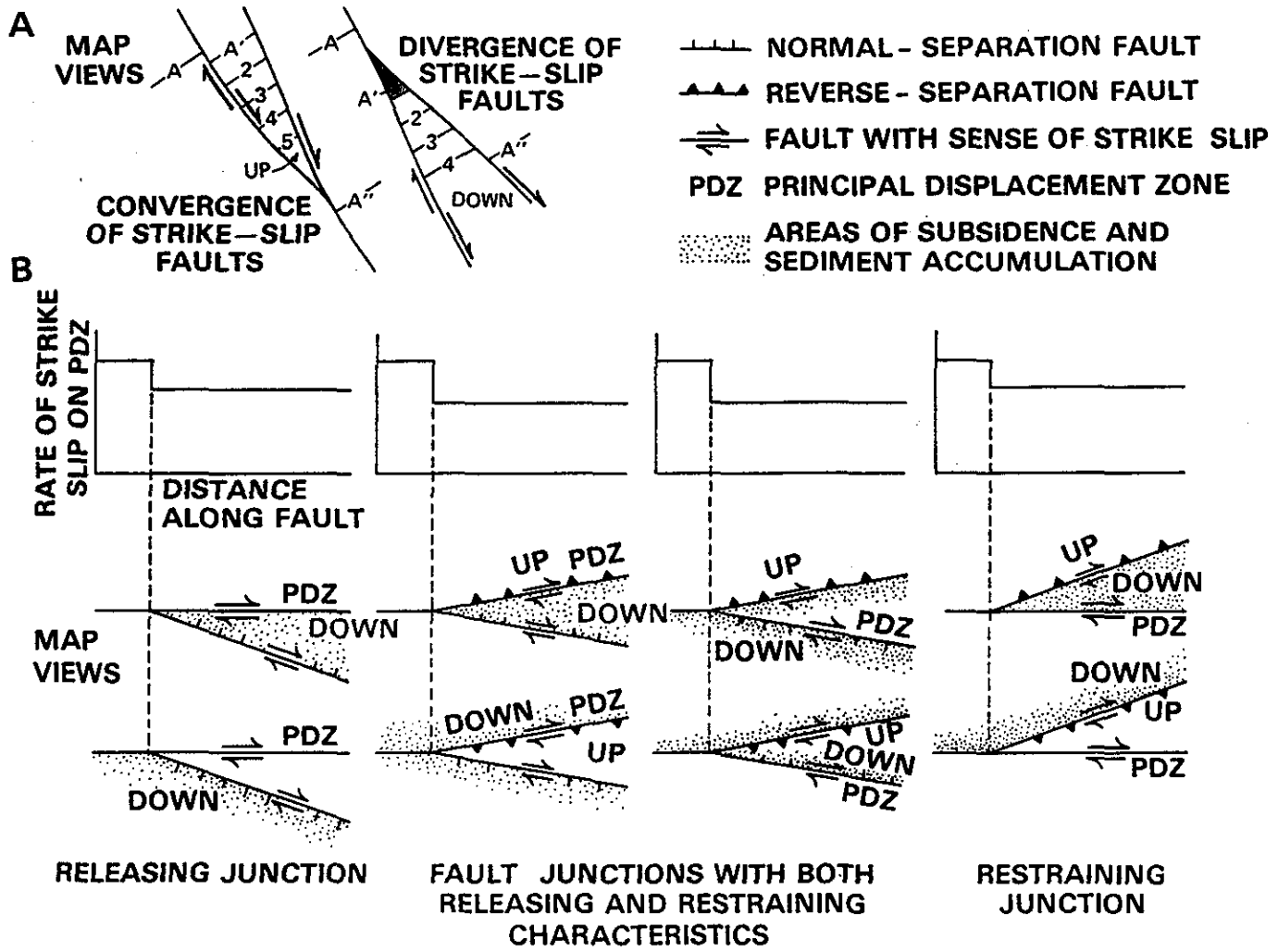



FIG. 12.—A) Sketch maps showing uplift of the tip of a fault wedge with convergence of right-slip faults, and subsidence of the tip with divergence (from Crowell, 1974b).

B) An alternative version of A, showing a range of possible results of slip along a bifurcating right-slip fault. See text for futher explanation.

tain Garden and Duanvale fault zones appears to have nucleated in Miocene time on northwest-striking normal faults that bounded a Paleogene graben (Fig. 2 of Mann et al., 1985 this volume). Other bends in strike-slip faults are due to the deformation of initially straight faults, as a result of (1) incompatible slip at a fault junction; (2) rotations within one or more adjacent blocks; or (3) intersection of a strike-slip fault with a zone of greater extensional or convergent strain. The development of the "big bend" of the San Andreas fault (Fig. 1) was attributed by Bohannon and Howell (1982) to incompatible displacement in late Cenozoic time on the San Andreas and Garlock faults (320 km of right slip, and 65 km of left slip, respectively; Smith, 1962; Smith and Ketner, 1970; Crowell, 1981b). As discussed above, this deformation was accompanied by counterclockwise rotation of the Mojave block between the faults (Fig. 2A; Morton and Hillhouse, 1985). Bends may also develop as a result of small-scale block rotation of the sort documented by Nicholson et al. (1985a, b; Fig. 6B). Şengör et al. (1985 this volume) describe fault bends due to the intersection of strike-slip faults with zones of accentuated extensional strain at the western end of the North Anatolian fault, and of accentuated convergent strain near the junction of the North Anatolian and East Anatolian faults in eastern Turkey (see their Figs. 10, 11, and 12).

Oversteps, and branching and braiding are fundamental features of many strike-slip fault zones and fault systems, and they develop by a number of mechanisms: (1) bending of initially straight faults; (2) direct and indirect interaction between faults; (3) segmentation of curved faults; (4) faulting within a weak zone oblique to possible failure planes; and (5) reactivation of pre-existing extension fractures (Crowell, 1974b; Freund, 1974; Segall and Pollard, 1980; 1983; Mann et al., 1983; Aydin and Nur, 1982a, 1985 this volume). Mann et al. (1983) proposed that pull-aparts evolve from incipient to mature ("extremely developed") basins through a sequence of closely related states. According to them, basins tend to form at releasing bends, and develop by way of spindle-shaped and "lazy S" (or "lazy Z") basins such as the La González Basin, Venezuela (Fig. 11A;

655163



Schubert, 1980), to rhomboidal basins such as the Dead Sea Rift (Fig. 11B; Zak and Freund, 1981; Manspeizer, 1985 this volume), and eventually, in some cases, to long narrow troughs floored by oceanic crust (e.g., the Cayman Trough of the northern Caribbean). In this model, oversteps arise by the propagation of secondary strike-slip faults in the vicinity of the releasing bend. A possible example of this branching process is the junction between the San Gabriel and San Andreas faults, the site of the Ridge Basin (Fig. 1). Between about 12 and 5 Ma, 13 km of sediment was deposited at a right bend along the San Gabriel fault, which at the same time experienced as much as 60 km of right slip (Crowell, 1982; Nilsen and McLaughlin, 1985 this volume). Beginning between 5 and 6 Ma, the San Gabriel fault ceased to be active, and strike-slip deformation was taken over by the San Andreas fault.

The interaction of parallel faults propagating from opposite directions is inherent in the models of Rodgers (1980) and Segall and Pollard (1980) for the evolution of pull-apart basins, and a possible example, the Soria Basin of northern Spain, is discussed in this volume by Guiraud and Seguret (1985). Theoretical studies indicate that significant interaction should occur between strike-slip faults if they are separated by less than twice the depth of faulting (Segall and Pollard, 1980). For strike-slip faults in California, where seismicity is observed to depths of 10 to 15 km, interaction is expected if faults are closer than 20 to 30 km. The other mechanisms listed above for generating oversteps are discussed elsewhere in this volume by Aydin and Nur (1985), and only briefly mentioned here. A consistent sense of overstepping along some curved fault zones suggests a relation between the sense of step and curvature (Aydin and Nur, 1985 this volume). An example of overstepping faults within an inappropriately oriented weak zone is the series of transform faults in the Gulf of California (Fig. 2 of Mann et al., 1983). The reactivation of pre-existing extension fractures appears to be largely a small-scale phenomenon (Segall and Pollard, 1983).

In the light of the foregoing discussion of the kinematics of strike-slip basins, we here consider the interpretation of one of the key geological elements needed to undertake a palinspastic reconstruction: piercing points of known age with which to derive the displacement history of the major strike-slip faults (e.g., Crowell, 1962, 1982, for offsets across the San Andreas and San Gabriel faults, California; and Freund et al., 1970, for offsets across the Dead Sea fault). Owing to the paucity of suitable geologic "lines," such reconstructions are commonly difficult. In the simplest case, the time of earliest movement on a strike-slip fault is given approximately by the age of the youngest rocks offset by the maximum amount ($T_1$ in Fig. 13A). For the San Andreas fault in southern California, this is late Miocene (Crowell, 1981a). The timing for the Dead Sea fault is less well constrained as approximately mid-Miocene, but definitely younger than basaltic dikes dated as about 20 Ma (Garfunkel, 1981), and the nature of this sort of uncertainty is shown diagrammatically in Figure 13A. Another difficulty arises if displacement varies along the fault as well as increasing with time. Strike-slip faults commonly branch and intersect, and in places accommodate differential extension or shortening. Figure 13 illustrates alternative interpretations of the displacement history of a hypothetical fault, given piercing points of known age ($T_0$, $T_1$, $T_2$, $T_3$), known displacement magnitude ($D_0$, $D_1$, $D_2$, $D_3$), and known location along one side of the fault ($L_0$, $L_1$, $L_2$, $L_3$). In one interpretation (Fig. 13A), the fault moves episodically over a long interval, beginning between times $T_1$ and $T_2$, and ending at $T_4$. For rocks of a given age, the magnitude of displacement is the same at all points along the fault. In the second interpretation (Fig. 13B), faulting is confined to a short interval between times $T_3$ and $T_4$. Piercing points of different ages indicate different magnitudes of displacement, because displacement varies along the fault. In reality, a given fault may exhibit displacement that is both variable and episodic, with the rate of movement changing from one interval of geologic time to another (not shown in Fig. 13). A given data set may also be incompatible with the extreme interpretations presented. The point of the illustration, however, is that in areas of complex deformation it is important to interpret the offset history of a given strike-slip fault in a regional plate-tectonic context, incorporating other stratigraphic clues to the timing of faulting.

### *Distinctive Aspects of the Stratigraphic Record*

Strike-slip basins are present in many different plate tectonic settings, and they are filled with sediments deposited in a variety of marine and non-marine environments, subject to a range of climatic conditions. In spite of these obvious differences, however, certain aspects of the stratigraphic record appear to be distinctive. These are (1) geological mismatches within and at the boundaries of basins, that is, features which document the occurrence of strike slip; (2) a tendency for longitudinal as well as lateral basin asymmetry, owing to the migration of depocenters with time; (3) evidence for episodic rapid subsidence, recorded by thick stratigraphic sections, and in some marine basins by rapid deepening; (4) the development of pronounced topographic relief, which is associated with abrupt lateral facies changes and local unconformities at basin margins; and (5) marked differences in stratigraphic thickness, facies geometry, and the occurrence of unconformities from one basin to another in the same region.

*Geological Mismatches.*—A geological mismatch occurs where rocks juxtaposed by a fault require a considerable amount of displacement to have taken place on the fault or on another structure cut by the fault. Such mismatches occur at sutures, in thrust and fold belts, and across some low-angle normal faults in extensional allochthons. They are also common in regions deformed by major strike-slip faults. The segment of the San Gabriel fault between the southern part of the Ridge Basin and the eastern Ventura Basin is a good example (Fig. 14; Crowell, 1982). Lateral facies relations, clast-size trends, and paleocurrent data suggest that conglomerate of the upper Miocene Modelo Formation of the Ventura Basin was derived from a nearby source to the northeast. The conglomerate consists of distinctive clasts of gabbro, norite, anorthosite, and gneiss as large as 1.5 m in diameter for which no nearby source is known across the

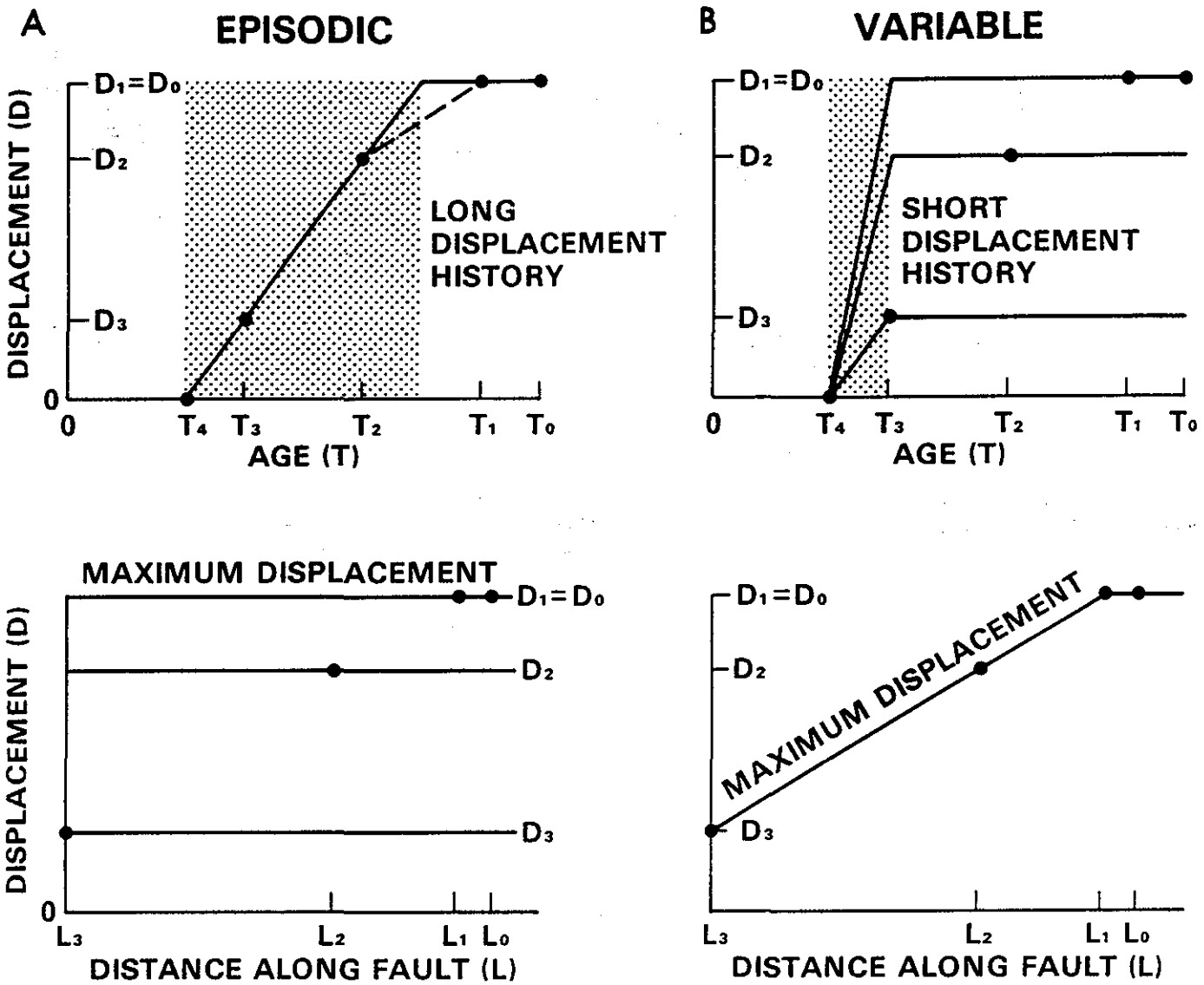



FIG. 13.—Alternative interpretations of the displacement history of a hypothetical fault, given piercing points of known age ($T_0$, $T_1$, $T_2$, $T_3$), known displacement magnitude ($D_0$, $D_1$, $D_2$, $D_3$), and known location along one side of the fault ($L_0$, $L_1$, $L_2$, $L_3$).

A) The fault moves episodically over a long interval, beginning between time $T_3$ and time $T_2$, and ending at $T_1$. For rocks of a given age, the magnitude of displacement is the same at all points along the fault. Note that by connecting displacement-age pairs, one might infer (perhaps incorrectly) that faulting began as early as time $T_3$, and that the slip rate increased after $T_2$ (dashed line).

B) Movement along the fault is confined to a short interval between times $T_3$ and $T_4$. Piercing points of different ages indicate different magnitudes of displacement, because displacement varies along the fault.

San Gabriel fault. Instead, that region is underlain by thick Miocene and older sedimentary rocks overlying a basement terrane quite different from that represented in the Modelo clasts. Immediately across the fault from the Modelo conglomerate, the Violin Breccia, also upper Miocene and also marine, was derived from a predominantly gneissic source to the southwest, where the basement is still largely covered by Miocene and older sedimentary rocks. The mismatch between sediments and suitable source rocks on both sides of the San Gabriel fault can be resolved, however, by removing between 35 and 60 km of right slip (Crowell, 1982). We emphasize that although evidence of this sort is important for documenting the magnitude or even occurrence of lateral offsets, the presence of similar geology on opposite sides of a fault at a particular locality does not necessarily preclude strike-slip deformation, a phenomenon that Crowell (1962) termed regional trace slip.

*Basin Asymmetry.*—Many sedimentary basins are asymmetrical, especially if faults occur preferentially along one side, and as in the case of grabens formed by regional extension (Harding, 1984), the sense of asymmetry in strike-slip basins may change from one profile to another (e.g., the Gulf of Elat; Ben-Avraham et al., 1979). The faults bounding strike-slip basins may be characterized by either normal separation (e.g., the Dead Sea Rift; Fig. 15A) or reverse separation (e.g., the Ventura Basin, California; Fig.

655165



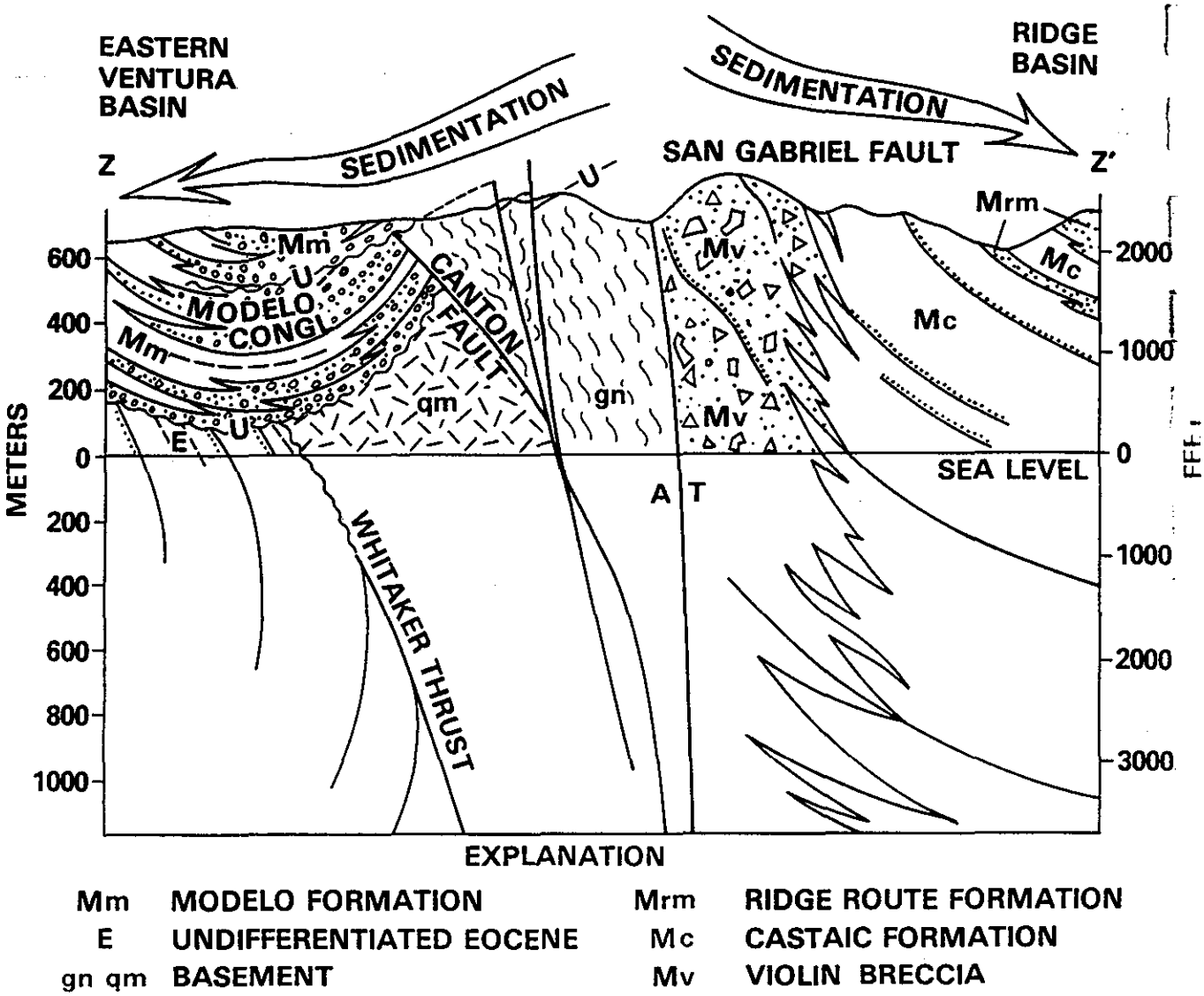
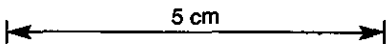



FIG. 14.—An example of a geological mismatch across a strike-slip fault: the San Gabriel fault, California (from Crowell, 1982; see Fig. 1 for location). The Modelo Conglomerate, derived from the northeast, is faulted against the Violin Breccia, derived from the southwest. T, displacement toward the observer; A, displacement away from the observer.

15B), or as discussed in the section on structural style, both normal and reverse faults may be present in the same basin (see Nilsen and McLaughlin, 1985 this volume). A particularly distinctive feature of strike-slip basins is the tendency for longitudinal as well as lateral asymmetry. The depocenter of the Dead Sea Basin, for example, has migrated northward more than 100 km from the site of the Arava Valley in the Miocene to the present Dead Sea (Fig. 11B; Zak and Freund, 1981; Manspeizer, 1985 this volume). Other basins with longitudinal asymmetry described in this volume are the Ridge Basin, California, and Hornelen Basin, Norway (Nilsen and McLaughlin, 1985), the Soria Basin of northern Spain (Guiraud and Seguret, 1985), the Nonacho Basin of Canada (Aspler and Donaldson, 1985), and possibly the Central Basin of Spitsbergen (Steel et al., 1985).

*Episodic Rapid Subsidence.*—Strike-slip basins are characterized by extremely rapid rates of subsidence (Fig. 16), even more rapid than many grabens and foreland basins and where there is an abundant sediment supply, by v thick stratigraphic sections in comparison with lateral ba dimensions (S. Y. Johnson, 1985; Nilsen and McLaughlin 1985, both in this volume). For example, about 13 km of sediment accumulated in the Ridge Basin in only 7 m (Crowell and Link, 1982), and 5 km of sediment was posited in the Vallecito-Fish Creek Basin in about 3.4 m.y (N. M. Johnson et al., 1983). The Ventura Basin subsid nearly 4 km in the past 1 m.y. (Fig. 15B; Yeats, 197 Marine basins and some deep lakes tend to become te porarily starved of sediment, a situation that promotes th accumulation of fine-grained organic-rich sediments s able for the generation of petroleum (Graham et al., 19 Link et al., 1985 this volume). Depending on local pattern of deformation, however, the subsidence in strike-slip ba sins is also episodic, and may end abruptly. The Vallec



Fish Creek Basin has been uplifted more than 5 km in the past 0.9 m.y. (N. M. Johnson et al., 1983).

*Local Facies Changes and Unconformities.*—Although not diagnostic of a strike-slip setting, many strike-slip basins form adjacent to uplifted blocks with pronounced topographic relief. As described in many of the papers that follow, this leads to very coarse sedimentary facies along some basin margins and to abrupt lateral facies changes. Local vertical movements of blocks result in localized unconformities.

*Contrasts Between Basins.*—Again, because of local tectonic controls, patterns of sedimentation vary markedly from one basin to another within the same region (see the description of Eocene sedimentation in Washington by Johnson, 1985 this volume). In the case of basins for which original geometry has been obscured by subsequent defor-

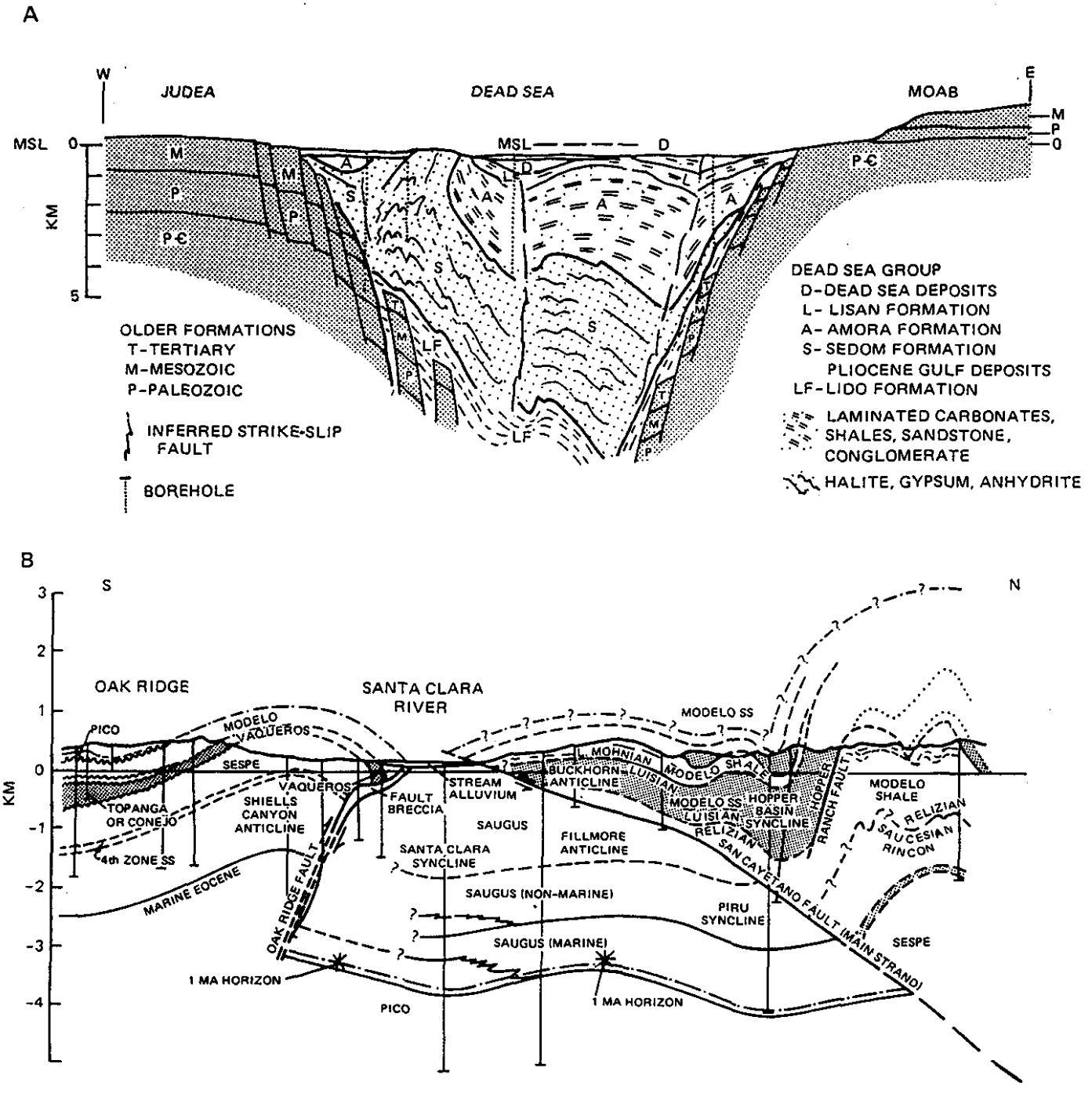
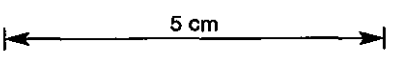



FIG. 15.—A comparison of strike-slip basins in profile.
A) The Dead Sea Rift, bounded by faults with normal separation (from Zak and Freund, 1981; see Fig. 11B for location).
B) The Ventura Basin, California, bounded by faults with reverse separation (from Yeats, 1983; see Fig. 1 for location).



655167

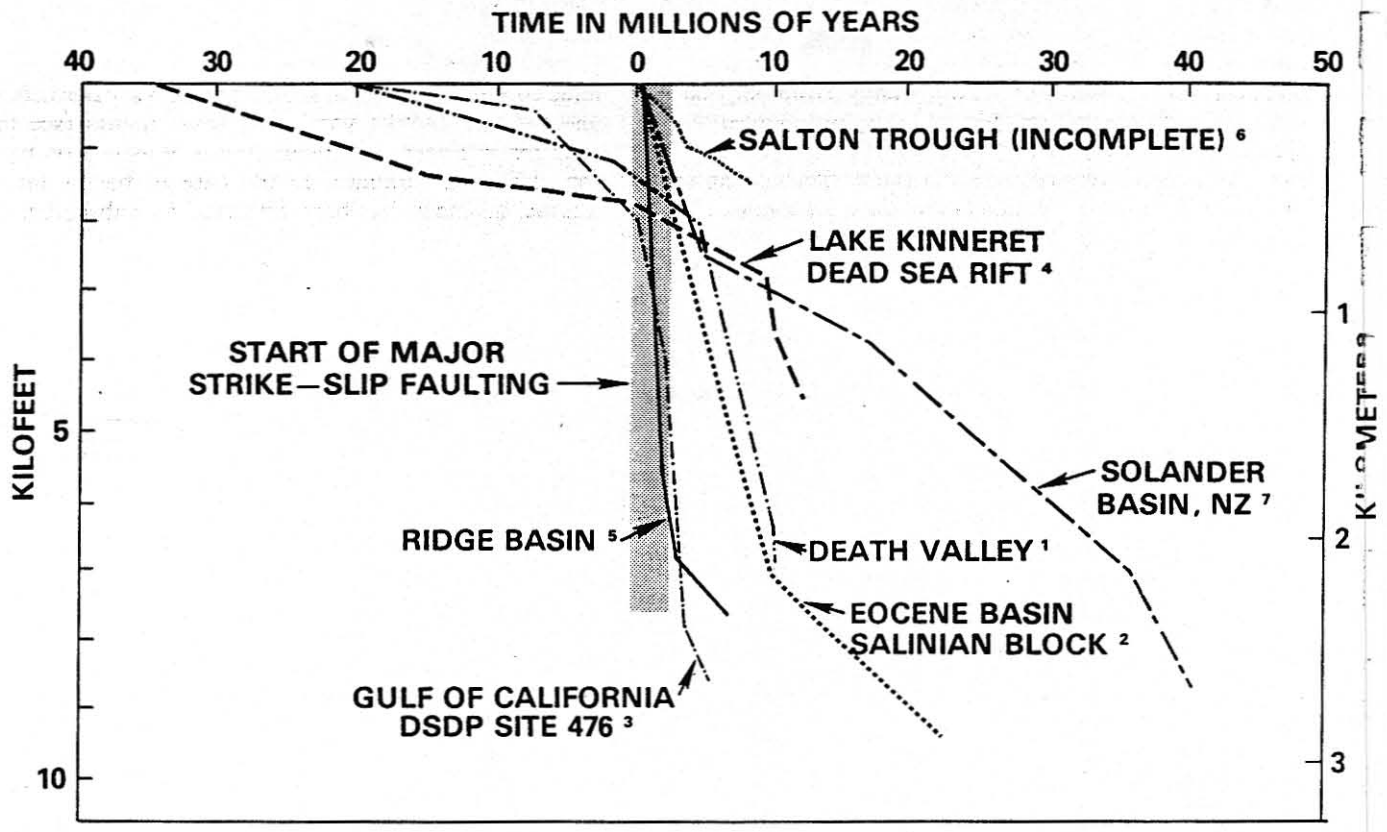



FIG. 16.—Tectonic subsidence curves for selected strike-slip basins. Tectonic subsidence is calculated by correcting cumulative stratigraphic thicknesses for the effects of sediment loading, sediment compaction, and water-depth changes. For each basin, the patterned area in the vicinity of th origin represents the approximate time of onset of major strike-slip deformation. Sources of data: 1, Hunt and Mabey (1966); 2, Graham (1976); Curray et al. (1982); 4, Ben-Avraham et al. (1981); 5, Crowell and Link (1982), and papers therein; 6, Kerr et al. (1979); 7, Norris and Cart (1980).

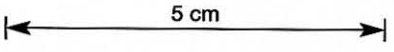
mation (e.g., many Paleozoic and Precambrian examples), regional stratigraphic comparisons may provide some of the more important clues that sedimentation was accompanied by strike-slip deformation (Heward and Reading, 1980; Aspler and Donaldson, 1985 this volume).

## ECONOMIC IMPORTANCE

Oil and gas are the most important resource exploited in strike-slip basins. Huff (1980) estimated that as much as 133 billion barrels has been discovered, but we regard this figure as rather high. The Dead Sea, known as Lake Asphaltitis to the ancient Greeks, was mentioned by the Latin authors Josephus and Tacitus as a source of asphalt used for calking ships and preparing medicines (Nissenbaum, 1978). In modern times, some of the most productive basins have been in California. About 10 billion barrels of oil have been produced from the Los Angeles, Ventura, Santa Maria, Salinas, and Cuyama Basins alone (Taylor, 1976). Current production from these basins is about 600,000 barrels of oil per day, and the ultimate recovery is estimated to be as much as 20 billion barrels of oil equivalent. The Point Arguello oil field, discovered in the offshore Santa Maria Basin in 1981, is the largest U.S. discovery since Prudhoe Bay, Alaska, with between 2.2 and 2.5 billion barrels of oil in place, and total recoverable reserves of between 300 and 500 million barrels (Crain et al., 1985). Oth northern California offshore basins are promising (Crouch and Bachman, 1985). Additional reserves may be disco ered in provinces affected by strike-slip deformation els where in the world, such as the southern Caribbean regio (Leonard, 1983), the Bering Sea (Marlow, 1979; Fisher 1982), the Dead Sea (Wilson et al., 1983), and parts China (Li Desheng, 1984). Individual strike-slip basins rang from very rich to non-productive, depending on such factors as the presence of source rocks, thermal history and maturation, migration potential, reservoir quality and dis tribution, occurrence of traps and seal, and preservation trapped hydrocarbons (Kingston et al., 1983b; Biddle and Christie-Blick, 1985b). Most important is the timing o maturation, migration and trap formation, because strike slip basins tend to be short-lived. Examples of commod ties, other than petroleum, found in strike-slip basins are ground water, coal and lignite, geothermal energy, an subsurface brines.

## CONCLUSIONS

(1) Structural patterns along strike-slip faults differ in de tail from simple predictions. The geometry of faults an folds along a given fault zone is generally a result of protracted, episodic deformation of heterogeneous sediment



and sedimentary rocks, involving the rotation of crustal blocks at a variety of scales, as well as strike slip, together with varying degrees of convergence and divergence, all superimposed on a pre-existing structural grain. On a regional scale, distinctive aspects of the structural style are the occurrence of en echelon structures, evidence for simultaneous shortening and extension, and random directions of vergence in associated thrusts and nappes.

(2) Basins form along strike-slip faults as a result of localized crustal extension and/or localized crustal shortening. The main processes leading to subsidence are mechanical thinning, thermal contraction, and loading due to the convergence of crustal blocks, amplified by the effects of sediment loading. The rifting stage is preferentially represented in the stratigraphic record of many strike-slip basins, because they are typically narrow, and in some cases detached (and therefore subject to less post-rift thermal subsidence), and many basins experience subsequent uplift and erosion. The importance of lithospheric flexure depends on the amount of extension involved in basin formation. Flexural effects are probably reduced during rifting.

(3) The location of depositional sites along strike-slip faults is controlled by crustal type and the configuration of preexisting crustal structures, variations in the motion of adjacent lithospheric plates, and the kinematic behavior of crustal blocks. A key factor influencing the development of sedimentary basins is the manner in which overall plate motion is accommodated by discrete slip on major faults, and by the rotation and internal deformation of blocks. Subsidence history cannot be determined with confidence from present fault geometry, which therefore provides a poor basis for basin classification.

(4) Distinctive aspects of the stratigraphic record along strike-slip faults are geological mismatches; a tendency for basins to be asymmetrical both longitudinally and laterally; thick stratigraphic sections representing short intervals of time; the occurrence of abrupt lateral facies changes and local unconformities; and marked differences in stratigraphic thickness, facies geometry, and occurrence of unconformities from one basin to another in the same region.

(5) A major frontier for research in strike-slip basins is that of integrated geophysical, geological and modelling studies in a variety of plate-tectonic settings. The geophysical work should include standard seismic reflection, seismic refraction, gravity, magnetic and heat flow measurements, together with paleomagnetic studies to establish the magnitude and timing of rotations, and the boundaries of the blocks experiencing rotation. The geological work should include structural, stratigraphic and sedimentological studies using outcrop, borehole and seismic reflection data, together with investigations of diagenesis and paleothermometry. Modelling should be directed at using all available data in quantitative tests of our notions of the processes that control the development of strike-slip basins.

## ACKNOWLEDGMENTS

This paper is an outgrowth of work conducted for Exxon Production Research Company, and we are grateful to that company for permission to publish and for support in the preparation of the manuscript. Christie-Blick acknowledges additional logistical support from an ARCO Foundation Fellowship. For stimulating discussions at various times about deformation and basins along strike-slip faults and for preprints of articles, we thank numerous geoscientists, but especially Tod Harding and Richard Vierbuchen (Exxon); Roger Bilham, Gerard Bond, Kathy Crane, Dennis Kent, Michelle Kominz, Craig Nicholson, Leonardo Seeber, Michael Steckler, Anthony Watts, and Patrick Williams (Lamont-Doherty Geological Observatory); John Crowell, Bruce Luyendyk and Arthur Sylvester (University of California, Santa Barbara); James Helwig and Jay Namson (ARCO); Ray Weldon (Caltech); M. J. Cheadle (University of Cambridge); William Dickinson (University of Arizona); and all the participants of the 1984 Research Symposium of the Society of Economic Paleontologists and Mineralogists on Strike-Slip Deformation, Basin Formation, and Sedimentation. Thom Davis and Ernie Duebendorfer kindly allowed us to use their unpublished mapping of neotectonic features along the San Andreas Fault to construct Figure 7. The manuscript benefitted from constructive reviews by Gerard Bond, Kevin Burke, Kathy Crane, James Helwig, Dennis Kent, Craig Nicholson, Harold Reading, and Arthur Sylvester.

## REFERENCES

AHORNER, L., 1975, Present-day stress field and seismotectonic block movements along major fault zones in central Europe: Tectonophysics, v. 19, p. 233–249.

ALBERS, J. P., 1967, Belt of sigmoidal bending and right-lateral faulting in the western Great Basin: Geological Society of America Bulletin, v. 78, p. 143–156.

ALLEN, C. R., 1957, San Andreas fault zone in San Gorgonio Pass, southern California: Geological Society of America Bulletin, v. 68, p. 315–350.

———, 1965, Transcurrent faults in continental areas, *in* A Symposium on Continental Drift: Philosophical Transactions of Royal Society of London, Series A, v. 258, p. 82–89.

ANADÓN, P., CABRERA, L., GUIMERÀ, J., AND SANTANACH, P., 1985, Paleogene strike-slip deformation and sedimentation along the southeastern margin of the Ebro Basin, *in* Biddle K. T., and Christie-Blick, N., eds., Strike-Slip Deformation, Basin Formation, and Sedimentation: Society of Economic Paleontologists and Mineralogists Special Publication No. 37, p. 303–318.

ANDERSON, E. M., 1951, The dynamics of faulting and dyke formation with applications to Britain: Edinburgh, Oliver and Boyd, 2nd edition, 206 p.

ARMSTRONG, R. L., 1968, Sevier orogenic belt in Nevada and Utah: Geological Society of America Bulletin, v. 79, p. 429–458.

———, 1978, Pre-Cenozoic Phanerozoic time scale—Computer file of critical dates and consequences of new and in-progress decay-constant revisions, *in* Cohee, G. V., Glaessner, M. F., and Hedberg, H. D., eds., Contributions to the Geologic Time Scale: American Association of Petroleum Geologists Studies in Geology No. 6, p. 73–91.

ASPLER, L. B., AND DONALDSON, J. A., 1985, The Nonacho Basin (Early Proterozoic), Northwest Territories, Canada: Sedimentation and deformation in a strike-slip setting, *in* Biddle K. T., and Christie-Blick, N., eds., Strike-Slip Deformation, Basin Formation, and Sedimentation: Society of Economic Paleontologists and Mineralogists Special Publication No. 37, p. 193–209.

ATWATER, T., 1970, Implications of plate tectonics for the Cenozoic tectonic evolution of western North America: Geological Society of America Bulletin, v. 81, p. 3513–3536.

ATWATER, T., AND MOLNAR, P., 1973, Relative motion of the Pacific and North American plates deduced from sea-floor spreading in the Atlantic, Indian, and South Pacific Oceans, *in* Kovach, R. L., et al., eds., Proceedings, Tectonic Problems of the San Andreas Fault System:

655169



Stanford University Publications in Geological Sciences, v. 13, p. 136–148.

AYDIN, A., AND NUR, A., 1982a, Evolution of pull-apart basins and their scale independence: Tectonics, v. 1, p. 91–105.

———, 1982b, Evolution of pull-apart basins and push-up ranges: Pacific Petroleum Geologists Newsletter: American Association of Petroleum Geologists, Pacific Section, Nov. 1982, p. 2–4.

———, 1985, The types and role of stepovers in strike-slip tectonics, *in* Biddle K. T., and Christie-Blick, N., eds., Strike-Slip Deformation, Basin Formation, and Sedimentation: Society of Economic Paleontologists and Mineralogists Special Publication No. 37, p. 35–44.

BALLANCE, P. F., 1980, Models of sediment distribution in non-marine and shallow marine environments in oblique-slip fault zones, *in* Ballance, P. F., and Reading, H. G., eds., Sedimentation in Oblique-Slip Mobile Zones: International Association of Sedimentologists Special Publication No. 4, p. 229–236.

BALLANCE, P. F., AND READING, H. G., eds., 1980a, Sedimentation in Oblique-Slip Mobile Zones: International Association of Sedimentologists Special Publication No. 4, 265 p.

———, 1980b, Sedimentation in oblique-slip mobile zones: an introduction, *in* Ballance, P. F., and Reading, H. G., eds., Sedimentation in Oblique-Slip Mobile Zones: International Association of Sedimentologists Special Publication No. 4, p. 1–5.

BALLY, A. W., ed., 1983, Seismic Expression of Structural Styles: American Association of Petroleum Geologists Studies in Geology Series, No. 15, 3 volumes.

BALLY, A. W., AND SNELSON, S., 1980, Realms of subsidence, *in* Miall, A. D., ed., Facts and Principles of World Petroleum Occurrence: Canadian Society of Petroleum Geologists Memoir 6, p. 9–94.

BARTLETT, W. L., FRIEDMAN, M., AND LOGAN, J. M., 1981, Experimental folding and faulting of rocks under confining pressure. Part IX. Wrench faults in limestone layers: Tectonophysics, v. 79, p. 255–277.

BARTOW, J. A., 1984, Geologic map and cross sections of the southeastern margin of the San Joaquin Valley, California: United States Geological Survey Miscellaneous Investigations Series Map I–1496, Scale 1:125,000.

BARTOW, J. A., AND MCDOUGALL, K., 1984, Tertiary stratigraphy of the southeastern San Joaquin Valley, California: United States Geological Survey Bulletin 1529-J, 41 p.

BEAUMONT, C., 1981, Foreland basins: Geophysical Journal of Royal Astronomical Society, v. 65, p. 291–329.

BECK, M. E., JR., 1980, Paleomagnetic record of plate-margin tectonic processes along the western margin of North America: Journal of Geophysical Research, v. 85, p. 7115–7131.

BELT, E. S., 1968, Post-Acadian rifts and related facies, eastern Canada, *in* Zen, E-An, White, W. S., Hadley, J. B., and Thompson, J. B., Jr., eds., Studies of Appalachian Geology, Northern and Maritime: New York, Wiley Interscience, p. 95–113.

BEN-AVRAHAM, Z., ALMAGOR, G., AND GARFUNKEL, Z., 1979, Sediments and structure of the Gulf of Elat (Aqaba)—northern Red Sea: Sedimentary Geology, v. 23, p. 239–267.

BEN-AVRAHAM, Z., GINZBURG, A., AND YUVAL, Z., 1981, Seismic reflection and refraction investigations of Lake Kinneret—central Jordan Valley, Israel: Tectonophysics, v. 80, p. 165–181.

BIDDLE, K. T., AND CHRISTIE-BLICK, N., 1985a, Glossary—Strike-slip deformation, basin formation, and sedimentation, *in* Biddle, K. T., and Christie-Blick, N., eds., Strike-Slip Deformation, Basin Formation, and Sedimentation: Society of Economic Paleontologists and Mineralogists Special Publication No. 37, p. 375–386.

BIDDLE, K. T., AND CHRISTIE-BLICK, N. H., 1985b, Basin formation, structural traps, and controls on hydrocarbon occurrence along wrench-fault zones: Offshore Technology Conference Paper OTC 4872, p. 291–295.

BILHAM, R., AND WILLIAMS, P., 1985, Sawtooth segmentation and deformation processes on the southern San Andreas fault, California: Geophysical Research Letters, v. 12, p. 557–560.

BIRD, P., AND ROSENSTOCK, R. W., 1984, Kinematics of present crust and mantle flow in southern California: Geological Society of America Bulletin, v. 95, p. 946–957.

BLAKE, M. C., JR., CAMPBELL, R. H., DIBBLEE, T. W., JR., HOWELL, D. G., NILSEN, T. H., NORMARK, W. R., VEDDER, J. C., AND SILVER, E. A., 1978, Neogene basin formation in relation to plate-tectonic evolution of San Andreas fault system, California: American Association of Petroleum Geologists Bulletin, v. 62, p. 344–372.

BOHANNON, R. G., AND HOWELL, D. G., 1982, Kinematic evolution the junction of the San Andreas, Garlock, and Big Pine faults, California: Geology, v. 10, p. 358–363.

BOIS, C., BOUCHE, P., AND PELET, R., 1982, Global geologic history a distribution of hydrocarbon reserves: American Association of Petroleum Geologists Bulletin, v. 66, p. 1248–1270.

BONATTI, E., AND CRANE, K., 1984, Oceanic fracture zones: Scientific American, v. 250, p. 40–51.

BRADLEY, D. C., 1982, Subsidence in Late Paleozoic basins in the northern Appalachians: Tectonics, v. 1, p. 107–123.

BRIDEN, J. C., TURNELL, H. B., AND WATTS, D. R., 1984, British paleomagnetism, Iapetus Ocean, and the Great Glen Fault: Geology, v. 12, p. 428–431.

BURCHFIEL, B. C., AND STEWART, J. H., 1966, "Pull-apart" origin of the central segment of Death Valley, California: Geological Society of America Bulletin, v. 77, p. 439–442.

BURCHFIEL, B. C., WALKER, D., DAVIS, G. A., AND WERNICKE, B., 1983, Kingston Range and related detachment faults—a major "breakaway" zone in the southern Great Basin: Geological Society of America Abstracts with Programs, v. 15, p. 536.

BURKE, K., MANN, P., AND KIDD, W., 1982, What is a ramp valley?: 11th International Congress on Sedimentology, Hamilton, Ontario, International Association of Sedimentologists, Abstracts of Papers, p. 40

BUTLER, R. W. H., 1982, The terminology of structures in thrust belts: Journal of Structural Geology, v. 4, p. 239–245.

CAMPBELL, J. D., 1958, En echelon folding: Economic Geology, v. 53, p. 448–472.

CAREY, S. W., 1955, The orocline concept in geotectonics: Royal Society of Tasmania Proceedings, v. 89, p. 255–288.

———, 1958, A tectonic approach to continental drift, *in* Carey, S. W., convenor, Continental Drift: A Symposium: Hobart, University of Tasmania, p. 177–355.

CEMEN, I., WRIGHT, L. A., DRAKE, R. E., AND JOHNSON, F. C., 1985, Cenozoic sedimentation and sequence of deformational events at the southeastern end of the Furnace Creek strike-slip fault zone, Death Valley region, California, *in* Biddle, K. T., and Christie-Blick, N., eds., Strike-Slip Deformation, Basin Formation, and Sedimentation: Society of Economic Paleontologists and Mineralogists Special Publication No. 37, p. 127–141.

CHAMBERLAIN, V. E., AND LAMBERT, R. St J., 1985, Cordilleria, a newly defined Canadian microcontinent: Nature, v. 314, p. 707–713.

CHAMPION, D. E., HOWELL, D. G., AND GROMME, C. S., 1984, Paleomagnetic and geologic data indicating 2500 km of northward displacement for the Salinian and related terranes, California: Journal of Geophysical Research, v. 89, p. 7736–7752.

CHEADLE, M. J., CZUCHRA, B. L., BYRNE, T., ANDO, C. J., OLIVER, J. E., BROWN, L. D., KAUFMAN, S., MALIN, P. E., AND PHINNEY, R. A., 1985, The deep crustal structure of the Mojave Desert, California, from COCORP seismic reflection data: Tectonics, in press.

CHINNERY, M. A., 1961, The deformation of the ground around surface faults: Seismological Society of America Bulletin, v. 51, p. 355–372.

———, 1963, The stress changes that accompany strike-slip faulting: Seismological Society of America Bulletin, v. 53, p. 921–932.

CHOUKROUNE, P., FRANCHETEAU, J., AND LE PICHON, X., 1978, In situ structural observations along Transform Fault A in the FAMOUS area Mid-Atlantic Ridge: Geological Society of America Bulletin, v. 89, p. 1013–1029.

CISOWSKI, S. M., 1984, Evidence for early Tertiary remagnetization of Devonian rocks from the Orcadian basin, northern Scotland, and associated transcurrent fault motion: Geology, v. 12, p. 369–372.

CLARK, M. M., 1972, Surface rupture along the Coyote Creek Fault, *in* The Borrego Mountain Earthquake of April 9, 1968: United States Geological Survey Professional Paper 787, p. 55–86.

———, 1973, Map showing recently active breaks along the Garlock and associated faults, California: United States Geological Survey Miscellaneous Investigations Series Map I–741.

CLAYTON, L., 1966, Tectonic depressions along the Hope Fault, a transcurrent fault in North Canterbury, New Zealand: New Zealand Journal of Geology and Geophysics, v. 9, p. 95–104.

CLOOS, E., 1955, Experimental analysis of fracture patterns: Geological Society of America Bulletin, v. 66, p. 241–256.

COCHRAN, J. R., 1983, Effects of finite rifting times on the development

of sedimentary basins: Earth and Planetary Science Letters, v. 66, p. 289–302.

CONEY, P. J., JONES, D. L., AND MONGER, J. W. H., 1980, Cordilleran suspect terranes: Nature, v. 288, p. 329–333.

COURTILLOT, V., TAPPONIER, P., AND VARET, J., 1974, Surface features associated with transform faults—A comparison between observed examples and an experimental model: Tectonophysics, v. 24, p. 317–329.

COX, A., 1980, Rotation of microplates in western North America, *in* Strangway, D. W., ed., *The Continental Crust and its Mineral Deposits*: Geological Association of Canada Special Paper 20, p. 305–321.

CRAIN, W. E., MERO, W. E., AND PATTERSON, D., 1985, Geology of the Point Arguello discovery: American Association of Petroleum Geologists Bulletin, v. 69, p. 537–545.

CROUCH, J. K., 1979, Neogene tectonic evolution of the California continental borderland and western Transverse Ranges: Geological Society of America Bulletin, Part I, v. 90, p. 338–345.

CROUCH, J. K., BACHMAN, S. B., AND SHAY, J. T., 1984, Post-Miocene compressional tectonics along the central California margin, *in* Crouch, J. K., and Bachman, S. B., eds., Tectonics and Sedimentation Along the California Margin: Society of Economic Paleontologists and Mineralogists, *Pacific Section*, v. 38, p. 37–54.

CROUCH, J., AND BACHMAN, S., 1985, California basins gain attention: American Association of Petroleum Geologists Explorer, April, p. 1, 8–9.

CROWELL, J. C., 1962, Displacement along the San Andreas fault, California: Geological Society of America Special Paper No. 71, 61 p.

———, 1974a, Sedimentation along the San Andreas fault, California, *in* Dott, R. H., Jr., and Shaver, R. H., eds., Modern and Ancient Geosynclinal Sedimentation: Society of Economic Paleontologists and Mineralogists Special Publication No. 19, p. 292–303.

———, 1974b, Origin of late Cenozoic basins in southern California, *in* Dickinson, W. R., ed., Tectonics and Sedimentation: Society of Economic Paleontologists and Mineralogists Special Publication No. 22, p. 190–204.

———, 1976, Implications of crustal stretching and shortening of coastal Ventura Basin, California, *in* Howell, D. G., ed., Aspects of the Geologic History of the California Continental Borderland: American Association of Petroleum Geologists, Pacific Section, Miscellaneous Publication 24, p. 365–382.

———, 1979, The San Andreas fault system through time: Journal of Geological Society of London, v. 136, p. 293–302.

———, 1981a, An outline of the tectonic history of southeastern California, *in* Ernst, W. G., ed., The Geotectonic Development of California (Rubey Volume 1): Englewood Cliffs, New Jersey, Prentice-Hall, p. 584–600.

———, 1981b, Juncture of San Andreas transform system and Gulf of California rift: Oceanologica Acta, Proceedings, 26th International Geological Congress, Paris, Geology of Continental Margins Symposium, p. 137–141.

———, 1982, The tectonics of Ridge Basin, southern California, *in* Crowell, J. C., and Link, M. H., eds., Geologic History of Ridge Basin, Southern California: Society of Economic Paleontologists and Mineralogists, Pacific Section, p. 25–42.

CROWELL, J. C., AND LINK, M. H., eds., 1982, *Geologic History of Ridge Basin, Southern California*: Society of Economic Paleontologists and Mineralogists, Pacific Section, 304 p.

CURRAY, J. R., AND MOORE, D. G., 1984, Geologic history of the mouth of the Gulf of California, *in* Crouch, J. K., and Bachman, S. B., eds., Tectonics and Sedimentation Along the California Continental Margin: Society of Economic Paleontologists and Mineralogists, Pacific Section, v. 38, p. 17–36.

CURRAY, J. R., AND MOORE, D. G., et al., 1982, Baja California passive margin transect: Sites 474, 475 and 476, *in* Curray, J. R., Moore, D. G., *et al.*, *Initial Reports of Deep Sea Drilling Project*, v. 64, Part 1, p. 35–210.

DAHLSTROM, C. D. A., 1970, Structural geology in the eastern margin of the Canadian Rocky Mountains: Bulletin of Canadian Petroleum Geology, v. 18, p. 332–406.

DAVIS, G. A., AND BURCHFIEL, B. C., 1973, Garlock fault: an intracontinental transform structure, southern California: Geological Society of America Bulletin, v. 84, p. 1407–1422.

DAVIS, T., AND LAGOE, M., 1984, Cenozoic structural development of the north-central Transverse Ranges and southern margin of the San Joaquin Valley: Geological Society of America Abstracts with Programs, v. 16, p. 484.

DETRICK, R. S., JR., AND PURDY, G. M., 1980, The crustal structure of the Kane fracture zone from seismic refraction studies: Journal of Geophysical Research, v. 85, p. 3759–3777.

DEWEY, J. F., 1982, Plate tectonics and the evolution of the British Isles: Journal of Geological Society of London, v. 139, p. 371–412.

DEWEY, J. F., AND PINDELL, J. L., 1985, Neogene block tectonics of eastern Turkey and northern South America: Continental applications of the finite difference method: Tectonics, v. 4, p. 71–83.

DIBBLEE, T. W., JR., 1977, Strike-slip tectonics of the San Andreas fault and its role in Cenozoic basin evolvement, *in* Late Mesozoic and Cenozoic Sedimentation and Tectonics in California: San Joaquin Geological Society Short Course, p. 26–38.

DICKINSON, W. R., 1978, *Plate tectonic evolution of sedimentary basins*, *in* Dickinson, W. R., and Yarborough, H., eds., Plate tectonics and hydrocarbon accumulation: American Association of Petroleum Geologists *Continuing Education* Course Note Series No. 1, p. 1–62.

D'ONFRO, P., AND GLAGOLA, P., 1983, Wrench fault, southeast Asia, *in* Bally, A. W., ed., Seismic Expression of Structural Styles, American Association of Petroleum Geologists Studies in Geology Series 15, v. 3, p. 4.2–9 to 4.2–12.

DOKKA, R. K., 1983, Displacements on late Cenozoic strike-slip faults of the central Mojave Desert, California: Geology, v. 11, p. 305–308.

DOKKA, R. K., AND MERRIAM, R. H., 1982, Late Cenozoic extension of northeastern Baja California, Mexico: Geological Society of America Bulletin, v. 93, p. 371–378.

DONATH, F. A., 1970, *Some information squeezed out of rock*: American Scientist, v. 58, p. 54–72.

DONOVAN, R. N., AND MEYERHOFF, A. A., 1982, Comment on 'Paleomagnetic evidence for a large (~2,000 km) sinistral offset along the Great Glen Fault during Carboniferous time:' Geology, v. 10, p. 604–605.

DOWNEY, M. W., 1984, Evaluating seals for hydrocarbon accumulations: American Association of Petroleum Geologists Bulletin, v. 68, p. 1752–1763.

EATON, G. P., 1982, The Basin and Range Province: Origin and tectonic significance: Annual Review of Earth and Planetary Sciences, v. 10, p. 409–440.

EISBACHER, G. H., 1985, Pericollisional strike-slip faults and syn-orogenic basins, Canadian Cordillera, *in* Biddle, K. T., and Christie-Blick, N., eds., 1985, Strike-Slip Deformation, Basin Formation, and Sedimentation: Society of Economic Paleontologists and Mineralogists Special Publication No. 37, p. 265–282.

EMMONS, R. C., 1969, Strike-slip rupture patterns in sand models: Tectonophysics, v. 7, p. 71–87.

ENSLEY, R. A., AND VEROSUB, K. L., 1982, Biostratigraphy and magnetostratigraphy of southern Ridge Basin, central Transverse Ranges, California, *in* Crowell, J. C., and Link, M. H., eds., Geologic History of Ridge Basin, Southern California: Society of Economic Paleontologists and Mineralogists, *Pacific Section*, p. 13–24.

FISHER, M. A., 1982, Petroleum geology of Norton Basin, Alaska: American Association of Petroleum Geologists Bulletin, v. 66, p. 286–301.

FITZGERALD, E. L., 1968, Structure of British Columbia foothills: American Association of Petroleum Geologists Bulletin, v. 52, p. 641–664.

FORSYTH, D. W., 1979, Lithospheric flexure: Reviews of Geophysics and Space Physics, v. 17, p. 1109–1114.

FOX, P. J., AND GALLO, D. G., 1984, A tectonic model for ridge-transform-ridge plate boundaries: Implications for the structure of oceanic lithosphere: Tectonophysics, v. 104, p. 205–242.

FRALICK, P. W., 1982, *Wrench basin type inferred from sedimentation* style: Examples from the Upper Paleozoic Cumberland Basin, Maritime, Canada: 11th International Congress on Sedimentology, Hamilton, Ontario, International Association of Sedimentologists, Abstracts of Papers, p. 38.

FREUND, R., 1970, Rotation of strike slip faults in Sistan, southeast Iran: Journal of Geology, v. 78, p. 188–200.

———, 1971, The Hope fault, a strike-slip fault in New Zealand: New Zealand Geological Survey Bulletin, v. 86, p. 1–49.

———, 1974, Kinematics of transform and transcurrent faults: Tectonophysics, v. 21, p. 93–134.

655171

———, 1982, The role of shear in rifting, *in* Pálmason, G., ed., Continental and Oceanic Rifts: American Geophysical Union Geodynamics Series, v. 8, p. 33–39.

FREUND, R., GARFUNKEL, Z., ZAK, I., GOLDBERG, M., WEISSBROD, T., AND DERIN, B., 1970, The shear along the Dead Sea rift: Philosophical Transactions of Royal Society of London, Series A, v. 267, p. 107–130.

FUIS, G. S., MOONEY, W. D., HEALY, J. H., MCMECHAN, G. A., AND LUTTER, W. J., 1984, A seismic refraction survey of the Imperial Valley region, California: Journal of Geophysical Research, v. 89, p. 1165–1189.

GAMOND, J. F., 1983, Displacement features associated with fault zones: a comparison between observed examples and experimental models: Journal of Structural Geology, v. 5, p. 33–45.

GARFUNKEL, Z., 1974, Model for the late Cenozoic tectonic history of the Mojave Desert, California, and for its relation to adjacent regions: Geological Society of America Bulletin, v. 85, p. 1931–1944.

———, 1981, Internal structure of the Dead Sea leaky transform (rift) in relation to plate kinematics: Tectonophysics, v. 80, p. 81–108.

GOGUEL, J., 1948, Introduction à l'étude mécanique des déformations de l'écorce terrestre: Mémoires, Carte Géologique Détaillée de la France, 2nd edition, 530 p.

GRAHAM, R. H., 1978, Wrench faults, arcuate fold patterns and deformation in the southern French Alps: Proceedings of Geological Association, v. 89, p. 125–142.

GRAHAM, S. A., 1976, Tertiary sedimentary tectonics of the central Salinian block of California [unpubl. Ph.D. dissertation]: Stanford, Stanford University, 510 p.

GRAHAM, S. A., AND WILLIAMS, L. A., 1985, Tectonic, depositional, and diagenetic history of Monterey Formation (Miocene), central San Joaquin Basin, California: American Association of Petroleum Geologists Bulletin, v. 69, p. 385–411.

GREEN, A. R., 1977, The evolution of the Earth's crust and sedimentary basin development: Offshore Technology Conference Paper OTC 2885, p. 67–72.

GREENHAUS, M. R., AND COX, A., 1979, Paleomagnetism of the Morro Rock-Islay Hill Complex as evidence for crustal block rotations in central coastal California: Journal of Geophysical Research, v. 84, p. 2393–2400.

GROSHONG, R. H., AND RODGERS, D. A., 1978, Left-lateral strike-slip fault model, *in* Wickham, J., and Denison, R., eds., Structural Style of Arbuckle Region: Geological Society of America Field Trip No. 3.

GUIRAUD, M., AND SEGURET, M., 1985, A releasing solitary overstep model for the late Jurassic—early Cretaceous (Wealdian) Soria strike-slip basin (northern Spain), *in* Biddle, K. T., and Christie-Blick, N., eds., Strike-Slip Deformation, Basin Formation, and Sedimentation: Society of Economic Paleontologists and Mineralogists Special Publication No. 37, p. 159–175.

GUTH, P. L., 1981, Tertiary extension north of the Las Vegas Valley shear zone, Sheep and Desert Ranges, Clark County, Nevada: Geological Society of America Bulletin, Part I, v. 92, p. 763–771.

GWINN, V. E., 1964, Thin-skinned tectonics in the Plateau and northwestern Valley and Ridge Provinces of the central Appalachians: Geological Society of America Bulletin, v. 75, p. 863–900.

HADLEY, D., AND KANAMORI, H., 1977, Seismic structure of the Transverse Ranges, California: Geological Society of America Bulletin, v. 88, p. 1469–1478.

HAMILTON, W., 1978, Mesozoic tectonics of the western United States, *in* Howell, D. G., and McDougall, K. A., eds., Mesozoic Paleogeography of the Western United States: Pacific Coast Paleogeography Symposium 2, Society of Economic Paleontologists and Mineralogists, Pacific Section, p. 33–70.

HARDING, T. P., 1974, Petroleum traps associated with wrench faults: American Association of Petroleum Geologists Bulletin, v. 58, p. 1290–1304.

———, 1983, Divergent wrench fault and negative flower structure, Andaman Sea, *in* Bally, A. W., ed., Seismic Expression of Structural Styles: American Association of Petroleum Geologists Studies in Geology, Series 15, v. 3, p. 4.2–1 to 4.2–8.

———, 1984, Graben hydrocarbon occurrences and structural style: American Association of Petroleum Geologists Bulletin, v. 68, p. 333–362.

———, 1985, Seismic characteristics and identification of negative flo structures, positive flower structures, and positive structural inversi American Association of Petroleum Geologists Bulletin, v. 69, p. 582–600.

HARDING, T. P., AND LOWELL, J. D., 1979, Structural styles, their pla tectonic habitats, and hydrocarbon traps in petroleum provinces: Am ican Association of Petroleum Geologists Bulletin, v. 63, p. 101 1058.

HARDING, T. P., GREGORY, R. F., AND STEPHENS, L. H., 1983, Convergen wrench fault and positive flower structure, Ardmore Basin, Oklahon *in* Bally, A. W., ed., Seismic Expression of Structural Styles: Am ican Association of Petroleum Geologists Studies in Geology, Series 15, v. 3, p. 4.2–13 to 4.2–17.

HARDING, T. P., VIERBUCHEN, R. C., AND CHRISTIE-BLICK, N., 198 Structural styles, plate-tectonic settings, and hydrocarbon traps of d vergent (transtensional) wrench faults, *in* Biddle, K. T., and Christi Blick, N., eds., Strike-Slip Deformation, Basin Formation, and Sedimentation: Society of Economic Paleontologists and Mineralogists Special Publication no. 37, p. 51–77.

HARLAND, W. B., 1971, Tectonic transpression in Caledonian Spitsbe gen: Geological Magazine, v. 108, p. 27–42.

HARLAND, W. B., COX, A. V., LLEWELLYN, P. G., PICTON, C. A. G., SMITH, A. G., AND WALTERS, R., 1982, A Geologic Time Scale: Cam bridge, Cambridge University Press, 131 p.

HARRIS, L. B., AND COBBOLD, P. R., 1984, Development of conjugat shear bands during simple shearing: Journal of Structural Geology, v. 7, p. 37–44.

HASZELDINE, R. S., 1984, Carboniferous North Atlantic paleogeography stratigraphic evidence for rifting, not megashear or subduction: Geological Magazine, v. 121, p. 443–463.

HEARN, T. M., AND CLAYTON, R. W., 1984, Crustal structure and tectonics in Southern California (abs.): EOS, v. 65, p. 992.

HERD, D. G., 1978, Intracontinental plate boundary east of Cape Mendocino, California: Geology, v. 6, p. 721–725.

HELWIG, J., 1974, Eugeosynclinal basement and a collage concept of orogenic belts, *in* Dott, R. H., Jr., and Shaver, R. H., eds., Modern and Ancient Geosynclinal Sedimentation: Society of Economic Paleontologists and Mineralogists Special Publication No. 19, p. 359–376.

HEWARD, A. P., AND READING, H. G., 1980, Deposits associated with a Hercynian to late Hercynian continental strike-slip system, Cantabrian Mountains, northern Spain, *in* Ballance, P. F., and Reading, H. G., eds., Sedimentation in Oblique-Slip Mobile Zones: International Association of Sedimentologists Special Publication No. 4, p. 105–125.

HILL, D. P., 1982, Contemporary block tectonics: California and Nevada: Journal of Geophysical Research, v. 87, p. 5433–5450.

HILL, M. L., AND TROXEL, B. W., 1966, Tectonics of Death Valley region, California: Geological Society of America Bulletin, v. 77, p. 435–438.

HOWELL, D. G., CROUCH, J. K., GREENE, H. G., MCCULLOCH, D. S., AND VEDDER, J. G., 1980, Basin development along the late Mesozoic and Cainozoic California margin: a plate tectonic margin of subduction, oblique subduction and transform tectonics, *in* Ballance, P. F., and Reading, H. G., eds., Sedimentation in Oblique-Slip Mobile Zones: International Association of Sedimentologists Special Publication No. 4, p. 43–62.

HUBBERT, M. K., 1937, Theory of scale models as applied to the study of geologic structures: Geological Society of America Bulletin, v. 48, p. 1459–1520.

HUFF, K. F., 1980, Frontiers of world exploration, *in* Miall, A. D., ed., Facts and Principles of World Petroleum Occurrence: Canadian Society of Petroleum Geologists Memoir 6, p. 343–362.

HUNT, C. B., AND MABEY, D. R., 1966, Stratigraphy and structure, Death Valley, California: United States Geological Survey Professional Paper 494-A, 162 p.

ILLIES, J. H., 1975, Intraplate tectonics in stable Europe as related to plate tectonics in the Alpine System: Geologische Rundschau, v. 64, p. 677–699.

ILLIES, J. H., AND GREINER, G., 1978, Rhinegraben and the Alpine System: Geological Society of America Bulletin, v. 89, p. 770–782.

IRVING, E., 1979, Paleopoles and paleolatitudes of North America and speculations about displaced terrains: Canadian Journal of Earth Sciences, v. 16, p. 669–694.

IRVING, E., AND STRONG, D. F., 1984, Palaeomagnetism of the Early Carboniferous Deer Lake Group, western Newfoundland: no evidence for *mid-Carboniferous displacement* of "Acadia:" Earth and Planetary Science Letters, v. 69, p. 379–390.

IRVING, E., MONGER, J. W. H., AND YOLE, R. W., 1980, New paleomagnetic evidence for displaced terranes in British Columbia, *in* Strangway, D. W., ed., The Continental Crust and its Mineral Deposits: Geological Association of Canada Special Paper 20, p. 441–456.

JACKSON, P. A., AND YEATS, R. S., 1982, Structural evolution of Carpinteria Basin, western Transverse Ranges, California: American Association of Petroleum Geologists Bulletin, v. 66, p. 805–829.

JARVIS, G. T., AND MCKENZIE, D. P., 1980, Sedimentary basin formation with finite extension rates: Earth and Planetary Science Letters, v. 48, p. 42–52.

JENNINGS, C. W., compiler, 1975, Preliminary fault and geologic map of southern California, in Crowell, J. C., ed, San Andreas Fault in Southern California: California Division of Mines and Geology Special Report 118, Scale 1:750,000.

JOHNSON, N. M., OFFICER, C. B., OPDYKE, N. D., WOODWARD, G. D., ZEITLER, P. K., AND LINDSAY, E. H., 1983, rates of late Cenozoic tectonism in the Vallecito-Fish Creek basin, western Imperial Valley, California: *Geology, v. 11, p. 664–667.*

JOHNSON, S. Y., 1985, Eocene strike-slip faulting and nonmarine basin formation in Washington, *in* Biddle, K. T., and Christie-Blick, N., eds., Strike-Slip Deformation, Basin Formation, and Sedimentation: Society of Economic Paleontologists and Mineralogists Special Publication No. 37, p. 283–302.

JONES, D. L., SILBERLING, N. J., AND HILLHOUSE, J., 1977, Wrangellia—A displaced terrane in northwestern North America: Canadian Journal of Earth Sciences, v. 14, p. 2565–2577.

JUNGER, A., 1976, Tectonics of the southern California borderland, *in* Howell, D. G., ed., Aspects of the Geologic History of the California Continental Borderland: American Association of Petroleum Geologists, Pacific Section, Miscellaneous Publication 24, p. 486–498.

KANTER, L. R., AND MCWILLIAMS, M. O., 1982, Rotation of the southernmost Sierra Nevada, California: Journal of Geophysical Research, v. 87, p. 3819–3830.

KARIG, D. E., 1980, Material transport within accretionary prisms and the "knocker" problem: Journal of Geology, v. 88, p. 27–39.

KARIG, D. E., AND JENSKY, W., 1972, The proto-Gulf of California: Earth and Planetary Science Letters, v. 17, p. 169–174.

KARSON, J. A., 1984, Variations in structure and petrology in the Coastal Complex, Newfoundland: anatomy of an oceanic fracture zone, *in* Gass, I. G., Lippard, S. J., and Shelton, A. W., eds., Ophiolites and Oceanic *Lithosphere: Geological Society of London, Special Publication No.* 13, p. 131–144.

KARSON, J. A., AND DICK, H. J. B., 1983, Tectonics of ridge-transform intersections at the Kane fracture zone: Marine Geophysical Researches, v. 6, p. 51–98.

KELTS, K., 1981, A comparison of some aspects of sedimentation and translational tectonics from the Gulf of California and the Mesozoic Tethys, northern Penninic margin: Eclogae Geologicae Helvetiae, v. 74, p. 317–338.

KENNEDY, W. Q., 1946, The Great Glen Fault: Quarterly Journal of Geological Society of London, v. 102, p. 41–76.

KENT, D. V., 1982, Paleomagnetic evidence for post-Devonian displacement of the Avalon platform (Newfoundland): Journal of Geophysical Research, v. 87, p. 8709–8716.

KENT, D. V., AND OPDYKE, N. D., 1978, Paleomagnetism of the Devonian Catskill red beds: Evidence for motion of the coastal New England–Canadian Maritime region relative to cratonic North America: Journal of Geophysical Research, v. 83, p. 4441–4450.

———, 1979, The Early Carboniferous paleomagnetic field of North America and its bearing on tectonics of the northern Appalachians: Earth and Planetary Science Letters, v. 44, p. 365–372.

———, 1985, Multicomponent magnetizations from the Mississippian Mauch Chunk Formation of the central Appalachians and their tectonic implications: Journal of Geophysical Research, v. 90, p. 5371–5383.

KERR, D. R., PAPPAJOHN, S., AND PETERSON, G. L., 1979, Neogene stratigraphic section at Split Mountain, eastern San Diego County, California, *in* Crowell, J. C., and Sylvester, A. G., eds., Tectonics of the Juncture Between the San Andreas Fault System and the Salton Trough, Southeastern California: Santa Barbara, California, Department of Geological Sciences, University of California, p. 111–123.

KING, P. B., 1969, Tectonic map of North America: United States Geological Survey, Scale 1:5,000,000.

KINGMA, J. T., 1958, Possible origin of piercement structures, local unconformities, and secondary basins in the Eastern Geosyncline, New Zealand: New Zealand Journal of Geology and Geophysics, v. 1, p. 269–274.

KINGSTON, D. R., DISHROON, C. P., AND WILLIAMS, P. A., 1983a, Global basin classification system: American Association of Petroleum Geologists Bulletin, v. 67, p. 2175–2193.

———, 1983b, Hydrocarbon plays and global basin classification: American Association of Petroleum Geologists Bulletin, v. 67, p. 2194–2198.

KLEMME, H. D., 1980, Petroleum basins—classifications and characteristics: Journal of Petroleum Geology, v. 3, p. 187–207.

LABOTKA, T. C., 1980, Petrology of a medium-pressure regional metamorphic terrane, Funeral Mountains, California: American Mineralogist, v. 65, p. 670–689.

———, 1981, Petrology of an andalusite-type regional metamorphic terrane, Panamint Mountains, California: Journal of Petrology, v. 22, p. 261–296.

LABOTKA, T. C., AND WARASILA, R., 1983, Ages of metamorphism in the central Panamint Mountains, California: Geological Society of America Abstracts with Programs, v. 15, p. 437.

LACHENBRUCH, A. H., AND SASS, J. H., 1980, Heat flow and energetics of the San Andreas fault zone: Journal of Geophysical Research, v. 85, p. 6185–6222.

LEHNER, P., AND BAKKER, G., 1983, Equatorial fracture zone (Romanche fracture), *in* Bally, A. W., ed., Seismic Expression of Structural Styles: American Association of Petroleum Geologists Studies in Geology, Series 15, v. 3, p. 4.2–25 *to* 4.2–29.

LENSEN, G. J., 1958, A method of graben and horst formation: Journal of Geology, v. 66, p. 579–587.

LEONARD, R., 1983, Geology and hydrocarbon accumulations, Columbus Basin, offshore Trinidad: American Association of Petroleum Geologists, v. 67, p. 1081–1093.

LEWIS, K. B., 1980, Quaternary sedimentation on the Hikurangi oblique-subduction and transform margin, New Zealand, *in* Ballance, P. F., and Reading, H. G., eds., Sedimentation in Oblique-Slip Mobile Zones: International Association of Sedimentologists Special Publication No. 4, p. 171–189.

LI DESHENG, 1984, Geologic evolution of petroliferous basins on continental shelf of China: American Association of Petroleum Geologists *Bulletin*, v. 68, p. 993–1003.

LINK, M. H., ROBERTS, M. T., AND NEWTON, M. S., 1985, Walker Lake Basin, Nevada: An example of late Tertiary (?) to Recent sedimentation in a basin adjacent to an active strike-slip fault, *in* Biddle, K. T., and Christie-Blick, N., eds., Strike-Slip Deformation, Basin Formation, and Sedimentation: Society of Economic Paleontologists and Mineralogists Special Publication No. 37, p. 105–125.

LOGAN, J. M., 1979, Brittle phenomena: Reviews of Geophysics and Space Physics, v. 17, p. 1121–1132.

LOGAN, J. M., FRIEDMAN, M., HIGGS, N. G., DENGO, C., AND SHIMAMOTO, T., 1979, *Experimental studies of simulated gouge and their application* to studies of natural fault zones: United States Geological Survey Open-File Report 79-1239, p. 305–343.

LONSDALE, P., 1978, Near-bottom reconnaissance of a fast-slipping transform zone at the Pacific-Nazca plate boundary: Journal of Geology, v. 86, p. 451–472.

LOWELL, J. D., 1972, Spitsbergen Tertiary orogenic belt and the Spitsbergen fracture zone: Geological Society of America Bulletin, v. 83, p. 3091–3102.

LUDMAN, A., 1981, Significance of transcurrent faulting in eastern Maine and location of the suture between Avalonia and North America: American Journal of Science, v. 281, p. 463–483.

LUYENDYK, B. P., KAMERLING, M. J., AND TERRES, R., 1980, Geometric model for Neogene crustal rotations in southern California: Geological Society of America Bulletin, Part I, v. 91, p. 211–217.

LUYENDYK, B. P., KAMERLING, M. J., TERRES, R. R., AND HORNAFIUS, J. S., 1985, Simple shear of southern California during Neogene time

655173



suggested by paleomagnetic declinations: Journal of Geophysical Research, in press.

MACDONALD, K. C., KASTENS, K., SPIESS, F. N., AND MILLER, S. P., 1979, Deep tow studies of the Tamayo transform fault: Marine Geophysical Researches, v. 4, p. 37–70.

MANDL, G., DE JONG, L. N. G., AND MALTHA, A., 1977, Shear zones in granular material: Rock Mechanics, v. 9, p. 95–144.

MANN, P., AND BRADLEY, D., 1984, Comparison of basin types in active and ancient strike-slip zones (abs.): American Association of Petroleum Geologists Bulletin, v. 68, p. 503.

MANN, P., AND BURKE, K., 1982, Basin formation at intersections of conjugate strike-slip faults: examples from southern Haiti: Geological Society of America Abstracts with Programs, v. 14, p. 555.

MANN, P., HEMPTON, M. R., BRADLEY, D. C., AND BURKE, K., 1983, Development of pull-apart basins: Journal of Geology, v. 91, p. 529–554.

MANN, P., DRAPER, G., AND BURKE, K., 1985, Neotectonics of a strike-slip restraining bend system, Jamaica, *in* Biddle, K. T., and Christie-Blick, N., eds., Strike-Slip Deformation, Basin Formation, and Sedimentation: Society of Economic Paleontologists and Mineralogists Special Publication No. 37, p. 211–226.

MANSPEIZER, W., 1985, The Dead Sea Rift: Impact of climate and tectonism on Pleistocene and Holocene sedimentation, *in* Biddle, K. T., and Christie-Blick, N., eds., Strike-slip Deformation, Basin Formation, and Sedimentation: Society of Economic Paleontologists and Mineralogists Special Publication No. 37, p. 143–158.

MARLOW, M. S., 1979, Hydrocarbon prospects in Navarin basin province, northwest Bering Sea shelf: Oil and Gas Journal, October 29, v. 77, p. 190–196.

MARLOW, M. S., AND COOPER, A. K., 1980, Mesozoic and Cenozoic structural trends under southern Bering Sea shelf: American Association of Petroleum Geologists Bulletin, v. 64, p. 2139–2155.

MCKENZIE, D., 1978, Some remarks on the development of sedimentary basins: Earth and Planetary Science Letters, v. 40, p. 25–32.

MENARD, H. W., AND ATWATER, T., 1969, Origin of fracture zone topography: Nature, v. 222, 1037–1040.

MIALL, A. D., 1985, Stratigraphic and structural predictions from a plate-tectonic model of an oblique-slip orogen: The Eureka Sound Formation (Campanian-Oligocene), northeast Canadian Arctic islands, *in* Biddle, K. T., and Christie-Blick, N., eds., Strike-Slip Deformation, Basin Formation, and Sedimentation: Society of Economic Paleontologists and Mineralogists Special Publication No. 37, p. 000–000.

MINSTER, J. B. AND JORDAN, T. H., 1978, Present-day plate motions: Journal of Geophysical Research, v. 83, p. 5331–5354.

———, 1984, Vector constraints on Quaternary deformation of the western United States east and west of the San Andreas fault, *in* Crouch, J. K., and Bachman, S. B., eds., Tectonics and Sedimentation Along the California margin: Society of Economic Paleontologists and Mineralogists, Pacific Section, v. 38, p. 1–16.

MINSTER, J. B., JORDAN, T. H., MOLNAR, P., AND HAINES, E., 1974, Numerical modelling of instantaneous plate tectonics: Geophysical Journal of Royal Astronomical Society, v. 36, p. 541–576.

MOLNAR, P., AND TAPPONNIER, P., 1975, Cenozoic tectonics of Asia: Effects of a continental collision: Science, v. 189, p. 419–426.

MOODY, J. D., AND HILL, M. J., 1956, Wrench-fault tectonics: Geological Society of America Bulletin, v. 67, p. 1207–1246.

MOORE, D. G., 1969, Reflection profiling studies of the California continental Borderland: Structure and Quarternary turbidite basins: Geological Society of America Special Paper 107, 138 p.

MORGENSTERN, N. R., AND TCHALENKO, J. S., 1967, Microscopic structures in kaolin subjected to direct shear: Géotechnique, v. 17, p. 309–328.

MORTON, J. L., AND HILLHOUSE, J. W., 1985, Paleomagnetism and K-Ar ages of Miocene basaltic rocks in the western Mojave Desert, California: manuscript.

MUTTER, J. C., AND DETRICK, R. S., 1984, Multichannel seismic evidence for anomalously thin crust at Blake Spur fracture zone: Geology, v. 12, p. 534–537.

NAMSON, J. S., DAVIS, T. L., AND LAGOE, M. B., 1985, Tectonic history and thrust-fold deformation style of seismically active structures near Coalinga, California: United States Geological Survey Professional Paper, submitted.

NARDIN, T. R., AND HENYEY, T. L., 1978, Pliocene-Pleistocene diastrophism of Santa Monica and San Pedro shelves, California continental borderland: American Association of Petroleum Geologists Bulletin, v. 62, p. 247–272.

NELSON, W. J., AND KRAUSSE, H.-F., 1981, The Cottage Grove fault system in southern Illinois: Illinois Institute of Natural Resources, State Geological Survey Division, Circular 522, 65 p.

NICHOLSON, C., SEEBER, L., WILLIAMS, P., AND SYKES, L. R., 1985a, Seismicity and fault kinematics through the eastern Transverse Ranges, California: Block rotation, strike-slip faulting and shallow-angle thrusting: Journal of Geophysical Research, in press.

NICHOLSON, C., SEEBER, L., WILLIAMS, P. L., AND SYKES, L. R., 1985b, Seismic deformation along the southern San Andreas fault, California: Implications for conjugate slip rotational block tectonics: Tectonics, submitted.

NILSEN, T. H., AND MCLAUGHLIN, R. J., 1985, Comparison of tectonic framework and depositional patterns of the Hornelen strike-slip basin of Norway and the Ridge and Little Sulphur Creek strike-slip basins of California, *in* Biddle, K. T., and Christie-Blick, N. eds., Strike Slip Deformation, Basin Formation, and Sedimentation: Society of Economic Paleontologists and Mineralogists Special Publication No. 37, p. 80–103.

NISSENBAUM, A., 1978, Dead Sea Asphalts—Historical aspects: American Association of Petroleum Geologists Bulletin, v. 62, p. 837–844.

NORRIS, R. J., AND CARTER, R. M., 1980, Offshore sedimentary basins at the southern end of the Alpine fault, New Zealand, *in* Ballance, P. F., and Reading, H. G., eds., Sedimentation in Oblique-Slip Mobile Zones: International Association of Sedimentologists Special Publication No. 4, p. 237–265.

ODONNE, F., AND VIALON, P., 1983, Analogue models of folds above a wrench fault: Tectonophysics, v. 99, p. 31–46.

OPDYKE, N. D., LINDSAY, E. H., JOHNSON, N. M., AND DOWNS, T., 1977, The paleomagnetism and magnetic polarity stratigraphy of the mammal-bearing section of Anza Borrego State Park, California: Quaternary Research, v. 7, p. 316–329.

PAGE, B. M., AND ENGEBRETSON, D. C., 1984, Correlation between the geologic record and computed plate motions for central California: Tectonics, v. 3, p. 133–155.

PALMER, A. R., 1983, The Decade of North American Geology 1983 time scale: Geology, v. 11, p. 503–504.

PARNELL, J. T., 1982, Comment on 'Paleomagnetic evidence for a large (2,000 km) sinistral offset along the Great Glen fault during Carboniferous time:' Geology, v. 10, p. 605.

PAVONI, N., 1961, Die Nordanatolische Horizontalverschiebung: Geologische Rundschau, v. 51, p. 122–139.

PERRODON, A., AND MASSE, P., 1984, Subsidence, sedimentation and petroleum systems: Journal of Petroleum Geology, v. 7, p. 5–26.

PERROUD, H., VAN DER VOO, R., AND BONHOMMET, N., 1984, Paleozoic evolution of the Armorica plate on the basis of paleomagnetic data: Geology, v. 12, p. 579–582.

PHILIP, H., AND MEGARD, F., 1977, Structural analysis of the superficial deformation of the 1969 Pariahuanca earthquakes (central Peru): Tectonophysics, v. 38, p. 259–278.

PITMAN, W. C., III, AND ANDREWS, J. A., 1985, Subsidence and thermal history of small pull-apart basins, *in* Biddle, K. T., and Christie-Blick, N., eds., Strike-Slip Deformation, Basin Formation, and Sedimentation: Society of Economic Paleontologists and Mineralogists Special Publication No. 37, p. 45–49.

PITTMAN, E. D., 1981, Effect of fault-related granulation on porosity and permeability of quartz sandstones, Simpson Group (Ordovician), Oklahoma: American Association of Petroleum Geologists Bulletin, v. 65, p. 2381–2387.

QUENNELL, A. M., 1958, The structural and geomorphic evolution of the Dead Sea Rift: Quarterly Journal of Geological Society of London, v. 114, p. 1–24.

RAMSAY, J. G., 1980, Shear zone geometry: a review: Journal of Structural Geology, v. 2, p. 83–99.

READING, H. G., 1980, Characteristics and recognition of strike-slip fault systems, *in* Ballance, P. F., and Reading, H. G., eds., Sedimentation in Oblique-Slip Mobiles Zones: International Association of Sedimentologists Special Publication No. 4, p. 7–26.

———, 1982, Sedimentary basins and global tectonics: Proceedings of

Geological Association, v. 93, p. 321–350.
RIEDEL, W., 1929, Zur Mechanik geologischer Brucherscheinungen: Zentrablatt für Mineralogie, Geologie und Pälaeontologie, v. 1929 B, p. 354–368.
RIXON, L. K., 1978, Clay modelling of the Fitzroy Graben: Bureau of Mineral Resources Journal of Australian Geology and Geophysics, v. 3, p. 71–76.
ROBERTS, M. T., 1983, Seismic example of complex faulting from northwest shelf of Palawan, Phillipines, *in* Bally, A. W., ed., Seismic Expression of Structural Styles: American Association of Petroleum Geologists Studies in Geology, Series 15, v. 3, p. 4.2–18 to 4.2–24.
RODGERS, D. A., 1980, Analysis of pull-apart basin development produced by en echelon strike-slip faults, *in* Ballance, P. F., and Reading, H. G., eds., Sedimentation in Oblique-Slip Mobile Zones: International Association of Sedimentologists Special Publication No. 4, p. 27–41.
RODGERS, J., 1963, Mechanics of Appalachian foreland folding in Pennsylvania and West Virginia: American Association of Petroleum Geologists Bulletin, v. 47, p. 1527–1536.
RON, H., FREUND, R., GARFUNKEL, Z., AND NUR, A., 1984, Block rotation by strike-slip faulting: structural and paleomagnetic evidence: Journal of Geophysical Research, v. 89, p. 6256–6270.
RON, H., AND EYAL, Y., 1985, Intraplate deformation by block rotation and mesostructures along the Dead Sea transform, northern Israel: Tectonics, v. 4, p. 85–105.
ROY, J. L., AND MORRIS, W. A., 1983, A review of paleomagnetic results from the Carboniferous of North America; the concept of Carboniferous geomagnetic field horizon markers: Earth and Planetary Science Letters, v. 65, p. 167–181.
ROYDEN, L. H., 1985, The Vienna Basin: A thin-skinned pull-apart basin, *in* Biddle, K. T., and Christie-Blick, N., eds., Strike-Slip Deformation, Basin Formation, and Sedimentation: Society of Economic Paleontologists and Mineralogists Special Publication No. 37, p. 319–338.
ROYDEN, L., AND KEEN, C. E., 1980, Rifting processes and thermal evolution of the continental margin of eastern Canada determined from subsidence curves: Earth and Planetary Science Letters, v. 51, p. 343–361.
ROYDEN, L. H., HORVÁTH, F., AND BURCHFIEL, B. C., 1982, Transform faulting, extension, and subduction in the Carpathian Pannonian region: Geological Society of America Bulletin, v. 93, p. 717–725.
SALVADOR, A., 1985, Chronostratigraphic and geochronometric scales in COSUNA stratsigraphic correlation charts of the United States: American Association of Petroleum Geologists Bulletin, v. 69, p. 181–189.
SBAR, M. L., 1982, Delineation and interpretation of seismotectonic domains in western North America: Journal of Geophysical Research, v. 87, p. 3919–3928.
SCHUBERT, C., 1980, Late-Cenozoic pull-apart basins, Boconó fault zone, Venezuelan Andes: Journal of Structural Geology, v. 2, p. 463–468.
SEARLE, R. C., 1979, Side-scan sonar studies of North Atlantic fracture zones: Journal of Geological Society of London, v. 136, p. 283–292.
———, 1983, Multiple, closely spaced transform faults in fast-slipping fracture zones: Geology, v. 11, p. 607–610.
SEGALL, P., AND POLLARD, D. D., 1980, Mechanics of discontinuous faults: Journal of Geophysical Research, v. 85, p. 4337–4350.
———, 1983, Nucleation and growth of strike slip faults in granite: Journal of Geophysical Research, v. 88, p. 555–568.
ŞENGÖR, A. M. C., BURKE, K., AND DEWEY, J. F., 1978, Rifts at high angles to orogenic belts: Tests for their origin and the Upper Rhine Graben as an example: American Journal of Science, v. 278, p. 24–40.
ŞENGÖR, A. M. C., GÖRÜR, N., AND ŞAROĞLU, F., 1985, Strike-slip faulting and related basin formation in zones of tectonic escape: Turkey as a case study, *in* Biddle, K. T., and Christie-Blick, N., eds., Strike-Slip Deformation, Basin Formation, and Sedimentation: Society of Economic Paleontologists and Mineralogists Special Publication No. 37, p. 227–264.
SHARP, R. V., 1976, Surface faulting in Imperial Valley during the earthquake swarm of January–February, 1975, Seismological Society of America Bulletin, v. 66, p.1145–1154.
———, 1977, Map showing the Holocene surface expression of the Brawley Fault, Imperial County, California: United States Geological Survey Miscellaneous Field Studies Map MF-838.
———, 1981, Variable rates of late Quaternary strike slip on the San Jacinto fault zone, southern California: Journal of Geophysical Research, v. 86, p. 1754–1762.
SIBSON, R. H., 1977, Fault rocks and fault mechanisms: Journal of Geological Society of London, v. 133, p. 191–213.
SIEH, K. E., AND JAHNS, R. H., 1984, Holocene activity of the San Andreas fault at Wallace Creek, California: Geological Society of America Bulletin, v. 95, p. 883–896.
SINHA, M. C., AND LOUDEN, K. E., 1983, The Oceanographer fracture zone–I. Crustal structure from seismic refraction studies: Geophysical Journal of Royal Astronomical Society, v. 75, p. 713–736.
SMITH, D. I., AND WATSON, J., 1983, Scale and timing of movements on the Great Glen fault, Scotland: Geology, v. 11, 523–526.
SMITH, G. I., 1962, Large lateral displacement on Garlock fault, California, as measured from offset dike swarm: American Association of Petroleum Geologists Bulletin, v. 46, p.85–104.
SMITH, G. I., AND KETNER, K. B., 1970, Lateral displacement on the Garlock fault, southeastern California, suggested by offset sections of similar metasedimentary rocks: United States Geological Survey Professional Paper 700-D, p. 1–9.
STECKLER, M. S., 1981, Thermal and mechanical evolution of Atlantic-type margins [unpubl. Ph.D. thesis]: New York, Columbia University, 261 p.
STECKLER, M. S., AND TEN BRINK, U. S., 1985, Replacement of the Gulf of Suez rift by the Dead Sea transform: The role of the hinge zones in rifting (abs.): EOS, v. 66, p. 364.
STECKLER, M. S., AND WATTS, A. B., 1982, Subsidence history and tectonic evolution of Atlantic-type continental margins, *in* Scrutton, R. A., ed., Dynamics of Passive Margins: American Geophysical Union Geodynamics Series, v. 6, p. 184–196.
STEEL, R., GJELBERG, J., HELLAND-HANSEN, W., KLEINSPEHN, K., NØTTVEDT, A., AND RYE-LARSEN, M., 1985, The Tertiary strike-slip basins and orogenic belt of Spitsbergen, *in* Biddle, K. T., and Christie-Blick, N., eds., Strike-Slip Deformation, Basin Formation, and Sedimentation: Society of Economic Paleontologists and Mineralogists Special Publication No. 37, p. 227–264.
STEWART, J. H., 1978, Basin-range structure in western North America: A review, *in* Smith, R. B., and Eaton, G. P., eds., Cenozoic tectonics and regional geophysics of the western Cordillera: Geological Society of America Memoir 152, p. 1–31.
———, 1983, Extensional tectonics in the Death Valley area, California: Transport of the Panamint Range structural block 80 km northwestward: Geology, v. 11, p. 153–157.
SUPPE, 1978, Cross section of southern part of northern Coast Ranges and Sacramento Valley, California: Geological Society of America Map and Chart Series, MC-28B.
SYKES, L. R., 1967, Mechanism of earthquakes and nature of faulting on the mid-oceanic ridges: Journal of Geophysical Research, v. 72, p. 2131–2153.
SYLVESTER, A. G., compiler, 1984, Wrench fault tectonics: American Association of Petroleum Geologists Reprint Series, No. 28, 374 p.
SYLVESTER, A. G., AND SMITH, R. R., 1976, Tectonic transpression and basement-controlled deformation in San Andreas fault zone, Salton Trough, California: American Association of Petroleum Geologists Bulletin, v. 60, p. 2081–2102.
TAYLOR, J. C., 1976, Geologic appraisal of the petroleum potential of offshore southern California: the borderland compared to onshore coastal basins: United States Geological Survey Circular 730, 43 p.
TCHALENKO, J. S., 1970, Similarities between shear zones of different magnitudes: Geological Society of America Bulletin, v. 81, p. 1625–1640.
TCHALENKO, J. S., AND AMBRASEYS, N. N., 1970, Structural analyses of the Dasht-e Bayaz (Iran) earthquake fractures: Geological Society of America Bulletin, v. 81, p. 41–60.
TERRES, R., AND CROWELL, J. C., 1979, Plate tectonic framework of the San Andreas-Salton Trough juncture, *in* Crowell, J. C., and Sylvester, A. G., eds., Tectonics of the Juncture Between the San Andreas Fault System and the Salton Trough, Southeastern California: Santa Barbara, California, Department of Geological Sciences, University of California, p. 15–25.
TERRES, R. R., AND SYLVESTER, A. G., 1981, Kinematic analysis of ro-

655175

tated fractures and blocks in simple shear: Seismological Society of American Bulletin, v. 71, p. 1593–1605.

TURCOTTE, D. L., LIU, J. Y., AND KULHAWY, F. H., 1984, The role of an intracrustal asthenosphere on the behavior of major strike-slip faults: Journal of Geophysical Research, v. 89, p. 5801–5816.

VAIL, P. R., MITCHUM, R. M., JR., TODD, R. G., WIDMIER, J. M., THOMPSON, S., JR., SANGREE, J. B., BUBB, J. N., AND HATELID, W. G., 1977, Seismic stratigraphy and global changes of sea level, *in* Payton, C. E., ed., Seismic Stratigraphy—Applications to Hydrocarbon Exploration: American Association of Petroleum Geologists Memoir 26, p. 49–212.

VAN DER VOO, R., 1982, Pre-Mesozoic paleomagnetism and plate tectonics: Annual Review of Earth and Planetary Sciences, v. 10, p. 191–220.

———, 1983, Paleomagnetic constraints on the assembly of the Old Red continent: Tectonophysics, v. 91, p. 271–283.

VAN DER VOO, R., AND SCOTESE, C. R., 1981, Paleomagnetic evidence for a large (~2,000 km) sinistral offset along the Great Glen Fault during Carboniferous time: Geology, v. 9, p. 583–589.

VAN DER VOO, R., FRENCH, A. N., AND FRENCH, R. B., 1979, A paleomagnetic pole position from the folded Upper Devonian Catskill red beds, and its tectonic implications: Geology, v. 7, p. 345–348.

VINK, G. E., MORGAN, W. J., AND ZHAO, W.-L., 1984, Preferential rifting of continents: A source of displaced terranes: Journal of Geophysical Research, v. 89, p. 10,072–10,076.

WATTS, A. B., 1983, The strength of the Earth's crust: Marine Technology Society Journal, v. 17, p. 5–17.

WEBB, T. H., AND KANAMORI, H., 1985, Earthquake focal mechanisms in the eastern Transverse Ranges and San Emigdio Mountains, southern California, and evidence for a regional decollement: Seismological Society of America Bulletin, v. 75, p. 737–757.

WEBER, G. E., AND LAJOIE, K. R., 1977, Late Pleistocene and Holocene tectonics of the San Gregorio fault zone between Moss Beach and Point Ano Nuevo, San Mateo County, California: Geological Society of America Abstracts with Programs, v. 9, p. 524.

WEERTMAN, J., 1965, Relationship between displacements on a free surface and the stress on a fault: Seismological Society of America Bulletin, v. 55, p. 945–953.

WELDON, R., AND HUMPHREYS, G., 1985, A kinematic model of southern California: Tectonics, in press.

WELDON, R. J., II, AND SIEH, K. E., 1985, Holocene rate of slip and tentative recurrence interval for large earthquakes on the San Andreas fault, Cajon Pass, southern California: Geological Society of American Bulletin, v. 96, p. 793–812.

WELDON, R. J., WINSTON, D. S., KIRSCHVINK, J. L., AND BURBANK, D. W., 1984, Magnetic stratigraphy of the Crowder Formation, Cajon Pass, southern California: Geological Society of America Abstracts with Programs, v. 16, p. 689.

WENTWORTH, C. M., BLAKE, M. C., JR., JONES, D. L., WALTER, A. W., AND ZOBACK, M. D., 1984, Tectonic wedging associated with emplacement of the Franciscan assemblage, California Coast Ranges, *in* Blake, M. C., Jr., ed., Franciscan Geology of Northern California: Society of Economic Paleontologists and Mineralogists, Pacific Section, v. 43, p. 163–173.

WERNICKE, B., SPENCER, J. E., BURCHFIEL, B. C., AND GUTH, P. L., 1982, Magnitude of crustal extension in the southern Great Basin: Geology, v. 10, p. 499–502.

WHITE, R. S., 1985, Seismic reflection profiling comes of age: Geological Magazine, v. 122, p. 199–201.

WILCOX, R. E., HARDING, T. P., AND SEELY, D. R., 1973, Basic wrench tectonics: American Association of Petroleum Geologists Bulletin, v. 57, p. 74–96.

WILSON, G., 1970, Wrench movements in the Aristarchus region of the Moon: Proceedings of Geological Association, v. 81, p. 595–608.

WILSON, J. E., KASHAI, E. L., AND CROKER, P., 1983, Hydrocarbon potential of Dead Sea Rift Valley: Oil and Gas Journal, v. 81, No. 25, June 20, p. 147–154.

WILSON, J. T., 1965, A new class of faults and their bearing on continental drift: Nature, v. 207, p. 343–347.

WINCHESTER, J. A., 1982, Comment on 'Paleomagnetic evidence for a large (~2,000 km) sinistral offset along the Great Glen fault during Carboniferous time:' Geology, v. 10, p. 487–488.

WISE, D. U., DUNN, D. E., ENGELDER, J. T., GEISER, P. A., HATCHER, R. D., KISH, S. A., ODOM, A. L., AND SCHAMEL, S., 1984, Fault-related rocks: Suggestions for terminology: Geology, v. 12, p. 391–394.

WRIGHT, L. A., AND TROXEL, B. W., 1970, Summary of regional evidence for right-lateral displacement in the western Great Basin: Discussion: Geological Society of America Bulletin, v. 81, p. 2167–2173.

YEATS, R. S., 1978, Neogene acceleration of subsidence rates in southern California: Geology, v. 6, p. 456–460.

———, 1981, Quaternary flake tectonics of the California Transverse Ranges: Geology, v. 9, p. 16–20.

———, 1983, Large-scale Quaternary detachments in Ventura Basin, southern California: Journal of Geophysical Research, v. 88, p. 569–583.

ZALAN, P. V., NELSON, E. P., WARME, J. E., AND DAVIS, T. L., 1985, The Piaui Basin: Rifting and wrenching in an equatorial Atlantic transform basin, *in* Biddle, K. T., and Christie-Blick, N., eds., Strike-Slip Deformation, Basin Formation, and Sedimentation: Society of Economic Paleontologists and Mineralogists Special Publication No. 37, p. 000–000.

ZAK, I., AND FREUND, R., 1981, Asymmetry and basin migration in the Dead Sea rift, *in* Freund, R., and Garfunkel, Z., eds., The Dead Sea Rift: Tectonophysics, v. 80, p.27–38.

ZIONY, J. I., AND YERKES, R. F., 1984, Fault slip-rate estimation for the Los Angeles region: Challenges and opportunities (abs.): Seismological Society of America, Eastern Section, Earthquake Notes, v. 55, No. 1, p. 8.

655176

# STRUCTURAL STYLES, PLATE-TECTONIC SETTINGS, AND HYDROCARBON TRAPS OF DIVERGENT (TRANSTENSIONAL) WRENCH FAULTS

T. P. HARDING AND R. C. VIERBUCHEN
*Exxon Production Research Company*
*P. O. Box 2189*
*Houston, Texas 77252-2189:*
AND
NICHOLAS CHRISTIE-BLICK
*Department of Geological Sciences and*
*Lamont-Doherty Geological Observatory*
*of Columbia University*
*Palisades, New York 10964*

ABSTRACT: A divergent (transtensional) wrench fault is one along which strike-slip deformation is accompanied by a component of extension. Faulting dominates the structural style and can initiate significant subsidence and sedimentation. The divergent wrench fault differs from other types of wrench faults by having mostly normal separation on successive profiles, negative flower structures, and a different suite of associated structures. En echelon faults, most with normal separation, commonly flank the zone, and some exhibit evidence of external rotation about vertical axes and have evidence of superimposed strike slip. Flexures associated with the wrench fault are formed predominantly by vertical components of displacement, and most are drag and forced folds parallel to and adjacent to the wrench. Hydrocarbon traps can occur in fault slices within the principal strike-slip zone, at culminations of forced folds, in the flanking tilted fault blocks, and within less common en echelon folds oblique to the zone.

Divergent wrench faults occur at active plate boundaries, in extensional and contractional continental settings, and within plates far from areas of pronounced regional deformation. Along transform margins and within wrench systems, divergent wrench styles tend to develop where major strands or segments of strands bend or splay toward the orientation of associated normal faults (e.g., elements of the San Andreas system in the Mecca Hills, California), and where major strands are regionally oblique to interplate slip lines (e.g., Dead Sea transform, Middle East). The style also develops at releasing fault oversteps and fault junctions (e.g., Ridge Basin, California), and locally where crustal blocks rotate between bounding wrench faults. In extensional settings, divergent wrench faults may form within graben doglegs and oversteps (e.g., between the Rhine and Bresse grabens, northern Europe), and they may separate regions that experienced different magnitudes of extension (e.g., Andaman Sea area). Many oceanic fracture zones have divergent wrench characteristics. The style has also been recognized in magmatic arcs (e.g., the Great Sumatran fault) and in both backarc and peripheral foreland settings (e.g., Lake Basin fault zone, Montana) near convergent plate boundaries, and in intra-plate settings (e.g., Cottage Grove fault, Illinois; Scipio-Albion trend, Michigan).

## INTRODUCTION AND PREVIOUS WORK

Divergent wrench zones are defined as those strike-slip systems within which the principal displacement zone and, in many cases, the adjacent associated structures are dominated by extensional characteristics. This article illustrates the structural style of divergent wrench zones and summarizes their known tectonic habitats and associated hydrocarbon traps.

Past discussions of wrench-fault styles have emphasized the contractional structures that accompany convergent strike slip (e.g., Wilcox et al., 1973; Sylvester and Smith, 1976). Several studies have shown individual structures attributable to extensional strike slip, but none has dealt with the full range of structural features that can be present. Nelson and Krausse (1981) presented the most thorough documentation, using an example from the Illinois basin where coal mining has provided unusually dense subsurface control. The results of that study are incorporated in our present work. The mechanics of oblique plate separation were discussed briefly by Harland (1971), and he first applied the term "transtension" to deformation in these zones. Wilcox et al. (1973) introduced the term "divergent wrench fault" and suggested that the structure along such faults is characterized by an increase in extensional block faulting and a decrease in en echelon folding. These authors described graben structures that were formed by divergent strike-slip deformation of a clay-cake model. Courtillot et al. (1974) also reproduced extensional strike-slip structures with a clay-cake model of a transform fault between simulated spreading centers. Earlier, Bishop (1968) documented fault patterns in New Zealand, portions of which are now recognized as essential elements of the structural style. Harding (1983) has recently illustrated a divergent wrench fault on seismic reflection data from the Andaman Sea and has established criteria for differentiating these zones from other styles on seismic profiles (Harding, 1985). D'Onfro and Glagola (1983) have published seismic reflection profiles of another divergent wrench zone in southeast Asia.

Our overview of divergent wrench systems presented here is drawn from these previous studies, from new field work in the Mecca Hills of southern California, and from additional seismic reflection profiles.

## EXTENSIONAL STRIKE-SLIP STYLES

Two important changes occur in the structures associated with wrench faults when strike slip is accompanied by significant divergence. First, lateral compression is decreased to the extent that en echelon folds and thrusts are present only diffusely or concentrated in localized settings. Second, regional extension enhances brittle deformation to the degree that the style is commonly dominated by faults.

Copyright © 1985, The Society of Economic Paleontologists and Mineralogists

655177



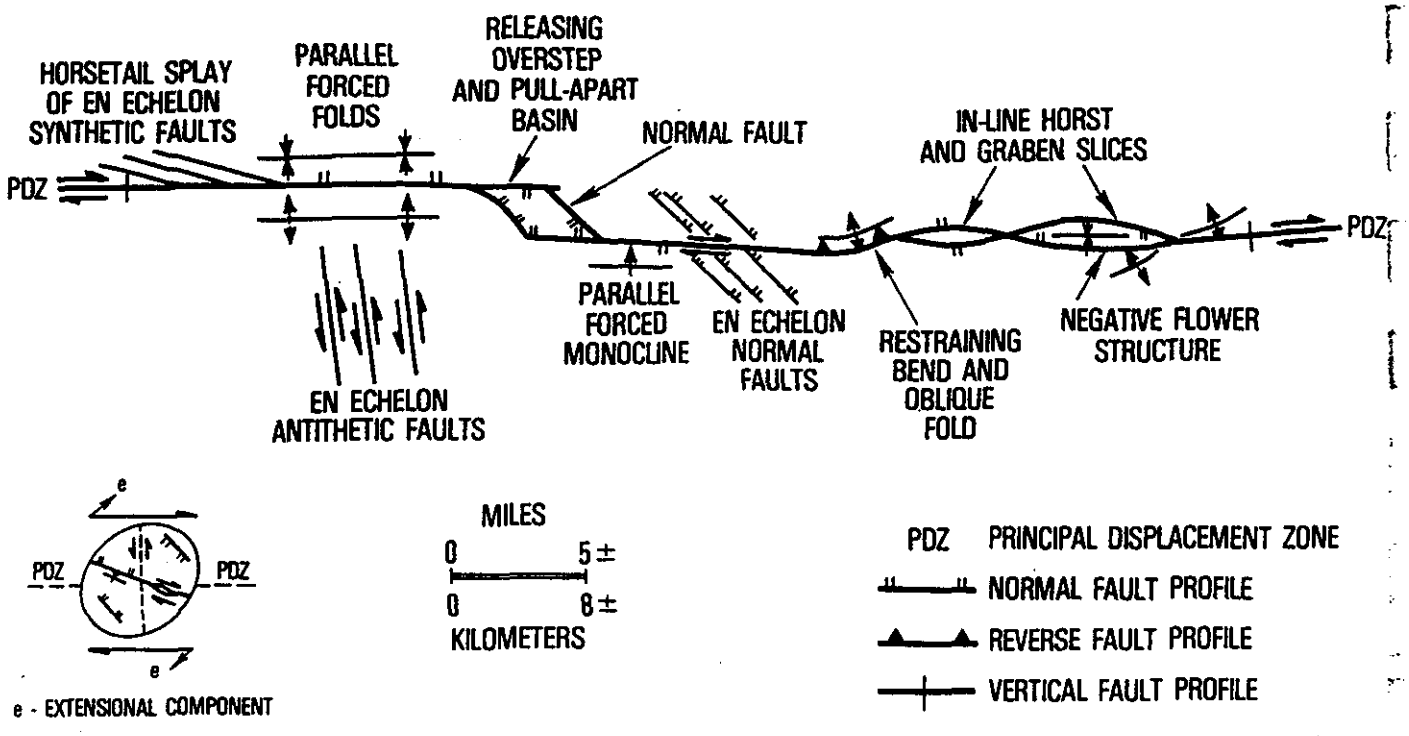
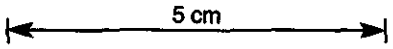



FIG. 1.—Assemblage of structures associated with divergent wrench faults and simplified strain ellipse for right-slip deformation (inset). Not all divergent wrench zones contain every feature and those structures present may be combined in different ways. The assemblage shown here is a composite of examples presented in this paper and others cited in the references.




### *Principal Strike-Slip Displacement Zone*

A linear, throughgoing principal displacement zone is the fundamental element of the structural assemblage (PDZ in Fig. 1). This zone accounts for most of the lateral displacement between opposing blocks. Other faults in the assemblage tend to be shorter and to have smaller displacements. In some cases, the deformation consists solely of the principal displacement zone; in other instances, the zone is flanked on one or both sides by associated external structures.

Tchalenko and Ambraseys (1970) demonstrated that the principal displacement zone is composed mostly of synthetic strike-slip faults (i.e., Riedel shears; Riedel, 1929) and interconnecting P shears. Strike slip along P shears is in the same sense as along the synthetic faults, but P shears and synthetic faults step in opposite senses (Fig. 2). The prediction of structures and their orientations shown in Figure 2 is simplistic, and is most applicable to the early stages of a single tectonic event and to one wrench zone. Protracted or episodic deformation involving two or more major wrench faults can be considerably more complex. Orientations of structures in left-slip systems may be determined by viewing Figures 1 and 2 in reverse image.

The overall dip of the principal displacement zones is thought to be near-vertical at depth in many instances, and where there is definitive control, faults with normal separation dominate in transverse profiles (i.e., hanging-wall block apparently downthrown; Fig. 3). As with other types of wrench faults, the direction of fault dip may change along

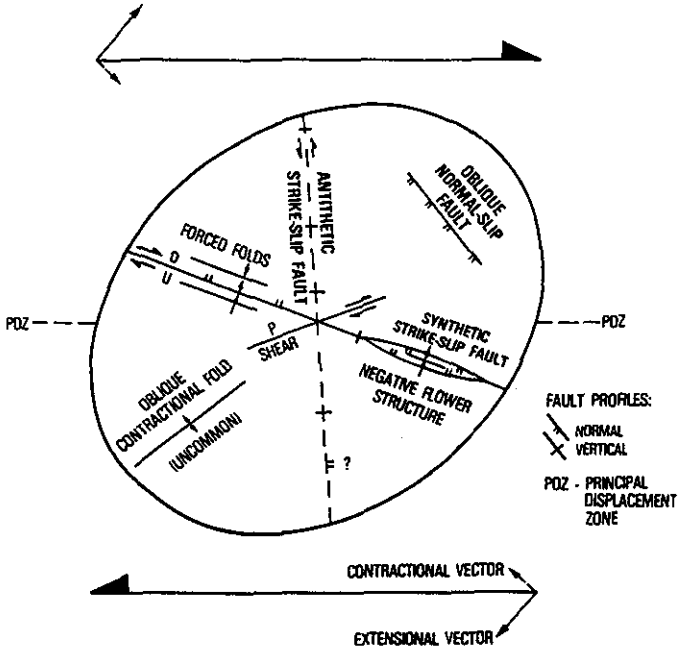



FIG. 2.—Strain ellipse with idealized orientations of main structures initiated along a right-lateral divergent wrench fault, compiled from clay-cake models and from geologic examples. Most of the structures and their orientations are present in other styles of wrench faults, but the comparative abundance of the various features differs significantly. Segments of the principal displacement zone (PDZ) that splay or bend to the right tend to have normal separation, but reverse faults can also be present depending on the way in which displacements are distributed along the PDZ.

655178



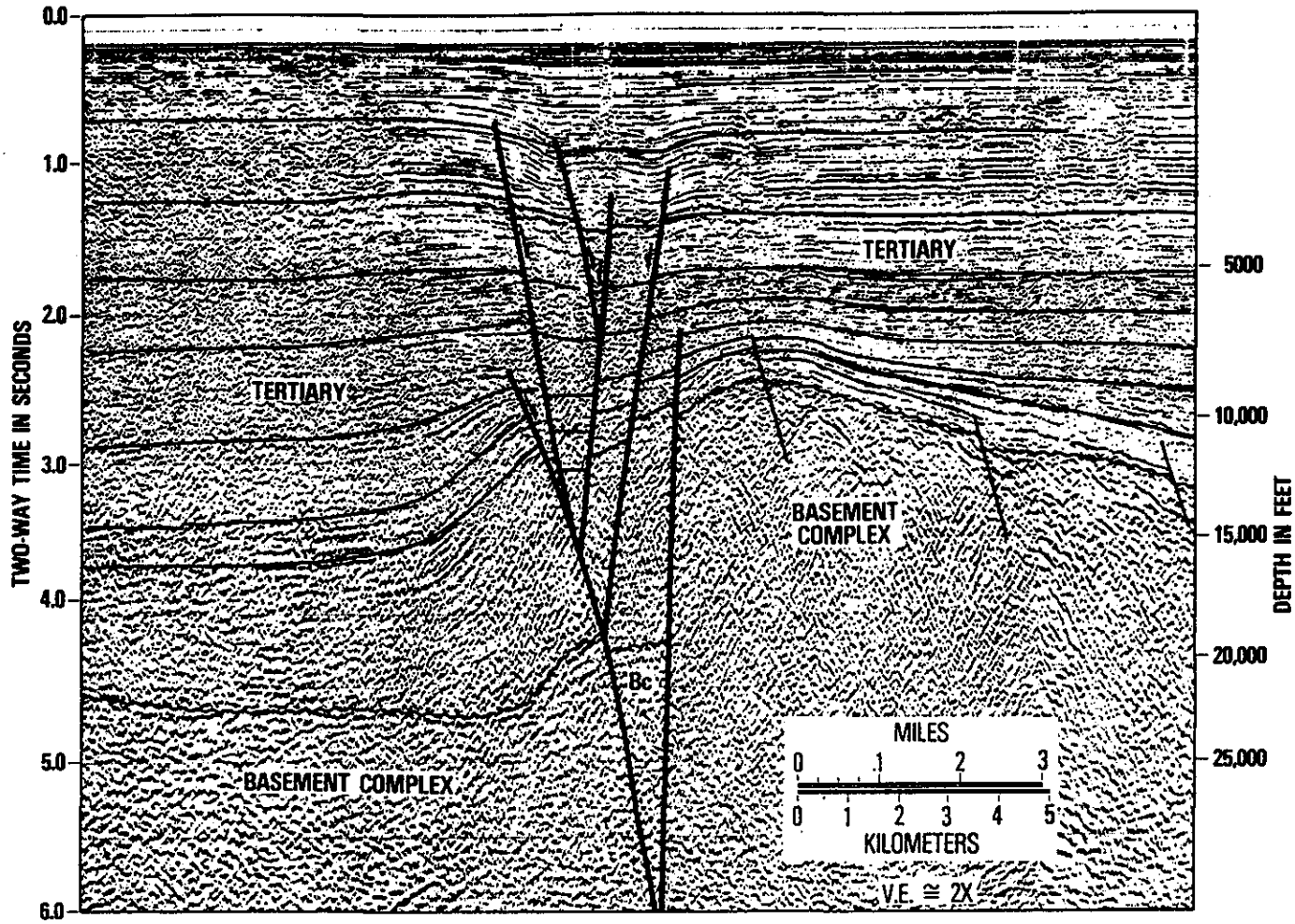



FIG. 3.—Seismic profile across a major fault zone in the Bering Sea. This area has undergone several deformations with different structural styles. Divergent wrench fault characteristics are most apparent in the younger Tertiary sediments above 2.0 seconds. Interpretation courtesy of W. A. Spindler (personal commun., 1984).

strike, and the apparently upthrown side can also change along strike or from one structural level to another. In some examples, the principal displacement zone appears to terminate abruptly at depth against a subhorizontal crustal detachment (Royden, 1985 this volume; Cheadle et al., in press).

Along some divergent wrench systems the principal displacement zone splays upward and outward at shallower levels (Emmons, 1969). The fault slices may form the core of a negative flower structure, which is defined as a shallow synform bounded by the upward and outward spreading strands of strike-slip faults that have mostly normal separation (above 2.0 seconds in Fig. 3; Harding and Lowell, 1979; D'Onfro and Glagola, 1983; Harding, 1983, 1985). The fold is termed a synform because at depth the flanks may have tilted independently and may never have been parts of an integrated flexure. Divergent wrench faults composed of a single strand may be more common, however.

Faults with reverse separation in transverse profile (i.e., hanging-wall block apparently upthrown) are present within some principal displacement zones. Contractional structures are throught to be most common where irregularities in the zone's trace cause opposing blocks to converge (e.g., restraining bend in Fig. 1; Crowell, 1974; Aydin and Nur, 1982). The contractional features commonly distinguish divergent wrench faults from normal-slip faults, which otherwise may have similar profile characteristics (Harding, 1985). However, successive intervals of normal slip and block rotation (in cross section) in areas of very great extension can over-steepen the initial normal faults so that they acquire reverse separation (Proffett, 1977). The presence of both normal and reverse separation then ceases to distinguish the two styles. Releasing bends (Crowell, 1974) and releasing oversteps (Christie-Blick and Biddle, 1985 this volume; see Fig. 1) may cause blocks to diverge and enhance the development of extensional strike-slip features. Several examples of these relationships are discussed below.

Most folds associated with the divergent wrench faults we have studied occur adjacent to and parallel with the principal displacement zone. In the absence of regional horizontal shortening, the more subtle vertical components of movement appear to be the major cause of fold formation.

5 cm

655179



The flexures resemble the forced folds that develop above normal fault blocks: anticlines or monoclinal knees adjacent to and parallel with the relatively higher side of the principal displacement zone; synclines or monoclinal ankle flexures adjacent to and parallel with the edge of the apparently down-dropped block. These flexures commonly bound negative flower structures at shallow levels (e.g., above 2.0 seconds in Fig. 3). Where the principal displacement zone consists of a single strand, a single monoclinal knee or ankle may face toward the relatively down-dropped block, or both high- and low-side flexures may be absent.

### *External Associated Structures*

Deformation of the terrane flanking the principal displacement zone may be negligible. The regional dip in several examples continues unchanged across the zone, and external structures are diffuse or absent (see shallower reflections on Fig. 3). In other examples, faults oblique to the trace of the principal displacement zone are the most common type of associated structure.

*External Faults.*—The external faults, where present, occur in belts along one or both sides of the throughgoing wrench and are en echelon or oblique to the trend of the zone: left-stepping for right-lateral systems (Fig. 1) and right-stepping for left-lateral zones (Fig. 4). The strike of the external faults ranges from slightly oblique to the principal displacement zone (e.g., synthetic or Riedel strike-slip faults; Riedel, 1929) to nearly transverse (e.g., antithetic or conjugate Riedel faults; Fig. 2). The external fault sets commonly contain several fault orientations, but most external faults tend to be subparallel to the direction predicted for normal faults by our simple strain ellipse. In addition, where control is sufficient for determination, most of the external faults are characterized by normal separation and steep dips.

The fault set of the Lake Basin fault zone is an example of a distinct right-stepping en echelon pattern (Fig. 4). There is no principal displacement zone at the surface, but a left-lateral divergent wrench fault is believed to be present at depth (Chamberlain, 1919; Alpha and Fanshawe, 1954; Smith, 1965). A segment of the Dasht-e Bayaz earthquake system studied by Tchalenko and Ambraseys (1970) in central Iran similarly consists solely of en echelon fractures. The relationships there are unusually clear and these authors interpreted the pattern as representative of an initial stage in the development of the throughgoing principal displacement zone.

Individual dislocations along the Lake Basin fault zone strike at angles of 30° to 70° (most are between 45° and 60°) to the overall trend and have been interpreted as normal faults (Smith, 1965). Seismic control near the west end of the zone demonstrates steep fault dips with normal and, possibly, several reverse separations (Fig. 5). The variety of trends and separations probably results from the interaction of two factors: (1) pre-deformational anisotropies, and (2) external rotation and reactivation of the faults.

External rotation may significantly alter the structural pattern, and the style is, therefore, best expressed in the early stages of deformation. Attempts to identify it in later stages on the basis of observed or reconstructed fault patterns may be misleading. The effects of rotation have been demonstrated on a small scale by means of earthquake fractures in southern California (Terres and Sylvester, 1981: Fig. 6A in Christie-Blick and Biddle, 1985 this volume). There, clockwise external rotation of a planar anisotropy oriented oblique to the right-slip Imperial fault occurred during the earthquake of 15 October 1979 (see inset map in Fig. 6 for location of Imperial fault). The earthquake fractures approximate en echelon normal faults, and antithetic strike slip was superimposed on them by the rotation. Both reverse and normal separations are present. The sense of external rotation matched the sense of strike slip on the Imperial fault, and imposed the antithetic displacements in a mechanism roughly analogous to the slip generated by inclining a row of dominoes. Such a mechanism has been discussed by Freund (1970), and also by Luyendyk et al. (1980) to explain how paleomagnetically determined block rotations of 70° to 80° may be accommodated in the Miocene tectonics of southern California.

*External Associated Folds.*—Folds outside the principal displacement zone are generally sparse. Where developed, they are oblique or en echelon to the master fault: left-step-

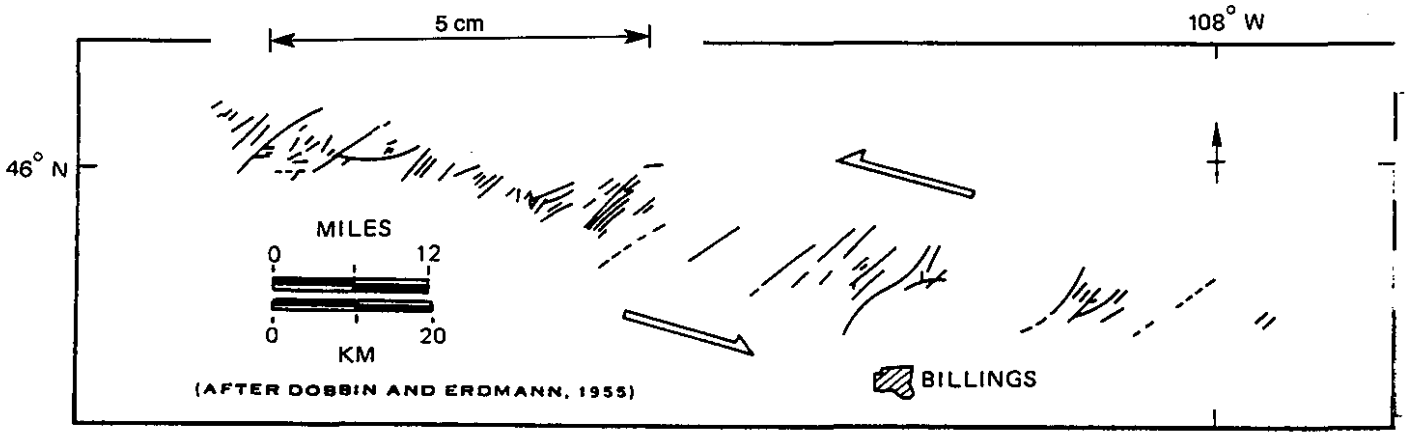



FIG. 4.—Surface map of Lake Basin fault zone, Montana. Orientations of most en echelon faults correspond with the idealized normal-fault direction in Figure 2 for left-lateral wrench faulting, but some faults are more nearly transverse and several are less oblique than predicted.

655180

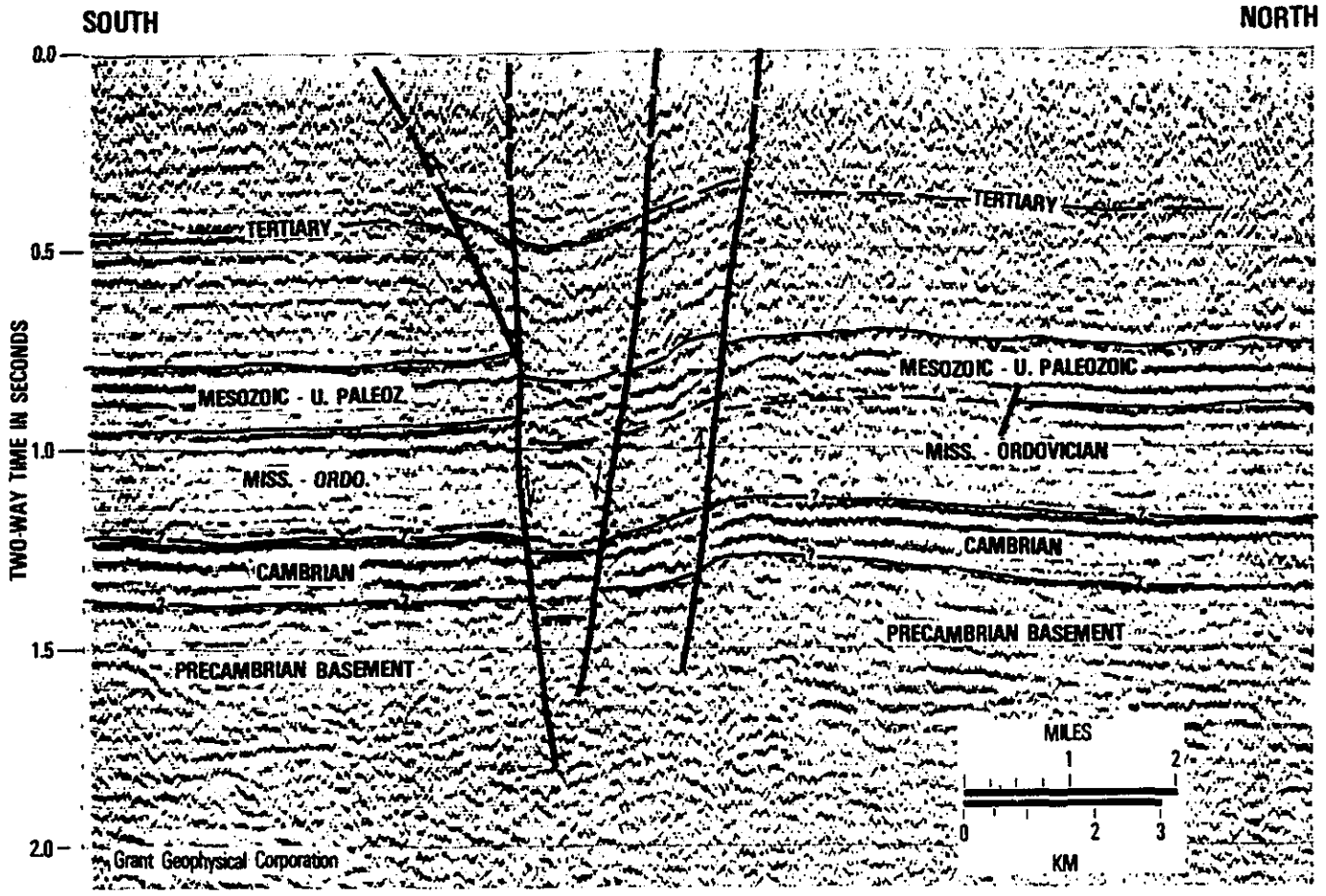



FIG. 5.—Seismic profile near west end of the Lake Basin fault zone. Zone includes both faults with normal separation and faults with reverse separation. Most faults dip steeply and they may converge at greater depth into a single, throughgoing principal displacement zone. The deformation has been dated as post-Paleocene and possibly post-Eocene by Alpha and Fanshawe (1954). Profile courtesy of Grant Geophysical Corporation, 1983; interpretation courtesy of G. H. Weisser (personal commun., 1983).

5 cm

ping for left-lateral faults and right-stepping (Fig. 1) for right-lateral faults. Where we have observed external folds, they result from localized convergent deformation, for example, at a restraining bend (Fig. 1). They may also form during an earlier, convergent phase of strike slip that had the same sense of offset as the subsequent divergent phase.

Other folds and faults may be inherited from earlier deformation unrelated to strike slip or may be superimposed by later tectonic events. Some of these structures could appear by coincidence to be congruent with the structural relationships of a wrench zone, and recognition of this disparity is a prerequisite for the correct analysis and identification of style.

## DIVERGENT WRENCH FAULTS OF THE MECCA HILLS

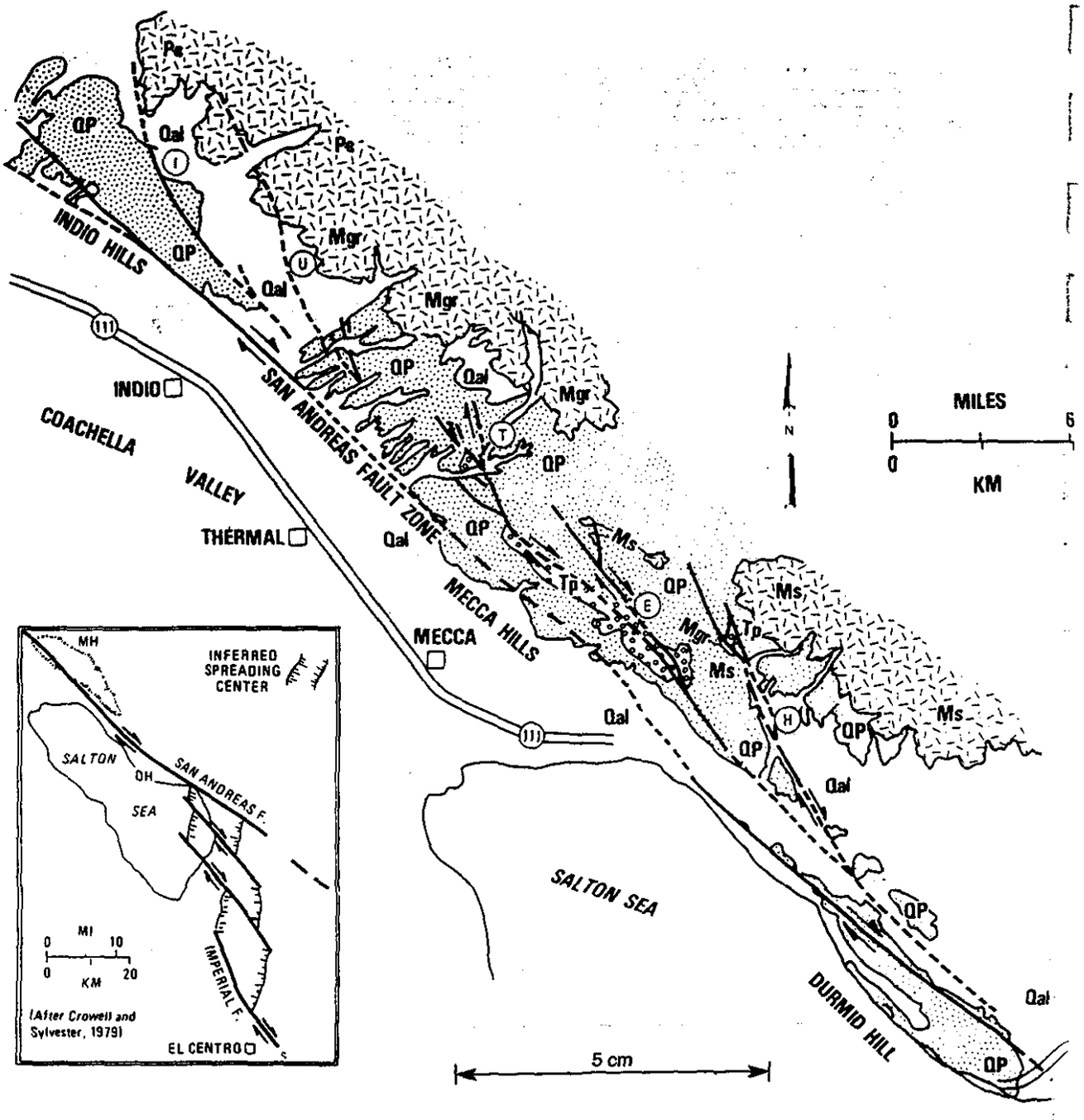
### *Plate-Tectonic Setting of the Mecca Hills Faults*

The Mecca Hills faults are three subparallel, right-slip faults that splay northward from the San Andreas wrench system along the northeast margin of the Salton Trough (Fig. 6). The divergent wrench style consists here almost solely of the principal displacement zone. The present tectonic framework originated around 4.5 Ma and is considered to be a northwestward continuation of the Gulf of California ridge-and-transform system (see inset map in Fig. 6; Crowell and Sylvester, 1979; Crowell, 1981). The subsurface axis of the trough lies within a releasing overstep (Fig. 1) between the San Andreas and Imperial faults. Their side-stepped pattern is indicated by earthquake epicenters and the surface traces of active faults (Rockwell and Sylvester, 1979). Away from the San Andreas and Imperial faults, the Salton Trough is flanked by high basement terranes that form the limbs of a broad arch (J. C. Crowell, personal commun., 1979).

On the northeast flank of the basin, convergent wrench faults dominate the structural style of the San Andreas and other major northwest-striking faults (Sylvester and Smith, 1976). The strike of the Mecca Hills splay faults is midway between that of the convergent strands and the north-south orientation predicted for normal faults associated with the San Andreas system (compare orientations with the strain ellipse of Fig. 2). Structural features typical of divergent wrench faults have been observed along three of the splays: the Painted Canyon, Eagle Canyon, and Hidden Springs

655181






**RECOGNIZED AND POTENTIAL DIVERGENT WRENCH FAULTS**

- (H) HIDDEN SPRINGS FAULT (FIG. 8)
- (E) NORTHERN SEGMENT OF EAGLE CANYON FAULT (FIG. 7)
- (T) THERMAL CANYON SPLAY OF PAINTED CANYON FAULT
- (U) UNNAMED FAULT
- (I) INDIO HILLS FAULT

- Qal RECENT ALLUVIUM
- QP PLIOCENE-PLEISTOCENE NONMARINE SEDIMENTS
- Tp PLIOCENE NONMARINE SEDIMENTS
- Mgr MESOZOIC (?) GRANITIC ROCKS
- Ms MESOZOIC OROCOPIA SCHIST
- Pc PRECAMBRIAN COMPLEX

(GENERALIZED AFTER ROGERS, 1965, AND JENNINGS, [illegible])

faults (Fig. 6). The investigation of two faults to the north with similar orientations is incomplete.

### *Evidence of Right Slip on the Mecca Hills Faults*

Fine-grained Pliocene rocks adjacent to the Painted Canyon fault are offset approximately 3 km from their source (A. G. Sylvester, personal commun., 1979). Along another portion of this fault, Hays (1957) reported distributions of rock colors that suggest about 0.8 km of right slip. In addition, the en echelon pattern of folds associated with the southeastern segments of the Painted Canyon and Eagle Canyon faults suggests right slip.

The distribution of Pliocene sedimentary rocks along the Eagle Canyon fault indicates right slip of 1.6 km (Hays, 1957). Along the southern segment of this fault the northwestern boundary of an en echelon fold set lies approximately 1.3 km farther southeast than its position across the fault (Fig. 7). The folds are thought to have formed mainly during accumulation of the right slip (Sylvester and Smith, 1976), but they could have developed independently, which would negate their validity as offset evidence.

Along the Hidden Springs fault, the northeast limit of a distinctive basal breccia is apparently offset 1.2 km right-laterally, but according to Hays (1957), irregularities in the original depositional pattern could account for much of this displacement. Near Shaver's Well, displacement on the Hidden Springs fault dies out rapidly into horsetail splays (Fig. 8). Here, tongues of a schist breccia are offset as much as 45 m right-laterally on individual faults (Hays, 1957).

### *Structural Styles of the Mecca Hills Faults*

Both the Painted Canyon and the Eagle Canyon faults have convergent strike-slip styles along their southern and central segments where they are closest to the San Andreas fault zone (Fig. 6). Along the central segment of the Eagle Canyon fault, beds are steeply dipping to overturned, the fault has a vertical or upthrust profile (segment with sawtooth symbols in Fig. 7), and drag folds are tight where present. Farther south, the limbs of tight, en echelon folds are offset across the fault, and it is difficult to differentiate these external structures from features of the principal displacement zone.

Deformation along the northern, divergent trace of the Eagle Canyon fault (segment with double tick symbol in Fig. 7) is much less intense and less complex than that to the south. A major normal fault, oriented north-south within the extensional sector predicted for the regional right-slip deformation, is the main external structure in this area (left of mid-point of Fig. 7). Beds dip 5° to 15° basinward across the area, with only minimal disruption. The principal displacement zone consists of a single strand with normal separation (Fig. 9). At the locality of Figure 9 (shown in Fig. 7), the zone's dip appears to flatten with depth, but this may be only a local irregularity. A gentle upturn of beds within the hanging-wall block locally reverses the basinward dip and forms a low-side syncline (Fig. 10). The syncline is thought to reflect the vertical component of the deformation. An accompanying high-side, forced anticline lies opposite the syncline only 0.5 km to the southeast (Fig. 7), and drag folds that demonstrate shortening are noticeably absent within the principal displacement zone. To the northwest, the Eagle Canyon fault terminates into a large horsetail structure composed of closely spaced, subvertical to vertical faults. There is little or no folding or other distortion of the regional dip of beds within the horsetail.

The Thermal Canyon fault (T in Fig. 6) is the north-northwest-striking splay of the Painted Canyon fault and is the segment of that system that has a divergent style. The contractional structures that dominate the southern portions of the Painted Canyon fault appear to be absent, and the principal displacement zone has normal separation. Horizontal slickenside striae are the only structural indication of strike slip.

The Hidden Springs fault (H in Fig. 6) is consistently oriented within the extensional sector of the regional right-slip deformation. The principal displacement zone of this fault generally dips steeply to vertically, and along much of its length has an extensional strike-slip style (Fig. 8). The zone terminates northward into a complex horsetail composed of several major fault strands. In a tributary canyon just south of Shaver's Well, the main faults bound narrow, steeply dipping slices. One strand splays upward and outward, forming a fault architecture similar to a negative flower structure (Fig. 11). Other subvertical faults within the canyon abut the throughgoing north-northwest-striking faults at high angles. Both the main strands and the external faults have abundant horizontal slickenside striae, but there is little or no evidence of horizontal shortening within the offset beds.

South-southeast of the horsetail, the strand of the Hidden Springs fault illustrated in Figure 11 turns eastward into the contractional sector of the deformation (i.e., turns subparallel to the orientation predicted for contractional structures associated with right slip; compare with Fig. 2), and forms a restraining bend (segment with sawtooth symbols in Fig. 8). The profile of the principal displacement zone opposite this bend is that of a downward-steepening reverse fault, and beds immediately adjacent to the fault are shortened by drag folding (Fig. 12).

## COTTAGE GROVE FAULT SYSTEM

### *Plate-Tectonic Setting of the Cottage Grove Fault System*

The structural style of the Cottage Grove fault system is dominated by external en echelon faults and has been elab-

FIG. 6.—Late Cenozoic tectonic framework of Salton Trough, California, in the vicinity of the Mecca Hills (inset), and location of divergent wrench faults identified along the northeast side of the San Andreas fault. Lack of continuous outcrops adjacent to the San Andreas fault makes it difficult to demonstrate a direct connection with the divergent wrench faults, but a splay configuration is inferred from the tectonic relationships. Abbreviations in inset map: MH, Mecca Hills; DH, Durmid Hill.

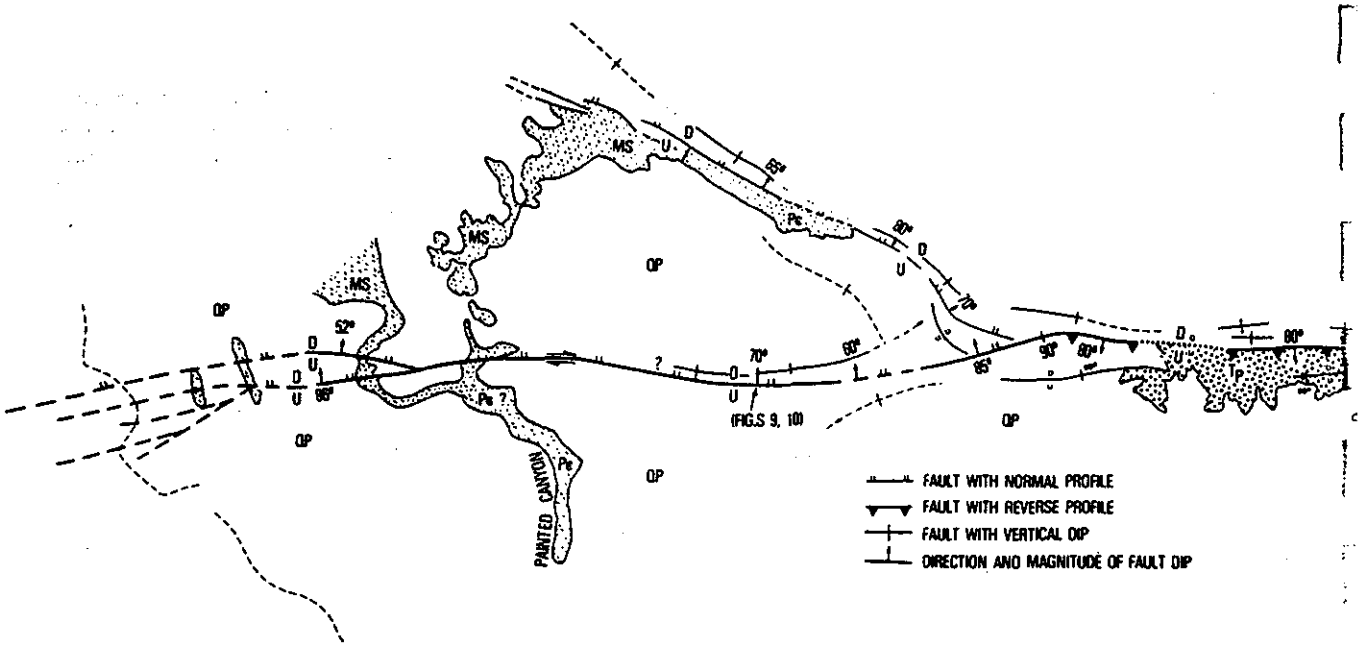



FIG. 7.—Generalized surface geologic map of the Eagle Canyon fault, Mecca Hills. Dating and correlation of stratigraphic units modified aft

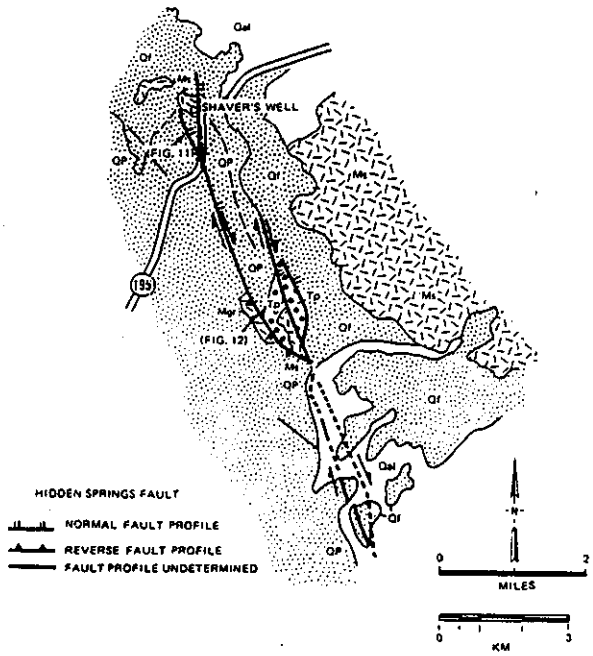



FIG. 8.—Generalized geologic map of northern segment of the Hidden Springs fault, Mecca Hills (after Jennings, 1967). Qf, Pleistocene fanglomerate; see Figure 6 for explanation of other symbols and for setting of fault.

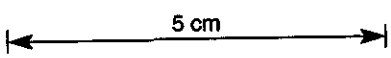
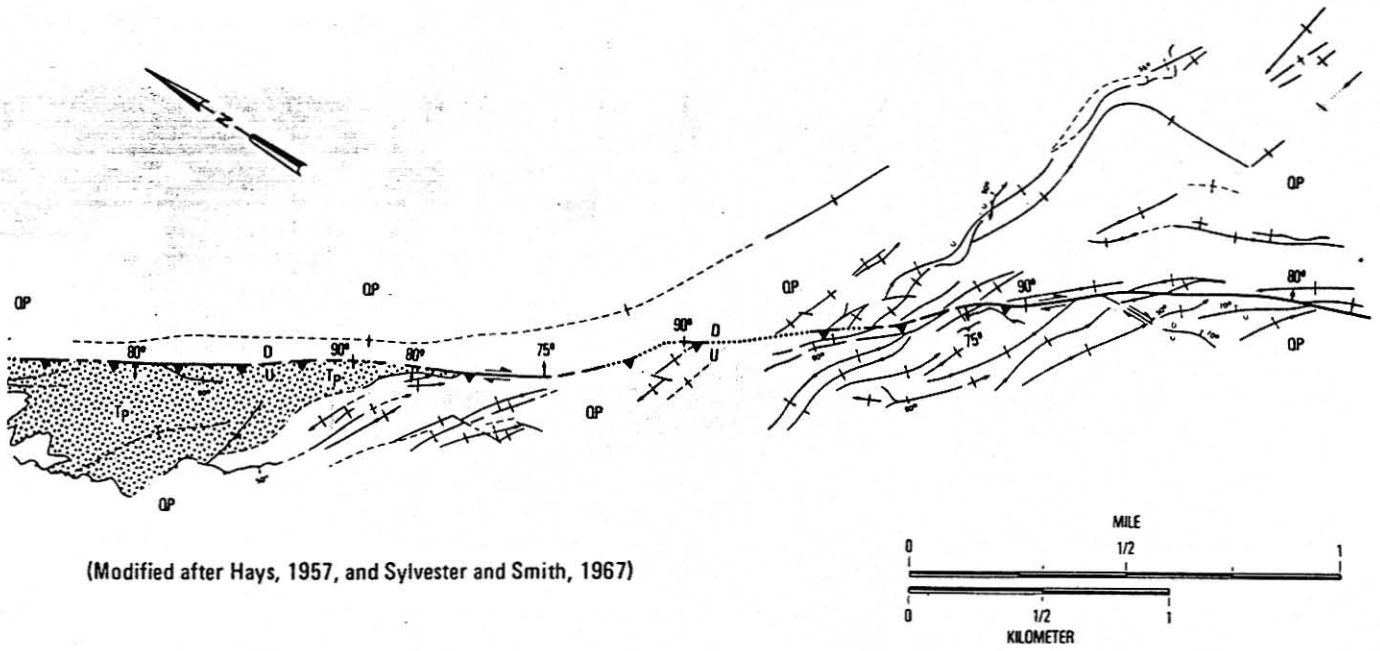






FIG. 9.—Profile of Eagle Canyon fault. Outcrop is approximately 25 m high. Exposed segments of fault surface are indicated by arrows. Basal Pliocene-Pleistocene conglomerates on left are juxtaposed against stratigraphically higher, lighter colored buff sandstones and pebbly sandstones of the hanging-wall block on the right. View toward northwest. See Figure 7 for location and Figure 10 for associated fold.




(Modified after Hays, 1957, and Sylvester and Smith, 1967)

Jennings (1967). See Figure 6 for explanation of symbols for rock units and setting of fault.

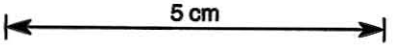





FIG. 10.—Drag syncline on eastern, relatively down-dropped side (foreground) of northern segment of the Eagle Canyon fault. Position of fault is indicated by arrow. Visible portion of cliff face is approximately 20 m high. Fault dips toward viewer and follows face of darker colored outcrop from left margin of photograph. View toward west-northwest. See Figure 7 for location and Figure 9 for profile of fault zone.

655185




FIG. 11.—Portion of a divergent horsetail at the northwest termination of the Hidden Springs fault. Exposure of faults is 12 to 15 m high. Splays are closely spaced and steeply dipping; most have horizontal slickenside striae here or in adjacent outcrops. Displaced Pliocene-Pleistocene gravels exhibit little or no folding. Faults merge downward into single, subvertical zone at right base of photo. View toward south-southeast. See Figure 8 for location. T, displacement toward viewer; A, away from viewer.

orately documented by Nelson and Krausse (1981; see their illustrations for further details of the style). The system trends east-west for possibly 110 km across the southwest flank of the Illinois Basin (Fig. 13). The basin is a gentle, intracratonic downwarp. The broad arches and domes at the periphery of the downwarp were formed by mid-Ordovician time, except the Pascola arch, which is thought to have developed in the late Paleozoic (Buschbach and Atherton, 1979; Sloss, 1979). The basement warps and adjacent forelands (Appalachian and Arkoma Basins in Fig. 13) separated the Illinois Basin from orogenic belts that were active on the southeast (Appalachian thrust front) and southwest during the late Paleozoic.

The origin of the intracratonic sag is uncertain, but it may be related to thermal contraction of lithosphere, extended during the formation of an earlier graben system (Ervin and McGinnis, 1975; Sloss, 1979). Aeromagnetic and gravity surveys have delineated a deeply buried northeast-trending trough, the Reelfoot rift of Ervin and McGinnis (1975) or the Mississippi Valley graben of Kane et al. (1981). The northeasternmost segment of this graben corresponds closely with the southward plunge of the Cambrian-Ordovician precursor of the Illinois Basin (Fig. 1 in Sloss, 1979). The Cottage Grove fault system may have developed along a segment of the older graben system (Heyl and Brock, 1961; Buschbach and Atherton, 1979).

Precise dating of the age of faulting is not possible because of the absence of stratigraphic section between the deformed Pennsylvanian beds and the surficial Pleistocene cover. Igneous dikes in the nearby fluorspar district (4 in Fig. 13) have been dated as 267 ± 20 Ma, or Early Permian (Zartman et al., 1967), and are similar compositionally to dikes intruded into extensional faults of the Cottage Grove system. Nelson and Krausse (1981) accept this as evidence of a late Paleozoic age for the wrench faulting.

### *Evidence of Right Slip on the Cottage Grove Fault System*

Clark and Royds (1948) were the first of a number of authors (e.g., Heyl and Brock, 1961; Wilcox et al., 1973)

to suggest that the Cottage Grove system contains structures that resulted from strike-slip deformation. Nelson and Krausse (1981) have recently summarized this structural evidence: (1) The orientations of structural elements generally repeat those predicted for right slip by the strain-ellipse and clay-cake models for right slip (compare Figs. 2 and 14; Wilcox et al., 1973). (2) The fault sets resemble the fracture systems developed along seismically active faults that have explicit evidence of lateral displacements (e.g., Fig. 8 in Tchalenko and Ambraseys, 1970). (3) The fault pattern and elements of the fold pattern are also similar to zones that have geologic evidence of historic strike slip (e.g., Bishop, 1967).

The boundaries of a Pennsylvanian stream deposit suggest as much as 1.6 km of right slip, but other channels limit the offset to a smaller amount. Nelson and Krausse (1981) have concluded that the maximum lateral displacement is on the order of several hundred meters.

### *Characteristics of the Principal Strike-Slip Displacement Zone*

The principal displacement zone includes the main faults of the Cottage Grove fault system and has structural characteristics typical of wrench zones. These are (1) subvertical faults, (2) inconsistent apparent upthrown side, (3) interchanging normal and reverse separations across the zone as a whole, and (4) narrow, steeply dipping, in-line horst and graben slices that form a braided swath and have normal and reverse separations on individual faults (Nelson and Krausse, 1981). Nelson and Krausse describe the master zone as typically tens to hundreds of meters wide, with vertical displacements as great as 60 m.

Discontinuities occur in the major strands of the principal displacement zone and are occupied by considerably shorter, northwest-striking en echelon faults (Fig. 15). These en echelon faults are steeply dipping, and most have normal separations. Some of the faults have horizontal slickenside striae and reverse separations that are interpreted by Nelson and Krausse (1981) as consequences of oblique slip. These authors, in an interpretation similar to ours and others (e.g., Tchalenko and Ambraseys, 1970), have interpreted the structure of the discontinuities as characteristic of an early stage in the development of the Cottage Grove system.

Folds associated with the known extent of the system lie immediately adjacent to the upthrown side of the principal displacement zone, and most trend subparallel with the zone (Fig. 16). The zone-parallel folds verge toward the appar-

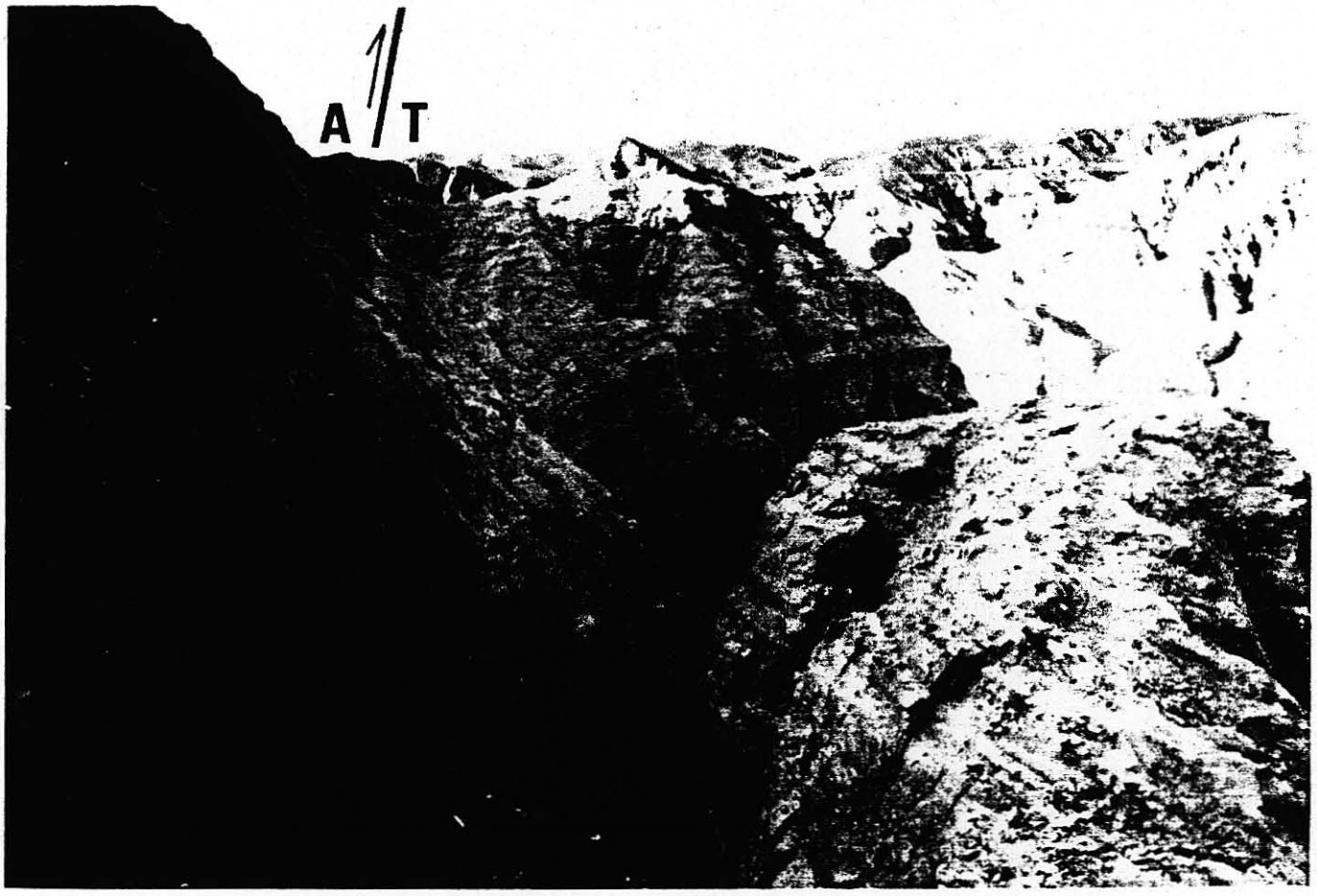



FIG. 12.—Steep upthrust profile at restraining bend in trace of the Hidden Springs fault. Fault bounds a large block of Mesozoic(?) granite on the left. Exposed segment is approximately 6 m high. Pliocene-Pleistocene sandstones and gravels in footwall on right are dragged steeply upward in apparent response to a vertical, convergent component of displacement. View toward the northwest. See Figure 8 for location. T, displacement toward viewer; A, away from viewer.

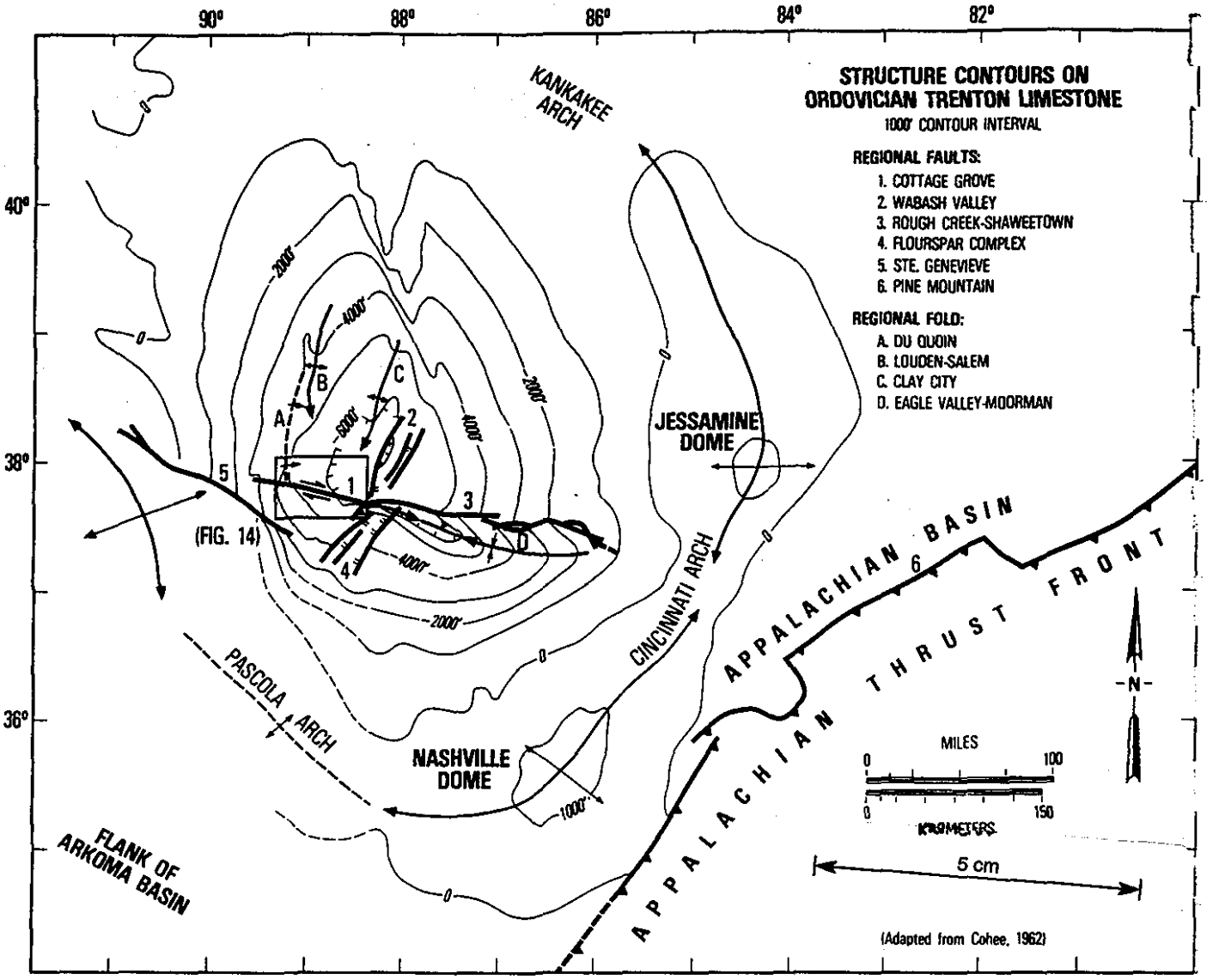



FIG. 13.—Intraplate tectonic setting of the Illinois Basin and Cottage Grove fault system (fault 1). Peripheral arches and flanks of foreland basins (Arkoma Basin, Appalachian Basin, and Black Warrior Basin south of Nashville Dome) separate the Illinois Basin from the convergent margin structures to the east (e.g., Appalachian Thrust Front) and south (south of Arkoma Basin).

ent down-dropped block (Figs. 15, 16). Nelson and Krausse (1981, p. 56) interpreted the structures as drape folds caused by vertical components of the deformation. Two small anticlines adjacent to the eastern portion of the principal displacement zone have a fundamentally different pattern. They lie oblique to the trend in a right-stepping en echelon pattern that is compatible with the right-slip deformation.

### *Characteristics of the External Structures*

Left-stepping en echelon faults are present within a belt 5 to 16 km wide along both sides of the entire mapped trace of the principal displacement zone (Fig. 14). Individual faults are as long as 11 km and have a maximum vertical separation of 20 m (Nelson and Krausse, 1981). The orientation of these faults relative to the principal displacement zone varies from that predicted for en echelon normal faults to the more nearly transverse trend anticipated for antithetic strike-slip faults (compare Figs. 2 and 14). Most dislocations are thought to be steeply dipping (60° to 90°) normal faults by Nelson and Krausse, and they consider faults on opposite sides of the principal displacement zone to have developed independently.

Nelson and Krausse (1981) also report that some of the external faults show evidence of oblique slip, such as oblique and horizontal slickenside striae, and changes in dip direction, separation sense (normal and reverse), and apparent upthrown side on individual dislocations. Strike slip may be dominant on a number of faults, and at several localities, reverse and normal separations occur on adjacent, parallel strands (Fig. 17). We suggest that, similar to the Lake Basin fault zone, external clockwise rotation of the blocks bounded by the en echelon faults occurred during wrench deformation and could have selectively rejuvenated some of the faults in a reverse- and strike-slip sense. In addition,

other breaks may have originated as antithetic strike-slip faults.

Several anticlines are west of the principal displacement zone and trend oblique to its projection (Bremen anticline, Wine Hill dome, and Campbell Hill anticline in Fig. 16). Their location and right-stepping en echelon map pattern suggest an extension of the zone of right-slip deformation. The folding may have been accentuated by shortening at a restraining bend formed where the system's inferred continuation trends more nearly due west.

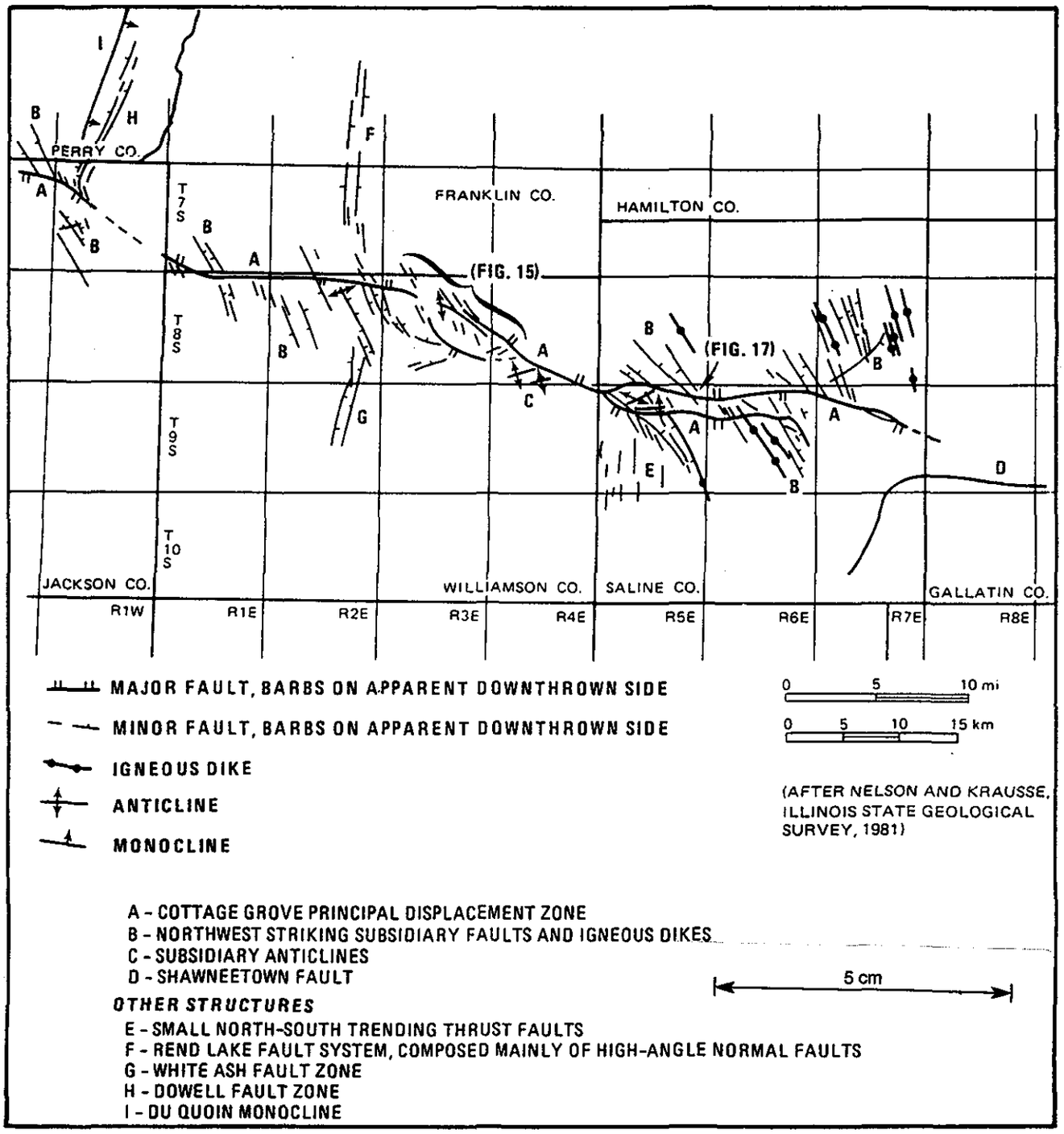



FIG. 14.—Main structural elements of the Cottage Grove fault system (subsidiary anticlines are incompletely shown; see Fig. 16). Structures D through I are considered not part of the Cottage Grove fault system by Nelson and Krausse (1981), and several are known to be of a different age. See Figure 13 for regional setting.

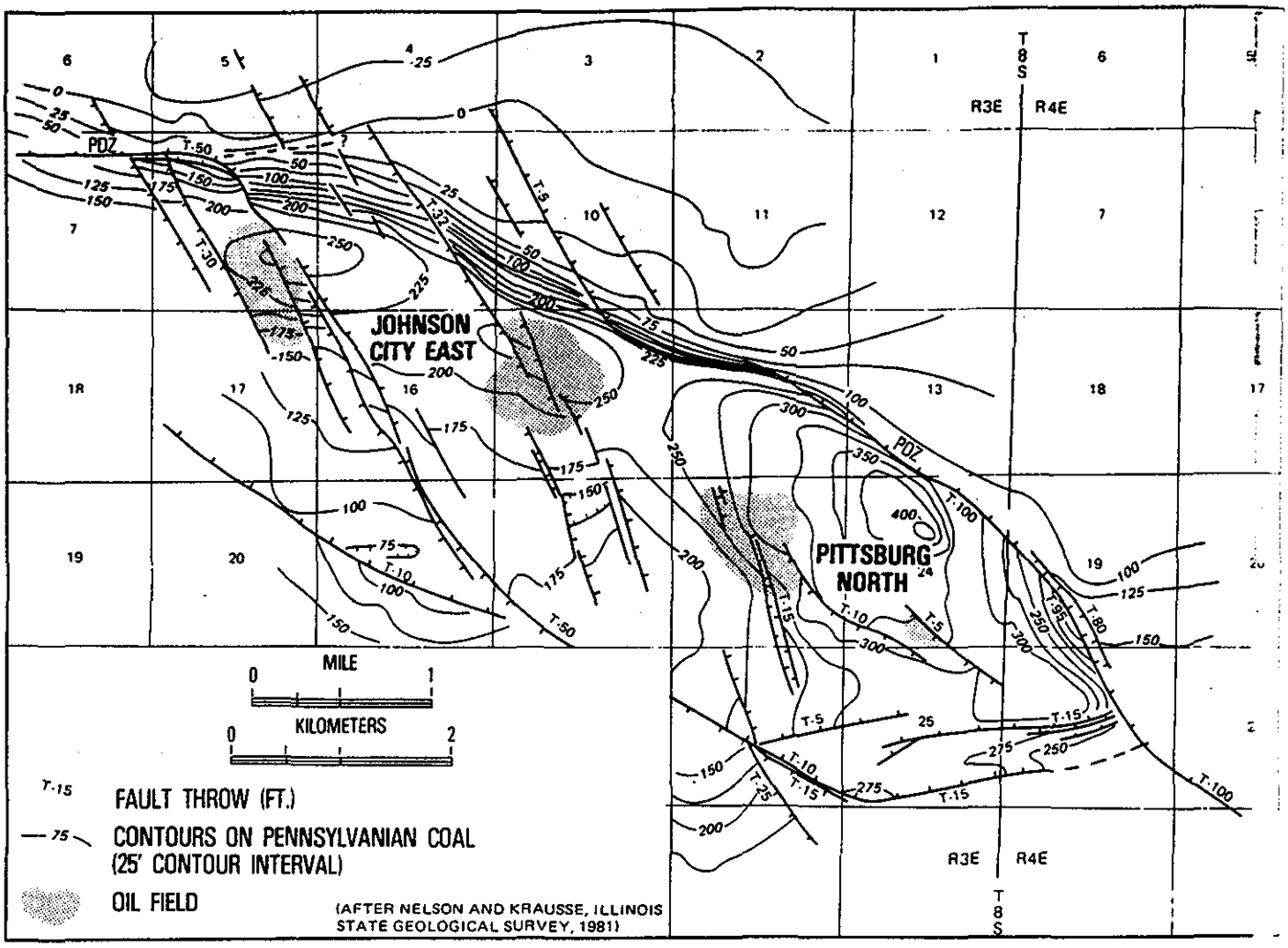



FIG. 15.—Detailed structure map of the principal displacement zone (PDZ) of the Cottage Grove fault system opposite the Pittsburg anticline (located in Figs. 14, 16). A gap in the PDZ occurs in Sections 8, 9, 10, 14, and 15 and is replaced by elements of an en echelon fault set. Other north-northwest-striking faults are external to the zone. The fold lies along the apparent high side of a projection of the PDZ and verges toward t relatively down-dropped, northeastern block.

5 cm

## ANDAMAN SEA FAULT

### *Plate-Tectonic Setting of the Andaman Sea Fault*

The Andaman Sea fault illustrates the profile characteristics of divergent wrench faults over a much greater range of depth than the Mecca Hills and Cottage Grove examples and further demonstrates the manifestation of the style in seismic reflection data. The wrench fault lies within the Andaman Sea region, a marginal basin bounded on the west by the Andaman-Nicobar Ridge and subduction zone, and on the east by the magmatic arc terranes of the Malay Peninsula (Fig. 18; C.C.O.P., 1981). On the eastern margin of the sea, north-striking normal faults were active from the Oligocene to the early Miocene (Curray et al., 1979). In the central portion of the sea, magnetic anomalies in oceanic crust demonstrate that seafloor spreading has been occurring there since at least 13.5 Ma (Lawver and Curray, 1981). Geophysical data and the trend of the central rift valley indicate that segments of the spreading ridge trer east-northeast to north-northeast and are linked by right-slip transform faults that strike north-northwest (Fig. 18).

### *Evidence for Right Slip on the Andaman Sea Fault*

The Andaman Sea fault trends north-northwest subpa allel to right-slip faults of similar age elsewhere in the re gion (Fig. 19; Eguchi et al., 1979). The zone has a numbe of features characteristic of wrench faults: (1) a relatively straight, throughgoing trace; (2) changes in the appare upthrown block that occur along strike (Fig. 19) and wi depth (Fig. 20); (3) flanking folds that have a right-stepping en echelon pattern near the northern end of the fault; and (4) a possible restraining bend suggested by reverse-sep ration faults at the zone's southern end. Several of the e echelon folds appear to be offset 2.5 to 3 km right-laterally (folds A-A′ and B-B′ in Fig. 19).

### *Structural Style of the Andaman Sea Region*

The structural assemblage of the Andaman Sea region repeats elements present in the above examples (compare Figs. 14, 16, and 19) and corroborates the observation that divergent strike slip has a unique and definable structural style. Deformation is characterized by a single major fault flanked by a set of discontinuous, oblique faults with normal separation (Fig. 19, and right side of Fig. 20).

The external fault set is asymmetric; dislocations are more numerous east of the principal displacement zone. Their profile characteristics are relatively simple and are repeated from one external fault to the next. The features suggestive of external rotation, cited for the Lake Basin and Cottage Grove zones, are absent. En echelon folds occur only near an apparent restraining bend formed where the wrench fault turns toward a more northwesterly course (north of profile 1 in Fig. 19). Elsewhere there are few if any structures

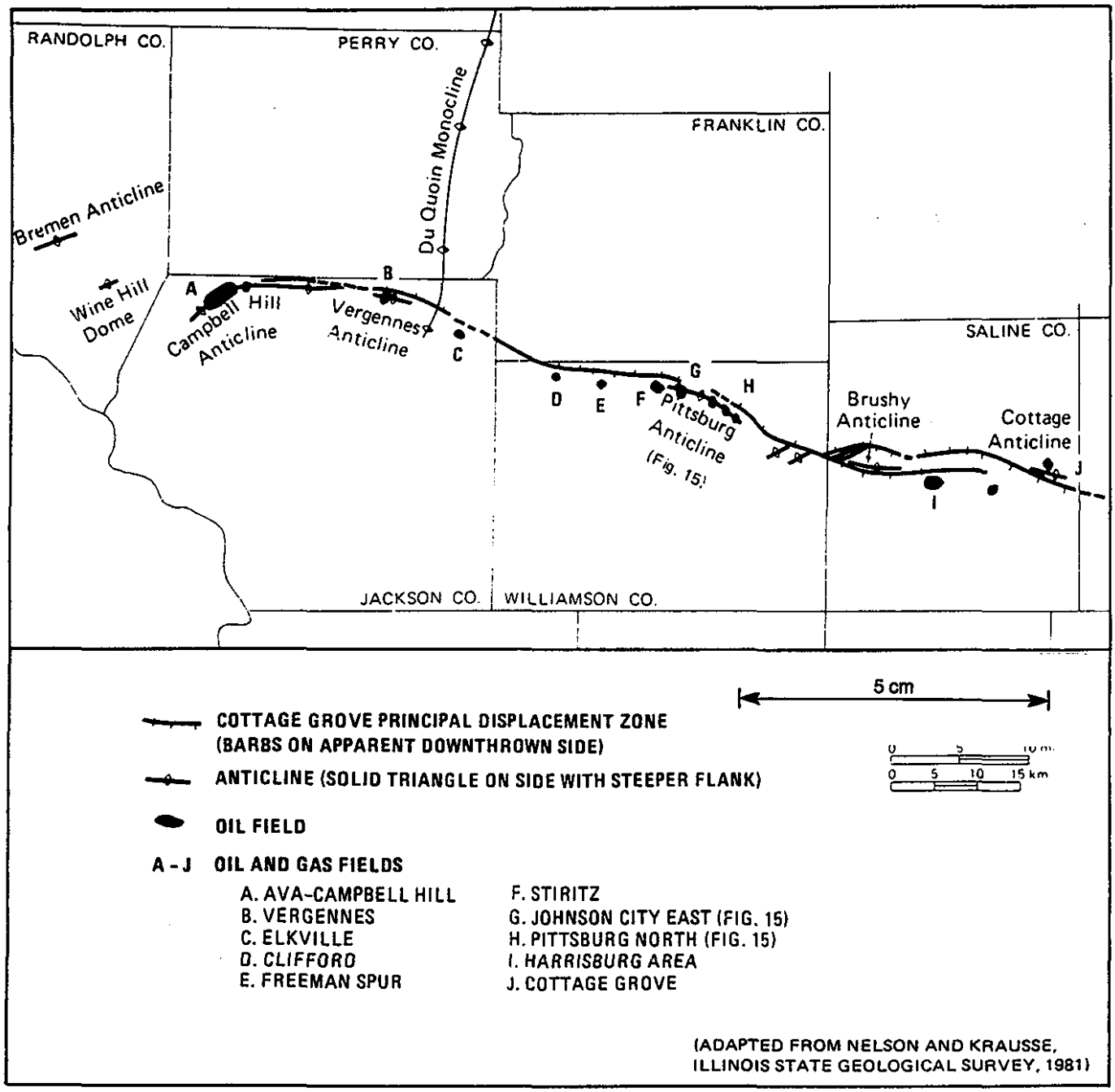



FIG. 16.—Map of the distribution of anticlines and oil and gas fields associated with the Cottage Grove fault system. Other oil and gas fields external to the system (most numerous to the north) are not shown. The inception of the Du Quoin monocline predates strike-slip deformation, and this structure is not considered to be part of the Cottage Grove system (Nelson and Krausse, 1981).

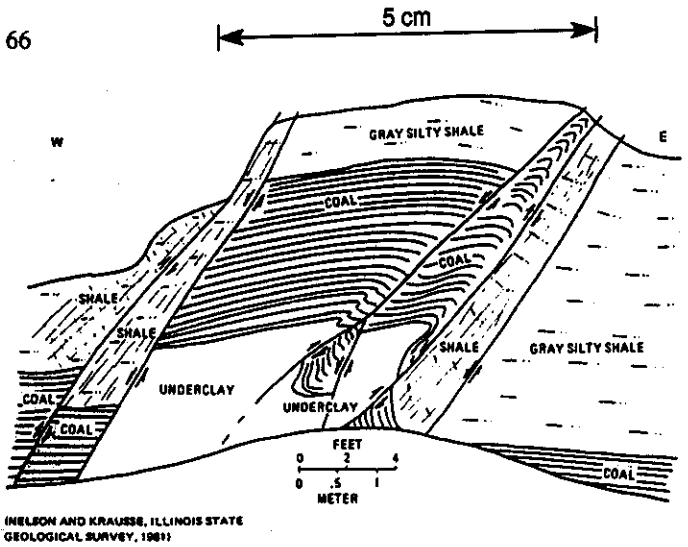



FIG. 17.—Detailed cross section of northwest-striking en echelon faults of the Cottage Grove fault system. Individual strands with reverse separation are tentatively interpreted as inverted normal faults that have undergone external rotation about a vertical axis. Other elements have retained at least part of their original normal separation. Beds within the fault zone are tightly folded. See Figure 14 for location.

indicative of regional shortening, and reflections from Neogene strata have consistent, low dips across the region (Figs. 20, 21).

The principal displacement zone is more complex and variable than the external normal faults (compare faults in Figs. 20 and 21). Its profile characteristics resemble those illustrated in Figures 3 and 5: (1) Faults splay upward and outward and most have normal separations; and (2) monoclinal flexures at the shoulders of the zone verge inward toward a central, down-dropped slice and bound a shallow synform (Fig. 21). Similar features characterize the seismic reflection profiles of another wrench fault in southeast Asia described by D'Onfro and Glagola (1983). A negative flower structure is present on profile 2 and includes a subsidiary fault with a reverse separation within Miocene strata on the zone's east side (Fig. 21). The reverse fault developed at a restraining bend within the zone's southern segment (Fig. 19). The shallow synform is not developed at profile 1, and a change in the dip separation at depth is the most distinctive expression of wrench faulting here (Fig. 20). The apparent upthrown block changes from the west side above 3.3 seconds to the east side below 3.5 seconds. The top of the basement in the western block is only approximated from regional control, but its displacement to deeper levels is corroborated by the presence of stratal reflections considerably below 3.5 seconds.

## PLATE-TECTONIC SETTINGS FOR EXTENSIONAL STRIKE SLIP

Divergent wrench faults occur in a wide variety of plate-tectonic settings, including transform, divergent, and convergent plate boundaries; extensional and contractional continental settings; and within plates far from areas of pronounced regional deformation (Fig. 22). Evidence for extensional strike slip is least common, however, in regions dominated by crustal shortening, or where there is minimal basement-involved deformation (e.g., passive continental margins). The zones and settings evolve through time (not shown in the instantaneous sketches of Fig. 22), and the faults may exhibit extensional strike-slip during only part of their history. Divergent segments may occur within systems that elsewhere have convergent styles (e.g., Fig. 22 a, b) or may dominate the entire length of the wrench zone (e.g., Fig. 22 d, e).

### *Transform Plate Boundary and Intra-Wrench Settings*

Divergent wrench styles tend to develop within transform or wrench systems (1) where the principal displacement zone bends or splays into the extensional sector of regional deformation (Fig. 22a); (2) at releasing fault oversteps and fault junctions (Fig. 22b); and (3) locally where crustal blocks rotate between bounding wrench faults (Fig. 22c).

The geometrically simplest habitat of divergent wrench style is a releasing splay or bend in a single wrench fault. A releasing splay develops where splay faults, when viewed down the trace of a right-slip zone, diverge away from the viewer on the right side of the master fault or converge with the zone in a direction away from the viewer on the left side (Fig. 22a). The converse is true for left-slip zones. The Mecca Hills faults are examples of right-slip releasing splays (Fig. 6).

A similar pattern of orientation change defines a releasing bend. The western segment on the Bocono fault adjacent to the La González Basin, northwestern Venezuela, is an example (Fig. 23a). Quaternary normal separation is on the order of several kilometers, and right slip is indicated by displaced drainages and stratigraphy, offset moraines, and seismicity (see references in Schubert, 1980). Other examples of releasing bends have been summarized recently by Mann et al. (1983).

The entire wrench system may have a divergent wrench style where a straight fault is consistently oblique to the regional interplate slip lines. The principal displacement zones of the Dead Sea transform south of Lebanon, for example, are predominantly of divergent wrench style judging from descriptions of surface features by Freund et al. (1970), Schulman and Bartov (1978), Garfunkel (1981), Eyal and Reches (1983), and Manspeizer (1985 this volume). Restoration of the 105 km of left slip documented along this zone includes a clockwise rotation of the eastern block (Figs. 4b to 9b in Freund et al., 1970), suggesting an oblique divergent plate motion of several degrees (see also Garfunkel, 1981). Plate-tectonic analyses of the Red Sea – Gulf of Aden area also imply extensional strike-slip along the Dead Sea transform (e.g., Le Pichon and Francheteau, 1978; Cochran, 1983; Mann et al., 1983). The inception of the folds in Israel that are oriented oblique to the Dead Sea transform, and interpreted by Freund (1965), Vroman (1967), and Wilcox et al. (1973) to be the result of wrench-related deformation, significantly predates the initiation of strike-slip (Eyal and Reches, 1983). In addition, Eyal and Reches (1983) have determined that the stress field related to the Dead Sea transform is different from the stress field involved in the development of the folds. The folds are therefore not considered an essential element of the divergent wrench style south of Lebanon.

Releasing oversteps and releasing fault junctions (Fig. 22b) also have patterns that result in the oblique separation of blocks, and they are similar to those defined for releasing splays and bends. Indeed, Mann et al. (1983) argued that oversteps generally evolve from bends in an earlier throughgoing fault, although other origins are possible (Aydin and Nur, 1985 this volume). A possible example of a releasing overstep characterized by divergent wrench style is the Hula graben of the northern Dead Sea rift (Fig. 23c; Freund et al., 1968). Numerous other examples of pull-apart basins are cited by Aydin and Nur (1982) and by Mann et al. (1983), but not all such basins are associated with divergent wrench faults. The southern San Andreas fault opposite the Salton trough, for example, is dominated by a convergent wrench fault style (Sylvester and Smith, 1976).

Extension occurs at releasing fault junctions in the manner discussed by Kingma (1958), Lensen (1959), and Crowell (1974). At the junction that bounds the Ridge Basin (Fig.

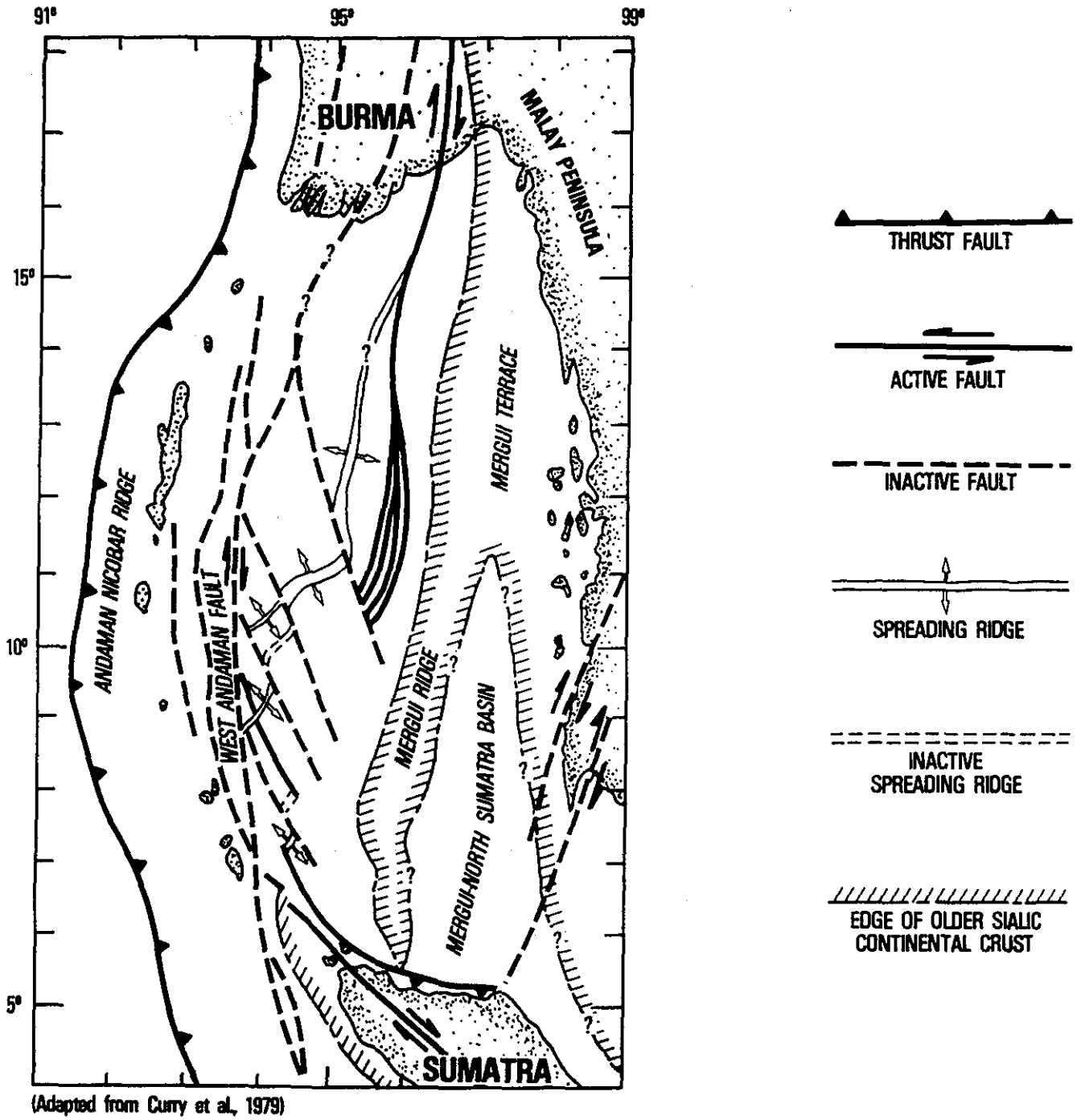



FIG. 18.—Tectonic framework of the Andaman Sea. Arrowheads have been added to identify spreading centers and are diagrammatic.

5 cm

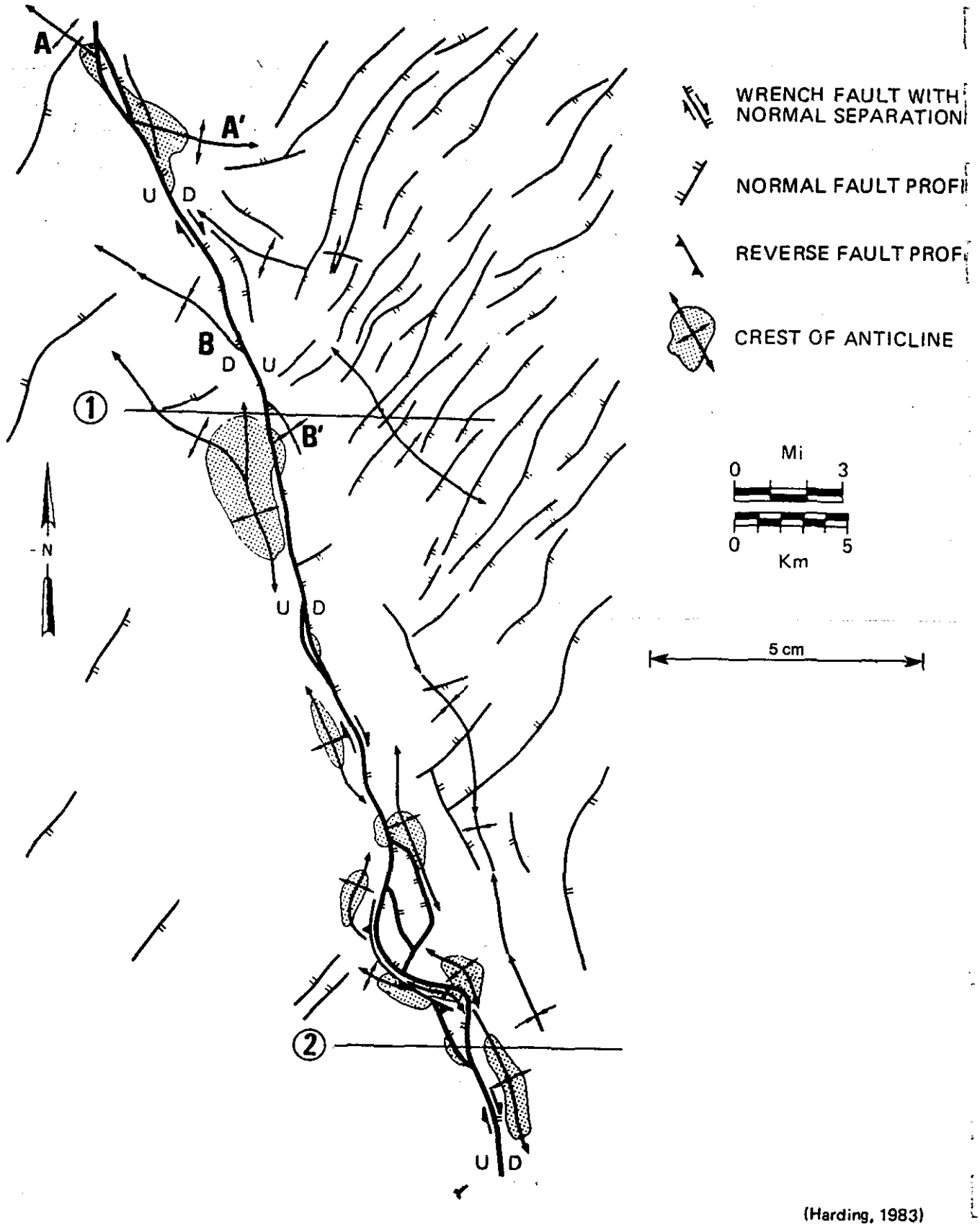



FIG. 19.—Tectonic map of structures mapped on a lower Miocene reflection and position of the Andaman Sea seismic profiles. A–A' and B–B' identify possibly correlative folds that appear to be offset in a right-lateral sense.

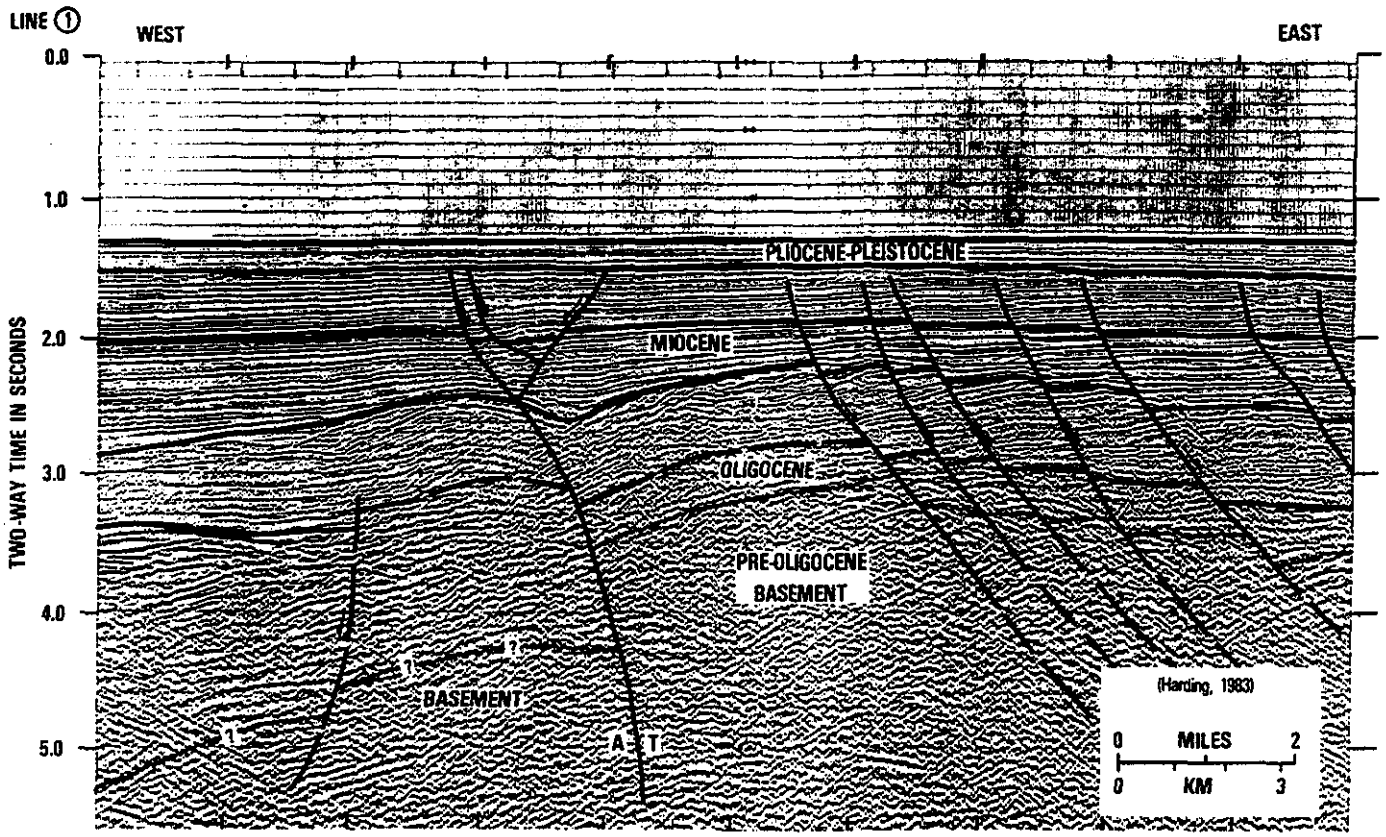



FIG. 20.—Interpreted seismic profile 1 across the Andaman Sea wrench fault. Deeper stratal reflections on west side of wrench fault (left center) indicate a change in the apparently down-dropped block at depth. Obliquely striking normal faults dip toward the right on eastern half of profile. See Figure 19 for structural setting of line. T, displacement toward viewer; A, displacement away from viewer.

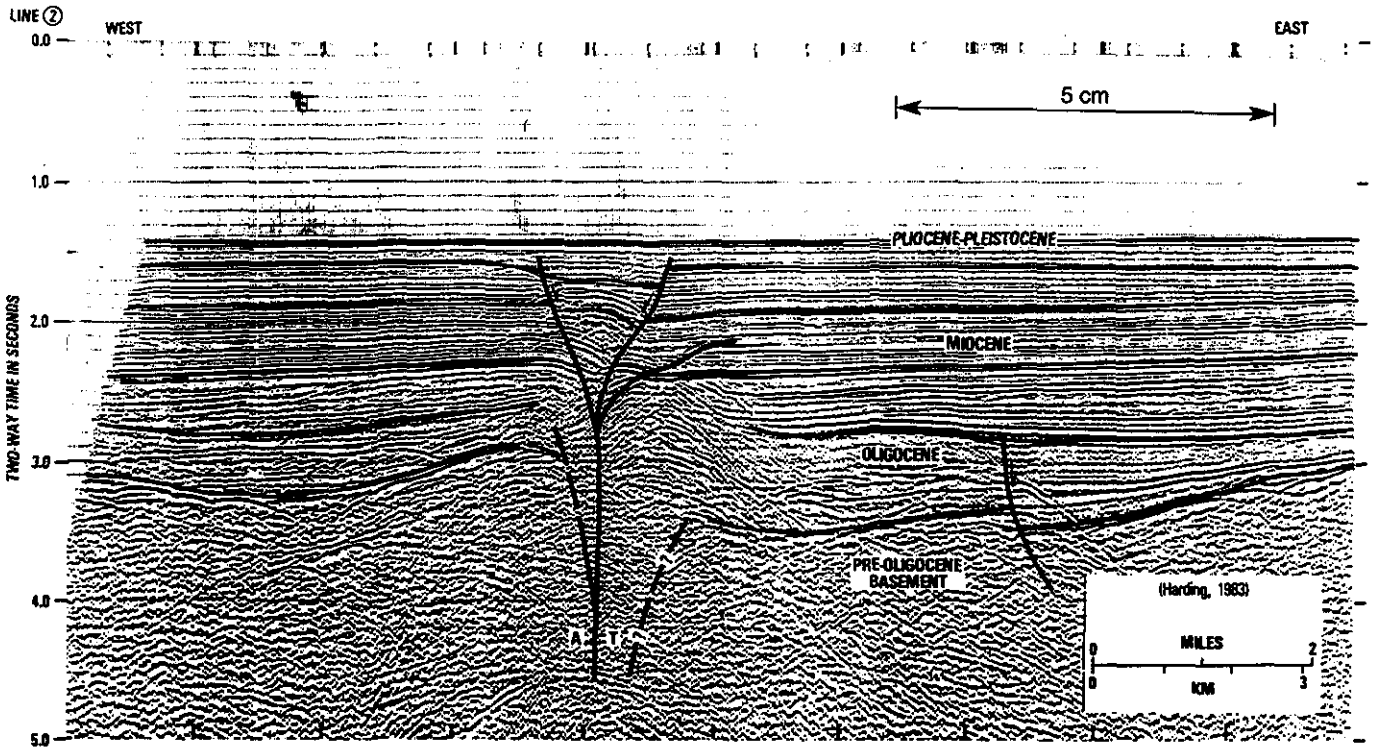
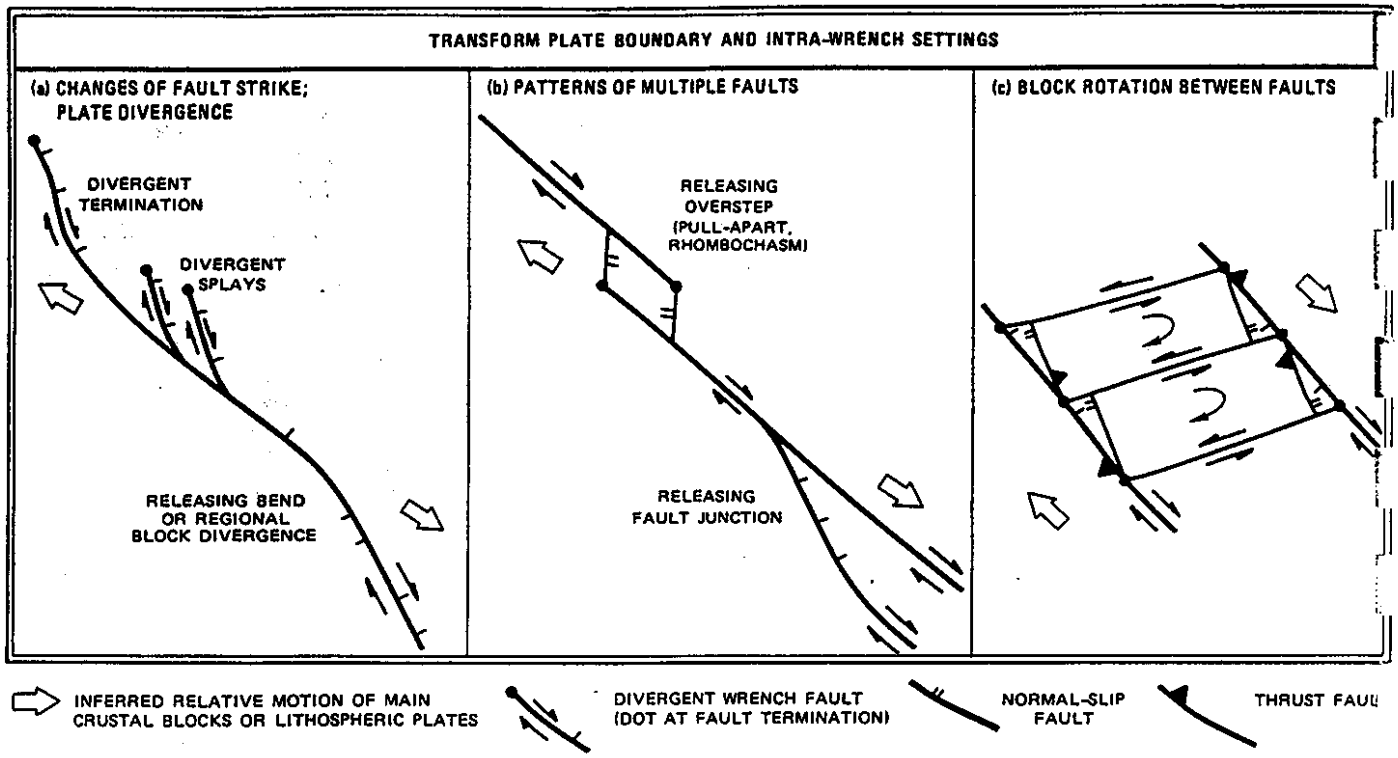
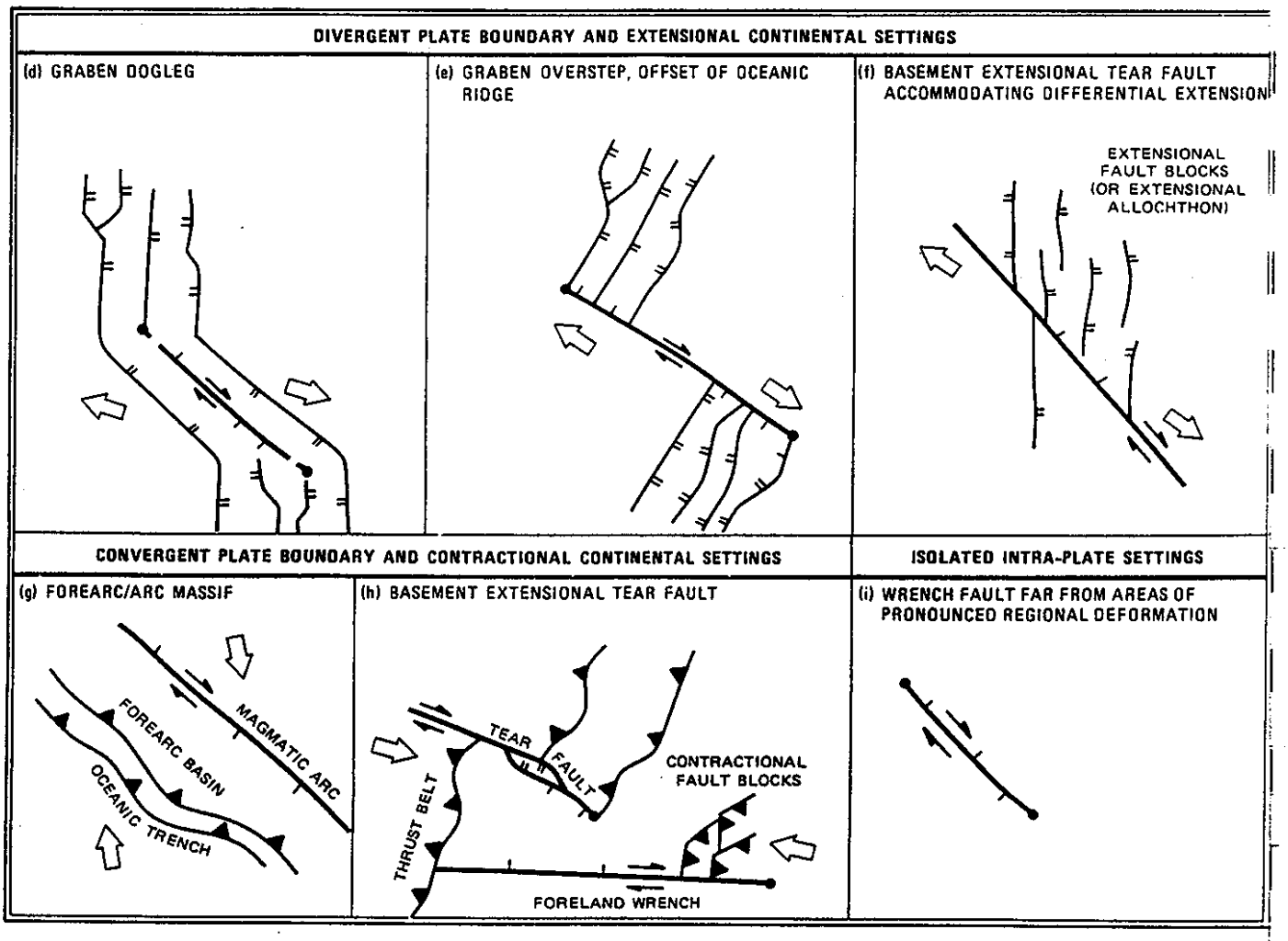



FIG. 21.—Interpreted seismic profile 2 across the Andaman Sea wrench fault. This profile illustrates the characteristics of a negative flower structure and changes in the development of the fault zone that occur along strike from profile 1 (compare with Fig. 20). See Figure 19 for structural setting of line. T, displacement toward viewer; A, displacement away from viewer.


TRANSFORM PLATE BOUNDARY AND INTRA-WRENCH SETTINGS
(a) CHANGES OF FAULT STRIKE; PLATE DIVERGENCE
DIVERGENT TERMINATION
DIVERGENT SPLAYS
RELEASING BEND OR REGIONAL BLOCK DIVERGENCE
(b) PATTERNS OF MULTIPLE FAULTS
RELEASING OVERSTEP (PULL-APART, RHOMBOCHASM)
RELEASING FAULT JUNCTION
(c) BLOCK ROTATION BETWEEN FAULTS
INFERRED RELATIVE MOTION OF MAIN CRUSTAL BLOCKS OR LITHOSPHERIC PLATES
DIVERGENT WRENCH FAULT (DOT AT FAULT TERMINATION)
NORMAL-SLIP FAULT
THRUST FAUL


DIVERGENT PLATE BOUNDARY AND EXTENSIONAL CONTINENTAL SETTINGS
(d) GRABEN DOGLEG
(e) GRABEN OVERSTEP, OFFSET OF OCEANIC RIDGE
(f) BASEMENT EXTENSIONAL TEAR FAULT ACCOMMODATING DIFFERENTIAL EXTENSION
EXTENSIONAL FAULT BLOCKS (OR EXTENSIONAL ALLOCHTHON)
CONVERGENT PLATE BOUNDARY AND CONTRACTIONAL CONTINENTAL SETTINGS
ISOLATED INTRA-PLATE SETTINGS
(g) FOREARC/ARC MASSIF
FOREARC BASIN
MAGMATIC ARC
OCEANIC TRENCH
(h) BASEMENT EXTENSIONAL TEAR FAULT
TEAR FAULT
CONTRACTIONAL FAULT BLOCKS
THRUST BELT
FORELAND WRENCH
(i) WRENCH FAULT FAR FROM AREAS OF PRONOUNCED REGIONAL DEFORMATION

23b), the San Gabriel fault was active from about 12 Ma to 5 Ma and has predominantly normal separation (Crowell, 1982). However, the adjacent Liebre fault, active from 8 Ma to between 6 and 5 Ma and approximately parallel to the San Gabriel, is characterized by reverse separation. This difference in style illustrates the fallibility of using patterns predicted from Figures 1 and 2 in areas where two or more deformational events are superimposed or where more than one major strike-slip fault is involved. In addition, the fault patterns shown in Figure 23 do not always result in basin subsidence.

A possible scheme for the rotation of crustal blocks between wrench faults is shown in Figure 22c (scale is uncertain). Abundant paleomagnetic evidence demonstrates widespread, predominantly clockwise rotation of crustal blocks in western North America during Cenozoic time (Beck, 1980; Luyendyk et al., 1980). Any significant block rotations similar to those shown in Figure 22c should lead to the initiation of sedimentary basins and to alternations of convergent and divergent wrench style where block corners alternately rotate toward or away from the throughgoing fault (indicated with normal- and thrust-fault symbols). These structural complexities have been corroborated by earthquake hypocentral location and first-motion studies in the eastern Transverse Ranges, California (Nicholson et al., 1985). The structural patterns that result from such rotational deformation are not included in Figures 1 and 2.

### *Divergent Plate Boundary and Extensional Continental Settings*

Well-known examples of divergent wrench faults within divergent plate boundaries and extensional continental settings are oriented oblique or transverse to the trend of normal fault systems. The most common are apparently localized in the vicinity of graben doglegs and oversteps (Fig. 22d; Harding, 1984). Doglegs are short, oblique graben segments connecting subparallel straightaways. Extensional strike slip can occur within the middle segment of the dogleg, particularly if the regional plate separation is oblique to that segment. Several transform faults in the northern Red Sea (see Fig. 1 in Coleman, 1974) may be interpreted in this manner. Freund (1982) has also observed that obliquely oriented strike-slip faults, not necessarily confined to doglegs, are an occasional part of graben structures. He has attributed the formation of these faults to rare instances of crustal attenuation parallel to the graben axis.

Graben oversteps occur where the ends of graben segments overlap and are not connected directly by normal faults (Fig. 22e). Continued extension ultimately causes strike slip along a line connecting the grabens (Courtillot et al., 1974). Zones of en echelon faults connect the overstepped ends of the Rhine and Bresse grabens and have been interpreted by Illies (see Fig. 10 in Illies, 1974) as left-lateral wrench zones or oblique-slip faults with left-slip components. The zones resemble the belts of external faults associated with divergent wrench faults, and he has compared the deformation to an incipient ridge-ridge transform fault system.

A somewhat different class of divergent wrench fault occurs in broad areas of pervasive regional extension, such as the Basin and Range Province of southeastern California and adjacent Nevada (Figs. 22f, 23d). There, wrench faults act as major basement tear faults, separating terranes that in late Cenozoic time experienced different amounts of extension (Wernicke et al., 1982; Burchfiel et al., 1983). These faults, however, do not necessarily have a divergent style throughout their lengths. Specific examples are the Garlock fault (Davis and Burchfiel, 1973), the Las Vegas Valley shear zone (Guth, 1981), and the Furnace Creek fault zone (Wright and Troxel, 1970; Stewart, 1983; Cemen et al., 1985 this volume). The Andaman Sea fault (Fig. 19) may also be an extensional tear fault. In both the Basin and Range and Andaman Sea examples, the associated normal faults are oblique rather than en echelon because they are of regional extent, and not arranged solely along wrench zones.

Divergent wrench faults are also known from oceanic regimes. The western rift zone of southwestern Iceland, for example, is connected to the Reykjanes segment of the North Atlantic mid-oceanic spreading center by an obliquely oriented zone of right-stepping, en echelon fissure swarms (Tryggvason, 1982). The swarms are geometrically similar to the en echelon normal faults between the Rhine and Bresse grabens. Elsewhere, many oceanic transform zones consist of valleys and ridges within and parallel to the principal displacement zone and of external, oblique slip faults (Fox and Gallo, 1984). The structural style of such fracture zones is similar to that of some continental divergent wrench faults, but the style does not develop in the same way. The transform valley is thought to be a manifestation of restricted partial melting at the relatively cold ridge-transform intersection. This results in reduced segregation of basaltic melt and thinner oceanic crust. Oblique faulted topography adjacent to the transform arises from reorientation of the principal stress axes as a result of welding of the upper mantle across the transform (Fox and Gallo, 1984).

### *Convergent Plate Boundary and Contractional Continental Settings*

We have recognized divergent wrench faults in three convergent margin and contractional continental settings thus far: arc massif, and both backarc and peripheral forelands (cf. Dickinson, 1974); additional settings are probable.

Regions of high heat flow and thin, weakened lithosphere, such as arc massifs, appear to have localized longitudinal wrench faults within convergent margin settings (Fig. 22g; Fitch, 1972). Along the axis of the central Barisan Mountains in Sumatra, the right-lateral Great Sumatran fault consists of a braided zone that includes in-line grabens, pull-apart basins, and linear topographic depressions. The structural depressions are bounded by major right-lateral faults and subordinate, but still important, normal faults

FIG. 22.—Cartoon of plate-tectonic settings and patterns of divergent strike-slip faulting. Examples are based on known occurrences (except style of fault in d, which is assumed), and are consistently drawn for a right-slip system to facilitate comparison. There is undoubtedly a greater variety of possible fault patterns and complexities than is shown. Scale is variable, and the patterns in one sketch may constitute local details of another.

655197

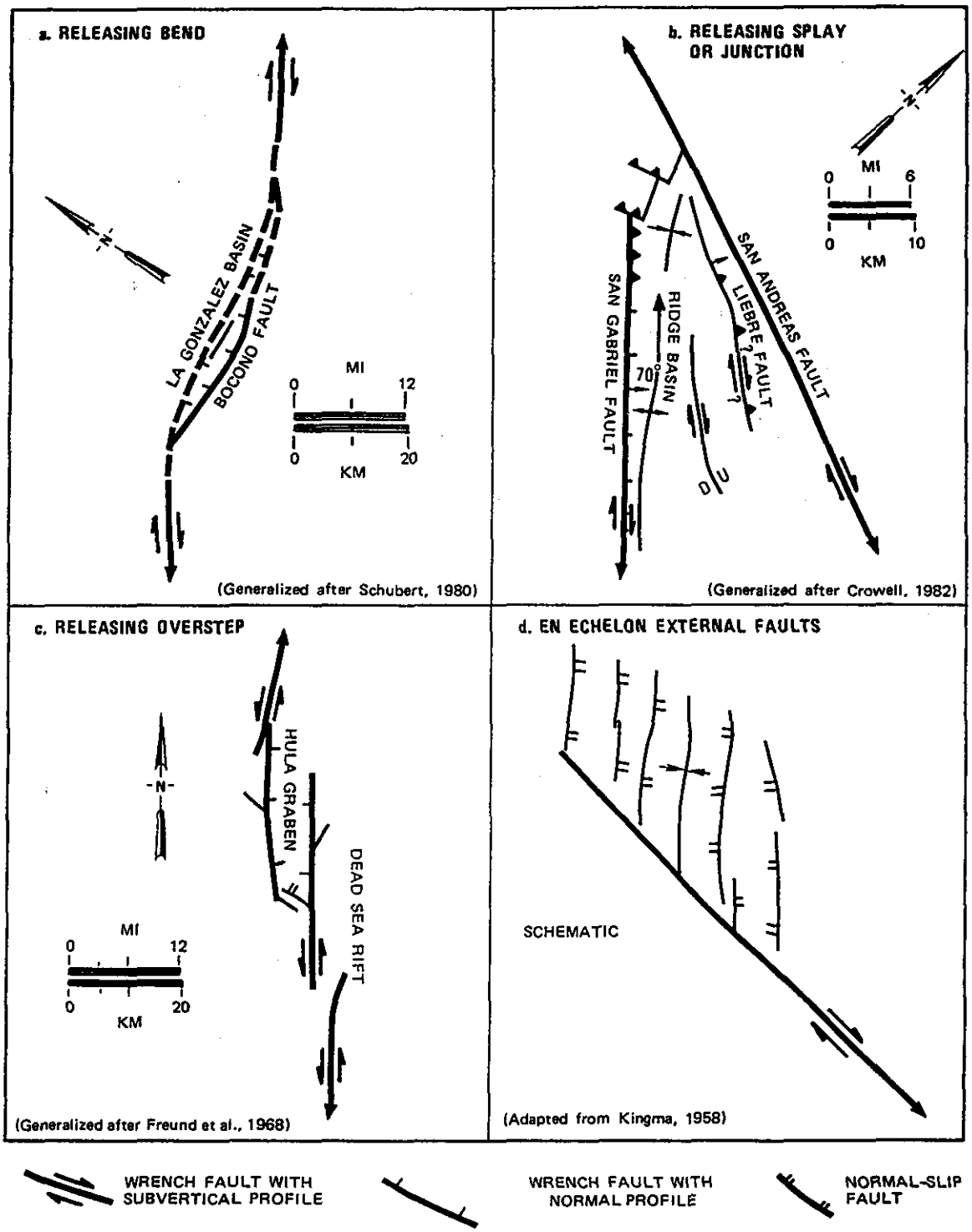
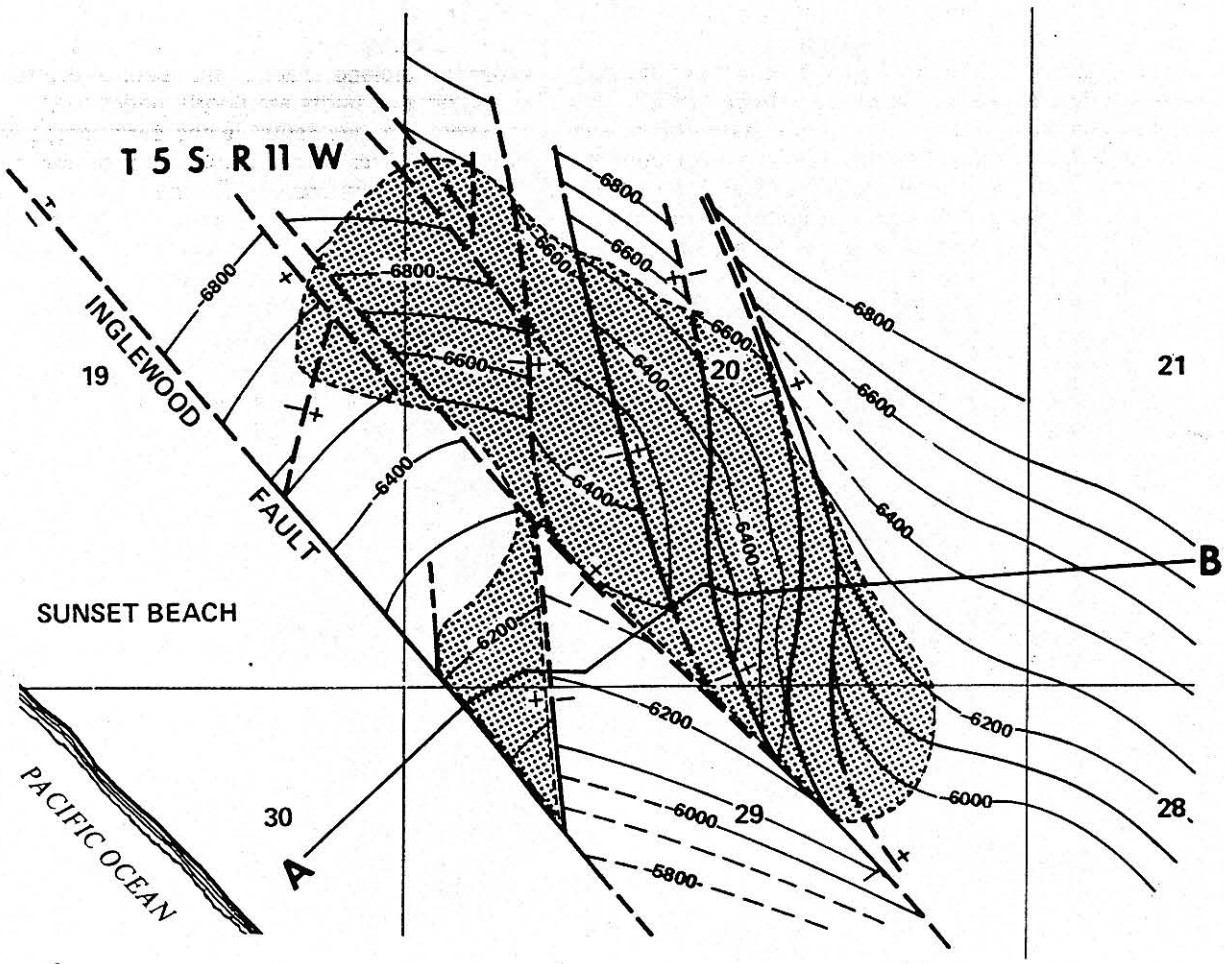
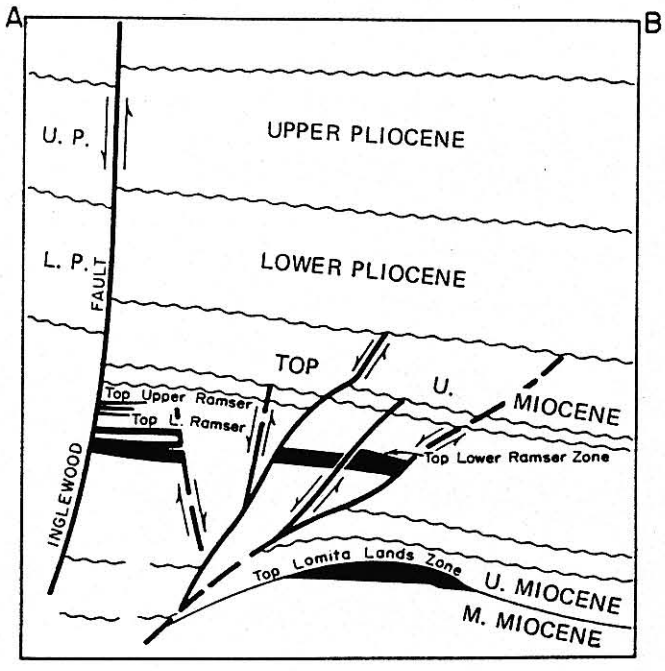



FIG. 23.—Four common patterns of strike-slip faults and secondary faults associated with strike slip that sometimes result in basin subsidence. Fault profile styles in (a) are from Giegengack (1977) and Schubert (1980). Fault profiles in (b) are generalized from descriptions in Crowell (1982); the reverse segment at northwest end of San Gabriel fault was superimposed on an earlier extensional profile. Fault profiles in (c) are from Horowitz (1973) and Schulman and Bartov (1978).

5 cm




(After Allen and Hazenbush, 1957)




(After California Div. Oil & Gas, 1961)

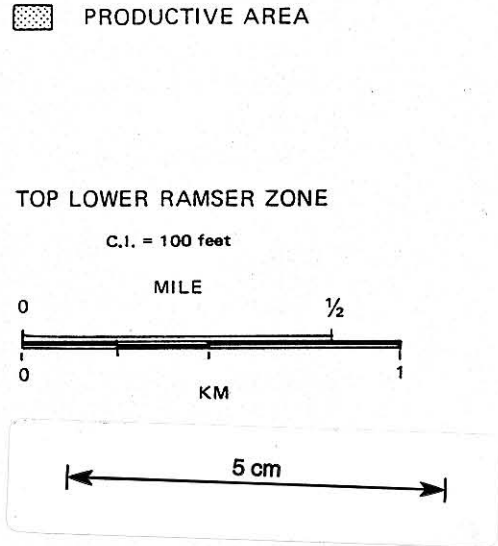



FIG. 24.—Structure of the Sunset Beach oil field, Los Angeles Basin, California. Shallow, north-south, en echelon fault blocks are closed southward by throughgoing, northwest-striking faults, and westward by normal faults. The Inglewood fault is part of the regional Newport-Inglewood wrench zone, which has a maximum right slip of 760 m on structural markers near the top of the Miocene (Harding, 1973).

655199

(see Fig. 9 in Posavec et al., 1973). Strike slip probably resulted from oblique encroachment between the Indian Ocean plate and the Sumatran plate in a setting roughly analogous to that shown in Figure 22g (Fitch, 1972). The extensional component of the strike slip is more difficult to explain, especially because of the dominance of contractional structures in the adjacent backarc (Hamilton, 1979, Plate I). The extension has been attributed to oceanward migration of the frontal parts of the Sumatran arc system by D. E. Karig and W. Jensky (in Hamilton, 1979). Dickinson (1974) related extension in arc massifs to crustal uplift and arching, and to volcano-tectonic subsidence. Recent unpublished work by T. R. Bultman and T. P. Harding indicates that contractional folds within the Sumatran back-arc basins may owe their oblique orientation to the Great Sumatran fault more to pre-existing basement grain than to right-slip tectonics as previously reported by Wilcox et al. (1973).

Wrench faults oriented oblique to the trend of major tectonic zones within the region of convergence may also have a divergent style (foreland wrench in Fig. 22h). The La Basin fault zone (Figs. 4, 5) has this orientation within orogenic foreland. Factors that control the strike-slip style of the oblique faults are poorly understood.

Several oblique faults in the peripheral foreland regi of the outer West Carpathians appear to have acted as tear separating eastern areas with continuing thrusting from areas in the west where thrusting was already complete (Royde 1985 this volume). The Vienna Basin is located at a co plex releasing overstep between at least three such faults (see pull-apart within extensional tear fault in Fig. 22h). each consisting of several branches with normal separatio Reflection seismic data, subsidence history, and heat-flo data suggest that the Vienna Basin is allochthonous, and that the bounding tear faults merge at depth with a gentl dipping crustal detachment (Royden, 1985 this volume Oblique tear faults, such as those of the Vienna Basin, a commonly late structures, and are invariably associated with belt-parallel extension, which is promoted by pronounce salients and re-entrants in the orogen (Dahlstrom, 1970).

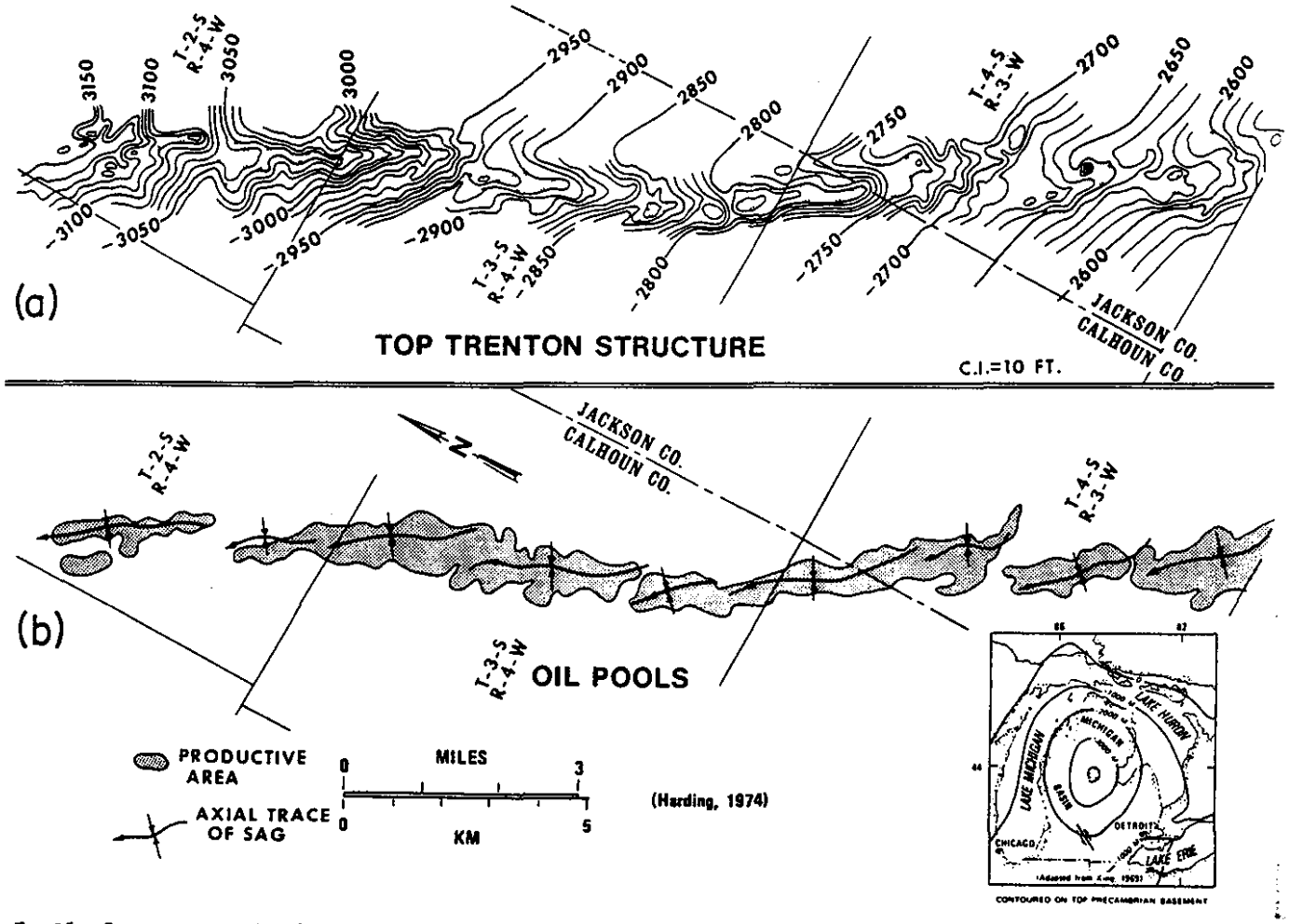



FIG. 25.—Structure map and setting (inset) of the Scipio-Albion trend, Michigan Basin, Michigan. (a) Map of central and northern parts of the field contoured on the top of the Ordovician Trenton Formation, which directly overlies the productive interval. (b) Pattern of sag axes determined from the structure contours.

5 cm

### *Intraplate Occurrences*

The Cottage Grove fault of the Illinois Basin illustrates the intracratonic setting of divergent wrench faults (Figs. 13, 22i), and the Scipio-Albion trend of the Michigan Basin provides another example (see the following discussion). Pre-existing zones of crustal weakness are recognized as a potentially important determinant of location and orientation. Convergent wrench faults are also known from mid-plate localities, but the cause of the mid-plate strike slip and controls on its style are unknown.

## HYDROCARBON TRAPS ASSOCIATED WITH DIVERGENT WRENCH FAULTS

Three main types of structural traps associated with divergent wrench faults are known to be productive (see also D'Onfro and Glagola, 1983): (1) fault slices within the principal displacement zone, (2) forced folds parallel to the high side of the principal displacement zone, and (3) en echelon fault blocks flanking either or both sides of the zone. The forced folds have the greatest potential for providing both effective and abundant trap opportunities (e.g., Figs. 16, 19). Most hydrocarbon accumulations along the Cottage Grove fault system are located near anticlinal culminations along the apparent high side of the principal displacement zone, but they are productive in very low volumes in this example. Subsidiary traps commonly associated with anticlines, such as up-plunge reservoir terminations (pinchout, truncation, etc.) and cross faults, increase the potential for hydrocarbon prospects at the forced folds (e.g., Fig. 15). External, oblique anticlines, such as the Campbell Hill anticline in Figure 16, may also provide additional fold closures, but are less common.

En echelon normal-fault blocks are productive in the Newport-Inglewood trend, California, and in several other wrench zones (Fig. 24; Harding, 1973, 1974; Barrows, 1974). The fault blocks are developed where the principal displacement zone has the characteristics of a divergent wrench fault. Effective closure is dependent on block tilt away from fault intersections and on fault seals, usually at both the oblique normal faults and the principal displacement zone (Weber et al., 1978; Smith, 1980).

A vertical linear zone of fractured, dolomitic limestone forms the reservoir for the hydrocarbon accumulation along the Scipio-Albion trend, Michigan. A sag overlies the zone and is thought to reflect the distribution of fractures (Fig. 25). Both the sag and the productive limits of the fractured reservoir have a segmented right-stepping, en echelon pattern that resembles the orientation of synthetic faults at the principal displacement zone of a left-slip system. The series of sags trends obliquely down the regional dip (inset map in Fig. 25), and there is little other discernible deformation. Divergent wrench faulting is interpreted to have formed the unique sag and its en echelon pattern while at the same time enhancing fracturing and limiting deformation to a narrow swath (Harding, 1974). Graben slices within the principal displacement zone of the Cottage Grove fault system are also intensely fractured (Nelson and Krausse, 1981).

Although potential traps occur along divergent wrench faults, it is thought that the limited extent of external structures, the paucity of folds, and the dependence on sealing faults for closure are all significant limiting factors. Trends developed where blocks move in a convergent sense (Harding, 1974) or with neither convergence nor divergence (Harding, 1973, 1976) should have larger numbers of effective structural traps.

## CONCLUSIONS

Our investigations indicate that some wrench zones contain a structural assemblage that is dominated by extensional features and that distinctive elements of this assemblage are repeated in a wide variety of tectonic settings. In the past, zones such as these may not have been properly recognized as wrench faults. The structural assemblage differs in important ways from the other wrench styles and constitutes a discrete structural style: (1) faulting dominates deformation adjacent to the principal displacement zone: (2) folds are for the most part oriented parallel to the principal displacement zone; and (3) the overall zone of deformation is typically relatively narrow. The structures may be combined in several ways. Some divergent wrench systems consist solely of a principal displacement zone with normal separation; other divergent wrench zones are composed of sets of en echelon normal faults; and still other systems have both elements. One result of their structural characteristics is that the potential for effective structural traps is not as great along divergent wrench faults as it is in regions of convergent or simple strike slip. The extensional characteristics of the style also make it difficult to differentiate divergent wrench faults from normal fault blocks, especially when interpreting seismic reflection data. In these instances it is necessary to determine both profile and map characteristics.

## ACKNOWLEDGMENTS

This study was originally conducted for Exxon Production Research Company and we are grateful to that company for its permission to publish. Exxon Company, U.S.A., provided the Bering Sea and Lake Basin seismic reflection profiles and the maps of the Scipio-Albion trend. Esso Exploration, Inc., supplied the Andaman Sea example. K. T. Biddle, C. A. Dengo, R. P. George, D. W. Phelps, and A. C. Tuminas, of Exxon Production Research Company, reviewed the manuscript, and R. W. Wiener provided regional data for the Illinois Basin. G. C. Bond, Kristian Meisling, K. R. Schmitt, and D. M. Worral also made helpful suggestions. Logistical support at Lamont-Doherty Geological Observatory was provided by an ARCO Foundation Fellowship to Christie-Blick. Lamont-Doherty Geological Observatory Contribution No. 3912 (Christie-Blick).

## *REFERENCES*

ALLEN, D. R., AND HAZENBUSH, G. C., 1957, Sunset oil field: California Division of Oil and Gas, California Oil Fields—Summary of Operations, v. 43, no. 2, p. 47–50.

ALPHA, A. G., AND FANSHAWE, J. R., 1954, Tectonics of northern Bighorn basin area and adjacent south-central Montana: Billings Geological Society Guidebook, 5th Annual Field Conference, Pryor Mountains-Northern Bighorn Basin, Montana, p. 72–79.

AYDIN, A., AND NUR, A., 1982, Evolution of pull-apart basins and their scale independence: Tectonics, v. 1, p. 91–105.

AYDIN, A., AND NUR, A., 1985, The types and role of stepovers in strike-slip tectonics, *in* Biddle, K. T., and Christie-Blick, N., eds., Strike-slip Deformation, Basin Formation and Sedimentation: Society of Economic Paleontologists and Mineralogists Special Publication No. 37, p. 35–44.

BARROWS, A. G., 1974, A review of the geology and earthquake history of the Newport-Inglewood structural zone, southern California: California Division Mines and Geology Special Report 114, 115 p.

BECK, M. E., JR., 1980, Paleomagnetic record of plate-margin tectonic processes along the western edge of North America: Journal of Geophysical Research, v. 85, p. 7115–7131.

BISHOP, D. G., 1968, The geometric relationships of structural features associated with major strike-slip faults in New Zealand: New Zealand Journal of Geology and Geophysics, v. 11, p. 405–417.

BURCHFIEL, B. C., WALKER, D., DAVIS, G. A., AND WERNICKE, B., 1983, Kingston Range and related detachment faults—a major "breakaway" zone in the southern Great Basin: Geological Society of America Abstracts with Programs, v. 15, p. 536.

BUSCHBACH, T. C., AND ATHERTON, E., 1979, History of the structural uplift of the southern margin of the Illinois basin, *in* Palmer, J. E., and Dutcher, R. R., eds., Depositional and Structural History of the Pennsylvanian System of the Illinois Basin, Part 2: Illinois State Geological Survey Guidebook Series 15a, Field trip 9, Ninth International Congress, Carboniferous Stratigraphy and Geology, p. 112–115.

CALIFORNIA DIVISION OF OIL AND GAS, 1961, California oil and gas fields maps and data sheets, part 2, Los Angeles–Ventura basins and central coastal regions: California Division of Oil and Gas, p. 496–913.

CEMEN, I., WRIGHT, L. A., DRAKE, R. E., AND JOHNSON, F. C., 1985, Cenozoic sedimentation and sequence of deformational events at the southeastern end of the Furnace Creek strike-slip fault zone, Death Valley region, California, *in* Biddle, K. T., and Christie-Blick, N., eds., Strike-Slip Deformation, Basin Formation, and Sedimentation: Society of Economic Paleontologists and Mineralogists Special Publication No. 37, p. 127–141.

CHAMBERLAIN, R. T., 1919, A peculiar belt of oblique faulting: Journal of Geology, v. 27, p. 602–613.

CHEADLE, M. J., CZUCHRA, B. L., BYRNE, T., ANDO, C. J., OLIVER, J. E., BROWN, L. O., KAUFMAN, S., MALM, P. E., AND PHINNEY, R. A., in press, The deep crustal structure of the Mojave Desert, California, from COCORP seismic reflection data: Tectonics.

CHRISTIE-BLICK, N., AND BIDDLE, K. T., 1985, Deformation and basin formation along strike-slip faults, *in* Biddle, K. T., and Christie-Blick, N., eds., Strike-Slip Deformation, Basin Formation, and Sedimentation: Society of Economic Paleontologists and Mineralogists Special Publication No. 37, p. 1–34.

CLARK, S. K., AND ROYDS, J. S., 1948, Structural trends and fault systems in Eastern Interior basin: American Association of Petroleum Geologists Bulletin, v. 32, p. 1728–1749.

COCHRAN, J. R., 1983, A model for development of Red Sea: American Association of Petroleum Geologists Bulletin, v. 67, p. 41–69.

COHEE, G. V., 1962, *Tectonic map of the United States: United States* Geological Survey and American Association of Petroleum Geologists, 1:2,500,000.

COLEMAN, R. G., 1974, Geologic background of the Red Sea, *in* Burk, C. A., and Drake, C. L., eds., The Geology of Continental Margins: New York, Springer-Verlag, p. 743–751.

COMMITTEE FOR COORDINATION OF JOINT PROSPECTING FOR MINERAL RESOURCES IN ASIAN OFFSHORE AREAS (C.C.O.P.), 1981, Studies in east Asian tectonics and resources (SEATAR): United Nations ESCAP, C.C.O.P. Technical Publication 7a, p. 37–50.

COURTILLOT, V., TAPPONNIER, P., AND VARET, J., 1974, Surface features associated with transform faults: a comparison between observed examples and an experimental model: Tectonophysics, v. 24, p. 317–329.

CROWELL, J. C., 1974, Origin of Late Cenozoic basins in southern California, *in* Dickinson, W. R., ed., Tectonics and Sedimentation: Society of Economic Paleontologists and Mineralogists Special Publication No. 22, p. 190–204.

———, 1981, Juncture of San Andreas transform system and Gulf of California rift: Oceanologica Acta, Proceedings, 26th International Geological Congress, Geology of Continental Margins Symposium, Paris, p. 137–141.

———, 1982, The tectonics of Ridge Basin, southern California, *in* Crowell, J. C., and Link, M. H., eds., Geologic History of Ridge Basin, Southern California: Society of Economic Paleontologists and Mineralogists, Pacific Section, p. 25–42.

CROWELL, J. C., AND SYLVESTER, A. G., eds., 1979, Tectonics of the *Juncture Between the San Andreas Fault System and the Salton Trough* Southeastern California—A Guidebook: Santa Barbara, California Department of Geological Sciences, University of California, 193

CURRAY, J. R., MOORE, D. G., LAWVER, L. A., EMMEL, F. J., RAITT, R. W., HENRY, M., AND KIECKHEFEIZ, R., 1979, Tectonics of the Andaman Sea and Burma, *in* Watkins, J. S., Montadert, L., and Dickenson, P. W., eds., Geological and Geophysical Investigations of Continental Margins: American Association of Petroleum Geologists Memoir p. 189–198.

DAHLSTROM, C. D. A., 1970, Structural geology in the eastern margin of the Canadian Rocky Mountains: Bulletin of Canadian Petroleum Geology, v. 18, p. 332–406.

DAVIS, G. A., AND BURCHFIEL, B. C., 1973, Garlock fault: an intracontinental transform structure, southern California: Geological Society of America Bulletin, v. 84, p. 1407–1422.

DICKINSON, W. R., 1974, Plate tectonics and sedimentation, *in* Dickson, W. R., ed., Tectonics and Sedimentation: Society of Economic Paleontologists and Mineralogists Special Publication No. 22, p. 27.

DOBBIN, C. E., AND ERDMAN, C. E., 1955, Structure contour map of Montana plains: United States Geological Survey Oil and Gas Investigation Map OM 178A, Scale 1:500,000.

D'ONFRO, P., AND GLAGOLA, P., 1983, Wrench fault, southeast Asia, *in* Bally, A. W., ed., *Seismic Expression of Structural Styles*, v. American Association of Petroleum Geologists Studies in Geology, ries 15, p. 4.2–9 to 4.2–12.

EGUCHI, T., UYEDA, S., AND MAKI, T., 1979, Seismotectonics and tectonic history of the Andaman sea: Tectonophysics, v. 57, p. 35–51

EMMONS, R. C., 1969, Strike-slip rupture patterns in sand models: Tonophysics, v. 7, No. 1, p. 71–87.

ERVIN, C. P., AND MCGINNIS, L. D., 1975, Reelfoot rift: reactivated precursor to the Mississippi embayment: Geological Society America Bulletin, v. 86, p. 1287–1295.

EYAL, Y., AND RECHES, ZE'EV, 1983, Tectonic analysis of the Dead rift region since the Late-Cretaceous based on mesostructures: Tectics, v. 2, p. 167–185.

FITCH, T. J., 1972, Plate convergence, transcurrent faults, and intern deformation adjacent to southeast Asia and the western Pacific: Jou of Geophysical Research, v. 77, p. 4432–4460.

FOX, P. J., AND GALLO, D. G., 1984, A tectonic model for ridge-transform-ridge plate boundaries: Implications for the structure of ocean lithosphere: Tectonophysics, v. 104, p. 205–242.

FREUND, R., 1965, A model of the structural development of Israel adjacent areas since Upper Cretaceous times: Geological Magazine 102, p. 189–205.

———, 1970, Rotation of strike slip faults in Sistan, southeast Iran: Journ of Geology, v. 78, p. 188–200.

———, 1982, The role of shear in rifting, *in* Pálmason, G., ed., C tinental and Oceanic Rifts: American Geophysical Union Geodynam Series, v. 8, p. 33–39.

FREUND, R., GARFUNKEL, Z., ZAK, I., GOLDBERG, M., WEISSBROD, T., DERIN, B., 1970, The shear along the Dead Sea rift: Philosoph Transactions of Royal Society of London, Series A, v. 267, p. 1 130.

GARFUNKEL, Z., 1981, Internal structure of the Dead Sea leaky transform (rift) in relation to plate kinematics: Tectonophysics, v. 80, p. 81–1

GIEGENGACK, R., 1977, Late Cenozoic tectonics of the Tabay-Estang graben, Venezuelan Andes, *in* Espejo, A., ed., Memorias del V C greso Geologico Venezolano: Ministerio de Energia y Minos, Caracas Tomo II, p. 721–737.

GUTH, P. L., 1981, Tertiary extension north of the Las Vegas Val shear zone, Sheep and Desert Ranges, Clark County, Nevada: G logical Society of America Bulletin, Part I, v. 92, p. 763–771.

HAMILTON, W., 1979, Tectonics of the Indonesian region: United State Geological Survey Professional Paper 1078, 345 p.

HARDING, T. P., 1973, Newport-Inglewood trend, California–an exam of wrenching style of deformation: American Association of Petrole Geologists Bulletin, v. 57, p. 97–116.

———, 1974, Petroleum traps associated with wrench faults: Americ

Association of Petroleum Geologists Bulletin, v. 58, p. 1290–1304.
———, 1976, Tectonic significance and hydrocarbon trapping consequences of sequential folding synchronous with San Andreas faulting, San Joaquin Valley, California: American Association of Petroleum Geologists Bulletin, v. 60, p. 356–378.
———, 1983, Divergent wrench fault and negative flower structure, Andaman Sea, *in* Bally, A. W., ed., Seismic Expression of Structural Styles, v. 3: American Association of Petroleum Geologists Studies in Geology, Series 15, p. 4.2–1 to 4.2–8.
———, 1984, Graben hydrocarbon occurrences and structural style: American Association of Petroleum Geologists Bulletin, v. 68, p. 333 to 362.
———, 1985, Seismic characteristics and identification of negative flower structures, positive flower structures and positive structural inversion: American Association of Petroleum Geologists Bulletin, v. 69, p. 582–600.
HARDING, T. P., AND LOWELL, J. D., 1979, Structural styles, their plate-tectonic habitats and hydrocarbon traps in petroleum provinces: American Association of Petroleum Geologists Bulletin, v. 63, p. 1016–1058.
HARLAND, W. B., 1971, Tectonic transpression in Caledonian Spitsbergen: Geological Magazine, v. 108, p. 27–42.
HAYS, W. H., 1957, Geology of the central Mecca Hills, Riverside County, California [unpubl. Ph.D. Thesis]: New Haven, Yale University, 324 p.
HEYL, A. V., JR., AND BROCK, M. R., 1961, Structural framework of the Illinois-Kentucky mining district and its relation to mineral deposits: United States Geological Survey Professional Paper 424-D, p. D3–D6.
HOROWITZ, A., 1973, Development of the Hula basin, Israel: Israel Journal Earth Sciences, v. 22, p. 107–139.
ILLIES, J. H., 1974, Taphrogenesis and plate tectonics, *in* Illies, J. H., and Fuchs, K., eds., Approaches to Taphrogenesis: Stuttgart, E. Schweizerbart'sche Verlagsbuchhandlung, p. 433–460.
JENNINGS, C., 1967, Salton Sea sheet, Geologic map of California, Olaf P. Jenkins edition: California Division of Mines and Geology, Scale 1:250,000.
KANE, M. F., HILDENBRAND, T. G., AND HENDRICKS, J. D., 1981, Model for the tectonic evolution of the Mississippi embayment and its contemporary seismicity: Geology, v. 9, p. 563–568.
KING, P. B., 1969, Tectonic map of North America: United States Geological Survey, Scale 1:5,000,000.
KINGMA, J. T., 1958, Possible origin of piercement structures, local unconformities, and secondary basins in the Eastern Geosyncline, New Zealand: New Zealand Journal of Geology and Geophysics, v. 1, p. 269–274.
LAWVER, L. A., AND CURRAY, J. R., 1981, Evolution of the Andaman Sea (abs.): EOS, Transactions of American Geophysical Union, v. 62, No. 45, p. 1044.
LENSEN, G. J., 1959, Secondary faulting and transcurrent splay-faulting at transcurrent fault intersections: New Zealand Journal of Geology and Geophysics, v. 2, p. 729–734.
LE PICHON, X., AND FRANCHETEAU, J., 1978, A plate-tectonic analysis of the Red Sea–Gulf of Aden area: Tectonophysics, v. 46, p. 369–406.
LUYENDYK, B. P., KAMERLING, M. J., AND TERRES, R., 1980, Geometric model for Neogene crustal rotations in southern California: Geological Society of America Bulletin, Part I, v. 91, p. 211–217.
MANN, P., HEMPTON, M. R., BRADLEY, D. C., AND BURKE, K., 1983, Development of pull-apart basins: Journal of Geology, v. 91, p. 529–554.
MANSPEIZER, W., 1985, The Dead Sea Rift: Impact of climate and tectonism on Pleistocene and Holocene sedimentation, *in* Biddle, K. T., and Christie-Blick, N., eds., Strike-Slip Deformation, Basin Formation, and Sedimentation: Society of Economic Paleontologists and Mineralogists Special Publication No. 37, p. 143–158.
NELSON, W. J., AND KRAUSSE, H.-F., 1981, The Cottage Grove fault system in southern Illinois: Illinois Institute of Natural Resources, State Geological Survey Division, Circular 522, 65 p.
NICHOLSON, C., SEEBER, L., WILLIAMS, P., AND SYKES, L. R., 1985, Seismicity and fault kinematics through the eastern Transverse Ranges, California: Block rotation, strike-slip faulting and shallow-angle thrusts: Journal of Geophysical Research, in press.
POSAVEC, M., TAYLOR, D., VAN LEEVEN, TH., AND SPECTOR, A., 1973, Tectonic controls of vulcanism and complex movements along the Sumatran fault system: Geological Society of Malaysia Bulletin, v. 6, p. 43–60.
PROFFETT, J. M., JR., 1977, Cenozoic geology of the Yerington district, Nevada, and implications for the nature and origin of Basin and Range faulting: Geological Society of America Bulletin, v. 88, p. 247–266.
RIEDEL, W., 1929, Zur mechanik geologischer Brucherscheinungen: Zentralblatt für Mineralogie and Paleontologie, v. 1929B, p. 354–368.
ROCKWELL, T., AND SYLVESTER, A. G., 1979, Neotectonics of the Salton Trough, *in* Crowell, J. C., and Sylvester, A. G., eds. Tectonics of the Juncture Between the San Andreas and the Salton Trough, Southeastern California—A Guidebook: Santa Barbara, California, Department of Geological Sciences, University of California, p. 41–52.
ROGERS, T. H., 1965, Santa Ana sheet, Geologic Map of California, Olaf P. Jenkins edition: California Division of Mines and Geology, Scale 1:250,000.
ROYDEN, L. H., 1985, The Vienna Basin: A thin-skinned pull-apart basin, *in* Biddle, K. T., and Christie-Blick, N., eds., Strike-Slip Deformation, Basin Formation, and Sedimentation: Society of Economic Paleontologists and Mineralogists Special Publication No. 37, p. 319–338.
SCHUBERT, C., 1980, Late-Cenozoic pull-apart basins, Boconó fault zone, Venezuelan Andes: Journal of Structural Geology, v. 2, p. 463–468.
SCHULMAN, N., AND BARTOV, Y., 1978, Tectonics and sedimentation along the rift valley, excursion Y2: 10th International Congress on Sedimentology, Jerusalem, International Association of Sedimentologists, Guidebook, p. 37–94.
SLOSS, L. L., 1979, Plate-tectonic implications of the Pennsylvanian System in the Illinois basin, *in* Palmer, J. E., and Dutcher, R. R., eds., Depositional and Structural History of the Pennsylvanian System of the Illinois Basin, Part 2: Illinois State Geological Survey Guidebook, Series 15a, Field trip 9, Ninth International Congress, Carboniferous Stratigraphy and Geology, p. 107–112.
SMITH, D. A., 1980, Sealing and nonsealing faults in Louisiana Gulf Coast salt basin: American Association of Petroleum Geologists Bulletin, v. 64, p. 145–172.
SMITH, J. G., 1965, Fundamental transcurrent faulting in northern Rocky Mountains: American Association of Petroleum Geologists Bulletin, v. 49, p. 1398–1409.
STEWART, J. H., 1983, Extensional tectonics in the Death Valley area, California: Transport of the Panamint Range structural block 80 km northwestward: Geology, v. 11, p. 153–157.
SYLVESTER, A. G., AND SMITH, R. R., 1976, Tectonic transpression and basement-controlled deformation in San Andreas fault zone, Salton trough, California: American Association of Petroleum Geologists Bulletin, v. 60, p. 2081–2102.
TCHALENKO, J. S., AND AMBRASEYS, N. N., 1970, Structural analysis of the Dasht-e Bayaz (Iran) earthquake fractures: Geological Society of America Bulletin, v. 81, p. 41–60.
TERRES, R. R., AND SYLVESTER, A. G., 1981, Kinematic analysis of rotated fractures and blocks in simple shear: Seismological Society of America Bulletin, v. 71, p. 1593–1605.
TRYGGVASON, E., 1982, Recent ground deformation in continental and oceanic rift zones, *in* Pálmason, G., ed., Continental and Oceanic Rifts: American Geophysical Union Geodynamics Series, v. 8, p. 17–29.
VROMAN, A. J., 1967, On the fold pattern of Israel and the Levant: Geological Survey of Israel Bulletin, v. 43, p. 23–32.
WEBER, K. J., MANDL, G., PILAAR, W. F., LEHNER, F., AND PRECIOUS, R. G., 1978, The role of faults in hydrocarbon migration and trapping in Nigerian growth fault structures: Offshore Technology Conference Paper OTC 3356, p. 2643–2652.
WERNICKE, B., SPENCER, J. E., BURCHFIEL, B. C., AND GUTH, P. L., 1982, Magnitude of crustal extension in the southern Great Basin: Geology, v. 10, p. 499–502.
WILCOX, R. E., HARDING, T. P., AND SEELY, D. R., 1973, Basic wrench tectonics: American Association of Petroleum Geologists Bulletin, v. 57, p. 74–96.
WRIGHT, L. A., AND TROXEL, B. W., 1970, Summary of regional evidence for right-lateral displacement in the western Great Basin: Discussion: Geological Society of America Bulletin, v. 81, p. 2167–2173.
ZARTMAN, R. E., BROCK, M. R., HEYL, A. V., AND THOMAS, H. H., 1967, K-Ar and Rb-Sr ages of some alkaline intrusive rocks from central and eastern United States: American Journal Science, v. 265, no. 10, p. 848–870.

655203

# COMPARISON OF TECTONIC FRAMEWORK AND DEPOSITIONAL PATTERNS OF THE HORNELEN STRIKE-SLIP BASIN OF NORWAY AND THE RIDGE AND LITTLE SULPHUR CREEK STRIKE-SLIP BASINS OF CALIFORNIA

TOR H. NILSEN[1] AND ROBERT J. MCLAUGHLIN
*U.S. Geological Survey*
*345 Middlefield Road*
*Menlo Park, California 94025*

ABSTRACT: Thick nonmarine sequences with similar facies and geometry may accumulate in basins that develop adjacent to strike-slip faults. Herein we compare three basins of different age and size whose tectonic and depositional characteristics suggest a similar origin and history.

The Hornelen Basin developed during the Middle and possibly Early Devonian in western Norway. The basin is bounded on the north and south by east-striking faults, and the northern fault is considered to have been a zone of major right-slip movement. The basin is 60–70 km long, 15–25 km wide, and about 1,250 km$^2$ in areal extent; its cumulative fill of 25,000 m was deposited at an estimated rate of 2.5 m/1,000 yr. The Ridge Basin developed during the Miocene and Pliocene between the right-lateral San Gabriel and San Andreas faults in southern California. The basin is 30–40 km long, 6–15 km wide, and about 400 km$^2$ in areal extent; its cumulative fill of 7,000–11,000 m was deposited at an estimated rate of about 3 m/1,000 yr. The three Little Sulphur Creek Basins probably developed between 4 and 2 Ma along the east side of the right-lateral Maacama fault zone in northern California. These basins cumulatively are about 12 km long, 1.5 to 2 km wide, and about 15 km$^2$ in areal extent; their cumulative fill of 5,000 m was deposited at an estimated rate of about 2.5 m/1,000 yr.

Coarse sedimentary breccia, which constitutes a relatively small volume of the fill, was deposited in each of these basins along the active right-slip fault margin as talus, landslide, and small but steep debris-flow-dominated alluvial fans. Along other margins of the basins, a much larger volume of the fill accumulated as larger streamflow-dominated alluvial fans, braided-stream, meandering-stream, fan-delta, and deltaic deposits. Lacustrine deposits that include turbidites and, locally in Ridge Basin, chemical precipitates, accumulated in the centers of the basins. The basin floors are generally tilted toward the margins with active right-slip faults so that the basin axes and the depocenters are subparallel to, and shifted toward, this margin. Sediment was transported toward the basin center from surrounding highlands and then longitudinally down the basin axis. The basin fills were syn-depositionally faulted and post-depositionally folded into large plunging synclines. The basins lengthened over time and contain thicknesses of sedimentary rocks that are comparable to or greater than their widths.

## INTRODUCTION

Sedimentary basins that develop along strike-slip faults have various shapes and sizes, and differ in the details of their tectonic and depositional history. These differences are related in part to the geometry and orientation of the principal bounding faults. Because the principal faults may be curved, braided, or en echelon, areas of compression (or transpression) may develop adjacent to or even within areas of extension (or transtension). Basins that are of pull-apart origin are common along strike-slip faults and may be filled with very thick sedimentary sequences.

The purpose of this paper is to compare the tectonic evolution, geometry, depositional framework, and geologic history of three well-studied basins that developed adjacent to major strike-slip faults. The three basins, the Hornelen Basin of western Norway, the Ridge Basin of southern California, and the Little Sulphur Creek Basins of northern California (Fig. 1), developed in continental settings and are filled chiefly, if not wholly, by nonmarine sedimentary rocks that include prominent lacustrine facies. Two of these three basins, the Ridge and Hornelen Basins, have long been used as models for sedimentation along strike-slip faults.

The three basins vary in size (Fig. 2), permitting interesting comparisons of their tectonic and depositional features. Although we have worked chiefly in the Little Sulphur Creek Basins, we feel confident in making the comparative analysis because of the excellent descriptions of the Hornelen Basin by R. J. Steel and his colleagues and of the Ridge Basin by J. C. Crowell, M. H. Link and their colleagues, whose work we heavily rely upon. The depositional aspects of the basins are emphasized herein, particularly the distribution of various facies and the style of basin sedimentation. The largest and oldest basin, the Devonian Hornelen Basin, is discussed first, then the intermediate-size Ridge Basin, and finally the small Little Sulphur Creek Basins.

## HORNELEN BASIN

### *Setting*

The Hornelen Basin is the largest and northernmost of four east-trending Devonian sedimentary basins that crop out along the west coast of Norway between Nordfjord and Sognefjord (Fig. 1A; Kolderup, 1904; Nilsen, 1973; Bryhni, 1975; Steel, 1976). The basin was mapped and its stratigraphy and sedimentology studied by Kolderup (1927), Bryhni (1964a,b,c; 1978), Steel et al. (1977, 1979), Larsen and Steel (1978), Steel and Aasheim (1978), Steel and Gloppen (1980), Gloppen and Steel (1981), and Pollard et al. (1982). Fossils of plants (Kolderup, 1904, 1915a,b; 1916; Nathorst, 1915; Hoeg, 1936) and freshwater crossopterygian fishes (Kiaer, 1918; Jarvik, 1949) indicate a Middle Devonian age for the uppermost strata in the basin.

The basin developed after the Late Silurian Caledonian orogeny, when the northwestern European (Baltica) and northeastern North American cratons were sutured by the closure of Iapetus, the proto-Atlantic Ocean (Gee, 1975). The suturing in western Norway caused the detachment and eastward thrusting of nappes onto the edge of the craton (Gee, 1978). The Devonian basins have been primarily regarded as pull-apart basins that formed grabens and half-grabens within a framework of post-Caledonian strike-slip

[1]Present address: RPI Pacific, Inc., 507 Seaport Court, Suite 101, Redwood City, California 94063

Copyright © 1985, The Society of Economic Paleontologists and Mineralogists

655204



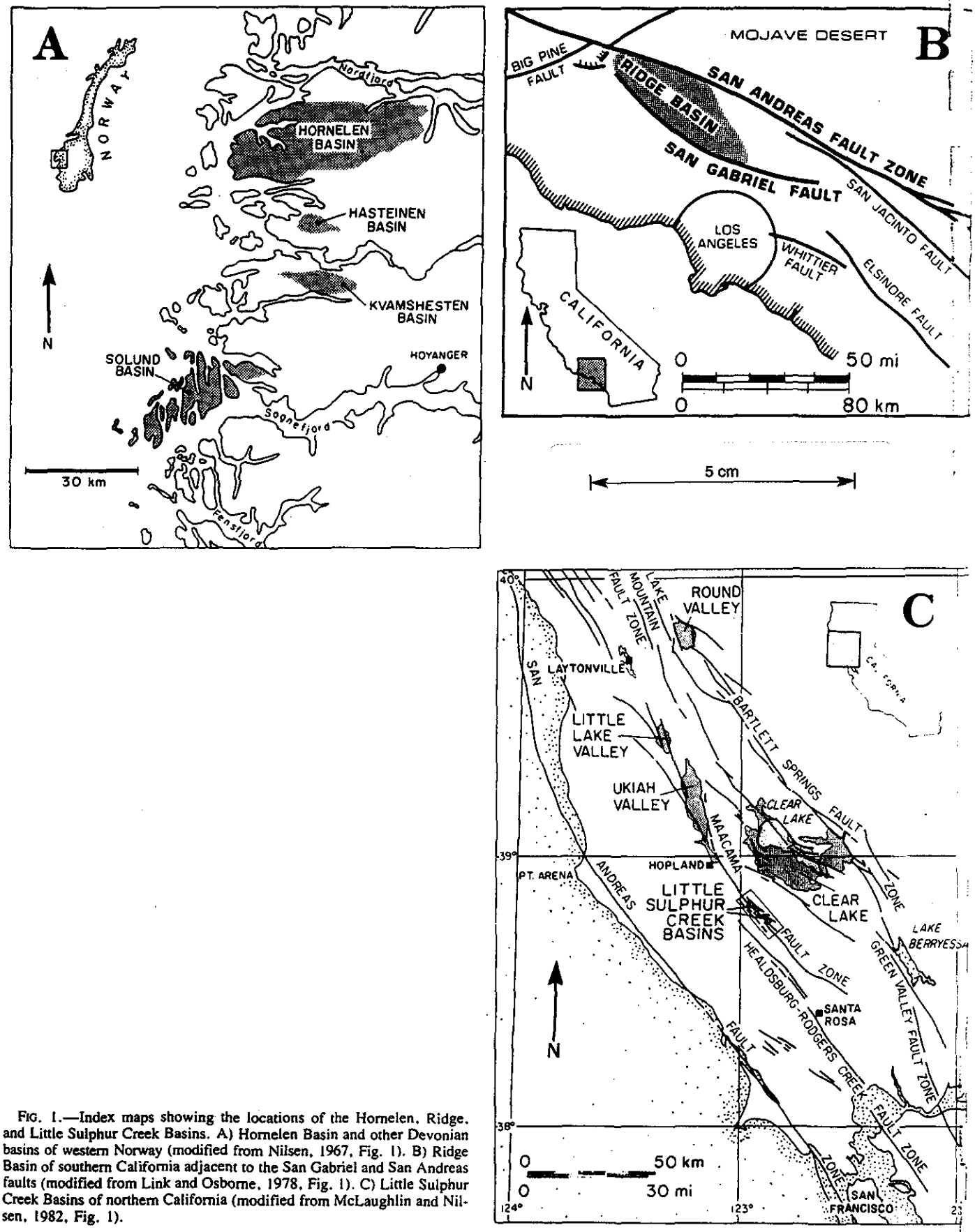



FIG. 1.—Index maps showing the locations of the Hornelen, Ridge, and Little Sulphur Creek Basins. A) Hornelen Basin and other Devonian basins of western Norway (modified from Nilsen, 1967, Fig. 1). B) Ridge Basin of southern California adjacent to the San Gabriel and San Andreas faults (modified from Link and Osborne, 1978, Fig. 1). C) Little Sulphur Creek Basins of northern California (modified from McLaughlin and Nilsen, 1982, Fig. 1).

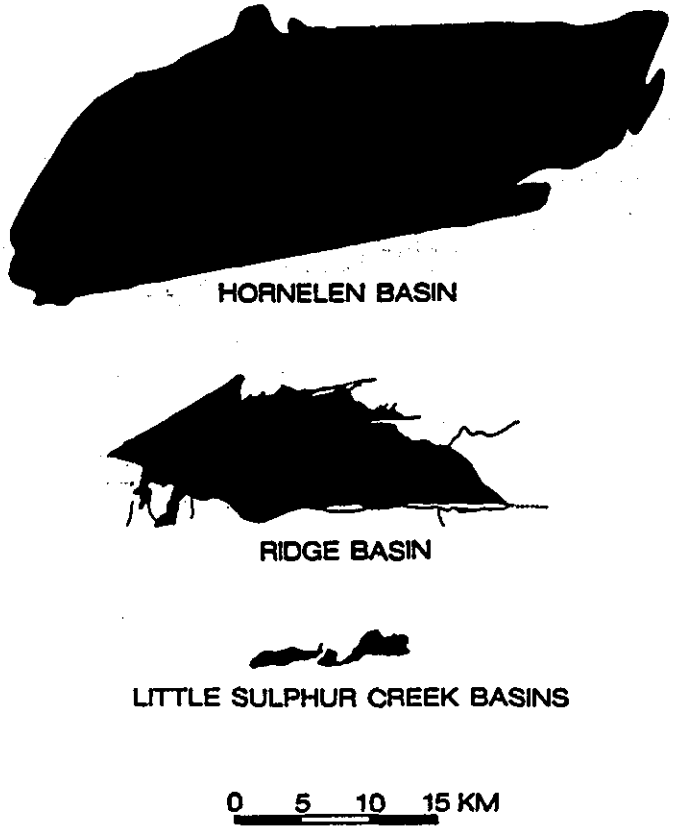



FIG. 2.—Outline maps of the Hornelen, Ridge, and Little Sulphur Creek Basins showing their relative sizes.

faulting (Steel and Gloppen, 1980).

The Hornelen Basin is 60–70 km long, 15–25 km wide, and occupies an area of 1,250 km$^2$ (Fig. 3). The strata in the axial part of the basin dip consistently eastward and attain a total stratigraphic thickness of 25,000 m. The northern and southern margins of the basin are formed by high-angle faults, the southern fault striking slightly north of east and the northern fault almost due east (Figs. 3 and 4A, B). The Devonian sedimentary rocks rest unconformably on pre-Devonian basement rocks along the western margin of the basin and rest with fault contact on basement rocks along the eastern margin of the basin (Fig. 4B).

Conglomerate is common around most of the basin margins and generally thins and pinches out toward the center of the basin (Fig. 3). The axial deposits are generally finer grained and consist of fine-grained conglomerate, sandstone, siltstone, and shale. No evidence of marine sedimentation has been observed.

The basement rocks that underlie and surround Hornelen Basin consist of two distinct types: (1) to the north, east, and south, Precambrian metamorphic rocks that include chiefly schist, gneiss and quartzite; and (2) to the west and probably beneath the basin, Cambrian, Ordovician, and Silurian shale, graywacke, basalt, gabbro, and granitic rocks.

### *Structure*

The Hornelen Basin forms a broad east-plunging syncline in which the synclinal axis is located close to the northern basin margin (Fig. 3). The basin fill is characterized by a step-like topography defined by basin-wide coarsening- and thickening-upward sequences (Fig. 4C). Beds along the

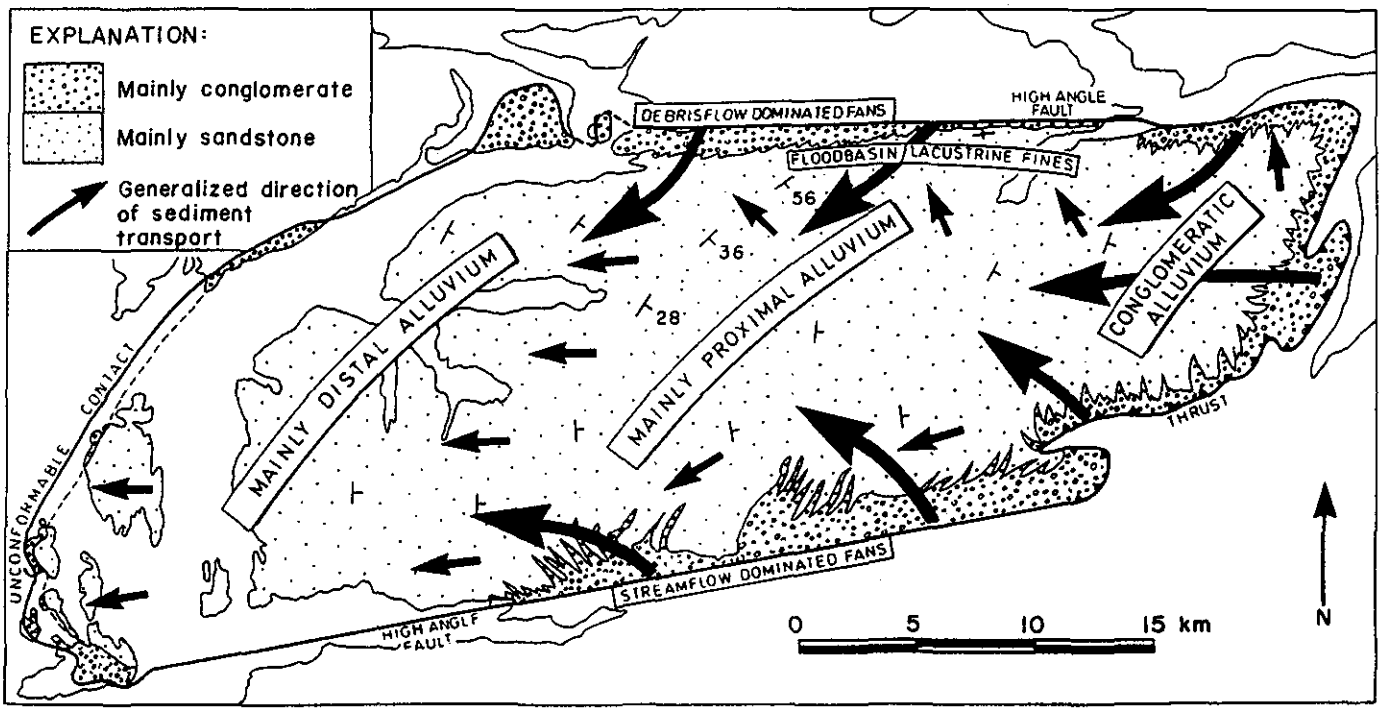
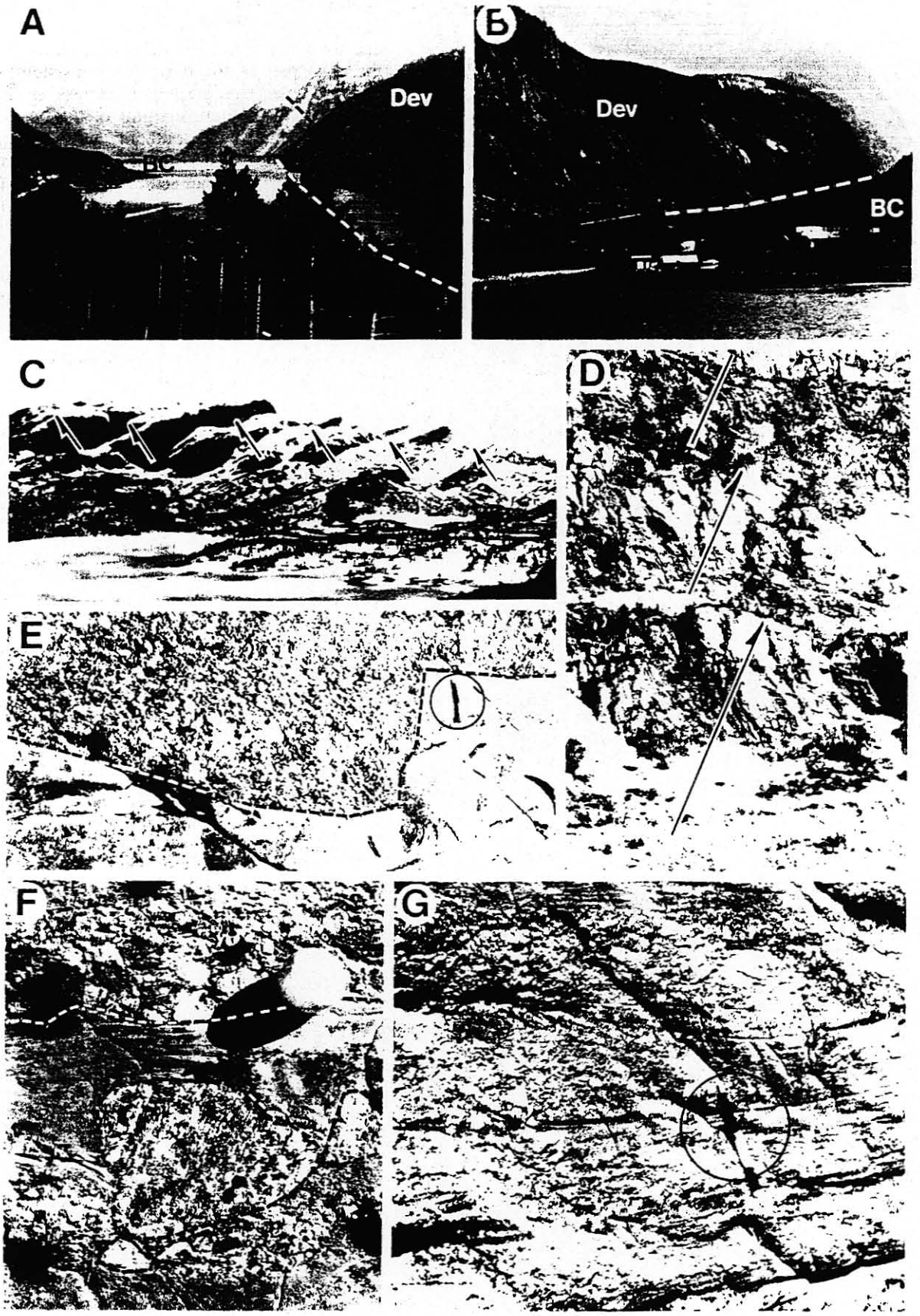



FIG. 3.—Simplified geologic and paleogeographic map of Hornelen Basin showing overall structural framework, major rock types, and generalized directions of sediment transport (from Steel and Aasheim, 1978, Fig. 1). For location, see figure 1A.

5 cm

655206



655207

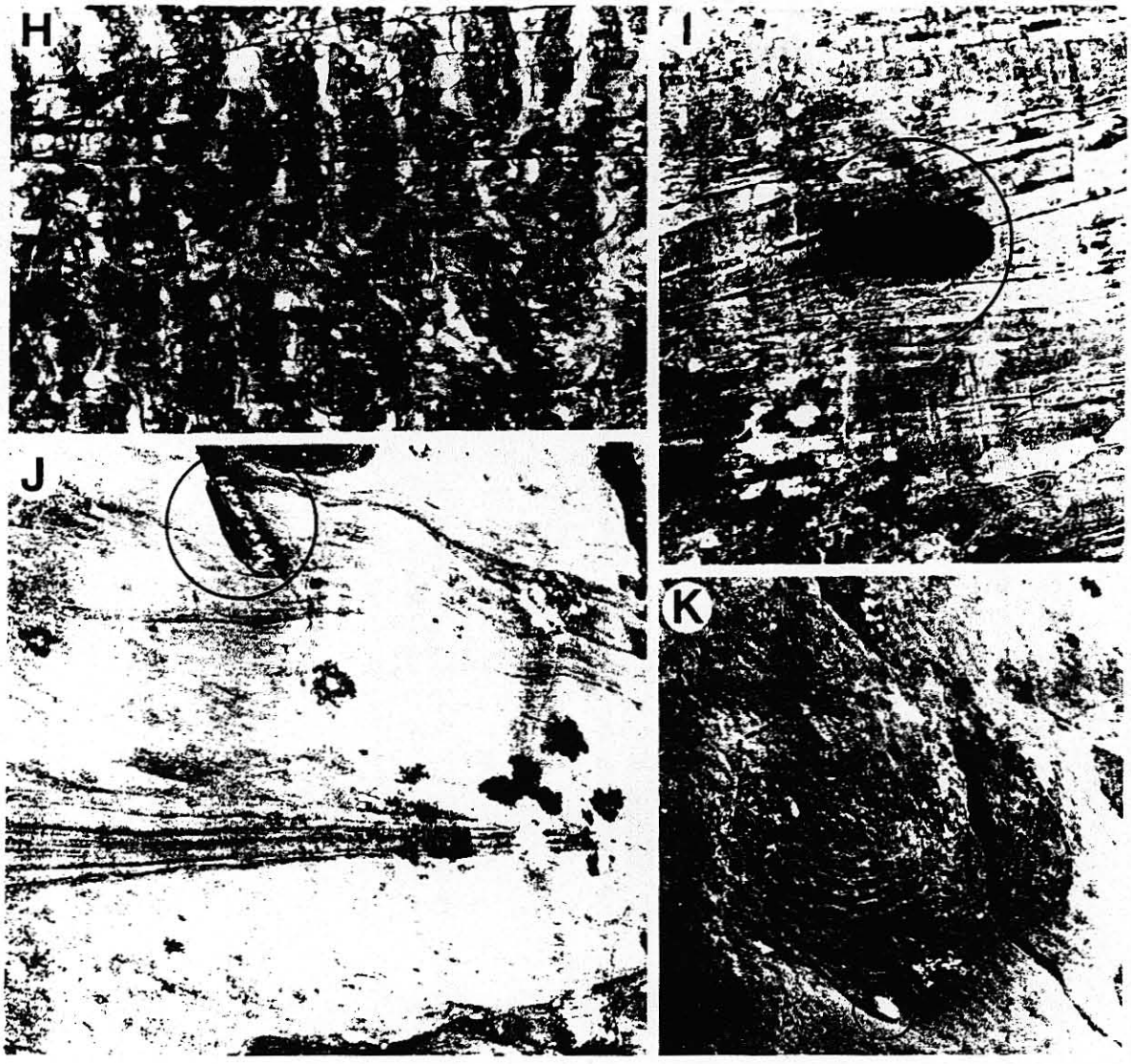



FIG. 4.—Photographs of Hornelen Basin and its chief depositional facies. A) view east along northern boundary fault (white dashed line) showing eastern faulted contact (dashed black line) of Devonian sedimentary rocks (Dev) on basement rocks (BC). B) view east along southern boundary fault (white dashed line) showing juxtaposition of Devonian sedimentary rocks (Dev) and basement rocks (BC). C) stacked 100-to-200-m-thick thickening- and coarsening-upward sequences (arrows) in the central part of the basin. D) stacked thickening- and coarsening-upward sequences (arrows) in streamflow-dominated alluvial-fan deposits along southern margin of basin. E) channeled base (dashed line) of subaerial conglomeratic debris-flow deposit of alluvial fan; pen circled for scale. F) poorly sorted and reverse-graded subaerial conglomeratic debris-flow of alluvial-fan deposit; apple for scale. G) well-stratified, interbedded conglomerate and sandstone of streamflow-dominated alluvial-fan deposit; pen circled for scale. H) wave-rippled, bioturbated, lacustrine siltstone deposited in axial part of basin; circle with diameter of 7 cm for scale. I) planar- and cross-stratified basin-axis fluvial deposits; mitten circled for scale. J) cross-stratified basin-axis fluvial deposits; knife circled for scale. K) synsedimentary deformation associated with upward expulsion of fluids and development of sandstone diapirs in basin-axis fluvial deposits; bottle cap circled for scale.

northern and southern margins of the basin, which are also organized into sequences of this type (Fig. 4D), are locally steeply dipping and have clearly been affected by post-depositional faulting along these margins. The faulted eastern margin of the basin has generally been interpreted as a thrust. The northern boundary fault can be traced both eastward and westward into the basement and the southern boundary fault can be traced westward into the basement (R. J. Steel, written commun., July, 1984).

### *Depositional Facies*

The deposits of Hornelen Basin have been studied in considerable detail and the general patterns of sedimentation are well understood (Fig. 5A, B). Small, debris-flow-dominated alluvial fans are present along the entire northern margin of the basin adjacent to that basin-margin fault, and larger streamflow-dominated alluvial fans are present along the entire southern margin of the basin adjacent to that ba-

655208

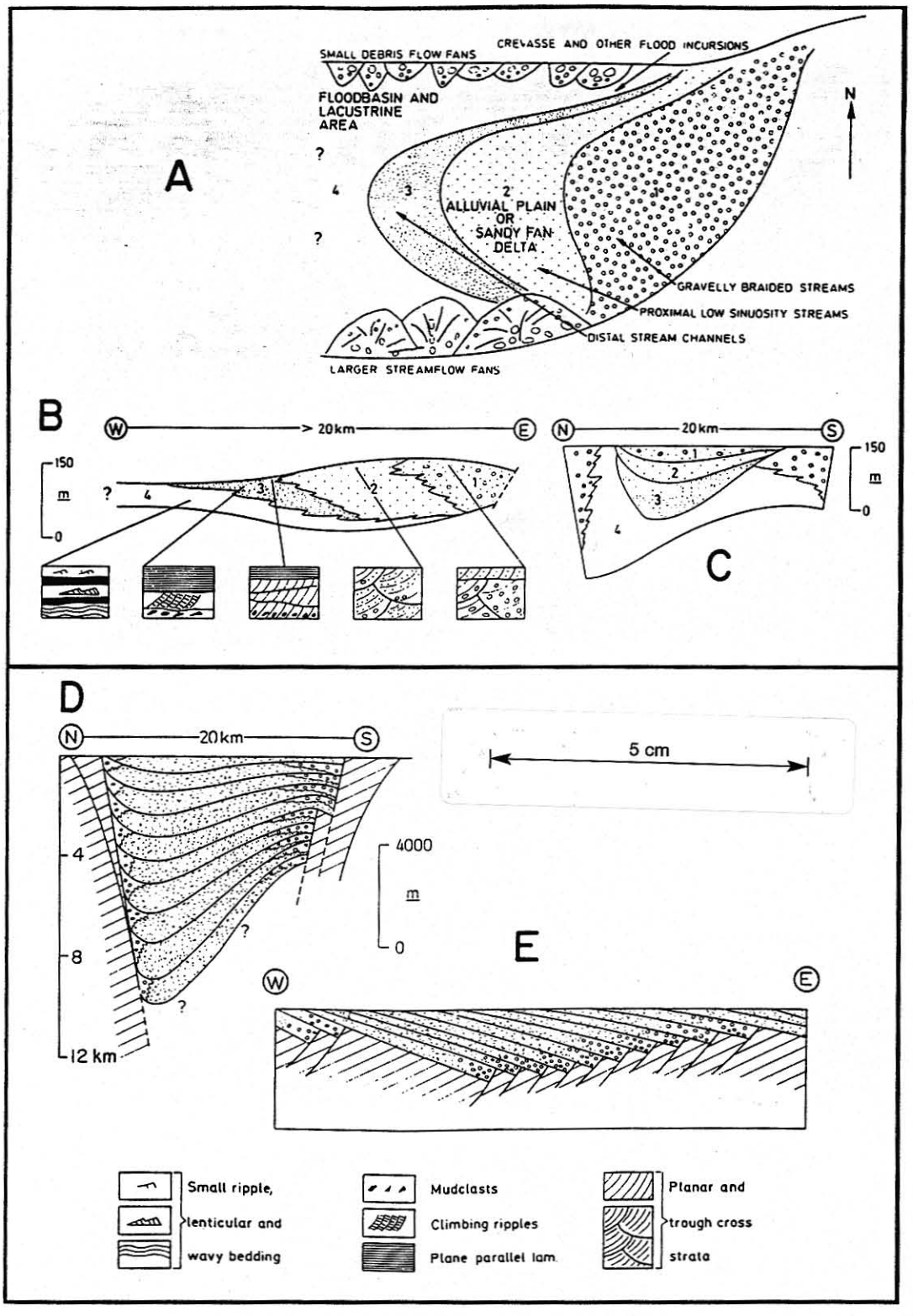



FIG. 5.—Structural and depositional framework of Hornelen Basin (modified from Steel and Gloppen, 1980, Fig. 9). A) general paleogeograph, and style of basin filling, showing three principal sources of detritus and distribution of depositional facies along the basin margins and in the basin axis. B) longitudinal east-west cross-section of the basin showing proximal-to-distal organization of depositional facies during progradation of a sing 100-to-200-m-thick sequence. C) transverse north-south cross-section showing lateral relations between basin-margin alluvial-fan deposits and basi axis fluvial and lacustrine deposits during progradation of a single 100-to-200-m-thick sequence. D) simplified transverse north-south cross-sectio showing vertical and horizontal stacking arrangement of multiple 100-to-200-m-thick sequences and asymmetry of the basin. E) inferred longitudinal east-west cross-section showing repetitive stacking of 100-to-200-m-thick sequences, eastward overstep of sedimentary sequence onto faulted basement surface, and eastward migration of basin depocenter.

sin-margin fault (Steel, 1976; Larsen and Steel, 1978; Steel and Aasheim, 1978; Gloppen and Steel, 1981). The axial part of the basin is dominated by fluvial and lacustrine facies; the fluvial sediments accumulated on a broad alluvial plain or sandy lacustrine fan-delta, fed by ephemeral low-sinuosity streams that prograded into lakes situated to the northwest (Steel and Aasheim, 1978).

The northern debris-flow-dominated alluvial fans generally have radii of 0.5–1.3 km, thicknesses of 100–200 m, and are characterized by relatively steep paleoslopes (Gloppen and Steel, 1981). The fans, which prograded into adjacent lacustrine environments, have a wedge-shaped geometry in which they thicken toward the basin-margin faults (Fig. 5C). These fans consist largely of subaerial and subaqueous conglomeratic debris-flow deposits characterized by poor sorting, poor rounding, general lack of stratification and clast orientation, packing that is either clast- or matrix-supported, reverse grading (Fig. 4F), and a positive correlation between bed thickness and maximum clast size (Gloppen and Steel, 1981). Angular clasts as large as 75 cm are locally present in these fan deposits. Bed thicknesses and the proportion of debris-flow deposits within the fans decrease southward. The fans are typically organized into overall thickening- and coarsening-upward sequences that are 100–200 m thick and similar thinner, smaller sequences that are 5–25 m thick (Gloppen and Steel, 1981).

The streamflow-dominated alluvial fans along the southern margin of the basin generally have radii of 2–4 km, thicknesses of 75–120 m, and are characterized by relatively gentle paleoslopes (Gloppen and Steel, 1981). Although these fan deposits are similar to the debris-flow-dominated fans in overall geometry and cyclical organization, they consist mostly of beds of conglomerate and conglomeratic sandstone characterized by better sorting, better rounding, parallel stratification and cross-stratification, well-developed clast orientation, packing that is generally clast-supported, normal grading, and a positive correlation between bed thickness and maximum clast size (Fig. 4G; Gloppen and Steel, 1981). The distal parts of these fans consist mostly of sheetflood deposits formed of laterally continuous alternating thin beds of nonchannelized fine-grained conglomerate and sandstone.

The axial deposits of Hornelen Basin are organized into about 200 basin-wide coarsening-upward sequences that average about 150 m in thickness and form the prominent step-like topography in the basin (Figs. 4C and 5D; Steel and Aasheim, 1978). These sequences can be divided in ascending order into four distinct facies: (1) floodplain and lacustrine deposits, dominantly mudstone, siltstone, and very fine grained sandstone that contain current, wave, and climbing ripple marks (Fig. 4H), wavy and lenticular bedding, mudcracks, shale rip-up clasts, syn-sedimentary slumps, trace fossils, and some thin-bedded turbidites; (2) alluvial deposits of several types, consisting for the most part of fine- to medium-grained, cross-stratified and parallel-stratified sandstone deposited by distal braided or meandering streams (Fig. 4I, J); (3) alluvial plain or sandy fan-delta deposits, dominated by pebbly or very coarse grained, cross-stratified or parallel-stratified sandstone; and (4) conglomeratic braided-stream deposits, dominated by massive, planar-, and cross-stratified conglomerate and sandstone that fills channels and contains well-sorted and well-rounded clasts of varied composition (Steel and Aasheim, 1978; Pollard et al., 1982). These axial depositional bodies thin and fine westward, extend for east-west distances of at least 20 km, and prograded westward and northwestward into the basin. The bodies generally thicken toward the northern basin margin and the floodplain and lacustrine deposits are more widely distributed adjacent to the northern basin margin, suggesting that the basin floor was generally tilted northward.

### *Paleocurrents and Maximum Clast Size*

Paleocurrent directions from the Hornelen Basin yield a pattern of lateral infilling of the basin from its northern and southern margins and westward transport down the axis of the basin (Figs. 3 and 5A; Brhyni, 1964a,b; Steel, 1976; Steel and Gloppen, 1980). Directions of sediment transport along the western margin of the basin indicate westward flow above the basal unconformity. Detailed paleocurrent studies of the small debris-flow-dominated alluvial fan deposits along the northern margin of the basin show patterns of sediment transport that are southward in proximal facies and westward in distal facies, concomitant with gradual decrease in the same directions of the average and maximum clast size of the conglomerate (Larsen and Steel, 1978; Steel and Aasheim, 1978; Gloppen and Steel, 1981). Analyses of the larger streamflow-dominated alluvial-fan deposits along the southern margin yield similar but reversed results, with the directions being toward the north and northwest (Fig. 5A; Steel and Gloppen, 1980; Gloppen and Steel, 1981). In the axial fluvial and lacustrine deposits, sediment transport was generally westward and the maximum clast sizes, where observed along correlative horizons, generally fine westward (Steel and Aasheim, 1978; Pollard et al., 1982).

### *Tectonic and Depositional History*

Steel and Gloppen (1981) concluded that Hornelen Basin formed as a result of Devonian strike-slip faulting. They thought that the northern basin-margin fault was the dominant fault that controlled sedimentation within the basin (Fig. 3); on the basis of the composition of clasts within the northern debris-flow-dominated alluvial fans, and projections of the sizes of the drainage areas for these fans, they concluded that the northern basin-margin fault was a right-lateral strike-slip fault. The southern boundary fault is thought to be a normal fault, however, chiefly because the conglomerate clasts can be readily matched with adjacent source areas.

The systematic westward displacement and overlapping of the depositional loci of alluvial fans along the northern and southern basin margins and of the axial facies suggests that the basin depocenter systematically migrated eastward through time (Fig. 5). As a result of this migration, the maximum thickness of sedimentary strata at any one place probably never exceeded 8,000 m, even though the cumulative stratigraphic thickness for the entire basin is about 25,000 m. The basin floor generally sloped westward, as indicated by the general directions of sediment transport in

the axial parts of the basin, but also had a northerly component of slope, as indicated by the concentration of lacustrine deposits along the northern margin of the basin (Fig. 5A,B,C). Although much coarse-grained sediment was transported into the basin as alluvial fans from its northern and southern margins, most of the sediment was transported axially into the basin from source areas to the east.

The 100-to-200-m-thick basin-wide coarsening-upward sequences in the fill of Hornelen Basin are thought by Steel and Gloppen (1980) to correspond to major episodes of horizontal displacement along basin-margin faults (Fig. 5D). The lowering of the basin floor along now buried west-dipping normal faults resulted in eastward migration of the basin depocenter (Fig. 5E); thinner coarsening-upward sequences were thought to result chiefly from vertical movement of the basin floor, which caused migration of the source area and progradation of depositional bodies into the basin. Abundant syn-sedimentary deformation, particularly in the basin-axis lacustrine and marginal lacustrine deposits, may record penecontemporaneous seismic activity (Fig. 4K).

## RIDGE BASIN

### *Setting*

The Ridge Basin is located between the San Andreas and San Gabriel faults in southern California (Fig. 1B) and w[as] mapped by Clements (1937), Eaton (1939), and Crowe[ll] (1950, 1954a). Its geologic history has recently been summarized in detail in a volume edited by Crowell and Link (1982a) that has an accompanying geologic map by Crow[ell] et al. (1982). The basin is 30 to 40 km long, 6 to [1]0 km wide, and covers an area of about 400 km$^2$ (Fig. 6). The basin developed in the Mohnian (late Miocene) an[d] continued to fill with sediment through the early Pleisto[cene], after which it was deformed and uplifted (Crowell, 1974a,b, 1975, 1982a; Crowell and Link, 1982b; Link, 1983).

During the late Miocene, the San Gabriel fault was a m[a]jor active strand of the San Andreas fault system (Crowell, 1952, 1954b, 1975), and the Ridge Basin formed east of a major bend in the fault. More than 60 km of right slip o[c]curred along the San Gabriel fault from late Miocene in[to]

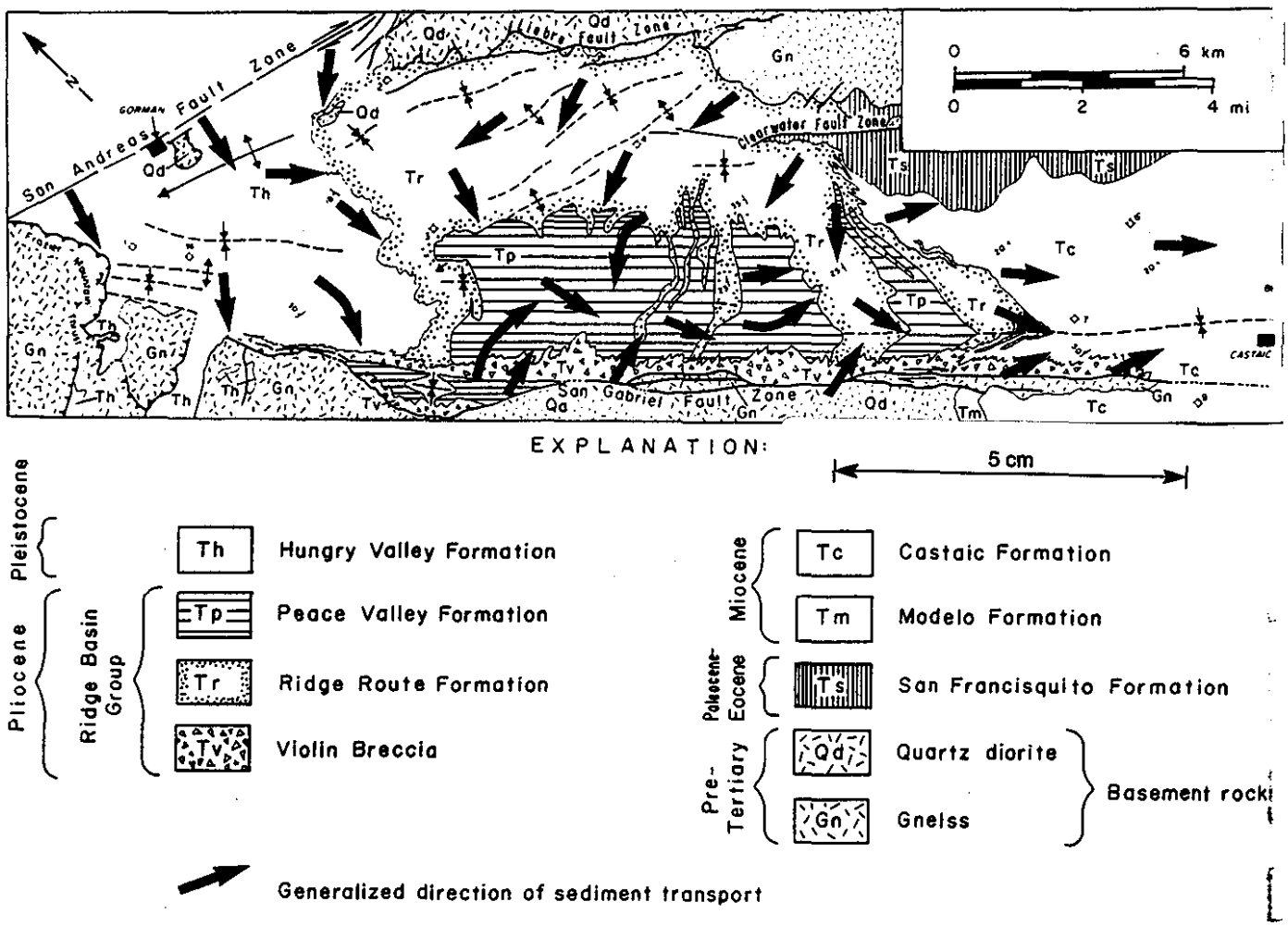



FIG. 6.—Generalized geologic map of Ridge Basin (modified from Link and Osborne, 1978, Fig. 3, after Crowell, 1954a, 1975) showing generalized directions of sediment transport (from Link, 1982c, Fig. 2). For location see Figure 1B.

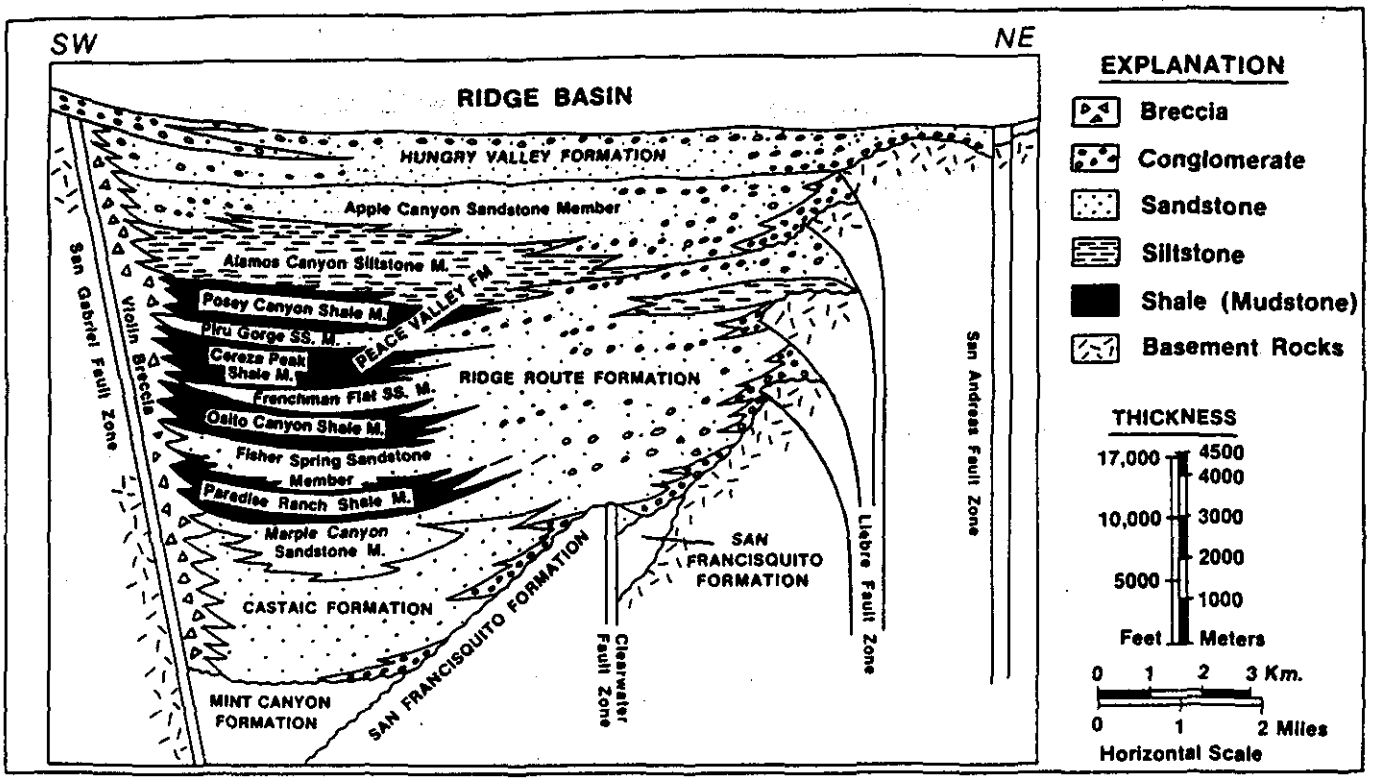



FIG. 7.—Generalized cross-section of Ridge Basin showing principal faults (from Crowell and Link, 1982b, Fig. 2).

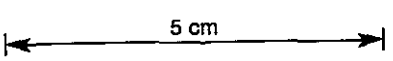
Pliocene time. During the Pleistocene, the modern trace of the San Andreas fault developed along the northeastern flank of the Ridge Basin, and active right slip shifted to this fault. As much as 240 km of displacement has taken place on the San Andreas fault in this region, offsetting the Ridge Basin from its chief source area, which was originally located to the northeast.

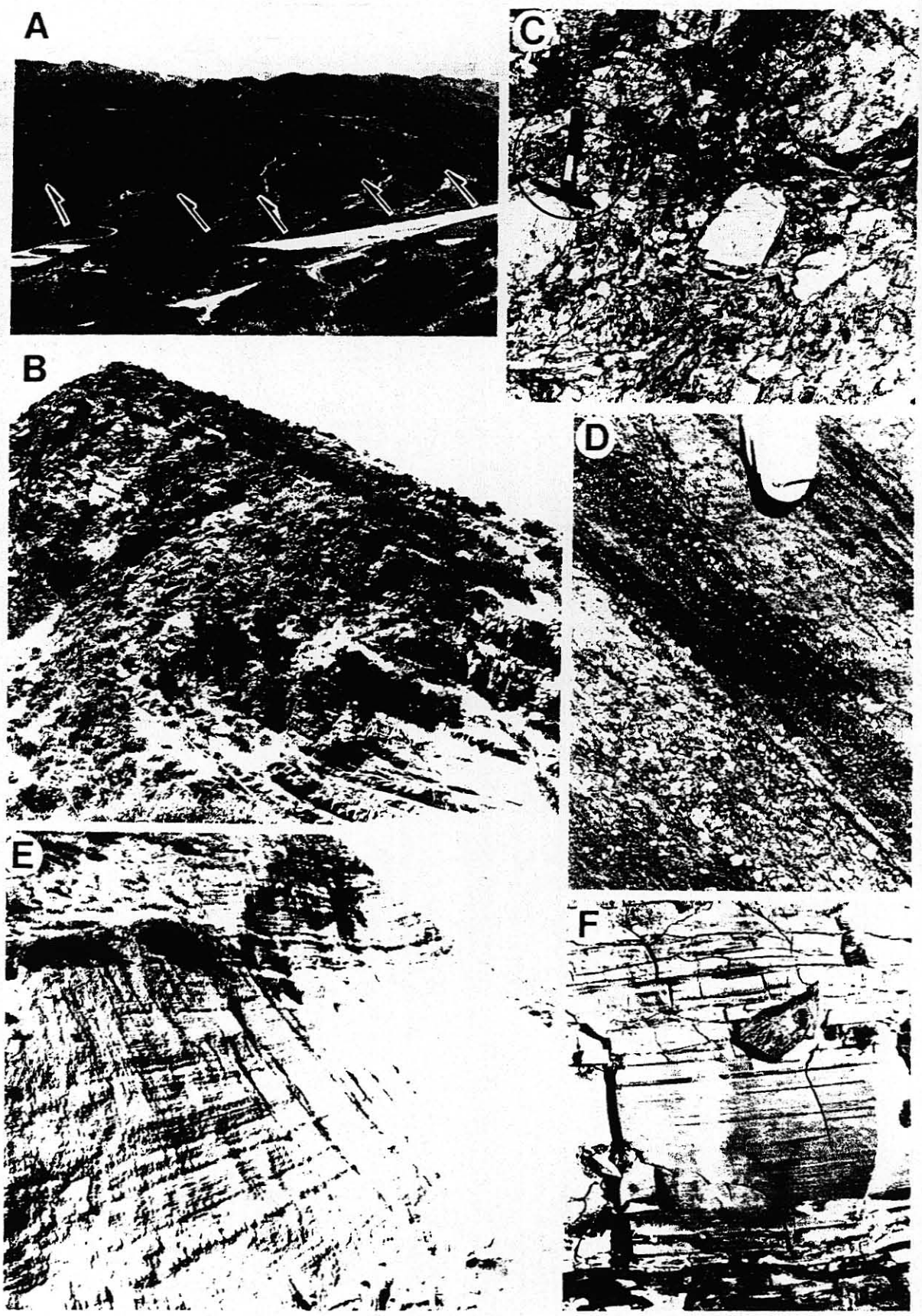
The Ridge Basin is filled with more than 13,500 m of sedimentary rocks (Fig. 7). The nonmarine Miocene Mint Canyon Formation forms the lowest part of the basin fill and it is overlain by the marine upper Miocene Castaic Formation, which is about 2,200 m thick. The remainder of the basin fill has been assigned to the nonmarine Ridge Basin Group (Crowell, 1975), which conformably overlies and laterally interfingers with the Castaic Formation. The Ridge Basin Group, which is 9,000–11,000 m thick, contains marine deposits in its lower 600 m. It consists of four formations: (1) the Violin Breccia, which is confined to the western margin of the basin, is about 11,000 m thick, and interfingers northeastward with the Castaic Formation and other units of the Ridge Basin Group; (2) the Peace Valley Formation, about 8,000 m thick, dominantly shale and siltstone, but also including an analcimic and ferroan dolomitic mudstone, deposited chiefly in the central part of the basin; (3) the Ridge Route Formation, about 9,000 m thick, dominantly conglomerate and sandstone, deposited chiefly along the eastern margin of the basin; and (4) the Hungry Valley Formation, about 1,100 m thick, dominantly conglomerate and sandstone, deposited basin-wide as the final stage of basin filling (Link, 1982a).

Ridge Basin is bounded both on the southwest and northeast and is also underlain by granite, quartz diorite, quartz monzonite, and gneiss of Precambrian to Mesozoic age (Figs. 6 and 7). These types of rocks, which also extend southeastward into the Mojave Desert province east of the San Andreas fault, as well as sandstone of the underlying San Francisquito Formation and Mint Canyon Formation, formed the chief source of detritus deposited in the Ridge Basin. Thus, the sandstone deposits of Ridge Basin are chiefly arkosic in composition (Link, 1982b), reflecting the dominantly granitic provenance (Link, 1982c).

### *Structure*

In northeast-southwest cross-section, the Ridge Basin has the appearance of a complex half-graben bounded by the San Gabriel fault on the southwest and the San Andreas fault on the northeast (Figs. 6 and 7). The Clearwater and Liebre fault zones are primarily high-angle reverse faults that were active during basin sedimentation. Paleomagnetic studies of the stratigraphic sequence of Ridge Basin by Ensley and Verosub (1982a,b) suggest that the Clearwater fault was tectonically active from 8.1 to 7.8 Ma, the southern branches of the Liebre fault were active from 7.3 to 6.1 Ma, and the northern branches of the Liebre fault were active from 6.0 to 5.0 Ma. They also concluded that the San Gabriel fault was active continuously from prior to 8.1 to 5.0 Ma and determined that the sedimentary rocks of Ridge Basin had not been rotated. The unconformable overlap of the Clearwater and Liebre faults by the base of the Hungry




A
B
C
D
E
F
5 cm

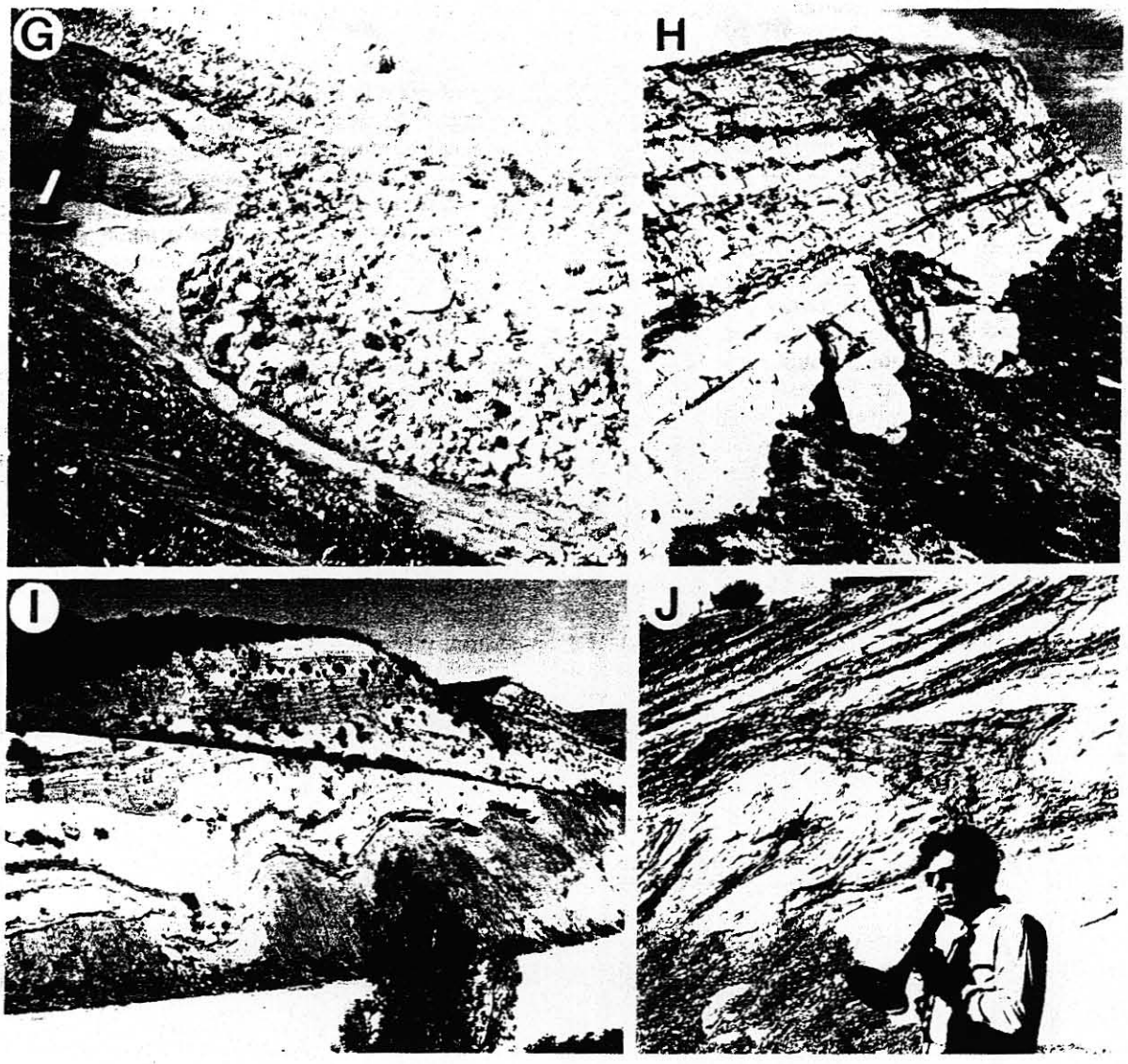



FIG. 8.—Photographs of Ridge Basin and its chief depositional facies. A) view eastward from ridge underlain by the Violin Breccia toward the axis of Ridge Basin showing stacked sequences (arrows) in the central part of the basin; interstate highway in middle of photograph for scale. B) view northwest of northeast-dipping beds of the Violin Breccia interfingering laterally from left to right with fine-grained and thin-bedded lacustrine deposits. C) typical appearance of proximal facies of the Violin Breccia; hammer circled for scale. D) reverse-graded distal subaqueous debris-flow deposits of the Violin Breccia; end of pocket knife for scale. E) thin-bedded lacustrine deposits of the Peace Valley Formation; geologists in lower right corner for scale. F) very thinly laminated analcimic lacustrine mudstone of the Peace Valley Formation; thickness of section shown is about 25 cm. G) channelized conglomeratic fluvial deposits of the Ridge Route Formation; note underlying bed with abundant climbing ripple lamination. H) deltaic sandstone member of the Ridge Route Formation that extends across most of Ridge Basin. I) large-scale basin-axis syn-sedimentary deformation. J) small-scale basin-axis syn-sedimentary deformation, J. C. Crowell for scale.

Valley Formation (Figs. 6 and 7) shows that the San Gabriel fault continued to move after the Liebre fault had become inactive, probably until the beginning of the Pleistocene (Crowell, 1975). The uppermost part of the basin fill, the Hungry Valley Formation, was deposited between 5.0 and 4.0 Ma, as the San Andreas fault zone became active. The Frazier Mountain thrust developed in the middle Pleistocene and subsequently became inactive and was folded (Crowell, 1982a).

The sedimentary fill of Ridge Basin forms a series of basin-wide northwest-dipping ridges (Fig. 8A). The fill has been folded into a broad asymmetric northwest-plunging syncline (Figs. 6 and 7) whose axis lies close to the southwestern flank of the basin, adjacent to outcrops of the Violin Breccia. The northwest-plunging strata of the Ridge Basin Group lap successively northwestward onto the basement so that the true thickness of the stratigraphic sequence at any point in the basin is less than 4,500 m, although the

655214

total measured stratigraphic sequence along the synclinal axis is more than 13,500 m (Crowell, 1975; Crowell and Link, 1982b).

### *Depositional Facies*

The general character and distribution of depositional facies in the Ridge Basin have been summarized by Link and Osborne (1978) and by Link (1983). The facies consist chiefly of (1) marine mudstone and turbidites of the Castaic Formation and the lower part of the Ridge Basin Group in the southeastern axial part of the basin, (2) alluvial fans of the Violin Breccia along the southwestern margin of the basin, (3) alluvial-fan, fan-delta, sublacustrine deltas, and fluvial deposits of the Ridge Route Formation along the northeastern margin of the basin, (4) shallow- and deep-lacustrine deposits of the Peace Valley Formation in the axial part of the basin, and (5) alluvial-fan and fluvial deposits of the Hungry Valley Formation (Figs. 6 and 7).

The Castaic Formation (Crowell, 1954b) and the lower part of the Ridge Route Formation consist dominantly of marine slope deposits and basin-axis turbidites (Link, 1982b). The Castaic Formation is more than 2,500 m thick in the southeastern end of Ridge Basin (Stitt, 1982). The unit rests unconformably on the Mint Canyon Formation and records a late Miocene marine transgression into the basin; foraminifers indicate initial shallow-marine conditions followed by moderately deep-marine conditions, and finally, shoaling of the environments accompanied by partly restricted circulation and the development of a silled basin (McDougall, 1982; Stanton, 1982). Water depths increased southeastward from less than 100 m in the northwest to as much as 1,500 m in the southeast (McDougall, 1982). The slope deposits consist chiefly of poorly bedded mudstone that contains large slide blocks, are slump-folded, and are cut by channels or small canyons filled with sandstone, conglomerate, and coquina; the basin-axis turbidites consist of channel, interchannel, and depositional-lobe deposits (Link, 1982d; Stitt, 1982).

The Violin Breccia accumulated as talus and steep alluvial cones adjacent to the San Gabriel fault (Crowell, 1982b). The breccia crops out for a distance of 34 km adjacent to the fault but extends northeastward toward the center of the basin for a distance of only 1.5 km, where it pinches out into lacustrine shale and siltstone of the axial Peace Valley Formation or sandstone members of the Ridge Route Formation (Fig. 8B). The Violin Breccia is as thick as 11,000 m and its lower part is marine. The proximal part of the Violin Breccia consists of unbedded massive rubble that contains blocks as large as 2 m long (Fig. 8C). To the northeast, it gradually fines, becomes better stratified, contains more interbedded mudstone, and its clasts are better rounded. The reverse grading at the base of many of the coarse-grained beds suggests deposition by subaerial and subaqueous debris flows (Fig. 8D). A landslide block about a kilometer in length is interbedded in the breccia at one location. The Violin Breccia is organized into very distinctive coarsening- and thickening-upward sequences. The conglomerate contains mostly clasts of gneiss and granite derived from the Alamo and Frazier Mountain areas, which are currently located along the northwestern margin of the Ridge Basin.

The basin-axis Peace Valley Formation consists chiefly of fine-grained lacustrine deposits that vary considerably in character because of fluctuations in lake level and transport of coarse-grained sediments into the lake along its margins (Smith, 1982a). The marginal lacustrine facies include shoreline, nearshore sandflat and mudflat, offshore bar, and fluvio-deltaic deposits, and the offshore lacustrine facies include turbidite and mudrock-carbonate deposits (Fig. 8E; Link and Osborne, 1978). Fossils from the Peace Valley Formation include molluscs (Young, 1982), ostracodes (Forester and Brouwers, 1982), algal stromatolites (Link et al., 1978), insects (Squires, 1979), and various invertebrate fossils that include freshwater fishes and bones of horses, turtles, camels, mastodons, ground sloths, and rhinoceroses (see summary in Welton and Link, 1982). Abundant plant fossils (Axelrod, 1982) and trace fossils (Smith et al., 1982) are present in both the Peace Valley Formation and intertongued coarser deposits of adjacent members of the Ridge Basin Group. Analcime, dolomite, and locally gypsum that are present within the Posey Canyon Shale Member and Alamos Canyon Siltstone Member of the Peace Valley Formation probably indicate brackish and alkaline conditions (Fig. 8F; Irvine, 1977; Smith, 1982b).

The Ridge Route Formation consists of more than 9,000 m of alluvial-fan, fluvial, and lacustrine shoreline deposits shed into the basin from source areas located on the northeast flank of Ridge Basin (Link, 1982e). The alluvial-fan deposits accumulated as conglomerate, breccia, and sandstone chiefly adjacent to basement that was uplifted along the Clearwater and Liebre fault zones (Fig. 7). The fan deposits grade basinward into fluvial deposits of meandering and braided types, which consist chiefly of cross-stratified conglomeratic sandstone and mudstone (Fig. 8G; Link, 1984). The shoreline deposits include nearshore, beach, delta, and fan-delta sequences that interfinger with the lacustrine beds of the Peace Valley Formation. A number of the prominent sandstone members of the Ridge Route Formation extend entirely across Ridge Basin to interfinger with the Violin Breccia (Figs. 6 and 8H); these units grade laterally into sublacustrine deltaic and turbidite complexes that were at times exposed as a result of falling lake levels (Harper and Osborne, 1982; Hollywood and Osborne, 1982; Link, 1982f; Wood and Osborne, 1982).

The youngest part of the Ridge Basin Group, the Hungry Valley Formation, is about 1,400 m thick and consists chiefly of a lower member deposited by braided streams and an upper member deposited as alluvial-fan deposits (Crowell, 1982c; Ramirez, 1983). The alluvial-fan deposits overlap the Liebre and San Gabriel fault zones, but are truncated by the San Andreas fault (Crowell, 1982c). The sedimentary rocks of the Hungry Valley Formation record final filling of Ridge Basin, and derivation of detritus from the Frazier Mountain area and various sources northeast of the San Andreas fault. Ramirez (1983) suggests that part of the San Bernardino Mountains, now located 220 km to the southeast of and across the San Andreas fault from Ridge Basin, formed the source area of much of the Hungry Valley Formation.

*Paleocurrents and Maximum Clast Size*

Paleocurrent measurements from the various stratigraphic units of the Ridge Basin Group indicate that (1) the Violin Breccia was derived from the southwestern margin of the basin across the San Gabriel fault, (2) the Ridge Route Formation was derived from the northeastern flank of the basin, with some units clearly shed off uplifts along the Clearwater and Liebre fault zones, (3) the axial deposits of the basin, which include parts of the Violin Breccia, Ridge Route Formation, and Peace Valley Formation, were generally transported southeastward down the axis of the basin, and (4) the younger Hungry Valley Formation was derived from the north, northwest, and west (Fig. 6; Link, 1982d). Paleowind directions were generally along the basin axis but toward the north-northwest (Link, 1982d).

The largest clasts in the Ridge Basin are found in the Violin Breccia adjacent to the San Gabriel fault margin. Angular blocks of basement rocks as large as several meters are found locally in the Violin Breccia, and the maximum sizes of the blocks generally increases toward the fault. Conglomerate along the northeastern margin of the basin contains generally more rounded fragments, although it is locally very coarse, including sedimentary breccia adjacent to the Clearwater and Liebre fault zones, and it generally increases in coarseness toward the northeastern basin margin. In the northwestern part of the basin and upper part of the Ridge Basin Group, conglomerate of the Hungry Valley Formation generally coarsens toward the northern basin margin.

*Tectonic and Depositional History*

The Ridge Basin developed as a stretched and sagged crustal wedge northeast of the San Gabriel fault in the area where the fault had a curvilinear trace (Crowell, 1982a). The San Gabriel fault was the principal zone of right slip during most of the history of the basin, and its curved trace led to uplift of a source area along the southwestern margin of the basin that migrated northwestward through time, shedding detritus that formed the Violin Breccia into the basin (Figs. 9, 10A; Crowell, 1974a, b; 1975; 1982b). The Clearwater and Liebre fault zones became active as the basin widened and grew, and most of the basin fill was transported into the basin by rivers draining source areas located to the northeast. The basin depocenter migrated northwestward through time as the source of the Violin Breccia moved northward along the southwest side of the San Gabriel fault (Fig. 10B); as a result, the successive alluvial fans that form the Violin Breccia become younger northwestward and form a shingled pattern that coincides with the northwestward migration of the depocenter. Within the axial part of the wedge-shaped basin, sediments were transported southeastward down the axis of the basin concurrently with northwestward migration of the depocenter. Abundant evidence of syn-sedimentary deformation in the basin fill suggests possible penecontemporaneous seismicity (Fig. 8I, J). When the principal locus of right slip transferred to the San Andreas fault, the other basin-margin faults became inactive, the basin was folded, uplifted, and transported northward about 220–240 km.

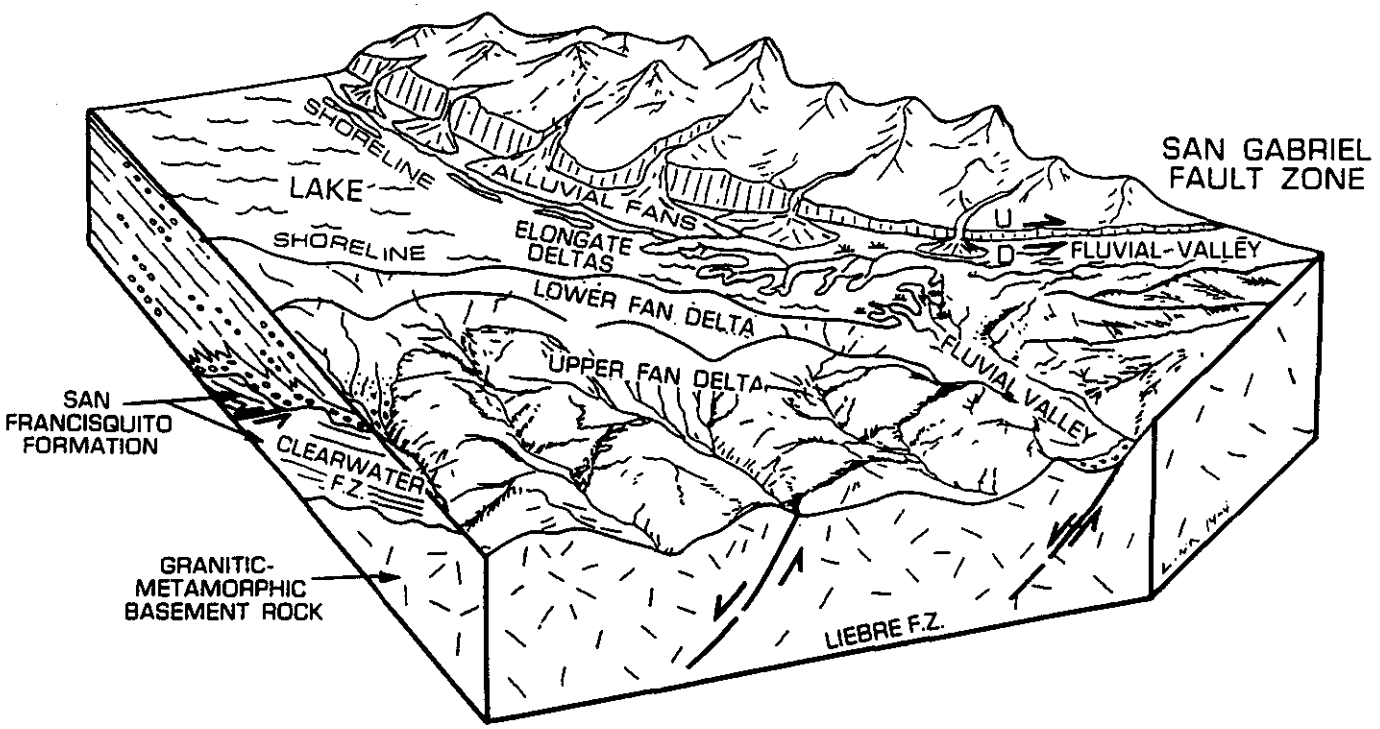



FIG. 9.—Depositional model for Ridge Basin (from Link, 1984, Fig. 13).

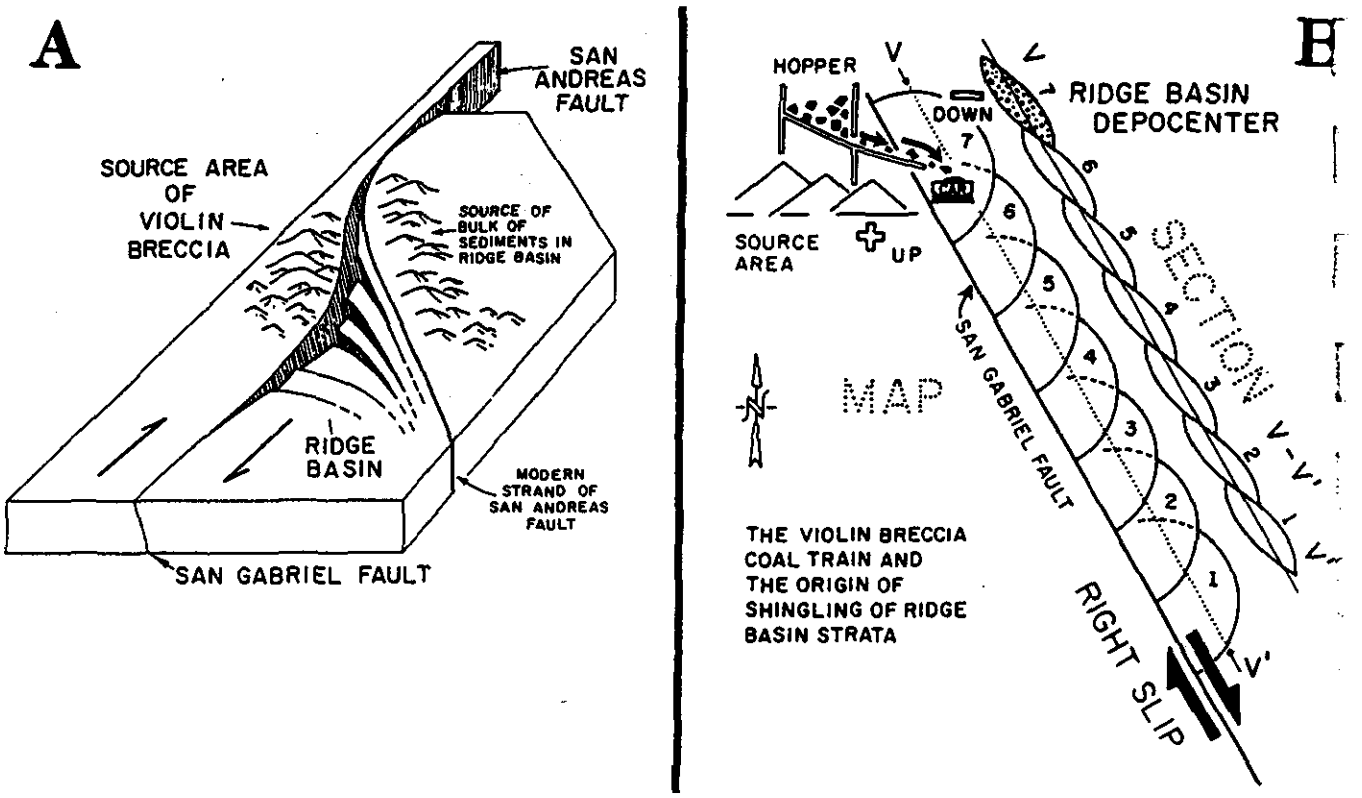



FIG. 10.—Tectonic and depositional models for origin and filling of Ridge Basin. A) block diagram showing origin of Ridge Basin east of the San Gabriel fault (from Crowell, 1974b, Fig. 5). B) model of Ridge Basin infilling and depocenter migration (from Crowell, 1982b, Fig. 9).

## LITTLE SULPHUR CREEK BASINS

### *Setting*

The Little Sulphur Creek Basins, which developed along the Maacama fault zone, form part of a large number of Neogene nonmarine sedimentary basins in northern California (Fig. 1C). The California Coast Ranges north of San Francisco are characterized by a wide zone of right-lateral shear associated with the San Andreas fault system (McLaughlin, 1978, 1981). In addition to the San Andreas fault itself, the Healdsburg–Rogers Creek, Maacama, Green Valley, and Bartlett Springs fault zones accommodate major amounts of right slip. As a result of oblique pull-apart extension between branching splays of these faults, sedimentary basins or depressions developed in the Pliocene and Pleistocene that include the Ukiah Valley, Little Lake Valley, Round Valley, Clear Lake Basin, and the three Little Sulphur Creek Basins.

The Little Sulphur Creek Basins extend along the Maacama fault zone for about 13 km (Fig. 11; McLaughlin and Nilsen, 1980, 1982; Nilsen et al., 1980). They are bounded on the southwest by branching splays of the active right-lateral Maacama fault zone that strike N30°–40°W (Fig. 12A). Conjugate thrusts that strike west and northwest, and left-lateral fault splays that also strike northwest, intersect the main northwest-striking fault zone, separating the basin fill into three distinct 1.5-to-2.0-km-wide pull-apart basins (Fig. 11). The basins have a cumulative fill of about 5,000 m.

Recent seismicity (Bufe et al., 1981) and youthful physiographic fault features associated with the Maacama fault zone indicate that it is still active (Donnelly et al., 1976; Herd and Helley, 1977; Herd, 1978; Pampeyan et al., 198[illegible]). First-motion solutions for several earthquakes indicate right-slip with maximum extension parallel to vectors oriented approximately N60°W–S60°E (Bufe et al., 1981). On the basis of offset of the Sonoma Volcanics, and of an offset of similar magnitude of late Mesozoic ophiolitic rocks (McLaughlin, 1981), maximum displacement along the Maacama fault zone is considered to be approximately [illegible] km or less.

The Little Sulphur Creek Basins are surrounded by complexly deformed late Mesozoic rocks that consist of (1) melange on the southeast and west, with abundant blocks of chert and blueschist, belonging to the Franciscan assemblage; (2) an intact terrane of weakly metamorphosed graywacke on the northeast and northwest, also assigned to the Franciscan assemblage; and (3) an ophiolite terrane on the southeast composed of ultramafic rocks, gabbro, diabase, mafic breccia, and basalt (Fig. 11). Almost all the sedimentary fill in the Little Sulphur Creek Basins appears to be derived from these three late Mesozoic terranes.

The age of the fill of the Little Sulphur Creek Basins is poorly known. However, on the basis of a mollusc-bearing clast of sandstone, regional stratigraphic and structural relations, and a probable genetic relation between the age of basin formation and the northward propagation of the San Andreas transform system during the Neogene (Blake et al.

1978; Dickinson and Snyder, 1979), the basins probably began to develop between 3 and 4 Ma and have been filled and deformed since then.

### *Structure*

The fill of the Little Sulphur Creek Basins has been deformed by tilting, folding, and probably by rotation between the basin-margin faults (Fig. 11). Tilting, indicated by very steeply dipping beds, is most prominent along the southwest side of the southeasternmost basin. In that area, conglomerate and breccia have vertical dips and are truncated against a major active strand of the Maacama fault zone. The basin fill forms a series of stacked basin-wide sequences that form northwest-dipping ridges that have been folded into a broad syncline (Fig. 12B). Synclinal axes of the southeastern and central basins plunge to the northwest. The synclinal axis of the northwestern basin plunges both northwestward and southeastward. Prominent right-lateral drag folds are locally present along the fault zone; in addition to the drag folds, major synclinal folds in the basin fill have axes that trend N40°–69°W, oblique to the trend of the Maacama fault zone. Along the northeast margins of the basins, beds are only slightly tilted, without noticeable oversteepening or drag folding, suggesting lesser uplift and deformation along that margin.

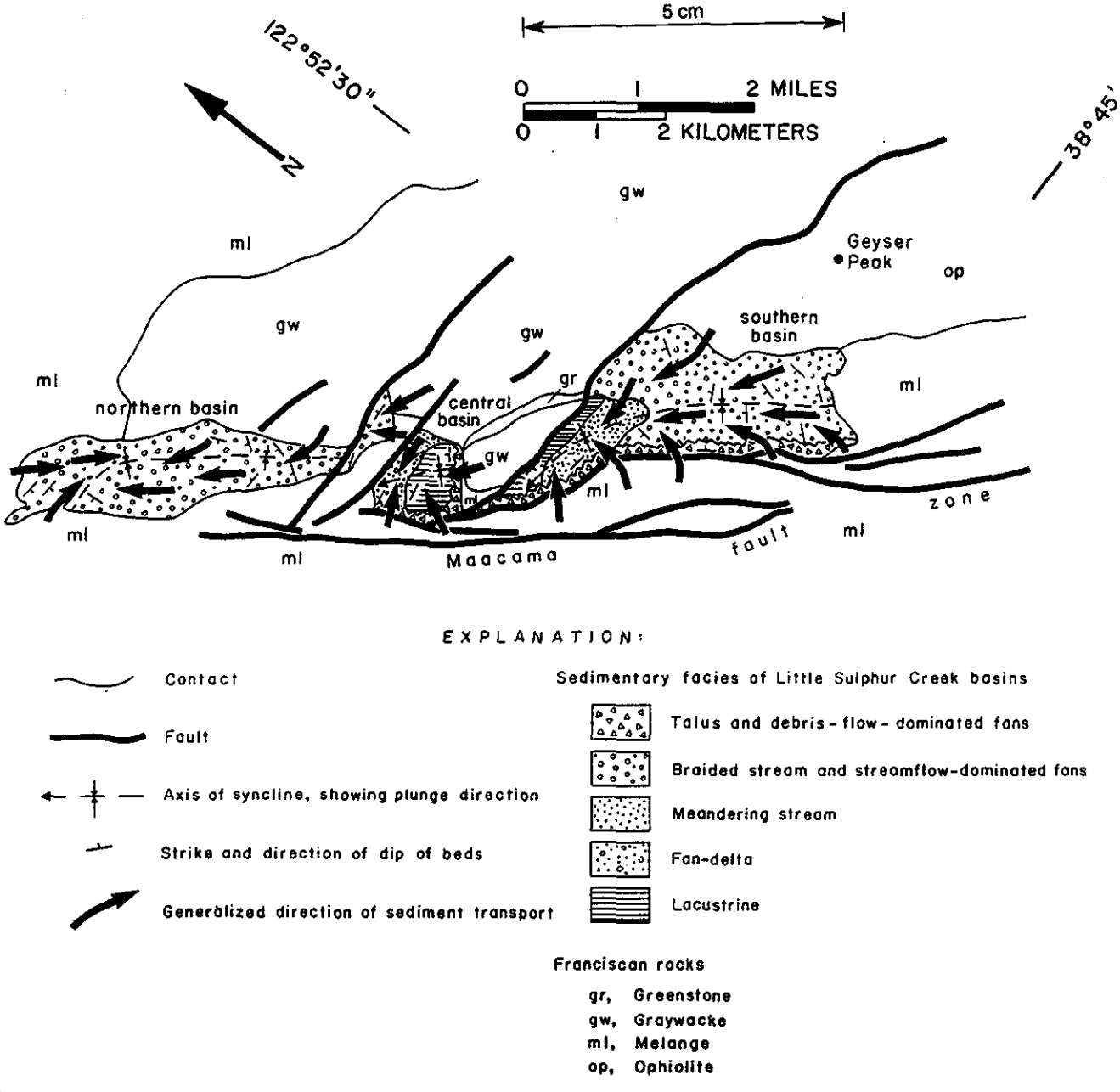
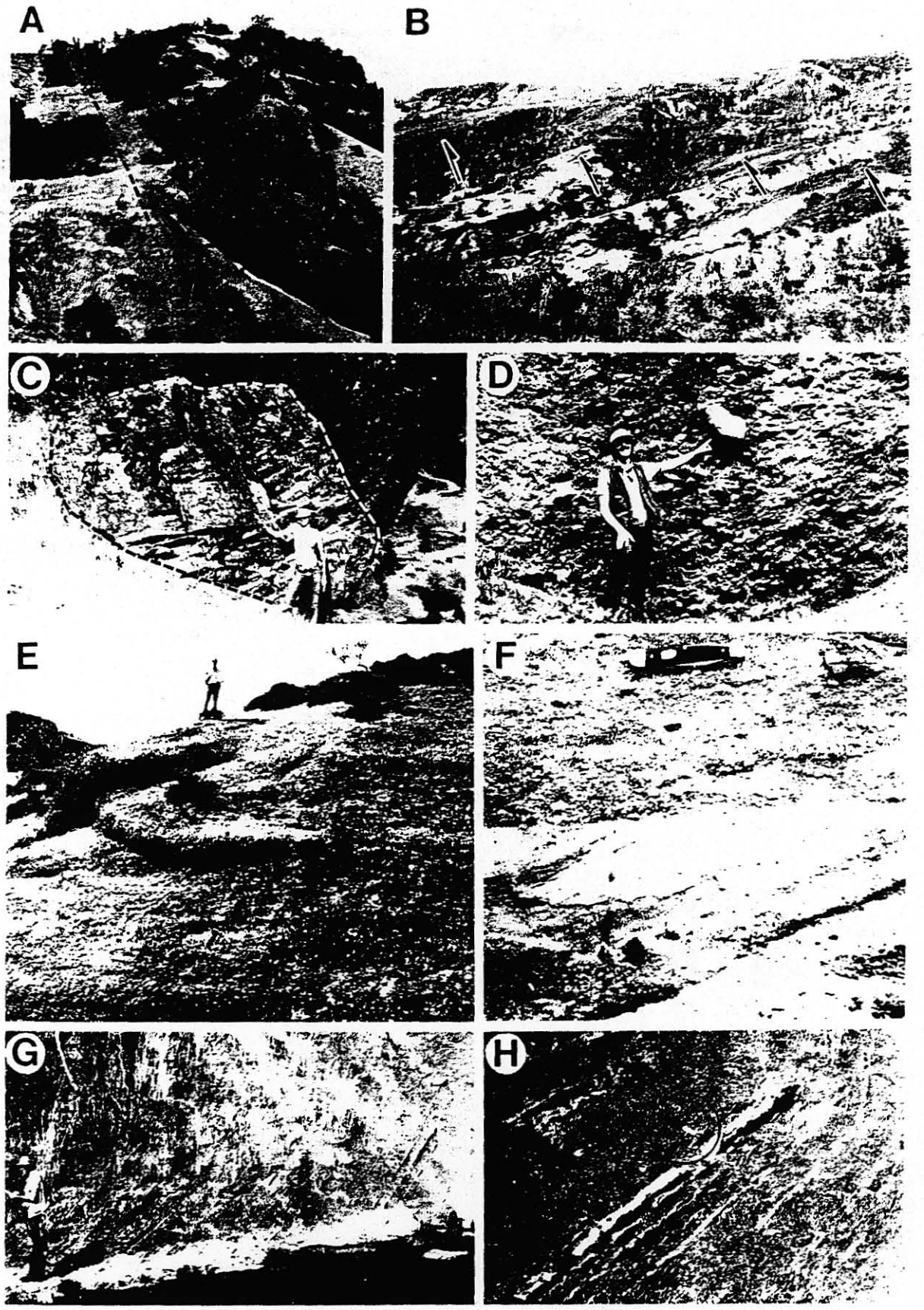



FIG. 11.—Generalized geologic map of the Little Sulphur Creek area, showing the three Little Sulphur Creek Basins, principal faults, distribution of surrounding rock types, depositional facies, and generalized directions of sediment transport. For location, see Figure 1C.

655218



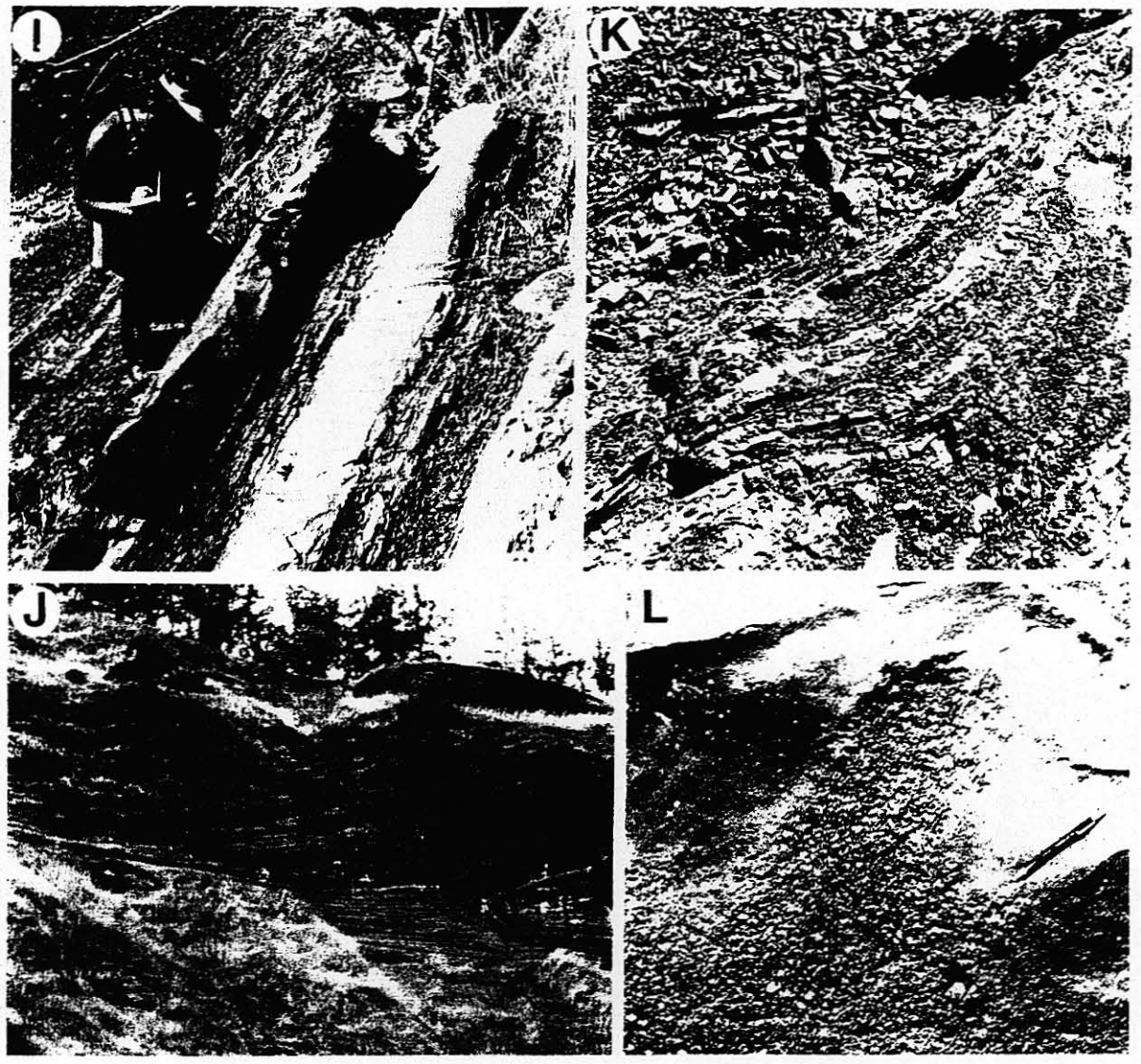



FIG. 12.—Photographs of Little Sulphur Basins and their chief depositional facies. A) view northwest along trace of Maacama fault zone (dashed line) showing outcrops of basin-margin conglomerate on ridge crest to right. B) view northeastward toward the axis of the basin showing stacked sequences (arrows) in the central part of the basins. C) large angular block of chert in talus and debris-flow-dominated alluvial-fan deposits along southwestern margin of the basin. D) poorly sorted debris-flow-dominated alluvial-fan deposits along southwestern margin of basin. E) well-stratified conglomerate and sandstone deposited by streamflow-dominated alluvial fans and braided streams. F) cross-stratified sandstone and interbedded conglomerate deposited by braided streams. G) thin-bedded basin-axis lacustrine deposits. H) basin-axis lacustrine turbidites; hammer circled for scale. I) fining- and thinning-upward sequence probably deposited by meandering stream in axial part of basin. J) conglomeratic fan-delta deposits that prograded southwestward (to left) over mollusc-bearing lacustrine mudstone and siltstone. K) syn-sedimentary slump in lacustrine-margin deposits. L) mass of conglomerate injected upward about 35 cm into pebbly siltstone.

### *Depositional Facies*

The distribution of nonmarine facies in the three Little Sulphur Creek Basins is complex and probably reflects an irregular paleogeography (Fig. 11). Conglomeratic braided-stream deposits dominate the sedimentary fill of the southern and northern basins. Other important deposits include fault-scarp talus and debris-flow breccia, meandering-stream, conglomeratic fan-delta, and lacustrine deposits (Fig. 13). Representative measured sections for each depositional facies were shown by McLaughlin and Nilsen (1982, Fig. 5).

The talus deposits include some conglomeratic debris-flows and landslides. Talus deposits are most prominent along the southwestern margin of the southern basin adjacent to the Maacama fault, where angular blocks of chert and blueschist as long as several meters are enclosed in coarse, unsorted and angular breccia (Fig. 12C). Abundant debris-flow conglomerate (Fig. 12D) intertongues with the extremely coarse talus deposits, and both grade laterally northeastward into braided-stream deposits. Debris-flow conglomerate is also common along most basin margins, where it interfingers toward the basin axes with braided-stream deposits.

The braided-stream deposits consist chiefly of fining-up-

655220

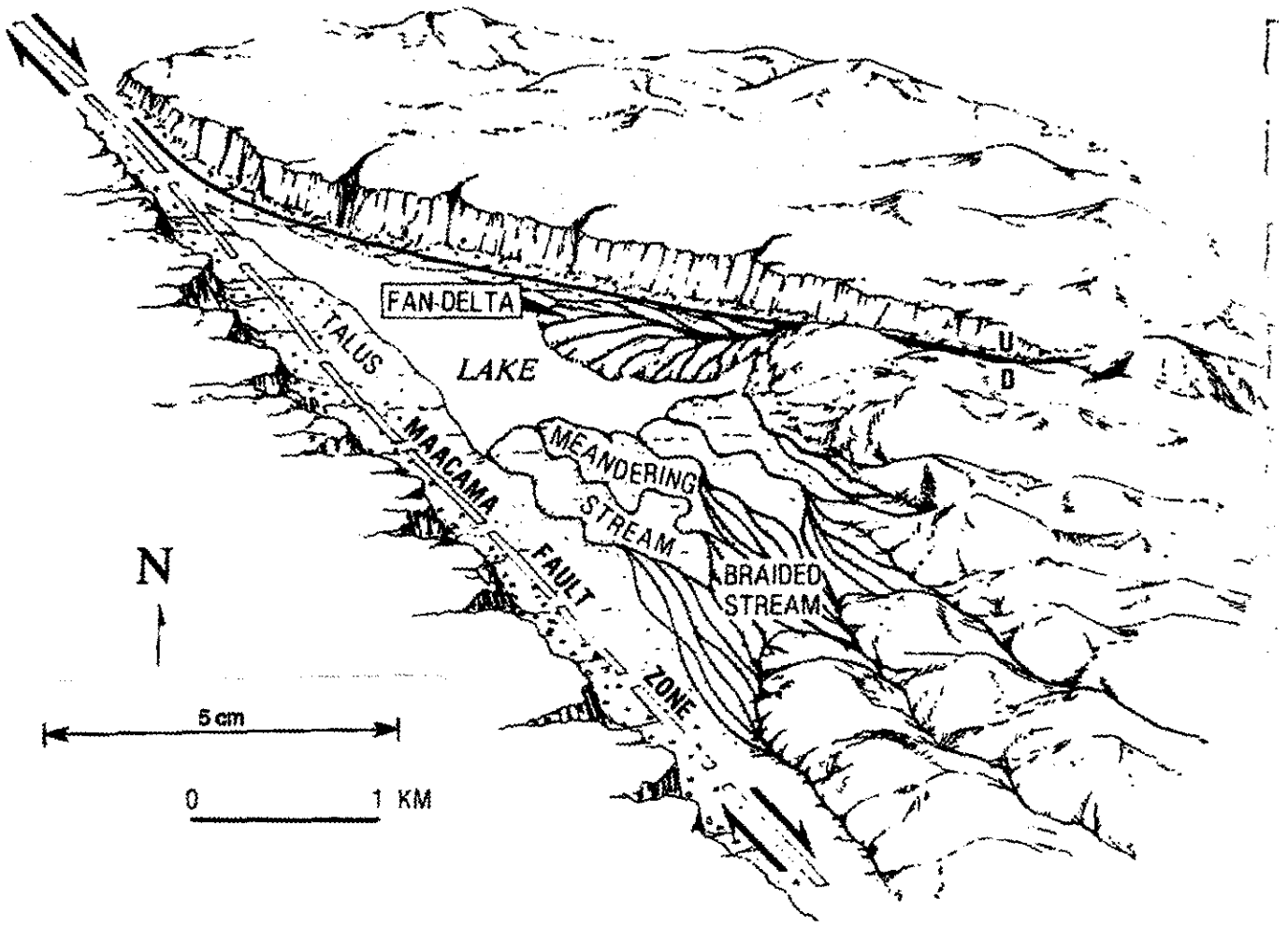



FIG. 13.—Depositional and tectonic model for the Little Sulphur Creek Basins showing the distribution of chief depositional facies (from McLaughlin and Nilsen, 1982, Fig. 9).

ward couplets of conglomerate and sandstone (Fig. 12E, F). Shale and mudstone are generally absent. Each of the conglomerate and sandstone couplets, which range from about 0.5 m to as much as 5 m in thickness, is thought to represent a gravel bar or flood unit developed in a braided-stream channel. The base of each couplet is channeled into underlying conglomerate, conglomeratic sandstone, or sandstone. Typically, the conglomerate is massive or crudely parallel-stratified, and the overlying sandstone is massive, parallel-stratified, or low-angle cross-stratified. The conglomerate has well-developed imbrication and long-axis orientation, which is characteristic of streamflow deposits.

Lacustrine deposits of both deep and shallow origin crop out at the northwest end of the southern basin and in the central basin (Fig. 12G, H). Shoreline deposits contain mud cracks and other features indicative of periodic desiccation. The deeper-water lacustrine deposits consist of thin-bedded turbidite sandstone and siltstone that alternate with variegated mudstone and claystone.

The meandering-stream deposits are abundant in the northwestern part of the southern basin (Fig. 12I). They consist of fining-upward sequences that are about 5 to 10 m thick. The fining-upward sequences consist, in ascending order, of a basal channeled conglomerate or sandstone that is massive or crudely parallel-stratified, trough cross-stratified sandstone, ripple-laminated sandstone and siltstone, and mudstone. The locally thick mudstone units that are floodplain deposits contain abundant disseminated tubular structures and nodules of calcium carbonate inferred to be of paleosol origin, thin seams of coal, and abundant plant debris. Some of these sequences may also be representative of braided streams, with extensive floodplain shale intervals.

The conglomeratic fan-delta deposits of the central basin contain conglomeratic beds that grade laterally through a zone of foresets with amplitudes locally greater than 10 m into thinly interbedded sandstone and mudstone (Fig. 12J). The fan-delta deposits prograde basinward into fossiliferous lacustrine strata. The well-defined topset, foreset, and bottomset beds of the fan delta resemble those of classical Gilbert-type deltas.

### *Paleocurrents and Maximum Clast Size*

Based on a total of 121 paleocurrent measurements of clast imbrication and long-axis orientation, cross-stratification, and flute and groove casts, McLaughlin and Nilsen

(1982, Fig. 7) demonstrated a pattern of basin infilling from the basin margins and longitudinal transport along the basin axes, toward the northwest and southeast (Fig. 11). The paleocurrent pattern suggests the presence of source areas on most margins of the basin. The predominant transport in the southern and central basins was toward the northwest along the basin axes in the direction of plunge of the basin synclines; in the northern basin it was toward the northwest and southeast, parallel to the basin axis.

Based on many measurements of maximum clast size in the basins, McLaughlin and Nilsen (1982, Fig. 6) determined that the largest clasts are located along the southwestern flank of the southernmost basin adjacent to the active Maacama fault zone. Here large angular clasts several meters long are embedded in generally finer-grained, angular conglomerate. These large clasts appear to represent blocks that slid or slumped into the basin along either a syndepositionally active fault zone or an uplifted block of basement rocks along the basin margin.

Cobble-sized debris that is generally well-rounded is common in many other parts of the basins, and forms a chief component of braided- and meandering-stream, fan-delta, and alluvial-fan deposits. Based on the overall pattern of paleocurrents, maximum clast sizes, depositional facies, and clast composition, it is clear that the chief source area of the basin fill was located to the southeast (Fig. 11).

### *Tectonic and Depositional History*

The depositional facies of the Little Sulphur Creek Basins and their relation to basin-margin faults strongly imply that deposition took place concurrently with uplift and with oblique slip along the Maacama fault zone (Fig. 14). The buttressing of the megabreccias against a major strand of the Maacama fault zone on the southwest side of the southern basin, and the sheared surfaces of numerous clasts in the megabreccias, suggests deposition as fault-scarp talus. Abundant syn-sedimentary slumps, dewatering structures, liquefaction features, and minor angular unconformities in finer-grained sediments, together with the megabreccias and structural setting, strongly suggest that basin-margin faults were seismically active during sedimentation, when much of the sedimentary fill was water-saturated (Fig. 12K, L).

Although very coarse sedimentary breccia was transported into the southern basin from the southwestern margin as talus cones, landslides, and debris flows, most detritus was transported into Little Sulphur Creek basins from the southeast, where braided-stream and debris-flow deposits form a proximal facies. The braided-stream deposits grade distally into meandering-stream deposits. Here, more extensive floodplains developed, and sand and silt were transported into a deep lake extending from the northwest end of the southern basin into the central basin. Turbidity currents were generated where the meandering streams entered into the lake when lake levels and/or stream discharge were high.

From the northeast margin of the central basin, a coarse-grained fan-delta prograded out into the lake, triggering turbidity currents along its front. The source of detritus for the fan-delta may have lain to the southeast, from which sediment was transported along the trend of a secondary west-trending fault that probably connected to the Maacama fault. Abundant macrofossils in bottomset beds indicate the presence of good faunal habitats within the lake. The lake probably emptied toward the northwest, and varied greatly in size and depth, responding to changing tectonic, climatic, and outlet conditions.

The basins appear to have formed initially by east-west oblique pull-apart between en echelon and branching splays of the Maacama fault zone that strike N30°–40°W (Fig. 14). Subsequently, the basin fill was deformed by tilting against basin-margin faults, with the greatest uplift along the southwest side of the basins. Continued uplift and right-lateral shear formed synclinal folds whose axes trend N40°–60°W (Fig. 14), approximately parallel with the direction of maximum extension.

## TECTONIC AND SEDIMENTOLOGIC COMPARISON

It is clear from our review of the tectonic and depositional framework of the Hornelen, Ridge, and Little Sulphur Creek Basins that, despite important differences in age, size, thickness of basin fill, and regional setting, the three basins are remarkably similar. In Figure 15, the basins are shown at roughly the same size and orientation to emphasize many of these similarities; the major controlling strike-slip fault is positioned along the left margin of each basin so that the style of infilling, distribution of depositional facies, and tectonic framework can be understood and compared.

Each basin is elongate parallel to the orientation of the major controlling strike-slip fault, and talus, landslide, and debris-flow-dominated alluvial fans were deposited along that margin of the basin. Each of the bounding strike-slip faults is dextral; although the amount of offset along the Hornelen margin is unknown, the San Gabriel and Maacama faults have known offsets of more than 60 km and about 20 km, respectively. In each basin, the major controlling strike-slip fault is throughgoing and forms a continuous bounding margin to the basin, although in the later history of Ridge Basin, the San Gabriel fault was unconformably overlapped by the Hungry Valley Formation as active strike-slip faulting shifted to the San Andreas fault. Because of the active strike slip, source areas along this margin migrated through time, resulting in a similar migration of the depocenter in the same direction.

The basins probably became longer and wider through time. Progressive basin-widening faulting along the margins of the basins opposite to the major strike-slip fault, either along high-angle reverse faults, oblique-slip faults, or normal faults, eventually yielded length-to-width ratios of between 3:1 and 5:1. This widening and lengthening process can be most clearly demonstrated in Ridge Basin, where the growth, cessation of movement, and eventual overlap of the Clearwater and Liebre faults can be documented in the field. In Ridge and Hornelen Basins, the migration of the depocenters in a direction parallel to the basin is also clearly demonstrable.

Each basin was subsequently folded into a broad, gently plunging syncline, although numerous subsidiary folds have been mapped, especially in Ridge Basin. The synclines generally plunge in the same direction that the depocenters

655222

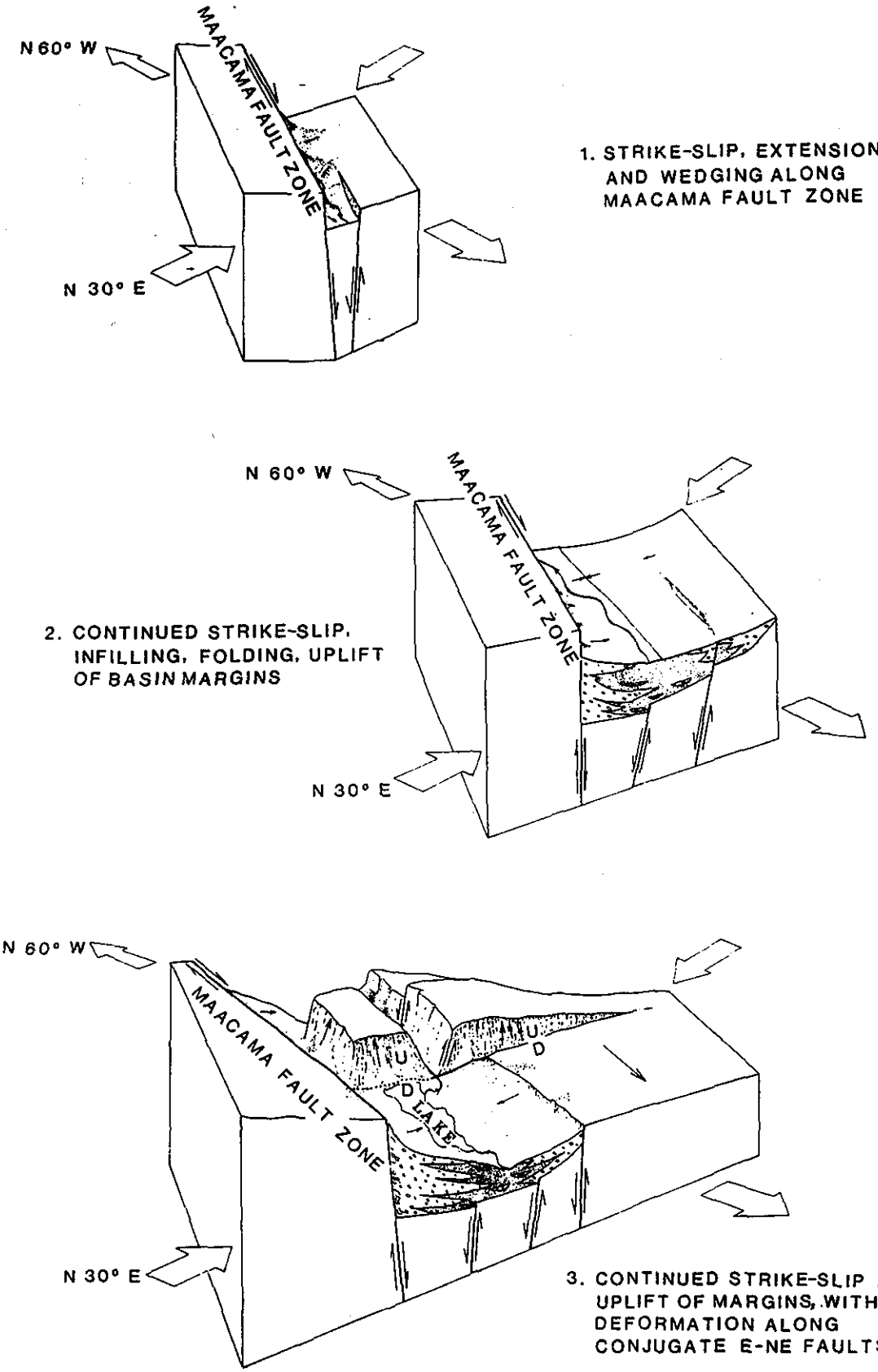



FIG. 14.—*Tectonic and sedimentary evolution of Little Sulphur Creek Basins within the framework of active strike-slip movement along the* Maacama fault (from McLaughlin and Nilsen, 1982, Fig. 8).

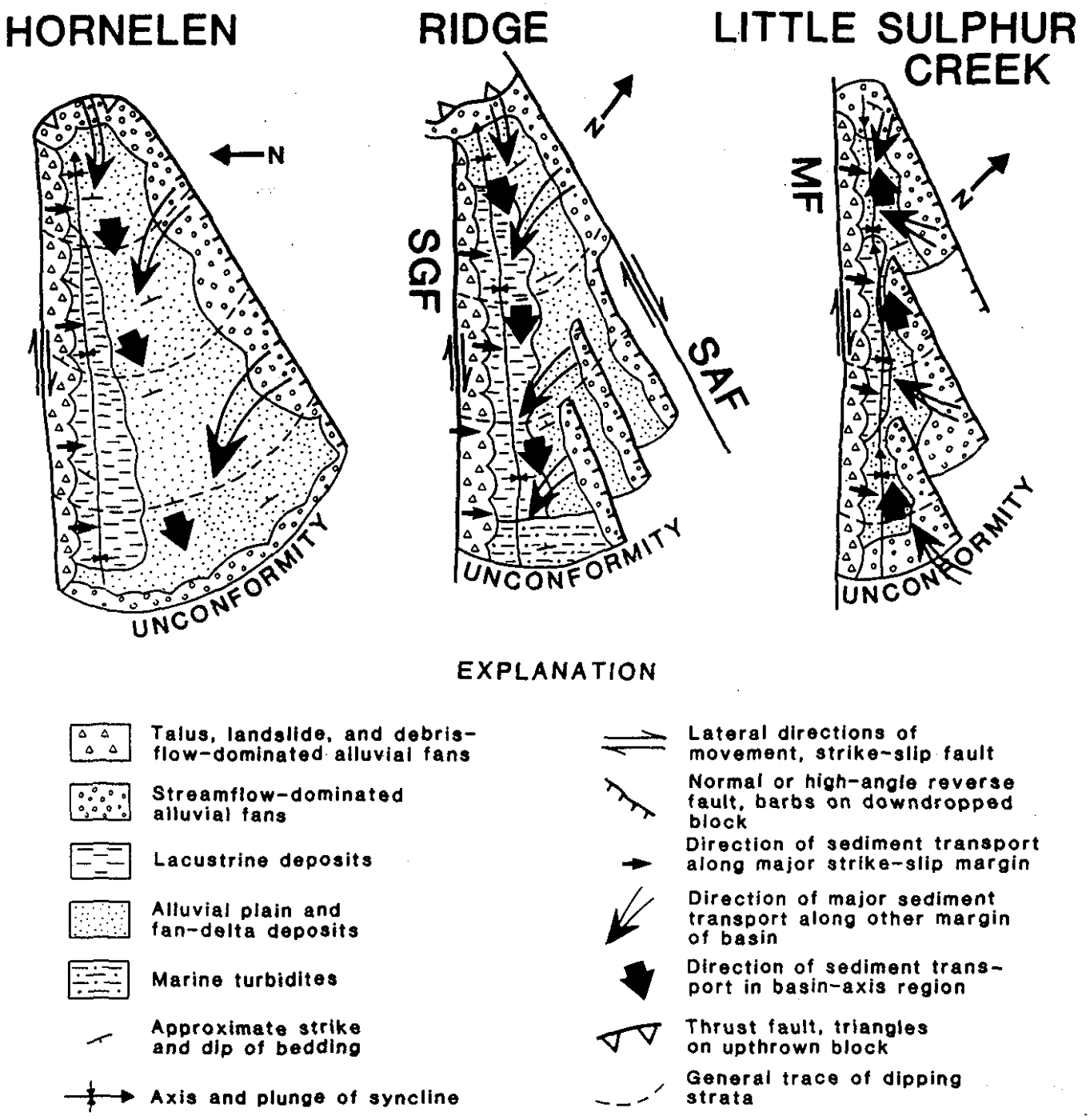



FIG. 15.—Tectonic and sedimentary comparison of Hornelen, Ridge, and Little Sulphur Creek Basins. Note that the scales are variable and that the three basins, of varying size, are drawn at roughly the same size for purposes of comparison. The basins have also been reoriented (see respective north arrows) to facilitate the comparison. Abbreviations: MF, Maacama fault; SAF, San Andreas fault; SGF, San Gabriel fault.

migrated, although the structural termination of each basin in the direction of plunge is different. Differently oriented thrust faults terminate the eastern and northwestern margins of Hornelen and Ridge Basins, respectively, and at the northwestern margin of the Little Sulphur Creek Basins, the plunge of the synclinal axis apparently reverses. The opposite end of the basins in each case is marked by a major unconformity.

The debris-flow-dominated alluvial-fan deposits adjacent to the major strike-slip-faulted margin form a narrow strip of coarser-grained deposits that extend generally less than 2 km into the basin-axis region. These alluvial fans were apparently small and steep, and in many areas shed debris directly into lakes of various depths. Subaerial debris-flow deposits can be traced laterally into sublacustrine debris-flow deposits.

655224

The distribution of the lacustrine facies in each basin shifted toward the active strike-slip basin margin, suggesting that the basin floors were tilted toward that margin. This tilting or slope of the basin floor explains the formation of larger streamflow-dominated alluvial fans along the opposite basin margin. These streamflow-dominated fans transported better sorted, better rounded, and generally finer-grained detritus that was deposited on larger and more gently sloping fans. The fans graded laterally into alluvial-plain and fan-delta deposits that were transported into the lakes. Most sediment was introduced into each basin from this opposite margin, and some coarse-grained units extend all the way across the basins to interfinger with the debris-flow-dominated alluvial-fan deposits.

Basin-axis sediment transport is markedly opposite to the direction of depocenter migration in Hornelen and Ridge Basins but generally in the same direction as the depocenter migration in the Little Sulphur Creek Basins, except at their northwestern end, where the paleocurrent directions appear to reverse. It is possible that major uplifts to the south related to volcanic activity yielded a northwesterly plunge of the basin floor of the Little Sulphur Creek Basins.

Sedimentation in each of the basins was rapid, as is typical for many basins generated along strike-slip faults. We calculate average sedimentation rates of 2.5 m/1,000 yr for Hornelen Basin, 3 m/1,000 yr for Ridge Basin, and 2.5 m/1,000 yr for the Little Sulphur Creek Basins, making conservative assumptions about the duration of basin filling from published time scales (Palmer, 1983). These sedimentation rates are very high and reflect active syn-depositional tectonism, basin development, uplift of surrounding source areas, subsidence of the basin floor, and lateral migration of basin depocenters. The history of each basin appears to be similar, including (1) rapid basin development adjacent to a major strike-slip fault during a phase of transtension, (2) basin lengthening and widening during continued active strike-slip faulting, and (3) rapid closure, folding and uplift of the basin fill during a phase of transpression. This last phase can be associated with shifting of strike-slip activity to another fault, as is the case with Ridge Basin, or to other complex changes in the style of strike-slip activity.

## SUMMARY AND CONCLUSIONS

Marine sedimentary basins that have developed along strike-slip faults have been of great interest because of the large amounts of petroleum resources found in them (Moody, 1973; Harding, 1974, 1976). For example, many of the Tertiary basins in California associated with the San Andreas fault system, such as the Los Angeles and Ventura Basins, have been extremely productive (Blake et al., 1978; Howell et al., 1980). The Ridge Basin in southern California, although petroleum has not been produced from it, has been extensively explored, because the fine-grained lacustrine facies has a very high content of total organic matter (Link and Smith, 1982) and the basal part of its fill consists of marine deposits.

In this paper we have compared two other well-studied basins with Ridge Basin in an attempt to gain a better understanding of the nature and organization of the sedimentary infilling of basins that develop adjacent to strike-s faults. Our comparison has yielded a surprisingly simi sedimentary and tectonic history in each case. We feel tha the following list of similar characteristics of the basins collectively significant for recognizing these basins as be of strike-slip origin and may have relevance for the gene recognition of basins developed adjacent to strike-slip faults. Not all of the criteria, of course, are applicable only to stri slip basins; many are also applicable to simple extensio rift basins as well.

(1) The basins were formed adjacent to important co tinental-margin or intracontinental strike-slip faults.

(2) Although the basins are fault-bounded along more than one margin, a major strike-slip fault forms the most prominent basin margin.

(3) The basins are elongate parallel to the major co trolling strike-slip fault.

(4) The basins are synclinal in overall structure.

(5) The basins were initially formed by extension a subsequently compressed and folded, probably as a resu of transtension followed by transpression.

(6) The basins are asymmetrical, with their structura deepest parts close to and subparallel to the major syn-c positionally active strike-slip margin.

(7) The basins do not contain any record of syn-dep sitional volcanism or plutonism. Volcanism may, howev be common in some other similar basins.

(8) The basins, although small, are characterized by a wide variety of depositional facies, including talus, lar slide, alluvial-fan, braided and meandering fluvial, delta fan-delta, shoreline, shallow and deep lacustrine, turbidit chemical precipitate, and algal limestone deposits.

(9) The basin fill is characterized dominantly by ax infilling, subparallel to the major strike-slip basin marg

(10) The basin-margin deposits are distinctive. Along the syn-depositionally active strike-slip margin, small debris-flow-dominated alluvial fans that contain coarse sedime tary breccia and conglomerate were deposited. Along t inactive or less active margins, larger streamflow-domi nated alluvial-fan and fluvial deposits that contain fin grained conglomerate and little breccia were deposited.

(11) The basin fill is characterized by abrupt facies changes.

(12) The basin fill was derived from multiple basin-m gin sources that changed through time as a result of c tinued lateral movement along the basin-margin faults.

(13) The basin fill has a varied and complex petrograph as a result of the multiple sources that change through ti and space.

(14) The basins contain very thick sedimentary section compared to their area.

(15) The basin fill is characterized by high rates of se mentation, roughly 2.5–3.0 m/1,000 yrs.

(16) The basins are characterized by depocenters tha migrated in the same direction as that of the source terr opposite the major strike-slip margin of the basin; this m gration direction is generally opposite to that of the genera flow of axial paleocurrents.

655225



(17) The basin fill is characterized by abundant syn-sedimentary slumping and deformation, possibly in response to seismicity along the basin margins.

These criteria may define some of the chief characteristics of certain types of basins that develop adjacent to strike-slip faults. The criteria are clearly developed for nonmarine basins and most of the aspects of the sedimentary facies will not be applicable to shallow- and deep-marine basins such as those of offshore New Zealand described in Ballance and Reading (1980), the Southern California Borderland (Moore, 1969), and the Caribbean region (Schubert, 1982).

Basins along strike-slip faults can originate in a number of different ways, and the depositional and tectonic styles of these basins vary accordingly. For example, basins can develop as a result of extension adjacent to regions of fault curvature, as suggested by Crowell (1974) for the Ridge Basin. Basins can also develop in areas where strike-slip faults bifurcate and diverge, producing alternating uplifted and downdropped blocks, and in areas where strike-slip faults are oriented in en echelon fashion (Quennell, 1958; Rodgers, 1980). Aydin and Nur (1982) concluded from an analysis of many pull-apart basins in the world that the basin width is controlled by the initial fault geometry and that the basin length is a function of increasing fault displacements.

Nevertheless, there appear to be a number of additional modern and ancient pull-apart basins associated with strike-slip faults, which have characteristics similar to the three basins described herein. Late Cenozoic basins in Venezuela along the Bocono fault zone appear to be almost identical (Schubert, 1980). A number of basins in the San Francisco Bay region of California have been filled in an analogous way (Aydin and Page, 1984). The Lake Hazar and other basins in eastern Turkey, along the East Anatolian fault, are currently being filled in a very similar manner (Hempton et al., 1983; Hempton and Dunne, 1984). Thus, the general style of basin tectonism and sedimentation in the three basins that we have compared is probably applicable to many other basins. In particular, the general cycle for strike-slip basins postulated by Reading (1980) of (1) transtension to form the basin, (2) basin filling, and (3) transpression to fold and uplift the basin fill, is directly applicable to the basins we have considered herein.

## ACKNOWLEDGMENTS

Nilsen acknowledges the following individuals for helpful field excursions: Inge Bryhni through the Hornelen Basin in 1964; Ron Steel through the Hornelen Basin in 1982; and John Crowell and Martin Link through the Ridge Basin on several occasions between 1973 and 1983. For our work in the Little Sulphur Creek Basins, we thank Henry Ohlin for assistance in field work at various times, E. A. Griffin for compilation of data, and G. G. Zuffa for help in measurement of sections and studies of sandstone petrography. We thank the many ranchers and property owners along Little Sulphur Creek for permitting us to work on their land. We also thank R. J. Steel, J. A. Bartow, R. H. Brady, M. H. Link, E. J. Helley, Harvey Kelsey and several other colleagues at the U.S. Geological Survey for helpful discussions of the Little Sulphur Creek Basins in the field. Finally, we thank J. A. Bartow, P. F. Ballance, Hugh McLean, R. J. Steel, and the editors of this volume for constructive reviews of this paper and Mary Milan for her patient and skillful typing.

## REFERENCES

AXELROD, D. I., 1982, Vegetation and climate during middle Ridge Basin deposition, *in* Crowell, J. C., and Link, M. H., eds., Geologic History of Ridge Basin, Southern California: Society of Economic Paleontologists and Mineralogists, Pacific Section, p. 247–252.

AYDIN, ATILLA, AND NUR, AMOS, 1982, Evolution of pull-apart basins and their scale independence: Tectonics, v. 1, p. 91–105.

AYDIN, ATILLA, AND PAGE, B. M., 1984, Diverse Pliocene-Quaternary tectonics in a transform environment, San Francisco Bay Region, California: Geological Society of America Bulletin, v. 95, p. 1303–1317.

BALLANCE, P. F., AND READING, H. G., eds., 1980, Sedimentation in oblique-slip mobile zones: International Association of Sedimentologists Special Publication No. 4, 265 p.

BLAKE, M. C., JR., CAMPBELL, R. H., DIBBLEE, T. W., JR., HOWELL, D. G., NILSEN, T. H., NORMARK, W. R., VEDDER, J. C., AND SILVER, E. A., 1978, Neogene basin formation in relation to plate-tectonic evolution of San Andreas fault system, California: American Association of Petroleum Geologists Bulletin, v. 62, p. 344–372.

BRYHNI, INGE, 1964a, Relasjonen mellom senkaledonsk tektonikk og sedimentasjon ved Hornelens og Hasteinens devon: Norges Geologiske Undersøkelse, v. 233, p. 10–25.

———, 1964b, Migrating basins on the Old Red Continent: Nature, v. 202, p. 384–385.

———, 1964c, Sediment structures in the Hornelen series: Norsk Geologisk Tiddskrift, v. 44, p. 486–488.

———, 1975, The West Norwegian basins of Old Red Sandstone: Ninth *International Congress of Sedimentology, Nice, France, Theme 5*, p. 111–117.

———, 1978, Flood deposits in the Hornelen Basin, west Norway (Old Red Sandstone): Norsk Geologisk Tidsskrift, v. 58, p. 273–300.

BUFE, C. G., MARKS, S. M., LESTER, F. W., LUDWIN, R. S., AND STICKNEY, M. C., 1981, Seismicity of the Geysers-Clear Lake region, *in* McLaughlin, R. J., and Donnelly-Nolan, J. M., eds., Research in the Geysers-Clear Lake Geothermal Area, Northern California: United States Geological Survey Professional Paper 1141, p. 129–137.

CLEMENTS, THOMAS, 1937, Structure of southeastern part of Tejon quadrangle, California: American Association of Petroleum Geologists Bulletin, v. 21, p. 212–232.

CROWELL, J. C., 1950, Geology of Hungry Valley area, southern California: American Association of Petroleum Geologists Bulletin, v. 34, p. 1623–1646.

———, 1952, Probable large lateral displacement on the San Gabriel fault, southern California: American Association of Petroleum Geologists Bulletin, v. 36, p. 2026–2035.

———, 1954a, Geology of the Ridge Basin area, California: California Division Mines Bulletin 170, Map sheet 7.

———, 1954b, Strike-slip displacement of the San Gabriel fault, southern California: California Division of Mines Bulletin 170, Ch. 4, p. 49–52.

———, 1974a, Origin of late Cenozoic basins in southern California, *in* Dickinson, W. R., ed., Tectonics and Sedimentation: Society of Economic Paleontologists and Mineralogists Special Publication No. 22, p. 190–204.

———, 1974b, Sedimentation along the San Andreas fault, California, *in* Dott, R. H., Jr., and Shaver, R. H., eds., Modern and Ancient Geosynclinal Sedimentation: Society of Economic Paleontologists and Mineralogists Special Publication No. 19, p. 292–303.

———, 1975, The San Gabriel fault and Ridge Basin, *in* Crowell, J. C., ed., San Andreas Fault in Southern California: California Division of Mines and Geology Special Report 118, p. 208–233.

———, 1982a, The tectonics of Ridge Basin, Southern California, *in* Crowell, J. C., and Link, M. H., eds., Geologic History of Ridge Basin, Southern California: Society of Economic Paleontologists and Mineralogists, Pacific Section, p. 25–42.

———, 1982b, The Violin Breccia, Ridge Basin, *in* Crowell, J. C., and

655226

Link, M. H., eds. Geologic History of Ridge Basin, Southern California: Society of Economic Paleontologists and Mineralogists, Pacific Section, p. 89–98.

———, 1982c, Pliocene Hungry Valley Formation, Ridge Basin, southern California, *in* Crowell, J. C., and Link, M. H., eds., Geologic History of Ridge Basin, Southern California: Society of Economic Paleontologists and Mineralogists, Pacific Section, p. 143–150.

CROWELL, J. C., AND LINK, M. H., eds. 1982a, Geologic history of Ridge Basin, southern California: Society of Economic Paleontologists and Mineralogists, Pacific Section, 304 p.

CROWELL, J. C., AND LINK, M. H., 1982b, Ridge Basin, southern California: Introduction, *in* Crowell, J. C., and Link, M. H., eds., Geologic History of Ridge Basin, Southern California: Society of Economic Paleontologists and Mineralogists, Pacific Section, p. 1–4.

CROWELL, J. C., ET AL., 1982, Geologic map and cross sections, Ridge Basin, southern California: Society of Economic Paleontologists and Mineralogists, Pacific Station, 2 plates, 5p.

DICKINSON, W. R., AND SNYDER, W. S., 1979, Geometry of triple junctions related to San Andreas transform: Journal of Geophysical Research, v. 84, B2, p. 561–572.

DONNELLY, J. M., MCLAUGHLIN, R. J., GOFF, F. E., AND HEARN, B. C., 1976, Active faulting in the Geysers-Clear Lake area, northern California: Geological Society of America Abstracts with Programs, v. 8., p. 369–370.

EATON, J. E., 1939, Ridge Basin, California: American Association of Petroleum Geologists Bulletin, v. 23, p. 517–558.

ENSLEY, R. A., AND VEROSUB, K. L., 1982a, Biostratigraphy and magnetostratigraphy of southern Ridge Basin, central Transverse Ranges, California, *in* Crowell, J. C., and Link, M. H., eds., Geologic History of Ridge Basin, Southern California: Society of Economic Paleontologists and Mineralogists, Pacific Section, p. 13–24.

ENSLEY, R. A., AND VEROSUB, K. L., 1982b, A magnetostratigraphy study of the sediments of the Ridge Basin, southern California and its tectonic and sedimentologic implications: Earth and Plantary Science Letters, v. 59, p. 192–207.

FORESTER, R. M., AND BROUWERS, E. M., 1982, Paleoenvironmental implications of some estuarine and non-marine ostracodes from Ridge Basin, southern California, *in* Crowell, J. C., and Link, M. H., eds., Geologic History of Ridge Basin, Southern California: Society of Economic Paleontologists and Mineralogists, Pacific Section, p. 239–246.

GEE, D. G., 1975, A tectonic model for the central part of the Scandinavian Caledonides: American Journal of Science, v. 275, p. 468–515.

———, 1978, Nappe displacement in the Scandinavian Caledonides: Tectonophysics, v. 47, p. 393–410.

GLOPPEN, T. G., AND STEEL, R. J., 1981, The deposits, internal structure and geometry in six alluvial fan-fan delta bodies (Devonian-Norway)—a study in the significance of bedding sequence in conglomerates, *in* Ethridge, R. G., and Flores, R. M., eds, Recent and Ancient Nonmarine Depositional Environments: Models for Exploration: Society of Economic Paleontologists and Mineralogists Special Publication No. 31, p. 49–69.

HARDING, T. P., 1974, Petroleum traps associated with wrench faults: American Association of Petroleum Geologists Bulletin, v. 58, p. 1290–1304.

———, 1976, Predicting productive trends related to wrench faults: World Oil, v. 182, p. 64–69.

HARPER, A. S., AND OSBORNE, R. H., 1982, Fluviolacustrine facies of the Fisher Springs Sandstone Member, Mio-Pliocene Ridge Route Formation, Ridge Basin, southern California, *in* Crowell, J. C., and Link, M. H., eds., Geologic History of Ridge Basin, Southern California: Society of Economic Paleontologists and Mineralogists, Pacific Section, p. 105–114.

HEMPTON, M. R., AND DUNNE, L. A., 1984, Sedimentation in pull-apart basins: Active examples in eastern Turkey: Journal of Geology, v. 92, p. 513–530.

HEMPTON, M. R., DUNNE, L. A., AND DEWEY, J. F., 1983, Sedimentation in an active strike-slip basin, southeastern Turkey: Journal of Geology, v. 91, p. 401–412.

HERD, D. G., 1978, Intracontinental plate boundary east of Cape Mendocino, California: Geology, v. 6, p. 721–725.

HERD, D. G., AND HELLEY, E. J., 1977, Faults with Quaternary displacement, northwestern San Francisco Bay Region, California: United States Geological Survey Miscellaneous Field Studies Map MF-818, Scale 1:125,000.

HOEG, O. E., 1936, Norges fossile flora: Naturen, v. 60, p. 53–94.

HOLLYWOOD, J. M., AND OSBORNE, R. H., 1982, Sedimentology of the Frenchman Flat Sandstone Member of the Ridge Route Formation, Ridge Basin, southern California, *in* Crowell, J. C., and Link, M. H., eds., Geologic History of Ridge Basin, Southern California: Society of Economic Paleontologists and Mineralogists, Pacific Section, p. 115–

HOWELL, D. G., CROUCH, J. K., GREEN, H. G., MCCULLOCH, D. S., VEDDER, J. G., 1980, Basin development along the late Mesozoic and Cainozoic California margin: A plate tectonic margin of subduction, oblique subduction and transform tectonics, *in* Ballance, P. F., and Reading, H. G., eds., 1980, Sedimentation in Oblique-Slip Mobile Zones: International Association of Sedimentologists Special Publication No. 4, p. 43–62.

IRVINE, P. H., 1977, The Posey Canyon Shale—a Pliocene lacustrine despoit of the Ridge Basin, southern California [unpubl. M.A. thesis]: Berkeley, University of California, 87 p.

JARVIK, ERIK, 1949, On the middle Devonian crossopterygians from the Hornelen field in western Norway: Universitet i Bergen Aarbok 1948, Naturvidenskap Raekke, No. 8, 48 p.

KIAER, J., 1918, Fiskerester fra den devoniske sandsten paa Norges kyst: Bergens Museum Aarbok, Naturvidenskap Raekke, No. 7, p. 17.

KOLDERUP, C. F., 1904, Vestlandets devonisk lagraekker: Naturen, p. 270–276.

———, 1915a, Vestlandets devonfelter og deres plantefossiler: Natu p. 217–232.

———, 1915b, Das vorkommen der pflanzenreste: Bergens Museu Aarbok 1914–1915, Naturvidenskap Raekke, No. 9, p. 1–11.

———, 1916, Vestnorges devon: Forhandlingen ved 16 Skandinav Naturforskermotet, p. 499–507.

———, 1927, Hornelen devonfelt: Bergens Museum Aarbok 1926, N turvidenskap Raekke, No. 6, p. 1–56.

LARSEN, V., AND STEEL, R. J., 1978, The sedimentary history of a d flow-dominated, Devonian alluvial fan—a study of textural inver Sedimentology, v. 25, p. 37–59.

LINK, M. H., 1982a, Stratigraphic nomenclature and age of Miocene strat Ridge Basin, southern California, *in* Crowell, J. C., and Link, M. eds., Geologic History of Ridge Basin, Southern California: Soc of Economic Paleontologists and Mineralogists, Pacific Section, p 12.

———, 1982b, Petrography and geochemistry of sedimentary rocks, Rid Basin, southern California, *in* Crowell, J. C., and Link, M. H., Geologic History of Ridge Basin, Southern California: Society of nomic Paleontologists and Mineralogists, Pacific Section, p. 159–

———, 1982c, Provenance, paleocurrents, and paleogeography of Rid Basin, southern California, *in* Crowell, J. C., and Link, M. H., Geologic History of Ridge Basin, Southern California: Society of nomic Paleontologists and Mineralogists, Pacific Station, p. 265–

———, 1982d, Slope and turbidite facies of the Miocene Castaic For mation and the lower part of the Marple Canyon Sandstone Membe Ridge Route Formation, Ridge Basin, southern California, *in* Crow J. C., and Link, M. H., eds., Geologic History of Ridge Basin, So ern California: Society of Economic Paleontologists and Mineralog Pacific Section, p. 79–88.

———, 1982e, Introduction to the facies of the Ridge Route Formati Ridge Basin, southern California, *in* Crowell, J. C., and Link, M. eds., Geologic History of Ridge Basin, Southern California: Soc of Economic Paleontologists and Mineralogists, Pacific Section, p. 99 104.

———, 1982f, Sedimentology of the upper Miocene Piru Gorge Sa stone Member of the Ridge Route Formation, Ridge Basin, south California, *in* Crowell, J. C., and Link, M. H., eds., Geologic His of Ridge Basin, Southern California: Society of Economic Paleonto ogists and Mineralogists, Pacific Section, p. 127–134.

———, 1983, Sedimentation, tectonics, and offset of Miocene-Plioc Ridge Basin, California, *in* Andersen, D. W., and Rymer, M. J., e Tectonics and Sedimentation Along Faults of the San Andreas System Society of Economic Paleontologists and Mineralogists, Pacific Sec tion, p. 17–31.

———, 1984, Fluvial facies of the Miocene Ridge Route Formati Ridge Basin, California, *in* Nilsen, T. H., ed., Fluvial Sedimenta and Related Tectonic Framework, Western North America: Special is sue of Sedimentary Geology, v. 38, p. 263–285.

LINK, M. H., AND OSBORNE, R. H., 1978, Lacustrine facies in the H

cene Ridge Basin Group: Ridge Basin, California, *in* Matter, Albert, and Tucker, M. E., eds., Modern and Ancient Lake Sediments: International Association of Sedimentologists Special Publication No. 2, p. 169–187.

LINK, M. H., OSBORNE, R. H., AND AWRAMIK, STANLEY, 1978, Lacustrine stromatolites and associated sediments of the Pliocene Ridge Route Formation, Ridge Basin, California: Journal of Sedimentary Petrology, v. 48, p. 143–178.

LINK, M. H., AND SMITH, P. R., 1982, Organic geochemistry of Ridge Basin, southern California, *in* Crowell, J. C., and Link, M. H., eds., Geologic History of Ridge Basin, Southern California: Society of Economic Paleontologists and Mineralogists, Pacific Section, p. 191–198.

MCDOUGALL, KRISTIN, 1982, Microfossil assemblages from the Castaic Formation, southern California, *in* Crowell, J. C., and Link, M. H., eds., Geologic History of Ridge Basin, Southern California: Society of Economic Paleontologists and Mineralogists, Pacific Section, p. 219–228.

MCLAUGHLIN, R. J., 1978, Preliminary geologic map and structural sections of the central Mayacmas Mountains and the Geysers steam field, Sonoma, Lake and Mendocino Counties, California: United States Geological Survey Open-File Map 78–389, scale 1:24,000, two sheets.

———, 1981, Tectonic setting of pre-Tertiary rocks and its relation to geothermal resources in the Geysers-Clear Lake area, *in* McLaughlin, R. J., and Donnelly-Nolan, J. M., eds., Research in the Geysers-Clear Lake Geothermal Area, Northern California: United States Geological Survey Professional Paper 1141, p. 3–23.

MCLAUGHLIN, R. J., AND NILSEN, T. H., 1980, Tectonic framework of the Neogene Little Sulphur Creek basins, Sonoma County, California: Geological Society of America Abstracts with Programs, v. 12, p. 119.

MCLAUGHLIN, R. J., AND NILSEN, T. H., 1982, Neogene non-marine sedimentation in small pull-apart basins of the San Andreas fault system, Sonoma County, California: Sedimentology, v. 29, p. 865–876.

MOODY, J. D., 1973, Petroleum exploration aspects of wrench fault tectonics: American Association of Petroleum Geologists Bulletin, v. 57, p. 449–476.

MOORE, D. G., 1969, Reflection profiling studies of the California continental borderland: Structure and Quaternary turbidite basins: Geological Society of America Special Paper No. 107, 142 p.

NATHORST, A. G., 1915, Zur Devonflora des westlichen Norwegens: Bergens Museum Aarbok 1914–1915, Naturvidenskap Raekke, No. 9, p. 12–23.

NILSEN, T. H., 1967, Old Red sedimentation in the Solund district, western Norway, *in* Oswald, D. H., ed., International Symposium on the Devonian System: Alberta Society of Petroleum Geologists, v. 2, p. 1101–1115.

———, 1973, Devonian (Old Red Sandstone) sedimentation and tectonics of Norway, *in* Pitcher, M. G., ed., Arctic Geology: American Association of Petroleum Geologists Memoir 19, p. 471–481.

NILSEN, T. H., MCLAUGHLIN, R. J., GRIFFIN, E. A., AND ZUFFA, G. G., 1980, Fluvial and lacustrine sedimentology of the Neogene Little Sulphur Creek basins, Sonoma County, California: Geological Society of America Abstracts with Programs, v. 12, p. 45.

PALMER, A. R., compiler, 1983, The Decade of North American Geology 1983 geologic time scale: Geology, v. 11, p. 503–504.

PAMPEYAN, E. H., HARSH, P. W., AND COAKLEY, J. M., 1981, Preliminary map showing recently active breaks along the Maacama fault zone between Hopland and Laytonville, Mendocino County, California: United States Geological Survey Miscellaneous Field Studies Map MF-1217, Scale 1:24,000, two sheets.

POLLARD, J. E., STEEL, R. J., AND UNDERSRUD, EINAR, 1982, Facies sequences and trace fossils in lacustrine/fan delta deposits, Hornelen Basin (M. Devonian), western Norway: Sedimentary Geology, v. 32, p. 63–87.

QUENNELL, A. M., 1958, The structural and geomorphic evolution of the Dead Sea Rift: Quarterly Journal of Geological Society of London, v. 114, p. 1–24.

RAMIREZ, V. R., 1983, Hungry Valley Formation: Evidence for 220 kilometers of post Miocene offset on the San Andreas fault, *in* Andersen, D. W., and Rymer, M. J., eds., Tectonics and Sedimentation Along Faults of the San Andreas System: Society of Economic Paleontologists and Mineralogists, Pacific Section, p. 33–44.

READING, H. G., 1980, Characteristics and recognition of strike-slip fault systems, *in* Ballance, P. F., and Reading, H. G., eds., 1980, Sedimentation in Oblique-Slip Mobile Zones: International Association of Sedimentologists Special Publication No. 4, p. 7–26.

RODGERS, D. A., 1980, Analysis of pull-apart basin development produced by *en echelon* strike-slip faults, *in* Ballance, P. F., and Reading, H. G., eds., 1980, Sedimentation in Oblique-Slip Mobile Zones: International Association of Sedimentologists Special Publication No. 4, p. 27–41.

SCHUBERT, CARLOS, 1980, Late Cenozoic pull-apart basins, Bocono fault zone, Venezuelan Andes: Journal of Structural Geology, v. 2, p. 463–468.

———, 1982, Origin of Cariaco basin, southern Caribbean Sea: Marine Geology, v. 47, p. 345–360.

SMITH, P. R., 1982a, Sedimentology and diagenesis of the Miocene Peace Valley Formation, Ridge Basin, southern California, *in* Crowell, J. C., and Link, M. H., eds., Geologic History of Ridge Basin, Southern California: Society of Economic Paleontologists and Mineralogists, Pacific Section, p. 151–158.

———, 1982b, Paleolimnology of Miocene lakes in Ridge Basin, southern California, *in* Crowell, J. C., and Link, M. H., eds. Geologic History of Ridge Basin, Southern California: Society of Economic Paleontologists and Mineralogists, Pacific Section, p. 259–264.

SMITH, P. R., HARPER, A. S., AND WOOD, M. F., 1982, Non-marine trace fossils in the Mio-Pliocene Ridge Basin Group, southern California, *in* Crowell, J. C., and Link, M. H., eds., Geologic History of Ridge Basin, Southern California: Society of Economic Paleontologists and Mineralogists, Pacific Section, p. 253–258.

SQUIRES, R. L., 1979, Middle Pliocene dragonfly nymphs, Ridge basin, Transverse Ranges, California: Journal of Paleontology, v. 53, p. 446–452.

STANTON, R. J., JR., 1982, Molluscan paleoecology and depositional environment of the Miocene Castaic Formation, Ridge Basin, southern California, *in* Crowell, J. C., and Link, M. H., eds., Geologic History of Ridge Basin, Southern California: Society of Economic Paleontologists and Mineralogists, Pacific Section, p. 211–218.

STEEL, R. J., 1976, Devonian basins of western Norway—sedimentary response to tectonism and to varying tectonic context: Tectonophysics, v. 36, p. 207–224.

STEEL, R. J., AND AASHEIM, S. M., 1978, Alluvial sand desposition in a rapidly subsiding basin (Devonian, Norway), *in* Miall, A. D., ed., Fluvial Sedimentology: Canadian Society of Petroleum Geologists Memoir 5, p. 385–412.

STEEL, R. J., AND GLOPPEN, T. G., 1980, Late Caledonian (Devonian) basin formation, western Norway: Signs of strike-slip tectonics during infilling, *in* Ballance, P. F., and Reading, H. G., eds., 1980, Sedimentation in Oblique-Slip Mobile Zones: International Association of Sedimentologists Special Publication No. 4, p. 79–103.

STEEL, R. J., MAEHLE, S., NILSEN, H., ROE, S. L., AND SPINNANGR, AANON, 1977, Coarsening-upward cycles in the alluvium of Hornelen Basin (Devonian) Norway: Sedimentary response to tectonic events: Geological Society of America Bulletin, v. 88, p. 1124–1134.

STEEL, R. J., MAEHLE, S., NILSEN, H., ROE, S. L., AND SPINNANGR, AANON, 1979, Reply to discussion by H. F. Garner: Geological Society of America Bulletin, v. 90, Part 1, p. 122–124.

STITT, L. T., 1982, Structure and late Miocene paleogeography of southern Ridge Basin, southern California, *in* Crowell, J. C., and Link, M. H., eds., Geologic History of Ridge Basin, Southern California: Society of Economic Paleontologists and Mineralogists, Pacific Section, p. 43–52.

WELTON, B. J., AND LINK, M. H., 1982, Vertebrate paleontology of Ridge Basin, southern California, *in* Crowell, J. C., and Link, M. H., eds., Geologic History of Ridge Basin, Southern California: Society of Economic Paleontologists and Mineralogists, Pacific Section, p. 205–210.

WOOD, M. F., AND OSBORNE, R. H., 1982, Sedimentology of the Mio-Pliocene Apple Canyon Sandstone Member, Ridge Route Formation, Ridge Basin, southern California, *in* Crowell, J. C., and Link, M. H., eds., Geologic History of Ridge Basin, Southern California: Society of Economic Paleontologists and Mineralogists, Pacific Section, p. 135–142.

YOUNG, D. R., 1982, Miocene molluscan paleontology of the Ridge Basin Group, Ridge Basin, southern California, *in* Crowell, J. C., and Link, M. H., eds., Geologic History of Ridge Basin, Southern California: Society of Economic Paleontologists and Mineralogists, Pacific Section, p. 219–228.

655228

# Aberfoyle Resources Limited

EXPLORATION DIVISION

OPEN FILE

TCR 93-3441

## EXPLORATION LICENCE 106/87

## LAKE MACKINTOSH

## TASMANIA

MICROFILMED
FICHE No. 012721 - 29B

MINES
FILE REF. EL106/87
15 JUN 1993
DOC. REF.
OFFICER | FOR ACTION | FOR INFO.
Sue Bolles | 94-97
RESUBMIT TO | DATE

Progress Report for the Period

April 1992 - April 1993

Volume 2 of 3

Appendices III - XI

Distribution

Aberfoyle - Burnie (1/3)
Aberfoyle - Hawthorn (2/3)
**Division of Mines (3/3)**

Internal Report No: Mackintosh 52

# APPENDIX III

**ABERFOYLE** 655230 MEMORANDUM

| | | | |
|---|---|---|---|
| Date | 9 June 1993 | Ref | JS:AAI |
| To | S Richardson | From | J Silic |
| At | Burnie | At | Hawthorn |
| Copies to | | Keep | |

Subject **MAC30 DHEM Data**

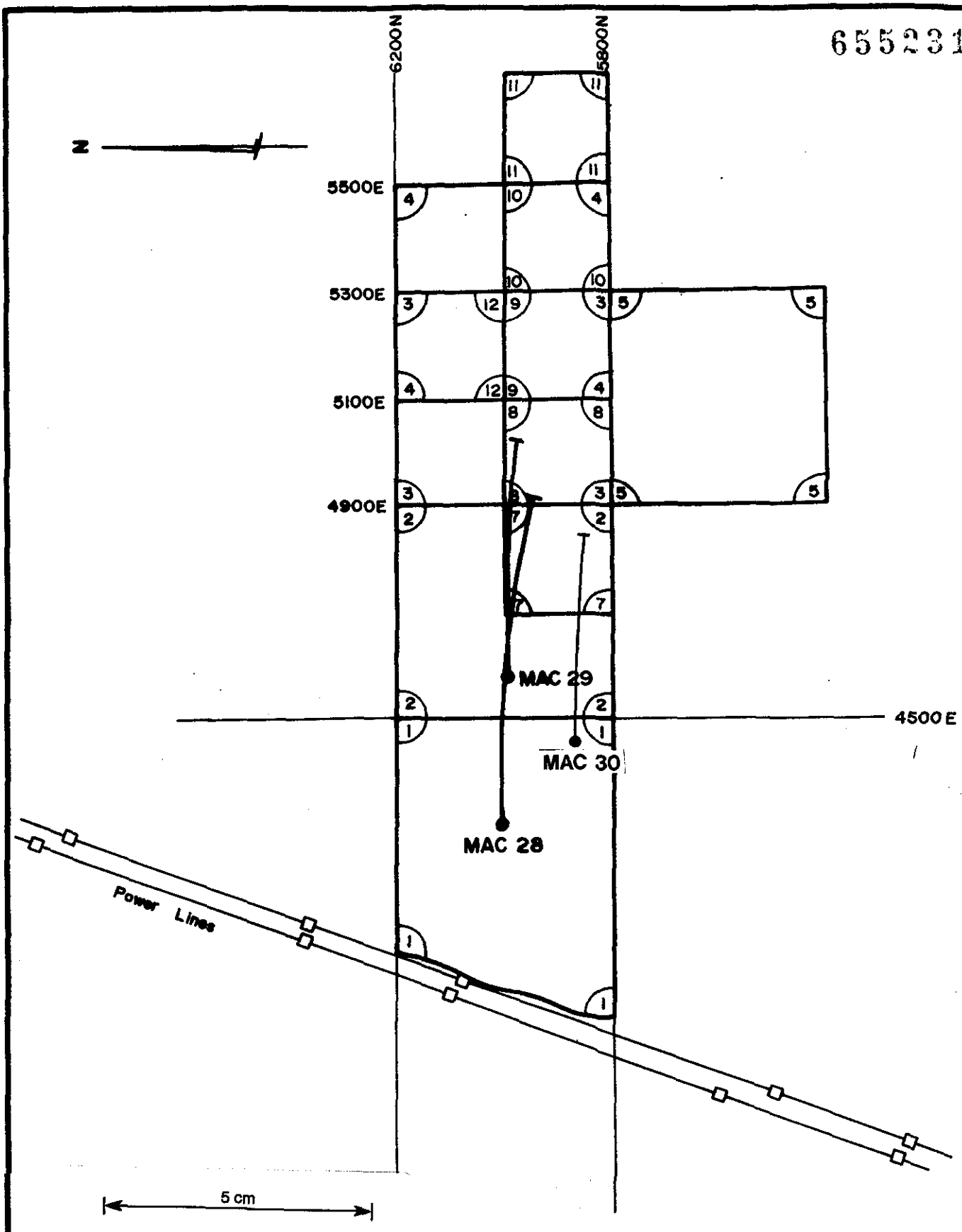
DHEM data was collected using the Zonge GDP-16 system operating at 32hz.

A response which could be interpreted as being due to an offhole conductive source is evident in the data set. In particular peaking of the response at 650 metres down the drillhole at medium times (eg Loop 5 data time windows 12-17) may be outlining a stationary current source.

Numerous attempts were made to reconcile this data set with the MAC28 response and the model interpreted from the MAC28 data set. As a result model interpreted from MAC28 data is now considered to be a highly unlikely scenario, however considering the difficulting of interpreting these data sets (evident from the beginning of this project) it is recommended that three component downhole EM data set be obtained in MAC28 before an alternative model is proposed to explain the MAC28, MAC30 response. This will be done as soon as a three component DHEM system becomes available in Australia (most likely the Crone DHEM system).

JOVAN SILIC

655231




# Aberfoyle Resources Limited

EXPLORATION DIVISION

| Revisions | | | |
|---|---|---|---|
| Init. | Date | Init. | Date |
| GLC | 10/91 | | |
| | | | |
| | | | |
| | | | |
| | | | |

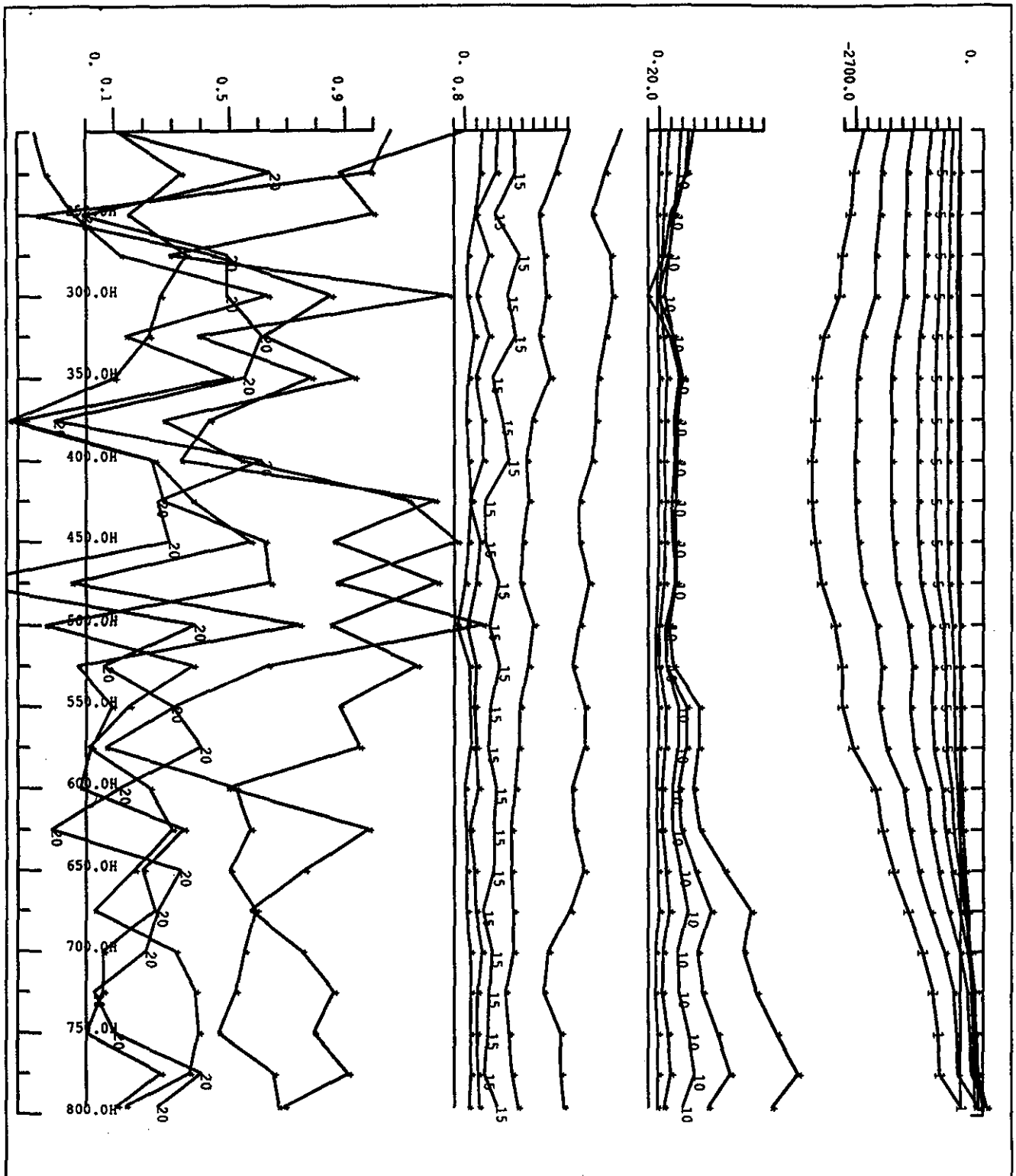
NORTH WEST TASMANIA

## MACKINTOSH EL 106/87

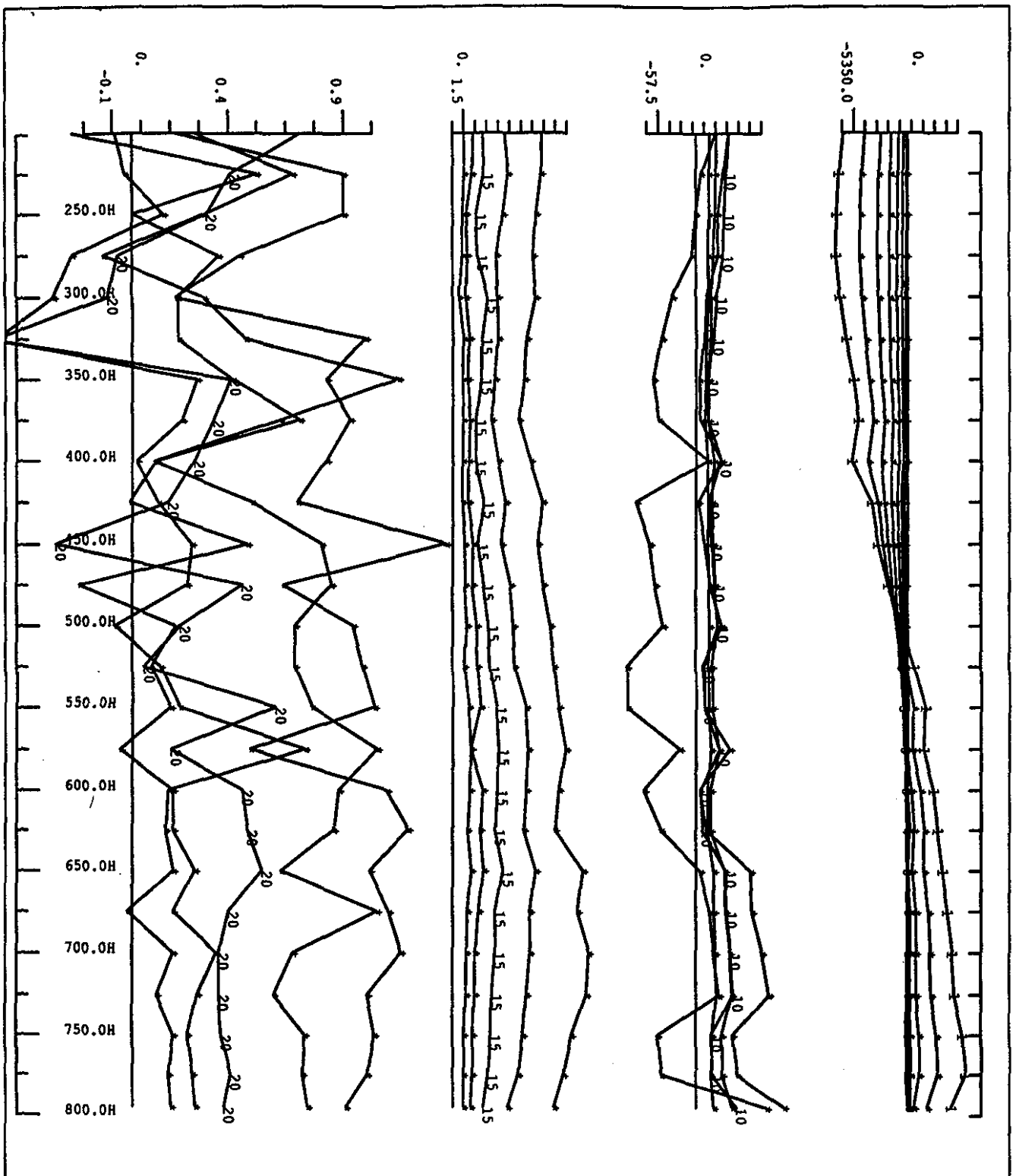
DDH MAC 28-30 - DHEM LOOPS

Location Code : K55/3 | Scale : 1 : 10000 | Date : August 1991

Compiled : JS
Drawn : JS
Traced : GLC
Checked : JS
Plate No. : MAC 334




MACKINTOSH EL
DHEM
LOOP 4
MAC 30
ALONGE HOLE COMPONENT
ZONGE GDP_16 32 HZ
ABERFOYLE RESOURCES
Scale 1: 3500.0 Plot no : 7




MACKINTOSH EL
DHEM
LOOP 5
MAC 30
ALONGE HOLE COMPONENT
ZONGE GDP_16 32 HZ
ABERFOYLE RESOURCES
Scale 1: 3500.0 Plot no : 8

# APPENDIX IV

# ABERFOYLE RESOURCES LTD. DRILL LOG

## MINES DEPARTMENT REPORT HEADER PAGE

**Drillhole Database name: mac**

**Report Grid: Mack**

**Report Legend follows:**

Collar Coordinate Reliability Flags

s = surveyed
m = measured
e = estimated

Assay, Composite, Geochem Bad Data Flag

Any element data that is bad will be recognised by an attached asterisk
example: 2.41*

# ABERFOYLE RESOURCES LTD. DRILL LOG

655236

| Area Code | Prospect | Report Grid | Dataset |
|---|---|---|---|
| mac | Mt.Charter | Mack | Header data set |

| Holename | Stored Grid |
|---|---|
| DDMA0032 | Mack |

**Hole Depth**
278.40

| Collar Easting | Collar Northing | Collar RL | Collar Depth |
|---|---|---|---|
| 4370.500s | 4876.100s | 805.60s | .00 |

| 1st Survey Depth | Survey Dip | Survey Azimuth | Survey Instrument |
|---|---|---|---|
| .00 | -77.50 | 232.00 | clinometer |

| Start Date and Time | End Date & Time |
|---|---|
| 01/12/1992 | 18/12/1992 |

| Geologist | Hole Objective |
|---|---|
| S.Richardson | Structural Targ |

| Work Proposal | Tenement |
|---|---|
| | E.L.106/87 |

| Area Code | Prospect | Report Grid | Dataset |
|---|---|---|---|
| mac | Mt.Charter | AMG | Header data set |

| Holename | Stored Grid |
|---|---|
| DDMA0032 | Mack |

**Hole Depth**
278.40

| Collar Easting | Collar Northing | Collar RL | Collar Depth |
|---|---|---|---|
| 389856.153s | 5391555.157s | 805.60s | .00 |

| 1st Survey Depth | Survey Dip | Survey Azimuth | Survey Instrument |
|---|---|---|---|
| .00 | -77.50 | 254.10 | clinometer |

| Start Date and Time | End Date & Time |
|---|---|
| 01/12/1992 | 18/12/1992 |

| Geologist | Hole Objective |
|---|---|
| S.Richardson | Structural Targ |

| Work Proposal | Tenement |
|---|---|
| | E.L.106/87 |

# ABERFOYLE RESOURCES LTD. DRILL LOG

| Area Code | Prospect | Report Grid | Dataset |
|---|---|---|---|
| mac | Mt.Charter | Mack | Survey data set |

| Holename | Stored Grid |
|---|---|
| DDMA0032 | Mack |

| Depth | Dip | Azi | Instrument |
|---|---|---|---|
| 0.00 | -77.50i | 232.00i | clinometer |
| 25.00 | -77.00i | 236.50i | eastman |
| 50.00 | -76.50i | 241.50i | eastman |
| 75.00 | -76.00i | 242.50i | eastman |
| 100.00 | -76.00i | 243.00i | eastman |
| 125.00 | -75.50i | 245.50i | eastman |
| 150.00 | -74.00i | 249.50i | eastman |
| 175.00 | -73.00i | 255.00i | eastman |
| 200.00 | -72.50i | 259.50i | eastman |
| 225.00 | -72.00i | 262.50i | eastman |
| 239.00 | -71.50i | 263.00i | eastman |
| 249.00 | -71.10i | 259.00i | eastman |
| 256.00 | -70.80i | 260.00i | eastman |
| 267.00 | -68.90i | 259.90i | eastman |
| 278.40 | -68.50i | 262.00i | eastman |

# ABERFOYLE RESOURCES LTD. DRILL LOG

| Area Code | Prospect | Report Grid | Dataset |
|---|---|---|---|
| mac | Mt.Charter | Mack | Drill log data set |

| Holename | Stored Grid |
|---|---|
| DDMA0032 | Mack |

| Item # | From | To | Contractor | Drill Rig | Drill Method | ID |
|---|---|---|---|---|---|---|
| 1.00 | 0.00 | 3.00 | Longyear | Longyear HD 44 | Tricone | 118 |
| 2.00 | 3.00 | 227.10 | Longyear | Longyear HD 44 | Diamond | 96 |
| 3.00 | 227.10 | 278.40 | Longyear | Longyear HD 44 | Diamond | 75 |

655240

# ABERFOYLE RESOURCES LTD. DRILL LOG

| Area Code | Prospect | Report Grid | Dataset |
|---|---|---|---|
| mac | Mt.Charter | Mack | Casing log data set |

| Holename | Stored Grid |
|---|---|
| DDMA0032 | Mack |

| Item | From | To | Casing Type | ID | L | Comments |
|---|---|---|---|---|---|---|
| 1.00 | ? | ? | ? | ? | ? | No casing or PVC in hole |

5 cm

Aberfoyle Resources Limited
EXPLORATION DIVISION

# DIAMOND DRILL LOG

PROJECT : _____

PROSPECT: _____

HOLE NO: MAC 32
PAGE: 1 of 7
LOGGED: SR
DATE: 5-1-93

## LITHOLOGY

| DEPTH | DRILL RUNS | CORE LOSS | ROCK NAME | DESCRIPTION |
|---|---|---|---|---|
| HW | | 1 | HA-bv/lv | Cy<br>Frags – HA – si+se+fy<br>– 1000 mm max.<br>– P<br>– A<br>Matrix – si+se+fy<br>– 10% |
| | | 2 | | |
| | | 3 | | |
| | | 4 | | Altered brecciated Dacite. |
| | | 5 | | |
| | | 6 | | |
| 29.9 | | 7 | | 5 |
| | | 8 | Y-mlv | Cy<br>Frags – HA<br>– 40mm<br>– m<br>– VE<br>matrix – si+se+fy<br>– 25% |
| 35.1 | | 9 | | |
| | | 10 | D-l/bv | LCy<br>Frags – D<br>– Ao<br>– P<br>– A<br>matrix – si+se<br>– 10% |
| FW | | | | |

## ALTERATION

P 4 si se fy
si P 3 L 4
Se P4

33.5
P 3 Se Si
Se 3 P
Si 1 P

## VEINING

| | | | |
|---|---|---|---|
| 13.7 | | | |
| | Int – 4<br>Thick – 100<br>min – Ba+Co | | 20–40°CA |
| 17.3 | | | |
| | 2 | 10 | BaCo |
| 23.8 | | | |
| | 4 | 300 | BaCo |
| 25.8 | | | |
| | 2 | 10 | BaCo |
| 29.9 | | | |
| | 1 | 5 | SiCo |
| 35.1 | | | |
| | 1 | 5 | SiCo |
| | 3 | 10 | Py |

## MINERALISATION

| | | |
|---|---|---|
| Vn<br>Ds | Py 5–10 | |
| 23.5 | | |
| Vn<br>Ds<br>Ds | Py 10<br>sp? 2 | |
| 29.9 | | |
| Ds | Py 5–10, Sp? 3–5<br>Cu tr | |
| 35.1 | | |
| Vn<br>(Ds) | Py 15 | |

## STRUCTURE

Tv CA

| | | | |
|---|---|---|---|
| 14.5 | 30 | 20 | Ru |
| 22.4 | 190 | ? | PuRu |
| 32.6 | 40 | 25 | Ru |
| 33.5 | 20 | 25 | PuRu |
| 35.1 | 10 | 20 | PuRu |
| 39.7 | 10 | 20 | Ru |

WEATHERING

VISUAL LOG

## REMARKS

CL 5m
25°

CL 18m
25°

Patchy cream coloured Sp? looks identical to Precious Metal mineralisation as at Que River.

CL 32m
30°

well developed stockwork pyrite. Alteration less intense. Veins predominantly at low angle to CA.

DEPTH

Aberfoyle Resources Limited
EXPLORATION DIVISION

# DIAMOND DRILL LOG

5 cm

PROJECT : MACKINTOSH

PROSPECT: MT CHARTER

655242

HOLE NO: MAC 32
PAGE: 2 of —
LOGGED: SR
DATE: 5-1-93

| DEPTH | DRILL RUNS | CORE LOSS | LITHOLOGY: ROCK NAME | LITHOLOGY: DESCRIPTION | ALTERATION | VEINING | MINERALISATION | STRUCTURE | WEATHERING | VISUAL LOG | REMARKS | DEPTH |
|---|---|---|---|---|---|---|---|---|---|---|---|---|
| 75 | | 11 | D-L\|bv | | | | | | | | Alteration decreasing | |
| 47 | | | | | 48.0 | 48.3 | 48.3 | | | | | |
| 49 | | 12 | | | P 2 Se | | Vn Py 3-5<br>Ds | 50.8 100 10 Ru | | | | |
| 51 | | | | | | | | 52.4 60 10 Ru | | | | |
| 53 | | 13 | | | | | | | | | | |
| 55 | | 14 | D-bv | Frags - D 150mm<br>Cy - P<br>- A<br>Matrix - a 10 | | | | 55.6 1 20 SL | | | CL 54m 30° | |
| 57 | | | | | 56.6 | | | 57.5 10 25 PuRu<br>58.2 10 30 PuRu | | | | |
| 59 | | 15 | Y-FW\|mLV | LCyGm<br>Frags - D?<br>- 90<br>- P<br>- V<br>Matrix - a 20 | P 1 Se Cl | | | | | | | |
| 61 | | | | | | | | 61.7 10 ? Ru | | | | |
| 63 | | 16 | | | | | 62.8 | 62.8 10 ? Ru<br>64.2 160 5 Ru | | | | |
| 65 | | | YD-LW\|bv\|aV | CyGm<br>Frags - D?<br>- 100<br>- P<br>- V<br>Matrix - a ~30-100% | | | Ds Py 1 | | | | Rock becomes more green due to chlorite. Unsure in composition but prob. still Dacitic | |
| 67 | | 17 | | | | | | | | | | |
| 69 | | 18 | | | | | | 68.5 3 10 PuRu<br>70.0 20 ? PuRu | | | CL 68m 25° | |
| 71 | | | | | | | | 70.7 10 ? Ru | | | | |
| 73 | | 19 | | | | | | | | | Generally broken core ≈ 60-96 m | |
| 75 | | | | | | | | 75.6 100 ? Ru | | | | |
| 77 | | 20 | | | | | | 76.8 10 ? Ru<br>77.9 10 5 PuRu | | | | |
| 79 | | | | | | | | | | | CL 80m 15° | |
| 81 | | 21 | | | 82.0 | | | 81.4 20 ? RuPu | | | | |
| 83 | | | | | P 2 Cl Se | | | | | | | |
| 85 | | 22 | 85.0 | | | | | | | | | |

Aberfoyle Resources Limited
EXPLORATION DIVISION

# DIAMOND DRILL LOG

PROJECT : MACKINTOSH
PROSPECT: MT CHARTER

6552 13

5 cm

HOLE NO : MAC 32
PAGE: 3 of 7
LOGGED: SR
DATE: 5-1-93

| DEPTH | DRILL RUNS | CORE LOSS | LITHOLOGY: ROCK NAME | LITHOLOGY: DESCRIPTION | ALTERATION | VEINING | MINERALISATION | STRUCTURE | WEATHERING | VISUAL LOG | REMARKS | DEPTH |
|---|---|---|---|---|---|---|---|---|---|---|---|---|
| 88 | | 23 | D-L | Cg Cm - Cm | | | | 89.8 640 ? Ru | | | massive lava | 88 |
| 90 | | | | | | | | | | | | 90 |
| 92 | | 24 | | | | | | | | | broad zones of broken core prob. faults at low angle to CA. | 92 |
| 94 | | | | 94.0 S | | | | | | | | 94 |
| 95.6 | | 25 | YD-Lv | Cg C Frags - D? - m -20 - SR Matrix - a -30 G1 | | | | 96.0 500 ? Ru | | | | 96 |
| 96 | | | | | | | | | | | | |
| 98 | | | D-Lv/L | LCg Frags - D -40 - P - A Matrix - SiSe - 10 | 97.5 P 3 Se Si P 3 SR P 1 Si | | | | | | | 98 |
| 100 | | 26 | | 100.5 S | 100.5 P 2 CL Se P 2 CL P 1 Se | | | 100.5 1 25 SL | | | Massive to finely feldspar phyric Dacite Lava. Moderate Se+Si+fy alteration resulting in Quartzite appearance. | 100 |
| 102 | | | | | | | | | | | | 102 |
| 104 | | 27 | D-L 104.5 | LCg Ru - LCg | 104.5 P 3 Se Si Py P 3 Se P 1 Si | 104.5 1 10 Si Py | 104.5 Ds Vn Py 3-5 | 105.7 70 20 Ru Lu | | | | 104 |
| 106 | | 28 | Q/D-L | LCg | | | | | | | | 106 |
| 108 | | | | | | | | | | | | 108 |
| 110 | | 29 | | | | | | 110.0 20 ? Ru 111.0 10 ? Ru | | | | 110 |
| 112 | | | | 113.0 | 113.0 P 3 Se Si Py | | | 113.0 2 2 Py | | | | 112 |
| 114 | | 30 | Q/D-Lv 114.5 | LCg Frags. - D (Fw) -30 - P - V Matrix - Se Si - 40 | 114.5 Ep 3 Py P 3 Se Si Py P 3 Se P 1 Si | | | 115.4 5 25 Py | | | | 114 |
| 116 | | | | | | | | | | | | 116 |
| 118 | | 31 | Q/D-L | | | | | 118.9 1 20 Py | | | | 118 |
| 120 | | | | | 121.3 121.9 P 2 CL Se P 3 Se Si Py P 3 Se P 1 Si | | 122.2 Ds Vn Py 5 | | | | CL 122 25° | 120 |
| 122 | | 32 | | | | | | | | | | 122 |
| 124 | | | | | | | | | | | | 124 |
| 126 | | 33 | | | | | | 127.8 10 35 Ru Lu | | | | 126 |
| 128 | | | | | | | | | | | | 128 |

Aberfoyle Resources Limited
EXPLORATION DIVISION

# DIAMOND DRILL LOG

655244

5 cm

PROJECT : MACKINTOSH
PROSPECT: MT. CHARTER

HOLE NO: MAC 32
PAGE: 4 of 7
LOGGED: SR
DATE: 5-1-93

| DEPTH | DRILL RUNS | CORE LOSS | LITHOLOGY: ROCK NAME | LITHOLOGY: DESCRIPTION | ALTERATION | VEINING | MINERALISATION | STRUCTURE | WEATHERING | VISUAL LOG | REMARKS | DEPTH |
|---|---|---|---|---|---|---|---|---|---|---|---|---|
| 131 | | 34 | Q/D-L | Gy | P 3 Se Si Py | 131.8 | 131.8 Vn Ds Py 5 | 130.6 1 25 Pn | | | 131 CL 25° | 131 |
| 133 | | | | | | 2 2c Ba Co | Vn sp tr (assoc w. Ba Vns) | 132.3 1 30 Pn | | | | 133 |
| 135 | | 35 | | | | 135.3 | | | | | Quellite altered mass. to wk. fol. Phy. D-L. | 135 |
| 137 | | | | | | 3 200 Ba Co | | 137.3 2o 25 Pn | | | | 137 |
| 139 | | 36 | | | | 137.8 2 10 Ba Co | | | | | | 139 |
| 141 | | | | | | 141.2 | | | | | | 141 |
| 143 | | 37 | | | | 1 5 Ba Co | | | | | | 143 |
| 145 | | | | | | 1 10 Si | | | | | | 145 |
| 147 | | 38 | | | | | | | | | | 147 |
| 149 | | | | | | 148.7 | | | | | | 149 |
| 151 | | | | | | 2 50 Ba Co | | | | | | 151 |
| 153 | | 39 | | | | 153.6 | | | | | | 153 |
| 155 | | | | | | 3 10 Ba Co Py | 154.8 Vn Ds Py 5-10 Stockwork. | 154.2 1 10 Pn | | | | 155 |
| 157 | | 40 | | | | 156.8 | | 154.8 1 40 Pn | | | | 157 |
| 159 | | | | | | 2 5 Si Co | | 155.7 1 40 Pn | | | | 159 |
| 161 | | 41 | | | | 161.4 | | 160.0 3 Pn 35 | | | | 161 |
| 163 | | | | | | 3 40 Si Py ± Cc ± Co | | 161.4 7o ? Pn | | | | 163 |
| 165 | | 42 | | | | | | | | | | 165 |
| 167 | | | | | | 166.6 | | | | | CL 167m 30° | 167 |
| 169 | | 43 | | | | 2 10 Si Py ± Co | | 169.9 1 30 Sl Pn | | | | 169 |
| 171 | | | | | | | | 170.5 1 20 Pn | | | | 171 |

Aberfoyle Resources Limited
EXPLORATION DIVISION

# DIAMOND DRILL LOG

PROJECT : MACKINTOSH
PROSPECT: MT CHALTER

6552 43

5 cm

HOLE NO : MAC 32
PAGE : 5 of 7
LOGGED : JR
DATE : 7-1-93

DEPTH | DRILL RUNS | CORE LOSS | LITHOLOGY: ROCK NAME | LITHOLOGY: DESCRIPTION | ALTERATION | VEINING | MINERALISATION | STRUCTURE | WEATHERING | VISUAL LOG | REMARKS | DEPTH

## LITHOLOGY

ROCK NAME: Q|D-L

DESCRIPTION:
182.8 Int Max Shape
VESICLES – 3 5 5
183.4

## ALTERATION

P 3 Se Si Py

189.5
P 2 Se Ca Si
190.4
P 2 Se Si Ca Py
P 2 Se
P 1 Si
PV 1 CL

## VEINING

172.8
3 20 Si Py ± C
174.8
3 50 Ba C ± Py
3 20 Si Py ± C
186.8
1 40 Ba C
2 5 Si Py
194.6
2 5 Si Py

## MINERALISATION

172.8
Vn Py 10–15
Ds
Vn Sp Cp Tr
186.8
Vn Py 5
Ds
207.7
Vn Py 10
Ds
209.2
Vn Py 5
Ds

## STRUCTURE

175.9 2 25 Pu
176.4 2 45 Ru Sl
187.8 1 30 Sl Pu
192.1 2 45 Pu
192.6 1 45 Pu
192.9 1 45 Pu
194.4 1 20 Sl Pu
196.1 1 40 Py Pu
196.5 1 40 Sl Pu
197.5 60 30 Pu
199.4 1 30 Pu Sl
201.7 10 30 Ru
202.9 5 40 Pu
203.2 1 40 Pu
204.1 20 ? Ru Pu
205.9 10 ? Ru
206.4 10 30 Ru
208.3 2 25 Sl Pu
214.7 10 45 Ru

## REMARKS

CL 188m
40°

Less altered + weakly chloritic

CL 207m
30°

Aberfoyle Resources Limited
EXPLORATION DIVISION

# DIAMOND DRILL LOG

PROJECT : MACKINTOSH
PROSPECT: MT CHARTER
655216

5 cm

HOLE NO : MAC 32
PAGE : 6 of 7
LOGGED : SR
DATE : 7-1-93

| DEPTH | DRILL RUNS | CORE LOSS | LITHOLOGY: ROCK NAME | LITHOLOGY: DESCRIPTION | ALTERATION | VEINING | MINERALISATION | STRUCTURE | WEATHERING | VISUAL LOG | REMARKS | DEPTH |
|---|---|---|---|---|---|---|---|---|---|---|---|---|
| 217 | | 54 | | | | 217.7 | | 217.5 10 2 PyPo | | | | 217 |
| 219 | | | | | | 2 200 BaCo<br>1 10 SiPy | | | | | CL 220m<br>40° | 219 |
| 221 | | 55 | | | | | | | | | | 221 |
| 223 | | | | | | | | 223.1 10 20 Py | | | | 223 |
| | | | | | | | | 224.0 1 20 SiPy<br>224.6 2 15 SiPy | | | | |
| 225 | | 56 | | | | | | | | | | 225 |
| 227 | | | | | 226.9 P 3 SeSiPy<br>Se P 3<br>Si P 1 | 226.9 1 5 Si ± C | | 227.5 60 20 PyPo<br>227.8 5 10 Py | | | | 227 |
| 229 | | 57 | 229.1 | 91 | | | | | | | Dominantly altered D-L but bands of Volcaniclastic to 30cm beginning to appear. | 229 |
| 231 | | | Q/D-L/LV | Lcy - Cy<br>Frags - D 30, P, A<br>matrix - SiSiPy 30% | | | | | | | | 231 |
| 233 | | | | | | | | | | | | 233 |
| 235 | | 58 | 235.1 | 5 | | | 235.0 Ds Py 3 | 235.0 110 25 PyPo | | | | 235 |
| | | | Y-mLv | Lcy br<br>Frags - D, Pc 20, M, SR<br>matrix - Se 20% | | | | | | | CL 237m<br>30° | |
| 237 | | | 238.8 | No Core - Navi Drill Cut. | 238.8 | 238.8 | 238.8 | 237.7 5 40 SiPy | | | | 237 |
| 239 | | | 241.9 | | 241.9 | 241.9 | 241.9 | | | | | 239 |
| 241 | | 59 | 242.1 | 5 | 242.1 P2 SeClSi<br>r2 Se<br>P1 Si<br>L2 Cl | | | | | | | 241 |
| 243 | | | D-L/Lv/bv | Cy<br>Frags - D 100, P, A<br>matrix - a 70% | | 1 5 Si ± Co | Ds Py 3 | | | | | 243 |
| 245 | | | | | | | | | | | | 245 |
| 247 | | 60 | | | 249.7 P 3 SeSi Py<br>P 3 Se<br>P 1 Si | | 247.7 Vn Py 5-10<br>Ds Vn GnSp Tr | | | | | 247 |
| 249 | | | | | | | | | | | | 249 |
| 251 | | | 250.4 | 51 | | | 250.4 Ds (Vn) Py 3 | | | | | 251 |
| 253 | | 61 | Y-mLv/bv | Cy<br>Frags - D, Pc 500, P, SR-A<br>matrix - SiSiPy 20% | | | | 254.1 5 20 PyPo | | | Y-mLv with Angular blocks of D-L → 50cm ? | 253 |
| 255 | | | | | | | | | | | CL 255m<br>30° | 255 |
| 257 | | | 256.8 | No Core - Navi Drill Cut | 256.8 | 256.8 | 256.8 | | | | | 257 |

PROJECT : _____

PROSPECT: _____

5 cm

Aberfoyle Resources Limited
EXPLORATION DIVISION

# DIAMOND DRILL LOG

655247

HOLE NO: MAc 32
PAGE: 7 of 7
LOGGED: SR
DATE: 7-1-93

| DEPTH | DRILL RUNS | CORE LOSS | LITHOLOGY: ROCK NAME | LITHOLOGY: DESCRIPTION | ALTERATION | VEINING | MINERALISATION | STRUCTURE | WEATHERING | VISUAL LOG | REMARKS | DEPTH |
|---|---|---|---|---|---|---|---|---|---|---|---|---|
| 260 | | | | N: Core – Navi Drill Cut. | | | | | | | | 260 |
| | | | | 260.8 | 260.8 | 260.8 | 260.8 | | | | | |
| 262 | | 62 | Y-mly/bv | Cm C Frags – Dsfc –Sgc –Sft-fh matrix – silsfy –20% | P 3 Se Silfy | 1 5 Si±Co | Ds (Vn) fy 3 | 262.4 30 15 Rulfy | | | | 262 |
| | | | 264.3 | 91 | | 263.5 | | 263.5 15 20 Rulfu | | | | |
| 264 | | | | | P 3 Se | 2 10 Si C | 265.1 | | | | | 264 |
| 266 | | | | Cm C | P 2 Si | 266.4 | Vn Ds fy 5-10 | | | | | 266 |
| | | 63 | | | | 267.4 300 Si | 267.6 | | | | | |
| 268 | | | Q/D-L | Fined massive lava. | | | Vn Ds fy 5-10 | 268.9 1 15 Ru Sc | | | | 268 |
| 270 | | | | | | 2 10 Si±Co | Vn Sf Gn ET | 270.7 50 20 Ru | | | | 270 |
| | | 64 | | | | 2 15 BaCo | | | | | CL 273m 30° | |
| 272 | | | | | | | | | | | | 272 |
| 274 | | | | | | 275.5 | 275.5 | | | | | 274 |
| 276 | | 65 | | | | 1 50 Silfy | Vn Ds fy 3-5 | | | | | 276 |
| 278 | | | | 278.4 | | | | | | | EOH 278.4m | 278 |
| 280 | | | | | | | | | | | | 280 |

# APPENDIX V

# ABERFOYLE RESOURCES LTD. DRILL LOG

655249

**Area Code** mac | **Prospect** Mt.Charter | **Report Grid** Mack | **Dataset** Geochemical data set

**Holename** DDMA0032 | **Stored Grid** Mack

| From | To | Sample | Type | Cu ppm | Pb ppm | Zn ppm | Ag ppm | Au ppm | Ba ppm | As ppm | Cr ppm | Zr ppm | Ti ppm | Ti/Zr |
|---|---|---|---|---|---|---|---|---|---|---|---|---|---|---|
| 0.00 | 13.70 | 622301 | cgri | 76 | 13 | 324 | 17.0 | 0.156 | 14300 | 670 | 14 | 178 | 3141 | 17.65 |
| 13.70 | 17.30 | 622302 | cgri | 106 | 9 | 1869 | 31.0 | 0.318 | 152100 | 613 | 17 | 143 | 2222 | 15.54 |
| 17.30 | 23.50 | 622303 | cgri | 108 | 45 | 1302 | 20.0 | 0.370 | 15900 | 440 | 17 | 152 | 2824 | 18.58 |
| 23.50 | 25.20 | 622304 | cgri | 240 | 20 | 3584 | 64.0 | 1.200 | 141300 | 858 | 17 | 142 | 2278 | 16.04 |
| 25.20 | 29.90 | 622305 | cgri | 268 | 46 | 4262 | 34.0 | 0.569 | 92500 | 991 | 12 | 138 | 2400 | 17.39 |
| 29.90 | 32.20 | 622306 | cgri | 268 | 64 | 3723 | 34.0 | 0.878 | 56200 | 642 | 15 | 135 | 2219 | 16.44 |
| 32.20 | 35.10 | 622308 | cgri | 47 | 14 | 84 | 3.0 | 0.036 | 3503 | 252 | 33 | 223 | 3209 | 14.39 |
| 35.10 | 48.30 | 622309 | cgri | 77 | 43 | 126 | 2.0 | 0.022 | 1227 | 304 | 15 | 209 | 2808 | 13.44 |
| 48.30 | 56.60 | 622310 | cgri | 58 | 36 | 217 | <2.0 | 0.021 | 1486 | 150 | 18 | 200 | 2801 | 14.01 |
| 56.60 | 62.80 | 622311 | cgri | 74 | 39 | 230 | <2.0 | 0.012 | 740 | 62 | 36 | 204 | 2962 | 14.52 |
| 62.80 | 74.00 | 622312 | cgri | 45 | <5 | 223 | <2.0 | 0.010 | 863 | 52 | 35 | 187 | 2702 | 14.45 |
| 74.00 | 85.00 | 622313 | cgri | 54 | 16 | 229 | <2.0 | 0.011 | 882 | 87 | 28 | 189 | 2818 | 14.91 |
| 85.00 | 100.50 | 622314 | cgri | 49 | <5 | 237 | <2.0 | 0.019 | 15900 | 44 | 17 | 209 | 2583 | 12.36 |
| 100.50 | 114.50 | 622315 | cgri | 55 | 12 | 94 | <2.0 | 0.011 | 1346 | 228 | 24 | 172 | 2404 | 13.98 |
| 114.50 | 123.00 | 622316 | cgri | 74 | 9 | 136 | <2.0 | 0.022 | 2959 | 118 | 15 | 178 | 2537 | 14.25 |
| 123.00 | 131.80 | 622317 | cgri | 69 | 11 | 73 | 2.0 | 0.055 | 2019 | 160 | 6 | 159 | 2579 | 16.22 |
| 131.80 | 141.20 | 622318 | cgri | 117 | 52 | 1743 | 5.0 | 0.106 | 25600 | 234 | 8 | 153 | 2462 | 16.09 |
| 141.20 | 148.70 | 622319 | cgri | 156 | 21 | 195 | 2.0 | 0.181 | 4516 | 207 | 15 | 154 | 2968 | 19.27 |
| 148.70 | 156.80 | 622320 | cgri | 171 | 21 | 1469 | 8.0 | 0.320 | 42300 | 402 | 14 | 156 | 2703 | 17.33 |
| 156.80 | 165.00 | 622322 | cgri | 104 | 68 | 170 | 4.0 | 0.467 | 2362 | 357 | 9 | 148 | 2739 | 18.51 |
| 165.00 | 172.80 | 622323 | cgri | 118 | 56 | 197 | 3.0 | 0.347 | 4149 | 279 | 6 | 158 | 2743 | 17.36 |
| 172.80 | 180.00 | 622324 | cgri | 163 | 17 | 698 | 5.0 | 0.442 | 26700 | 314 | 11 | 152 | 2477 | 16.30 |
| 180.00 | 186.80 | 622325 | cgri | 255 | 24 | 1346 | 4.0 | 0.361 | 40200 | 226 | 9 | 154 | 2336 | 15.17 |
| 186.80 | 194.60 | 622326 | cgri | 190 | 50 | 378 | 3.0 | 0.584 | 10000 | 174 | <5 | 164 | 2758 | 16.82 |
| 194.60 | 207.70 | 622327 | cgri | 417 | 53 | 326 | 2.0 | 0.540 | 4320 | 189 | <5 | 154 | 2789 | 18.11 |
| 207.70 | 217.70 | 622328 | cgri | 536 | 22 | 594 | 2.0 | 0.353 | 11200 | 195 | 9 | 168 | 2904 | 17.29 |
| 217.70 | 226.90 | 622329 | cgri | 168 | 7 | 249 | <2.0 | 0.484 | 30500 | 147 | 16 | 165 | 2766 | 16.76 |
| 226.90 | 235.10 | 622330 | cgri | 72 | 19 | 155 | <2.0 | 0.266 | 8200 | 115 | 5 | 194 | 1955 | 10.08 |
| 235.10 | 242.10 | 622331 | cgri | 57 | 18 | 65 | <2.0 | 0.047 | 2112 | 45 | 79 | 179 | 2944 | 16.45 |
| 242.10 | 250.40 | 622332 | cgri | 100 | 155 | 431 | <2.0 | 0.086 | 2836 | 91 | 111 | 147 | 3032 | 20.63 |
| 250.40 | 264.30 | 622333 | cgri | 113 | 32 | 243 | 7.0 | 0.093 | 3779 | 108 | 58 | 180 | 2409 | 13.38 |
| 264.30 | 278.40 | 622334 | cgri | 155 | <5 | 162 | <2.0 | 0.377 | 23600 | 130 | 6 | 176 | 1724 | 9.80 |

32 samples

# ABERFOYLE RESOURCES LTD. DRILL LOG

**Area Code** mac | **Prospect** Mt.Charter | **Report Grid** Mack | **Dataset** Geochemical data set

**Holename** DDMA0032 | **Stored Grid** Mack

| From | To | SiO2 % | TiO2 % | Al2O3 % | Fe2O3 % | MnO % | MgO % | CaO % | Na2O % | K2O % | P2O5 % | LOI % | TOTAL % |
|---|---|---|---|---|---|---|---|---|---|---|---|---|---|
| 0.00 | 13.70 | 59.70 | 0.52 | 14.56 | 7.58 | 0.02 | 0.90 | 0.27 | 0.06 | 5.17 | 0.25 | 7.24 | 104.44 |
| 13.70 | 17.30 | 48.50 | 0.37 | 8.33 | 6.40 | 0.06 | 0.60 | 0.10 | 0.17 | 2.93 | 0.10 | 7.23 | 100.53 |
| 17.30 | 23.50 | 62.40 | 0.47 | 13.03 | 7.14 | 0.02 | 0.80 | 0.15 | <0.05 | 4.51 | 0.21 | 6.56 | 103.41 |
| 23.50 | 25.20 | 49.00 | 0.38 | 8.92 | 6.66 | 0.03 | 0.60 | 0.12 | 0.22 | 3.19 | 0.12 | 8.03 | 101.48 |
| 25.20 | 29.90 | 54.20 | 0.40 | 9.97 | 7.21 | 0.02 | 0.60 | 0.15 | 0.20 | 3.40 | 0.17 | 7.20 | 101.81 |
| 29.90 | 32.20 | 59.20 | 0.37 | 10.44 | 6.84 | 0.02 | 0.70 | 0.14 | 0.37 | 3.71 | 0.16 | 6.32 | 101.88 |
| 32.20 | 35.10 | 61.60 | 0.54 | 17.88 | 5.15 | 0.01 | 1.20 | 0.01 | 0.05 | 6.22 | 0.16 | 5.64 | 102.61 |
| 35.10 | 48.30 | 61.40 | 0.47 | 16.44 | 6.64 | 0.01 | 1.20 | 0.03 | 0.06 | 5.68 | 0.19 | 6.52 | 103.92 |
| 48.30 | 56.60 | 63.00 | 0.47 | 16.53 | 5.66 | 0.01 | 1.90 | 0.06 | <0.05 | 5.40 | 0.20 | 5.83 | 102.96 |
| 56.60 | 62.80 | 61.90 | 0.49 | 17.14 | 5.72 | 0.03 | 3.50 | 0.17 | 0.07 | 4.76 | 0.19 | 5.51 | 101.70 |
| 62.80 | 74.00 | 65.80 | 0.45 | 16.62 | 4.71 | 0.04 | 3.00 | 0.09 | <0.05 | 4.63 | 0.20 | 4.38 | 100.38 |
| 74.00 | 85.00 | 64.70 | 0.47 | 16.61 | 4.92 | 0.04 | 2.90 | 0.18 | 0.15 | 4.70 | 0.20 | 4.46 | 100.22 |
| 85.00 | 100.50 | 64.30 | 0.43 | 15.55 | 4.38 | 0.03 | 3.20 | 0.09 | 0.07 | 4.35 | 0.22 | 4.77 | 100.21 |
| 100.50 | 114.50 | 66.20 | 0.40 | 14.68 | 5.81 | 0.02 | 1.30 | 0.29 | <0.05 | 4.99 | 0.20 | 4.92 | 102.38 |
| 114.50 | 123.00 | 68.10 | 0.42 | 14.50 | 4.75 | 0.01 | 1.00 | 0.24 | 0.08 | 5.16 | 0.19 | 4.44 | 102.28 |
| 123.00 | 131.80 | 67.60 | 0.43 | 14.31 | 4.97 | 0.01 | 0.90 | 0.33 | <0.05 | 4.90 | 0.25 | 4.84 | 102.50 |
| 131.80 | 141.20 | 66.00 | 0.41 | 12.98 | 4.46 | 0.01 | 0.80 | 0.32 | 0.05 | 4.27 | 0.24 | 4.34 | 100.83 |
| 141.20 | 148.70 | 69.50 | 0.50 | 13.65 | 4.16 | 0.01 | 0.90 | 0.32 | 0.16 | 4.97 | 0.26 | 4.24 | 102.00 |
| 148.70 | 156.80 | 64.20 | 0.45 | 12.04 | 4.64 | 0.02 | 0.80 | 0.32 | 0.20 | 4.16 | 0.24 | 4.92 | 105.94 |
| 156.80 | 165.00 | 67.70 | 0.46 | 13.43 | 5.56 | 0.02 | 1.00 | 0.34 | <0.05 | 4.70 | 0.25 | 4.89 | 102.79 |
| 165.00 | 172.80 | 66.60 | 0.46 | 13.56 | 5.66 | 0.02 | 1.10 | 0.36 | 0.08 | 4.69 | 0.25 | 5.11 | 102.72 |
| 172.80 | 180.00 | 65.50 | 0.41 | 11.62 | 5.56 | 0.04 | 0.90 | 0.54 | 0.05 | 4.02 | 0.23 | 5.40 | 102.16 |
| 180.00 | 186.80 | 65.50 | 0.39 | 11.30 | 4.49 | 0.05 | 0.80 | 0.43 | 0.09 | 3.88 | 0.22 | 5.67 | 101.61 |
| 186.80 | 194.60 | 67.20 | 0.46 | 13.89 | 4.94 | 0.03 | 1.00 | 0.37 | 0.15 | 4.62 | 0.26 | 4.90 | 102.06 |
| 194.60 | 207.70 | 66.30 | 0.47 | 13.98 | 5.82 | 0.02 | 1.20 | 0.38 | <0.05 | 4.51 | 0.27 | 5.18 | 102.33 |
| 207.70 | 217.70 | 63.90 | 0.48 | 13.25 | 6.44 | 0.05 | 1.40 | 0.43 | <0.05 | 4.30 | 0.28 | 5.72 | 102.20 |
| 217.70 | 226.90 | 63.70 | 0.46 | 12.44 | 7.34 | 0.02 | 1.50 | 0.36 | 0.06 | 3.97 | 0.25 | 4.98 | 101.46 |
| 226.90 | 235.10 | 72.50 | 0.33 | 12.76 | 3.06 | 0.01 | 0.70 | 0.20 | <0.05 | 4.33 | 0.12 | 3.64 | 100.83 |
| 235.10 | 242.10 | 64.30 | 0.49 | 16.40 | 5.14 | 0.01 | 1.00 | 0.30 | 0.06 | 5.47 | 0.22 | 4.80 | 102.00 |
| 242.10 | 250.40 | 66.50 | 0.50 | 15.67 | 4.49 | 0.02 | 1.10 | 0.34 | 0.25 | 5.20 | 0.25 | 4.18 | 101.36 |
| 250.40 | 264.30 | 69.90 | 0.40 | 14.82 | 3.15 | 0.02 | 0.80 | 0.25 | 0.08 | 4.93 | 0.17 | 2.98 | 99.85 |
| 264.30 | 278.40 | 71.70 | 0.29 | 10.70 | 3.83 | 0.01 | 0.60 | 0.15 | 0.07 | 3.59 | 0.11 | 3.71 | 100.62 |

# ABERFOYLE RESOURCES LTD. DRILL LOG

**Area Code** mac
**Prospect** Mt.Charter
**Report Grid** Mack
**Dataset** Geochemical data set

**Holename** DDMA0032
**Stored Grid** Mack

| From | To | S % | P205/Ti | Altn.In |
|---|---|---|---|---|
| 0.00 | 13.70 | 6.60 | 0.48 | 94.84 |
| 13.70 | 17.30 | 8.80 | 0.28 | 92.89 |
| 17.30 | 23.50 | 6.35 | 0.44 | 98.15 |
| 23.50 | 25.20 | 8.40 | 0.32 | 91.77 |
| 25.20 | 29.90 | 7.95 | 0.42 | 91.95 |
| 29.90 | 32.20 | 7.35 | 0.43 | 89.63 |
| 32.20 | 35.10 | 3.80 | 0.29 | 99.20 |
| 35.10 | 48.30 | 5.10 | 0.40 | 98.71 |
| 48.30 | 56.60 | 3.70 | 0.42 | 99.86 |
| 56.60 | 62.80 | 2.10 | 0.39 | 97.18 |
| 62.80 | 74.00 | 0.37 | 0.45 | 99.48 |
| 74.00 | 85.00 | 0.83 | 0.42 | 95.84 |
| 85.00 | 100.50 | 1.00 | 0.51 | 97.92 |
| 100.50 | 114.50 | 3.40 | 0.50 | 96.32 |
| 114.50 | 123.00 | 3.05 | 0.46 | 95.06 |
| 123.00 | 131.80 | 3.70 | 0.59 | 95.39 |
| 131.80 | 141.20 | 4.05 | 0.58 | 93.20 |
| 141.20 | 148.70 | 2.80 | 0.51 | 92.44 |
| 148.70 | 156.80 | 9.28 | 0.53 | 90.51 |
| 156.80 | 165.00 | 4.20 | 0.55 | 95.16 |
| 165.00 | 172.80 | 4.40 | 0.55 | 92.94 |
| 172.80 | 180.00 | 4.95 | 0.55 | 89.29 |
| 180.00 | 186.80 | 4.35 | 0.57 | 90.00 |
| 186.80 | 194.60 | 3.10 | 0.57 | 91.53 |
| 194.60 | 207.70 | 3.70 | 0.57 | 94.54 |
| 207.70 | 217.70 | 4.60 | 0.59 | 93.75 |
| 217.70 | 226.90 | 2.90 | 0.55 | 92.87 |
| 226.90 | 235.10 | 2.20 | 0.38 | 97.10 |
| 235.10 | 242.10 | 3.65 | 0.45 | 94.73 |
| 242.10 | 250.40 | 2.60 | 0.51 | 91.44 |
| 250.40 | 264.30 | 1.95 | 0.43 | 94.55 |
| 264.30 | 278.40 | 3.25 | 0.37 | 95.01 |

655252 PAGE 1 OF 1

CORE GRIND SAMPLING

HOLE No. MAC32

DATE 8-1-93

| No. | SAMPLE NUMBER | INTERVAL | ELEMENTS REQUIRED | ST | SAMPLE NUMBER | INTERVAL | ELEMENTS REQUIRED | ST |
|---|---|---|---|---|---|---|---|---|
| 1 | 622301 | 0-13.7 | | | 622333 | 250.4-264.3 | | |
| 2 | 302 | 13.7-17.3 | | 3.6 | 622334 | 264.3-278.4 | | |
| 3 | 303 | 17.3-23.5 | | 6.2 | | | | |
| 4 | 304 | 23.5-25.2 | | 1.7 | | | | |
| 5 | 305 | 25.2-29.9 | | 4.7 | | | | |
| 6 | 306 | 29.9-32.2 | | 2.3 | | | | |
| 7 | 307 | STANDARD | | | | | | |
| 8 | 308 | 32.2-35.1 | | | | | | |
| 9 | 309 | 35.1-48.3 | | | | | | |
| 10 | 310 | 48.3-56.6 | | | | | | |
| 11 | 311 | 56.6-62.8 | | | | | | |
| 12 | 312 | 62.8-74.0 | | | | | | |
| 13 | 313 | 74.0-85.0 | | | | | | |
| 14 | 314 | 85.0-100.5 | | | | | | |
| 15 | 315 | 100.5-114.5 | | | | | | |
| 16 | 316 | 114.5-123.0 | | | | | | |
| 17 | 317 | 123.0-131.8 | | | | | | |
| 18 | 318 | 131.8-141.2 | | | | | | |
| 19 | 319 | 141.2-148.7 | | | | | | |
| 20 | 320 | 148.7-156.8 | | | | | | |
| 21 | 321 | STANDARD | | | | | | |
| 22 | 322 | 156.8-165.0 | | | | | | |
| 23 | 323 | 165.0-172.8 | | | | | | |
| 24 | 324 | 172.8-180.0 | | | | | | |
| 25 | 325 | 180.0-186.8 | | | | | | |
| 26 | 326 | 186.8-194.6 | | | | | | |
| 27 | 327 | 194.6-207.7 | | | | | | |
| 28 | 328 | 207.7-217.7 | | | | | | |
| 29 | 329 | 217.7-226.9 | | | | | | |
| 30 | 330 | 226.9-235.1 | | | | | | |
| 31 | 331 | 235.1-242.1 | | | | | | |
| 32 | 622332 | 242.1-250.4 | | | | | | |

655253

# ANALABS

A Division of Inchcape Inspection and Testing Services Australia Pty. Ltd. A.C.N. 004 591 664

Phone (004) 316837 | 14 Thirkell St. COOEE TAS 7320 | Fax (004) 318890

## ANALYTICAL REPORT No. 100560.60.09261

THIS REPORT MUST BE READ IN CONJUNCTION WITH THE ACCOMPANYING ANALYTICAL DATA

INVOICE TO:
Aberfoyle Resources Limited
Exploration Division
P.O. Box 952
BURNIE TAS 7320

| ORDER No. | PROJECT |
|---|---|
| 2163 | |

| DATE RECEIVED | RESULTS REQUIRED |
|---|---|
| 29/01/93 | ASAP |

| No. OF PAGES OF RESULTS | DATE REPORTED | No. OF COPIES | TOTAL No. OF SAMPLES |
|---|---|---|---|
| 6 | 09/03/93 | 1 | 34 |

| SAMPLE NUMBERS | SAMPLE DESCRIPTION | ELEMENT/METHOD |
|---|---|---|
| 622301/34 | CG Prep : GP031 | Cu,Pb,Zn,Ag/GA101, Ag/GA104 |
| | | Au,Au(R),Au(S)/GG309 |
| | | Ba,As,Cr,Zr/GX401, Ba/GX406 |
| | | Whole Rock Analysis/OX408 |

RESULTS TO
Mr R de Bomford
Aberfoyle Resources Limited
P.O. Box 952
BURNIE TAS 7320

RESULTS TO

RESULTS TO

REMARKS

MAC-32 GRINDS

AUTHORISED OFFICER

655254

# ANALABS

A Division of Inchcape Testing Services (Australia) Pty. Ltd.
A.C.N. 004 591 664

# ANALYTICAL DATA

| SAMPLE PREFIX | REPORT No. | REPORT DATE | CLIENT ORDER No. | PAGE |
|---|---|---|---|---|
| | 100560.60.09261 | 09/03/93 | 2163 | 1 OF 6 |

| BE No. | SAMPLE No. | Depth | Cu | Pb | Zn | Ag | Ag | Au | Au(R) | Au(S) | Ba |
|---|---|---|---|---|---|---|---|---|---|---|---|
| 1 | 622301 | 0 | 76 | 13 | 324 | 17 | - | 0.156 | - | - | - |
| 2 | 622302 | 13.7 | 106 | 9 | 1869 | - | 31 | 0.318 | - | - | - |
| 3 | 622303 | 17.3 | 108 | 45 | 1302 | - | 20 | 0.370 | - | - | - |
| 4 | 622304 | 23.5 | 240 | 20 | 3584 | 0.27 | 64 | 1.200 | 0.55 | - | - |
| 5 | 622305 | 25.2 | 268 | 46 | 4262 | - | 34 | 0.569 | - | 0.581 | - |
| 6 | 622306 | 29.9 | 268 | 64 | 3723 | - | 34 | 0.878 | - | - | - |
| 7 | 622307 | 32.2 STD | 125 | 185 | 2289 | <2 | - | 0.011 | - | - | 1139 |
| 8 | 622308 | 35.1 | 47 | 14 | 84 | 3 | - | 0.036 | - | - | 3503 |
| 9 | 622309 | | 77 | 43 | 126 | 2 | - | 0.022 | - | - | 1227 |
| 10 | 622310 | | 58 | 36 | 217 | <2 | - | 0.021 | - | - | 1486 |
| 11 | 622311 | | 74 | 39 | 230 | <2 | - | 0.012 | - | - | 740 |
| 12 | 622312 | | 45 | <5 | 223 | <2 | - | 0.010 | 0.012 | - | 863 |
| 13 | 622313 | | 54 | 16 | 229 | <2 | - | 0.011 | - | - | 882 |
| 14 | 622314 | | 49 | <5 | 237 | <2 | - | 0.019 | - | - | - |
| 15 | 622315 | | 55 | 12 | 94 | <2 | - | 0.011 | - | - | 1346 |
| 16 | 622316 | | 74 | 9 | 136 | <2 | - | 0.022 | - | - | 2959 |
| 17 | 622317 | | 69 | 11 | 73 | 2 | - | 0.055 | - | - | 2019 |
| 18 | 622318 | | 117 | 52 | 1743 | 5 | - | 0.106 | - | - | - |
| 19 | 622319 | | 156 | 21 | 195 | 2 | - | 0.181 | - | - | 4516 |
| 20 | 622320 | | 171 | 21 | 1469 | 8 | - | 0.320 | - | - | - |
| 21 | 622321 | STD | 123 | 190 | 2230 | <2 | - | 0.008 | - | - | 1062 |
| 22 | 622322 | | 104 | 68 | 170 | 4 | - | 0.467 | 0.467 | - | 2362 |
| 23 | 622323 | | 118 | 56 | 197 | 3 | - | 0.347 | - | - | 4149 |
| 24 | 622324 | | 163 | 17 | 698 | 5 | - | 0.442 | - | 0.450 | - |
| 25 | 622325 | | 255 | 24 | 1346 | 4 | - | 0.361 | - | - | - |

Results in ppm unless otherwise specified
T = element present; but concentration too low to measure
X = element concentration is below detection limit
- = element not determined

AUTHORISED OFFICER

655255

# ANALABS

A Division of Inchcape Testing Services (Australia) Pty. Ltd.
A.C.N. 004 591 664

## ANALYTICAL DATA

| SAMPLE PREFIX | REPORT No. | REPORT DATE | CLIENT ORDER No. | PAGE |
|---|---|---|---|---|
| | 100560.60.09261 | 09/03/93 | 2163 | 2 OF 6 |

| IBE No. | SAMPLE No. | Cu | Pb | Zn | Ag | Ag | Au | Au(R) | Au(S) | Ba |
|---|---|---|---|---|---|---|---|---|---|---|
| 1 | 622326 | 190 | 50 | 378 | 3 | - | 0.584 | - | - | - |
| 2 | 622327 | 417 | 53 | 326 | 2 | - | 0.540 | - | - | 4320 |
| 3 | 622328 | 536 | 22 | 594 | 2 | - | 0.353 | - | - | - |
| 4 | 622329 | 168 | 7 | 249 | <2 | - | 0.484 | - | - | - |
| 5 | 622330 | 72 | 19 | 155 | <2 | - | 0.266 | - | - | - |
| 6 | 622331 | 57 | 18 | 65 | <2 | - | 0.047 | - | - | 2112 |
| 7 | 622332 | 100 | 155 | 431 | <2 | - | 0.086 | - | - | 2836 |
| 8 | 622333 | 113 | 32 | 243 | 7 | - | 0.093 | - | - | 3779 |
| 9 | 622334 | 155 | <5 | 162 | <2 | - | 0.377 | - | - | - |
| 10 | | | | | | | | | | |
| 11 | | | | | | | | | | |
| 12 | | | | | | | | | | |
| 13 | | | | | | | | | | |
| 14 | | | | | | | | | | |
| 15 | | | | | | | | | | |
| 16 | | | | | | | | | | |
| 17 | | | | | | | | | | |
| 18 | | | | | | | | | | |
| 19 | | | | | | | | | | |
| 20 | | | | | | | | | | |
| 21 | | | | | | | | | | |
| 22 | | | | | | | | | | |
| 23 | DETECTION | 4 | 5 | 4 | 2 | 10 | 0.008 | 0.008 | 0.008 | 10 |
| 24 | UNITS | ppm | ppm | ppm | ppm | ppm | ppm | ppm | ppm | ppm |
| 25 | METHOD | GA101 | GA101 | GA101 | GA101 | GA104 | GG309 | GG309 | GG309 | GX401 |

Results in ppm unless otherwise specified
T = element present; but concentration too low to measure
X = element concentration is below detection limit
- = element not determined

AUTHORISED OFFICER

655256

# ANALABS

A Division of Inchcape Testing Services (Australia) Pty. Ltd.
A.C.N. 004 591 664

# ANALYTICAL DATA

| SAMPLE PREFIX | REPORT No. | REPORT DATE | CLIENT ORDER No. | PAGE |
|---|---|---|---|---|
| | 100560.60.09261 | 09/03/93 | 2163 | 3 OF 6 |

| TUBE No. | SAMPLE No. | Ba | As | Cr | Zr | Ti | S | Al2O3 | SiO2 | TiO2 |
|---|---|---|---|---|---|---|---|---|---|---|
| 1 | 622301 | 1.43 | 670 | 14 | 178 | 3141 | 6.600 | 14.56 | 59.7 | 0.52 |
| 2 | 622302 | 15.21 | 613 | 17 | 143 | 2222 | 8.800 | 8.33 | 48.5 | 0.37 |
| 3 | 622303 | 1.59 | 440 | 17 | 152 | 2824 | 6.350 | 13.03 | 62.4 | 0.47 |
| 4 | 622304 | 14.13 | 858 | 17 | 142 | 2278 | 8.400 | 8.92 | 49.0 | 0.38 |
| 5 | 622305 | 9.25 | 991 | 12 | 138 | 2400 | 7.950 | 9.97 | 54.2 | 0.40 |
| 6 | 622306 | 5.62 | 642 | 15 | 135 | 2219 | 7.350 | 10.44 | 59.2 | 0.37 |
| 7 | 622307 | - | 20 | 973 | 86 | 2677 | 0.035 | 15.13 | 51.4 | 0.45 |
| 8 | 622308 | - | 252 | 33 | 223 | 3209 | 3.800 | 17.88 | 61.6 | 0.54 |
| 9 | 622309 | - | 304 | 15 | 209 | 2808 | 5.100 | 16.44 | 61.4 | 0.47 |
| 10 | 622310 | - | 150 | 18 | 200 | 2801 | 3.700 | 16.53 | 63.0 | 0.47 |
| 11 | 622311 | - | 62 | 36 | 204 | 2962 | 2.100 | 17.14 | 61.9 | 0.49 |
| 12 | 622312 | - | 52 | 35 | 187 | 2702 | 0.370 | 16.62 | 65.8 | 0.45 |
| 13 | 622313 | - | 87 | 28 | 189 | 2818 | 0.830 | 16.61 | 64.7 | 0.47 |
| 14 | 622314 | 1.59 | 44 | 17 | 209 | 2583 | 1.000 | 15.55 | 64.3 | 0.43 |
| 15 | 622315 | - | 228 | 24 | 172 | 2404 | 3.400 | 14.68 | 66.2 | 0.40 |
| 16 | 622316 | - | 118 | 15 | 178 | 2537 | 3.050 | 14.50 | 68.1 | 0.42 |
| 17 | 622317 | - | 160 | 6 | 159 | 2579 | 3.700 | 14.31 | 67.6 | 0.43 |
| 18 | 622318 | 2.56 | 234 | 8 | 153 | 2462 | 4.050 | 12.98 | 66.0 | 0.41 |
| 19 | 622319 | - | 207 | 15 | 154 | 2968 | 2.800 | 13.65 | 69.5 | 0.50 |
| 20 | 622320 | 4.23 | 402 | 14 | 156 | 2703 | 9.280 | 12.04 | 64.2 | 0.45 |
| 21 | 622321 | - | 18 | 935 | 85 | 2701 | 0.035 | 15.09 | 51.5 | 0.45 |
| 22 | 622322 | - | 357 | 9 | 148 | 2739 | 4.200 | 13.43 | 67.7 | 0.46 |
| 23 | 622323 | - | 279 | 6 | 158 | 2743 | 4.400 | 13.56 | 66.6 | 0.46 |
| 24 | 622324 | 2.67 | 314 | 11 | 152 | 2477 | 4.950 | 11.62 | 65.5 | 0.41 |
| 25 | 622325 | 4.02 | 226 | 9 | 154 | 2336 | 4.350 | 11.30 | 65.5 | 0.39 |

Results in ppm unless otherwise specified
T = element present; but concentration too low to measure
X = element concentration is below detection limit
- = element not determined

AUTHORISED OFFICER

655257

**ANALABS**

A Division of Inchcape Testing Services (Australia) Pty. Ltd.
A.C.N. 004 591 664

# ANALYTICAL DATA

| SAMPLE PREFIX | REPORT No. | REPORT DATE | CLIENT ORDER No. | PAGE |
|---|---|---|---|---|
| | 100560.60.09261 | 09/03/93 | 2163 | 4 OF 6 |

| TUE No. | SAMPLE No. | Ba | As | Cr | Zr | Ti | S | Al2O3 | SiO2 | TiO2 |
|---|---|---|---|---|---|---|---|---|---|---|
| 1 | 622326 | 1.00 | 174 | <5 | 164 | 2758 | 3.100 | 13.89 | 67.2 | 0.46 |
| 2 | 622327 | - | 189 | <5 | 154 | 2789 | 3.700 | 13.98 | 66.3 | 0.47 |
| 3 | 622328 | 1.12 | 195 | 9 | 168 | 2904 | 4.600 | 13.25 | 63.9 | 0.48 |
| 4 | 622329 | 3.05 | 147 | 16 | 165 | 2766 | 2.900 | 12.44 | 63.7 | 0.46 |
| 5 | 622330 | 0.82 | 115 | 5 | 194 | 1955 | 2.200 | 12.76 | 72.5 | 0.33 |
| 6 | 622331 | - | 45 | 73 | 179 | 2944 | 3.650 | 16.40 | 64.3 | 0.49 |
| 7 | 622332 | - | 91 | 111 | 147 | 3032 | 2.600 | 15.67 | 66.5 | 0.50 |
| 8 | 622333 | - | 108 | 58 | 180 | 2409 | 1.950 | 14.82 | 69.9 | 0.40 |
| 9 | 622334 | 2.36 | 130 | 6 | 176 | 1724 | 3.250 | 10.70 | 71.7 | 0.29 |
| 10 | | | | | | | | | | |
| 11 | | | | | | | | | | |
| 12 | | | | | | | | | | |
| 13 | | | | | | | | | | |
| 14 | | | | | | | | | | |
| 15 | | | | | | | | | | |
| 16 | | | | | | | | | | |
| 17 | | | | | | | | | | |
| 18 | | | | | | | | | | |
| 19 | | | | | | | | | | |
| 20 | | | | | | | | | | |
| 21 | | | | | | | | | | |
| 22 | | | | | | | | | | |
| 23 | DETECTION | 0.01 | 2 | 5 | 5 | 60 | 0.005 | 0.05 | 0.1 | 0.01 |
| 24 | UNITS | % | ppm | ppm | ppm | ppm | % | % | % | % |
| 25 | METHOD | GX406 | GX401 | GX401 | GX401 | OX408 | OX408 | OX408 | OX408 | OX408 |

Results in ppm unless otherwise specified
*T = element present; but concentration too low to measure*
X = element concentration is below detection limit
– = element not determined

AUTHORISED OFFICER

655258

# ANALABS

A Division of Inchcape Testing Services (Australia) Pty. Ltd.
A.C.N. 004 591 664

## ANALYTICAL DATA

| SAMPLE PREFIX | REPORT No. | REPORT DATE | CLIENT ORDER No. | PAGE |
|---|---|---|---|---|
| | 100560.60.09261 | 09/03/93 | 2163 | 5 OF 6 |

| TU No. | SAMPLE No. | Fe2O3 | MnO | CaO | K2O | MgO | P2O5 | Na2O | LOI | TOTAL |
|---|---|---|---|---|---|---|---|---|---|---|
| 1 | 622301 | 7.58 | 0.02 | 0.27 | 5.17 | 0.9 | 0.251 | 0.06 | 7.24 | 104.44 |
| 2 | 622302 | 6.40 | 0.06 | 0.10 | 2.93 | 0.6 | 0.104 | 0.17 | 7.23 | 100.53 |
| 3 | 622303 | 7.14 | 0.02 | 0.15 | 4.51 | 0.8 | 0.208 | <0.05 | 6.56 | 103.41 |
| 4 | 622304 | 6.66 | 0.03 | 0.12 | 3.19 | 0.6 | 0.120 | 0.22 | 8.03 | 101.48 |
| 5 | 622305 | 7.21 | 0.02 | 0.15 | 3.40 | 0.6 | 0.169 | 0.20 | 7.20 | 101.81 |
| 6 | 622306 | 6.84 | 0.02 | 0.14 | 3.71 | 0.7 | 0.160 | 0.37 | 6.32 | 101.88 |
| 7 | 622307 | 9.85 | 0.87 | 3.87 | 1.27 | 7.5 | 0.197 | 3.53 | 5.30 | 99.53 |
| 8 | 622308 | 5.15 | 0.01 | 0.01 | 6.22 | 1.2 | 0.157 | 0.05 | 5.64 | 102.61 |
| 9 | 622309 | 6.64 | 0.01 | 0.03 | 5.68 | 1.2 | 0.188 | 0.06 | 6.52 | 103.92 |
| 10 | 622310 | 5.66 | 0.01 | 0.06 | 5.40 | 1.9 | 0.197 | <0.05 | 5.83 | 102.96 |
| 11 | 622311 | 5.72 | 0.03 | 0.17 | 4.76 | 3.5 | 0.191 | 0.07 | 5.51 | 101.70 |
| 12 | 622312 | 4.71 | 0.04 | 0.09 | 4.63 | 3.0 | 0.201 | <0.05 | 4.38 | 100.38 |
| 13 | 622313 | 4.92 | 0.04 | 0.18 | 4.70 | 2.9 | 0.198 | 0.15 | 4.46 | 100.22 |
| 14 | 622314 | 4.38 | 0.03 | 0.09 | 4.35 | 3.2 | 0.221 | 0.07 | 4.77 | 100.21 |
| 15 | 622315 | 5.81 | 0.02 | 0.29 | 4.99 | 1.3 | 0.201 | <0.05 | 4.92 | 102.38 |
| 16 | 622316 | 4.75 | 0.01 | 0.24 | 5.16 | 1.0 | 0.194 | 0.08 | 4.44 | 102.28 |
| 17 | 622317 | 4.97 | 0.01 | 0.33 | 4.90 | 0.9 | 0.255 | <0.05 | 4.84 | 102.50 |
| 18 | 622318 | 4.46 | 0.01 | 0.32 | 4.27 | 0.8 | 0.237 | 0.05 | 4.34 | 100.83 |
| 19 | 622319 | 4.16 | 0.01 | 0.32 | 4.97 | 0.9 | 0.257 | 0.16 | 4.24 | 102.00 |
| 20 | 622320 | 4.64 | 0.02 | 0.32 | 4.16 | 0.8 | 0.240 | 0.20 | 4.92 | 105.94 |
| 21 | 622321 | 9.83 | 0.87 | 3.83 | 1.28 | 7.6 | 0.200 | 3.56 | 5.21 | 99.57 |
| 22 | 622322 | 5.56 | 0.02 | 0.34 | 4.70 | 1.0 | 0.251 | <0.05 | 4.89 | 102.79 |
| 23 | 622323 | 5.66 | 0.02 | 0.36 | 4.69 | 1.1 | 0.254 | 0.08 | 5.11 | 102.72 |
| 24 | 622324 | 5.56 | 0.04 | 0.54 | 4.02 | 0.9 | 0.227 | 0.05 | 5.40 | 102.16 |
| 25 | 622325 | 4.49 | 0.05 | 0.43 | 3.88 | 0.8 | 0.222 | 0.09 | 5.67 | 101.61 |

Results in ppm unless otherwise specified
T = element present; but concentration too low to measure
X = element concentration is below detection limit
– = element not determined

AUTHORISED OFFICER

655259

# ANALABS

A Division of Inchcape Testing Services (Australia) Pty. Ltd.
A.C.N. 004 591 664

## ANALYTICAL DATA

| SAMPLE PREFIX | REPORT No. | REPORT DATE | CLIENT ORDER No. | PAGE |
|---|---|---|---|---|
| | 100560.60.09261 | 09/03/93 | 2163 | 6 OF 6 |

| TU No. | SAMPLE No. | Fe2O3 | MnO | CaO | K2O | MgO | P2O5 | Na2O | LOI | TOTAL |
|---|---|---|---|---|---|---|---|---|---|---|
| 1 | 622326 | 4.94 | 0.03 | 0.37 | 4.62 | 1.0 | 0.264 | 0.15 | 4.90 | 102.06 |
| 2 | 622327 | 5.82 | 0.02 | 0.38 | 4.51 | 1.2 | 0.266 | <0.05 | 5.18 | 102.33 |
| 3 | 622328 | 6.44 | 0.05 | 0.43 | 4.30 | 1.4 | 0.284 | <0.05 | 5.72 | 102.20 |
| 4 | 622329 | 7.34 | 0.02 | 0.36 | 3.97 | 1.5 | 0.252 | 0.06 | 4.98 | 101.46 |
| 5 | 622330 | 3.06 | 0.01 | 0.20 | 4.33 | 0.7 | 0.124 | <0.05 | 3.64 | 100.83 |
| 6 | 622331 | 5.14 | 0.01 | 0.30 | 5.47 | 1.0 | 0.219 | 0.06 | 4.80 | 102.00 |
| 7 | 622332 | 4.49 | 0.02 | 0.34 | 5.20 | 1.1 | 0.253 | 0.25 | 4.18 | 101.36 |
| 8 | 622333 | 3.15 | 0.02 | 0.25 | 4.93 | 0.8 | 0.173 | 0.08 | 2.98 | 99.85 |
| 9 | 622334 | 3.83 | 0.01 | 0.15 | 3.59 | 0.6 | 0.107 | 0.07 | 3.71 | 100.62 |
| 10 | | | | | | | | | | |
| 11 | | | | | | | | | | |
| 12 | | | | | | | | | | |
| 13 | | | | | | | | | | |
| 14 | | | | | | | | | | |
| 15 | | | | | | | | | | |
| 16 | | | | | | | | | | |
| 17 | | | | | | | | | | |
| 18 | | | | | | | | | | |
| 19 | | | | | | | | | | |
| 20 | | | | | | | | | | |
| 21 | | | | | | | | | | |
| 22 | | | | | | | | | | |
| 23 | DETECTION | 0.01 | 0.01 | 0.01 | 0.01 | 0.1 | 0.005 | 0.05 | 0.01 | 0.01 |
| 24 | UNITS | % | % | % | % | % | % | % | % | % |
| 25 | METHOD | OX408 | OX408 | OX408 | OX408 | OX408 | OX408 | OX408 | OX408 | OX408 |

Results in ppm unless otherwise specified
T = element present; but concentration too low to measure
X = element concentration is below detection limit
– = element not determined

AUTHORISED OFFICER

# APPENDIX VI

# ABERFOYLE RESOURCES LTD. DRILL LOG

## MINES DEPARTMENT REPORT HEADER PAGE

**Drillhole Database name: mac**

**Report Grid: Mack**

**Report Legend follows:**

Collar Coordinate Reliability Flags

s = surveyed
m = measured
e = estimated

Assay, Composite, Geochem Bad Data Flag

Any element data that is bad will be recognised by an attached asterisk
example: 2.41*

# ABERFOYLE RESOURCES LTD. DRILL LOG

| Area Code | Prospect | Report Grid | Dataset |
|---|---|---|---|
| mac | Mt. Charter | Mack | Header data set |

| Holename | Stored Grid |
|---|---|
| DDMA0033 | Mack |

**Hole Depth**
910.70

| Collar Easting | Collar Northing | Collar RL | Collar Depth |
|---|---|---|---|
| 3719.700s | 4534.900s | 800.70s | .00 |

| 1st Survey Depth | Survey Dip | Survey Azimuth | Survey Instrument |
|---|---|---|---|
| .00 | -70.00 | 66.00 | clinometer |

| Start Date and Time | End Date & Time |
|---|---|
| 08/01/1993 | 18/02/1993 |

| Geologist | Hole Objective |
|---|---|
| S.Richardson | Structural Targ |

| Work Proposal | Tenement |
|---|---|
| | E.L.106/87 |

655263

# ABERFOYLE RESOURCES LTD. DRILL LOG

| Area Code | Prospect | Report Grid | Dataset |
|---|---|---|---|
| mac | Mt. Charter | AMG | Header data set |

| Holename | Stored Grid |
|---|---|
| DDMA0033 | Mack |

**Hole Depth**
910.70

| Collar Easting | Collar Northing | Collar RL | Collar Depth |
|---|---|---|---|
| 389124.801s | 5391483.872s | 800.70s | .00 |

| 1st Survey Depth | Survey Dip | Survey Azimuth | Survey Instrument |
|---|---|---|---|
| .00 | -70.00 | 88.10 | clinometer |

| Start Date and Time | End Date & Time |
|---|---|
| 08/01/1993 | 18/02/1993 |

| Geologist | Hole Objective |
|---|---|
| S.Richardson | Structural Targ |

| Work Proposal | Tenement |
|---|---|
| | E.L.106/87 |

655264

# ABERFOYLE RESOURCES LTD. DRILL LOG

| Area Code | Prospect | Report Grid | Dataset |
|---|---|---|---|
| mac | Mt. Charter | Mack | Survey data set |

| Holename | Stored Grid |
|---|---|
| DDMA0033 | Mack |

| Depth | Dip | Azi | Instrument |
|---|---|---|---|
| 0.00 | -70.00i | 66.00i | clinometer |
| 25.00 | -70.00i | 66.00i | eastman |
| 50.00 | -70.00i | 66.00i | eastman |
| 75.00 | -71.00i | 66.50i | eastman |
| 100.00 | -70.00i | 69.25i | eastman |
| 125.00 | -69.75i | 69.50i | eastman |
| 150.00 | -69.25i | 69.50i | eastman |
| 175.00 | -69.00i | 70.00i | eastman |
| 200.00 | -68.50i | 70.00i | eastman |
| 225.00 | -68.25i | 71.00i | eastman |
| 250.00 | -68.25i | 72.00i | eastman |
| 275.00 | -67.00i | 72.00i | eastman |
| 300.00 | -66.50i | 70.50i | eastman |
| 325.00 | -66.75i | 69.50i | eastman |
| 350.00 | -66.50i | 70.00i | eastman |
| 375.00 | -67.00i | 70.50i | eastman |
| 400.00 | -67.00i | 70.50i | eastman |
| 425.00 | -67.00i | 70.50i | eastman |
| 450.00 | -67.00i | 71.00i | eastman |
| 475.00 | -67.00i | 71.50i | eastman |
| 500.00 | -66.50i | 72.00i | eastman |
| 525.00 | -66.00i | 72.50i | eastman |
| 550.00 | -65.75i | 73.00i | eastman |
| 575.00 | -65.50i | 73.75i | eastman |
| 600.00 | -65.00i | 75.75i | eastman |
| 625.00 | -65.00i | 78.00i | eastman |
| 650.00 | -64.50i | 79.00i | eastman |
| 675.00 | -64.50i | 79.75i | eastman |
| 700.00 | -64.25i | 80.00i | eastman |
| 725.00 | -64.25i | 80.00i | eastman |
| 750.00 | -64.25i | 80.50i | eastman |
| 775.00 | -64.25i | 81.00i | eastman |
| 800.00 | -64.00i | 82.00i | eastman |
| 825.00 | -64.00i | 83.00i | eastman |
| 850.00 | -64.00i | 84.00i | eastman |
| 875.00 | -64.00i | 85.00i | eastman |
| 900.00 | -64.00i | 85.00i | eastman |
| 910.70 | -64.00i | 85.00i | eastman |

# ABERFOYLE RESOURCES LTD. DRILL LOG

| Area Code | Prospect | Report Grid | Dataset |
|---|---|---|---|
| mac | Mt. Charter | Mack | Drill log data set |

| Holename | Stored Grid |
|---|---|
| DDMA0033 | Mack |

| Item # | From | To | Contractor | Drill Rig | Drill Method | ID |
|---|---|---|---|---|---|---|
| 1.00 | 0.00 | 1.50 | Longyear | Longyear HD 44 | Tricone | 118 |
| 2.00 | 1.50 | 232.90 | Longyear | Longyear HD 44 | Diamond | 96 |
| 3.00 | 232.90 | 910.70 | Longyear | Longyear HD 44 | Diamond | 75 |

# ABERFOYLE RESOURCES LTD. DRILL LOG

| Area Code | Prospect | Report Grid | Dataset |
|---|---|---|---|
| mac | Mt. Charter | Mack | Casing log data set |

| Holename | Stored Grid |
|---|---|
| DDMA0033 | Mack |

| Item | From | To | Casing Type | ID | L | Comments |
|---|---|---|---|---|---|---|
| 1.00 | 0.00 | 1.50 | HQ | 77.8 | y | ? |
| 2.00 | 0.00 | 910.70 | 40mm Cl.18 PVC | 40mm | y | ? |

# Aberfoyle Resources Limited

EXPLORATION DIVISION

HOLE No. MAC 33

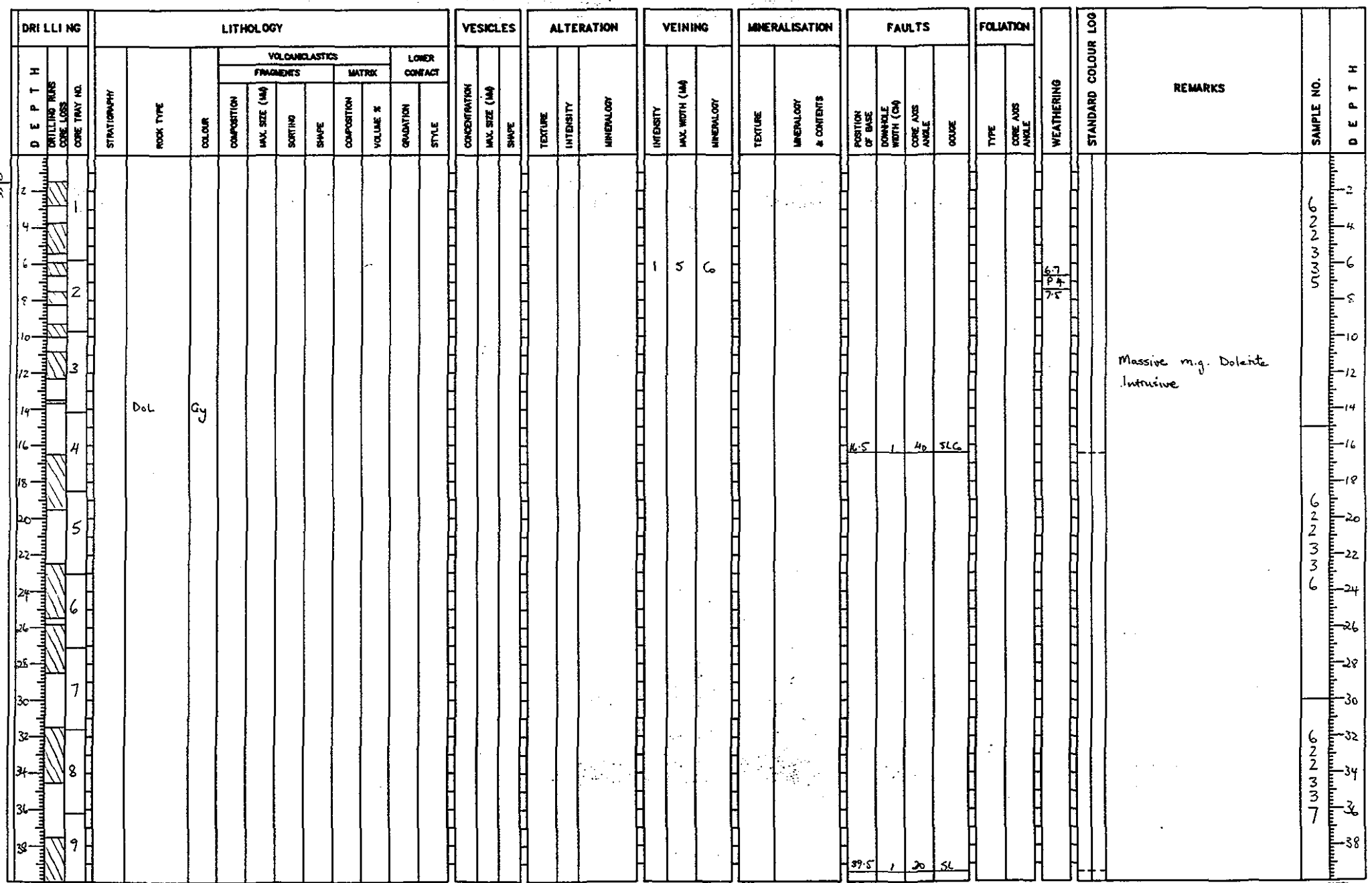
PAGE 1 OF 23

GEO. SL

DATE 20-1-93

5 cm

# DIAMOND DRILL LOG




65522

log31931.mor

# Aberfoyle Resources Limited

EXPLORATION DIVISION

HOLE No. MAC 33

PAGE 2 OF 23

GEO. SR

DATE 20-1-93

5 cm

# DIAMOND DRILL LOG

| DRILLING | | | LITHOLOGY | | | | | | | | | | | VESICLES | | | ALTERATION | | | VEINING | | | MINERALISATION | | FAULTS | | | | FOLIATION | | WEATHERING | STANDARD COLOUR LOG | REMARKS | SAMPLE NO. | DEPTH |
|---|---|---|---|---|---|---|---|---|---|---|---|---|---|---|---|---|---|---|---|---|---|---|---|---|---|---|---|---|---|---|---|---|---|---|
| DEPTH | DRILLING RUNS | CORE LOSS | STRATIGRAPHY | ROCK TYPE | COLOUR | VOLCANICLASTICS: FRAGMENTS: COMPOSITION | FRAGMENTS: MAX. SIZE (MM) | FRAGMENTS: SORTING | FRAGMENTS: SHAPE | MATRIX: COMPOSITION | MATRIX: VOLUME % | LOWER CONTACT: GRADATION | LOWER CONTACT: STYLE | CONCENTRATION | MAX. SIZE (MM) | SHAPE | TEXTURE | INTENSITY | MINERALOGY | INTENSITY | MAX. WIDTH (MM) | MINERALOGY | TEXTURE | MINERALOGY & CONTENTS | POSITION OF BASE | DOWNHOLE WIDTH (CM) | CORE AXIS ANGLE | GOUGE | TYPE | CORE AXIS ANGLE | | | | | |
| 42 | | 10 | | | | | | | | | | | | | | | | | | | | | | | | | | | | | | | | 42 |
| 44 | | | | | | | | | | | | | | | | | | | | | | | | | | | | | | | | | | 44 |
| 46 | | | | | | | | | | | | | | | | | | | | | | | | | | | | | | | | | 6223388 | 46 |
| 48 | | 11 | | | | | | | | | | | | | | | | | | | | | | | | | | | | | | | | 48 |
| 50 | | | | | | | | | | | | | | | | | | | | | | | | | | | | | | | | | | 50 |
| 52 | | 12 | | | | | | | | | | | | | | | | | | | | | | | | | | | | | | | | 52 |
| 54 | | | | DoL | Gy | | | | | | | | | | | | | | | 1 | 5 | G | | | | | | | | | | | | 54 |
| 56 | | 13 | | | | | | | | | | | | | | | | | | | | | | | | | | | | | | | | 56 |
| 58 | | | | | | | | | | | | | | | | | | | | | | | | | 58.4 | 40 | ? | Ru | | | | | | 58 |
| 60 | | 14 | | | | | | | | | | | | | | | | | | | | | | | | | | | | | | | 6223389 | 60 |
| 62 | | | | | | | | | | | | | | | | | | | | | | | | | | | | | | | | | | 62 |
| 64 | | 15 | | | | | | | | | | | | | | | | | | | | | | | | | | | | | | | | 64 |
| 66 | | | | | | | | | | | | | | | | | | | | | | | | | | | | | | | | | | 66 |
| 68 | | 16 | | | | | | | | | | | | | | | | | | | | | | | | | | | | | | | | 68 |
| 70 | | | | | | | | | | | | | | | | | | | | | | | | | | | | | | | | | | 70 |
| 72 | | | | | | | | | | | | | | | | | | | | | | | | | | | | | | | | | | 72 |
| 74 | | 17 | | 73.6 | | | | | | | | 90 | I | | | | | | | | | | 73.6 | | 74.5 | 90 | 30? | Ru60 | | | | | Chilled margin of a few cm. in dk. shale is below. | | 74 |
| 76 | | | | SW | Bk | | | | | | | S | | | | | | | | | | | Ds, No, Bt | Py3 | | | | | Bt | 80° | | | | | 76 |
| 78 | | 18 | QRS | 77.55 | | | | | | | | S | C | | | | | | | | | | 77.55 | | | | | | 75.0 | | | | | | 78 |
| | | | | 77.7 | | | | | | | | S | C | | | | | | | | | | 77.7 | | | | | | Bt | 70° | | | | | |
| | | | | SW | Bk | | | | | | | | | | | | | | | | | | Ds, Bt | Py3 | | | | | 77.6 | | | | | | |

6555698

log@1993Laser

# Aberfoyle Resources Limited

EXPLORATION DIVISION

HOLE No. MAC 33

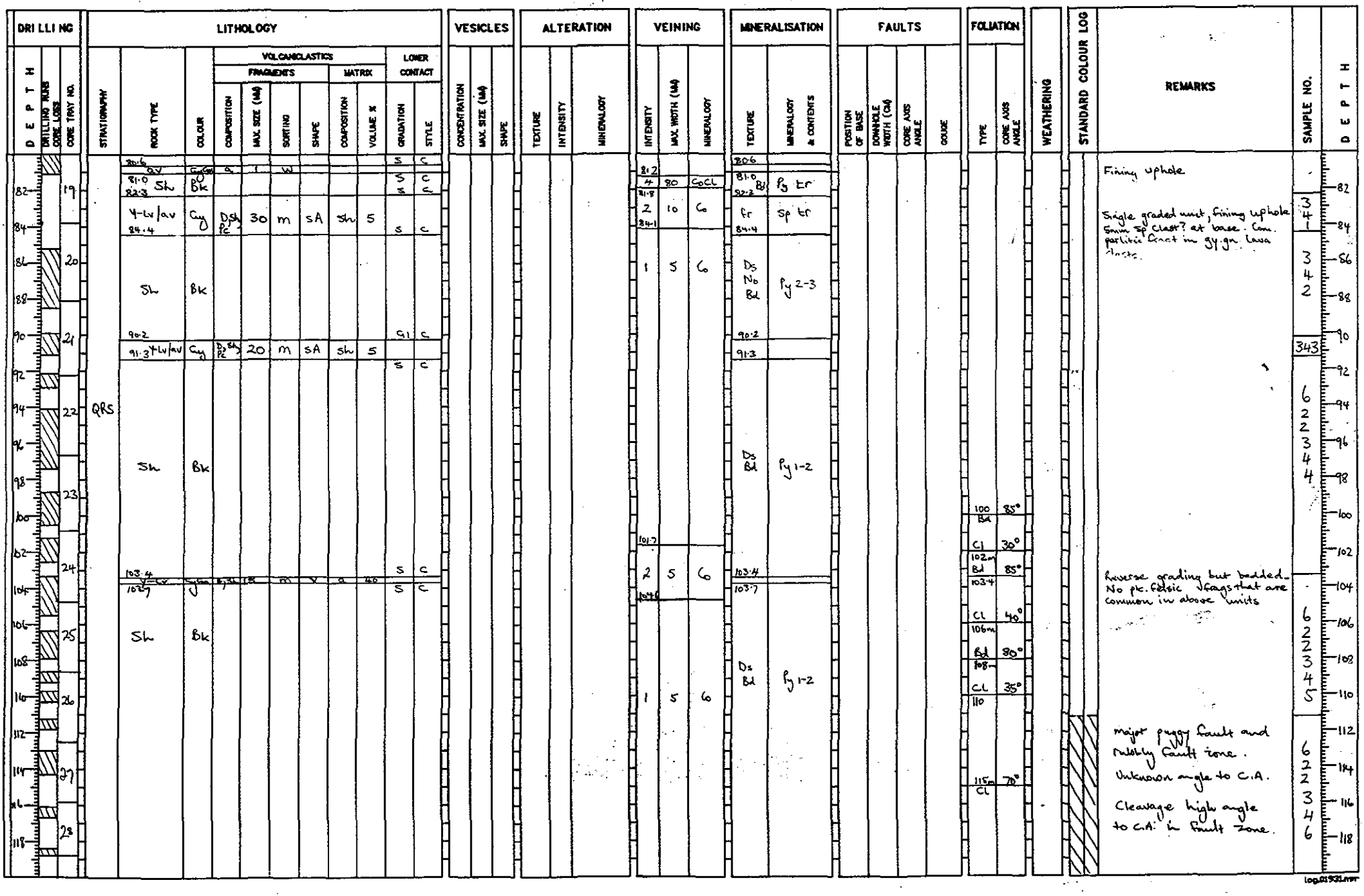
PAGE 3 OF 23

GEO. SR

DATE 20-1-93

5 cm

# DIAMOND DRILL LOG




6552369

# Aberfoyle Resources Limited

EXPLORATION DIVISION

HOLE No. MAC33

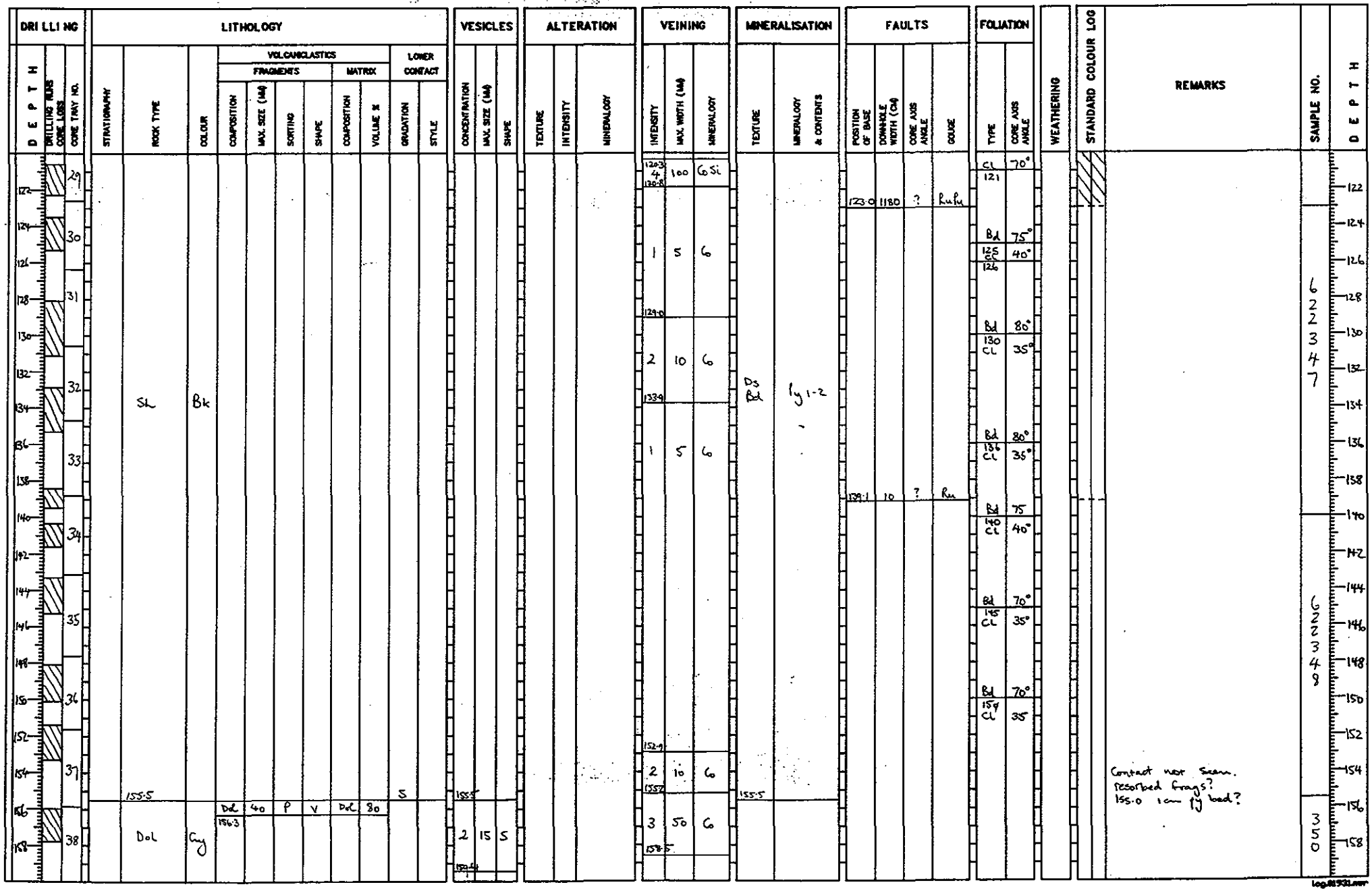
PAGE 4 OF 23

GEO. SR

DATE 26-1-93

5 cm

# DIAMOND DRILL LOG



# Aberfoyle Resources Limited

EXPLORATION DIVISION

HOLE No. MAC 33

PAGE 5 OF 23

GEO. SK

DATE 26-1-93

5 cm

# DIAMOND DRILL LOG

| DRILLING | | | LITHOLOGY | | | | | | | | | | VESICLES | | | ALTERATION | | | VEINING | | | MINERALISATION | | FAULTS | | | | FOLIATION | | WEATHERING | STANDARD COLOUR LOG | REMARKS | SAMPLE NO. | DEPTH |
|---|---|---|---|---|---|---|---|---|---|---|---|---|---|---|---|---|---|---|---|---|---|---|---|---|---|---|---|---|---|---|---|---|---|
| | | | | | | VOLCANICLASTICS | | | | | | LOWER CONTACT | | | | | | | | | | | | | | | | | | | | | |
| | | | | | | FRAGMENTS | | | | MATRIX | | | | | | | | | | | | | | | | | | | | | | | |
| DEPTH | DRILLING RUNS CORE LOSS | CORE TRAY NO. | STRATIGRAPHY | ROCK TYPE | COLOUR | COMPOSITION | MAX. SIZE (MM) | SORTING | SHAPE | COMPOSITION | VOLUME % | GRADATION | STYLE | CONCENTRATION | MAX. SIZE (MM) | SHAPE | TEXTURE | INTENSITY | MINERALOGY | INTENSITY | MAX. WIDTH (MM) | MINERALOGY | TEXTURE | MINERALOGY & CONTENTS | POSITION OF BASE | DOWNHOLE WIDTH (CM) | CORE AXIS ANGLE | GOUGE | TYPE | CORE AXIS ANGLE | | | | |
| 162 | | 39 | | | | | | | | | | | | | | | | | | | | | | | | | | | | | | | 162 |
| 164 | | | | DoL | GD | | | | | | | | | | | | | | 2 | 200 | G | | | | | | | | | | | | 164 |
| 166 | | 40 | | | | | | | | | | | | | | | | | | | | | | | | | | | | | | | 166 |
| 168 | | | | | | | | | | | | | | | | | | | | | | | | | | | | | | | | | 168 |
| 170 | | | | | | | | | | | | S | | K98 1 | 3 | S | | | | | | | 170·5 | | | | | | | | | 170 |
| | | 41 | | 170·5 | | | | | | | | | | 170·5 | | | | | 170·9 | | | | | | | | | | | | | |
| 172 | | | | | | | | | | | | | | | | | | | | | | | | | | | | | BL | 85° | | Contact not seen | 172 |
| 174 | | 42 | | | | | | | | | | | | | | | | | 1 | 10 | G | | | | | | | 172 | | | | | 174 |
| 176 | | | QRS | SH | BK | | | | | | | | | | | | | | | | | DS BL | PY 1-2 | | | | | BL | 85° | | | | 176 |
| 178 | | 43 | | | | | | | | | | | | | | | | | | | | | | | | | | 177 | | | | | 178 |
| 180 | | | | | | | | | | | | | | | | | | | | | | | | | | | | CL | 30° | | | | 180 |
| 182 | | 44 | | | | | | | | | | | | | | | | | | | | | | | | | | 180 | | | | | 182 |
| 184 | | | | | | | | | | | | | | | | | | | | | | | | | | | | BL | 85° | | | | 184 |
| 186 | | 45 | | | | | | | | | | | | | | | | | | | | | | | | | | 182 | | | | | 186 |
| 188 | | | | | | | | | | | | | | | | | | | | | | | | | | | | | | | | | 188 |
| 190 | | 46 | | | | | | | | | | | | | | | | | | | | | | 190·5 | 50 | ? | | | | | | | 190 |
| 192 | | | | | | | | | | | | | | | | | | | | | | | | | | | | | | | | | 192 |
| 194 | | 47 | | | | | | | | | | | | | | | | | | | | | | | | | | BL | 85° | | | | 194 |
| 196 | | | | | | | | | | | | | | | | | | | | | | | | | | | | 192 | | | | | 196 |
| 198 | | 48 | | | | | | | | | | | | | | | | | | | | | | | | | | | | | | | 198 |
| | | | | | | | | | | | | | | | | | | | | | | | | | | | | 197 CL | 35° | | | | |

65521-1

# Aberfoyle Resources Limited

EXPLORATION DIVISION

HOLE No. MAC 33

PAGE 6 OF 23

GEO. SR

DATE 26-1-93

5 cm

# DIAMOND DRILL LOG

DRILLING: DEPTH | DRILLING RUNS | CORE LOSS | CORE TRAY NO.

LITHOLOGY: STRATIGRAPHY | ROCK TYPE | COLOUR | VOLCANICLASTICS: FRAGMENTS: COMPOSITION | MAX. SIZE (MM) | SORTING | SHAPE; MATRIX: COMPOSITION | VOLUME % | LOWER CONTACT: GRADATION | STYLE

VESICLES: CONCENTRATION | MAX. SIZE (MM) | SHAPE

ALTERATION: TEXTURE | INTENSITY | MINERALOGY

VEINING: INTENSITY | MAX. WIDTH (MM) | MINERALOGY

MINERALISATION: TEXTURE | MINERALOGY & CONTENTS

FAULTS: POSITION OF BASE | DOWNHOLE WIDTH (CM) | CORE AXIS ANGLE | GOUGE

FOLIATION: TYPE | CORE AXIS ANGLE

WEATHERING

STANDARD COLOUR LOG

REMARKS

SAMPLE NO. | DEPTH

| DEPTH | STRATIGRAPHY | ROCK TYPE | COLOUR | VOLCANICLASTICS: FRAGMENTS: COMPOSITION | MAX. SIZE (MM) | SORTING | SHAPE; MATRIX: COMPOSITION | VOLUME % | LOWER CONTACT: GRADATION | STYLE | VESICLES: CONCENTRATION | MAX. SIZE (MM) | SHAPE | ALTERATION: TEXTURE | INTENSITY | MINERALOGY | VEINING: INTENSITY | MAX. WIDTH (MM) | MINERALOGY | MINERALISATION: TEXTURE | MINERALOGY & CONTENTS | FAULTS: POSITION OF BASE | DOWNHOLE WIDTH (CM) | CORE AXIS ANGLE | GOUGE | FOLIATION: TYPE | CORE AXIS ANGLE | WEATHERING | REMARKS | SAMPLE NO. |
|---|---|---|---|---|---|---|---|---|---|---|---|---|---|---|---|---|---|---|---|---|---|---|---|---|---|---|---|---|---|---|
| 202 | | | | | | | | | | | | | | | | | | | | | | | | | | Cl | 30° | | | |
| 204 | | | | | | | | | | | | | | | | | | | | | | | | | | Bd | 30° | | | |
| 206 | QRS | Sh | Blk | | | | | | | | | | | | | | | | | | | | | | | 202 | | | | |
| 208 | | | | | | | | | | | | | | | | | | | | | | 207.0 | | | | Bd | 70° | | Increase in Py content - mostly as irregular veinlets and nodules. | |
| 210 | | | | | | | | | | | | | | | | | | | | | Ds Bd No | Py 2-3 | | | | 207 | | | | |
| 212 | | | | | | | | | | | | | | | | | | | | | | | | | | Bd | 60° | | Bedding changes orientation approaching Basalt. | |
| 214 | | | | | | | | | | | | | | | | | | | | | | | | | | 210 | | | | |
| 216 | | 216.1 | | | | | | | S | C | 216.9 | | | 216.1 | | | | | | | | 216.1 | | | | Cl | 30° | | | |
| 218 | | B-bx/Sh 218.9 | gybk | B | 70 | P | A | Sh | 25 | gl | 218.9 | 2 | SE | 218.9 | | | | | | | | 218.9 | | | | 211 | | | | |
| 220 | | | | | | | | Si,a | 20 | | | | | | R | 3 | Si | | | | | | | | | Cl | 25° | | | |
| 222 | | | | | | | | 231.6 | | | | | | | R | 2 | Se Cl | | | | | | | | | 214 | | | | |
| 224 | RS | YB-Lt/bx | gyGn | B Q | 200 | P | V | Si,Se Co | 15 | | Fr | 10 | SE | | Fr | 1 | Se Cl | 2 | 10 | C | Ds Vn | Py 2 | 221.4 | 20 | ? | Ru | 215 | 55° | | | |
| 226 | | | | | | | | | | | 3 | | | | Fr | 3 | Si Se | | | | | | 221.6 | 10 | ? | Ru | Bd | | | | |
| 228 | | | | | | | | | | | | | | | Ma | 4 | Si | 2382 | | | | | 222.6 | 10 | ? | Ru | | | | | |
| 230 | | | | | | | | | | | | | | | | | | | | | | | 228.9 | 10 | ? | Pu Sh | | | | | |
| 232 | | | | | | | | | | | | | | | | | | 3 | 10 | C | | | | | | | | | | | |
| 234 | | | | | | | | | | | | | | | | | | 2344 | | | | 234.4 | 2344 | 10 | 70° | Pu Ru | | | | | |
| 236 | | | | | | | | | | | | | | | | | | 1 | 20 | Si Co | Ds Vn | Py 3-5 Sp Tr 235.7 | | | | | | | | | |
| 238 | | | | | | | | | | | | | | | | | | | | | Ds | Sp 3 Gn 2 Py Tr 239.2 | | | | | | | | | |

HQ / NQ

Increase in Py content - mostly as irregular veinlets and nodules.

Bedding changes orientation approaching Basalt.

Pepperitic interval

Faulted conformable contact.

A complexly altered and mineralised interval. Frags massive to amygdal. gy.gn se+cl to gy. bleached Si+Se ± diseam sp.fm. Matrix varies from Se+Cl to Si+Co to Si. Blotchy irregular Co common to abundant.

Common disseminated sp+cp in altered gy. bleached siliceous frags + in matrix.

6223533 | 6223534 | 6223535 | 6223536

log.01931.wor

# Aberfoyle Resources Limited

EXPLORATION DIVISION

HOLE No. MAC 33

PAGE 7 OF 23

GEO. S.R.

DATE 29-1-93

5 cm

# DIAMOND DRILL LOG

| DRILLING | | | | LITHOLOGY | | | | | | | | | | VESICLES | | | ALTERATION | | | VEINING | | | MINERALISATION | | FAULTS | | | | FOLIATION | | | | | | |
|---|---|---|---|---|---|---|---|---|---|---|---|---|---|---|---|---|---|---|---|---|---|---|---|---|---|---|---|---|---|---|---|---|---|---|
| | | | | | | | VOLCANICLASTICS | | | | | | LOWER CONTACT | | | | | | | | | | | | | | | | | | | | | | |
| | | | | | | | FRAGMENTS | | | | MATRIX | | | | | | | | | | | | | | | | | | | | | | | | |
| DEPTH | DRILLING RUNS | CORE LOSS | CORE TRAY NO. | STRATIGRAPHY | ROCK TYPE | COLOUR | COMPOSITION | MAX. SIZE (MM) | SORTING | SHAPE | COMPOSITION | VOLUME % | GRADATION | STYLE | CONCENTRATION | MAX. SIZE (MM) | SHAPE | TEXTURE | INTENSITY | MINERALOGY | INTENSITY | MAX. WIDTH (MM) | MINERALOGY | TEXTURE | MINERALOGY & CONTENTS | POSITION OF BASE | DOWNHOLE WIDTH (CM) | CORE AXIS ANGLE | GOUGE | TYPE | CORE AXIS ANGLE | WEATHERING | STANDARD COLOUR LOG | REMARKS | SAMPLE NO. | DEPTH |
| 242 | 59 | | | PLS | | | | | | | | | | | | | | | | | | | | | | | | | | | | | | 242 |
| 244 | | | | | | | | | | | | | | | | | | | | | | | | | | | | | | | | | | 244 |
| 246 | 60 | | | | | | | | | | | | | | | | | | | | | | | | | 246.6 | 10 | ? | ku | | | | | 246 |
| 248 | | | | | | | | | | | | | | | | | | | | | | | | | | | | | | | | | | 248 |
| 250 | | | | | | | | | | | | | | | | | | | | | | | | | | | | | | | | | | 250 |
| 252 | 61 | | | | | | | | | | | | | | | | | | | | | | | | | | | | | | | | | 252 |
| 254 | | | | | | | | | | | | | G2 | | | | 254.4 | | | | | | | | 254.4 | | | | | | | | | 254 |
| 256 | | | | | B-L/bV | GyGn | B | 500 | P | V | SiSe | 20 | | | | | | Ma | 3 | Si Se Ca | | | | Ds (Vn) | Sp Gn Py Tr | | | | | | | | | 256 |
| 258 | | | | | | | | | | | | | | | | | | LFr | 2 | Si Se | | | | | | | | | | | | | | 258 |
| 260 | 62 | | | | 259.1 | | | | | | | | | | 259.1 | | | Fr | 1 | Se Cl | 259.1 | | | 259.1 | | | | | | | | 258.1 Ca V. | | | 260 |
| 262 | | | | | No Core | | | | | | | | | | | | | | | | | | | | | | | | | | | | | 262 |
| | | | | | 262.9 | | | | | | | | | | 262.9 | | 262.9 | P | 1 | Si | 262.9 | | | 262.9 | | | | | | | | | | | |
| | | | | | B-L | | | | | | | | S | | 2 | 10 | SE | | | | | | | | | | | | | | | | | | |
| 264 | | | | | 263.5 | | | | | | | | | | 263.5 | | | L | 3 | Si Se | | | | | | | | | | | | | Prob. lge block. | | 264 |
| | | | | PLS | B-L/bV | GyGn | B | 200 | P | V | SiSe | 20 | S | | Fg 2 | 10 | S | | | | 2 | 10 | Ca | Ds (Vn) | Gn Tr Sp 1 | | | | | | | | | | |
| 266 | 63 | | | | 265.1 B-L 266.6 | | | | | | | | S | | 265.1 2 | 20 | S | P | 1 | Si | 266.9 | | | | | | | | | | | | | lge block? | | 266 |
| 268 | | | | | B-L/bV | GyGn | B | 500 | P | V | SiSe | 20 | | | 266.6 Fr 2 | 10 | S | Ma | 3 | Si Se Ca | | | | | | | | | | | | | | Basalt weakly Fd. phyric Very siliceous matrix w variably siliceous frags; most Se+Cl altd. Wk. dissem Sp+Gn min associated with Si+Se altn. | | 268 |
| 270 | | | | | | | | | | | | | | | | | | LFr | 2 | Si Se | | | | | | | | | | | | | | | 270 |
| 272 | 64 | | | | | | | | | | | | | | | | | Fr | 1 | Se Cl | 2 | 100 | Si Tr | | | | | | | | | | | | 272 |
| 274 | | | | | | | | | | | | | | | | | | | | | 275.9 | | | | | | | | | | | | | | 274 |
| 276 | 65 | | | | | | | | | | | | | | | | | | | | | | | | | 279.6 | 1 | 5° | SL | | | | | | 276 |
| 278 | | | | | | | | | | | | | | | | | | | | | | | | | | | | | | | | | | 278 |

Tr 622279 250.0m

log01931.mnr

Aberfoyle Resources Limited
EXPLORATION DIVISION

HOLE No. MAC 33
PAGE 8 OF 23
GEO. SR
DATE 3-2-93

5 cm

# DIAMOND DRILL LOG

| DRILLING | | | | LITHOLOGY | | | | | | | | | | VESICLES | | | ALTERATION | | | VEINING | | | MINERALISATION | | FAULTS | | | | FOLIATION | | | | | | |
|---|---|---|---|---|---|---|---|---|---|---|---|---|---|---|---|---|---|---|---|---|---|---|---|---|---|---|---|---|---|---|---|---|---|---|
| DEPTH | DRILLING RUNS | CORE LOSS | CORE TRAY NO. | STRATIGRAPHY | ROCK TYPE | COLOUR | VOLCANICLASTICS FRAGMENTS COMPOSITION | FRAGMENTS MAX. SIZE (MM) | FRAGMENTS SORTING | FRAGMENTS SHAPE | VOLCANICLASTICS MATRIX COMPOSITION | MATRIX VOLUME % | LOWER CONTACT GRADATION | LOWER CONTACT STYLE | CONCENTRATION | MAX. SIZE (MM) | SHAPE | TEXTURE | INTENSITY | MINERALOGY | INTENSITY | MAX. WIDTH (MM) | MINERALOGY | TEXTURE | MINERALOGY & CONTENTS | POSITION OF BASE | DOWNHOLE WIDTH (DM) | CORE AXIS ANGLE | DUCTILE | TYPE | CORE AXIS ANGLE | WEATHERING | STANDARD COLOUR LOG | REMARKS | SAMPLE NO. | DEPTH |
| 282 | | | 66 | | | | | | | | | | | | | | | | | | 2 | 20 | G | | | | | | | | | | | 282 |
| 284 | | | | | | | | | | | | | | | | | | | | | 1 | 10 | Si Ep | | | | | | | | | | Vesicular frags become increasingly rare with depth. | | 284 |
| 286 | | | 67 | | | | | | | | | | | | | | | | | | | | | | | | | | | | | | | 286 |
| 288 | | | | | 288.2 | | | | | | | | S | | 288.2 | | | 288.2 | | | | | | | | | | | | | | | | 622366 | 288 |
| 290 | | | | | B-L 290.7 | cgfm | | | | | | | S | | 290.7 | 2 | 5 | V | 290.7 | L | 1 | Si | 290.7 | | | | | | | | | | | | | 290 |
| 292 | | | 68 | | B-L/bv 292.5 | cgfm | BQ | 200 | P | V | Sise | 20 | | | | | | | UFr | 2 | SiSe | | | | | | | | | | | | | | | 292 |
| 294 | | | | | No Core 297.5 | | | | | | | | | | | | | | Ma | 3 | SiSeCo | 292.5 | | | 292.5 | | | | | | | | | No SAMPLE | | 294 |
| 296 | | | | | | | | | | | | | | | | | | | | | 297.5 | | | | | | | | | | | | | | 296 |
| 298 | | | 69 | | B-Lv 301.1 | cgfm | BQ | 60 | P | A | SiSe | 20 | S | | 301.1 | | | Fr | 1 | CL | 2 | 10 | SiEp | Ds Vn | Sp1 CnTr | | | | | | | | | | 622361 | 298 |
| 300 | | | | | | | | | | | | | | | | | | | LFr | 2 | SiSe | 299.0 | | | | | | | | | | | | | 300 |
| 302 | | | | | B-L 305.5 | cgfm | | | | | | | S | | 305.5 | 1 | 3 | V | Ma | 3 | SiSeCo | 1 | 10 | SiSp | Vn (Ds) | Sp2 CnTr | 301.1 | | | | | | | | | 302 |
| 304 | | | | | | | | | | | | | | | | | | | L | 1 | Si | 2 | 10 | G | | | | | | | | | | | 304 |
| 306 | | | 70 | | | | | | | | | | | | | | | | | | | 1 | 5 | SiEp | | | 305.5 | | | | | | | | 306 |
| 308 | | | | | B-L/bv | DGy Gn | AP,Q | 200 | P | V | SiSe | 20 | | | | | | | Ma | 3 | SiSeCo | | | | Ds Vn | Sp1 CnTr | | | | | | | | | Fragments become darker green => more chloritic less amygdaloidal and more prominently feldspar phyric. Smaller frags in the altered matrix are bleached cream and often look like dacite. | | 308 |
| 310 | | | | | | | | | | | | | | | | | | | LFr | 2 | SiSe | | | | 308.8 | | | | | | | | | | 310 |
| 312 | | | 71 | | | | | | | | | | | | | | | | Fr | 1 | CL | | | | Ds Vn | Sp2 CnTr | | | | | | | | 622362 | 312 |
| 314 | | | | | | | | | | | | | | | | | | | | | | | | | | | | | | | | | | | 314 |
| 316 | | | 72 | | | | | | | | | | | | | | | | | | | | | | | | | | | | | | | | 316 |
| 318 | | | | | | | | | | | | | | | | | | | | | | | | | | | | | | | | | | | 318 |

log#193.wor

Aberfoyle Resources Limited
EXPLORATION DIVISION

HOLE No. WMC-93
PAGE 9 OF 23
GEO. SR
DATE 3-2-93

5 cm

# DIAMOND DRILL LOG

| DRILLING | | | LITHOLOGY | | | | | | | | | | VESICLES | | | ALTERATION | | | VEINING | | | MINERALISATION | | FAULTS | | | | FOLIATION | | WEATHERING | STANDARD COLOUR LOG | REMARKS | SAMPLE NO. | DEPTH |
|---|---|---|---|---|---|---|---|---|---|---|---|---|---|---|---|---|---|---|---|---|---|---|---|---|---|---|---|---|---|---|---|---|---|
| DEPTH | DRILLING AIDS CORE LOSS | CORE TRAY NO. | STRATIGRAPHY | ROCK TYPE | COLOUR | VOLCANICLASTICS FRAGMENTS COMPOSITION | VOLCANICLASTICS FRAGMENTS MAX. SIZE (MM) | VOLCANICLASTICS FRAGMENTS SORTING | VOLCANICLASTICS FRAGMENTS SHAPE | VOLCANICLASTICS MATRIX COMPOSITION | VOLCANICLASTICS MATRIX VOLUME % | LOWER CONTACT GRADATION | LOWER CONTACT STYLE | CONCENTRATION | MAX. SIZE (MM) | SHAPE | TEXTURE | INTENSITY | MINERALOGY | INTENSITY | MAX. WIDTH (MM) | MINERALOGY | TEXTURE | MINERALOGY & CONTENTS | POSITION OF BASE | DOWNHOLE WIDTH (CM) | CORE AXIS ANGLE | GOUGE | TYPE | CORE AXIS ANGLE | | | | | |
| 322 | | | | | | | | | | | | S | | | | 320.3 | | | | | | | 320.3 | | | | | | | | | TS 622280 320.8m | 622363 | 322 |
| 324 | | 73 | | B-L | Cgfn | | | | | | | | | | | P | 1 | Si | | | | | Ds | Sp 2 Cn Tr | | | | | | | | | | 324 |
| 326 | | | | | | | | | | | | | | | | | | | | | | | | | | | | | | | | | | 326 |
| 328 | | | | | | | | | | | | G1 | | | | 328.6 | | | | | | | | | | | | | | | | | | 328 |
| 330 | | 74 | | B-Lv | Cgfn | B | 40 | P | A | SiSe | 30 | | | | | Ma | 3 | Si Se Ca | 2 | 10 | Ca | 331.6 | | | | | | | | | | | | 622364 | 330 |
| 332 | | | | | | | | | | | | G1 | | | | | | | 1 | 5 | Si Ep | | | | | | | | | | | | | 332 |
| 334 | | 75 | | B-L/Lv | Cgfn | | 30 | P | V | SeCl | 10 | G1 | | | | | | | | | | | | | | | | | | | | | | 334 |
| 336 | | | | 335.6 | | | | | | | | | | | | | | | | | | | | | | | | | | | | | | 336 |
| 338 | | | | | | | | | | | | | | | | | | | | | | | Ds Cn | Sp 1-2 Tr | | | | | | | | | 622365 | 338 |
| 340 | | 76 | | | | | | | | | | | | | | | | | | | | | | | | | | | | | | TS 622281 340.4m | | 340 |
| 342 | | | | B-Lv/bv | Cgfn | B | 100 | P | V | SiSe | 20 | | | | | | | | | | | | | | | | | | | | | | | 342 |
| 344 | | | | | | | | | | | | | | | | | | | | | | | | | | | | | | | | Dk green CL. alt. B? or A? fangs in Si+Se altd matrix of ash and fine lapilli sized material Hyaloclastite? | | 344 |
| 346 | | 77 | | | | | | | | | | | | | | | | | | | | | | | | | | | | | | | | 346 |
| 348 | | | | | | | | | | | | | | | | | | | | | | | | | | | | | | | | | 622366 | 348 |
| 350 | | | | | | | | | | | | | | | | | | | | | | | | | | | | | | | | | | 350 |
| 352 | | 78 | | | | | | | | | | | | | | | | | | | | | | | | | | | | | | | | 352 |
| 354 | | | | | | | | | | | | | | | | | | | | | | | | | | | | | | | | | | 354 |
| 356 | | | | | | | | | | | | | | | | | | | | | | | | | | | | | | | | | | 356 |
| 358 | | 79 | | | | | | | | | | | | | | | | | | | | | | | | | | | | | | | | 358 |
| | | | | 359.0 | | | | | | | | F | | | | 359.0 | | | | | | | 359.0 | | 359.0 | 50 | 10? | Ru | | | | | |

log/0193L.wor

65293

Aberfoyle Resources Limited
EXPLORATION DIVISION

HOLE No. MAC 55
PAGE 10 OF 23
GEO. SR
DATE

5 cm

# DIAMOND DRILL LOG

DRILLING: DEPTH; DRILLING RUNS / CORE LOSS; CORE TRAY NO.

LITHOLOGY: STRATIGRAPHY; ROCK TYPE; COLOUR; VOLCANICLASTICS — FRAGMENTS: COMPOSITION, MAX. SIZE (MM), SORTING, SHAPE; MATRIX: COMPOSITION, VOLUME %; LOWER CONTACT: GRADATION, STYLE

VESICLES: CONCENTRATION, MAX. SIZE (MM), SHAPE

ALTERATION: TEXTURE, INTENSITY, MINERALOGY

VEINING: INTENSITY, MAX. WIDTH (MM), MINERALOGY

MINERALISATION: TEXTURE, MINERALOGY & CONTENTS

FAULTS: POSITION OF BASE, DOWNHOLE WIDTH (CM), CORE AXIS ANGLE, GOUGE

FOLIATION: TYPE, CORE AXIS ANGLE

WEATHERING

STANDARD COLOUR LOG

REMARKS

SAMPLE NO.

DEPTH

| DEPTH | CORE TRAY NO. | ROCK TYPE | COLOUR | LITHOLOGY | VESICLES | ALTERATION | VEINING | MINERALISATION | FAULTS | REMARKS | SAMPLE NO. |
|---|---|---|---|---|---|---|---|---|---|---|---|
| 362 | 80 | B-pl | Cyfm | | 1 15 SE | | 3 10 Co | Ds Vn Sp pairs | | ← TS 622282 362.8m Common black cherty interpillow sediment | 622368 |
| 364 | | | | | | | | | | Lacks prominent disseminated Sp of previous units. An obvious change in the nature of min and in lithology. | |
| 366 | 81 | | | | | | | | 368.2 120 ? Ru | | |
| 368 | | | | | | | | | | | |
| 370 | | | | | | | | | | | |
| 372 | 82 | 372.6 | | | | 372.6 | | | | | |
| 374 | | B-Lv/bv | Cyfm | B,Cl 500 P V Si5e 10 | | Ma 2 Si | | | | Large (>30cm) blocks of (amygdaloidal) basalt with abundant dk gn. Cl. altered clasts and totally bleached B? clasts. Smallest Congl and mechanic often Si altd. | 622369 |
| 376 | | | | | | | | | | | |
| 378 | 83 | 379.0 | | S | | | | | | | |
| 380 | | B-L | Cyfn | | | L 1 Co | | | | | 622370 |
| 382 | | | | | | | | | | | |
| 384 | 84 | | | | | | 384.6 | | | | |
| 386 | | | | | | P 2 Cl | 2 5 Co | | 387.5 20 65 Ru Pu | | |
| 388 | 85 | 389.1 | | G1 | 389.1 | 389.1 | 388.3 | 389.1 | | | |
| 390 | | YA-Lv | Dcy Grn | A (Si A) 50 P V SiEp 20 | | L 3 Si | | Ds Sp Gn Tr | | sequence again becoming feldspar phyric | 622371 |
| 392 | | 392.1 | | G2 | | 392.1 | | | | | |
| 394 | 86 | A-L/Lv | Cyfm | A 30 P V Si4 L10 | | L 3 Ep<br>L 3 Si<br>P 2 EpSi | | | | Domainally altered lava | 622372 |
| 396 | | | | | | | | | | | |
| 398 | 87 | | | | | | | | | | |

65516

log81931.wor

Aberfoyle Resources Limited

EXPLORATION DIVISION

HOLE No. MAC 05

PAGE 11 OF 23

GEO. SR

DATE 5-2-93

5 cm

# DIAMOND DRILL LOG

DRILLING: DEPTH; DRILLING RUNS; CORE LOSS; CORE TRAY NO.

LITHOLOGY: STRATIGRAPHY; ROCK TYPE; COLOUR; VOLCANICLASTICS — FRAGMENTS: COMPOSITION, MAX. SIZE (MM), SORTING, SHAPE; MATRIX: COMPOSITION, VOLUME %; LOWER CONTACT: GRADATION, STYLE

VESICLES: CONCENTRATION; MAX. SIZE (MM); SHAPE

ALTERATION: TEXTURE; INTENSITY; MINERALOGY

VEINING: INTENSITY; MAX. WIDTH (MM); MINERALOGY

MINERALISATION: TEXTURE; MINERALOGY & CONTENTS

FAULTS: POSITION OF BASE; DOWNHOLE WIDTH (CM); CORE AXIS ANGLE; GOUGE

FOLIATION: TYPE; CORE AXIS ANGLE

WEATHERING

STANDARD COLOUR LOG

REMARKS

SAMPLE NO.

DEPTH

| DEPTH | CORE TRAY NO. | ROCK TYPE | COLOUR | VESICLES | ALTERATION | VEINING | MINERALISATION |
|---|---|---|---|---|---|---|---|
| 403.5 | | | | | | | |
| 404 | 88 | | | | | 2 50 SiCl | Ds Vn SpGnTr |
| 406 | | | | | | | |
| 408 | | A-L/W | cgy gn | | | | |
| 410 | 89 | | | | | | |
| 412 | | | | | | | |
| 414 | | | | | | | |
| 416 | 90 | | | | | | |
| 418 | | | | | | | |
| 420 | | | | | | | |
| 422 | 91 | | | | | | |
| 423.5 | | | | 423.5 | 423.5 | | 423.5 |
| 424 | | | | | | | |
| 426 | | | | 1 10 SE | L 3 Ep | | |
| 428 | 92 | A-L | cgy gn | | | | |
| 430 | | | | | | | |
| 431.5 | | | | 431.5 | 431.5 | | |
| 432 | 93 | A-L/W | cgy gn | | | | |
| 434 | | | A | | | 1 5 G | |
| 435.5 | | | | | | 1 5 Si | |
| 436 | 94 | | | | | | |
| 438 | | | | | | | |

REMARKS:

local pyrhotite in Si veins. Devonian?

Domainal Si ± Ep alth. of finely fd phyric A? Lava. with possibly some minor true volcaniclastic.

412.5 ORIENTATION

Ts 622283 427.3m

Ts 622284 438.2

SAMPLE NO.: 622373; 622374; 622375; 622376

DEPTH: 402, 404, 406, 408, 410, 412, 414, 416, 418, 420, 422, 424, 426, 428, 430, 432, 434, 436, 438

log.01SR1.mm

Aberfoyle Resources Limited
EXPLORATION DIVISION

HOLE NO. M -
PAGE 12 OF 23
GEO. SR
DATE 5-2-93

5 cm

# DIAMOND DRILL LOG

DRILLING | LITHOLOGY | VESICLES | ALTERATION | VEINING | MINERALISATION | FAULTS | FOLIATION | WEATHERING | STANDARD COLOUR LOG | REMARKS | SAMPLE NO. | DEPTH

DEPTH | DRILLING RUNS | CORE LOSS | CORE TRAY NO.

LITHOLOGY: STRATIGRAPHY | ROCK TYPE | COLOUR | VOLCANICLASTICS: FRAGMENTS: COMPOSITION, MAX. SIZE (MM), SORTING, SHAPE; MATRIX: COMPOSITION, VOLUME % | LOWER CONTACT: GRADATION, STYLE

VESICLES: CONCENTRATION, MAX. SIZE (MM), SHAPE

ALTERATION: TEXTURE, INTENSITY, MINERALOGY

VEINING: INTENSITY, MAX. WIDTH (MM), MINERALOGY

MINERALISATION: TEXTURE, MINERALOGY & CONTENTS

FAULTS: POSITION OF BASE, DOWNHOLE WIDTH (CM), CORE AXIS ANGLE, GOUGE

FOLIATION: TYPE, CORE AXIS ANGLE

| DEPTH | CORE TRAY NO. | ROCK TYPE | COLOUR | FRAG. COMP. | FRAG. MAX SIZE (MM) | FRAG. SORTING | FRAG. SHAPE | MATRIX COMP. | MATRIX VOLUME % | LOWER CONTACT GRADATION | LOWER CONTACT STYLE |
|---|---|---|---|---|---|---|---|---|---|---|---|
| 442 | | | | | | | | | | | |
| 444 | 95 | | | | | | | | | | |
| 446 | | A-L/Lv | Cy/Gn | A | 50 | P | V | Si/Se | 20 | | |
| 448 | 96 | | | | | | | | | | |
| 450 | | | | | | | | | | | |
| 451.4 | | | | | | | | | | G1 | |
| 452 | | A-L | Cy/Gn | | | | | | | | |
| 454.3 | 97 | | | | | | | | | G1 | |
| 455.7 | | A-Lv | Cy/Gn | A | 40 | P | V | Si/Se | 60 | F | |
| 456 | | | | | | | | | | | |
| 458 | | A-L/Lv | Cy/Gn | A | 50 | P | V | Si/Se | 50 | | |
| 460 | 98 | | | | | | | | | | |
| 462 | | | | | | | | | | | |
| 464 | 99 | | | | | | | | | | |
| 466 | | | | | | | | | | | |
| 468 | 100 | | | | | | | | | | |
| 470 | | | | | | | | | | | |
| 472 | | | | | | | | | | | |
| 474 | 101 | | | | | | | | | | |
| 476 | | | | | | | | | | | |
| 478 | 102 | | | | | | | | | | |

| DEPTH | CONCENTRATION | MAX. SIZE (MM) | SHAPE |
|---|---|---|---|
| 454 | 1 | 10 | V |
| 454.3 | | | |

| DEPTH | TEXTURE | INTENSITY | MINERALOGY |
|---|---|---|---|
| | L | 3 | Ep |
| | Ma | 2 | Si Se |
| | Fl | 1 | Cc |
| 451.4 | | | |
| | L | 3 | Ep |
| 454.3 | | | |
| | Ma | 1 | Si Se |

| DEPTH | INTENSITY | MAX. WIDTH (MM) | MINERALOGY |
|---|---|---|---|
| 454.3 | 1 | 5 | G |

| DEPTH | TEXTURE | MINERALOGY & CONTENTS |
|---|---|---|
| 454.3 | Ds | Py 1 |

| DEPTH | POSITION OF BASE | DOWNHOLE WIDTH (CM) | CORE AXIS ANGLE | GOUGE |
|---|---|---|---|---|
| 466.6 | 466.6 | 10 | 90 | 25 | Ru |

| DEPTH | TYPE | CORE AXIS ANGLE |
|---|---|---|
| 446.5 | FB | 10° |

REMARKS

Probably domainally altd lava.

Flow banding?!

More massive lava.

Feldspar phyric below 454.3m only locally.

Major Fault at low angle to CA.

Massive to locally wkly fd. phyric (pk. Ab) lava with local weak pseudofragmental texture from dominl Si Se alt'n.
TS 622285
468.2

SAMPLE NO.: 622377 | 622378 | 622379

DEPTH: 442 | 444 | 446 | 448 | 450 | 452 | 454 | 456 | 458 | 460 | 462 | 464 | 466 | 468 | 470 | 472 | 474 | 476 | 478

log8193.wor

95-22-06

Aberfoyle Resources Limited

EXPLORATION DIVISION

HOLE NO. MAD--

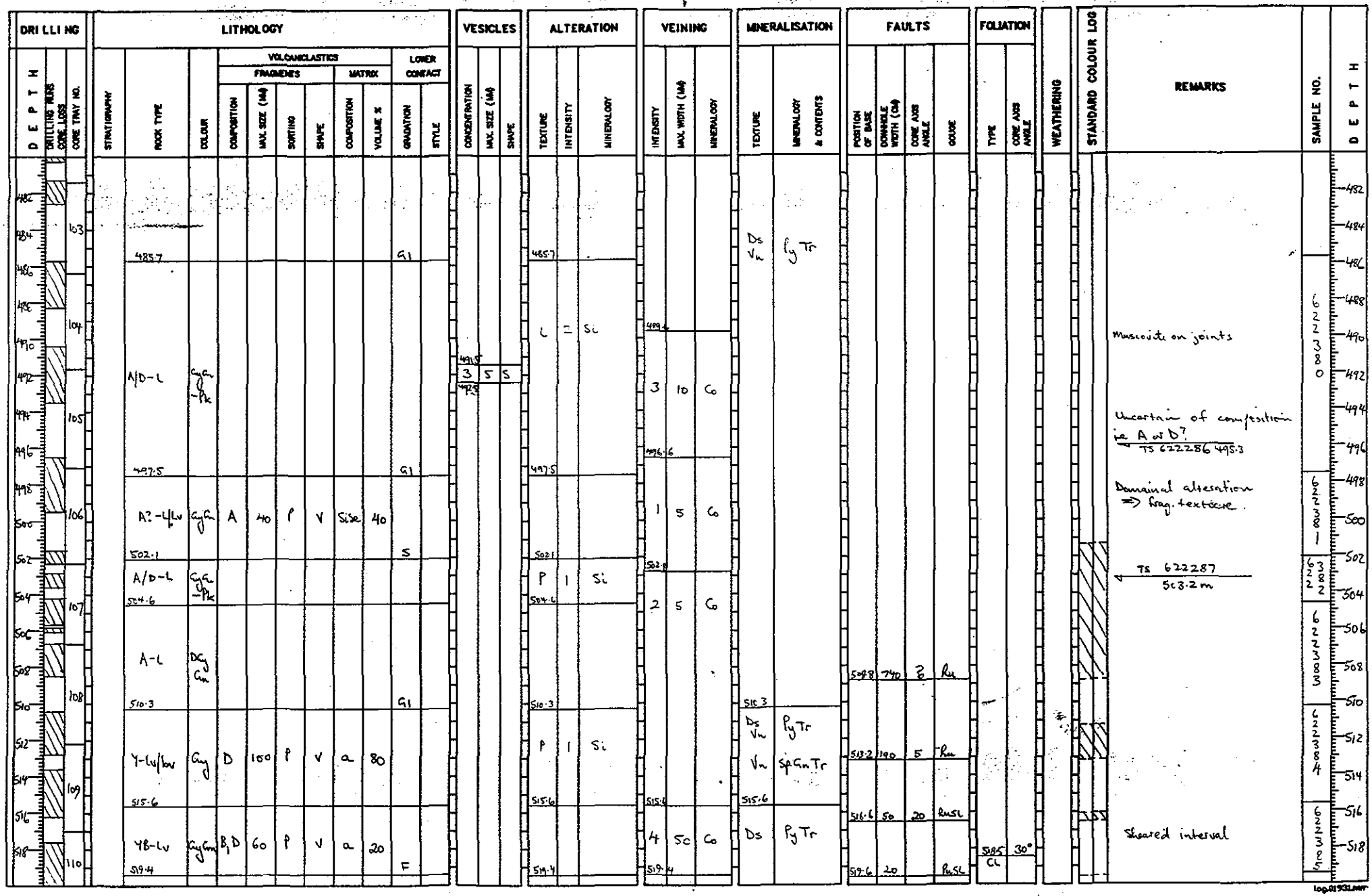
PAGE 13 OF 23

GEO. SK

DATE 5-2-93

5 cm

# DIAMOND DRILL LOG



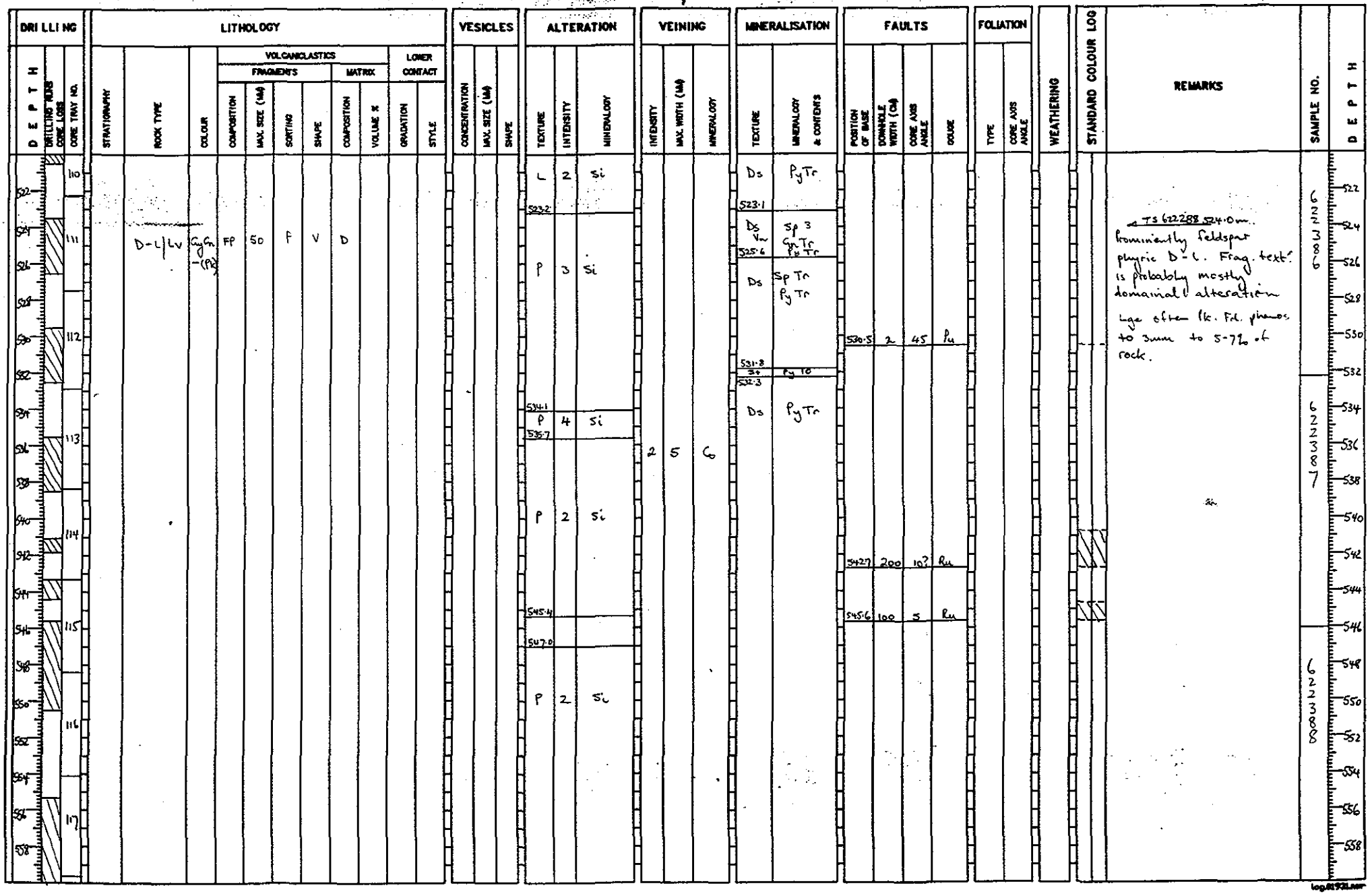

log.01931.wmf

Abermoyle Resources Limited
EXPLORATION DIVISION

HOLE NO. mA4
PAGE 14 OF 23
GEO. SR
DATE 10-2-93

5 cm

# DIAMOND DRILL LOG




log.dr92.wor

0555

Aberfoyle Resources Limited

EXPLORATION DIVISION

HOLE NO. MA[illegible]

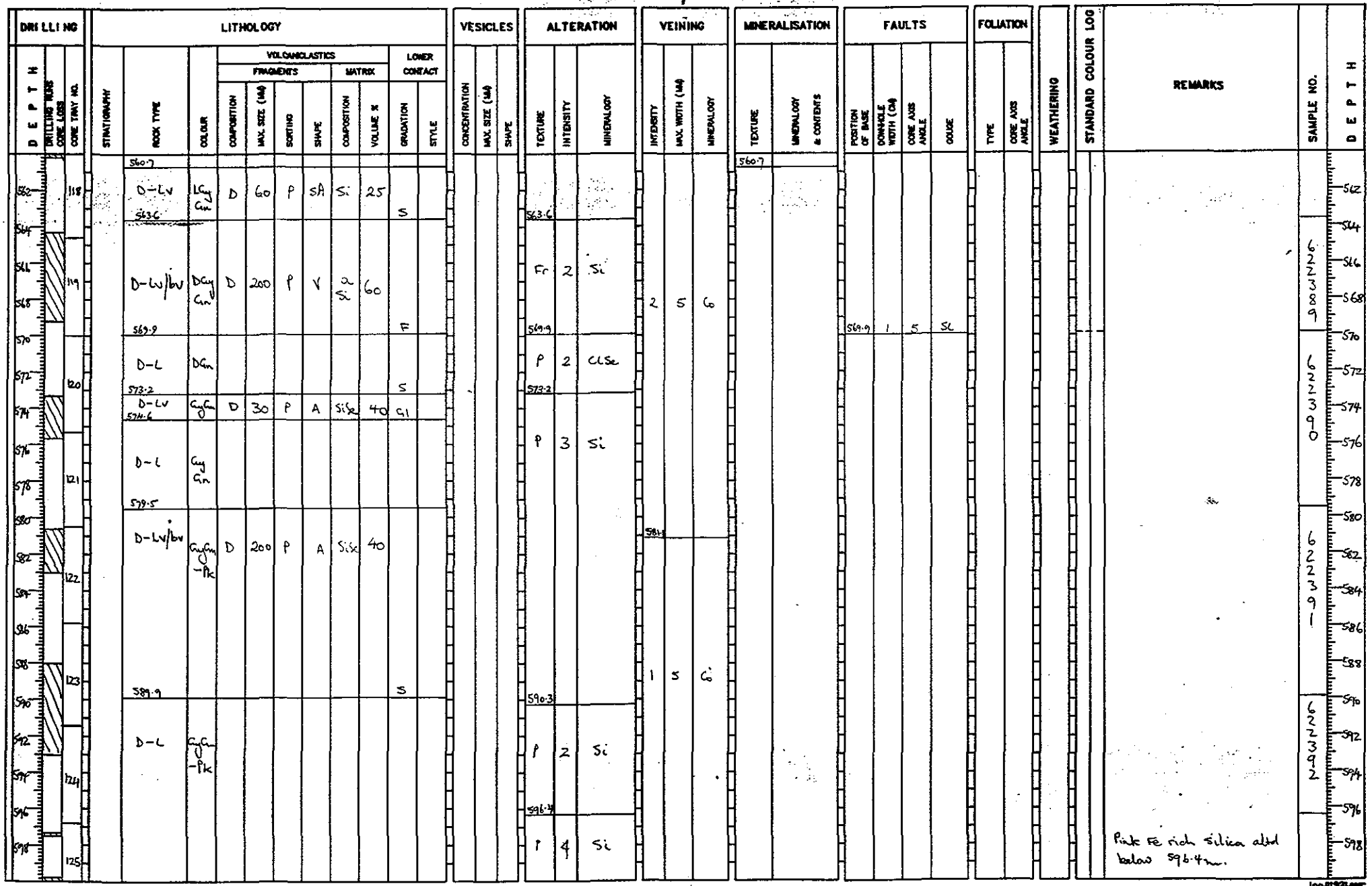
PAGE 15 OF 23

GEO. SR

DATE 10-2-93

5 cm

# DIAMOND DRILL LOG



Aberfoyle Resources Limited

EXPLORATION DIVISION

HOLE No. MH-93

PAGE 16 OF 23

GEO. SR

DATE 11-2-93

5 cm

# DIAMOND DRILL LOG

| DRILLING | | | LITHOLOGY | | | | | | | | | | VESICLES | | | ALTERATION | | | VEINING | | | MINERALISATION | | FAULTS | | | | FOLIATION | | WEATHERING | STANDARD COLOUR LOG | REMARKS | SAMPLE NO. | DEPTH |
|---|---|---|---|---|---|---|---|---|---|---|---|---|---|---|---|---|---|---|---|---|---|---|---|---|---|---|---|---|---|---|---|---|---|
| DEPTH | DRILLING RUNS / CORE LOSS | CORE TRAY NO. | STRATIGRAPHY | ROCK TYPE | COLOUR | VOLCANICLASTICS: FRAGMENTS: COMPOSITION | VOLCANICLASTICS: FRAGMENTS: MAX. SIZE (MM) | VOLCANICLASTICS: FRAGMENTS: SORTING | VOLCANICLASTICS: FRAGMENTS: SHAPE | VOLCANICLASTICS: MATRIX: COMPOSITION | VOLCANICLASTICS: MATRIX: VOLUME % | LOWER CONTACT: GRADATION | LOWER CONTACT: STYLE | CONCENTRATION | MAX. SIZE (MM) | SHAPE | TEXTURE | INTENSITY | MINERALOGY | INTENSITY | MAX. WIDTH (MM) | MINERALOGY | TEXTURE | MINERALOGY & CONTENTS | POSITION OF BASE | DOWNHOLE WIDTH (CM) | CORE AXIS ANGLE | GOUGE | TYPE | CORE AXIS ANGLE | | | | SAMPLE NO. | DEPTH |
| 602 | | | | | | | | | | | | | | | | | | | | | | | | | | | | | | | | | 602 |
| 604 | | | | | | | | | | | | | | | | | | | | | | | | | | | | | | | | | 604 |
| 606 | | 126 | | | | | | | | | | | | | | | | | | | | | | | | | | | | | | | 606 |
| 608 | | | | | 609.7 | | | | | | | | | | | f | 4 | Si | | | | | | | | | | | | | | 608 |
| 610 | | | | | Dg Gn | | | | | | | | | | | 610.7 | | | | | | | | | | | | | | | | | 610 |
| 612 | | 127 | | | | | | | | | | | | | | | | | | | | | | | | | | | | | | | 612 |
| 614 | | | | B-L | 613.4 | | | | | | | S | | 613.4 | | | | | 613.4 | | | | | | | | | | | | | | 614 |
| 616 | | 128 | | | Gn | | | | | | | | | 2 | 10 | E | L | 3 | Ep | 1 | 5 | G | | | | | | | | | | | | 616 |
| 618 | | | | | | | | | | | | | | | | | | | | 2 | 20 | G | | | | | | | | | | | | 618 |
| 620 | | | | | 621.1 | | | | | | | S | | 621.1 | | | | | 621.1 | | | | 621.1 | | | | | | | | | | | 620 |
| 622 | | 129 | | | | | | | | | | | | | | | | | | | | | Ds | Sp 1 | | | | | | | | | | 622 |
| 624 | | | | FP-mLv | Gn | | | | | | | | | | | | | | | 2 | 50 | Si Tr | $V_N$ | | | | | | | | | | | 624 |
| 626 | | | | | | | | | | | | | | | | | | | | | | | | | | | | | | | | | 626 |
| 628 | | 130 | | | | | | | | | | | | | | | | | | | | | | | | | | | | | | | 628 |
| 630 | | | | | 631.1 | | | | | | | G1 | | 631.1 | | | | | 631.1 | | | | 631.1 | | | | | | | | | | | 630 |
| 632 | | | | B-pl | Gn | | | | | | | | | 2 | 30 | S | | | | 2 | 10 | G | | | | | | | | | | | | 632 |
| 634 | | 131 | | | | | | | | | | | | | | | | | | 1 | 10 | Si Tr | | | | | | | | | | | | 634 |
| 636 | | | | | 637.1 | | | | | | | G2 | | | | | | | | | | | | | | | | | | | | | | 636 |
| 638 | | 132 | | | | | | | | | | | | 639 | | | | | | 698.2 | | | | | | | | | | | | | | 638 |
| | | | | | | | | | | | | | | | | | | | | 3 | 15 | Tr Si | | | | | | | | | | | | |

Sharp but brecciated base to pink Si alt'n zone.

Sharp - drilled? - top

Brecciated base.

Fine to coarse flecks and rare wisps to cm of dk brown Sp.

TS 622289 625.5m

Bottom 50cm is weakly polymict

Only minor inter pillow sediment.

Pillowed top to bulk of basaltic unit below.

log.0193.mwr

Aberfoyle Resources Limited
EXPLORATION DIVISION

HOLE No. MA-[illegible]
PAGE 17 OF 23
GEO. SR
DATE 15-2-93

5 cm

# DIAMOND DRILL LOG

DRILLING: DEPTH | DRILLING RUNS | CORE LOSS | CORE TRAY NO.

LITHOLOGY: STRATIGRAPHY | ROCK TYPE | COLOUR | VOLCANICLASTICS: FRAGMENTS: COMPOSITION | MAX. SIZE (MM) | SORTING | SHAPE; MATRIX: COMPOSITION | VOLUME % | LOWER CONTACT: GRADATION | STYLE

VESICLES: CONCENTRATION | MAX. SIZE (MM) | SHAPE

ALTERATION: TEXTURE | INTENSITY | MINERALOGY

VEINING: INTENSITY | MAX. WIDTH (MM) | MINERALOGY

MINERALISATION: TEXTURE | MINERALOGY & CONTENTS

FAULTS: POSITION OF BASE | DOWNHOLE WIDTH (CM) | CORE AXIS ANGLE | GOUGE

FOLIATION: TYPE | CORE AXIS ANGLE

WEATHERING

STANDARD COLOUR LOG

REMARKS | SAMPLE NO. | DEPTH

| DEPTH | CORE TRAY NO. | ROCK TYPE | COLOUR | VESICLES | ALTERATION | VEINING | MINERALISATION |
|---|---|---|---|---|---|---|---|
| 642 | | | | 3 30 SE | | 2 10 Co | Vn Sp Tr |
| 643·0 | | | | | | 644·9 | |
| 644 | 133 | | | | | | |
| 646 | | | | | L 1 SiSe | 1 10 EpSi | |
| | | | | | | 2 10 Co | |
| 647·7 | | | | | | | |
| 648 | 134 | B-L | cgfm | 2 15 SE | | 4 10 Co | |
| 649·78 | | | | | | | |
| 650 | | | | | | | |
| 652 | | | | | | 3 20 Co | |
| 654 | 135 | | | | | 2 10 EpSiTr | |
| 655·4 | | | | | 663·0 | | |
| 656 | | | | | L 4 Si | | |
| 655·5 | | | | | | | |
| 658 | | | | 3 20 S | | 657·6 | |
| 659·0 | | | | | | | |
| 660 | 136 | | | | | | |
| 661·9 | | | | | | | |
| 662 | | | | | L 1 SiSe | 2 20 Co | |
| 664 | | | | 2 30 S | | | |
| 665 | 137 | | | | | 667·1 | |
| 666 | | | | | | | |
| 668 | | | | | | | |
| 669·0 | | | | | | 4 20 Co | |
| 670 | | | | | | | |
| 672 | 138 | | | 1 10 S | 672·0 | 672·0 | 672·0 |
| 672·0 | | | | | | | |
| 674 | | A-Lv | cgfm | | | 1 10 Co | |
| 676 | 139 | | | | | 2 50 Si | |
| 678 | | | | | | | |

REMARKS: Prominently feldspar phyric but appears to be dacitic
TS 622276 676·0m

SAMPLE NO.: 622198 | 622399

DEPTH: 642 644 646 648 650 652 654 656 658 660 662 664 666 668 670 672 674 676 678

6555 6563

log.0193.wor

Aberfoyle Resources Limited

EXPLORATION DIVISION

HOLE No. MAC 55

PAGE 18 OF 23

GEO. SK

DATE 15-2-93

5 cm

# DIAMOND DRILL LOG

DRILLING | LITHOLOGY | VESICLES | ALTERATION | VEINING | MINERALISATION | FAULTS | FOLIATION | WEATHERING | STANDARD COLOUR LOG | REMARKS | SAMPLE NO. | DEPTH

DEPTH | DRILLING RUNS / CORE LOSS | CORE TRAY NO. | STRATIGRAPHY | ROCK TYPE | COLOUR | VOLCANICLASTICS: FRAGMENTS: COMPOSITION, MAX. SIZE (MM), SORTING, SHAPE; MATRIX: COMPOSITION, VOLUME % | LOWER CONTACT: GRADATION, STYLE | VESICLES: CONCENTRATION, MAX. SIZE (MM), SHAPE | ALTERATION: TEXTURE, INTENSITY, MINERALOGY | VEINING: INTENSITY, MAX. WIDTH (MM), MINERALOGY | MINERALISATION: TEXTURE, MINERALOGY & CONTENTS | FAULTS: POSITION OF BASE, DOWNHOLE WIDTH (CM), CORE AXIS ANGLE, GOUGE | FOLIATION: TYPE, CORE AXIS ANGLE | WEATHERING | STANDARD COLOUR LOG | REMARKS | SAMPLE NO. | DEPTH

| DEPTH | CORE TRAY NO. | ROCK TYPE | COLOUR | FRAGMENTS COMPOSITION | FRAGMENTS MAX. SIZE (MM) | FRAGMENTS SORTING | FRAGMENTS SHAPE | MATRIX COMPOSITION | MATRIX VOLUME % | LOWER CONTACT GRADATION | LOWER CONTACT STYLE | ALTERATION TEXTURE | ALTERATION INTENSITY | ALTERATION MINERALOGY | VEINING INTENSITY | VEINING MAX. WIDTH (MM) | VEINING MINERALOGY | MINERALISATION TEXTURE | MINERALISATION MINERALOGY & CONTENTS |
|---|---|---|---|---|---|---|---|---|---|---|---|---|---|---|---|---|---|---|---|
| 682 | 140 | | | | | | | | | | | | | | | | | | |
| 684 | | | | | | | | | | | | | | | | | | | |
| 686 | 141 | | | | | | | | | | | | | | | | | | |
| 688 | | | | | | | | | | | | | | | | | | | |
| 690 | | A-Lv | Cgrn | FP | 50 | P | V | SiSeQ | 20 | | | P | 1 | Si | | | | Ds | PyTr |
| 692 | 142 | | | | | | | | | | | LMa | 2 | Si | | | | | |
| 694 | | | | | | | | | | | | | | | | | | | |
| 696 | | | | | | | | | | | | | | | | | | | |
| 698 | 143 | | | | | | | | | | | | | | | | | | |
| 700 | | | | | | | | | | | | | | | | | | | |
| 702 | 144 | | | | | | | | | | | | | | | | | | |
| 704 | | | | | | | | | | | | | | | | | | | |
| 706 | | | | | | | | | | | | | | | | | | | |
| 708 | 145 | | | | | | | | | | | | | | | | | | |
| 710 | | | | | | | | | | | | | | | | | | | |
| 712 | | | | | | | | | | | | | | | 712.4 | | | | |
| 714 | 146 | | | | | | | | | | | | | | 2 | 20 | 6 | | |
| 716 | | | | | | | | | | G1 | | | | | | | | | |
| 718 | 147 | 716.4 A-L | | | | | | | | | | 716.4 L | 1 | Si | | | | | |

Feldspar phyric lavas w. domainal alteration?

SAMPLE NO.: 622400, 622401

DEPTH: 682, 684, 686, 688, 690, 692, 694, 696, 698, 700, 702, 704, 706, 708, 710, 712, 714, 716, 718

65523

log.0193.wmf

Aberfoyle Resources Limited

EXPLORATION DIVISION

HOLE No. MAC 33

PAGE 19 OF 23

GEO. SR

DATE 23-2-93

# DIAMOND DRILL LOG

5 cm

| DRILLING | | | LITHOLOGY | | | | | | | | | | VESICLES | | | ALTERATION | | | VEINING | | | MINERALISATION | | FAULTS | | | | FOLIATION | | | | | |
|---|---|---|---|---|---|---|---|---|---|---|---|---|---|---|---|---|---|---|---|---|---|---|---|---|---|---|---|---|---|---|---|---|
| DEPTH | DRILLING RUNS / CORE LOSS | CORE TRAY NO. | STRATIGRAPHY | ROCK TYPE | COLOUR | VOLCANICLASTICS: FRAGMENTS: COMPOSITION | FRAGMENTS: MAX. SIZE (MM) | FRAGMENTS: SORTING | FRAGMENTS: SHAPE | MATRIX: COMPOSITION | MATRIX: VOLUME % | LOWER CONTACT: GRADATION | LOWER CONTACT: STYLE | CONCENTRATION | MAX. SIZE (MM) | SHAPE | TEXTURE | INTENSITY | MINERALOGY | INTENSITY | MAX. WIDTH (MM) | MINERALOGY | TEXTURE | MINERALOGY & CONTENTS | POSITION OF BASE | DOWNHOLE WIDTH (CM) | CORE AXIS ANGLE | GOUGE | TYPE | CORE AXIS ANGLE | WEATHERING | STANDARD COLOUR LOG | REMARKS | SAMPLE NO. | DEPTH |
| 722 | | | | A-L | Cgy | | | | | | | | | | | | L | 1 | Si | | | | | | | | | | | | | | | 722 |
| 724 | | 148 | | | Mcg | | | | | | | | | | | | L | 1 | Se | 2 | 20 | 6 | | | | | | | | | | | Aphyric to weakly fd phyric A? lava | 622402 | 724 |
| 726 | | | | | | | | | | | | | | | | | | | | | | | | | | | | | | | | | | 726 |
| 728 | | | | | | | | | | | | | | | | | | | | 728.7 | | | | | | | | | | | | | | 728 |
| 730 | | 149 | | | | | | | | | | | | | | | | | | 3 | 20 | 6 | Ds | PyTr | | | | | | | | | | 730 |
| 732 | | | | | | | | | | | | | | | | | | | | | | | | | | | | | | | | | | 732 |
| 734 | | | | | | | | | | | | | | | | | | | | | | | | | | | | | | | | TS 622290 733.6m | 622403 | 734 |
| 736 | | 150 | | | | | | | | | | | | | | | | | | | | | | | | | | | | | | | | 736 |
| 738 | | | | | | | | | | | | | | | | | | | | | | | | | | | | | | | | | | 738 |
| 740 | | | | | | | | | | | | | | | | | | | | 739.2 | | | | | | | | | | | | | | 740 |
| 742 | | 151 | | | | | | | | | | | | | | | | | | | | | | | 741.4 | 170 | 15° | Pu/Sm | | | | | | 742 |
| 744 | | | | | | | | | | | | | | | | | | | | 2 | 10 | 6 | | | | | | | | | | | | 744 |
| 746 | | 152 | | | | | | | | | | | | | | | | | | | | | | | | | | | | | | | | 746 |
| 748 | | | | | | | | | | | | | | | | | | | | | | | | | | | | | | | | | | 748 |
| 750 | | | | 750.5 | | | | | | | | G1 | | | | | 750.5 | | | | | | | | | | | | | | | | | 750 |
| 752 | | 153 | | A-L/LV | Cgy Gn | FP | 50 | P | V | Si | 20 | | | | | | Mg | 2 | Si | | | | | | | | | | | | | | | 622405 | 752 |
| 754 | | | | 755.7 | | | | | | | | S | | | | | 755.7 | | | | | | | | | | | | | | | | | 754 |
| 756 | | 154 | | | | | | | | | | | | | | | | | | | | | | | | | | | | | | | 622407 | 756 |
| 758 | | | | | | | | | | | | | | | | | | | | | | | | | | | | | | | | | | 758 |

65523

Aberfoyle Resources Limited

EXPLORATION DIVISION

HOLE NO. MAD...

PAGE 20 OF 23

GEO. SR

DATE 23-2-93

# DIAMOND DRILL LOG

5 cm

| DEPTH | DRILLING RUNS / CORE LOSS | CORE TRAY NO. | STRATIGRAPHY | ROCK TYPE | COLOUR | LITHOLOGY: VOLCANICLASTICS FRAGMENTS COMPOSITION | FRAGMENTS MAX. SIZE (MM) | FRAGMENTS SORTING | FRAGMENTS SHAPE | MATRIX COMPOSITION | MATRIX VOLUME % | LOWER CONTACT GRADATION | LOWER CONTACT STYLE | VESICLES CONCENTRATION | VESICLES MAX. SIZE (MM) | VESICLES SHAPE | ALTERATION TEXTURE | ALTERATION INTENSITY | ALTERATION MINERALOGY | VEINING INTENSITY | VEINING MAX. WIDTH (MM) | VEINING MINERALOGY | MINERALISATION TEXTURE | MINERALISATION MINERALOGY & CONTENTS | FAULTS POSITION OF BASE | FAULTS DOWNHOLE WIDTH (CM) | FAULTS CORE AXIS ANGLE | FAULTS GOUGE | FOLIATION TYPE | FOLIATION CORE AXIS ANGLE | WEATHERING | STANDARD COLOUR LOG | REMARKS | SAMPLE NO. | DEPTH |
|---|---|---|---|---|---|---|---|---|---|---|---|---|---|---|---|---|---|---|---|---|---|---|---|---|---|---|---|---|---|---|---|---|---|---|---|---|
| 762 | | 155 | | | | | | | | | | | | | | | P | 1 | Sscl | | | | | | | | | | | | | | | | | 762 |
| 764 | | | | | | | | | | | | | | | | | | | | | | | | | | | | | | | | | | | | 764 |
| 766 | | | | | | | | | | | | | | | | | | | | | | | | | | | | | | | | | | | | 766 |
| 768 | | 156 | | A-L/Lv | Gy/Gn | A, FP | 60 | P | V | Sil Cl | 10 | | | | | | | | | | | | | | | | | | | | | | | | | | 768 |
| 770 | | | | | | | | | | | | | | | | | | | | | 2 | 10 | Cc | | | | | | | | | | | | | 770 |
| 772 | | 157 | | | | | | | | | | | | | | | | | | | | | | | Ds | Py Tr | | | | | | | | | | 772 |
| 774 | | | | | | | | | | | | | | | | | | | | | | | | | | | | | | | | | | | | 774 |
| 776 | | | | | | | | | | | | | | | | | | | | | | | | | | | | | | | | | | | | 776 |
| 778 | | 158 | | | | | | | | | | | | | | | | | | | | | | | | | | | | | | | | | | 778 |
| 780 | | | | | | | | | | | | | | | | | | | | | | | | | | | | | | | | | | | | 780 |
| 782 | | | | | | | | | | | | | | | | | | | | | | | | | | | | | | | | | | | | 782 |
| 784 | | 159 | | | | | | | | | | S | | | | | | | | | | | | | | | | | | | | | | | | 784 |
| 786 | | | | | | | | | | | | | | | | | | | | | | | | | | | | | | | | | | | | 786 |
| 788 | | | | | | | | | | | | | | | | | | | | | | | | | | | | | | | | | | | | 788 |
| 790 | | 160 | | A-L | Gy/Gn | | | | | | | | | | | | | | | | | | | | | | | | | | | | | | | | 790 |
| 792 | | | | | | | | | | | | | | | | | | | | | | | | | | | | | | | | | | | | 792 |
| 794 | | 161 | | | | | | | | | | | | | | | | | | | | | | | | | | | | | | | | | | 794 |
| 796 | | | | | | | | | | | | | | | | | | | | | | | | | | | | | | | | | | | | 796 |
| 798 | | | | | | | | | | | | | | | | | | | | | | | | | | | | | | | | | | | | 798 |

784.0

785.5

789.5 2 5 V

791.3

789.9 P 1 Si

789.9

FB 791.5 30°

FB 792.5 0°

FB 795.0 20°

FB 796.0 80°

FB 798.0 30°

Only locally feldspar phyric unit of same composition as above

Domainially altered lava

Chilled? top 1m.

Becomes clast bearded? @ ≈ 0-30° CA below this point. Alteration banding?

TS 622278 791.4m

622408

622409

622410

65536

log8193User

Aberfoyle Resources Limited
EXPLORATION DIVISION

HOLE No. MAC 55
PAGE 21 OF 23
GEO. SR
DATE 23-2-93

5 cm

# DIAMOND DRILL LOG

DRILLING: DEPTH | DRILLING RUNS | CORE LOSS | CORE TRAY NO.

LITHOLOGY: STRATIGRAPHY | ROCK TYPE | COLOUR | VOLCANICLASTICS: FRAGMENTS: COMPOSITION, MAX. SIZE (MM), SORTING, SHAPE; MATRIX: COMPOSITION, VOLUME % | LOWER CONTACT: GRADATION, STYLE

VESICLES: CONCENTRATION | MAX. SIZE (MM) | SHAPE

ALTERATION: TEXTURE | INTENSITY | MINERALOGY

VEINING: INTENSITY | MAX. WIDTH (MM) | MINERALOGY

MINERALISATION: TEXTURE | MINERALOGY & CONTENTS

FAULTS: POSITION OF BASE | DOWNHOLE WIDTH (CM) | CORE AXIS ANGLE | DIP/DIR

FOLIATION: TYPE | CORE AXIS ANGLE

WEATHERING

STANDARD COLOUR LOG

REMARKS

SAMPLE NO. | DEPTH

| DEPTH | TRAY | ROCK TYPE | COLOUR | LITHOLOGY | VESICLES | ALTERATION | VEINING | MINERALISATION | FAULTS | FOLIATION | REMARKS | SAMPLE NO. |
|---|---|---|---|---|---|---|---|---|---|---|---|---|
| 802 | 162 | | | | 800.1 | | 801.6 | | | | 801.4 Base of flow banding<br>Feldspar phyric at base | 622410 |
| 804 | | | | | | | 2 20 6 | Ds PyTr | | | | |
| 805.7 | | | | S | | 805 | | 805.7 | | | | |
| 806 | 163 | av/FLV | Cy/Gn/Pk | a 2 W | | | | Vn SpTr<br>Ds PyTr | | 809.5 Bk 30° | massive to locally bedded well sorted fg/cg. v/c sandstone. | 622411 |
| 808 | | | | | | | | | | | | |
| 810 | 164 | | | | | | | | | | | |
| 812 | | | | | | | | | | | Fragment size increases downhole. | |
| 814 | | 814.4 | | C2 | | | | | | | are py HA frags. | |
| 816 | 165 | A-av/mfv | Cy/Gn | A (HA) 20 m V a 30 | | | | | | | TS 622291 813.2 | |
| 818 | | 818.8 | | S | 818.8 | | | | | | | |
| 820 | | 819.2 av/FLV 821.4 | | S S | 819.2 821.4 | 820.4 | | 821.4 | | | | 4-2 |
| 822 | 166 | B-L 823.4 | LGy | F | 2 5 S | P 2 SeCo | | | 823.4 1 15 Pw | | | 4-3 |
| 824 | | | | | 823.9 | 823.4 | | | | | | |
| 826 | 167 | Ss | Cy | S | 827.7 | 827.7 | 827.7 | | | Bd 827.6 80° | | 4-4 |
| 828 | | B-L 829.0 | Cy/Gn | S | 3 20 S | F 1 Co | 3 30 Co 829.0 | | | Bd 80° | | 415 |
| 830 | | | | | 829.6 | 829.0 | | | | 830 | | |
| 832 | 168 | Ss/Sh | Cy/Bk | | | | 1 10 6 | | | Bd 80° | 831.3 ORIENTATION | 622416 |
| 834 | | | | | | | | | | 835 | | |
| 836 | 169 | | | | | | | | | Bd 90 | | |
| 838 | | | | | | | | | | 840 | 838.3 x Bedding younging uphole | |

Log:8193Laser

6655

Aberfoyle Resources Limited

EXPLORATION DIVISION

HULL No. MAC 22

PAGE 22 OF 23

GEO. SR

DATE 24-2-93

# DIAMOND DRILL LOG

5 cm

DRILLING | LITHOLOGY | VESICLES | ALTERATION | VEINING | MINERALISATION | FAULTS | FOLIATION | WEATHERING | STANDARD COLOUR LOG | REMARKS | SAMPLE NO. | DEPTH

DEPTH | DRILLING RUNS | CORE LOSS | CORE TRAY NO.

STRATIGRAPHY | ROCK TYPE | COLOUR | VOLCANICLASTICS: FRAGMENTS: COMPOSITION, MAX. SIZE (MM), SORTING, SHAPE; MATRIX: COMPOSITION, VOLUME % | LOWER CONTACT: GRADATION, STYLE

VESICLES: CONCENTRATION, MAX. SIZE (MM), SHAPE

ALTERATION: TEXTURE, INTENSITY, MINERALOGY

VEINING: INTENSITY, MAX. WIDTH (MM), MINERALOGY

MINERALISATION: TEXTURE, MINERALOGY & CONTENTS

FAULTS: POSITION OF BASE, DOWNHOLE WIDTH (CM), CORE AXIS ANGLE, GOUGE

FOLIATION: TYPE, CORE AXIS ANGLE

WEATHERING

STANDARD COLOUR LOG

REMARKS

SAMPLE NO.

DEPTH

| DEPTH | DRILLING RUNS | CORE LOSS | CORE TRAY NO. |
|---|---|---|---|
| 842 | | | |
| 844 | | | 170 |
| 846 | | | |
| 848 | | | 171 |
| 850 | | | |
| 852 | | | |
| 854 | | | 172 |
| 856 | | | |
| 858 | | | |
| 860 | | | 173 |
| 862 | | | |
| 864 | | | |
| 866 | | | 174 |
| 868 | | | |
| 870 | | | |
| 872 | | | 175 |
| 874 | | | |
| 876 | | | 176 |
| 878 | | | |

| STRATIGRAPHY | ROCK TYPE | COLOUR | VOLCANICLASTICS: FRAGMENTS: COMPOSITION | MAX. SIZE (MM) | SORTING | SHAPE | MATRIX: COMPOSITION | VOLUME % | LOWER CONTACT: GRADATION | STYLE |
|---|---|---|---|---|---|---|---|---|---|---|
| | | | | | | | | | | |
| | 846.2 | | | | | | | | SI | |
| | Ss | Grey | | | | | | | | |
| | 861.4 | | | | | | | | SI | |
| | Ss/Sh | Grey-Blk | | | | | | | | |

| VESICLES: CONCENTRATION | MAX. SIZE (MM) | SHAPE |
|---|---|---|
| | | |

| ALTERATION: TEXTURE | INTENSITY | MINERALOGY |
|---|---|---|
| | | |

| VEINING: INTENSITY | MAX. WIDTH (MM) | MINERALOGY |
|---|---|---|
| 1 | 10 | Q |

| MINERALISATION: TEXTURE | MINERALOGY & CONTENTS |
|---|---|
| | |

| FAULTS: POSITION OF BASE | DOWNHOLE WIDTH (CM) | CORE AXIS ANGLE | GOUGE |
|---|---|---|---|
| | | | |

| FOLIATION: TYPE | CORE AXIS ANGLE |
|---|---|
| Bd 845 | 80° |
| Bd 856 | 80° |
| Bd 866 | 85° |
| Bd 870 | 85° |
| Bd 876.5 | 50 |

| WEATHERING |
|---|
| |

| STANDARD COLOUR LOG |
|---|
| |

| REMARKS |
|---|
| Near massive Ss interval |
| 866.6 ORIENTATION |
| Bedding becoming more disrupted and at shallower angle to CA. |

| SAMPLE NO. | DEPTH |
|---|---|
| 62247 | 842 |
| | 844 |
| | 846 |
| | 848 |
| | 850 |
| | 852 |
| | 854 |
| | 856 |
| | 858 |
| 62248 | 860 |
| | 862 |
| | 864 |
| | 866 |
| | 868 |
| | 870 |
| | 872 |
| | 874 |
| | 876 |
| | 878 |

65588

log81938.mor

Abermoyle Resources Limited
EXPLORATION DIVISION

HOLE NO. MAD--
PAGE 23 OF 23
GEO. SR
DATE 24-2-93

5 cm

# DIAMOND DRILL LOG

DRILLING: DEPTH | DRILLING RUNS | CORE LOSS | CORE TRAY NO.
LITHOLOGY: STRATIGRAPHY | ROCK TYPE | COLOUR | VOLCANICLASTICS: FRAGMENTS: COMPOSITION | MAX. SIZE (MM) | SORTING | SHAPE; MATRIX: COMPOSITION | VOLUME % | LOWER CONTACT: GRADATION | STYLE
VESICLES: CONCENTRATION | MAX. SIZE (MM) | SHAPE
ALTERATION: TEXTURE | INTENSITY | MINERALOGY
VEINING: INTENSITY | MAX. WIDTH (MM) | MINERALOGY
MINERALISATION: TEXTURE | MINERALOGY & CONTENTS
FAULTS: POSITION OF BASE | DOWNHOLE WIDTH (CM) | CORE AXIS ANGLE | GOUGE
FOLIATION: TYPE | CORE AXIS ANGLE
WEATHERING
STANDARD COLOUR LOG
REMARKS
SAMPLE NO.
DEPTH

| DEPTH | CORE TRAY NO. | ROCK TYPE | COLOUR | GRADATION | STYLE |
|---|---|---|---|---|---|
| 882 | 177 | | | | |
| 884 | | | | | |
| 886 | 178 | | | | |
| 888 | | | | | |
| 890 | | 890·1 | | 51 | |
| 892 | 179 | | | | |
| 894 | | | | | |
| 896 | | | | | |
| 898 | 180 | Ss | GD | | |
| 900 | | | | | |
| 902 | | | | | |
| 904 | 181 | | | | |
| 906 | | | | | |
| 908 | 182 | | | | |
| 910 | | | | | |
| 912 | | | | | |
| 914 | | | | | |
| 916 | | | | | |
| 918 | | | | | |

VEINING: 1 | 10 | C

| FAULTS: POSITION OF BASE | DOWNHOLE WIDTH (CM) | CORE AXIS ANGLE | GOUGE |
|---|---|---|---|
| 885·1 | 20 | 35 | RuSL |
| 890·1 | 5 | 5 | SL |

| FOLIATION: TYPE | CORE AXIS ANGLE |
|---|---|
| 883 | 65° |
| BA | |
| BA | 45° |
| 889 | |
| BA | 35° |
| 892 | |
| 897·5 | 75° |
| BA | |
| 905 | 65° |
| BA | |
| 907 | 70° |
| BA | |

STANDARD COLOUR LOG: ZZZ

905·2 ORIENTATION ⇒ Bedding flat.

EOH 910·7 m

65529

log01932.wor

**SAMPLE NUMBER: MAC 33 622279** 250.0 m

**SUMMARY: This rock is a monomict basaltic lava breccia derived from a poorly augite-phyric basalt, with distinctive large reacted and rounded plagioclase xenocrysts.**

**HAND SPECIMEN:**

This is a dark grey-green and strongly altered apparently polymict basaltic to andesitic lava breccia with fragments to at least several cm long

**THIN SECTION DESCRIPTION:**

This sample is a basaltic lava breccia, and despite the appearance in hand specimen strongly suggesting a polymict origin, thin section examination shows that it is a monomict lava breccia. The apparent variation in hand specimen of the lava fragments is attributable to variable styles and intensities of alteration. The rock was an augite-phyric basalt with occasional altered olivine phenocrysts and very distinctive and unusual strongly resorbed plagioclase phenocrysts. The augite phenocrysts make up about 2 modal% of the rock and are mainly small (<0.5mm long), although occasional larger euhedral crystals to 2mm long are present. Augite phenocrysts are mainly fresh stubby prisms, often in clots of three or four crystals, although some clots composed of more than twenty crystals are also present. Former olivine phenocrysts are mainly smaller than 1 mm long and are not very common; they are replaced by polycrystalline quartz and minor chlorite. There are quite a few rather large (to 3mm long) strongly rounded and reacted (resorbed) former plagioclase phenocrysts (albitized) in this lava breccia that are obviously out of equilibrium in this magma. They occur within fragments, not between fragments, and are clearly xenocrystal, probably derived from pre-existing dacitic magmas that used the same plumbing as this basaltic magma. The groundmass of the lava fragments varies slightly in texture from devitrified to spherulitic glass with tiny albite microlites and more granular augite crystals, to slightly more slowly-cooled basalt in which the devitrified glass is far more strongly charged with oriented and stouter plagioclase microlites.

The fragments in this sample have very diffuse and reacted margins against the inter-fragment matrix. The latter varies significantly in texture from rather coarse-grained polygonal quartz - prehnite-hematite intergrowths in most recrystallized areas, to more typical still relatively coarse-grained quartzo-feldspathic intergrowths with abundant interstitial and patchy chlorite.

This sample may have been the quenched and autobrecciated (hydrofractured) upper part of a basaltic lava flow that has suffered moderate hydrothermal alteration (mainly silica-alteration).

SAMPLE NUMBER: MAC 33 622280 320·8m

**SUMMARY: This rock is a rather well-preserved plagioclase+ augite-phyric dacitic lava with rare resorbed quartz and hornblende phenocrysts, and a low-grade regional burial metamorphic assemblage.**

HAND SPECIMEN:

This is a pale grey, massive, plagioclase-phyric dacitic lava with diffuse patchy silica alteration of the groundmass, and calcite-quartz veinlets.

THIN SECTION DESCRIPTION:

The protolith of this sample was probably very close mineralog- ically and texturally to sample 622286, being a sparsely plagioclase-phyric almost trachytic-textured lava with occasional augite microphenocrysts. However, the presence of a few distinct reacted and resorbed quartz phenocrysts or xenocrysts is one difference from 622286. Plagioclase phenocrysts make up about 1-2 modal% of this sample, and are small tabular to blocky albitized prisms, and augite phenocrysts are much less common fresh small (<0.3mm long) equigranular prisms. Two small resorbed phenocrysts of pleochroic hornblende are present, with ultra fine-grained reaction rims.

The groundmass of this sample was vitrophyric, composed of abundant tiny albite microlites and far less abundant tiny granular augite crystals set in devitrified glass. The latter has recrystallized to a very fine-grained rather murky quartzo-feldspathic material containing tiny fluffy leucoxene grains. Occasional small vesicles and tension gashes are filled by coarse-grained polycrystalline quartz and some fibrous epidote and pale green chlorite.

This is a well-preserved plagioclase+augite-phyric dacitic lava with a low-grade burial metamorphic mineral assemblage (albite-chlorite-silica-epidote-leucoxene).

SAMPLE NUMBER: MAC 33 622281 340.4m

**SUMMARY: This rock is a former sparsely plagioclase-phyric dacitic to rhyolitic lava breccia or hyaloclastite in which the brecciated texture has been enhanced by strong hydrothermal silica alteration.**

HAND SPECIMEN:

This is a strongly hydrothermally altered felsic lava breccia with dark clasts of plagioclase-phyric lava in a silica-altered matrix. Some clasts are several cm across.

THIN SECTION DESCRIPTION:

This sample is a former dacitic to rhyolitic lava breccia or hyaloclastite that has suffered strong 'false brecciation' and hydrothermal alteration. Fragments are widely dispersed, angular, and consist of a few modal% of small albitized plagioclase phenocrysts (<1mm across) and a single obvious quartz phenocryst, in a vitrophyric groundmass charged with tiny albite microlites set in devitrified glass. Epidote fans and granules are common in many plagioclase phenocrysts. The latter has recrystallized to an exceptionally fine-grained, low-birefringent silica-chlorite-leucoxene material with occasional spots of secondary quartz and patches of epidote.

The matrix in which the lava fragments are immersed consists of relatively coarse-grained polycrystalline silica containing subordinate anhedral albite grains and pale green chlorite. Less abundant phases in the silica-rich matrix are crystalline epidote in the most coarse-grained areas and segregations, sometimes intergrown with not uncommon red hematite.

The angular sharply-bounded fragments in this sample (though not all) suggest that this was a hyaloclastitic lava breccia. Subsequent quite strong hydrothermal alteration has enhanced the brecciation, leading to silica flooding and further disaggregation of the lava breccia.

SAMPLE NUMBER: MAC 33 622282 362.8m

SUMMARY: This rock is an augite+sparsely olivine-phyric basaltic lava with a prehnite-pumpellyite grade regional metamorphic overprint.

HAND SPECIMEN:

This is a very sparsely vesicular, finely augite-phyric basaltic lava.

THIN SECTION DESCRIPTION:

This sample is a texturally very well-preserved augite+sparsely olivine-phyric basaltic lava. About 5-8 modal% of the sample is made up of small prismatic euhedra of perfectly fresh augite phenocrysts and microphenocrysts. Many of these show significant compositional zoning, and multi-crystal clots of smaller, more anhedral or subhedral crystals are common. Small (<0.5mm long) euhedral former olivine phenocrysts make up <<<1 modal% of the rock, and are totally replaced by polycrystalline silica. There are no plagioclase phenocrysts or microphenocrysts in this sample.

The groundmass of this rock contains a few vesicles filled by polycrystalline quartz, hematite and epidote, and a few discontinuous, en echelon streaks of strained polycrystalline calcite. The groundmass consists of abundant tiny acicular to microlitic albitized plagioclase laths and less abundant small granular equidimensional augite all set in devitrified glass. The latter has recrystallized to anhedral quartz patches with subordinate chlorite and tiny fluffy leucoxene spots.

This is an augite-phyric basaltic lava typical of the Hellyer basalt, with a low-grade regional burial metamorphic overprint.

SAMPLE NUMBER: MAC 33 622283 427.3m

**SUMMARY: This rock is a plagioclase-phyric acid andesite lava with an unusual formerly vitrophyric groundmass texture.**

HAND SPECIMEN:

This is a massive slightly plagioclase-phyric basaltic to andesitic lava with occasional epidote segregations.

THIN SECTION DESCRIPTION:

This sample is a massive moderately plagioclase-phyric andesitic lava with about 8-10 modal% of albitized plagioclase phenocrysts that are mainly discrete tabular prisms less than 1mm long, occasionally containing granular epidote inclusions and patchy hematite dust. There are no clear former mafic phenocrysts.

The groundmass texture of this sample is most unusual, with blebby areas to about 2mm across with trachytic textures that look almost like lapilli. These blebs often have cores of polycrystalline secondary quartz. Interstitial areas between the rounded blebs make up from about 5 to 15 modal% of the rock, and are much darker coloured, being composed of an exceptionally fine-grained messy epidote-rich aggregate with minor chlorite, that overprints the original texture. Perfectly rounded vesicles are present throughout the rock, making up a few modal% of the sample, and being filled by radiating secondary quartz. Several quartz-epidote veinlets cut the sample, and carry a small amount of rather yellow Fe-rich sphalerite

This rock is probably a vitrophyric-textured lava of acid andesite composition, judging by the abundance of epidote and the hand specimen appearance. .

SAMPLE NUMBER: MAC 33 622284 438.2m

**SUMMARY: This rock is formerly glassy acid andesite to dacite lava breccia that has suffered hydrothermal alteration that produced false brecciation accompanied by silica-chlorite alteration.**

**HAND SPECIMEN:**

This is an almost black autobrecciated or false brecciated felsic lava breccia with common small plagioclase phenocrysts.

**THIN SECTION DESCRIPTION:**

This sample is a very complex lava breccia that has suffered strong silica alteration and accompanying 'false' brecciation. The rock was probably initially a lava breccia, with jigsaw fit fragments of moderately plagioclase-phyric acid andesite lava. Some of these have well-preserved perlitic cracks preserved, attesting to the originally glassy nature of this lava breccia. In most of the fragments, plagioclase phenocrysts and microphenocrysts make up about 3-5 modal% of the rock and are small (< 1mm) tabular albitized crystals with variably intense very fine-grained messy epidote overprinting. The groundmass of the best-preserved fragments is a mosaic-textured very fine-grained quartzo-feldspathic intergrowth with tiny albite microlites throughout. A few fragments are strongly chlorite-altered, although these are usually smaller than the well-preserved fragments. The inter-fragment areas are coarser-grained and cleaner quartz-dominated intergrowths, and fragments no longer show any evidence of jigsaw fit, and have been thoroughly disaggregated.

This sample was probably a polymict, glassy, plagioclase-phyric acid andesite to dacite lava breccia. Initial chlorite-silica hydrothermal alteration of fragment margins and inter-fragmental areas was followed by silica flooding and further disaggregation of the original breccia texture.

SAMPLE NUMBER: MAC 33 622285 468.2m

**SUMMARY: This rock is a hydrothermally-altered sparsely plagioclase-phyric dacitic hyaloclastite in which the brecciation has been enhanced by the passage of, and alteration by the hydrothermal fluids, that produced silicification of matrix areas.**

HAND SPECIMEN:

This is a hydrothermally altered (partially silicified) dacitic to andesitic lava breccia or hyaloclastite with pinkish ultra-fine-grained silica in more intensely altered areas between darker green lava fragments that are up to several mm long.

THIN SECTION DESCRIPTION:

This sample is, in many respects, very similar to the altered hyaloclastite 622289. It consists of darker coloured fragments from 1cm to <1mm of perlitically-cracked, formerly glassy lavas containing around 1-2 modal% of small, tabular albitized plagioclase phenocrysts to about 0.3mm long. The once-glassy groundmass of these fragments has devitrified and recrystallized to either a murky strongly chlorite-altered material containing tiny albite microlites, or else to a clearer fine-grained quartzo-feldspathic aggregates with limited sericite-calcite overprint. In the chloritized areas, the perlitic cracks are picked out by trails of quartz.

The formerly glassy lava fragments are immersed in a pervasive 'matrix' of rather cleaner, sugary quartzo-feldspathic material that contains occasional quartz-chlorite spots, and common larger areas of calcite overprinting. In much of this section, the matrix is volumetrically far more abundant than the fragments. This sample was initially a hyaloclastite or subaqueous chill breccia in which the brecciation has been enhanced during hydrothermal alteration.

SAMPLE NUMBER: MAC 33 622286 495.3m

**SUMMARY: This rock is a trachytic-textured dacitic lava with a low-grade burial metamorphic overprint.**

HAND SPECIMEN:

*This is a grey to pinkish grey altered felsic to intermediate* near aphyric lava with a few small calcite veinlets.

THIN SECTION DESCRIPTION:

This sample is a sparsely plagioclase-phyric trachytic-textured dacitic to acid andesite lava. Small tabular prismatic phenocrysts of albitized plagioclase to about 1mm maximum length make up around 1-2 modal% of the rock, and contain abundant chlorite inclusions. Some are overprinted by dusty prehnite and intergrown calcite. There were apparently no mafic silicate phenocrysts in this sample, but small FeTi oxide microphenocrysts are scattered through the rock and are altered to an intergrowth of chlorite, magnetite and sphene.

The groundmass of this sample is a fine-grained aggregate composed of small oriented albite laths set in volumetrically subordinate devitrified glass that has recrystallized to a quartzo-feldspathic intergrowth. This produces a rather swirling pilotaxitic or trachytic texture, interrupted by segregations of anhedral secondary quartz that occasionally coalesce to form veinlets of polycrystalline quartz. Small blebs and patches of chlorite are not uncommon through the groundmass, but the sample shows no sign of significant chlorite (hydrothermal) alteration. A *few calcite veinlets cut the sample and one thicker vein (7mm* wide) consists of intergrown calcite and quartz, with at least one crystal of barite growing in the vein.

This is a low-grade burial metamorphosed, sparsely plagioclase-phyric dacitic lava.

SAMPLE NUMBER: MAC 33 622287 503.2m

**SUMMARY: This rock is a formerly glassy, very well-preserved plagioclase-phyric dacitic lava with a low-grade regional burial metamorphic alteration assemblage.**

**HAND SPECIMEN:**

This is a dark red plagioclase-phyric massive felsic lava.

**THIN SECTION DESCRIPTION:**

This sample is a plagioclase-phyric texturally rather distinctive dacitic to rhyolitic lava. It consists of around 5-8 modal% of albitized plagioclase phenocrysts set in a formerly glassy groundmass. The plagioclase phenocrysts are mainly less than 1mm long, and usually occur in multi-crystal clots up to a few mm across. There is no convincing evidence for the original presence of any mafic phenocrysts in this lava.

The groundmass of this rock was originally glassy to spherulitic, and is composed of a very clean quartzo-feldspathic intergrowth dominated by tiny microlites of albite that merge at their margins into the anhedral quartzo-feldspathic intergrowth that makes up most of the groundmass. Throughout the groundmass there are abundant small to several mm-sized angular fracture fillings and irregular patches of secondary quartz and unusually crystalline sericite (muscovite?) and sphene. The latter is perfectly euhedral and up to almost 1mm long crystals in places.

This is a very well-preserved formerly glassy dacitic lava.

SAMPLE NUMBER: MAC 33 622288 524.0m

SUMMARY: This rock is a perlitically-cracked, formerly glassy, sparsely plagioclase-phyric dacitic lava.

HAND SPECIMEN:

This is a dark green sparsely plagioclase-phyric dacitic lava with quite clearly visible perlitic cracking.

THIN SECTION DESCRIPTION:

This sample is a well-preserved dacitic lava with about 3-5 modal% of albitized plagioclase phenocrysts in a perlitically-cracked groundmass. The plagioclase phenocrysts are up to several mm long, and occur as subhedral to euhedral, prismatic to blocky crystals, often aggregated in clots of three or four crystals. They are generally slightly sericite altered. Small euhedral to subhedral former augite phenocrysts, mainly less than 0.4mm long, are not uncommon, although most occur interstitially in clots of plagioclase phenocrysts. They are invariably altered to green chlorite. The same applies to small FeTi oxide phenocrysts that are altered to messy leucoxene.

The groundmass of this sample was undoubtedly originally glassy, and preserves abundant areas of strong perlitic cracking, in which the cracks are defined by fine-grained chloritic aggregates separating domains of fine-grained quartzo-feldspathic material after original glass. Tiny albite microlites are scattered in the quartzo-feldspathic material after glass. Other components in the altered glass are quite common fine-grained flaky chlorite and very fine-grained fluffy leucoxene granules. The distribution of groundmass chlorite is rather patchy, and in some parts of the thin section it is quite intensely developed. Narrow quartz- and quartz-calcite veinlets are not uncommon, and the latter define faults along which the quartz veins have been offset by up to a cm. Small trails and aggregates of an unidentified opaque phase (probably pyrite) are present throughout the groundmass, although they are modally insignificant.

This is a well-preserved formerly glassy dacitic lava.

SAMPLE NUMBER: MAC 33 622289 625·5m

**SUMMARY: This rock is a hyaloclastite or hydrofractured dacitic lava breccia derived from a plagioclase-phyric dacitic lava.**

**HAND SPECIMEN:**

This is a plagioclase-phyric mid-grey weakly autobrecciated dacitic lava with fragments up to 2cm across, but mostly much smaller.

***THIN SECTION DESCRIPTION:***

This sample in thin section was clearly a glassy dacitic lava that suffered limited hydrofracturing during eruption and cooling. Cores of fragments show well-preserved perlitic cracks, and in these best preserved areas, the rock can be seen to be composed of around 5 modal% of albitized plagioclase phenocrysts that commonly contain abundant inclusions of granular yellow epidote and minor chlorite. No convincing former mafic silicate phenocrysts are present, and occasional small FeTi oxide phenocrysts are altered to leucoxene. The groundmass of these fragments was glassy, and has perlitic cracks preserved by narrow lines of chlorite; the glass has recrystallized to a fairly fine-grained murky quartzo-feldspathic intergrowth. Other less well-preserved fragments show no perlitic cracks and a heavy overprinting by very fine-grained, messy epidote.

The 'matrix' areas between fragments are clearer or 'cleaner' than the fragments themselves, probably due to some degree of silicification of the former granulated glass that probably existed along the fragment boundaries and in the cracks produced between fragments during hyaloclastitic brecciation. The texture of the matrix areas is little different from that of the fragments, except that the secondary sugary quartz grains are slightly coarser-grained. No jig-saw fit fragments are obvious, so the sample protolith was probably brecciated during eruption to the extent that fragments were disaggregated. The low-grade burial metamorphic assemblage is prehnite-pumpellyite facies.

**SAMPLE NUMBER:** 622276 MAC-33, 676m

655201

**SUMMARY:**

This is a weakly hyaloclastic silicic andesitic lava in which the original brecciation has been enhanced by later low-grade hydrothermal alteration.

**HAND SPECIMEN:**

This is a dark grey plagioclase-phyric dacitic lava that shows a feint hyaloclastitic or pseudo-brecciated texture.

**THIN SECTION:**

This is a plagioclase-phyric formerly glassy lava with abundant well-preserved areas of perlitic cracking separated by domains in which the original perlitic texture has been disrupted due to more intense alteration related to fluid focussing.

The rock consists of around 3-5 modal% of fairly small, mainly euhedral albitized plagioclase phenocrysts (<1mm long) that sometimes occur in clots of two or three crystals. Many have distinctive rows of chloritized melt inclusions, and small fans of prehnite are not uncommon replacing parts of plagioclase phenocrysts and small areas of groundmass. There are no former mafic phenocrysts in this sample, and the not uncommon small phenocrysts of FeTi oxide are totally replaced by messy leucoxenitic intergrowths.

The groundmass of this sample was undoubtedly entirely glassy, as perlitic cracks are well preserved and picked out by very fine-grained chlorite. The abundance of chlorite decreases sharply into inter-fragment domains, that are dominated by very fine-grained silica and sericite. This has produced a texture in both hand specimen and thin section in which it is very difficult to decide whether the rock was originally composed of angular glassy lava fragments (a hyaloclastite) or whether the texture is a false brecciation due to hydrothermal alteration. The alteration is fairly low-grade, and dominated by silica. A few small veinlets of calcite transect the slide, and a number of small trails of very fine- grained euhedral magnetite or pyrite are also present.

I think that this rock was probably from the upper portion of a cooling unit, and that it cracked and shattered, without being too disaggregated, during eruption in water. The cracks focussed later hydrothermal alteration, which enhanced the original vague brecciated texture (hyaloclastitic?) to produce what is best classified as a false brecciated texture.

The abundance of chlorite in this sample is certainly more than I would expect to see in a 'normal' Que-Hellyer dacite, and suggests that this rock is more probably a silicic andesite.

SAMPLE NUMBER: MAC 33 622290 733.6m

**SUMMARY: This rock is a plagioclase+sparsely augite-phyric dacitic lava with a low-grade (chlorite-sericite-albite-silica) burial metamorphic assemblage.**

HAND SPECIMEN:

This is a mid- to dark green, sparsely plagioclase-phyric andesitic lava with abundant small chlorite spots and at the edge of the thin section chip, a darker green lithic fragment (or possibly contact with an adjacent flow).

THIN SECTION DESCRIPTION:

This sample is a plagioclase +sparse augite-phyric andesitic to dacitic lava with around 10-12 modal% of plagioclase phenocrysts and probably less than one modal% of altered augite phenocrysts. The plagioclase phenocrysts vary from blocky to tabular prisms that often occur in clots of three or four crystals, reaching a few mm in size. They are usually fairly strongly overprinted by sericite. Former augite phenocrysts are mainly smaller than 0.5mm long, with distinctive stubby prismatic euhedral shapes, and all are pseudomorphed by green chlorite. Former FeTi oxide phenocrysts are altered to leucoxenitic aggregates. A number of lithic fragments are present in the section. The largest is more than 1cm across and is composed of a quenched intergrowth of long, bladed albitized plagioclase and chloritized augite crystals. Two others are composed of small euhedral plagioclase and chloritized augite crystals and appear to be small, cognate microgabbroic clots, probably ripped from the walls of the conduit during passage of this lava to the surface.

The groundmass of this sample was probably mainly glassy, with a common indistinct patches in which tiny plagioclase microlites had nucleated. The glass has devitrified to a very fine-grained quartzo-feldspathic intergrowth that is quite heavily laced by a mesh of sericite, and also contains common small clots of chlorite and leucoxenitized opaques. Some meandering stylolitic pressure solution boundaries transect the rock, and are defined by concentrations of altered insoluble oxides.

This is a low-grade burial metamorphosed dacitic lava, probably transitional to an acid andesite.

**SAMPLE NUMBER:** 622277 MAC-33, 753.3m

**SUMMARY:**

This is a quite strongly altered (silica-chlorite-pyrite±calcite), weakly plagioclase-phyric, formerly glassy silicic andesite lava, originally very similar petrographically to 622276.

**HAND SPECIMEN:**

Despite coming from 77m deeper in the hole, this sample is very similar to the preceding rock in hand specimen, except for a weak network of very fine fractures, and probably a larger volume of more altered (inter-fragment) material than 622276.

**THIN SECTION:**

The protolith of this sample was almost certainly identical to that of the preceding sample 622276. It was a totally glassy, weakly plagioclase-phyric andesitic to dacitic rock with well-preserved perlitic cracks, albitized plagioclase phenocrysts (with some clayey alteration), and a weak hyaloclastitic texture. However, this sample has been notably more altered than 276, with coarsening of the chloritic seams that nucleate along the perlitic cracks, and far more common and coarser-grained polygonal secondary silica. Streaky calcite is more common than in 276, and disseminated idiomorphic pyrite crystals to almost 0.5mm across are not uncommon. The latter sometimes have rims and pressure fringes of green chlorite.

The texture is now definitely a false-brecciated texture, and it is not possible to judge whether this is simply an amplification of an original hyloclastite texture, or solely due to alteration of a more massive glassy lava flow. I would suggest that the former is more likely.

**SAMPLE NUMBER:** 266678, MAC-33 791.4m

**SUMMARY:**

This is a silicic andesite lava with moderate silica-chlorite alteration, and is similar in most respects to the two preceding samples except that it was less glassy, and apparently more massive than 622276 or 622277.

**HAND SPECIMEN:**

This is a dark grey, sparsely plagiolcase-phyric meta-andesitic lava with irregular alteration banding of lighter-coloured, finer-grained material, and a few calcite veinlets.

**THIN SECTION:**

This is a quite altered and recrystallized sparsely plagioclase-phyric andesitic lava. Former plagioclase phenocrysts make up around 1-3 modal% of this sample, and are totally albitized subhedral prisms usually less than 0.5mm long. Most have been almost completely replaced by very fine-grained sericite. There are no mafic phenocrysts in this rock, but small apatite microphenocrysts are not uncommon, and totally leucoxene-altered FeTi oxide phenocrysts are common.

The groundmass of this sample was weakly vesicular, glassy to vitrophyric, being composed of glass charged with tiny acicular plagioclase microlites. The glass has devitrified and crystallized to a patchy mosaic quartzo-feldspathic intergrowth, and conatins abundant very fine-grained sericite and common chlorite, plus many small angular patches of secondary quartz. Former vesicles are filled by polygonal quartz, and minor chlorite and epidote. The streaky to banded nature nature of the silica-chlorite alteration, best defined by modal variation in chlorite abundance, produces almost a weak schistosity in the rock, although the hand specimen lacks any sign of a weak parting. Calcite veinlets are also quite common.

This sample was, like 276 and 277, a silicic andesite lava. To me, it contains more chlorite (in a rock in which the chloritization is not pronounced) than typical MRV dacites, and in that respect is closer to an andesite. However, the abundant quartzo-feldspathic groundmass, the absence of mafic phenocrysts, and the relative paucity of plagioclase phenocrysts, are all features more typical of dacites. I suggest that it falls somewhere along the andesite to dacite spectrum.

SAMPLE NUMBER: MAC 33 622291 813.2m

**SUMMARY: This rock is probably a former lithic crystal tuff composed of small fragments (<2mm) of glassy plagioclase-phyric andesitic lava, and vitric ash. It has suffered strong chlorite-epidote alteration.**

HAND SPECIMEN:

This is a strongly altered dark green plagioclase-phyric andesitic lava or crystal lithic tuff.

THIN SECTION DESCRIPTION:

This sample is a difficult one to diagnose with certainty, due to strong alteration obliterating the primary texture to the extent that it is not immediately obvious whether this is a lava or a lithic crystal tuff. The rock certainly contains four or five distinct lithic fragments to about 2mm long, with quartzo-feldspathic groundmasses, small plagioclase phenocrysts and abundant secondary magnetite, but the remainder of the rock appears at first to have been a plagioclase-phyric glassy andesitic lava. Plagioclase phenocrysts are totally replaced by dense sericite, and there appear to have been few if any former mafic phenocrysts.

The groundmass of the rock is unusual. It was evidently largely glassy, and is now composed of an almost isotropic material probably made up of fine-grained epidote and chlorite, with a fine sericite web pervading it. Textural changes in the isotopic material are sudden, and suggest a fragmental texture in many places. I suggest that this was a lithic crystal tuff composed of small lapilli-sized fragments of glassy andesite in a matrix of vitric ash, all of which have totally altered to the same messy epidote-chlorite material upon devitrification and alteration.

655206

# ANALABS

A Division of Inchcape Inspection and Testing Services Australia Pty. Ltd. A.C.N. 004 591 864

7 APR 1993

Phone (004) 316837 | 14 Thirkell St. CODEE TAS 7320 | Fax (004) 318890

## ANALYTICAL REPORT No. 100560.60.09358

THIS REPORT MUST BE READ IN CONJUNCTION WITH THE ACCOMPANYING ANALYTICAL DATA

INVOICE TO:

Aberfoyle Resources Limited
Exploration Division
P.O. Box 952
BURNIE TAS 7320

| ORDER No. | PROJECT |
|---|---|
| 2739 | MAC-33 |

| DATE RECEIVED | RESULTS REQUIRED |
|---|---|
| 09/03/93 | ASAP |

| No. OF PAGES OF RESULTS | DATE REPORTED | No. OF COPIES | TOTAL No. OF SAMPLES |
|---|---|---|---|
| 3 | 06/04/93 | 1 | 16 |

| SAMPLE NUMBERS | SAMPLE DESCRIPTION | ELEMENT/METHOD |
|---|---|---|
| 622276/91 | DC Prep : GP033 - CHROME FREE BOWLS | Cu,Pb,Zn,Ag/GA101<br>Ba,As,Cr,Zr/GX401<br>WHOLE ROCK ANALYSIS/OX408 |

RESULTS TO:

Mr R de Bomford
Aberfoyle Resources Limited
P.O. Box 952
BURNIE TAS 7320

RESULTS TO:

RESULTS TO:

REMARKS

MAC-33 PET.

AUTHORISED OFFICER

655307

# ANALABS

A Division of Inchcape Testing Services (Australia) Pty. Ltd.
A.C.N. 004 591 664

## ANALYTICAL DATA

| SAMPLE PREFIX | REPORT No. | REPORT DATE | CLIENT ORDER No. | PAGE |
|---|---|---|---|---|
| | 100560.60.09358 | 06/04/93 | 2739 | 1 OF 3 |

| IBE No. | SAMPLE No. | Cu | Pb | Zn | Ag | Ba | As | Cr | Zr | Ti |
|---|---|---|---|---|---|---|---|---|---|---|
| 1 | 622276 | 11 | <5 | 83 | <2 | 1789 | 13 | 21 | 193 | 2250 |
| 2 | 622277 | 4 | <5 | 49 | <2 | 140 | <2 | 12 | 178 | 2150 |
| 3 | 622278 | <4 | <5 | 29 | <2 | 1069 | <2 | <5 | 164 | 3320 |
| 4 | 622279 | 46 | 654 | 814 | <2 | 2416 | 15 | 87 | 185 | 4480 |
| 5 | 622280 | 53 | 72 | 3689 | <2 | 1407 | 6 | 21 | 170 | 4260 |
| 6 | 622281 | 24 | 243 | 2496 | <2 | 1798 | 16 | 13 | 182 | 4850 |
| 7 | 622282 | 37 | 8 | 252 | <2 | 782 | 9 | 160 | 167 | 3920 |
| 8 | 622283 | 55 | 105 | 211 | <2 | 2261 | 6 | 9 | 164 | 3130 |
| 9 | 622284 | 5 | <5 | 80 | <2 | 1954 | <2 | 7 | 171 | 3220 |
| 10 | 622285 | 7 | <5 | 84 | <2 | 276 | 2 | 8 | 170 | 3070 |
| 11 | 622286 | 6 | <5 | 32 | <2 | 2569 | <2 | 6 | 156 | 2920 |
| 12 | 622287 | <4 | <5 | 16 | <2 | 1619 | <2 | 7 | 232 | 2070 |
| 13 | 622288 | 14 | 17 | 649 | <2 | 2302 | 24 | <5 | 234 | 2180 |
| 14 | 622289 | 18 | 38 | 1058 | <2 | 1768 | 7 | 71 | 237 | 2660 |
| 15 | 622290 | 5 | <5 | 60 | <2 | 854 | 2 | 15 | 243 | 3170 |
| 16 | 622291 | 25 | <5 | 73 | <2 | 1913 | 3 | 26 | 172 | 5950 |
| 17 | | | | | | | | | | |
| 18 | | | | | | | | | | |
| 19 | | | | | | | | | | |
| 20 | | | | | | | | | | |
| 21 | | | | | | | | | | |
| 22 | | | | | | | | | | |
| 23 | DETECTION | 4 | 5 | 4 | 2 | 10 | 2 | 5 | 5 | 60 |
| 24 | UNITS | ppm | ppm | ppm | ppm | ppm | ppm | ppm | ppm | ppm |
| 25 | METHOD | GA101 | GA101 | GA101 | GA101 | GX401 | GX401 | GX401 | GX401 | GX401 |

*Results in ppm unless otherwise specified*
T = element present; but concentration too low to measure
X = element concentration is below detection limit
– = element not determined

AUTHORISED OFFICER

655308

# ANALABS

A Division of Inchcape Testing Services (Australia) Pty. Ltd.
A.C.N. 004 591 664

## ANALYTICAL DATA

| SAMPLE PREFIX | REPORT No. | REPORT DATE | CLIENT ORDER No. | PAGE |
|---|---|---|---|---|
| | 100560.60.09358 | 06/04/93 | 2739 | 2 OF 3 |

| IBE No. | SAMPLE No. | Al2O3 | SiO2 | TiO2 | Fe2O3 | MnO | CaO | K2O | MgO | P2O5 |
|---|---|---|---|---|---|---|---|---|---|---|
| 1 | 622276 | 13.71 | 69.00 | 0.38 | 5.38 | 0.14 | 1.12 | 2.38 | 1.48 | 0.085 |
| 2 | 622277 | 13.68 | 64.20 | 0.36 | 4.47 | 0.13 | 4.13 | 0.47 | 1.42 | 0.099 |
| 3 | 622278 | 14.75 | 67.90 | 0.55 | 3.79 | 0.11 | 2.61 | 3.51 | 0.50 | 0.169 |
| 4 | 622279 | 13.96 | 59.10 | 0.75 | 8.15 | 0.38 | 4.30 | 2.35 | 4.51 | 0.270 |
| 5 | 622280 | 14.60 | 59.40 | 0.71 | 7.16 | 0.45 | 4.86 | 1.80 | 3.39 | 0.325 |
| 6 | 622281 | 15.82 | 55.60 | 0.81 | 8.32 | 0.47 | 4.63 | 2.04 | 3.62 | 0.362 |
| 7 | 622282 | 13.74 | 54.90 | 0.65 | 8.34 | 0.33 | 7.43 | 1.08 | 5.89 | 0.260 |
| 8 | 622283 | 15.36 | 62.20 | 0.52 | 6.23 | 0.22 | 4.41 | 2.82 | 1.91 | 0.281 |
| 9 | 622284 | 14.86 | 62.70 | 0.54 | 7.14 | 0.23 | 2.88 | 3.03 | 2.14 | 0.281 |
| 0 | 622285 | 16.19 | 61.50 | 0.51 | 7.98 | 0.19 | 1.63 | 1.54 | 2.70 | 0.284 |
| 1 | 622286 | 14.83 | 66.00 | 0.49 | 2.71 | 0.09 | 3.13 | 3.85 | 0.72 | 0.262 |
| 12 | 622287 | 14.45 | 71.70 | 0.35 | 2.01 | 0.04 | 1.10 | 4.83 | 0.20 | 0.085 |
| 3 | 622288 | 14.52 | 68.30 | 0.36 | 4.66 | 0.11 | 1.22 | 3.34 | 1.17 | 0.079 |
| 14 | 622289 | 13.73 | 67.00 | 0.44 | 5.60 | 0.25 | 2.85 | 2.72 | 2.07 | 0.207 |
| 5 | 622290 | 17.70 | 59.10 | 0.53 | 5.81 | 0.16 | 3.29 | 3.73 | 1.26 | 0.138 |
| 16 | 622291 | 16.44 | 56.50 | 0.99 | 9.35 | 0.17 | 1.93 | 3.84 | 3.62 | 0.187 |
| | | | | | | | | | | |
| 8 | | | | | | | | | | |
| 19 | | | | | | | | | | |
| 0 | | | | | | | | | | |
| 21 | | | | | | | | | | |
| 22 | | | | | | | | | | |
| 3 | DETECTION | 0.01 | 0.01 | 0.01 | 0.01 | 0.01 | 0.01 | 0.01 | 0.05 | 0.005 |
| 24 | UNITS | % | % | % | % | % | % | % | % | % |
| 5 | METHOD | OX408 | OX408 | OX408 | OX408 | OX408 | OX408 | OX408 | OX408 | OX408 |

*Results in ppm unless otherwise specified*
T = element present; but concentration too low to measure
X = element concentration is below detection limit
– = element not determined

AUTHORISED OFFICER

655209

# ANALABS

A Division of Inchcape Testing Services (Australia) Pty. Ltd.
A.C.N. 004 591 664

## ANALYTICAL DATA

| SAMPLE PREFIX | REPORT No. | REPORT DATE | CLIENT ORDER No. | PAGE |
|---|---|---|---|---|
| | 100560.60.09358 | 06/04/93 | 2739 | 3 OF 3 |

| TUBE No. | SAMPLE No. | S | Na2O | LOI | TOTAL | | | | | |
|---|---|---|---|---|---|---|---|---|---|---|
| 1 | 622276 | 0.180 | 3.83 | 2.02 | 99.67 | | | | | |
| 2 | 622277 | 0.370 | 5.80 | 4.54 | 99.64 | | | | | |
| 3 | 622278 | 0.020 | 3.16 | 2.86 | 99.90 | | | | | |
| 4 | 622279 | 0.170 | 2.72 | 2.88 | 99.50 | | | | | |
| 5 | 622280 | 0.290 | 3.61 | 2.90 | 99.54 | | | | | |
| 6 | 622281 | 0.160 | 3.49 | 4.22 | 99.58 | | | | | |
| 7 | 622282 | 0.040 | 3.38 | 3.73 | 99.80 | | | | | |
| 8 | 622283 | 0.050 | 3.18 | 2.35 | 99.53 | | | | | |
| 9 | 622284 | 0.060 | 3.00 | 2.76 | 99.62 | | | | | |
| 10 | 622285 | 0.240 | 3.94 | 2.79 | 99.52 | | | | | |
| 11 | 622286 | 0.010 | 4.63 | 2.88 | 99.60 | | | | | |
| 12 | 622287 | <0.005 | 4.28 | 0.88 | 99.96 | | | | | |
| 13 | 622288 | 0.420 | 3.18 | 2.31 | 99.64 | | | | | |
| 14 | 622289 | 0.060 | 2.79 | 1.94 | 99.69 | | | | | |
| 15 | 622290 | 0.160 | 3.82 | 4.38 | 100.04 | | | | | |
| 16 | 622291 | 0.120 | 2.06 | 4.31 | 99.57 | | | | | |
| 17 | | | | | | | | | | |
| 18 | | | | | | | | | | |
| 19 | | | | | | | | | | |
| 20 | | | | | | | | | | |
| 21 | | | | | | | | | | |
| 22 | | | | | | | | | | |
| | DETECTION | 0.005 | 0.05 | 0.01 | 0.01 | | | | | |
| | UNITS | % | % | % | % | | | | | |
| | METHOD | OX408 | OX408 | OX408 | OX408 | | | | | |

Results in ppm unless otherwise specified
T = element present; but concentration too low to measure
X = element concentration is below detection limit
– = element not determined

AUTHORISED OFFICER

# APPENDIX VII

# ABERFOYLE RESOURCES LTD. DRILL LOG

**Area Code** mac | **Prospect** Mt. Charter | **Report Grid** Mack | **Dataset** Geochemical data set

**Holename** DDMA0033 | **Stored Grid** Mack

| From | To | Sample Type | Cu ppm | Pb ppm | Zn ppm | Ag ppm | Au ppm | Ba ppm | As ppm | Cr ppm | Zr ppm | Ti ppm | Ti/Zr |
|---|---|---|---|---|---|---|---|---|---|---|---|---|---|
| 0.00 | 15.00 | 622335 cgri | 55 | 8 | 95 | <2.0 | <0.008 | 476 | 2 | 746 | 84 | 3140 | 37.38 |
| 15.00 | 30.00 | 622336 cgri | 55 | 6 | 78 | <2.0 | <0.008 | 456 | 2 | 766 | 89 | 3270 | 36.74 |
| 30.00 | 45.00 | 622337 cgri | 44 | <5 | 74 | <2.0 | <0.008 | 443 | 4 | 762 | 84 | 3150 | 37.50 |
| 45.00 | 60.00 | 622338 cgri | 41 | <5 | 78 | <2.0 | <0.008 | 456 | 3 | 789 | 74 | 2900 | 39.19 |
| 60.00 | 73.60 | 622339 cgri | 50 | 5 | 88 | <2.0 | <0.008 | 417 | <2 | 840 | 76 | 2950 | 38.82 |
| 73.60 | 82.30 | 622340 cgri | 94 | 41 | 166 | <2.0 | <0.008 | na | na | na | na | na | ? |
| 82.30 | 84.40 | 622341 cgri | 70 | 59 | 329 | <2.0 | <0.008 | na | na | na | na | na | ? |
| 84.40 | 90.20 | 622342 cgri | 105 | 44 | 145 | <2.0 | <0.008 | na | na | na | na | na | ? |
| 90.20 | 91.30 | 622343 cgri | 41 | 135 | 500 | <2.0 | <0.008 | na | na | na | na | na | ? |
| 91.30 | 103.40 | 622344 cgri | 77 | 37 | 153 | <2.0 | <0.008 | na | na | na | na | na | ? |
| 103.40 | 111.20 | 622345 cgri | 73 | 15 | 92 | <2.0 | <0.008 | na | na | na | na | na | ? |
| 111.20 | 123.00 | 622346 cgri | 80 | 42 | 160 | <2.0 | <0.008 | na | na | na | na | na | ? |
| 123.00 | 140.00 | 622347 cgri | 115 | 33 | 200 | <2.0 | <0.008 | na | na | na | na | na | ? |
| 140.00 | 155.50 | 622348 cgri | 86 | 30 | 135 | <2.0 | <0.008 | na | na | na | na | na | ? |
| 155.50 | 170.50 | 622350 cgri | 47 | 9 | 99 | <2.0 | <0.008 | 529 | <2 | 709 | 80 | 3070 | 38.37 |
| 170.50 | 185.00 | 622351 cgri | 71 | 34 | 148 | <2.0 | <0.008 | na | na | na | na | na | ? |
| 185.00 | 200.00 | 622352 cgri | 120 | 22 | 176 | <2.0 | <0.008 | na | na | na | na | na | ? |
| 200.00 | 216.10 | 622353 cgri | 80 | 17 | 137 | <2.0 | <0.008 | na | na | na | na | na | ? |
| 216.10 | 218.90 | 622354 cgri | 86 | 18 | 83 | <2.0 | <0.008 | 864 | 30 | 131 | 179 | 4770 | 26.65 |
| 218.90 | 234.40 | 622355 cgri | 63 | 57 | 323 | <2.0 | <0.008 | 1783 | 12 | 109 | 195 | 4720 | 24.21 |
| 234.40 | 239.20 | 622356 cgri | 84 | 1130 | 2178 | <2.0 | <0.008 | 1770 | 5 | 128 | 190 | 4670 | 24.58 |
| 239.20 | 254.40 | 622357 cgri | 71 | 1050 | 1086 | <2.0 | <0.008 | 1382 | 13 | 124 | 193 | 4790 | 24.82 |
| 254.40 | 266.60 | 622358 cgri | 74 | 155 | 312 | <2.0 | <0.008 | 1469 | 20 | 104 | 182 | 4500 | 24.73 |
| 266.60 | 276.00 | 622359 cgri | 83 | 875 | 1246 | <2.0 | <0.008 | 1769 | 13 | 67 | 175 | 4230 | 24.17 |
| 276.00 | 292.50 | 622360 cgri | 110 | 905 | 2090 | <2.0 | <0.008 | 1817 | 17 | 64 | 187 | 4430 | 23.69 |
| 297.50 | 308.80 | 622361 cgri | 115 | 41 | 1146 | <2.0 | <0.008 | 1915 | 7 | 44 | 171 | 4520 | 26.43 |
| 308.80 | 320.30 | 622362 cgri | 58 | 68 | 1815 | <2.0 | <0.008 | 2537 | 10 | 41 | 182 | 4690 | 25.77 |
| 320.30 | 328.60 | 622363 cgri | 220 | 935 | 4238 | <2.0 | <0.008 | 1358 | 2 | 38 | 178 | 4660 | 26.18 |
| 328.60 | 335.60 | 622364 cgri | 130 | 17 | 2728 | <2.0 | <0.008 | 1456 | 19 | 39 | 174 | 4710 | 27.07 |
| 335.60 | 348.00 | 622365 cgri | 115 | 490 | 3079 | <2.0 | <0.008 | 2038 | 8 | 33 | 180 | 4770 | 26.50 |
| 348.00 | 359.00 | 622366 cgri | 88 | 29 | 1450 | <2.0 | <0.008 | 1531 | 5 | 34 | 185 | 4740 | 25.62 |
| 359.00 | 372.60 | 622368 cgri | 83 | 83 | 706 | <2.0 | <0.008 | 1113 | 18 | 165 | 163 | 4040 | 24.79 |
| 372.60 | 379.00 | 622369 cgri | 140 | 52 | 216 | <2.0 | <0.008 | 1449 | 7 | 173 | 166 | 4040 | 24.34 |
| 379.00 | 389.10 | 622370 cgri | 130 | 25 | 188 | <2.0 | <0.008 | 1158 | 9 | 164 | 173 | 3920 | 22.66 |
| 389.10 | 392.10 | 622371 cgri | 145 | 1030 | 1723 | <2.0 | <0.008 | 140 | 46 | 21 | 178 | 3210 | 18.03 |
| 392.10 | 402.00 | 622372 cgri | 180 | 770 | 807 | <2.0 | <0.008 | 1415 | 16 | 19 | 180 | 3410 | 18.94 |
| 402.00 | 412.00 | 622373 cgri | 265 | 765 | 1610 | <2.0 | <0.008 | 1812 | 13 | 15 | 168 | 3180 | 18.93 |
| 412.00 | 423.50 | 622374 cgri | 253 | 310 | 710 | <2.0 | <0.008 | 1702 | 12 | 20 | 173 | 3200 | 18.50 |
| 423.50 | 431.50 | 622375 cgri | 195 | 120 | 463 | <2.0 | <0.008 | 1700 | 13 | 14 | 168 | 3190 | 18.99 |
| 431.50 | 443.00 | 622376 cgri | 190 | 6 | 449 | <2.0 | <0.008 | 1574 | 11 | 15 | 166 | 3120 | 18.80 |
| 443.00 | 454.30 | 622377 cgri | 150 | 30 | 307 | <2.0 | <0.008 | 1757 | 3 | 14 | 168 | 3120 | 18.57 |
| 454.30 | 470.00 | 622378 cgri | 56 | <5 | 143 | <2.0 | <0.008 | 414 | 4 | 17 | 173 | 3170 | 18.32 |
| 470.00 | 485.70 | 622379 cgri | 47 | <5 | 123 | <2.0 | <0.008 | 803 | 2 | 16 | 177 | 3180 | 17.97 |
| 485.70 | 497.50 | 622380 cgri | 85 | <5 | 104 | <2.0 | <0.008 | 1456 | 6 | 13 | 166 | 3080 | 18.55 |
| 497.50 | 502.10 | 622381 cgri | 46 | <5 | 105 | <2.0 | <0.008 | 1530 | <2 | 12 | 164 | 3130 | 19.09 |
| 502.10 | 504.60 | 622382 cgri | 56 | <5 | 83 | <2.0 | <0.008 | 1075 | <2 | 11 | 158 | 2820 | 17.85 |
| 504.60 | 510.30 | 622383 cgri | 27 | <5 | 132 | <2.0 | <0.008 | 845 | 7 | 19 | 182 | 3170 | 17.42 |
| 510.30 | 515.60 | 622384 cgri | 60 | 30 | 953 | <2.0 | <0.008 | 625 | 32 | 143 | 194 | 2670 | 13.76 |
| 515.60 | 519.40 | 622385 cgri | 72 | 155 | 404 | <2.0 | <0.008 | 220 | 28 | 756 | 79 | 2170 | 27.47 |
| 519.40 | 532.30 | 622386 cgri | 83 | 36 | 339 | <2.0 | <0.008 | 1137 | 14 | 16 | 230 | 2280 | 9.91 |
| 532.30 | 546.00 | 622387 cgri | 70 | <5 | 118 | <2.0 | <0.008 | 1476 | 2 | 13 | 225 | 2300 | 10.22 |
| 546.00 | 563.60 | 622388 cgri | 158 | <5 | 146 | <2.0 | <0.008 | 1673 | 5 | 10 | 215 | 2270 | 10.56 |
| 563.60 | 569.90 | 622389 cgri | 196 | <5 | 216 | <2.0 | <0.008 | 2795 | 3 | 19 | 235 | 2330 | 9.91 |
| 569.90 | 579.50 | 622390 cgri | 67 | <5 | 122 | <2.0 | <0.008 | 1102 | 3 | 14 | 210 | 2260 | 10.76 |
| 579.50 | 589.90 | 622391 cgri | 107 | <5 | 116 | <2.0 | <0.008 | 1526 | 2 | 5 | 231 | 2040 | 8.83 |
| 589.90 | 596.40 | 622392 cgri | 48 | <5 | 97 | <2.0 | <0.008 | 1359 | <2 | 12 | 241 | 2240 | 9.29 |
| 596.40 | 609.70 | 622393 cgri | 94 | 7 | 97 | <2.0 | <0.008 | 1563 | <2 | 7 | 226 | 2100 | 9.29 |
| 609.70 | 613.40 | 622394 cgri | 49 | <5 | 123 | <2.0 | <0.008 | 1487 | <2 | 12 | 239 | 2200 | 9.21 |
| 613.40 | 621.10 | 622395 cgri | 91 | 6 | 124 | <2.0 | <0.008 | 813 | 6 | 85 | 141 | 5870 | 41.63 |
| 621.10 | 631.10 | 622396 cgri | 81 | 247 | 918 | <2.0 | <0.008 | 1564 | 10 | 82 | 226 | 2750 | 12.17 |
| 631.10 | 651.00 | 622397 cgri | 230 | 33 | 291 | <2.0 | <0.008 | 997 | 11 | 474 | 155 | 3010 | 19.42 |
| 651.00 | 672.00 | 622398 cgri | 221 | <5 | 515 | <2.0 | <0.008 | 855 | 10 | 411 | 151 | 2820 | 18.68 |
| 672.00 | 687.00 | 622399 cgri | 205 | <5 | 317 | <2.0 | <0.008 | 1386 | 10 | 131 | 178 | 2500 | 14.04 |
| 687.00 | 702.00 | 622400 cgri | 239 | <5 | 225 | <2.0 | <0.008 | 1015 | 3 | 17 | 189 | 2480 | 13.12 |
| 702.00 | 716.40 | 622401 cgri | 214 | <5 | 214 | <2.0 | <0.008 | 1058 | <2 | 17 | 203 | 2660 | 13.10 |
| 716.40 | 728.00 | 622402 cgri | 265 | <5 | 244 | <2.0 | <0.008 | 1067 | 2 | 16 | 189 | 2580 | 13.65 |
| 728.00 | 739.70 | 622403 cgri | 198 | <5 | 195 | <2.0 | <0.008 | 819 | <2 | 12 | 194 | 2490 | 12.84 |
| 739.70 | 751.00 | 622404 cgri | 194 | 5 | 199 | <2.0 | <0.008 | 965 | <2 | 20 | 197 | 2510 | 12.74 |
| 751.00 | 755.70 | 622405 cgri | 245 | <5 | 253 | <2.0 | <0.008 | 335 | 3 | 19 | 197 | 2550 | 12.94 |
| 755.70 | 769.00 | 622407 cgri | 144 | <5 | 187 | <2.0 | <0.008 | 1174 | 9 | 45 | 166 | 4050 | 24.40 |
| 769.00 | 784.00 | 622408 cgri | 66 | <5 | 126 | <2.0 | <0.008 | 934 | <2 | 25 | 168 | 3760 | 22.38 |
| 784.00 | 795.00 | 622409 cgri | 64 | <5 | 94 | <2.0 | <0.008 | 978 | 4 | 12 | 152 | 3450 | 22.70 |
| 795.00 | 805.70 | 622410 cgri | 46 | <5 | 83 | <2.0 | <0.008 | 783 | 2 | 13 | 148 | 3040 | 20.40 |
| 805.70 | 818.80 | 622411 cgri | 77 | 41 | 423 | <2.0 | <0.008 | 1035 | 11 | 72 | 148 | 4790 | 32.36 |

**Area Code** mac
**Prospect** Mt. Charter
**Report Grid** Mack
**Dataset** Geochemical data set

**Holename** DDMA0033
**Stored Grid** Mack

| From | To | Sample | Type | Cu ppm | Pb ppm | Zn ppm | Ag ppm | Au ppm | Ba ppm | As ppm | Cr ppm | Zr ppm | Ti ppm | Ti/Zr |
|---|---|---|---|---|---|---|---|---|---|---|---|---|---|---|
| 818.80 | 821.40 | 622412 | cgri | 91 | <5 | 118 | <2.0 | <0.008 | 320 | 8 | 273 | 96 | 3170 | 33.02 |
| 821.40 | 823.40 | 622413 | cgri | 90 | <5 | 98 | <2.0 | <0.008 | 216 | 9 | 1068 | 33 | 1950 | 59.09 |
| 823.40 | 827.70 | 622414 | cgri | 60 | <5 | 85 | <2.0 | <0.008 | 180 | 15 | 394 | 144 | 1960 | 13.61 |
| 827.70 | 829.00 | 622415 | cgri | 79 | <5 | 94 | <2.0 | <0.008 | 165 | 4 | 870 | 47 | 1820 | 38.72 |
| 829.00 | 844.00 | 622416 | cgri | 43 | 5 | 75 | <2.0 | <0.008 | 294 | 7 | 355 | 188 | 2800 | 14.89 |
| 844.00 | 859.00 | 622417 | cgri | 32 | <5 | 70 | <2.0 | <0.008 | 233 | 5 | 435 | 167 | 2390 | 14.31 |
| 859.00 | 874.00 | 622418 | cgri | 25 | 7 | 92 | <2.0 | <0.008 | 369 | 7 | 399 | 181 | 2570 | 14.20 |

# ABERFOYLE RESOURCES LTD. DRILL LOG

**Area Code** mac | **Prospect** Mt. Charter | **Report Grid** Mack | **Dataset** Geochemical data set

**Holename** DDMA0033 | **Stored Grid** Mack

| From | To | SiO2 % | TiO2 % | Al2O3 % | Fe2O3 % | MnO % | MgO % | CaO % | Na2O % | K2O % | P2O5 % | LOI % | TOTAL % |
|---|---|---|---|---|---|---|---|---|---|---|---|---|---|
| 0.00 | 15.00 | 50.70 | 0.52 | 13.95 | 8.67 | 0.18 | 9.71 | 8.61 | 1.52 | 1.03 | 0.13 | 4.61 | 99.62 |
| 15.00 | 30.00 | 51.20 | 0.55 | 13.45 | 8.73 | 0.16 | 10.55 | 9.71 | 1.67 | 1.05 | 0.13 | 2.98 | 100.20 |
| 30.00 | 45.00 | 51.00 | 0.53 | 13.26 | 8.69 | 0.16 | 10.75 | 9.96 | 1.53 | 1.02 | 0.13 | 3.20 | 100.27 |
| 45.00 | 60.00 | 48.80 | 0.48 | 12.76 | 8.80 | 0.17 | 11.30 | 10.12 | 1.61 | 0.84 | 0.12 | 4.50 | 99.55 |
| 60.00 | 73.60 | 49.50 | 0.49 | 12.83 | 8.55 | 0.16 | 10.99 | 9.65 | 1.07 | 0.72 | 0.11 | 5.55 | 99.65 |
| 73.60 | 82.30 | na | na | na | na | na | na | na | na | na | na | na | na |
| 82.30 | 84.40 | na | na | na | na | na | na | na | na | na | na | na | na |
| 84.40 | 90.20 | na | na | na | na | na | na | na | na | na | na | na | na |
| 90.20 | 91.30 | na | na | na | na | na | na | na | na | na | na | na | na |
| 91.30 | 103.40 | na | na | na | na | na | na | na | na | na | na | na | na |
| 103.40 | 111.20 | na | na | na | na | na | na | na | na | na | na | na | na |
| 111.20 | 123.00 | na | na | na | na | na | na | na | na | na | na | na | na |
| 123.00 | 140.00 | na | na | na | na | na | na | na | na | na | na | na | na |
| 140.00 | 155.50 | na | na | na | na | na | na | na | na | na | na | na | na |
| 155.50 | 170.50 | 47.50 | 0.51 | 12.92 | 8.33 | 0.16 | 9.95 | 10.07 | 1.34 | 0.44 | 0.12 | 8.55 | 99.94 |
| 170.50 | 185.00 | na | na | na | na | na | na | na | na | na | na | na | na |
| 185.00 | 200.00 | na | na | na | na | na | na | na | na | na | na | na | na |
| 200.00 | 216.10 | na | na | na | na | na | na | na | na | na | na | na | na |
| 216.10 | 218.90 | 59.20 | 0.80 | 14.41 | 9.84 | 0.23 | 3.58 | 1.44 | 1.71 | 2.25 | 0.29 | 5.74 | 101.81 |
| 218.90 | 234.40 | 54.10 | 0.79 | 14.68 | 9.03 | 0.24 | 4.78 | 5.29 | 2.81 | 1.39 | 0.31 | 5.47 | 99.61 |
| 234.40 | 239.20 | 55.30 | 0.78 | 14.54 | 8.74 | 0.29 | 5.22 | 3.93 | 3.19 | 1.28 | 0.29 | 5.35 | 99.51 |
| 239.20 | 254.40 | 56.30 | 0.80 | 14.55 | 9.28 | 0.40 | 4.97 | 4.18 | 3.59 | 1.25 | 0.31 | 3.66 | 99.58 |
| 254.40 | 266.60 | 54.60 | 0.75 | 14.57 | 9.01 | 0.43 | 4.63 | 6.83 | 3.01 | 1.58 | 0.32 | 3.76 | 99.96 |
| 266.60 | 276.00 | 55.40 | 0.71 | 14.82 | 8.09 | 0.45 | 3.93 | 7.09 | 2.75 | 1.64 | 0.29 | 4.13 | 99.60 |
| 276.00 | 292.50 | 55.80 | 0.74 | 15.74 | 8.56 | 0.51 | 4.10 | 5.30 | 3.14 | 1.57 | 0.32 | 3.67 | 99.66 |
| 297.50 | 308.80 | 55.20 | 0.75 | 15.24 | 8.99 | 0.50 | 3.96 | 5.56 | 2.84 | 1.85 | 0.31 | 4.31 | 99.64 |
| 308.80 | 320.30 | 55.60 | 0.78 | 15.63 | 8.70 | 0.55 | 3.76 | 5.04 | 2.55 | 2.32 | 0.33 | 4.30 | 99.70 |
| 320.30 | 328.60 | 56.80 | 0.78 | 15.42 | 8.44 | 0.38 | 3.43 | 4.47 | 3.64 | 1.47 | 0.35 | 3.55 | 99.59 |
| 328.60 | 335.60 | 56.60 | 0.79 | 15.53 | 9.15 | 0.36 | 3.57 | 3.76 | 3.35 | 1.60 | 0.34 | 4.32 | 99.71 |
| 335.60 | 348.00 | 55.10 | 0.80 | 15.84 | 8.88 | 0.47 | 3.77 | 4.63 | 2.98 | 2.24 | 0.35 | 4.35 | 99.69 |
| 348.00 | 359.00 | 53.90 | 0.79 | 15.34 | 9.27 | 0.40 | 3.95 | 5.41 | 2.76 | 1.83 | 0.35 | 5.53 | 99.70 |
| 359.00 | 372.60 | 52.50 | 0.67 | 13.58 | 8.41 | 0.28 | 5.32 | 8.98 | 2.56 | 1.51 | 0.26 | 5.73 | 99.91 |
| 372.60 | 379.00 | 55.50 | 0.67 | 14.02 | 9.00 | 0.24 | 5.92 | 7.10 | 2.04 | 1.77 | 0.23 | 3.01 | 99.57 |
| 379.00 | 389.10 | 52.10 | 0.65 | 14.00 | 9.25 | 0.34 | 6.25 | 8.45 | 2.01 | 1.43 | 0.25 | 4.82 | 99.59 |
| 389.10 | 392.10 | 60.00 | 0.54 | 15.99 | 7.43 | 0.23 | 2.60 | 2.41 | 5.95 | 0.23 | 0.24 | 3.14 | 100.27 |
| 392.10 | 402.00 | 60.10 | 0.57 | 15.98 | 7.17 | 0.28 | 2.24 | 4.05 | 3.58 | 2.25 | 0.26 | 2.55 | 99.60 |
| 402.00 | 412.00 | 60.80 | 0.53 | 15.91 | 6.97 | 0.29 | 1.99 | 4.88 | 2.82 | 2.49 | 0.27 | 2.38 | 99.69 |
| 412.00 | 423.50 | 60.70 | 0.53 | 15.71 | 7.40 | 0.29 | 2.21 | 4.62 | 2.62 | 2.60 | 0.27 | 2.44 | 99.64 |
| 423.50 | 431.50 | 61.80 | 0.53 | 15.65 | 6.57 | 0.24 | 1.97 | 4.59 | 2.95 | 2.36 | 0.28 | 2.91 | 99.96 |
| 431.50 | 443.00 | 60.70 | 0.52 | 15.26 | 7.16 | 0.22 | 1.93 | 5.32 | 2.85 | 2.41 | 0.26 | 2.99 | 99.70 |
| 443.00 | 454.30 | 61.20 | 0.52 | 15.23 | 6.97 | 0.22 | 1.92 | 4.59 | 2.95 | 2.60 | 0.27 | 3.31 | 99.76 |
| 454.30 | 470.00 | 60.30 | 0.53 | 15.86 | 8.03 | 0.18 | 2.93 | 1.89 | 3.47 | 1.61 | 0.28 | 4.38 | 99.61 |
| 470.00 | 485.70 | 60.80 | 0.53 | 15.52 | 8.17 | 0.21 | 2.56 | 2.27 | 2.77 | 2.19 | 0.29 | 4.28 | 99.67 |
| 485.70 | 497.50 | 60.80 | 0.51 | 15.50 | 6.43 | 0.18 | 1.83 | 3.62 | 3.99 | 2.42 | 0.26 | 4.05 | 99.71 |
| 497.50 | 502.10 | 59.20 | 0.52 | 15.36 | 8.08 | 0.22 | 2.42 | 3.03 | 4.26 | 2.52 | 0.27 | 4.33 | 100.21 |
| 502.10 | 504.60 | 66.90 | 0.47 | 14.39 | 4.27 | 0.13 | 1.28 | 2.48 | 4.92 | 1.70 | 0.26 | 3.22 | 100.06 |
| 504.60 | 510.30 | 58.70 | 0.53 | 16.40 | 8.91 | 0.22 | 3.79 | 1.29 | 3.79 | 1.54 | 0.30 | 3.98 | 99.60 |
| 510.30 | 515.60 | 59.90 | 0.45 | 16.12 | 6.70 | 0.18 | 3.57 | 1.58 | 5.38 | 0.77 | 0.12 | 4.17 | 99.73 |
| 515.60 | 519.40 | 41.90 | 0.36 | 10.62 | 6.41 | 0.33 | 5.87 | 15.57 | 2.43 | 0.25 | 0.13 | 15.50 | 99.67 |
| 519.40 | 532.30 | 66.10 | 0.38 | 14.95 | 5.18 | 0.13 | 1.71 | 1.35 | 3.96 | 2.52 | 0.09 | 2.79 | 99.71 |
| 532.30 | 546.00 | 66.50 | 0.38 | 14.55 | 5.56 | 0.15 | 1.04 | 2.39 | 3.78 | 2.27 | 0.08 | 3.10 | 99.80 |
| 546.00 | 563.60 | 66.60 | 0.38 | 14.47 | 5.39 | 0.13 | 1.00 | 2.36 | 3.60 | 2.94 | 0.09 | 2.83 | 99.88 |
| 563.60 | 569.90 | 65.80 | 0.39 | 15.07 | 6.19 | 0.13 | 1.27 | 1.30 | 2.53 | 4.59 | 0.09 | 2.35 | 99.72 |
| 569.90 | 579.50 | 68.10 | 0.38 | 14.40 | 3.98 | 0.10 | 1.12 | 1.98 | 4.37 | 2.36 | 0.09 | 2.79 | 99.73 |
| 579.50 | 589.90 | 71.50 | 0.34 | 14.09 | 2.17 | 0.05 | 0.38 | 1.39 | 4.16 | 3.91 | 0.08 | 1.62 | 99.74 |
| 589.90 | 596.40 | 65.40 | 0.37 | 15.41 | 6.56 | 0.16 | 1.24 | 1.91 | 3.91 | 3.23 | 0.09 | 2.03 | 99.75 |
| 596.40 | 609.70 | 71.10 | 0.35 | 14.40 | 2.33 | 0.05 | 0.27 | 1.30 | 4.18 | 4.46 | 0.08 | 1.33 | 99.87 |
| 609.70 | 613.40 | 65.30 | 0.37 | 15.27 | 6.94 | 0.16 | 1.58 | 1.37 | 4.14 | 2.62 | 0.09 | 2.37 | 100.26 |
| 613.40 | 621.10 | 50.80 | 0.98 | 15.05 | 9.64 | 0.31 | 4.77 | 8.27 | 3.26 | 1.13 | 0.35 | 5.02 | 99.63 |
| 621.10 | 631.10 | 65.40 | 0.46 | 14.31 | 5.64 | 0.23 | 2.12 | 3.56 | 3.05 | 2.29 | 0.19 | 2.19 | 99.55 |
| 631.10 | 651.00 | 54.80 | 0.50 | 12.38 | 7.54 | 0.27 | 6.40 | 9.20 | 2.31 | 1.51 | 0.27 | 4.32 | 99.58 |
| 651.00 | 672.00 | 53.40 | 0.47 | 12.63 | 7.49 | 0.34 | 5.79 | 10.22 | 2.42 | 1.36 | 0.26 | 5.42 | 99.84 |
| 672.00 | 687.00 | 60.80 | 0.42 | 13.63 | 5.81 | 0.22 | 2.59 | 5.39 | 3.55 | 1.88 | 0.14 | 4.98 | 99.53 |
| 687.00 | 702.00 | 65.90 | 0.41 | 14.69 | 4.53 | 0.12 | 1.32 | 2.77 | 4.39 | 2.04 | 0.10 | 3.32 | 99.76 |
| 702.00 | 716.40 | 65.60 | 0.44 | 14.95 | 5.45 | 0.15 | 1.42 | 2.23 | 4.37 | 2.00 | 0.11 | 3.05 | 99.84 |
| 716.40 | 728.00 | 66.20 | 0.43 | 14.33 | 3.94 | 0.12 | 1.02 | 3.29 | 3.94 | 2.88 | 0.11 | 3.29 | 99.57 |
| 728.00 | 739.70 | 64.70 | 0.42 | 14.30 | 3.84 | 0.12 | 1.03 | 4.13 | 3.53 | 2.98 | 0.11 | 4.46 | 99.72 |
| 739.70 | 751.00 | 64.70 | 0.42 | 14.59 | 4.52 | 0.13 | 1.16 | 3.27 | 3.41 | 3.25 | 0.11 | 4.18 | 99.79 |
| 751.00 | 755.70 | 63.00 | 0.43 | 14.28 | 5.62 | 0.15 | 1.95 | 3.63 | 4.29 | 1.21 | 0.11 | 4.63 | 99.61 |
| 755.70 | 769.00 | 59.10 | 0.68 | 15.06 | 9.51 | 0.22 | 2.86 | 2.14 | 2.97 | 2.07 | 0.20 | 4.30 | 99.58 |
| 769.00 | 784.00 | 60.80 | 0.63 | 15.27 | 7.42 | 0.19 | 2.25 | 3.23 | 3.43 | 1.96 | 0.19 | 4.42 | 99.82 |
| 784.00 | 795.00 | 62.70 | 0.58 | 13.72 | 4.49 | 0.15 | 0.70 | 5.90 | 3.21 | 2.81 | 0.16 | 5.28 | 99.72 |
| 795.00 | 805.70 | 62.90 | 0.51 | 14.20 | 4.82 | 0.16 | 1.05 | 4.81 | 3.89 | 2.06 | 0.15 | 4.86 | 99.51 |
| 805.70 | 818.80 | 56.40 | 0.80 | 15.09 | 8.13 | 0.19 | 4.17 | 3.70 | 3.13 | 2.38 | 0.17 | 5.29 | 99.69 |

**Area Code** mac | **Prospect** Mt. Charter | **Report Grid** Mack | **Dataset** Geochemical data set

**Holename** DDMA0033 | **Stored Grid** Mack

| From | To | SiO2 % | TiO2 % | Al2O3 % | Fe2O3 % | MnO % | MgO % | CaO % | Na2O % | K2O % | P2O5 % | LOI % | TOTAL % |
|---|---|---|---|---|---|---|---|---|---|---|---|---|---|
| 818.80 | 821.40 | 51.40 | 0.53 | 13.62 | 8.34 | 0.16 | 7.13 | 6.27 | 0.57 | 2.01 | 0.14 | 9.33 | 99.78 |
| 821.40 | 823.40 | 39.30 | 0.32 | 11.79 | 8.08 | 0.25 | 7.54 | 14.70 | 0.13 | 1.50 | 0.11 | 16.19 | 100.04 |
| 823.40 | 827.70 | 68.90 | 0.33 | 6.36 | 3.90 | 0.16 | 3.19 | 7.22 | <0.05 | 1.14 | 0.10 | 8.25 | 99.86 |
| 827.70 | 829.00 | 33.50 | 0.30 | 10.68 | 7.92 | 0.34 | 8.17 | 18.27 | 0.67 | 0.68 | 0.10 | 18.93 | 99.69 |
| 829.00 | 844.00 | 63.20 | 0.47 | 9.16 | 5.03 | 0.14 | 5.33 | 5.79 | 0.14 | 1.72 | 0.11 | 8.49 | 99.80 |
| 844.00 | 859.00 | 68.60 | 0.40 | 7.55 | 4.50 | 0.13 | 5.22 | 4.24 | 0.23 | 1.27 | 0.09 | 7.18 | 99.50 |
| 859.00 | 874.00 | 67.50 | 0.43 | 8.65 | 4.93 | 0.12 | 5.37 | 3.98 | 0.34 | 1.61 | 0.12 | 6.77 | 99.96 |

Area Code: mac
Prospect: Mt. Charter
Report Grid: Mack

Dataset: Geochemical data set

Holename: DDMA0033
Stored Grid: Mack

| From | To | S % | P205/Ti | Altn.In |
|---|---|---|---|---|
| 0.00 | 15.00 | 0.02 | 0.26 | 51.46 |
| 15.00 | 30.00 | 0.01 | 0.23 | 50.48 |
| 30.00 | 45.00 | 0.01 | 0.24 | 50.60 |
| 45.00 | 60.00 | 0.04 | 0.26 | 50.86 |
| 60.00 | 73.60 | 0.05 | 0.22 | 52.21 |
| 73.60 | 82.30 | na | ? | ? |
| 82.30 | 84.40 | na | ? | ? |
| 84.40 | 90.20 | na | ? | ? |
| 90.20 | 91.30 | na | ? | ? |
| 91.30 | 103.40 | na | ? | ? |
| 103.40 | 111.20 | na | ? | ? |
| 111.20 | 123.00 | na | ? | ? |
| 123.00 | 140.00 | na | ? | ? |
| 140.00 | 155.50 | na | ? | ? |
| 155.50 | 170.50 | 0.04 | 0.23 | 47.66 |
| 170.50 | 185.00 | na | ? | ? |
| 185.00 | 200.00 | na | ? | ? |
| 200.00 | 216.10 | na | ? | ? |
| 216.10 | 218.90 | 2.36 | 0.36 | 64.92 |
| 218.90 | 234.40 | 0.75 | 0.39 | 43.24 |
| 234.40 | 239.20 | 0.59 | 0.37 | 47.72 |
| 239.20 | 254.40 | 0.26 | 0.39 | 44.46 |
| 254.40 | 266.60 | 0.43 | 0.42 | 38.69 |
| 266.60 | 276.00 | 0.27 | 0.41 | 36.15 |
| 276.00 | 292.50 | 0.25 | 0.43 | 40.18 |
| 297.50 | 308.80 | 0.11 | 0.41 | 40.89 |
| 308.80 | 320.30 | 0.10 | 0.43 | 44.48 |
| 320.30 | 328.60 | 0.84 | 0.45 | 37.66 |
| 328.60 | 335.60 | 0.34 | 0.43 | 42.10 |
| 335.60 | 348.00 | 0.23 | 0.44 | 44.13 |
| 348.00 | 359.00 | 0.12 | 0.45 | 41.43 |
| 359.00 | 372.60 | 0.13 | 0.39 | 37.18 |
| 372.60 | 379.00 | 0.05 | 0.34 | 45.69 |
| 379.00 | 389.10 | 0.07 | 0.38 | 42.34 |
| 389.10 | 392.10 | 1.51 | 0.44 | 25.29 |
| 392.10 | 402.00 | 0.57 | 0.46 | 37.05 |
| 402.00 | 412.00 | 0.33 | 0.51 | 36.78 |
| 412.00 | 423.50 | 0.22 | 0.52 | 39.92 |
| 423.50 | 431.50 | 0.10 | 0.52 | 36.48 |
| 431.50 | 443.00 | 0.10 | 0.50 | 34.69 |
| 443.00 | 454.30 | 0.03 | 0.52 | 37.48 |
| 454.30 | 470.00 | 0.14 | 0.53 | 45.86 |
| 470.00 | 485.70 | 0.09 | 0.54 | 48.52 |
| 485.70 | 497.50 | 0.08 | 0.52 | 35.83 |
| 497.50 | 502.10 | 0.05 | 0.53 | 40.39 |
| 502.10 | 504.60 | 0.07 | 0.56 | 28.71 |
| 504.60 | 510.30 | 0.12 | 0.56 | 51.20 |
| 510.30 | 515.60 | 0.76 | 0.27 | 38.41 |
| 515.60 | 519.40 | 0.32 | 0.36 | 25.37 |
| 519.40 | 532.30 | 0.58 | 0.23 | 44.34 |
| 532.30 | 546.00 | 0.03 | 0.22 | 34.92 |
| 546.00 | 563.60 | 0.04 | 0.23 | 39.80 |
| 563.60 | 569.90 | 0.02 | 0.22 | 60.47 |
| 569.90 | 579.50 | 0.06 | 0.24 | 35.40 |
| 579.50 | 589.90 | 0.02 | 0.23 | 43.60 |
| 589.90 | 596.40 | 0.00 | 0.24 | 46.13 |
| 596.40 | 609.70 | 0.01 | 0.23 | 46.33 |
| 609.70 | 613.40 | 0.02 | 0.24 | 43.25 |
| 613.40 | 621.10 | 0.06 | 0.36 | 33.85 |
| 621.10 | 631.10 | 0.08 | 0.42 | 40.02 |
| 631.10 | 651.00 | 0.08 | 0.53 | 40.73 |
| 651.00 | 672.00 | 0.05 | 0.54 | 36.13 |
| 672.00 | 687.00 | 0.11 | 0.33 | 33.33 |
| 687.00 | 702.00 | 0.17 | 0.24 | 31.94 |
| 702.00 | 716.40 | 0.04 | 0.26 | 34.13 |
| 716.40 | 728.00 | 0.07 | 0.26 | 35.04 |
| 728.00 | 739.70 | 0.10 | 0.26 | 34.36 |
| 739.70 | 751.00 | 0.09 | 0.25 | 39.77 |
| 751.00 | 755.70 | 0.26 | 0.26 | 28.52 |
| 755.70 | 769.00 | 0.53 | 0.29 | 49.10 |
| 769.00 | 784.00 | 0.07 | 0.30 | 38.73 |
| 784.00 | 795.00 | 0.05 | 0.28 | 27.81 |
| 795.00 | 805.70 | 0.06 | 0.29 | 26.33 |
| 805.70 | 818.80 | 0.23 | 0.21 | 48.95 |

**Area Code** mac

**Prospect** Mt. Charter

**Report Grid** Mack

**Dataset** Geochemical data set

**Holename** DDMA0033

**Stored Grid** Mack

| From | To | S % | P2O5/Ti | Altn.In |
|---|---|---|---|---|
| 818.80 | 821.40 | 0.26 | 0.26 | 57.20 |
| 821.40 | 823.40 | 0.07 | 0.35 | 37.87 |
| 823.40 | 827.70 | 0.25 | 0.30 | 37.65 |
| 827.70 | 829.00 | 0.15 | 0.35 | 31.85 |
| 829.00 | 844.00 | 0.20 | 0.24 | 54.31 |
| 844.00 | 859.00 | 0.10 | 0.23 | 59.22 |
| 859.00 | 874.00 | 0.16 | 0.27 | 61.77 |

655217



CORE GRIND SAMPLING

HOLE No. MAC 033

DATE 1-3-93

| No. | SAMPLE NUMBER | INTERVAL | ELEMENTS REQUIRED | ST | SAMPLE NUMBER | INTERVAL | ELEMENTS REQUIRED | ST |
|---|---|---|---|---|---|---|---|---|
| 1 | 622335 | 0-15 | WHOLE ROCK + TRACE | | 622366 | 348.0-359.0 | WHOLE ROCK + TRACE | |
| 2 | 336 | 15-30 | | | * 367 | STANDARD | | |
| 3 | 337 | 30-45 | | | 368 | 359.0-372.6 | | |
| 4 | 338 | 45-60 | | | 369 | 372.6-379.0 | | |
| 5 | 339 | 60-73.6 | | | 370 | 379.0-389.1 | | |
| 6 | 340 | 73.6-82.3 | Cu Pb Zn Ag Au | | 371 | 389.1-392.1 | | |
| 7 | 341 | 82.3-84.4 | | | 372 | 392.1-402.0 | | |
| 8 | 342 | 84.4-90.2 | | | 373 | 402.0-412.0 | | |
| 9 | 343 | 90.2-91.3 | | | 374 | 412.0-423.5 | | |
| 10 | 344 | 91.3-103.4 | | | 375 | 423.5-431.5 | | |
| 11 | 345 | 103.4-111.2 | | | 376 | 431.5-443.0 | | |
| 12 | 346 | 111.2-123.0 | | | 377 | 443.0-454.3 | | |
| 13 | 347 | 123.0-140.0 | | | 378 | 454.3-470.0 | | |
| 14 | 348 | 140.0-155.5 | | | 379 | 470.0-485.7 | | |
| 15 | * 349 | STANDARD | WHOLE ROCK + TRACE | | 380 | 485.7-497.5 | | |
| 16 | 350 | 155.5-170.5 | " " | | 381 | 497.5-502.1 | | |
| 17 | 351 | 170.5-185.0 | Cu Pb Zn Ag Au | | 382 | 502.1-504.6 | | |
| 18 | 352 | 185.0-200.0 | | | 383 | 504.6-510.3 | | |
| 19 | 353 | 200.0-216.1 | | | 384 | 510.3-515.6 | | |
| 20 | 354 | 216.1-218.9 | WHOLE ROCK + TRACE | | 385 | 515.6-519.4 | | |
| 21 | 355 | 218.9-234.4 | | | 386 | 519.4-532.3 | | |
| 22 | 356 | 234.4-239.2 | | | 387 | 532.3-546.0 | | |
| 23 | 357 | 239.2-254.4 | | | 388 | 546.0-563.6 | | |
| 24 | 358 | 254.4-266.6 | | | 389 | 563.6-569.9 | | |
| 25 | 359 | 266.6-276.0 | | | 390 | 569.9-579.5 | | |
| 26 | 360 | 276.0-292.5 | | | 391 | 579.5-589.9 | | |
| 27 | NO SAMPLE | 292.5-297.5 | | | 392 | 589.9-596.4 | | |
| 28 | 361 | 297.5-308.8 | | | 393 | 596.4-609.7 | | |
| 29 | 362 | 308.8-320.3 | | | 394 | 609.7-613.4 | | |
| 30 | 363 | 320.3-328.6 | | | 395 | 613.4-621.1 | | |
| 31 | 364 | 328.6-335.6 | | | 396 | 621.1-631.1 | | |
| 32 | 365 | 335.6-348.0 | | | 397 | 631.1-651.0 | | |

655218

CORE GRIND SAMPLING

HOLE No. MAC 033

DATE 1-3-93

| No. | SAMPLE NUMBER | INTERVAL | ELEMENTS REQUIRED | ST | SAMPLE NUMBER | INTERVAL | ELEMENTS REQUIRED | ST |
|---|---|---|---|---|---|---|---|---|
| 1 | 622398 | 651.0 - 672.0 | WHOLE ROCK + TRACE | | | | | |
| 2 | 399 | 672.0 - 687.0 | | | | | | |
| 3 | 400 | 687.0 - 702.0 | | | | | | |
| 4 | 401 | 702.0 - 716.4 | | | | | | |
| 5 | 402 | 716.4 - 728.0 | | | | | | |
| 6 | 403 | 728.0 - 739.7 | | | | | | |
| 7 | 404 | 739.7 - 751.0 | | | | | | |
| 8 | 405 | 751.0 - 755.7 | | | | | | |
| 9 | * 406 | STANDARD | | | | | | |
| 10 | 407 | 755.7 - 769.0 | | | | | | |
| 11 | 408 | 769.0 - 784.0 | | | | | | |
| 12 | 409 | 784.0 - 795.0 | | | | | | |
| 13 | 410 | 795.0 - 805.7 | | | | | | |
| 14 | 411 | 805.7 - 818.8 | | | | | | |
| 15 | 412 | 818.8 - 821.4 | | | | | | |
| 16 | 413 | 821.4 - 823.4 | | | | | | |
| 17 | 414 | 823.4 - 827.7 | | | | | | |
| 18 | 415 | 827.7 - 829.0 | | | | | | |
| 19 | 416 | 829.0 - 844.0 | | | | | | |
| 20 | 417 | 844.0 - 859.0 | | | | | | |
| 21 | 418 | 859.0 - 874.0 | | | | | | |
| 22 | | | | | | | | |
| 23 | | | | | | | | |
| 24 | | | | | | | | |
| 25 | | | | | | | | |
| 26 | | | | | | | | |
| 27 | | | | | | | | |
| 28 | | | | | | | | |
| 29 | | | | | | | | |
| 30 | | | | | | | | |
| 31 | | | | | | | | |
| 32 | | | | | | | | |

655319

# ANALABS

A Division of Inchcape Inspection and Testing Services Australia Pty. Ltd. A.C.N. 004 591 864

RECEIVED 21 APR 1993

Phone (004) 316837 | 14 Thirkell St. COOEE TAS 7320 | Fax (004) 318890

## ANALYTICAL REPORT No. 100560.60.09357

THIS REPORT MUST BE READ IN CONJUNCTION WITH THE ACCOMPANYING ANALYTICAL DATA

INVOICE TO: Aberfoyle Resources Limited
Exploration Division
P.O. Box 952
BURNIE TAS 7320

| ORDER No. | PROJECT |
|---|---|
| 2738 | MAC-33 |

| DATE RECEIVED | RESULTS REQUIRED |
|---|---|
| 09/03/93 | ASAP |

| No. OF PAGES OF RESULTS | DATE REPORTED | No. OF COPIES |
|---|---|---|
| 10 | 20/04/93 | 1 |

TOTAL No. OF SAMPLES: 84

| SAMPLE NUMBERS | SAMPLE DESCRIPTION | ELEMENT/METHOD |
|---|---|---|
| 92335/418 | CG Prep : GP031 - CHROME FREE BOWLS | Cu,Pb,Zn,Ag/GA101 |
| | | Au,Au(R)/GG309 |
| | | Ba,As,Cr,Zr/GX401 |
| | | WHOLE ROCK ANALYSIS/GX408 |

RESULTS TO: Mr R de Bomford
Aberfoyle Resources Limited
Exploration Division
P.O. Box 952
BURNIE TAS 7320

RESULTS TO:

RESULTS TO:

REMARKS

AMENDED Ti RESULTS

INSUFFICIENT SAMPLE FOR Au(S) RESULT

MAC-33
GRINDS

AUTHORISED OFFICER

655220

# ANALABS

A Division of Inchcape Testing Services (Australia) Pty. Ltd.
A.C.N. 004 591 664

## ANALYTICAL DATA

| SAMPLE PREFIX | REPORT No. | REPORT DATE | CLIENT ORDER No. | PAGE |
|---|---|---|---|---|
| | 100560.60.09357 | 20/04/93 | 2738 | 1 OF 10 |

| JBE No. | SAMPLE No. | Cu | Pb | Zn | Ag | Au | Au(R) | Ba | As | Cr |
|---|---|---|---|---|---|---|---|---|---|---|
| 1 | 622335 | 55 | 8 | 95 | <2 | <0.008 | - | 476 | 2 | 746 |
| 2 | 622336 | 55 | 6 | 78 | <2 | <0.008 | - | 456 | 2 | 766 |
| 3 | 622337 | 44 | <5 | 74 | <2 | <0.008 | - | 443 | 4 | 762 |
| 4 | 622338 | 41 | <5 | 78 | <2 | <0.008 | - | 456 | 3 | 789 |
| 5 | 622339 | 50 | 5 | 88 | <2 | <0.008 | - | 417 | <2 | 840 |
| 6 | 622340 | 94 | 41 | 166 | <2 | <0.008 | - | - | - | - |
| 7 | 622341 | 70 | 59 | 329 | <2 | <0.008 | - | - | - | - |
| 8 | 622342 | 105 | 44 | 145 | <2 | <0.008 | - | - | - | - |
| 9 | 622343 | 41 | 135 | 500 | <2 | <0.008 | - | - | - | - |
| 10 | 622344 | 77 | 37 | 153 | <2 | <0.008 | - | - | - | - |
| 11 | 622345 | 73 | 15 | 92 | <2 | <0.008 | <0.008 | - | - | - |
| 12 | 622346 | 80 | 42 | 160 | <2 | <0.008 | - | - | - | - |
| 13 | 622347 | 115 | 33 | 200 | <2 | <0.008 | - | - | - | - |
| 14 | 622348 | 86 | 30 | 135 | <2 | <0.008 | - | - | - | - |
| 15 | 622349 | 125 | 200 | 2180 | <2 | 0.014 | - | 1136 | 18 | 951 |
| 16 | 622350 | 47 | 9 | 99 | <2 | <0.008 | - | 529 | <2 | 709 |
| 17 | 622351 | 71 | 34 | 148 | <2 | <0.008 | - | - | - | - |
| 18 | 622352 | 120 | 22 | 176 | <2 | <0.008 | - | - | - | - |
| 19 | 622353 | 80 | 17 | 137 | <2 | <0.008 | - | - | - | - |
| 20 | 622354 | 86 | 18 | 83 | <2 | <0.008 | - | 864 | 30 | 131 |
| 21 | 622355 | 63 | 57 | 323 | <2 | <0.008 | - | 1783 | 12 | 109 |
| 22 | 622356 | 84 | 1130 | 2178 | <2 | <0.008 | <0.008 | 1770 | 5 | 128 |
| 23 | 622357 | 71 | 1050 | 1086 | <2 | <0.008 | - | 1382 | 13 | 124 |
| 24 | 622358 | 74 | 155 | 312 | <2 | <0.008 | - | 1469 | 20 | 104 |
| 25 | 622359 | 83 | 875 | 1246 | <2 | <0.008 | - | 1769 | 13 | 67 |

Results in ppm unless otherwise specified
T = element present; but concentration too low to measure
X = element concentration is below detection limit
- = element not determined

AUTHORISED OFFICER

655221

# ANALABS

A Division of Inchcape Testing Services (Australia) Pty. Ltd.
A.C.N. 004 591 664

## ANALYTICAL DATA

| SAMPLE PREFIX | REPORT No. | REPORT DATE | CLIENT ORDER No. | PAGE |
|---|---|---|---|---|
| | 100560.60.09357 | 20/04/93 | 2738 | 2 OF 10 |

| JBE No. | SAMPLE No. | Cu | Pb | Zn | Ag | Au | Au(R) | Ba | As | Cr |
|---|---|---|---|---|---|---|---|---|---|---|
| 1 | 622360 | 110 | 905 | 2090 | <2 | <0.008 | - | 1817 | 17 | 64 |
| 2 | 622361 | 115 | 41 | 1146 | <2 | <0.008 | - | 1915 | 7 | 44 |
| 3 | 622362 | 58 | 68 | 1815 | <2 | <0.008 | - | 2537 | 10 | 41 |
| 4 | 622363 | 220 | 935 | 4238 | <2 | <0.008 | - | 1358 | 2 | 38 |
| 5 | 622364 | 130 | 17 | 2728 | <2 | <0.008 | - | 1456 | 19 | 39 |
| 6 | 622365 | 115 | 490 | 3079 | <2 | <0.008 | - | 2038 | 8 | 33 |
| 7 | 622366 | 88 | 29 | 1450 | <2 | <0.008 | - | 1531 | 5 | 34 |
| 8 | 622367 | 135 | 193 | 2191 | <2 | <0.008 | - | 1120 | 18 | 1010 |
| 9 | 622368 | 83 | 83 | 706 | <2 | <0.008 | - | 1113 | 18 | 165 |
| 10 | 622369 | 140 | 52 | 216 | <2 | <0.008 | - | 1449 | 7 | 173 |
| 11 | 622370 | 130 | 25 | 188 | <2 | <0.008 | - | 1158 | 9 | 164 |
| 12 | 622371 | 145 | 1030 | 1723 | <2 | <0.008 | <0.008 | 140 | 46 | 21 |
| 13 | 622372 | 180 | 770 | 807 | <2 | <0.008 | - | 1415 | 16 | 19 |
| 14 | 622373 | 265 | 765 | 1610 | <2 | <0.008 | - | 1812 | 13 | 15 |
| 15 | 622374 | 253 | 310 | 710 | <2 | <0.008 | - | 1702 | 12 | 20 |
| 16 | 622375 | 195 | 120 | 463 | <2 | <0.008 | - | 1700 | 13 | 14 |
| 17 | 622376 | 190 | 6 | 449 | <2 | <0.008 | - | 1574 | 11 | 15 |
| 18 | 622377 | 150 | 30 | 307 | <2 | <0.008 | - | 1757 | 3 | 14 |
| 19 | 622378 | 56 | <5 | 143 | <2 | <0.008 | - | 414 | 4 | 17 |
| 20 | 622379 | 47 | <5 | 123 | <2 | <0.008 | - | 803 | 2 | 16 |
| 21 | 622380 | 85 | <5 | 104 | <2 | <0.008 | - | 1456 | 6 | 13 |
| 22 | 622381 | 46 | <5 | 105 | <2 | <0.008 | <0.008 | 1530 | <2 | 12 |
| 23 | 622382 | 56 | <5 | 83 | <2 | <0.008 | - | 1075 | <2 | 11 |
| 24 | 622383 | 27 | <5 | 132 | <2 | <0.008 | - | 845 | 7 | 19 |
| 25 | 622384 | 60 | 30 | 953 | <2 | <0.008 | - | 625 | 32 | 143 |

Results in ppm unless otherwise specified
T = element present; but concentration too low to measure
X = element concentration is below detection limit
– = element not determined

AUTHORISED OFFICER

655222

# ANALABS

A Division of Inchcape Testing Services (Australia) Pty. Ltd.
A.C.N. 004 591 664

## ANALYTICAL DATA

| SAMPLE PREFIX | REPORT No. | REPORT DATE | CLIENT ORDER No. | PAGE |
|---|---|---|---|---|
| | 100560.60.09357 | 20/04/93 | 2738 | 3 OF 10 |

| TUBE No. | SAMPLE No. | Cu | Pb | Zn | Ag | Au | Au(R) | Ba | As | Cr |
|---|---|---|---|---|---|---|---|---|---|---|
| 1 | 622385 | 72 | 155 | 404 | <2 | <0.008 | - | 220 | 28 | 756 |
| 2 | 622386 | 83 | 36 | 339 | <2 | <0.008 | - | 1137 | 14 | 16 |
| 3 | 622387 | 70 | <5 | 118 | <2 | <0.008 | - | 1476 | 2 | 13 |
| 4 | 622388 | 158 | <5 | 146 | <2 | <0.008 | - | 1673 | 5 | 10 |
| 5 | 622389 | 196 | <5 | 216 | <2 | <0.008 | - | 2795 | 3 | 19 |
| 6 | 622390 | 67 | <5 | 122 | <2 | <0.008 | - | 1102 | 3 | 14 |
| 7 | 622391 | 107 | <5 | 116 | <2 | <0.008 | - | 1526 | 2 | 5 |
| 8 | 622392 | 48 | <5 | 97 | <2 | <0.008 | - | 1359 | <2 | 12 |
| 9 | 622393 | 94 | 7 | 97 | <2 | <0.008 | - | 1563 | <2 | 7 |
| 10 | 622394 | 49 | <5 | 123 | <2 | <0.008 | - | 1487 | <2 | 12 |
| 11 | 622395 | 91 | 6 | 124 | <2 | <0.008 | - | 813 | 6 | 85 |
| 12 | 622396 | 81 | 247 | 918 | <2 | <0.008 | <0.008 | 1564 | 10 | 82 |
| 13 | 622397 | 230 | 33 | 291 | <2 | <0.008 | - | 997 | 11 | 474 |
| 14 | 622398 | 221 | <5 | 515 | <2 | <0.008 | - | 855 | 10 | 411 |
| 15 | 622399 | 205 | <5 | 317 | <2 | <0.008 | - | 1386 | 10 | 131 |
| 16 | 622400 | 239 | <5 | 225 | <2 | <0.008 | - | 1015 | 3 | 17 |
| 17 | 622401 | 214 | <5 | 214 | <2 | <0.008 | - | 1058 | <2 | 17 |
| 18 | 622402 | 265 | <5 | 244 | <2 | <0.008 | - | 1067 | 2 | 16 |
| 19 | 622403 | 198 | <5 | 195 | <2 | <0.008 | - | 819 | <2 | 12 |
| 20 | 622404 | 194 | 5 | 199 | <2 | <0.008 | - | 965 | <2 | 20 |
| 21 | 622405 | 245 | <5 | 253 | <2 | <0.008 | - | 335 | 3 | 19 |
| 22 | 622406 | 128 | 189 | 2215 | <2 | <0.008 | <0.008 | 1128 | 18 | 927 |
| 23 | 622407 | 144 | <5 | 187 | <2 | <0.008 | - | 1174 | 9 | 45 |
| 24 | 622408 | 66 | <5 | 126 | <2 | <0.008 | - | 934 | <2 | 25 |
| 25 | 622409 | 64 | <5 | 94 | <2 | <0.008 | - | 978 | 4 | 12 |

Results in ppm unless otherwise specified
T = element present; but concentration too low to measure
X = element concentration is below detection limit
- = element not determined

AUTHORISED OFFICER

655223

# ANALABS

A Division of Inchcape Testing Services (Australia) Pty. Ltd.
A.C.N. 004 591 664

## ANALYTICAL DATA

| SAMPLE PREFIX | REPORT No. | REPORT DATE | CLIENT ORDER No. | PAGE |
|---|---|---|---|---|
| | 100560.60.09357 | 20/04/93 | 2738 | 4 OF 10 |

| JBE No. | SAMPLE No. | Cu | Pb | Zn | Ag | Au | Au(R) | Ba | As | Cr |
|---|---|---|---|---|---|---|---|---|---|---|
| 1 | 622410 | 46 | <5 | 83 | <2 | <0.008 | - | 783 | 2 | 13 |
| 2 | 622411 | 77 | 41 | 423 | <2 | <0.008 | - | 1035 | 11 | 72 |
| 3 | 622412 | 91 | <5 | 118 | <2 | <0.008 | - | 320 | 8 | 273 |
| 4 | 622413 | 90 | <5 | 98 | <2 | <0.008 | - | 216 | 9 | 1068 |
| 5 | 622414 | 60 | <5 | 85 | <2 | <0.008 | - | 180 | 15 | 394 |
| 6 | 622415 | 79 | <5 | 94 | <2 | <0.008 | - | 165 | 4 | 870 |
| 7 | 622416 | 43 | 5 | 75 | <2 | <0.008 | - | 294 | 7 | 355 |
| 8 | 622417 | 32 | <5 | 70 | <2 | <0.008 | - | 233 | 5 | 435 |
| 9 | 622418 | 25 | 7 | 92 | <2 | <0.008 | - | 369 | 7 | 399 |
| 0 | | | | | | | | | | |
| 1 | | | | | | | | | | |
| 12 | | | | | | | | | | |
| 3 | | | | | | | | | | |
| 14 | | | | | | | | | | |
| 5 | | | | | | | | | | |
| 16 | | | | | | | | | | |
| 7 | | | | | | | | | | |
| 8 | | | | | | | | | | |
| 19 | | | | | | | | | | |
| 0 | | | | | | | | | | |
| 21 | | | | | | | | | | |
| 22 | | | | | | | | | | |
| 3 | DETECTION | 4 | 5 | 4 | 2 | 0.008 | 0.008 | 10 | 2 | 5 |
| 24 | UNITS | ppm | ppm | ppm | ppm | ppm | ppm | ppm | ppm | ppm |
| 5 | METHOD | GA101 | GA101 | GA101 | GA101 | GG309 | GG309 | GX401 | GX401 | GX401 |

Results in ppm unless otherwise specified
T = element present; but concentration too low to measure
X = element concentration is below detection limit
– = element not determined

AUTHORISED OFFICER

655324

# ANALABS

A Division of Inchcape Testing Services (Australia) Pty. Ltd.
A.C.N. 004 591 664

## ANALYTICAL DATA

| SAMPLE PREFIX | REPORT No. | REPORT DATE | CLIENT ORDER No. | PAGE |
|---|---|---|---|---|
| | 100560.60.09357 | 20/04/93 | 2738 | 5 OF 10 |

| JBE No. | SAMPLE No. | Zr | Ti | Al2O3 | SiO2 | TiO2 | Fe2O3 | MnO | CaO | K2O |
|---|---|---|---|---|---|---|---|---|---|---|
| 1 | 622335 | 84 | 3140 | 13.95 | 50.70 | 0.52 | 8.67 | 0.18 | 8.61 | 1.03 |
| 2 | 622336 | 89 | 3270 | 13.45 | 51.20 | 0.55 | 8.73 | 0.16 | 9.71 | 1.05 |
| 3 | 622337 | 84 | 3150 | 13.26 | 51.00 | 0.53 | 8.69 | 0.16 | 9.96 | 1.02 |
| 4 | 622338 | 74 | 2900 | 12.76 | 48.80 | 0.48 | 8.80 | 0.17 | 10.12 | 0.84 |
| 5 | 622339 | 76 | 2950 | 12.83 | 49.50 | 0.49 | 8.55 | 0.16 | 9.65 | 0.72 |
| 6 | 622349 | 84 | 2610 | 15.12 | 51.70 | 0.44 | 10.06 | 0.87 | 3.87 | 1.19 |
| 7 | 622350 | 80 | 3070 | 12.92 | 47.50 | 0.51 | 8.33 | 0.16 | 10.07 | 0.44 |
| 8 | 622354 | 179 | 4770 | 14.41 | 59.20 | 0.80 | 9.84 | 0.23 | 1.44 | 2.25 |
| 9 | 622355 | 195 | 4720 | 14.68 | 54.10 | 0.79 | 9.03 | 0.24 | 5.29 | 1.39 |
| 0 | 622356 | 190 | 4670 | 14.54 | 55.30 | 0.78 | 8.74 | 0.29 | 3.93 | 1.28 |
| 1 | 622357 | 193 | 4790 | 14.55 | 56.30 | 0.80 | 9.28 | 0.40 | 4.18 | 1.25 |
| 12 | 622358 | 182 | 4500 | 14.57 | 54.60 | 0.75 | 9.01 | 0.43 | 6.83 | 1.58 |
| 3 | 622359 | 175 | 4230 | 14.82 | 55.40 | 0.71 | 8.09 | 0.45 | 7.09 | 1.64 |
| 14 | 622360 | 187 | 4430 | 15.74 | 55.80 | 0.74 | 8.56 | 0.51 | 5.30 | 1.57 |
| 5 | 622361 | 171 | 4520 | 15.24 | 55.20 | 0.75 | 8.99 | 0.50 | 5.56 | 1.85 |
| 16 | 622362 | 182 | 4690 | 15.63 | 55.60 | 0.78 | 8.70 | 0.55 | 5.04 | 2.32 |
| 7 | 622363 | 178 | 4660 | 15.42 | 56.80 | 0.78 | 8.44 | 0.38 | 4.47 | 1.47 |
| 8 | 622364 | 174 | 4710 | 15.53 | 56.60 | 0.79 | 9.15 | 0.36 | 3.76 | 1.60 |
| 19 | 622365 | 180 | 4770 | 15.84 | 55.10 | 0.80 | 8.88 | 0.47 | 4.63 | 2.24 |
| 0 | 622366 | 185 | 4740 | 15.34 | 53.90 | 0.79 | 9.27 | 0.40 | 5.41 | 1.83 |
| 21 | 622367 | 82 | 2580 | 14.98 | 51.50 | 0.43 | 9.99 | 0.88 | 3.83 | 1.15 |
| 22 | 622368 | 163 | 4040 | 13.58 | 52.50 | 0.67 | 8.41 | 0.28 | 8.98 | 1.51 |
| 3 | 622369 | 166 | 4040 | 14.02 | 55.50 | 0.67 | 9.00 | 0.24 | 7.10 | 1.77 |
| 24 | 622370 | 173 | 3920 | 14.00 | 52.10 | 0.65 | 9.25 | 0.34 | 8.45 | 1.43 |
| 5 | 622371 | 178 | 3210 | 15.99 | 60.00 | 0.54 | 7.43 | 0.23 | 2.41 | 0.23 |

Results in ppm unless otherwise specified
T = element present; but concentration too low to measure
X = element concentration is below detection limit
– = element not determined

AUTHORISED OFFICER

655225

**ANALABS**

A Division of Inchcape Testing Services (Australia) Pty. Ltd.
A.C.N. 004 591 664

# ANALYTICAL DATA

| SAMPLE PREFIX | REPORT No. | REPORT DATE | CLIENT ORDER No. | PAGE |
|---|---|---|---|---|
| | 100560.60.09357 | 20/04/93 | 2738 | 6 OF 10 |

| JBE No. | SAMPLE No. | Zr | Ti | Al2O3 | SiO2 | TiO2 | Fe2O3 | MnO | CaO | K2O |
|---|---|---|---|---|---|---|---|---|---|---|
| 1 | 622372 | 180 | 3410 | 15.98 | 60.10 | 0.57 | 7.17 | 0.28 | 4.05 | 2.25 |
| 2 | 622373 | 168 | 3180 | 15.91 | 60.80 | 0.53 | 6.97 | 0.29 | 4.88 | 2.49 |
| 3 | 622374 | 173 | 3200 | 15.71 | 60.70 | 0.53 | 7.40 | 0.29 | 4.62 | 2.60 |
| 4 | 622375 | 168 | 3190 | 15.65 | 61.80 | 0.53 | 6.57 | 0.24 | 4.59 | 2.36 |
| 5 | 622376 | 166 | 3120 | 15.26 | 60.70 | 0.52 | 7.16 | 0.22 | 5.32 | 2.41 |
| 6 | 622377 | 168 | 3120 | 15.23 | 61.20 | 0.52 | 6.97 | 0.22 | 4.59 | 2.60 |
| 7 | 622378 | 173 | 3170 | 15.86 | 60.30 | 0.53 | 8.03 | 0.18 | 1.89 | 1.61 |
| 8 | 622379 | 177 | 3180 | 15.52 | 60.80 | 0.53 | 8.17 | 0.21 | 2.27 | 2.19 |
| 9 | 622380 | 166 | 3080 | 15.50 | 60.80 | 0.51 | 6.43 | 0.18 | 3.62 | 2.42 |
| 0 | 622381 | 164 | 3130 | 15.36 | 59.20 | 0.52 | 8.08 | 0.22 | 3.03 | 2.52 |
| 1 | 622382 | 158 | 2820 | 14.39 | 66.90 | 0.47 | 4.27 | 0.13 | 2.48 | 1.70 |
| 12 | 622383 | 182 | 3170 | 16.40 | 58.70 | 0.53 | 8.91 | 0.22 | 1.29 | 1.54 |
| 3 | 622384 | 194 | 2670 | 16.12 | 59.90 | 0.45 | 6.70 | 0.18 | 1.58 | 0.77 |
| 14 | 622385 | 79 | 2170 | 10.62 | 41.90 | 0.36 | 6.41 | 0.33 | 15.57 | 0.25 |
| 5 | 622386 | 230 | 2280 | 14.95 | 66.10 | 0.38 | 5.18 | 0.13 | 1.35 | 2.52 |
| 16 | 622387 | 225 | 2300 | 14.55 | 66.50 | 0.38 | 5.56 | 0.15 | 2.39 | 2.27 |
| 7 | 622388 | 215 | 2270 | 14.47 | 66.60 | 0.38 | 5.39 | 0.13 | 2.36 | 2.94 |
| 8 | 622389 | 235 | 2330 | 15.07 | 65.80 | 0.39 | 6.19 | 0.13 | 1.30 | 4.59 |
| 19 | 622390 | 210 | 2260 | 14.40 | 68.10 | 0.38 | 3.98 | 0.10 | 1.98 | 2.36 |
| 0 | 622391 | 231 | 2040 | 14.09 | 71.50 | 0.34 | 2.17 | 0.05 | 1.39 | 3.91 |
| 21 | 622392 | 241 | 2240 | 15.41 | 65.40 | 0.37 | 6.56 | 0.16 | 1.31 | 3.23 |
| 22 | 622393 | 226 | 2100 | 14.40 | 71.10 | 0.35 | 2.33 | 0.05 | 1.30 | 4.46 |
| 3 | 622394 | 239 | 2200 | 15.27 | 65.30 | 0.37 | 6.94 | 0.16 | 1.37 | 2.62 |
| 24 | 622395 | 141 | 5870 | 15.05 | 50.80 | 0.98 | 9.64 | 0.31 | 8.27 | 1.13 |
| 5 | 622396 | 226 | 2750 | 14.31 | 65.40 | 0.46 | 5.64 | 0.23 | 3.56 | 2.29 |

Results in ppm unless otherwise specified
T = element present; but concentration too low to measure
X = element concentration is below detection limit
– = element not determined

AUTHORISED OFFICER

655226

# ANALABS

A Division of Inchcape Testing Services (Australia) Pty. Ltd.
A.C.N. 004 591 664

## ANALYTICAL DATA

| SAMPLE PREFIX | REPORT No. | REPORT DATE | CLIENT ORDER No. | PAGE |
|---|---|---|---|---|
| | 100560.60.09357 | 20/04/93 | 2738 | 7 OF 10 |

| JBE No. | SAMPLE No. | Zr | Ti | Al2O3 | SiO2 | TiO2 | Fe2O3 | MnO | CaO | K2O |
|---|---|---|---|---|---|---|---|---|---|---|
| 1 | 622397 | 155 | 3010 | 12.38 | 54.80 | 0.50 | 7.54 | 0.27 | 9.20 | 1.51 |
| 2 | 622398 | 151 | 2820 | 12.63 | 53.40 | 0.47 | 7.49 | 0.34 | 10.22 | 1.36 |
| 3 | 622399 | 178 | 2500 | 13.63 | 60.80 | 0.42 | 5.81 | 0.22 | 5.39 | 1.88 |
| 4 | 622400 | 189 | 2480 | 14.69 | 65.90 | 0.41 | 4.53 | 0.12 | 2.77 | 2.04 |
| 5 | 622401 | 203 | 2660 | 14.95 | 65.60 | 0.44 | 5.45 | 0.15 | 2.23 | 2.00 |
| 6 | 622402 | 189 | 2580 | 14.33 | 66.20 | 0.43 | 3.94 | 0.12 | 3.29 | 2.88 |
| 7 | 622403 | 194 | 2490 | 14.30 | 64.70 | 0.42 | 3.84 | 0.12 | 4.13 | 2.98 |
| 8 | 622404 | 197 | 2510 | 14.59 | 64.70 | 0.42 | 4.52 | 0.13 | 3.27 | 3.25 |
| 9 | 622405 | 197 | 2550 | 14.28 | 63.00 | 0.43 | 5.62 | 0.15 | 3.63 | 1.21 |
| 10 | 622406 ✱ | 88 | 2730 | 15.13 | 51.50 | 0.45 | 10.03 | 0.88 | 3.79 | 1.19 |
| 11 | 622407 | 166 | 4050 | 15.06 | 59.10 | 0.68 | 9.51 | 0.22 | 2.14 | 2.07 |
| 12 | 622408 | 168 | 3760 | 15.27 | 60.80 | 0.63 | 7.42 | 0.19 | 3.23 | 1.96 |
| 13 | 622409 | 152 | 3450 | 13.72 | 62.70 | 0.58 | 4.49 | 0.15 | 5.90 | 2.81 |
| 14 | 622410 | 149 | 3040 | 14.20 | 62.90 | 0.51 | 4.82 | 0.16 | 4.81 | 2.06 |
| 15 | 622411 | 148 | 4790 | 15.09 | 56.40 | 0.80 | 8.13 | 0.19 | 3.70 | 2.38 |
| 16 | 622412 | 96 | 3170 | 13.62 | 51.40 | 0.53 | 8.34 | 0.16 | 6.27 | 2.01 |
| 17 | 622413 | 33 | 1950 | 11.79 | 39.30 | 0.32 | 8.08 | 0.25 | 14.70 | 1.50 |
| 18 | 622414 | 144 | 1960 | 6.36 | 68.90 | 0.33 | 3.90 | 0.16 | 7.22 | 1.14 |
| 19 | 622415 | 47 | 1820 | 10.68 | 33.50 | 0.30 | 7.92 | 0.34 | 18.27 | 0.68 |
| 20 | 622416 | 188 | 2800 | 9.16 | 63.20 | 0.47 | 5.03 | 0.14 | 5.79 | 1.72 |
| 21 | 622417 | 167 | 2390 | 7.55 | 68.60 | 0.40 | 4.50 | 0.13 | 4.24 | 1.27 |
| 22 | 622418 | 181 | 2570 | 8.65 | 67.50 | 0.43 | 4.93 | 0.12 | 3.98 | 1.61 |
| 23 | DETECTION | 5 | 60 | 0.01 | 0.01 | 0.01 | 0.01 | 0.01 | 0.01 | 0.01 |
| 24 | UNITS | ppm | ppm | % | % | % | % | % | % | % |
| 25 | METHOD | GX401 | OX408 | OX408 | OX408 | OX408 | OX408 | OX408 | OX408 | OX408 |

Results in ppm unless otherwise specified
T = element present; but concentration too low to measure
X = element concentration is below detection limit
– = element not determined

AUTHORISED OFFICER

655227

# ANALABS

A Division of Inchcape Testing Services (Australia) Pty. Ltd.
A.C.N. 004 591 664

## ANALYTICAL DATA

| SAMPLE PREFIX | REPORT No. | REPORT DATE | CLIENT ORDER No. | PAGE |
|---|---|---|---|---|
| | 100560.60.09357 | 20/04/93 | 2738 | 8 OF 10 |

| JBE No. | SAMPLE No. | MgO | P2O5 | S | Na2O | LOI | TOTAL | | | |
|---|---|---|---|---|---|---|---|---|---|---|
| 1 | 622335 | 9.71 | 0.134 | 0.020 | 1.52 | 4.61 | 99.62 | | | |
| 2 | 622336 | 10.55 | 0.129 | 0.010 | 1.67 | 2.98 | 100.20 | | | |
| 3 | 622337 | 10.75 | 0.129 | 0.010 | 1.53 | 3.20 | 100.27 | | | |
| 4 | 622338 | 11.30 | 0.125 | 0.040 | 1.61 | 4.50 | 99.55 | | | |
| 5 | 622339 | 10.99 | 0.106 | 0.050 | 1.07 | 5.55 | 99.65 | | | |
| 6 | 622349 | 7.53 | 0.192 | 0.050 | 3.38 | 5.60 | 100.04 | | | |
| 7 | 622350 | 9.95 | 0.117 | 0.040 | 1.34 | 8.55 | 99.94 | | | |
| 8 | 622354 | 3.58 | 0.291 | 2.360 | 1.71 | 5.74 | 101.81 | | | |
| 9 | 622355 | 4.78 | 0.310 | 0.750 | 2.81 | 5.47 | 99.61 | | | |
| 10 | 622356 | 5.22 | 0.288 | 0.590 | 3.19 | 5.35 | 99.51 | | | |
| 11 | 622357 | 4.97 | 0.308 | 0.260 | 3.59 | 3.66 | 99.58 | | | |
| 12 | 622358 | 4.63 | 0.315 | 0.430 | 3.01 | 3.76 | 99.96 | | | |
| 13 | 622359 | 3.93 | 0.288 | 0.270 | 2.75 | 4.13 | 99.60 | | | |
| 14 | 622360 | 4.10 | 0.319 | 0.250 | 3.14 | 3.67 | 99.66 | | | |
| 15 | 622361 | 3.96 | 0.306 | 0.110 | 2.84 | 4.31 | 99.64 | | | |
| 16 | 622362 | 3.76 | 0.332 | 0.100 | 2.55 | 4.30 | 99.70 | | | |
| 17 | 622363 | 3.43 | 0.353 | 0.840 | 3.64 | 3.55 | 99.59 | | | |
| 18 | 622364 | 3.57 | 0.338 | 0.340 | 3.35 | 4.32 | 99.71 | | | |
| 19 | 622365 | 3.77 | 0.352 | 0.230 | 2.98 | 4.35 | 99.69 | | | |
| 20 | 622366 | 3.95 | 0.353 | 0.120 | 2.76 | 5.53 | 99.70 | | | |
| 21 | 622367 | 7.53 | 0.192 | 0.040 | 3.39 | 5.69 | 99.66 | | | |
| 22 | 622368 | 5.32 | 0.261 | 0.130 | 2.56 | 5.73 | 99.91 | | | |
| 23 | 622369 | 5.92 | 0.226 | 0.050 | 2.04 | 3.01 | 99.57 | | | |
| 24 | 622370 | 6.25 | 0.248 | 0.070 | 2.01 | 4.82 | 99.59 | | | |
| 25 | 622371 | 2.60 | 0.237 | 1.510 | 5.95 | 3.14 | 100.27 | | | |

Results in ppm unless otherwise specified
T = element present; but concentration too low to measure
X = element concentration is below detection limit
– = element not determined

AUTHORISED OFFICER

655228

# ANALABS

A Division of Inchcape Testing Services (Australia) Pty. Ltd.
A.C.N. 004 591 664

## ANALYTICAL DATA

| SAMPLE PREFIX | REPORT No. | REPORT DATE | CLIENT ORDER No. | PAGE |
|---|---|---|---|---|
| | 100560.60.09357 | 20/04/93 | 2738 | 9 OF 10 |

| BE No. | SAMPLE No. | MgO | P2O5 | S | Na2O | LOI | TOTAL | | | |
|---|---|---|---|---|---|---|---|---|---|---|
| 1 | 622372 | 2.24 | 0.264 | 0.570 | 3.58 | 2.55 | 99.60 | | | |
| 2 | 622373 | 1.99 | 0.268 | 0.330 | 2.82 | 2.38 | 99.69 | | | |
| 3 | 622374 | 2.21 | 0.275 | 0.220 | 2.62 | 2.44 | 99.64 | | | |
| 4 | 622375 | 1.97 | 0.276 | 0.100 | 2.95 | 2.91 | 99.96 | | | |
| 5 | 622376 | 1.93 | 0.262 | 0.100 | 2.85 | 2.99 | 99.70 | | | |
| 6 | 622377 | 1.92 | 0.272 | 0.030 | 2.95 | 3.31 | 99.76 | | | |
| 7 | 622378 | 2.93 | 0.283 | 0.140 | 3.47 | 4.38 | 99.61 | | | |
| 8 | 622379 | 2.56 | 0.286 | 0.090 | 2.77 | 4.28 | 99.67 | | | |
| 9 | 622380 | 1.83 | 0.265 | 0.080 | 3.99 | 4.05 | 99.71 | | | |
| 10 | 622381 | 2.42 | 0.275 | 0.050 | 4.26 | 4.33 | 100.21 | | | |
| 11 | 622382 | 1.28 | 0.265 | 0.070 | 4.92 | 3.22 | 100.06 | | | |
| 12 | 622383 | 3.79 | 0.295 | 0.120 | 3.79 | 3.98 | 99.60 | | | |
| 13 | 622384 | 3.57 | 0.123 | 0.760 | 5.38 | 4.17 | 99.73 | | | |
| 14 | 622385 | 5.87 | 0.130 | 0.320 | 2.43 | 15.50 | 99.67 | | | |
| 15 | 622386 | 1.71 | 0.087 | 0.580 | 3.96 | 2.79 | 99.71 | | | |
| 16 | 622387 | 1.04 | 0.083 | 0.030 | 3.78 | 3.10 | 99.80 | | | |
| 17 | 622388 | 1.00 | 0.087 | 0.040 | 3.60 | 2.83 | 99.88 | | | |
| 18 | 622389 | 1.27 | 0.087 | 0.020 | 2.53 | 2.35 | 99.72 | | | |
| 19 | 622390 | 1.12 | 0.092 | 0.060 | 4.37 | 2.79 | 99.73 | | | |
| 20 | 622391 | 0.38 | 0.079 | 0.020 | 4.16 | 1.62 | 99.74 | | | |
| 21 | 622392 | 1.24 | 0.088 | <0.005 | 3.91 | 2.03 | 99.75 | | | |
| 22 | 622393 | 0.27 | 0.082 | 0.010 | 4.18 | 1.33 | 99.87 | | | |
| 23 | 622394 | 1.58 | 0.087 | 0.020 | 4.14 | 2.37 | 100.26 | | | |
| 24 | 622395 | 4.77 | 0.353 | 0.060 | 3.26 | 5.02 | 99.63 | | | |
| 25 | 622396 | 2.12 | 0.195 | 0.080 | 3.05 | 2.19 | 99.55 | | | |

Results in ppm unless otherwise specified
T = element present; but concentration too low to measure
X = element concentration is below detection limit
– = element not determined

AUTHORISED OFFICER

655229

# ANALABS

A Division of Inchcape Testing Services (Australia) Pty. Ltd.
A.C.N. 004 591 664

# ANALYTICAL DATA

| SAMPLE PREFIX | REPORT No. | REPORT DATE | CLIENT ORDER No. | PAGE |
|---|---|---|---|---|
| | 100560.60.09357 | 20/04/93 | 2738 | 10 OF 10 |

| TYPE No. | SAMPLE No. | MgO | P2O5 | S | Na2O | LOI | TOTAL | | | |
|---|---|---|---|---|---|---|---|---|---|---|
| | 622397 | 6.40 | 0.266 | 0.080 | 2.31 | 4.32 | 99.58 | | | |
| 2 | 622398 | 5.79 | 0.256 | 0.050 | 2.42 | 5.42 | 99.84 | | | |
| | 622399 | 2.59 | 0.139 | 0.110 | 3.55 | 4.98 | 99.53 | | | |
| 4 | 622400 | 1.32 | 0.100 | 0.170 | 4.39 | 3.32 | 99.76 | | | |
| | 622401 | 1.42 | 0.113 | 0.040 | 4.37 | 3.05 | 99.84 | | | |
| | 622402 | 1.02 | 0.110 | 0.070 | 3.94 | 3.29 | 99.57 | | | |
| | 622403 | 1.03 | 0.111 | 0.100 | 3.53 | 4.46 | 99.72 | | | |
| | 622404 | 1.16 | 0.107 | 0.090 | 3.41 | 4.18 | 99.79 | | | |
| 9 | 622405 | 1.95 | 0.111 | 0.260 | 4.29 | 4.63 | 99.61 | | | |
| | 622406 | 7.50 | 0.190 | 0.040 | 3.41 | 5.64 | 99.78 | | | |
| 11 | 622407 | 2.86 | 0.200 | 0.530 | 2.97 | 4.30 | 99.58 | | | |
| 12 | 622408 | 2.25 | 0.187 | 0.070 | 3.43 | 4.42 | 99.82 | | | |
| | 622409 | 0.70 | 0.165 | 0.050 | 3.21 | 5.28 | 99.72 | | | |
| 14 | 622410 | 1.05 | 0.149 | 0.060 | 3.89 | 4.86 | 99.51 | | | |
| | 622411 | 4.17 | 0.170 | 0.230 | 3.13 | 5.29 | 99.69 | | | |
| 16 | 622412 | 7.13 | 0.139 | 0.260 | 0.57 | 9.33 | 99.78 | | | |
| 17 | 622413 | 7.54 | 0.113 | 0.070 | 0.13 | 16.19 | 100.04 | | | |
| | 622414 | 3.19 | 0.100 | 0.250 | <0.05 | 8.25 | 99.86 | | | |
| 19 | 622415 | 8.17 | 0.105 | 0.150 | 0.67 | 18.93 | 99.69 | | | |
| 20 | 622416 | 5.33 | 0.114 | 0.200 | 0.14 | 8.49 | 99.80 | | | |
| 21 | 622417 | 5.22 | 0.092 | 0.100 | 0.23 | 7.18 | 99.50 | | | |
| 22 | 622418 | 5.37 | 0.115 | 0.160 | 0.34 | 6.77 | 99.96 | | | |
| 23 | DETECTION | 0.05 | 0.005 | 0.005 | 0.05 | 0.01 | 0.01 | | | |
| 24 | UNITS | % | % | % | % | % | % | | | |
| 25 | METHOD | OX408 | OX408 | OX408 | OX408 | OX408 | OX408 | | | |

Results in ppm unless otherwise specified
T = element present; but concentration too low to measure
X = element concentration is below detection limit
– = element not determined

AUTHORISED OFFICER

# APPENDIX VIII

# ABERFOYLE RESOURCES LTD. DRILL LOG

## MINES DEPARTMENT REPORT HEADER PAGE

**Drillhole Database name: mac**

**Report Grid: Mack**

**Report Legend follows:**

Collar Coordinate Reliability Flags

s = surveyed
m = measured
e = estimated

Assay, Composite, Geochem Bad Data Flag

Any element data that is bad will be recognised by an attached asterisk
example: 2.41*

655232

# ABERFOYLE RESOURCES LTD. DRILL LOG

| Area Code | Prospect | Report Grid | Dataset |
|---|---|---|---|
| mac | Muchison Zone | Mack | Header data set |

| Holename | Stored Grid |
|---|---|
| DDMA0034 | Mack |

**Hole Depth**
31.00

| Collar Easting | Collar Northing | Collar RL | Collar Depth |
|---|---|---|---|
| 3431.000m | 5719.000m | 681.60m | .00 |

| 1st Survey Depth | Survey Dip | Survey Azimuth | Survey Instrument |
|---|---|---|---|
| .00 | -75.00 | 315.00 | Clinometer |

| Start Date and Time | End Date & Time |
|---|---|
| 06/01/1993 | 09/01/1993 |

| Geologist | Hole Objective |
|---|---|
| S.Richardson | Structural Targ |

| Work Proposal | Tenement |
|---|---|
| | E.L.106/87 |

655233

# ABERFOYLE RESOURCES LTD. DRILL LOG

| Area Code | Prospect | Report Grid | Dataset |
|---|---|---|---|
| mac | Muchison Zone | AMG | Header data set |

| Holename | Stored Grid |
|---|---|
| DDMA0034 | Mack |

**Hole Depth**
31.00

| Collar Easting | Collar Northing | Collar RL | Collar Depth |
|---|---|---|---|
| 389302.799m | 5392689.590m | 681.60m | .00 |

| 1st Survey Depth | Survey Dip | Survey Azimuth | Survey Instrument |
|---|---|---|---|
| .00 | -75.00 | 337.10 | Clinometer |

| Start Date and Time | End Date & Time |
|---|---|
| 06/01/1993 | 09/01/1993 |

| Geologist | Hole Objective |
|---|---|
| S.Richardson | Structural Targ |

| Work Proposal | Tenement |
|---|---|
| | E.L.106/87 |

# ABERFOYLE RESOURCES LTD. DRILL LOG

| Area Code | Prospect | Report Grid | Dataset |
|---|---|---|---|
| mac | Muchison Zone | Mack | Survey data set |

| Holename | Stored Grid |
|---|---|
| DDMA0034 | Mack |

| Depth | Dip | Azi | Instrument |
|---|---|---|---|
| 0.00 | -75.00m | 315.00m | Clinometer |
| 16.00 | -74.25m | 308.50m | eastman |
| 31.00 | -72.50m | 299.00m | eastman |

# ABERFOYLE RESOURCES LTD. DRILL LOG

| Area Code | Prospect | Report Grid | Dataset |
|---|---|---|---|
| mac | Muchison Zone | Mack | Drill log data set |

| Holename | Stored Grid |
|---|---|
| DDMA0034 | Mack |

| Item # | From | To | Contractor | Drill Rig | Drill Method | ID |
|---|---|---|---|---|---|---|
| 1.00 | 0.00 | 3.00 | F.Ortner | F49J Modified | Tricone | 118 |
| 2.00 | 3.00 | 31.00 | F.Ortner | F49J Modified | Diamond | 96 |

655236

# ABERFOYLE RESOURCES LTD. DRILL LOG

| Area Code | Prospect | Report Grid | Dataset |
|---|---|---|---|
| mac | Muchison Zone | Mack | Casing log data set |

| Holename | Stored Grid |
|---|---|
| DDMA0034 | Mack |

| Item | From | To | Casing Type | ID | L | Comments |
|---|---|---|---|---|---|---|
| 1.00 | ? | ? | ? | ? | ? | No casing or PVC in hole |

Aberfoyle Resources Limited

EXPLORATION DIVISION

HOLE NO. Mac 24

PAGE 1 OF 1

GEO. SR

DATE 11-2-93

5 cm

# DIAMOND DRILL LOG

| DRILLING | | | | LITHOLOGY | | | | | | | | | | VESICLES | | | ALTERATION | | | VEINING | | | MINERALISATION | | FAULTS | | | | FOLIATION | | WEATHERING | STANDARD COLOUR LOG | REMARKS | SAMPLE NO. | DEPTH |
|---|---|---|---|---|---|---|---|---|---|---|---|---|---|---|---|---|---|---|---|---|---|---|---|---|---|---|---|---|---|---|---|---|---|---|
| DEPTH | DRILLING RUNS | CORE LOSS | CORE TRAY NO. | STRATIGRAPHY | ROCK TYPE | COLOUR | VOLCANICLASTICS: FRAGMENTS: COMPOSITION | VOLCANICLASTICS: FRAGMENTS: MAX. SIZE (MM) | VOLCANICLASTICS: FRAGMENTS: SORTING | VOLCANICLASTICS: FRAGMENTS: SHAPE | VOLCANICLASTICS: MATRIX: COMPOSITION | VOLCANICLASTICS: MATRIX: VOLUME % | LOWER CONTACT: GRADATION | LOWER CONTACT: STYLE | CONCENTRATION | MAX. SIZE (MM) | SHAPE | TEXTURE | INTENSITY | MINERALOGY | INTENSITY | MAX. WIDTH (MM) | MINERALOGY | TEXTURE | MINERALOGY & CONTENTS | POSITION OF BASE | DOWNHOLE WIDTH (CM) | CORE AXIS ANGLE | COUDE | TYPE | CORE AXIS ANGLE | | | | | |
| 2 | | | 1 | | | | | | | | | | | | | | | | | | | | | | | | | | 1·C CL | 35° | | | | | 2 |
| 4 | | | | | | | | | | | | | | | | | | | | | | | | | | | | | | | | | | | 4 |
| 6 | | | 2 | | | | | | | | | | | | | | | | | | | | | | | | | | 5·C BCL CL | 25° 25° | | | | | 6 |
| 8 | | | 3 | | | | | | | | | | | | | | | | | | | | | | | | | | | | 9·0 | | | | 8 |
| 10 | | | | | | | | | | | | | | | | | | | | | | | | Dx | Py Tr | | | | | | Qx P2 | | | | 10 |
| 12 | | | 4 | | | | | | | | | | | | | | | | | | | | | | | | | | | | | | | | 12 |
| 14 | | | | QRS | SW | BK | | | | | | | | | | | | | | | | | | | | | | | | | N·0 | | | | 14 |
| 16 | | | 5 | | | | | | | | | | | | | | | | | | | | | | | | | | | | | | | | 16 |
| 18 | | | | | | | | | | | | | | | | | | | | | | | | | | | | | | | | | | | 18 |
| 20 | | | 6 | | | | | | | | | | | | | | | | | | | | | | | | | | 20·C CL | 50° | | | | | 20 |
| 22 | | | | | | | | | | | | | | | | | | | | | | | | | | | | | | | | | | | 22 |
| 24 | | | 7 | | | | | | | | | | | | | | | | | | | | | | | | | | | | | | | | 24 |
| 26 | | | | | | | | | | | | | | | | | | | | | | | | | | | | | 25·0 BCL CL | 30° 45° | | | | | 26 |
| 28 | | | 8 | | | | | | | | | | | | | | | | | | | | | | | | | | | | | | | | 28 |
| 30 | | | 9 | | | | | | | | | | | | | | | | | | | | | | | | | | 30 BCL CL | 15° 35 | | | HOLE ABANDONED 31·0m | | 30 |
| 32 | | | | | | | | | | | | | | | | | | | | | | | | | | | | | | | | | | | 32 |
| 34 | | | | | | | | | | | | | | | | | | | | | | | | | | | | | | | | | | | 34 |
| 36 | | | | | | | | | | | | | | | | | | | | | | | | | | | | | | | | | | | 36 |
| 38 | | | | | | | | | | | | | | | | | | | | | | | | | | | | | | | | | | | 38 |

6555334

# APPENDIX IX

MINES DEPARTMENT REPORT HEADER PAGE

Drillhole Database name: mac

Report Grid: Mack

Report Legend follows:

Collar Coordinate Reliability Flags

s = surveyed
m = measured
e = estimated

Assay, Composite, Geochem Bad Data Flag

Any element data that is bad will be recognised by an attached asterisk
example: 2.41*

# ABERFOYLE RESOURCES LTD. DRILL LOG

| Area Code | Prospect | Report Grid | Dataset |
|---|---|---|---|
| mac | Murchison Zone | Mack | Header data set |

| Holename | Stored Grid |
|---|---|
| DDMA0035 | Mack |

**Hole Depth**
1189.60

| Collar Easting | Collar Northing | Collar RL | Collar Depth |
|---|---|---|---|
| 3560.600s | 5944.970s | 700.10s | .00 |

| 1st Survey Depth | Survey Dip | Survey Azimuth | Survey Instrument |
|---|---|---|---|
| .00 | -71.00 | 264.00 | theodolite |

| Start Date and Time | End Date & Time |
|---|---|
| 14/01/1993 | 23/02/1993 |

| Geologist | Hole Objective |
|---|---|
| S.Richardson | Structural Targ |

| Work Proposal | Tenement |
|---|---|
| | E.L.106/87 |

# ABERFOYLE RESOURCES LTD. DRILL LOG

| Area Code | Prospect | Report Grid | Dataset |
|---|---|---|---|
| mac | Murchison Zone | AMG | Header data set |

| Holename | Stored Grid |
|---|---|
| DDMA0035 | Mack |

**Hole Depth**
1189.60

| Collar Easting | Collar Northing | Collar RL | Collar Depth |
|---|---|---|---|
| 389507.892s | 5392850.199s | 700.10s | .00 |

| 1st Survey Depth | Survey Dip | Survey Azimuth | Survey Instrument |
|---|---|---|---|
| .00 | -71.00 | 286.10 | theodolite |

| Start Date and Time | End Date & Time |
|---|---|
| 14/01/1993 | 23/02/1993 |

| Geologist | Hole Objective |
|---|---|
| S.Richardson | Structural Targ |

| Work Proposal | Tenement |
|---|---|
| | E.L.106/87 |

# ABERFOYLE RESOURCES LTD. DRILL LOG

| Area Code | Prospect | Report Grid | Dataset |
|---|---|---|---|
| mac | Murchison Zone | Mack | Survey data set |

| Holename | Stored Grid |
|---|---|
| DDMA0035 | Mack |

| Depth | Dip | Azi | Instrument |
|---|---|---|---|
| 0.00 | -71.00i | 264.00i | theodolite |
| 25.00 | -71.00i | 264.00i | eastman |
| 50.00 | -71.00i | 264.00i | eastman |
| 75.00 | -71.00i | 264.50i | eastman |
| 100.00 | -71.00i | 265.25i | eastman |
| 125.00 | -71.00i | 266.25i | eastman |
| 150.00 | -70.50i | 266.75i | eastman |
| 175.00 | -70.25i | 267.50i | eastman |
| 200.00 | -70.25i | 268.50i | eastman |
| 225.00 | -70.00i | 269.50i | eastman |
| 250.00 | -69.25i | 270.00i | eastman |
| 275.00 | -69.25i | 270.75i | eastman |
| 300.00 | -69.00i | 271.00i | eastman |
| 325.00 | -69.00i | 271.50i | eastman |
| 350.00 | -69.00i | 273.00i | eastman |
| 375.00 | -68.75i | 274.50i | eastman |
| 400.00 | -68.00i | 275.00i | eastman |
| 425.00 | -66.75i | 275.50i | eastman |
| 450.00 | -66.00i | 277.00i | eastman |
| 475.00 | -66.00i | 278.50i | eastman |
| 500.00 | -66.00i | 279.50i | eastman |
| 525.00 | -66.00i | 280.00i | eastman |
| 550.00 | -66.00i | 280.50i | eastman |
| 575.00 | -66.00i | 280.50i | eastman |
| 600.00 | -66.00i | 280.50i | eastman |
| 625.00 | -66.00i | 280.50i | eastman |
| 650.00 | -66.00i | 281.00i | eastman |
| 675.00 | -66.00i | 283.00i | eastman |
| 700.00 | -66.00i | 283.50i | eastman |
| 725.00 | -66.00i | 283.75i | eastman |
| 750.00 | -66.00i | 284.50i | eastman |
| 775.00 | -66.00i | 284.50i | eastman |
| 800.00 | -65.80i | 285.00i | eastman |
| 825.00 | -65.50i | 285.00i | eastman |
| 850.00 | -65.25i | 285.50i | eastman |
| 875.00 | -65.00i | 287.50i | eastman |
| 900.00 | -64.80i | 288.50i | eastman |
| 925.00 | -64.50i | 289.00i | eastman |
| 950.00 | -64.50i | 289.50i | eastman |
| 975.00 | -64.50i | 290.00i | eastman |
| 1000.00 | -64.40i | 290.00i | eastman |
| 1025.00 | -64.25i | 290.50i | eastman |
| 1050.00 | -64.00i | 290.50i | eastman |
| 1075.00 | -64.00i | 291.00i | eastman |
| 1100.00 | -64.00i | 292.00i | eastman |
| 1125.00 | -64.00i | 292.50i | eastman |
| 1150.00 | -63.80i | 293.00i | eastman |
| 1175.00 | -63.50i | 293.25i | eastman |
| 1189.60 | -63.50i | 294.00i | eastman |

# ABERFOYLE RESOURCES LTD. DRILL LOG

655343

| Area Code | Prospect | Report Grid | Dataset |
|---|---|---|---|
| mac | Murchison Zone | Mack | Drill log data set |

| Holename | Stored Grid |
|---|---|
| DDMA0035 | Mack |

| Item # | From | To | Contractor | Drill Rig | Drill Method | ID |
|---|---|---|---|---|---|---|
| 1.00 | 0.00 | 7.00 | F.Ortner | F49J Modified | Tricone/Diamond | 118 |
| 2.00 | 7.00 | 222.00 | F.Ortner | F49J Modified | Diamond | 96 |
| 3.00 | 222.00 | 1189.60 | F.Ortner | F49J Modified | Diamond | 75 |

# ABERFOYLE RESOURCES LTD. DRILL LOG

**Area Code** mac
**Prospect** Murchison Zone
**Report Grid** Mack
**Dataset** Casing log data set

**Holename** DDMA0035
**Stored Grid** Mack

| Item | From | To | Casing Type | ID | L | Comments |
|---|---|---|---|---|---|---|
| 1.00 | 0.00 | 1.00 | HW | 101.6 | y | Old HW Placed at collar |
| 2.00 | 0.00 | 1189.60 | 40mm Cl.18 PVC | 40mm | y | ? |

# Aberfoyle Resources Limited

EXPLORATION DIVISION

HOLE No. MAC55
PAGE 1 OF 30
GEO. HJK
DATE 22-1-93

5 cm

# DIAMOND DRILL LOG

| DEPTH | DRILLING RUNS | CORE LOSS | CORE TRAY NO. | STRATIGRAPHY | ROCK TYPE | COLOUR | LITHOLOGY: VOLCANICLASTICS FRAGMENTS COMPOSITION | FRAGMENTS MAX. SIZE (MM) | FRAGMENTS SORTING | FRAGMENTS SHAPE | MATRIX COMPOSITION | MATRIX VOLUME % | LOWER CONTACT GRADATION | LOWER CONTACT STYLE | VESICLES CONCENTRATION | VESICLES MAX. SIZE (MM) | VESICLES SHAPE | ALTERATION TEXTURE | ALTERATION INTENSITY | ALTERATION MINERALOGY | VEINING INTENSITY | VEINING MAX. WIDTH (MM) | VEINING MINERALOGY | MINERALISATION TEXTURE | MINERALISATION MINERALOGY & CONTENTS | FAULTS POSITION OF BASE | FAULTS DOWNHOLE WIDTH (CM) | FAULTS CORE AXIS ANGLE | FAULTS GOUGE | FOLIATION TYPE | FOLIATION CORE AXIS ANGLE | WEATHERING | STANDARD COLOUR LOG | REMARKS | SAMPLE NO. | DEPTH |
|---|---|---|---|---|---|---|---|---|---|---|---|---|---|---|---|---|---|---|---|---|---|---|---|---|---|---|---|---|---|---|---|---|---|---|---|---|---|
| 2 | | | | | 2.9 | | | | | | | | | | | | | | | | | | | | | | | | | | | | | | Tricone to 2.9m | | 2 |
| 4 | | | | | | | | | | | | | | | | | | | | | | | | | | | | | | | | | | | | | 4 |
| 6 | | | 1 | PLS | FP-bv | OrGn | FP | >60 | P | ArsA | FP | 60 | G1 | | | | | A | 2 | SiAbEp | | | | | | | | | | | | | | 04 | | HQ | SAMPLE 89 | 6 |
| 8 | | | | | 9.3 | | | | | | | | | | | | | | | | | | | | | | | | | | | | 9.3 | | | | 8 |
| 10 | | | 2 | | FP-bv | GnOr | FP | >60 | P | ArsA | FP | 60 | G1 | | | | | | | | | | | | | | | | | | | | 02 | | 11.0m lost water | | 10 |
| 12 | | | | | 13.4 | | | | | | | | | | | | | | | | | 13.0 | | | | | | | | | | | 13.4 | | | | 12 |
| 14 | | | | | | | | | | | | | | | | | | | | | | | | | | | | | | | | | | | | | 14 |
| 16 | | | 3 | | FP-bv | OrGn | FP | >60 | P | ArsA | FP | 60 | S | | | | | | | | 1 | 20 | SiCO | | | | | | | | | | 03 | | 16.2m dropped core | | 16 |
| 18 | | | | | | | | | | | | | | | | | | | | | | | | | | | | | | | | | | | | | 18 |
| 20 | | | | | 20.2 | | | | | | | | | | | | | | | | | | | | | | 19.0 | 1 | 30 | SIOx | | 20.2 | | | 20 |
| 22 | | | 4 | | FP-bv 21.9 | GnGy | FP | >60 | P | ArsA | FPSi | 60 | S | | | | | | | | | | | | | | | | | | | 01 | 21.9 | | Joint planes oxidised FP frags wkly silicified but also epidote altered. | | 22 |
| | | | | | 22.6 FP-bv | OrBr | FP | >60 | P | ArsA | FP | 60 | S | | | | | | | | | | | | | | | | | | | 03 | 22.6 | | 21.9-22.6 - Cv Si fault planes? to 1cm | | |
| 24 | | | | | | | | | | | | | | | | | | | | | | 23.2 | | | | | | | | | | | | Fe staining on joint planes +/- dendritic Mn oxide. | | 24 |
| 26 | | | 5 | | FP-bv | GnGy | FP | >50 | P | ArsA | FP | 50 | S | | | | | | | | | | | | | | | | | | | 01 | | | | 26 |
| 28 | | | | | | | | | | | | | | | | | | | | | | | | | | | | | | | | | | | | | 28 |
| 30 | | | 6 | | 29.6 30.1 FP-bv | Or | FP | >40 | P | A | FP | 50 | S | | | | | | | | | | | | | | | | | | | 03 | 29.6 | | | 30.1 | 30 |
| 32 | | | | | FP-bv | GnGy | FP | >40 | P | sAAn | FP | 40 | | | | | | A | 3 | Si(Ab) | | | | | JP Ds | Pytr Gntr | | | | | | | 30.1 | | 31.1m Gn grain <0.2mm | | 32 |
| 34 | | | 7 | | | | | | | | | | | | | | | | | | | | | | JP | Pytr | | | | | | | | | | 34 |
| 36 | | | | | | | | | | | | | | | | | | | | | | | | | | | 36 | 1 | 65 | Ox | | | | | | 36 |
| 38 | | | 8 | | | | | | | | | | | | | | | | | | | | | | | | | | | | | | | | | | 38 |
| 40 | | | | | | | | | | | | | | | | | | | | | | | | | | | | | | | | | | | | | 40 |

39.2 dropped core

log.0193.wor

# Aberfoyle Resources Limited

EXPLORATION DIVISION

HOLE No. MAC 22

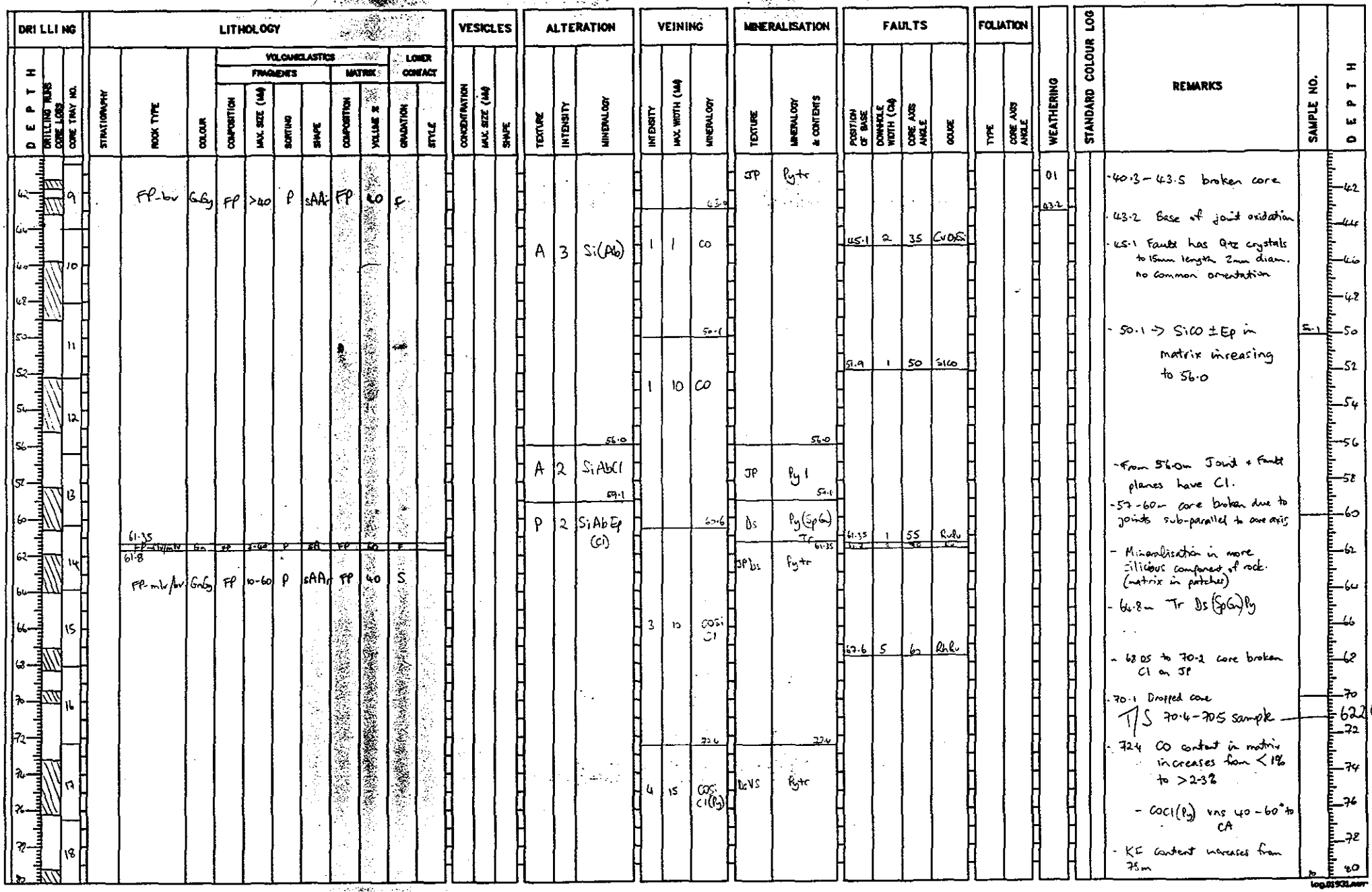
PAGE 2 OF 30

GEO. HJK

DATE 22-1-93

5 cm

# DIAMOND DRILL LOG



Aberfoyle Resources Limited

EXPLORATION DIVISION

HOLE No. MAL 55

PAGE 3 OF 30

GEO. HJK

DATE 25-1-93

5 cm

# DIAMOND DRILL LOG

DRILLING | LITHOLOGY | VESICLES | ALTERATION | VEINING | MINERALISATION | FAULTS | FOLIATION | WEATHERING | STANDARD COLOUR LOG | REMARKS | SAMPLE NO. | DEPTH

| DEPTH | DRILLING RUNS / CORE LOSS | CORE TRAY NO. | STRATIGRAPHY | ROCK TYPE | COLOUR | VOLCANICLASTICS: FRAGMENTS: COMPOSITION | FRAGMENTS: MAX. SIZE (MM) | FRAGMENTS: SORTING | FRAGMENTS: SHAPE | MATRIX: COMPOSITION | MATRIX: VOLUME % | LOWER CONTACT: GRADATION | LOWER CONTACT: STYLE |
|---|---|---|---|---|---|---|---|---|---|---|---|---|---|
| 80 | | | | 80.2 FP-bx | Pc | FP | >100 | P | AR | FP | 40 | G1 | |
| 82 | | 19 | | | | | | | | | | | |
| 84 | | | | | | | | | | | | | |
| 86 | | 20 | | | | | | | | | | | |
| 88 | | | | | | | | | | | | | |
| 90 | | 21 | | 91.9 | | | | | | | | | |
| 92 | | | | FP. lv | Pc | FP | 360 | P | sAA, | FP | 35 | G1 | |
| 94 | | 22 | | 96.9 | | | | | | | | | |
| 96 | | | | | | | | | | | | | |
| 98 | | 23 | | FP-bx | Pc | FP | 60 | P | sA | FP CO | 40 | | |
| 100 | | | | | | | | | | | | | |
| 102 | | 24 | | | | | | | | | | | |
| 104 | | | | | | | | | | | | | |
| 106 | | 25 | | | | | | | | | | | |
| 108 | | | | | | | | | | | | | |
| 110 | | 26 | | | | | | | | | | | |
| 112 | | | | | | | | | | | | | |
| 114 | | 27 | | | | | | | | | | | |
| 116 | | | | | | | | | | | | | |
| 118 | | | | | | | | | | | | | |
| 120 | | 28 | | | | | | | | | | | |

| VESICLES: CONCENTRATION | VESICLES: MAX. SIZE (MM) | VESICLES: SHAPE |
|---|---|---|
| | | |

| ALTERATION: TEXTURE | ALTERATION: INTENSITY | ALTERATION: MINERALOGY |
|---|---|---|
| P | 2 | SiPvEp(Cl) |
| | | 82 |
| P | 5 | SiAb |
| | | 82.5 |
| PL | 2 | SiAbEp |

| VEINING: INTENSITY | VEINING: MAX. WIDTH (MM) | VEINING: MINERALOGY |
|---|---|---|
| 4 | 15 | CoSiCl (Ep) |
| | | 82.7 |
| 3 | 8 | CoSi Cl |
| | | 89.2 |
| 1 | 5 | SiCO |
| | | 102.5 |
| 2 | 70 | SiCOCl Ep |
| | | 108.6 |
| 2 | 5 | CO |

| MINERALISATION: TEXTURE | MINERALOGY & CONTENTS |
|---|---|
| | 82.4 |
| VS | Py 1 |
| | 82.5 |
| Ds | Py tr |
| | 103.6 |
| JPDs | Py tr |

| FAULTS: POSITION OF BASE | FAULTS: DOWNHOLE WIDTH (CM) | FAULTS: CORE AXIS ANGLE | FAULTS: GOUGE |
|---|---|---|---|
| 82.8 | 30 | 40 | PuRu (CoSi) |
| 86.05 | 1 | 45 | SiCOCl |
| 90 | 1 | 5 | SiCICO |
| 94.15 | 1 | 50 | SiCO |

| FOLIATION: TYPE | FOLIATION: CORE AXIS ANGLE |
|---|---|
| | |

| WEATHERING |
|---|
| |

| STANDARD COLOUR LOG |
|---|
| |

REMARKS

- alteration intensity increase to fault, from fragment to pervasive
- fault has SiCO (10mm) on margins and PuRu core (multiple movements)
- alteration pervasive and less siliceous
- 83.0 to ~90m patches primarily pumpellyite rich.
- less CO in matrix after 82.8m
- possibly vesicular from 25.0m
- variable amounts of CO in matrix
- Ep more common in FP frags, SiAb in matrix ± CO
- fragment edges well defined

SAMPLE NO.

DEPTH

log01932.wor

9559

Aberfoyle Resources Limited
EXPLORATION DIVISION

HOLE No. MAC 22
PAGE 4 OF 30
GEO. HJK
DATE 25-1-93

5 cm

# DIAMOND DRILL LOG

| DRILLING | | | LITHOLOGY | | | | | | | | | | VESICLES | | | ALTERATION | | | VEINING | | | MINERALISATION | | FAULTS | | | | FOLIATION | | WEATHERING | STANDARD COLOUR LOG | REMARKS | SAMPLE NO. | DEPTH |
|---|---|---|---|---|---|---|---|---|---|---|---|---|---|---|---|---|---|---|---|---|---|---|---|---|---|---|---|---|---|---|---|---|---|
| DEPTH | DRILLING RUNS CORE LOSS | CORE TRAY NO. | STRATIGRAPHY | ROCK TYPE | COLOUR | VOLCANICLASTICS FRAGMENTS COMPOSITION | FRAGMENTS MAX. SIZE (MM) | FRAGMENTS SORTING | FRAGMENTS SHAPE | MATRIX COMPOSITION | MATRIX VOLUME % | LOWER CONTACT GRADATION | LOWER CONTACT STYLE | CONCENTRATION | MAX. SIZE (MM) | SHAPE | TEXTURE | INTENSITY | MINERALOGY | INTENSITY | MAX. WIDTH (MM) | MINERALOGY | TEXTURE | MINERALOGY & CONTENTS | POSITION OF BASE | DOWNHOLE WIDTH (CM) | CORE AXIS ANGLE | GOUGE | TYPE | CORE AXIS ANGLE | | | | | |
| 122 | | | | | | | | | | | | | | | | | | | | | | | | | | | | | | | | | | 122 |
| 124 | | 29 | | | | | | | | | | | | | | | | | | | | | | | | | | | | | | | | 124 |
| 126 | | | | | | | | | | | | | | | | | | | 2 | 5 | CO | | | | | | | | | | | | | 126 |
| 128 | | 30 | | | | | | | | | | | | | | | PL | 2 | SiAbEp | | | | JPDs | Py tr | 128.8 | 1 | 10 | COCiSi | | | | | 128 |
| 130 | | | | | | | | | | | | | | | | | | | | | | | | | | | | | | | | | | 130 |
| 132 | | 31 | | | | | | | | | | | | | | | | | | | | | | | | | | | | | | | | 132 |
| 134 | | | | | | | | | | | | | | | | | | | | | | | | | | | | | | | | | | 134 |
| 136 | | 32 | PLS | FP-bv | Pc | FP | 60 | P | sA | FP Co | 40 | G1 | | | | | | | | | | | | | | | | | | | | | | 136 |
| 138 | | | | | | | | | | | | | | | | | | | | | | | | | | | | | | | | | | 138 |
| 140 | | 33 | | | | | | | | | | | | | | | | | | | | | | | | | | | | | | | | 140 |
| 142 | | | | | | | | | | | | | | | | | | | | | | | | | | | | | | | | | | 142 |
| 144 | | 34 | | 144.9 | | | | | | | | | | | | | | | 144.37 | | | 144.8 | | 144.1 | | | | | | | | | | 144 |
| 146 | | | | | | | | | | | | | | | | | L | 4 | SiAb | | | | JPVs | Py1Sp1Gn1tr | 144.8 | 5 | 90 | PoCoSi | | | | | 146 |
| 148 | | 35 | | | | | | | | | | | | | | | | | | 3 | 15 | CoSi | | | 146.1 | 5 | 50 | PoRo | | | | | 148 |
| 150 | | | | FP-bv | Pc | FP | >60 | P | sAA | FP Si | 50 | | | | | | | | | 2 | 10 | CoSi | | | 146.6 | 150 | 20 | RoPo | | | | Fault to 1476 has Sp(pale) and Gn crystals in Po + Ro (to 1mm) | | 150 |
| 152 | | 36 | | | | | | | | | | | | | | | | | | | | | | | | | | | | | | | | 152 |
| 154 | | | | | | | | | | | | | | | | | | | 154.9 | | | 154.9 | | | | | | | | | | | | 154 |
| 156 | | 37 | | | | | | | | | | | | | | | P | 5 | Si(Ab) | 4 | 10 | Si Co (Sp) | VSDs | Sp2Gn1Py1 | | | | | | | | | Sp is pale in disseminations and dark in VS occurence (remobilised Devonian?) | | 156 |
| 158 | | | | | | | | | | | | | | | | | | | 158.2 | | | 158.2 | | 158.2 | | | | | | | | | | 158 |
| 160 | | 38 | | | | | | | | | | | | | | | P | 3 | Si(Ab) | 3 | 20 | CoSiEp (Sp) | VS | Sp tr Gn tr Py1 | 159 | 1 | 30 | CoCiSi | | | | | 160 |
| 162 | | | | | | | | | | | | | | | | | | | | | | | | | | | | | | | | | | 162 |

log2193.wor

Aberfoyle Resources Limited

EXPLORATION DIVISION

SCALE 1:1 | PAGE 5 OF 30 | GEO. HJK | DATE 26-1-93

5 cm

# DIAMOND DRILL LOG

DRILLING: DEPTH; DRILLING RUNS; CORE LOSS; CORE TRAY NO.

LITHOLOGY: STRATIGRAPHY; ROCK TYPE; COLOUR; VOLCANICLASTICS — FRAGMENTS: COMPOSITION, MAX. SIZE (MM), SORTING, SHAPE; MATRIX: COMPOSITION, VOLUME %; LOWER CONTACT: GRADATION, STYLE

VESICLES: CONCENTRATION, MAX. SIZE (MM), SHAPE

ALTERATION: TEXTURE, INTENSITY, MINERALOGY

VEINING: INTENSITY, MAX. WIDTH (MM), MINERALOGY

MINERALISATION: TEXTURE, MINERALOGY & CONTENTS

FAULTS: POSITION OF BASE, DOWNHOLE WIDTH (CM), CORE AXIS ANGLE, GOUGE

FOLIATION: TYPE, CORE AXIS ANGLE

WEATHERING

STANDARD COLOUR LOG

REMARKS

SAMPLE NO.

DEPTH

| DEPTH | CORE TRAY NO. | STRATIGRAPHY | ROCK TYPE | COLOUR | FRAG COMP | FRAG MAX SIZE (MM) | FRAG SORTING | FRAG SHAPE | MATRIX COMP | MATRIX VOLUME % | LOWER CONTACT GRADATION | LOWER CONTACT STYLE | VESICLES CONC. | VESICLES MAX SIZE (MM) | VESICLES SHAPE | ALTERATION TEXTURE | ALTERATION INTENSITY | ALTERATION MINERALOGY | VEINING INTENSITY | VEINING MAX WIDTH (MM) | VEINING MINERALOGY | MINERALISATION TEXTURE | MINERALISATION MINERALOGY & CONTENTS | FAULTS POSITION OF BASE | FAULTS DOWNHOLE WIDTH (CM) | FAULTS CORE AXIS ANGLE | FAULTS GOUGE | FOLIATION TYPE | FOLIATION CORE AXIS ANGLE | WEATHERING | SAMPLE NO. | REMARKS |
|---|---|---|---|---|---|---|---|---|---|---|---|---|---|---|---|---|---|---|---|---|---|---|---|---|---|---|---|---|---|---|---|---|
| 160–162 | | | | | | | | | | | | | | | | | | | | | | | | | | | | | | | | |
| 162–164 | 39 | PLS | FP-bx | Pc | FP | >150 | P | sAA | FP Si | 50 | G2 | | | | | P | 3 | Si (Ab) | 3 | 20 | Cos Ep | Dx VS | Pyl Sptr Gntr | | | | | | | | | 162.1 Gn in vein (5% of content of vein) |
| 164–166 | | | | | | | | | | | | | | | | | | 164.9 | | | | | | | | | | | | | | 165.1m Gn grain 5x1.5mm |
| 166–168 | 40 | | | | | | | | | | | | | | | L | 4 | KFSi 165.7 | | | 166 | | 165.7 | | | | | | | | | <1% combined s/phides. |
| 168–170 | | | | | | | | | | | | | | | | AF | U | Si (Ab) (Ep) | 2 | 7 | Cos: (GSp) | Dx VS JP | Pyt Sptr Gntr | | | | | | | | 168.1–168.2 sample 62651 |
| 170–172 | 41 | | | | | | | | | | | | | | | | | | | | 172.3 | | | | | | | | | | | Ds Sp dk Br |
| 172–174 | | | | | | | | | | | | | | | | | | | 3 | 10 | Cos: Ep (Sp) | | | 174.1 | 1 | 35 | S1 Cos Sp | | | | 172.0 onwards Co content of matrix increases. |
| 174–176 | 42 | | | | | | | | | | | | | | | | | | | | 192.3 | | | | | | | | | | | @ 175.95m 10cm Pale Gn bleached Angular fragment, very siliceous ± Gn blotches + Ds Sp RABr |
| 176–178 | | | | | | | | | | | | | | | | | | | | | | | | | | | | | | | | |
| 178–180 | | | | | | | | | | | | | | | | | | | | | | | | | | | | | | | | |
| 180–182 | 43 | | | | | | | | | | | | | | | | | | | | | | | | | | | | | | | 181.4 'Fibrous' SiCO vns 10mm wide ± VC Sp 55° to CA. |
| 182–184 | | | | | | | | | | | | | | | | | | | | | | | | | | | | | | | | |
| 184–186 | | | | | | | | | | | | | | | | | | | | | | | | | | | | | | | | Ep alt'n restricted to less silicified fragments. |
| 186–188 | 44 | | | | | | | | | | | | | | | | | 187.1 | 2 | 20 | COCl Si | | | | | | | | | | | 191 → 192+ possible wk. cleavage developed in patches – resembles vesicle alignment? – no consistent orientation? |
| 188–190 | | | | | | | | | | | | | | | | LF | 3 | Si (Ab) Cl Ep | | | | | | | | | | | | | | |
| 189.5 | | | | | | | | | | | | | 188.5 | | | | | | | | | | | | | | | | | | | |
| 190–192 | 45 | | FP-1? | Pc | | | | | | | | | 2 | 10 | E | | | | | | 191.1 | | | | | | | | | | | Fragments Cl²+ Ep altered in locally Si altd matrix vesicles? or deformed Co matrix. |
| 192–194 | | | | | | | | | | | | | | | | | | | | | | | | | | | | | | | | |
| 194–196 | 46 | | | | | | | | | | | | | | | | | | 2 | 10 | COSi (Ep) | | | | | | | | | | | 187.1 → 199.7 very mottled appearance – Dk Gn pseudo-fragments with PkBr blotches in LGnGy 'matrix' |
| 196–198 | | | | | | | | | | | | | | | | | | | | | | | | | | | | | | | | |
| 198–200 | 47 | | | | | | | | | | | | | | | | | 199.7 | | | | | 199.7 | | | | | | | | | 3p to 5mm PkBr blebs in Co |

log/0193/mer

6651

Aberfoyle Resources Limited

EXPLORATION DIVISION

HOLE NO. [illegible]

PAGE 6 OF 30

GEO. HJK

DATE 22-1-93

# DIAMOND DRILL LOG

5 cm

| DRILLING | | | LITHOLOGY | | | | | | | | | | VESICLES | | | ALTERATION | | | VEINING | | | MINERALISATION | | FAULTS | | | | FOLIATION | | WEATHERING | STANDARD COLOUR LOG | REMARKS | SAMPLE NO. | DEPTH |
|---|---|---|---|---|---|---|---|---|---|---|---|---|---|---|---|---|---|---|---|---|---|---|---|---|---|---|---|---|---|---|---|---|---|
| DEPTH | DRILLING RUNS CORE LOSS | CORE TRAY NO. | STRATIGRAPHY | ROCK TYPE | COLOUR | VOLCANICLASTICS: FRAGMENTS COMPOSITION | FRAGMENTS MAX. SIZE (MM) | FRAGMENTS SORTING | FRAGMENTS SHAPE | MATRIX COMPOSITION | MATRIX VOLUME % | LOWER CONTACT GRADATION | LOWER CONTACT STYLE | CONCENTRATION | MAX. SIZE (MM) | SHAPE | TEXTURE | INTENSITY | MINERALOGY | INTENSITY | MAX. WIDTH (MM) | MINERALOGY | TEXTURE | MINERALOGY & CONTENTS | POSITION OF BASE | DOWNHOLE WIDTH (CM) | CORE AXIS ANGLE | GOUGE | TYPE | CORE AXIS ANGLE | | | | | |
| 202 | | | | | | | | | | | | | | | | | | | | | | | | | | | | | | | | Vesicles variable in size, shape and concentrations | | 202 |
| 204 | | 48 | | | | | | | | | | | | | | | | | | | | | | | | | | | | | | | | 204 |
| 206 | | | PLS | FP-1? | Pc | | | | | | | G2 | | 2 | 10 | E | L | S | Si Ab | 3 | 10 | Cosi (Py) | Ds | Pytr Spty | | | | | | | | | | 206 |
| 208 | | 49 | | | | | | | | | | | | | | | | | 206.3 | | | 2061 | | 206.7 | | | | | | | | 2062-209.1 Fault - multiple movements Py / Co | | 208 |
| 210 | | | | | | | | | | | | | | | | | | | | 1 | 5 | Co 2067 | | | 208.1 | 140 | 10 | Co Ru Bx | | | | | 210 |
| 212 | | 50 | | | | | | | | | | | | | | | L | C | Ti (Py) 211.4 | 1 | 35 | Cosi | | | | | | | | | | -[illegible] texture very patchy | 211 | 212 |
| 214 | | | | | | | | | | | | | | | | | AF | 2 | Si 214.2 | | | | | | | | | | | | | | | 214 |
| 216 | | 51 | | | | | | | | | | | | | | | P | S | Si (Py) 216.9 | | | | Ds | Pytr | | | | | | | | | | 216 |
| 218 | | | | | | | | | | | | | | | | | | | | | | | | | | | | | | | | | | 218 |
| 220 | | 52 | | | | | | | | | | | | | | | AF | 2 | Si | | | | | | | | | | | | | | | 220 |
| 222 | | | | 222.75 | | | | | | | | | | | | | | | 222.75 | | | | | | | | | | | | | | | 222 |
| 224 | | 53 | | | | | | | | | | | | | | | | | | | | | | | | | | | | | | | | 224 |
| 226 | | | | | | | | | | | | | | | | | | | | | | 2268 | | | | | | | | | | | | 226 |
| 228 | | | | FP-bx/1 | Pc | FP | 80 | P | SAR | FP | 50 | G1 | | | | | AF | 3 | Si Py | 3 | 100 | Cosi Cl | | | | | | | | | | | | | 228 |
| 230 | | 54 | | | | | | | | | | | | | | | | | | | | | | | | | | | | | | | | 230 |
| 232 | | | | | | | | | | | | | | | | | | | | | | 235.2 | | | | | | | | | | | | 232 |
| 234 | | | | | | | | | | | | | | | | | | | | 4 | 30 | Cos Cl ? | | | 237.3 | 5 | 20 | Pu Ru | | | | | 234 |
| 236 | | 55 | | | | | | | | | | | | | | | | | 237.3 | | | 238.7 | | | | | | | | | | | | 236 |
| 238 | | | | FP-1 | Gabr | | | | | | | G1 | | | | | P | 4 | Si | 4 | 5 | Si Co | | | | | | | | | | | | | 238 |
| 240 | | | | | | | | | | | | | | | | | | | | | | | | | | | | | | | | | | 240 |

7S622652

239.2 - 239.85

log.01931.wor

# Aberfoyle Resources Limited

EXPLORATION DIVISION

HOLE No. MHC 55
PAGE 7 OF 30
GEO. HJK
DATE 28-1-93

5 cm

# DIAMOND DRILL LOG

DRILLING: DEPTH | DRILLING RUNS | CORE LOSS | CORE TRAY NO.

LITHOLOGY: STRATIGRAPHY | ROCK TYPE | COLOUR | VOLCANICLASTICS: FRAGMENTS (COMPOSITION | MAX. SIZE (MM) | SORTING | SHAPE) | MATRIX (COMPOSITION | VOLUME %) | LOWER CONTACT (GRADATION | STYLE)

VESICLES: CONCENTRATION | MAX. SIZE (MM) | SHAPE

ALTERATION: TEXTURE | INTENSITY | MINERALOGY

VEINING: INTENSITY | MAX. WIDTH (MM) | MINERALOGY

MINERALISATION: TEXTURE | MINERALOGY & CONTENTS

FAULTS: POSITION OF BASE | DOWNHOLE WIDTH (CM) | CORE AXIS ANGLE | GOUGE

FOLIATION: TYPE | CORE AXIS ANGLE

WEATHERING

STANDARD COLOUR LOG

REMARKS | SAMPLE NO. | DEPTH

| DEPTH | CORE TRAY NO. | ROCK TYPE | COLOUR | FRAGMENTS: COMPOSITION / MAX. SIZE (MM) / SORTING / SHAPE | MATRIX: COMPOSITION / VOLUME % | LOWER CONTACT: GRADATION / STYLE | VESICLES: CONCENTRATION / MAX. SIZE (MM) / SHAPE | ALTERATION: TEXTURE / INTENSITY / MINERALOGY | VEINING: INTENSITY / MAX. WIDTH (MM) / MINERALOGY | MINERALISATION: TEXTURE / MINERALOGY & CONTENTS | FAULTS: POSITION OF BASE / DOWNHOLE WIDTH (CM) / CORE AXIS ANGLE / GOUGE | FOLIATION: TYPE / CORE AXIS ANGLE | REMARKS | SAMPLE NO. |
|---|---|---|---|---|---|---|---|---|---|---|---|---|---|---|
| 262 | 56 | | | | | | | P C Si 263.5 | U 5 Si00 | | 262.45 1 45 SiCl | | | |
| 264 | | | | | | | | | | | 263.45 | | | |
| 266 | 57 | FP-1 | Gnbi | | | G1 | | L 3 SiAb | 5 30 Si00 | Di Py tr | | | Massive lava ± patchy alteration | |
| 268 | | | | | | | | | 268.8 | | | | | |
| 270 | 58 | | | | | | | | | | 271.9 1 45 SiCO(?) | | | |
| 272 | | | | | | | | | | | | | | |
| 274 | | | | | | | | | 3 20 Si00 | | | | | |
| 276 | 59 | | | | | | | | | | | | | |
| 278 | | | | | | | | | | | | | | |
| 280 | | | | | | | | | | | | | | |
| 282 | | | | | | | | | | | | | | |
| 284 | 60 | | | | | | | | | | | | | |
| 286 | | | | | | | | | | | | | | |
| 288 | | | | | | | | | | | | | | |
| 290 | | | | | | | | | | | | | | |
| 292 | | | | | | | | | | | | | | |
| 294 | 61 | | | | | | | | | | | | | |
| 296 | | | | | | | | | | | | | | |
| 298 | | | | | | | | | | | | | | |
| 300 | | | | | | | | | | | | | | |
| 302 | | | | | | | | | | | | | | |
| 304 | 62 | | | | | | | | | | | | | |
| 306 | | | | | | | | | | | | | | |
| 308 | | | | | | | | | | | | | | |
| 310 | | | | | | | | | | | | | | |
| 312 | | | | | | | | | | | | | | |
| 314 | 63 | | | | | | | | | | | | | |
| 316 | | | | | | | | | | | | | | |
| 318 | | | | | | | | | | | | | | |
| 320 | | | | | | | | | | | | | | |

256.7

FP-mlv | Pc | FP Si | 60 | M | A | FP Si | 60 | S | 262.45

B-bv 264.2 | Pc | Bpl FP | >50 | P | sA | FP Si | 40 | S | 262.45 | 5 10 V 266.2

B-pl | DGn | 5 20 ES | P 1 Ep(SiAb) Fu 270.7 | 3 10 Cb 270.8

L 2 Cl(AbSi) Ep | 3 20 Cb(Si)

VeDs Py 5 Sp1 Gn tr 266.2 | IP Py 10 270.7 | SP Py 2

259.9 10 50 RuPu
260.5 2 35 RuSi
262.8 2 80 PuRu

Massive lava ± patchy alteration

possibly polymict, matrix becomes finer downwards from FP to cherty (av?) hyaloclastite?

260.80-260.90 T/S 622653

Basalt breccia zone with numerous SiCO cavity veins - may be fault zone at contact

vesicles filled ± CO, SiAb, Py.

- IP Py and Ch patchy in width - up to 0.5m
- Pillows average ~30cm between Ch bands and chilled margins ± Py.
- Ch - 20% of rock to 276.0m

log.01931.wwr

# Abitibi Resources Limited
EXPLORATION DIVISION

HOLE NO. [illegible]
PAGE 1 OF 30
GEO. HJK
DATE 28-1-93

5 cm

# DIAMOND DRILL LOG

DRILLING | LITHOLOGY | VESICLES | ALTERATION | VEINING | MINERALISATION | FAULTS | FOLIATION | WEATHERING | STANDARD COLOUR LOG | REMARKS | SAMPLE NO. | DEPTH

DRILLING: DEPTH; DRILLING RUNS; CORE LOSS; CORE TRAY NO.

LITHOLOGY: STRATIGRAPHY; ROCK TYPE; COLOUR; VOLCANICLASTICS — FRAGMENTS: COMPOSITION, MAX. SIZE (MM), SORTING, SHAPE; MATRIX: COMPOSITION, VOLUME %; LOWER CONTACT: GRADATION, STYLE

VESICLES: CONCENTRATION; MAX. SIZE (MM); SHAPE

ALTERATION: TEXTURE; INTENSITY; MINERALOGY

VEINING: INTENSITY; MAX. WIDTH (MM); MINERALOGY

MINERALISATION: TEXTURE; MINERALOGY & CONTENTS

FAULTS: POSITION OF BASE; DOWNHOLE WIDTH (CM); CORE AXIS ANGLE; GOUGE

FOLIATION: TYPE; CORE AXIS ANGLE

WEATHERING

STANDARD COLOUR LOG

REMARKS

SAMPLE NO.

DEPTH

| DEPTH | ROCK TYPE | COLOUR | REMARKS |
|---|---|---|---|
| 290 | | | |
| 292 | | | |
| 294 | | | |
| 296 | | | |
| 298 | | | |
| 300 | | | |
| 302 | | | |
| 304 | | | |
| 306 | | | |
| 308 | | | |
| 310 | | | |
| 312 | | | |
| 314 | | | |
| 316 | | | |
| 318 | | | |
| 320 | | | |

| | | | | | | | | | | | | | | | | | | | | | | | | | |
|---|---|---|---|---|---|---|---|---|---|---|---|---|---|---|---|---|---|---|---|---|---|---|---|---|---|
| 290 | | | | | | | | | | | | | | | | | | | | | | | | | |
| 292 | | | | | | | | | | | | | | | | | | | | | | | | | |
| 294 | | | | | | | | | | | | | | | | | | | | | | | | | |
| 296 | | | | | | | | | | | | | | | | | | | | | | | | | |
| 298 | | | | | | | | | | | | | | | | | | | | | | | | | |
| 300 | | | | | | | | | | | | | | | | | | | | | | | | | |
| 302 | | | | | | | | | | | | | | | | | | | | | | | | | |
| 304 | | | | | | | | | | | | | | | | | | | | | | | | | |
| 306 | | | | | | | | | | | | | | | | | | | | | | | | | |
| 308 | | | | | | | | | | | | | | | | | | | | | | | | | |
| 310 | | | | | | | | | | | | | | | | | | | | | | | | | |
| 312 | | | | | | | | | | | | | | | | | | | | | | | | | |
| 314 | | | | | | | | | | | | | | | | | | | | | | | | | |
| 316 | | | | | | | | | | | | | | | | | | | | | | | | | |
| 318 | | | | | | | | | | | | | | | | | | | | | | | | | |
| 320 | | | | | | | | | | | | | | | | | | | | | | | | | |

| DEPTH | DRILLING RUNS | CORE LOSS | CORE TRAY NO. |
|---|---|---|---|
| 290 | | | |
| 292 | | | |
| 294 | | | |
| 296 | | | |
| 298 | | | |
| 300 | | | |
| 302 | | | |
| 304 | | | |
| 306 | | | |
| 308 | | | |
| 310 | | | |
| 312 | | | |
| 314 | | | |
| 316 | | | |
| 318 | | | |
| 320 | | | |

| STRATIGRAPHY | ROCK TYPE | COLOUR | VOLCANICLASTICS — FRAGMENTS: COMPOSITION | FRAGMENTS: MAX. SIZE (MM) | FRAGMENTS: SORTING | FRAGMENTS: SHAPE | MATRIX: COMPOSITION | MATRIX: VOLUME % | LOWER CONTACT: GRADATION | LOWER CONTACT: STYLE |
|---|---|---|---|---|---|---|---|---|---|---|
| | S-pl | DGn | | | | | | | F | |
| | 311.5 | | | | | | | | | |
| | B-pl/bx | G | | | | | | | | |

| VESICLES: CONCENTRATION | VESICLES: MAX. SIZE (MM) | VESICLES: SHAPE |
|---|---|---|
| 5 | 20 | ES |

| ALTERATION: TEXTURE | ALTERATION: INTENSITY | ALTERATION: MINERALOGY |
|---|---|---|
| L | 1 | C1 Ep (Mo) 297.0 |
| fm | 1 | FuSe (Mo Ep) |
| | | 303.2 |
| PS | 3 | C1 |
| | | 34 |
| L | 3 | FuSe(Ep) |

| VEINING: INTENSITY | VEINING: MAX. WIDTH (MM) | VEINING: MINERALOGY |
|---|---|---|
| 3 | 20 | COSi |
| | | 296.9 |
| 4 | 15 | COSi |
| | | 315.1 |
| 4 | 70 | COSiTPy |
| | | 315.5 |
| 6 | 20 | COSi |

| MINERALISATION: TEXTURE | MINERALOGY & CONTENTS |
|---|---|
| IP | Py2 |
| | 297 |
| IPDs | Pytr |
| | 315.1 |
| VSDS | Sph Gal Py tr |
| | 315.5 |
| Ds | Pytr |

| FAULTS: POSITION OF BASE | DOWNHOLE WIDTH (CM) | CORE AXIS ANGLE | GOUGE |
|---|---|---|---|
| 296.2 | 5 | 35 | CORUCA |
| 304.6 | 1 | 10 | CORSI |
| 313.7 | 220 | 20 | RuCOSi |

| FOLIATION: TYPE | FOLIATION: CORE AXIS ANGLE |
|---|---|
| VA | 55 |
| 295.2 | |
| VA | 50 |
| 307.4 | |

IP chert vleat 3% of core.

Zones of veinlets with Cl alteration from 297m →

vesicles infilled with CO rims, Si cores.

309.90 – 310.20 m IPCh band

minor Py in fault.

This basalt has less IPCh and more breccia zones & CO matrix.

Cl Altered vesicles common after (Si) rare chalcedonic

SAMPLE NO. 311.5

6555559

log21931.wor

# Aberfoyle Resources Limited

EXPLORATION DIVISION

HOLE No. MME55

PAGE 1 OF 30

GEO. HJK

DATE 28-1-93

5 cm

# DIAMOND DRILL LOG

| DRILLING | | | LITHOLOGY | | | | | | | | | | VESICLES | | | ALTERATION | | | VEINING | | | MINERALISATION | | FAULTS | | | | FOLIATION | | | | | | |
|---|---|---|---|---|---|---|---|---|---|---|---|---|---|---|---|---|---|---|---|---|---|---|---|---|---|---|---|---|---|---|---|---|---|
| DEPTH | DRILLING RUNS / CORE LOSS | CORE TRAY NO. | STRATIGRAPHY | ROCK TYPE | COLOUR | VOLCANICLASTICS: FRAGMENTS: COMPOSITION | FRAGMENTS: MAX. SIZE (MM) | FRAGMENTS: SORTING | FRAGMENTS: SHAPE | MATRIX: COMPOSITION | MATRIX: VOLUME % | LOWER CONTACT: GRADATION | LOWER CONTACT: STYLE | CONCENTRATION | MAX. SIZE (MM) | SHAPE | TEXTURE | INTENSITY | MINERALOGY | INTENSITY | MAX. WIDTH (MM) | MINERALOGY | TEXTURE | MINERALOGY & CONTENTS | POSITION OF BASE | DOWNHOLE WIDTH (CM) | CORE AXIS ANGLE | GOUGE | TYPE | CORE AXIS ANGLE | WEATHERING | STANDARD COLOUR LOG | REMARKS | SAMPLE NO. | DEPTH |
| | | | | B-pl/bx | Gn | | | | | | | | | 5 | 20 | ES | L | 3 | Fu Se (ep) 326.1 | 4 | 20 | CO Si | Bx | Py tr | | | | | | | | | Some Fu in CO vns CO matrix where elev. | | 322 |
| | | | | | | | | | | | | | | | | | A | 2 | Se CO (Fu) | | | 327.1 | | | | | | | | | | No faulting obvious | | 330 |
| | | | | | | | | | | | | | | | | | | | | 3 | 20 | CO | | 335 | | | | | | | | | | | 334 |
| | | | | 337.1 | | | | | | | | | | 5 | 8 | ES | | | | | | 337.1 | VSDs | Py2Spl | | | | | | | | | Sp also as vesicle filling | | 336 |
| | | | | B-bx | Pc | B-pl? | >80 | P | sA | CO | 30 | G1 | | | | 335.5 | | | | 2 | 12 | CO Si | Ba Py | tr | | | | | | | | | | | 340 |
| | | | | 341.5 | | | | | | | | | | | | | | | 341.5 | | | 341.5 | | | | | | | | | | | | 342 |
| | | | | B-bx | Pc | B | 120 | P | sA | B | 20 | G1 | | 1 | 3 | EI | F | 3 | Se CO | 1 | 5 | CO | | | | | | | | | | | vesicles in bx & frags - none visible in matrix | | 344 |
| | | | | 344.0 | | | | | | | | | | | | FVu | | | 344 | | | 344.2 | | | | | | | | | | | | |
| | | | | B-bx | Pc | B | >200 | P | AAr | CO | 45 | S | | 4 | 10 | SE | F | 4 | Si Po Se | 4 | 50 | CO Si | | | | | | | | | | | 332-340 may represent zone of very intense CO alteration - already high Fe content + earlier v. intense vesicles | | 346 |
| | | | | | | | | | | | | | | | | | | | 354.30 | | | 348.2 | | | | | | | | | | | | 348 |
| | | | | | | | | | | | | | | | | | | | | 1 | 5 | CO(Si) | | | | | | | | | | | | 350 |
| | | | | | | | | | | | | | | | | | | | | | | | | 354.3 | | | | | | | | | | 352 |
| | | | | | | | | | | | | | | | | | | | | | | 354.4 | VSDs | Py tr Sp tr Gn tr Cp tr | | | | | | | | | | 354 |
| | | | | B-l/bx | Gn | | | | | | | | | 1 | 10 | SE | L | 3 | Si Po Se | 2 | 15 | Tr Si Ep | | | | | | | | | | | | | 358 |
| | | | | | | | | | | | | | | | | | | | | | | | | | | | | | | | | | | 360 |

65533

log.01931.swr

Aberfoyle Resources Limited

EXPLORATION DIVISION

HOLE NO. M.[illegible]

PAGE 10 OF 30

GEO. HJK

DATE 29-1-93

5 cm

# DIAMOND DRILL LOG

DRILLING | DEPTH | DRILLING RUNS | CORE LOSS | CORE TRAY NO.

LITHOLOGY | STRATIGRAPHY | ROCK TYPE | COLOUR | VOLCANICLASTICS: FRAGMENTS: COMPOSITION, MAX. SIZE (MM), SORTING, SHAPE; MATRIX: COMPOSITION, VOLUME %; LOWER CONTACT: GRADATION, STYLE

VESICLES | CONCENTRATION | MAX. SIZE (MM) | SHAPE

ALTERATION | TEXTURE | INTENSITY | MINERALOGY

VEINING | INTENSITY | MAX. WIDTH (MM) | MINERALOGY

MINERALISATION | TEXTURE | MINERALOGY & CONTENTS

FAULTS | POSITION OF BASE | DOWNHOLE WIDTH (CM) | CORE AXIS ANGLE | GOUGE

FOLIATION | TYPE | CORE AXIS ANGLE

WEATHERING

STANDARD COLOUR LOG

REMARKS

SAMPLE NO.

DEPTH

| DEPTH | RUNS | CORE LOSS | TRAY NO. | ROCK TYPE | COLOUR | FRAG COMP | FRAG MAX SIZE (MM) | FRAG SORTING | FRAG SHAPE | MATRIX COMP | MATRIX VOLUME % | LOWER CONTACT GRADATION | LOWER CONTACT STYLE | VESICLES CONC. | VESICLES MAX SIZE (MM) | VESICLES SHAPE | ALTERATION TEXTURE | ALTERATION INTENSITY | ALTERATION MINERALOGY | VEINING INTENSITY | VEINING MAX WIDTH (MM) | VEINING MINERALOGY | MINERALISATION TEXTURE | MINERALISATION MINERALOGY & CONTENTS | FAULTS POSITION OF BASE | FAULTS DOWNHOLE WIDTH (CM) | FAULTS CORE AXIS ANGLE | FAULTS GOUGE | FOLIATION TYPE | FOLIATION CORE AXIS ANGLE | SAMPLE NO. |
|---|---|---|---|---|---|---|---|---|---|---|---|---|---|---|---|---|---|---|---|---|---|---|---|---|---|---|---|---|---|---|---|---|
| 364 | | | | | | | | | | | | | | 1 | 10 | | | | | | | | | | | | | | | | | |
| 366 | | | 81 | | | | | | | | | G1 | | | | | | | | | | | | | | | | | | | | |
| 368 | | | | | | | | | | | | | | | | | | | | 1 | 5 | COSi | | | | | | | | | | |
| 370 | | | 80 | | | | | | | | | | | | | | | | | | | | | | | | | | | | | |
| 372 | | | | | | | | | | | | | | | | | | | | | | | | | | | | | | | | |
| 374 | | | | | | | | | | | | | | | | | F | 3 | C1 | 3 | 20 | COSiC1 | | | 373.6 | | | | | | | |
| 376 | | | 81 | | | | | | | | | | | | | | | | | | | | | | | | | | | | | |
| 378 | | | | | | | | | | | | | | | | | L | 3 | SiAlSe Ep | 1 | 3 | C0 | | | | 378.9 | 1 | 30 | C1S1R | | | |
| 380 | | | | | | | | | | | | | | | | | | | | | | | | | | | | | | | | |
| 382 | | | 82 | | | | | | | | | | | | | | | | | | | | | | | | | | | | | |
| 384 | | | | | | | | | | | | | | | | | L | 4 | SiAlo(C1) | 4 | 40 | S160 | | | | | | | | | | |
| 386 | | | 83 | | | | | | | | | | | | | | | | | | | | | | | | | | | | | |
| 388 | | | | | | | | | | | | | | | | | | | | | | | | | | | | | | | | |
| 390 | | | | | | | | | | | | | | | | | | | | | | | | | | | | | | | | |
| 392 | | | 84 | | | | | | | | | | | | | | | | | | | | | | | | | | | | | |
| 394 | | | | | | | | | | | | | | | | | | | | | | | | | | | | | | | | |
| 396 | | | | 395.3 | | | | | | | | | | | | | | | | | | | | | | 395.4 | 10 | 20 | CO | | | 395.5 |
| 398 | | | 85 | B-W/1 | GrGy | B-1 | >400 | P | SA | B-1 Co | 30 | G1 | | | | | F | 4 | SiAlOEp | 2 | 140 | COSi EpC1 | | | | | | | | | | |
| 400 | | | | | | | | | | | | | | | | | | | | | | | | | | | | | | | | |

frags Ep altd throughout

vesicles restricted to "lapilli"

no obvious faults

T/S 622656 376.7 - 376.8

- may be a weakly epiclastic lava

400.3

log.01931.swr

Aberfoyle Resources Limited
EXPLORATION DIVISION

HOLE NO. MRC55
PAGE 11 OF 30
GEO. HJK
DATE 2-2-93

5 cm

# DIAMOND DRILL LOG

DRILLING: DEPTH | DRILLING RUNS | CORE LOSS | CORE TRAY NO.

LITHOLOGY: STRATIGRAPHY | ROCK TYPE | COLOUR | VOLCANICLASTICS: FRAGMENTS: COMPOSITION | MAX. SIZE (MM) | SORTING | SHAPE | MATRIX: COMPOSITION | VOLUME % | LOWER CONTACT: GRADATION | STYLE

VESICLES: CONCENTRATION | MAX. SIZE (MM) | SHAPE

ALTERATION: TEXTURE | INTENSITY | MINERALOGY

VEINING: INTENSITY | MAX. WIDTH (MM) | MINERALOGY

MINERALISATION: TEXTURE | MINERALOGY & CONTENTS

FAULTS: POSITION OF BASE | DOWNHOLE WIDTH (CM) | CORE AXIS ANGLE | GOUGE

FOLIATION: TYPE | CORE AXIS ANGLE

WEATHERING

STANDARD COLOUR LOG

REMARKS | SAMPLE NO. | DEPTH

| DEPTH | CORE TRAY NO. | ROCK TYPE | COLOUR | ALTERATION: TEXTURE | INTENSITY | MINERALOGY | VEINING: INTENSITY | MAX. WIDTH (MM) | MINERALOGY | MINERALISATION: TEXTURE | MINERALOGY & CONTENTS |
|---|---|---|---|---|---|---|---|---|---|---|---|
| 400 | | 400.3 | | | | 400.3 | | | | | 400.3 |
| 402 | 86 | | | | | | | | 405.1 | | |
| 404 | | | | | | | 2 | 5 | COSI | | |
| 406 | 3 | | | | | | | | | | |
| 408 | | | | | | | | | 413.8 | | |
| 410 | | | | | | | | | | | |
| 412 | | | | | | | | | | | |
| 414 | 88 | B-I/Bx | Pc | L | 4 | SiAlt(Cl) | 1 | 10 | SE | Ds | Pyr |
| 416 | | | | | | | | | | | |
| 418 | | | | | | | | | | | |
| 420 | 89 | | | | | | | | | | |
| 422 | | | | | | | | | | | |
| 424 | 90 | | | | | | 2 | 10 | COEP SI | | |
| 426 | | | | | | | | | 426.5 | | |
| 428 | | | | | | | | | | | |
| 430 | 91 | | | | | | 1 | 5 | COSI EP | | |
| 432 | | | | | | | | | | | |
| 434 | | | | | | | | | | | |
| 436 | 92 | | | | | | | | | | |
| 438 | | | | | | | | | | | |

REMARKS

404.65 – 404.20m
Pk "frag" S. Ab alt'd. B-I

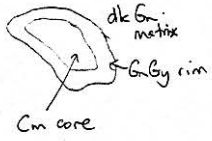
– no significant faulting.

– fibrous veins 413.8 – 418.5m

– very unusual rock similar to B-I previously – may or may not be IV

– pseudofragmental texture ± "frags" S. Ab alt'd, "matrix" Cl alt'd
426.50 – 426.65 T/S 692655

– "frags" apparently more vesicular than "matrix" + ± zoned alt'n edges eg. 429.3m




413.8 onwards – more fragmental in appearance

SAMPLE NO. 692655

log.01931.wor

Aberfoyle Resources Limited
EXPLORATION DIVISION

HOLE NO. MH-33
PAGE 12 OF 30
GEO. HJK
DATE 2-2-93

5 cm

# DIAMOND DRILL LOG

| DRILLING | | | LITHOLOGY | | | | | | | | | | | VESICLES | | | ALTERATION | | | VEINING | | | MINERALISATION | | FAULTS | | | | FOLIATION | | WEATHERING | STANDARD COLOUR LOG | REMARKS | SAMPLE NO. | DEPTH |
|---|---|---|---|---|---|---|---|---|---|---|---|---|---|---|---|---|---|---|---|---|---|---|---|---|---|---|---|---|---|---|---|---|---|---|
| DEPTH | DRILLING RUNS CORE LOSS | CORE TRAY NO. | STRATIGRAPHY | ROCK TYPE | COLOUR | VOLCANICLASTICS FRAGMENTS COMPOSITION | FRAGMENTS MAX. SIZE (MM) | FRAGMENTS SORTING | FRAGMENTS SHAPE | MATRIX COMPOSITION | MATRIX VOLUME % | LOWER CONTACT GRADATION | LOWER CONTACT STYLE | CONCENTRATION | MAX. SIZE (MM) | SHAPE | TEXTURE | INTENSITY | MINERALOGY | INTENSITY | MAX. WIDTH (MM) | MINERALOGY | TEXTURE | MINERALOGY & CONTENTS | POSITION OF BASE | DOWNHOLE WIDTH (CM) | CORE AXIS ANGLE | GOUGE | TYPE | CORE AXIS ANGLE | | | | | |
| 442 | | 93 | | | | | | | | | | | | | | | | | | | | | | | | | | | | | | | | 442 |
| 444 | | | | | | | | | | | | | | | | | L | 4 | Si Ab(Cl) | 1 | 5 | Cosi Ep | Ds | Pytr | | | | | | | | | | 444 |
| 446 | | 94 | | | | | | | | | | | | | | | | | | | | | | | | | | | | | | | ↓ very "fragmental" 449.4 not very "fragmental" | | 446 |
| 448 | | | | | | | | | | | | | | | | | | | | | | 449.4 | | | | | | | | | | | | | 448 |
| 450 | | 95 | | B-1/bv | Pc | | | | | | | G2 | | 1 | 10 | SE | L | 2 | Si Ab Cl | 4 | 20 | Si Ep Cl 449.4 | | | 449.6 | 15 | | Rh Ab | | | | | | | 450 |
| 452 | | | | | | | | | | | | | | | | | | | | | | | | | | | | | | | | | | | 452 |
| 454 | | | | | | | | | | | | | | | | | | | | | | | | | | | | | | | | | | | 454 |
| 456 | | 96 | | | | | | | | | | | | | | | | | | 2 | 50 | Ep Si Cl | | | | | | | | | | | minor Hc in vns. most Ep vns fibrous ± 40-50° to CA. | | 456 |
| 458 | | | | | | | | | | | | | | | | | | | | | | | | | | | | | | | | | | | 458 |
| 460 | | | | | | | | | | | | | | | | | | | | | | | | | | | | | | | | | 460.6 - orientation - vesicular 'frags' with zoned edges fairly common but less than up to 449.4cm | | 460 |
| 462 | | 97 | | | | | | | | | | | | | | | | | | | | | | | | | | | | | | | | | 462 |
| 464 | | | | | | | | | | | | | | | | | | | | | | | | | | | | | | | | | | | 464 |
| 466 | | | | | | | | | | | | | | | | | | | | | | | | | | | | | | | | | | | 466 |
| 468 | | 98 | | | | | | | | | | | | | | | | | | | | | | | | | | | | | | | | | 468 |
| 470 | | | | | | | | | | | | | | | | | | | | | | | | | | | | | | | | | | | 470 |
| 472 | | | | | | | | | | | | | | | | | | | | | | | | | | | | | | | | | | | 472 |
| 474 | | 99 | | | | | | | | | | | | | | | | | 473 | | | 474.9 | | | | | | | | | | | | | 474 |
| 476 | | | | B-bv | Pc | B-1 | 240 | P | sR | B-1 | 40 | | | | | | LF | 3 | Si Ab Cl | 1 | 15 | Cosi Ep | | | | | | | | | | | | | 476 |
| 478 | | 100 | | | | | | | | | | | | | | | | | | | | | | | | | | | | | | | | | 478 |
| 480 | | | | | | | | | | | | | | | | | | | | | | | | | | | | | | | | | | | 480 |

log01933.wor

96556

# Aberfoyle Resources Limited

EXPLORATION DIVISION

HOLE No. MAC35
PAGE 13 OF 30
GEO. HJK
DATE 3-2-93

5 cm

# DIAMOND DRILL LOG

## DRILLING

DEPTH | DRILLING RUNS | CORE LOSS | CORE TRAY NO.

CORE TRAY NO.: 101, 102, 103, 104, 105, 106, 107

## LITHOLOGY

STRATIGRAPHY | ROCK TYPE | COLOUR | VOLCANICLASTICS: FRAGMENTS: COMPOSITION, MAX. SIZE (MM), SORTING, SHAPE; MATRIX: COMPOSITION, VOLUME % | LOWER CONTACT: GRADATION, STYLE

| ROCK TYPE | COLOUR | COMPOSITION | MAX. SIZE (MM) | SORTING | SHAPE | COMPOSITION | VOLUME % |
|---|---|---|---|---|---|---|---|
| B. bx | R | B-1 | 240 | P | sR | B-1 | 40 |

## VESICLES

CONCENTRATION | MAX. SIZE (MM) | SHAPE

| CONCENTRATION | MAX. SIZE (MM) | SHAPE |
|---|---|---|
| 2 | 12 | ES |

## ALTERATION

TEXTURE | INTENSITY | MINERALOGY

| TEXTURE | INTENSITY | MINERALOGY |
|---|---|---|
| LF | 3 | Si Ab Cl |
| | | 493 |
| P | 3 | Si Cl |
| | | 493.9 |
| FL | 3 | Si Ab |

## VEINING

INTENSITY | MAX. WIDTH (MM) | MINERALOGY

| INTENSITY | MAX. WIDTH (MM) | MINERALOGY |
|---|---|---|
| 1 | 15 | Cosi Ep |
| | | 486 |
| 2 | 300 | Ep Si Co Cl |
| | | 493 |
| 4 | 15 | Co Si Cl |
| | | 493.9 |
| 3 | 60 | Ep Si Co |

## MINERALISATION

TEXTURE | MINERALOGY & CONTENTS

| TEXTURE | MINERALOGY & CONTENTS |
|---|---|
| Ds | Pyr |

## FAULTS

POSITION OF BASE | DOWNHOLE WIDTH (CM) | CORE AXIS ANGLE | GOUGE

| POSITION OF BASE | DOWNHOLE WIDTH (CM) | CORE AXIS ANGLE | GOUGE |
|---|---|---|---|
| 513.2 | 10 | 25 | Co Si Cl |

## FOLIATION

TYPE | CORE AXIS ANGLE

## WEATHERING

## STANDARD COLOUR LOG

## REMARKS

- most fags have zoned boundaries, are more vesicular than "matrix" (may be function of Si Ab alteration preserving them in appearance)

Orientation 496.6m

- veins fibrous

Ep+Si → intergrown ← "Si" core

vein @ 510.4m also has tremolite.

V. minor JP fy.

## SAMPLE NO.

## DEPTH

DEPTH: 482, 484, 486, 488, 490, 492, 494, 496, 498, 500, 502, 504, 506, 508, 510, 512, 514, 516, 518, 520

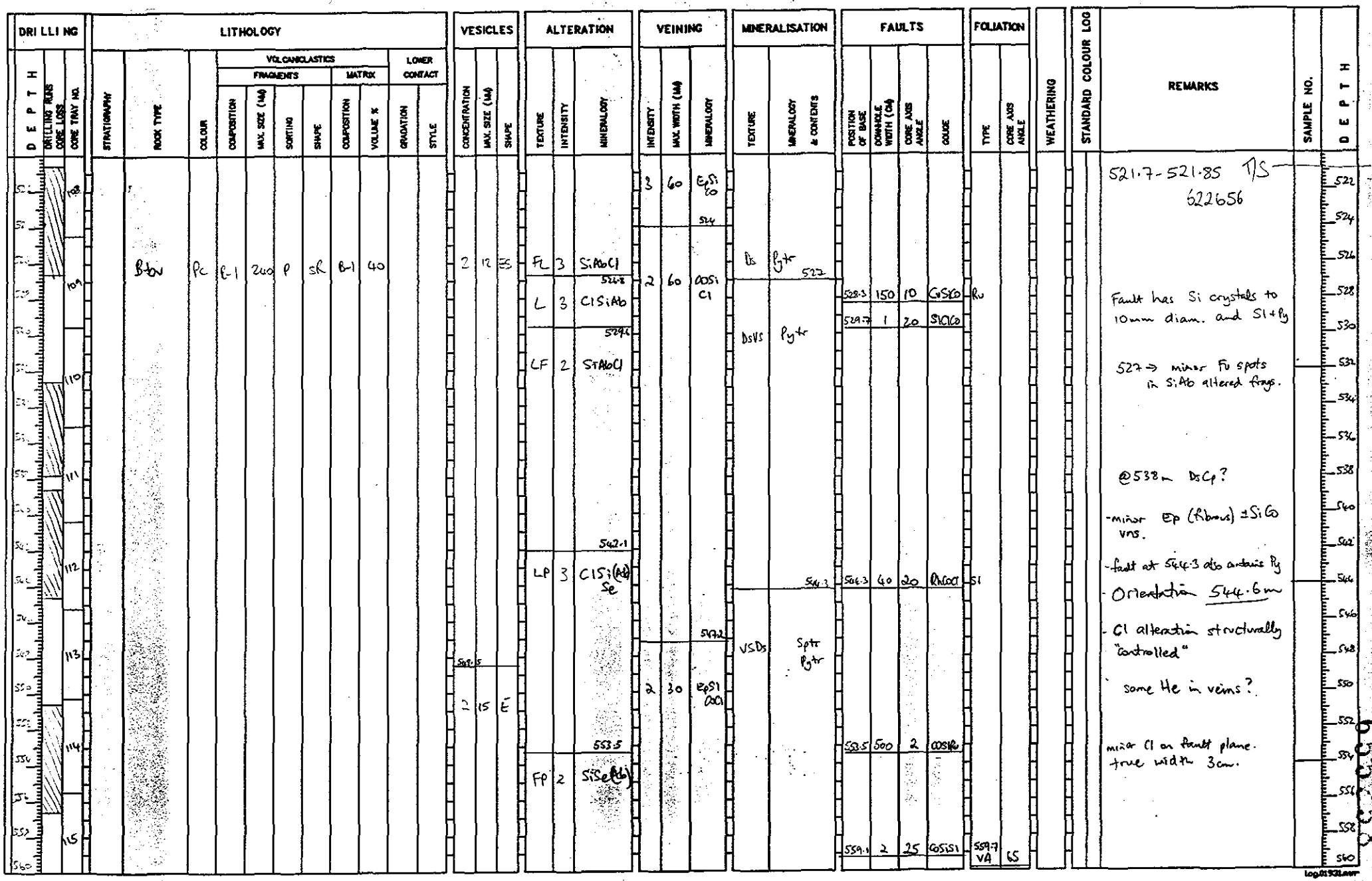
log.0193.wwr

Aberfoyle Resources Limited
EXPLORATION DIVISION

HOLE NO. MA-...
PAGE 16 OF 30
GEO. NJK
DATE 3-2-93

5 cm

# DIAMOND DRILL LOG



# Aberfoyle Resources Limited
EXPLORATION DIVISION

HOLE No. MAC 55
PAGE 15 OF 30
GEO. HJK
DATE 5-2-93

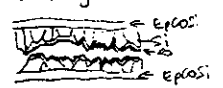
5 cm

# DIAMOND DRILL LOG

| DEPTH | DRILLING RUNS / CORE LOSS | CORE TRAY NO. | STRATIGRAPHY | ROCK TYPE | COLOUR | VOLCANICLASTICS: FRAGMENTS: COMPOSITION | FRAGMENTS: MAX. SIZE (MM) | FRAGMENTS: SORTING | FRAGMENTS: SHAPE | MATRIX: COMPOSITION | MATRIX: VOLUME % | LOWER CONTACT: GRADATION | LOWER CONTACT: STYLE | VESICLES: CONCENTRATION | VESICLES: MAX. SIZE (MM) | VESICLES: SHAPE | ALTERATION: TEXTURE | ALTERATION: INTENSITY | ALTERATION: MINERALOGY | VEINING: INTENSITY | VEINING: MAX. WIDTH (MM) | VEINING: MINERALOGY | MINERALISATION: TEXTURE | MINERALISATION: MINERALOGY & CONTENTS | FAULTS: POSITION OF BASE | FAULTS: DOWNHOLE WIDTH (CM) | FAULTS: CORE AXIS ANGLE | FAULTS: GOUGE | FOLIATION: TYPE | FOLIATION: CORE AXIS ANGLE | WEATHERING | STANDARD COLOUR LOG | REMARKS | SAMPLE NO. | DEPTH |
|---|---|---|---|---|---|---|---|---|---|---|---|---|---|---|---|---|---|---|---|---|---|---|---|---|---|---|---|---|---|---|---|---|---|---|---|
| 562 | | | | | | | | | | | | | | 2 | 15 | E | Fp | 2 | Si Se (Al) | | | | Vs Ds | Epsi Pytr | | | | | | | | | | | 562 |
| 564 | 116 | | | | | | | | | | | | | | | | | | | 1 | 30 | Epsi Co | | | | | | | | | | | | | 564 |
| 566 | | | | | | | | | | | | | | | | | | | | | | | | | | | | | | | | | | | 566 |
| 568 | | | | | | | | | | | | | | | | | | | | | | | | | 568 | 562.5 | 90 | 10 | Cosi Co | | | | | 568 |
| 570 | 117 | | | | | | | | | | | | | | | | | | | | | | Ds | Pytr | | | | | | | | | | | 570 |
| 572 | | | | | | | | | | | | | | | | | | | | | | | | | 572 | | | | | | | | | | 572 |
| 574 | | 118 | | B-bv | Pc | B-1 | 240 | P | SR | B-1 | 40 | S | | | | | | | | | | | | | | | | | | | | | | | 574 |
| 576 | | | | | | | | | | | | | | | | | | | | | | | | | | | | | | | | | | | 576 |
| 578 | | | | | | | | | | | | | | | | | | | | 2 | 10 | Si Co Ep | | | | | | | | | | | | | 578 |
| 580 | | 119 | | | | | | | | | | | | | | | | | | | | | | | 582.7 | | | | | | | | | | 580 |
| 582 | | | | | | | | | | | | | | | | | | | | | | | | | | | | | | | | | | | 582 |
| 584 | | | | 584.5 | | | | | | | | | | | | | | | | 3 | 15 | Ep | | | 584.5 | | | | | | | | | | 584 |
| 586 | | 120 | | B-lv | Pc | B-1 | 60 | P | sAA | SeSi | 50 | S | | 585.1 | | | | | | 3 | 20 | Co Si | | | | 585.4 | 1 | 50 | Pu | | | | | | 586 |
| 588 | | | | 588.6 | | | | | | | | | | | | | | | | | | | | | 585.6 | 3 | 10 | Si Co Si | | | | | | 588 |
| 590 | 121 | | 590.3 | B-bv | Pc | B-1 | 80 | P | SR | B-1 | 40 | GI | | 1 | 10 | SE | | | | 3 | 2 | Si Co | | | | | | | | | | | | | | 590 |
| 592 | | | | 588.3 | | | | | | | | | | 588.3 | | | | | | | | | | | | | | | | | | | | | | 592 |
| | | | | B-flv | Pc | B-1 | 10 | M | sA | B-1 | 50 | S | | 589.8 | | | C | 4 | Se Cl | | | | | | 589.8 | 589.3 | 80 | 15 | Pu Co | | | | | | |
| | | | | B-flv | Gr | | | | | | | S | | 590.3 | 30 | E | Fm | 3 | Se | | | | | | | | | | | | | | | | |
| | | | | B-flv/mV | Pc | B-1 | 15 | M | sA | B-1 | 50 | S | | 590.5 | | | | | | | | | | | | | | | | | | | | | | |
| | | | | 591.3 B-l/pl | Gr | | | | | | | S | | 591.3 | 40 | E | LF | 3 | Se (Cl) | | | | | | | | | | | | | | | | |
| | | | | 591.5 B-flv/mV | Pc | B-1 | 300 | M | sA | B-1 | 60 | F | | 591.5 | | | | | | | | | | | | | | | | | | | | | | |
| 594 | | | | | | | | | | | | | | | | | | | | | | | | | | | | | | | | | | | 594 |
| 596 | | 122 | | | | | | | | | | | | | | | | | | | | | | | 596.5 | | | | | | | | | | 596 |
| 598 | | | | | | | | | | | | | | | | | | | | 5 | 15 | Co Si Ep | | | | | | | | | | | | | 598 |
| 600 | | 123 | | | | | | | | | | | | | | | | | | | | | | | | | | | | | | | | | 600 |

REMARKS

Co as overgrowths on Si xals




true width ≈ 3cm

– 573.6m CuSi fault just in core

–veining sub-parallel to core

586.6 orientation

+ SiCo in fault

582.3 B-lv
2 flags of 2.2m of B-l/pl ± altd rims

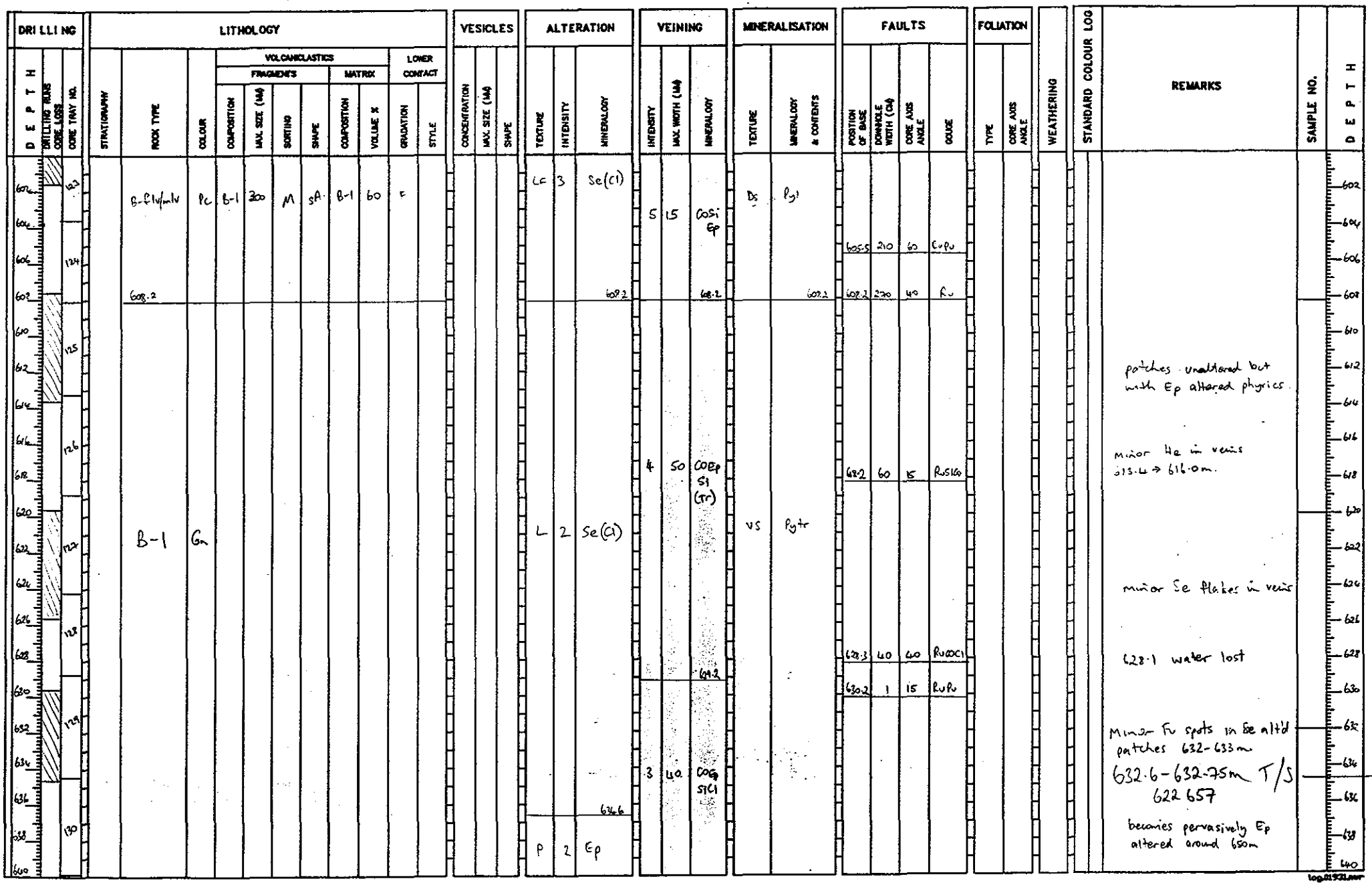
log81931.wrr

Aberfoyle Resources Limited
EXPLORATION DIVISION

HOLE No. MAC 55
PAGE 16 OF 30
GEO. HJK
DATE 9-2-93

5 cm

# DIAMOND DRILL LOG



Aberfoyle Resources Limited
EXPLORATION DIVISION

HOLE No. MAC 55
PAGE 17 OF 30
GEO. HJK
DATE 9-2-93

5 cm

# DIAMOND DRILL LOG

| DRILLING | | | LITHOLOGY | | | | | | | | | | VESICLES | | | ALTERATION | | | VEINING | | | MINERALISATION | | FAULTS | | | | FOLIATION | | WEATHERING | STANDARD COLOUR LOG | REMARKS | SAMPLE NO. | DEPTH |
|---|---|---|---|---|---|---|---|---|---|---|---|---|---|---|---|---|---|---|---|---|---|---|---|---|---|---|---|---|---|---|---|---|---|
| DEPTH | DRILLING RUNS CORE LOSS | CORE TRAY NO. | STRATIGRAPHY | ROCK TYPE | COLOUR | VOLCANICLASTICS FRAGMENTS COMPOSITION | FRAGMENTS MAX. SIZE (MM) | FRAGMENTS SORTING | FRAGMENTS SHAPE | VOLCANICLASTICS MATRIX COMPOSITION | MATRIX VOLUME % | LOWER CONTACT GRADATION | LOWER CONTACT STYLE | CONCENTRATION | MAX. SIZE (MM) | SHAPE | TEXTURE | INTENSITY | MINERALOGY | INTENSITY | MAX. WIDTH (MM) | MINERALOGY | TEXTURE | MINERALOGY & CONTENTS | POSITION OF BASE | DOWNHOLE WIDTH (CM) | CORE AXIS ANGLE | GOUGE | TYPE | CORE AXIS ANGLE | | | | | |
| 662 | | 131 | | | | | | | | | | | | | | | | | | | | | | | | | | | | | | | | 662 |
| 664 | | | | | | | | | | | | | | | | P | 2 | Ep | | | | | | | | | | | | | | | | 664 |
| 666 | | | | | | | | | | | | | | | | | | | | | | | | 666.2 | 5 | 10 | CO SiCl | | | | minor Ru | | 666 |
| 668 | | 132 | | | | | | | | | | | | | | | | | | | | | | | | | | | | | | | | 668 |
| 650 | | | | | | | | | | | | | | | | | | | | | | | | | | | | | | | | | | 650 |
| 652 | | | | | | | | | | | | | | | | | | | | | | | | 651.6 | 5 | 5 | CO SiCl | | | | same fault as @ 6462m | | 652 |
| 654 | | 133 | | | | | | | | | | | | | | | | | | | | | | 653.8 | 5 | 30 | Si Ru Po | | | | | | 654 |
| 656 | | | | | | | | | | | | | | | | | | | | | | | | | | | | | | | | 660-680m Basalt appearance varies from pale green Ep alt'd to dark with Ep (± Ab?) altered phyrics to patchy Si Ab altered zones to patchy Se altered zones | | 656 |
| 658 | | 134 | | B-1 | Gn | | | | | | | G2 | | | | | | | | | | | | | | | | | | | | | | 658 |
| 660 | | | | | | | | | | | | | | | | | | | | | | | | 660.3 | 2 | 20 | Si Co | | | | | | 660 |
| 662 | | | | | | | | | | | | | | | | | | | | 3 | 40 | Co Ep Si Cl | Vs | Pytr | | | | | | | | | 662 |
| 664 | | 135 | | | | | | | | | | | | | | L | 2 | Se | 653.5 | | | | | | | | | | | | | | | 664 |
| 666 | | | | | | | | | | | | | | | | | | | 655.3 | | | | | | | | | | | | | | | 666 |
| 668 | | | | | | | | | | | | | | | | | | | | | | | | | | | | | | | | | | 668 |
| 670 | | 136 | | B-1 | Gn | | | | | | | G2 | | | | | | | | | | | | | | | | | | | | | | 670 |
| 672 | | | | | | | | | | | | | | | | | | | | | | | | | | | | | | | | | | 672 |
| 674 | | 137 | | B-1/b | Gn | | | | | | | G2 | | | | L | 3 | Si Ab Se Ep | 666.8 | | | | | | | | | | | | | | | 674 |
| 676 | | | | | | | | | | | | | | | | | | | | 3 | 20 | Co Si Ep | | | | | | | | | | | | 676 |
| 678 | | | | | | | | | | | | | | | | | | | | | | | | | | | | | | | | | | 678 |
| 680 | | 138 | | | | | | | | | | | | | | | | | | | | | | | | | | | | | | | | 680 |

65563

log.01931.wor

Aberfoyle Resources Limited

EXPLORATION DIVISION

HOLE No. MAC-35

PAGE 18 OF 30

GEO. NJK

DATE 9-2-93

5 cm

# DIAMOND DRILL LOG

| DRILLING | | | LITHOLOGY | | | | | | | | | | VESICLES | | | ALTERATION | | | VEINING | | | MINERALISATION | | FAULTS | | | | FOLIATION | | | | | |
|---|---|---|---|---|---|---|---|---|---|---|---|---|---|---|---|---|---|---|---|---|---|---|---|---|---|---|---|---|---|---|---|---|
| DEPTH | DRILLING RUNS / CORE LOSS | CORE TRAY NO. | STRATIGRAPHY | ROCK TYPE | COLOUR | VOLCANICLASTICS: FRAGMENTS: COMPOSITION | FRAGMENTS: MAX. SIZE (MM) | FRAGMENTS: SORTING | FRAGMENTS: SHAPE | MATRIX: COMPOSITION | MATRIX: VOLUME % | LOWER CONTACT: GRADATION | LOWER CONTACT: STYLE | CONCENTRATION | MAX. SIZE (MM) | SHAPE | TEXTURE | INTENSITY | MINERALOGY | INTENSITY | MAX. WIDTH (MM) | MINERALOGY | TEXTURE | MINERALOGY & CONTENTS | POSITION OF BASE | DOWNHOLE WIDTH (CM) | CORE AXIS ANGLE | GOUGE | TYPE | CORE AXIS ANGLE | WEATHERING | STANDARD COLOUR LOG | REMARKS | SAMPLE NO. | DEPTH |
| 680 | | | | B-1/bv | Gn | | | | | | | C2 | | | | | | | | | | | | | | | | | | | | | | 680 |
| 682 | | | | 683.7 | | | | | | | | | | | | L | 3 | Si Ab Se Ep | 3 | 20 | Cs Si Ep | | | | | | | | | | | - 682.6m 30cm frag. of buff colour Si Ab ± Fu alteration | | 682 |
| 684 | | 139 | | | | | | | | | | | | | | | | 688.2 | | | 689.3 | | | 684 | 20 | 40 | Ru Si | | | | | | | 684 |
| 686 | | | | | | | | | | | | | | | | | | | | | | | | | | | | | | | | | | 686 |
| 688 | | | | | | | | | | | | | | | | | | | | | | | | | | | | | | | | | | 688 |
| 690 | | 140 | | | | | | | | | | | | | | | | | | | | VS | Pyr | | | | | | | | | | | 690 |
| 692 | | | | B-1 | Gn | | | | | | | | | | | DL | 3 | Ep (Se) | | | | | | | | | | | | | | | | 692 |
| 694 | | 141 | | | | | | | | | | | | | | | | | | | | | | | | | | | | | | | | 694 |
| 696 | | | | | | | | | | | | | | | | | | | | | | | | | | | | | | | | | | 696 |
| 698 | | | | | | | | | | | | | | | | | | | | | | | | | | | | | | | | | | 698 |
| 700 | | 142 | | | | | | | | | | | | | | | | | | | | | | | | | | | | | | | | 700 |
| 702 | | | | | | | | | | | | | | | | | | 705.8 | | | 2 | 10 | Cs Si Ep | | | | | | | | | | | 702 |
| 704 | | | | | | | | | | | | | | | | | | | | | | | | | | | | | | | | | | 704 |
| 706 | | 143 | | | | | | | | | | | | | | | | | | | | | | | | | | | | | | | | 706 |
| 708 | | | | | | | | | | | | | | | | SP | 3 | Cl (Se) | | | | | | 709.1 | 200 | 25 | Ru Pu Go | | | | | major fault? | | 708 |
| 710 | | | | | | | | | | | | | | | | | | 709.8 | | | | | | | | | | | | | | | | 710 |
| 712 | | 144 | | | | | | | | | | | | | | P | 2 | Ep Cl | | | | | | | | | | | | | | | | 712 |
| 714 | | | | | | | | | | | | | | | | | | 712.5 | | | | | | 714 | 50 | 30 | Ru Pu Go | | | | | same fault or splay of above | | 714 |
| 716 | | | | | | | | | | | | | | | | L | 3 | Si Ab Cl Ep | | | | | | | | | | | | | | | | 716 |
| 718 | | 145 | | | | | | | | | | | | | | | | | | | | | | | | | | | | | | | | 718 |
| 720 | | | | | | | | | | | | | | | | | | | | | | | | | | | | | | | | | | 720 |

622658

log.01931.wor

Aberfoyle Resources Limited

EXPLORATION DIVISION

HOLE NO. MA-33

PAGE 17 OF 30

GEO. HK

DATE 10-2-92

5 cm

# DIAMOND DRILL LOG

| DRILLING | | | LITHOLOGY | | | | | | | | | | VESICLES | | | ALTERATION | | | VEINING | | | MINERALISATION | | FAULTS | | | | FOLIATION | | WEATHERING | STANDARD COLOUR LOG | REMARKS | SAMPLE NO. | DEPTH |
|---|---|---|---|---|---|---|---|---|---|---|---|---|---|---|---|---|---|---|---|---|---|---|---|---|---|---|---|---|---|---|---|---|---|
| DEPTH | DRILLING RUNS CORE LOSS | CORE TRAY NO. | STRATIGRAPHY | ROCK TYPE | COLOUR | VOLCANICLASTICS FRAGMENTS COMPOSITION | VOLCANICLASTICS FRAGMENTS MAX. SIZE (MM) | VOLCANICLASTICS FRAGMENTS SORTING | VOLCANICLASTICS FRAGMENTS SHAPE | VOLCANICLASTICS MATRIX COMPOSITION | VOLCANICLASTICS MATRIX VOLUME % | LOWER CONTACT GRADATION | LOWER CONTACT STYLE | CONCENTRATION | MAX. SIZE (MM) | SHAPE | TEXTURE | INTENSITY | MINERALOGY | INTENSITY | MAX. WIDTH (MM) | MINERALOGY | TEXTURE | MINERALOGY & CONTENTS | POSITION OF BASE | DOWNHOLE WIDTH (CM) | CORE AXIS ANGLE | GOUGE | TYPE | CORE AXIS ANGLE | | | | | |
| 722 | | 146 | | | | | | | | | | | | | | C | 3 | Si Pb Cl Ep | 2 | 10 | Cosi Ep | VS | Py tr | | | | | | | | 721.6 cave in. | | 722 |
| | | | | | | | | | | | | | | | | | | 724.1 | | | | | | 723.2 | 10 | 15 | RuPb | | | | | | |
| 724 | | | | | | | | | | | | | | | | | | | | | | | | 724.1 | 20 | 15 | RuCoSi | | | | | | 724 |
| 726 | | 147 | | | | | | | | | | | | | | | | | | | | | | | | | | | | | | | 726 |
| 728 | | | | | | | | | | | | | | | | P | 2 | Ep | | | | | | | | | | | | | | | 728 |
| 730 | | | | | | | | | | | | | | | | | | | | | | | | | | | | | | | | | 730 |
| 732 | | 148 | | | | | | | | | | | | | | | | | | | | | | | | | | | | | | Ep alt'n of phenocrysts | | 732 |
| 734 | | | | | | | | | | | | | | | | | | | | | | | | 733.7 | 20 | 15 | RuCo | | | | | | 734 |
| 736 | | | | | | | | | | | | | | | | | | | | | | | | | | | | | | | | | 736 |
| 738 | | 149 | | B-1 | G | | | | | | | F | | | | | | | | | | | | | | | | | | | | | 738 |
| 740 | | | | | | | | | | | | | | | | | | | | | 740.2 | | | | | | | | | | | | 740 |
| 742 | | | | | | | | | | | | | | | | | | | 4 | 10 | Co He Si | | | | | | | | | | | | 742 |
| 744 | | 150 | | | | | | | | | | | | | | | | | | | | | | | | | | | | | | | 744 |
| 746 | | | | | | | | | | | | | | | | | | | | | 746.7 | | | 746.7 | 70 | 10 | RuRuBr | | | | | 746.7 | 746 |
| | | | | 746.7 | | | | | | | | | | | | | | | | | | | | | | | | | | | | | | |
| 748 | | 151 | | | | | | | | | | | | | | P | 2 | Cl Ep | | | | | | | | | | | | | | | 748 |
| 750 | | | | | | | | | | | | | | | | | | 748.7 | | | | | | | | | | | | | | | 750 |
| 752 | | 152 | | B-1/bx | Pc | | | | | | | | | | | P | 2 | Ep | 5 | 20 | Si Co He | | | | | | | | | | | | 751.6 ORIENTATION | | 752 |
| 754 | | | | | | | | | | | | | | | | | | | | | | | | | | | | | | | | Feldspar phyric in appearance? has CO matrix, widened veined. | | 754 |
| 756 | | | | | | | | | | | | | | | | | | | | | | | | | | | | | | | | 7575 - 757.6m T/S 622659 | | 756 |
| 758 | | 153 | | | | | | | | | | | | | | | | | | | | | | | | | | | | | | | | 758 |
| 760 | | | | | | | | | | | | | | | | | | | | | | | | | | | | | | | | | | 760 |

log.0193.wor

622659

# Aberfoyle Resources Limited

EXPLORATION DIVISION

HOLE No. MAC 35
PAGE 20 OF 30
GEO. HJK
DATE 11-2-93

5 cm

# DIAMOND DRILL LOG

| DRILLING | | | LITHOLOGY | | | | | | | | | | VESICLES | | | ALTERATION | | | VEINING | | | MINERALISATION | | FAULTS | | | | FOLIATION | | WEATHERING | STANDARD COLOUR LOG | REMARKS | SAMPLE NO. | DEPTH |
|---|---|---|---|---|---|---|---|---|---|---|---|---|---|---|---|---|---|---|---|---|---|---|---|---|---|---|---|---|---|---|---|---|---|
| DEPTH | DRILLING RUNS CORE LOSS | CORE TRAY NO. | STRATIGRAPHY | ROCK TYPE | COLOUR | VOLCANICLASTICS: FRAGMENTS: COMPOSITION | FRAGMENTS: MAX. SIZE (MM) | FRAGMENTS: SORTING | FRAGMENTS: SHAPE | MATRIX: COMPOSITION | MATRIX: VOLUME % | LOWER CONTACT: GRADATION | LOWER CONTACT: STYLE | CONCENTRATION | MAX. SIZE (MM) | SHAPE | TEXTURE | INTENSITY | MINERALOGY | INTENSITY | MAX. WIDTH (MM) | MINERALOGY | TEXTURE | MINERALOGY & CONTENTS | POSITION OF BASE | DOWNHOLE WIDTH (CM) | CORE AXIS ANGLE | GOUGE | TYPE | CORE AXIS ANGLE | | | | | |
| 762 | | | | B-V/bv | Pc | | | | | | | F | | | | P | 2 | Ep | 5 | 20 | Clo Ep | V: | Py+c | 764.2 | 1 | 30 | Sl Clo | | | | | | | 762 |
| 764 | | 154 | | | | | | | | | | | | | | | | | | | 764.7 | | | | | | | | | | | | | 764 |
| 766 | | | | | | | | | | | | | | | | | | | 2 | 10 | Cosi Hc | | | | | | | | | | | | | 766 |
| 768 | | | | | | | | | | | | | | | | | | | | | 768.2 | | | | | | | | | | | | | 768 |
| 770 | | 155 | | 770 | | | | | | | | | | | | | | 770 | | | | | | 770.3 | 0.3 | 50 | Kaol | | | | | Se on faults | | 770 |
| 772 | | | | B-1 | Gr | | | | | | | F | | | | LP | 2 | Cl(Se) | 2 | 60 | Cosi | | | 772 | 1 | 20 | Cl Clo | | | | | | | 772 |
| 774 | | 156 | | | | | | | | | | | | | | | | | | | 775 | | | 773.2 | 3 | 40 | Sil Pyr | | | | | | | 774 |
| 776 | | | | | | | | | | | | | | | | | | | | | | | | 776.6 | 5 | 30 | Pyr Clo | | | | | | | 776 |
| 778 | | | | 778.1 | | | | | | | | | | | | | | 778.1 | 1 | 10 | Cl | | | 778.1 | 1 | 30 | Cosi | | | | | | | 778 |
| 780 | | 157 | | B/D-lv | Pc | D FP | 250 | P | Sb SA | B | 60 | | | | | A | 2 | Cl Si | | | | | | | | | | | | | | | | 780 |
| 782 | | | | | | | | | | | | | | | | | | | | | | | | | | | | | | | | | | 782 |
| 784 | | | | | | | | | | | | | | | | | | | | | | | | | | | | | | | | | | 784 |
| 786 | | 158 | | | | | | | | | | | | | | | | | | | | | | | | | | | | | | | | 786 |
| 788 | | | | | | | | | | | | | | | | | | | | | 787.2 | | | 788.4 | 2 | 35 | Pyr Clo | | | | | | | 788 |
| 790 | | | | | | | | | | | | | | | | | | | | | | | | | | | | | | | | | | 790 |
| 792 | | 159 | | | | | | | | | | | | | | | | | | | | | | | | | | | | | | | | 792 |
| 794 | | | | | | | | | | | | | | | | | | | | | | | | | | | | | | | | | | 794 |
| 796 | | | | | | | | | | | | | | | | | | | | | | | | | | | | | | | | | | 796 |
| 798 | | 160 | | 798 | | | | | | | | | | | | 798 | | | | | | | | | | | | | | | | | | 798 |
| 800 | | | | B-1 | Gr | | | | | | | | | 3 | 15 | ES | P | 1 | Cl Se Ep | 3 | 20 | Cosi Ep | | | | | | | | | | | | | 800 |

Se on faults

D flags small ~5mm increasing with depth

7859-7860m TS 622660

- Minor zones of concentrations of D flags

65536

log01931.wor

Aberfoyle Resources Limited
EXPLORATION DIVISION

HOLE NO. MA-[illegible]
PAGE 21 OF 30
GEO. HJK
DATE 11-2-93

5 cm

# DIAMOND DRILL LOG

DRILLING: DEPTH; DRILLING RUNS; CORE LOSS; CORE TRAY NO.

LITHOLOGY: STRATIGRAPHY; ROCK TYPE; COLOUR; VOLCANICLASTICS — FRAGMENTS: COMPOSITION, MAX. SIZE (MM), SORTING, SHAPE; MATRIX: COMPOSITION, VOLUME %; LOWER CONTACT: GRADATION, STYLE

VESICLES: CONCENTRATION; MAX. SIZE (MM); SHAPE

ALTERATION: TEXTURE; INTENSITY; MINERALOGY

VEINING: INTENSITY; MAX. WIDTH (MM); MINERALOGY

MINERALISATION: TEXTURE; MINERALOGY & CONTENTS

FAULTS: POSITION OF BASE; DOWNHOLE WIDTH (CM); CORE AXIS ANGLE; GOUGE

FOLIATION: TYPE; CORE AXIS ANGLE

WEATHERING

STANDARD COLOUR LOG

REMARKS

SAMPLE NO.

DEPTH

| DEPTH | DRILLING RUNS / CORE LOSS | CORE TRAY NO. | STRATIGRAPHY | ROCK TYPE | COLOUR | VOLCANICLASTICS: FRAGMENTS — COMPOSITION | FRAGMENTS — MAX. SIZE (MM) | FRAGMENTS — SORTING | FRAGMENTS — SHAPE | MATRIX — COMPOSITION | MATRIX — VOLUME % | LOWER CONTACT — GRADATION | LOWER CONTACT — STYLE | VESICLES — CONCENTRATION | VESICLES — MAX. SIZE (MM) | VESICLES — SHAPE | ALTERATION — TEXTURE | ALTERATION — INTENSITY | ALTERATION — MINERALOGY | VEINING — INTENSITY | VEINING — MAX. WIDTH (MM) | VEINING — MINERALOGY | MINERALISATION — TEXTURE | MINERALISATION — MINERALOGY & CONTENTS | FAULTS — POSITION OF BASE | FAULTS — DOWNHOLE WIDTH (CM) | FAULTS — CORE AXIS ANGLE | FAULTS — GOUGE | FOLIATION — TYPE | FOLIATION — CORE AXIS ANGLE | WEATHERING | REMARKS |
|---|---|---|---|---|---|---|---|---|---|---|---|---|---|---|---|---|---|---|---|---|---|---|---|---|---|---|---|---|---|---|---|---|
| 802 | | 161 | | G-1 | G | | | | | | | F | | 3 | 15 | ES | P | 1 | ClSe Ep | 3 | 20 | SiCa Ep | VS | Py tr | 803.9 | 2 | 25 | Si(Cl) | | | | |
| 804 | | | | | | | | | | | | | | | | | | | | | | | | | | | | | | | | |
| 806 | | 162 | | 806.9 | | | | | | | | | | | | 806.9 | | | 806.9 | | | | | 806.9 | | 806.9 | 2 | 60 | Clay | | | | |
| 808 | | | | | | | | | | | | | | | | | | | | | | | | | | | | | | | | |
| 810 | | 163 | | | | | | | | | | | | | | | | | | | | | | | | | | | | | | |
| 812 | | | | | | | | | | | | | | | | | | | | | | | | | | | | | | | | |
| 814 | | | | | | | | | | | | | | | | | | | | | | | | VSDs | Py, Sph(Gn) Cpy tr | | | | | | | |
| 816 | | | | | | | | | | | | | | | | | | | | | | | | | | | | | | | | |
| 818 | | 164 | | D-lv | Pc | FP | 300 | P | A | SiSe (Cl) | 30 | | | | | | FL | S | Si(Cl) (Se) | | | | | | | | | | | | | |
| 820 | | | | | | | | | | | | | | | | | | | | | | | | | | | | | | | | |
| 822 | | 165 | | | | | | | | | | | | | | | | | | | | | | | | | | | | | | |
| 824 | | | | | | | | | | | | | | | | | | | | | | 824 | | | | | | | | | | |
| 826 | | | | | | | | | | | | | | | | | | | | | | | | | | | | | | | | |
| 828 | | 166 | | | | | | | | | | | | | | | | | | | | | | | | | | | | | | |
| 830 | | | | | | | | | | | | | | | | | | | | | | | | | | | | | | | | |
| 832 | | | | | | | | | | | | | | | | | | | | 2 | 10 | COSi Cl | | | | | | | | | | |
| 834 | | 167 | | | | | | | | | | | | | | | | | | | | | | | | | | | | | | |
| 836 | | | | | | | | | | | | | | | | | | | | | | | | | 836.5 | | | | | | | |
| 838 | | 168 | | | | | | | | | | | | | | | | | | | | | | D | Py tr | | | | | | | |
| 840 | | | | | | | | | | | | | | | | | | | | | | | | | | | | | | | | |

Dacite is FP & some lags GyGn others PkBr

some zones more massive.

832-6 ORIENTATION

log.01931.wwr

Aberfoyle Resources Limited
EXPLORATION DIVISION

HOLE No. MAC 55
PAGE 22 OF 30
GEO. HJK
DATE 12-2-93

5 cm

# DIAMOND DRILL LOG

| DRILLING | | | LITHOLOGY | | | | | | | | | | VESICLES | | | ALTERATION | | | VEINING | | | MINERALISATION | | FAULTS | | | | FOLIATION | | | | | | |
|---|---|---|---|---|---|---|---|---|---|---|---|---|---|---|---|---|---|---|---|---|---|---|---|---|---|---|---|---|---|---|---|---|---|
| DEPTH | DRILLING RUNS / CORE LOSS | CORE TRAY NO. | STRATIGRAPHY | ROCK TYPE | COLOUR | VOLCANICLASTICS: FRAGMENTS: COMPOSITION | FRAGMENTS: MAX. SIZE (MM) | FRAGMENTS: SORTING | FRAGMENTS: SHAPE | VOLCANICLASTICS: MATRIX: COMPOSITION | MATRIX: VOLUME % | LOWER CONTACT: GRADATION | LOWER CONTACT: STYLE | CONCENTRATION | MAX. SIZE (MM) | SHAPE | TEXTURE | INTENSITY | MINERALOGY | INTENSITY | MAX. WIDTH (MM) | MINERALOGY | TEXTURE | MINERALOGY & CONTENTS | POSITION OF BASE | DOWNHOLE WIDTH (CM) | CORE AXIS ANGLE | GOUGE | TYPE | CORE AXIS ANGLE | WEATHERING | STANDARD COLOUR LOG | REMARKS | SAMPLE NO. | DEPTH |
| 842 | | | | | | | | | | | | | | | | | | | | | | | | | | | | | | | | | | 842 |
| 844 | | 169 | | | | | | | | | | | | | | | | | | | | | | | | | | | | | | | | 844 |
| 846 | | | | | | | | | | | | | | | | | | | 2 | 10 | Calc Cl | | | | | | | | | | | | | 846 |
| 848 | | | | | | | | | | | | | | | | | | | | | 847 | | | | | | | | | | | | | 848 |
| 850 | | 170 | | | | | | | | | | | | | | | FL | 5 | Si (Cl) (Se) | | | | Ds | Pyr | | | | | | | | | | 850 |
| 852 | | | | D-lv | Pc | FPD | 300 | P | SA | Si Se(Cl) | 30 | | | | | | | | | 3 | 40 | Si Cl | | | | | | | | | | | | | 852 |
| 854 | | 171 | | | | | | | | | | | | | | | | | | | 854 | | | | | | | | | | | | | 854 |
| 856 | | | | | | | | | | | | | | | | | | | | | | | | | | | | | | | | | | 856 |
| 858 | | | | | | | | | | | | | | | | | | | | | | | | | 859 | 10 | 45 | RuPu | | | | | | 858 |
| 860 | | 172 | | | | | | | | | | | | | | | | | | | | | | | | | | | | | | | | 860 |
| 862 | | | | | | | | | | | | | | | | | | | | | 862.2 | | | | | | | | | | | | | 862 |
| 864 | | | | | | | | | | | | | | | | | | | | | | | | | | | | | | | | | | 864 |
| 866 | | 173 | | | | | | | | | | | | | | | | | | | | | | | | | | | | | | | | 866 |
| 868 | | | | | | | | | | | | | | | | | | | | | | | | | | | | | | | | | | 868 |
| 870 | | 174 | | | | | | | | | | | | | | | | | 2 | 15 | Cosi Cl | | | | | | | | | | | | | 870 |
| 872 | | | | | | | | | | | | | | | | | | | | | 873 | | | | | | | | | | | | | 872 |
| 874 | | | | | | | | | | | | | | | | | | | | | | | | | | | | | | | | | | 874 |
| 876 | | 175 | | | | | | | | | | | | | | | | | 1 | 10 | Cosi Cl | | | | | | | | | | | | | 876 |
| 878 | | | | | | | | | | | | | | | | | | | | | | | | | 773.1 | 2 | 10 | RuPu | | | | | | 878 |
| 880 | | | | | | | | | | | | | | | | | | | | | | | | | | | | | | | | | | 880 |

patches of Pl+Se alth ±Si

Some large lags have banded appearance

log.01931.wor

6955369

Aberfoyle Resources Limited

EXPLORATION DIVISION

HOLE No. MAC 55

PAGE 23 OF 30

GEO. HJK

DATE 15-2-93

5 cm

# DIAMOND DRILL LOG

DRILLING: DEPTH | DRILLING RUNS | CORE LOSS | CORE TRAY NO.

LITHOLOGY: STRATIGRAPHY | ROCK TYPE | COLOUR | VOLCANICLASTICS: FRAGMENTS: COMPOSITION | MAX. SIZE (MM) | SORTING | SHAPE; MATRIX: COMPOSITION | VOLUME % | LOWER CONTACT: GRADATION | STYLE

VESICLES: CONCENTRATION | MAX. SIZE (MM) | SHAPE

ALTERATION: TEXTURE | INTENSITY | MINERALOGY

VEINING: INTENSITY | MAX. WIDTH (MM) | MINERALOGY

MINERALISATION: TEXTURE | MINERALOGY & CONTENTS

FAULTS: POSITION OF BASE | DOWNHOLE WIDTH (CM) | CORE AXIS ANGLE | GOUGE

FOLIATION: TYPE | CORE AXIS ANGLE

WEATHERING

STANDARD COLOUR LOG

REMARKS

SAMPLE NO.

DEPTH

| DEPTH | ROCK TYPE | COLOUR | COMPOSITION | MAX. SIZE (MM) | SORTING | SHAPE | COMPOSITION | VOLUME % | GRADATION | STYLE |
|---|---|---|---|---|---|---|---|---|---|---|
| 895.8 | D-1v | Pc | FP D | 300 | P | SA | Si Se Cl | 30 | G1 | |
| 897.3 | FP-av | GGy | EP FP | <5 | W | SA | L | 60 | G1 | |
| 908.9 | D-1/bv | | | | | | | | S | |
| 913.8 | FP-av | GnGy | FP | <6 | W | SA | L | 50 | S | |
| | D-1/bv | PkGn | | | | | | | | |

| DEPTH | TEXTURE | INTENSITY | MINERALOGY |
|---|---|---|---|
| 895.8 | FL | 5 | Si (Clse) |
| 897.3 | P | 2 | SeCl |
| 908.9 | FL | 5 | Si (SeCl) |
| 913.8 | P | 2 | SeCl |
| 914 | P | 5 | Si |
| | F | 5 | Se |

| DEPTH | INTENSITY | MAX. WIDTH (MM) | MINERALOGY |
|---|---|---|---|
| 895.6 | 1 | 10 | coSi Cl |
| 898 | 4 | 70 | Co |
| 908.4 | 1 | 10 | Co |
| 911.8 | 3 | 10 | SiCo |
| | 4 | 90 | CoSi |

| DEPTH | TEXTURE | MINERALOGY & CONTENTS |
|---|---|---|
| 895.6 | Ds | Pyr |
| | DsVs | Pyr |

| DEPTH | POSITION OF BASE | DOWNHOLE WIDTH (CM) | CORE AXIS ANGLE | GOUGE |
|---|---|---|---|---|
| 894.2 | 894.2 | 2 | 30 | RuSR |
| 911.8 | 911.8 | 3 | 35 | CoRuSl |

REMARKS

TS 622661
881.0 m.

892.6m ORIENTATION

siliceous

622662
909.7 – 909.85 TS

no bedding apparent
- Ne + Cl altd flags in (Pyr) mafic matrix
- not siliceous

TS 622663 915.5m
siliceous

SAMPLE NO. 622553

log81931.mor

# Aberfoyle Resources Limited

EXPLORATION DIVISION

HOLE No. MFC 55
PAGE 24 OF 30
GEO. HJK
DATE 17-2-93

5 cm

# DIAMOND DRILL LOG

**DRILLING** — DEPTH; DRILLING RUNS; CORE LOSS; CORE TRAY NO.

**LITHOLOGY** — STRATIGRAPHY; ROCK TYPE; COLOUR; VOLCANICLASTICS (FRAGMENTS: COMPOSITION, MAX. SIZE (MM), SORTING, SHAPE; MATRIX: COMPOSITION, VOLUME %); LOWER CONTACT (GRADATION, STYLE)

**VESICLES** — CONCENTRATION; MAX. SIZE (MM); SHAPE

**ALTERATION** — TEXTURE; INTENSITY; MINERALOGY

**VEINING** — INTENSITY; MAX. WIDTH (MM); MINERALOGY

**MINERALISATION** — TEXTURE; MINERALOGY & CONTENTS

**FAULTS** — POSITION OF BASE; DOWNHOLE WIDTH (CM); CORE AXIS ANGLE; GOUGE

**FOLIATION** — TYPE; CORE AXIS ANGLE

**WEATHERING**

**STANDARD COLOUR LOG**

**REMARKS**

**SAMPLE NO.**

**DEPTH**

| DEPTH | Drilling runs / core loss / core tray no. | Rock type | Colour | Lithology: volcaniclastics — fragments: composition; max. size (mm); sorting; shape — matrix: composition; volume % — lower contact: gradation; style | Vesicles: concentration; max. size (mm); shape | Alteration: texture; intensity; mineralogy | Veining: intensity; max. width (mm); mineralogy | Mineralisation: texture; mineralogy & contents | Faults: position of base; downhole width (cm); core axis angle; gouge | Foliation: type; core axis angle | Weathering | Standard colour log | Remarks | Sample no. | Depth |
|---|---|---|---|---|---|---|---|---|---|---|---|---|---|---|---|
| 922 | | D-l/gr | Pkgy | | | F 5 Se | 4 90 Qtz | DisVn Pyr | 920.8 2 2 Qtz | | | | P 5 Si altd matrix. | | 922 |
| 924 | TT4 | | | | | | | | | | | | | | 924 |
| 926 | | | | | | | | | | | | | Mainly Plc with Gn pebbles. | | 926 |
| 928 | | | | | | | | | | | | | | | 928 |
| 930 | TT5 | | | | | | | | 931.4 5 30 RuSiCl | | | | | | 930 |
| 932 | | 933.2 | | | | 933.2 | | | | | | | | | 932 |
| 934 | TT6 | | | | | | | | | | | | | | 934 |
| 936 | | FP-av? 937.8 | GrGy | FP <6 W SA L 50 | | P 2 SeCl 937.8 | | | | | | | Similar to previous @ 928.9 - 933.8m | | 936 |
| 938 | | | | | | | | | 938.6 2 30 RuQSi | | | | + Se on fault | | 938 |
| 940 | TT7 | D-l/mW | Pc | | | | 938.7 | | | | | | | | 940 |
| 942 | | | | | | FA 4 SiSe | | | | | | | | | 942 |
| 944 | TT8 | | | | | | 943.3 | | | | | | | | 944 |
| 946 | | | | | | 946.2 | 4 30 CoSi | | | | | | | | 946 |
| 948 | | | | | | | | | 947.8 190 30 RuQCo | | | | + Py, core angle ranges 10° to 70° | | 948 |
| 950 | TT9 | | | | | L 4 Si 951.2 | | | | | | | 949.6m ORIENTATION. | | 950 |
| 952 | | | | | | | | | | | | | | | 952 |
| 954 | TT10 | | | | | P 5 Si (Se) | | | 954.7 5 30 CoQSi | | | | clots Se (Fu?) throughout | | 954 |
| 956 | | | | | | | | | | | | | | | 956 |
| 958 | | | | | | | | | | | | | | | 958 |
| 960 | TT11 | | | | | | | | | | | | | | 960 |

65538

log01931.wor

Aberfoyle Resources Limited

EXPLORATION DIVISION

HOLE NO. MRC33

PAGE 25 OF 30

GEO. HJK

DATE 17-2-93

5 cm

# DIAMOND DRILL LOG

DRILLING: DEPTH | DRILLING RUNS | CORE LOSS | CORE TRAY NO.

LITHOLOGY: STRATIGRAPHY | ROCK TYPE | COLOUR | VOLCANICLASTICS: FRAGMENTS: COMPOSITION | MAX. SIZE (MM) | SORTING | SHAPE; MATRIX: COMPOSITION | VOLUME % | LOWER CONTACT: GRADATION | STYLE

VESICLES: CONCENTRATION | MAX. SIZE (MM) | SHAPE

ALTERATION: TEXTURE | INTENSITY | MINERALOGY

VEINING: INTENSITY | MAX. WIDTH (MM) | MINERALOGY

MINERALISATION: TEXTURE | MINERALOGY & CONTENTS

FAULTS: POSITION OF BASE | DOWNHOLE WIDTH (CM) | CORE AXIS ANGLE | GOUGE

FOLIATION: TYPE | CORE AXIS ANGLE

WEATHERING

STANDARD COLOUR LOG

REMARKS | SAMPLE NO. | DEPTH

| DEPTH | ROCK TYPE | COLOUR | FRAGMENTS: COMPOSITION | MAX. SIZE (MM) | SORTING | SHAPE | MATRIX: COMPOSITION | VOLUME % | LOWER CONTACT: GRADATION | STYLE | ALTERATION: TEXTURE | INTENSITY | MINERALOGY | VEINING: INTENSITY | MAX. WIDTH (MM) | MINERALOGY | MINERALISATION: TEXTURE | MINERALOGY & CONTENTS | FAULTS: POSITION OF BASE | DOWNHOLE WIDTH (CM) | CORE AXIS ANGLE | GOUGE | REMARKS |
|---|---|---|---|---|---|---|---|---|---|---|---|---|---|---|---|---|---|---|---|---|---|---|---|
| 962 | D-l/mlv | Pc | | | | | | | F? | | P | 5 | Si | | | | Dlk | Pytr | | | | | changes from pervasive Si altn to more patchy Si ± Cl ± Se. |
| 962.7 | | | | | | | | | | | | | 962.9 | 4 | 30 | Cosi | | 962.9 | | | | | |
| 964 | | | | | | | | | | | | | | | | | | | 964.4 | 70 | 25 | RuPo | + Co + Si |
| 966 | | | | | | | | | | | | | | | | 967 | | | | | | | |
| 968 | D/FP-mlv | Pc | FP | >50 | P | sA | SiSe | 40 | | | A-F | 4 | SiSe | | | | | | 968.6 | 70 | 30 | RuCo | Lower Si content (alteration wise) |
| 970 | | | | | | | | | | | | | | | | | | | 970.1 | 40 | 20 | RuSiCo | |
| 972 | | | | | | | | | | | | | | 2 | 20 | CoSi Cl | | | | | | | VS Sptr over narrow intervals which are more intensely veined ± Si + Co vns ± Cl. |
| 974 | | | | | | | | | | | | | | | | | Ds. | Pytr | 975 | 3 | 25 | CoCSi | |
| 976 | | | | | | | | | | | | | | | | | | | | | | | Pk siliceous fags common. |
| 978 | | | | | | | | | | | | | | | | | | | | | | | |
| 980 | | | | | | | | | | | | | | | | | | | | | | | 980.3 – 980.45 m T/S 622664 |
| 982 | | | | | | | | | | | | | | | | 977.4 | | | 982.6 | 2 | 20 | SiCoCl | |
| 984 | | | | | | | | | | | | | | | | | | | | | | | |
| 986 | | | | | | | | | | | | | | | | | | | | | | | |
| 988 | | | | | | | | | | | | | | | | | | | | | | | |
| 990 | | | | | | | | | | | | | | 2 | 10 | CoSi | | | 991 | 1 | 35 | SiCl | |
| 992 | | | | | | | | | | | | | | | | | | | 991.7 | 10 | 15 | RhCoBr | numerous faults ± Si Cl ± Co ± Py ± Se |
| 994 | | | | | | | | | | | | | | | | | VS. | Pyl Sptr | | | | | |
| 996 | | | | | | | | | | | | | | | | | | | | | | | |
| 998 | | | | | | | | | | | AL | 4 | Si | | | | | | | | | | 999.2 ⇒ Pk patches of intense Si altn |
| 1000 | | | | | | | | | | | | | 999.2 | | | | | | | | | | |

DRILLING: CORE TRAY NO. 192 | 193 | 194 | 195 | 196 | 197 | 198

65569

log.01931.mrr

Abermoyle Resources Limited

EXPLORATION DIVISION

HOLE NO. MAR...

PAGE 26 OF 30

GEO. HJK

DATE 19-2-93

5 cm

# DIAMOND DRILL LOG

DRILLING: DEPTH; DRILLING RUNS; CORE LOSS; CORE TRAY NO.

LITHOLOGY: STRATIGRAPHY; ROCK TYPE; COLOUR; VOLCANICLASTICS — FRAGMENTS: COMPOSITION, MAX. SIZE (MM), SORTING, SHAPE; MATRIX: COMPOSITION, VOLUME %; LOWER CONTACT: GRADATION, STYLE

VESICLES: CONCENTRATION; MAX. SIZE (MM); SHAPE

ALTERATION: TEXTURE; INTENSITY; MINERALOGY

VEINING: INTENSITY; MAX. WIDTH (MM); MINERALOGY

MINERALISATION: TEXTURE; MINERALOGY & CONTENTS

FAULTS: POSITION OF BASE; DOWNHOLE WIDTH (CM); CORE AXIS ANGLE; GOUGE

FOLIATION: TYPE; CORE AXIS ANGLE

WEATHERING

STANDARD COLOUR LOG

REMARKS

SAMPLE NO.

DEPTH

| DEPTH | ROCK TYPE | COLOUR | FRAGMENTS: COMPOSITION | FRAGMENTS: MAX. SIZE (MM) | FRAGMENTS: SORTING | FRAGMENTS: SHAPE | MATRIX: COMPOSITION | MATRIX: VOLUME % | LOWER CONTACT: GRADATION | LOWER CONTACT: STYLE | CORE TRAY NO. |
|---|---|---|---|---|---|---|---|---|---|---|---|
| 1002 | | | | | | | | | | | 199 |
| 1004 | | | | | | | | | | | |
| 1006 | D/FP-Mix | lc | FP | >50 | P | SA | Dic | 40 | F | | 200 |
| 1008 | | | | | | | | | | | |
| 1010 | | | | | | | | | | | |
| 1012 | | | | | | | | | | | 201 |
| 1014 | | | | | | | | | | | |
| 1016 | | | | | | | | | | | |
| 1018 | | | | | | | | | | | 202 |
| 1020 | | | | | | | | | | | |
| 1020.8 | | | | | | | | | | | |
| 1022 | | | | | | | | | | | 203 |
| 1024 | | | | | | | | | | | |
| 1026 | D-1 | Pc | | | | | | | | | 204 |
| 1028 | | | | | | | | | | | |
| 1030 | | | | | | | | | | | |
| 1032 | | | | | | | | | | | 205 |
| 1034 | | | | | | | | | | | |
| 1036 | | | | | | | | | | | |
| 1038 | | | | | | | | | | | 206 |
| 1040 | | | | | | | | | | | |

| DEPTH | TEXTURE | INTENSITY | MINERALOGY |
|---|---|---|---|
| | AL | 4 | Si |
| 1002.6 | | | |
| | P | 5 | Si(Fe) |
| 1006.9 | | | |
| | AF | 5 | Si |
| 1021.1 | | | |
| | P | 4 | SeSi |
| 1025.3 | | | |
| | P | 5 | Si(He) |

| DEPTH | INTENSITY | MAX. WIDTH (MM) | MINERALOGY |
|---|---|---|---|
| 1000.2 | 4 | 10 | CoSi |
| 1009.6 | | | |
| | 1 | 10 | CoSi |
| 1013.6 | | | |
| | 2 | 30 | CoSi |
| 1006.5 | | | |
| | 3 | 25 | SiCo (Cl) |

| DEPTH | TEXTURE | MINERALOGY & CONTENTS |
|---|---|---|
| | Vc | Py tr |
| 1009.6 | | |
| | Ds | Py tr |

| POSITION OF BASE | DOWNHOLE WIDTH (CM) | CORE AXIS ANGLE | GOUGE |
|---|---|---|---|
| 1011.8 | 5 | 65 | RuPu |
| 1017.8 | 40 | 15 | Ru |
| 1021.3 | 60 | 30 | RuCoSi |
| 1022.1 | 5 | 10 | RuPu |
| 1022.8 | 2 | 15 | RuPu |
| 1024.6 | 20 | 15 | PuRuBrSi |
| 1027.3 | 2 | 50 | RuPu |

REMARKS:

Pk alteration

1009.6 m ORIENTATION

Broken zone 1016.70 - 1017.80

multiple generations of movement also Cv, Co, Ru, Cl

Rd Br (He rich) in colour

SAMPLE NO.

DEPTH

log01931.xls

0 93 99

Aberfoyle Resources Limited

EXPLORATION DIVISION

HOLE No. MAC 55

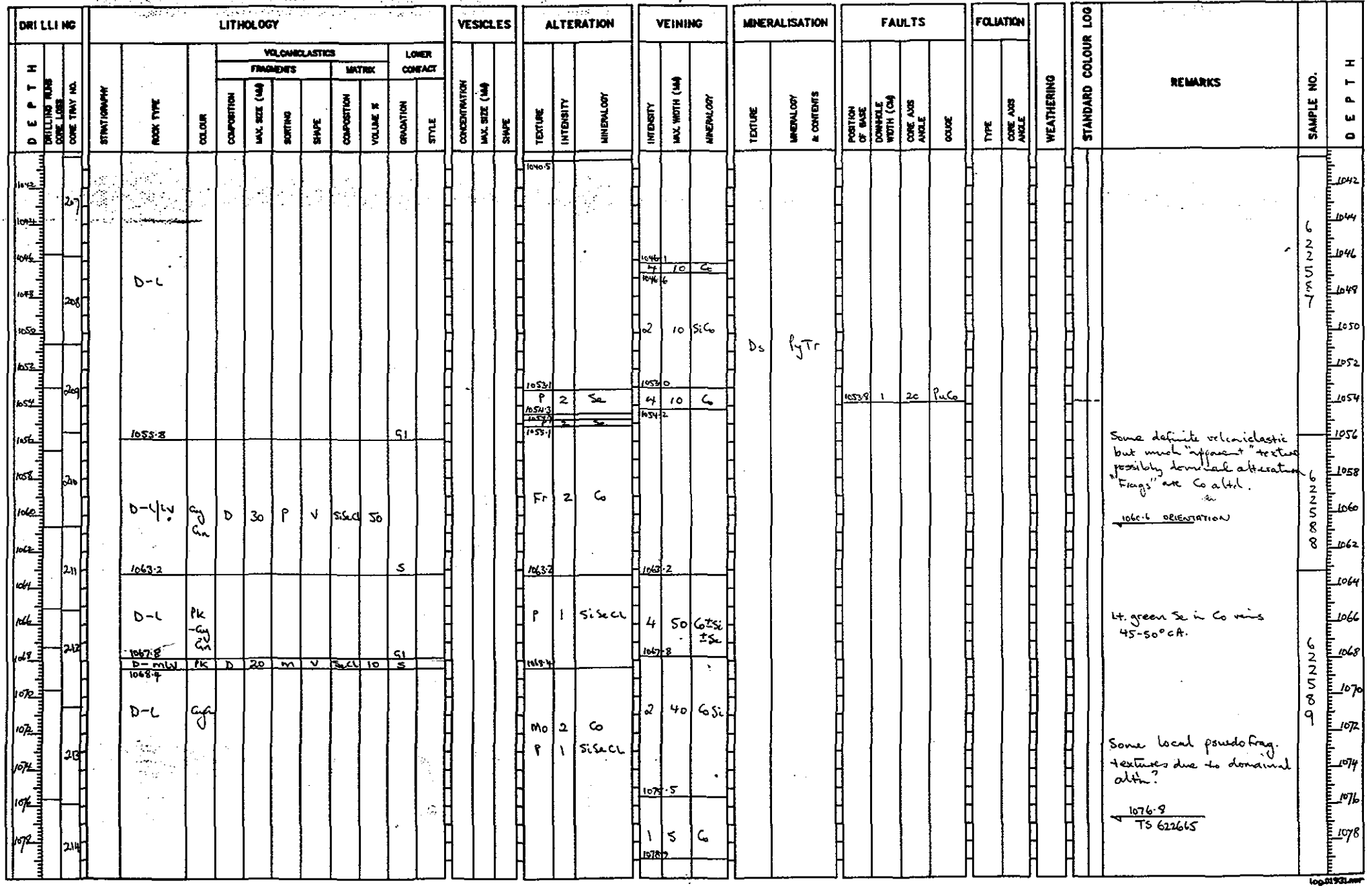
PAGE 27 OF 30

GEO. SK

DATE 24-2-93

5 cm

# DIAMOND DRILL LOG




69551

# Aberfoyle Resources Limited

EXPLORATION DIVISION

HOLE No. MAC 35

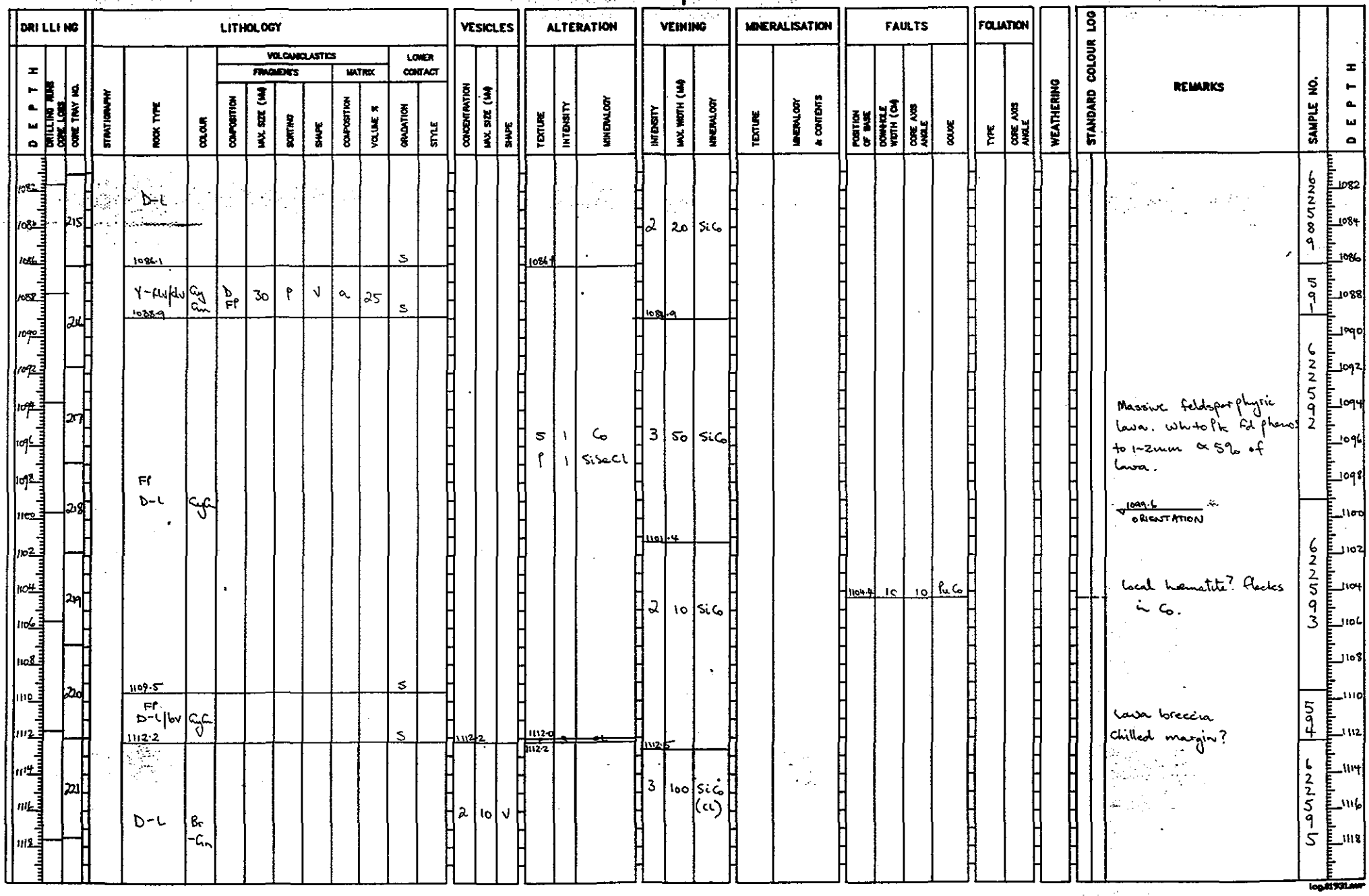
PAGE 28 OF 30

GEO. SR

DATE 24-2-93

5 cm

# DIAMOND DRILL LOG




log81931.mar

# Aberfoyle Resources Limited
EXPLORATION DIVISION

HOLE No. MAC35
PAGE 29 OF 30
GEO. SR
DATE 24-2-93

5 cm

# DIAMOND DRILL LOG

DRILLING: DEPTH | DRILLING RUNS | CORE LOSS | CORE TRAY NO.

LITHOLOGY: STRATIGRAPHY | ROCK TYPE | COLOUR | VOLCANICLASTICS: FRAGMENTS: COMPOSITION | MAX. SIZE (MM) | SORTING | SHAPE; MATRIX: COMPOSITION | VOLUME % | LOWER CONTACT: GRADATION | STYLE

VESICLES: CONCENTRATION | MAX. SIZE (MM) | SHAPE

ALTERATION: TEXTURE | INTENSITY | MINERALOGY

VEINING: INTENSITY | MAX. WIDTH (MM) | MINERALOGY

MINERALISATION: TEXTURE | MINERALOGY & CONTENTS

FAULTS: POSITION OF BASE | DOWNHOLE WIDTH (CM) | CORE AXIS ANGLE | GOUGE

FOLIATION: TYPE | CORE AXIS ANGLE

WEATHERING

STANDARD COLOUR LOG

REMARKS | SAMPLE NO. | DEPTH

| DEPTH | ROCK TYPE | COLOUR | LITHOLOGY | VESICLES | ALTERATION | VEINING | MINERALISATION | REMARKS | SAMPLE NO. |
|---|---|---|---|---|---|---|---|---|---|
| 1122 | | | | | | | | | |
| 1124 | | | | | | | | Weakly Fd. phyric and weakly vesicular flow? unit. or shallow intrusive | 622596 |
| 1126 | D-L | | | 2 10 V | P 2 Si; S 1 Cb | 3 10 Cb | | Common fine Cb veinlets ⇒ local stockwork. | |
| 1128 | | | | | | | | Brown colour ⇒ FeOx? | |
| 1130 | | | | | | | | | |
| 1132 | | | | | | | | TS 622466 1133.1m | |
| 1134 | | | | | | | | | |
| 1135.3 | | | | 1135.3 | 1135.3 | 1135.3 | Ds PyTr | | |
| 1136 | FP D-L. | Cg Grn | | | P 3 Cl | | | | 622597 |
| 1138 | | | | | 1136.7 1138.0 P 1 SeCb | | | | |
| 1140 | | | | | 1138.4 | | | | |
| 1142 | | | | | | 2 10 Si Cb (±Cl) | | Pk FP D? to aphyric lava. | |
| 1144 | | | | | | | | | |
| 1146 | | | | | | | | | |
| 1148 | | | | | P 1 SeClCb | 1148.3 | | | |
| 1150 | | | | | | | | | |
| 1150.9 | | | | | | | | | |
| 1152 | | | | | | | | | 622598 |
| 1154 | FP D-L/bx | Cg Grn | FP 60 P V Si Cl 10 | | | 1 10 Cb | | TS 622667 1155.0 | |
| 1156 | | | | | | | | | |
| 1158 | | | | | | | | 1159.7 ORIENTATION | |

622569

# Aberfoyle Resources Limited

EXPLORATION DIVISION

HOLE No. MAC 35

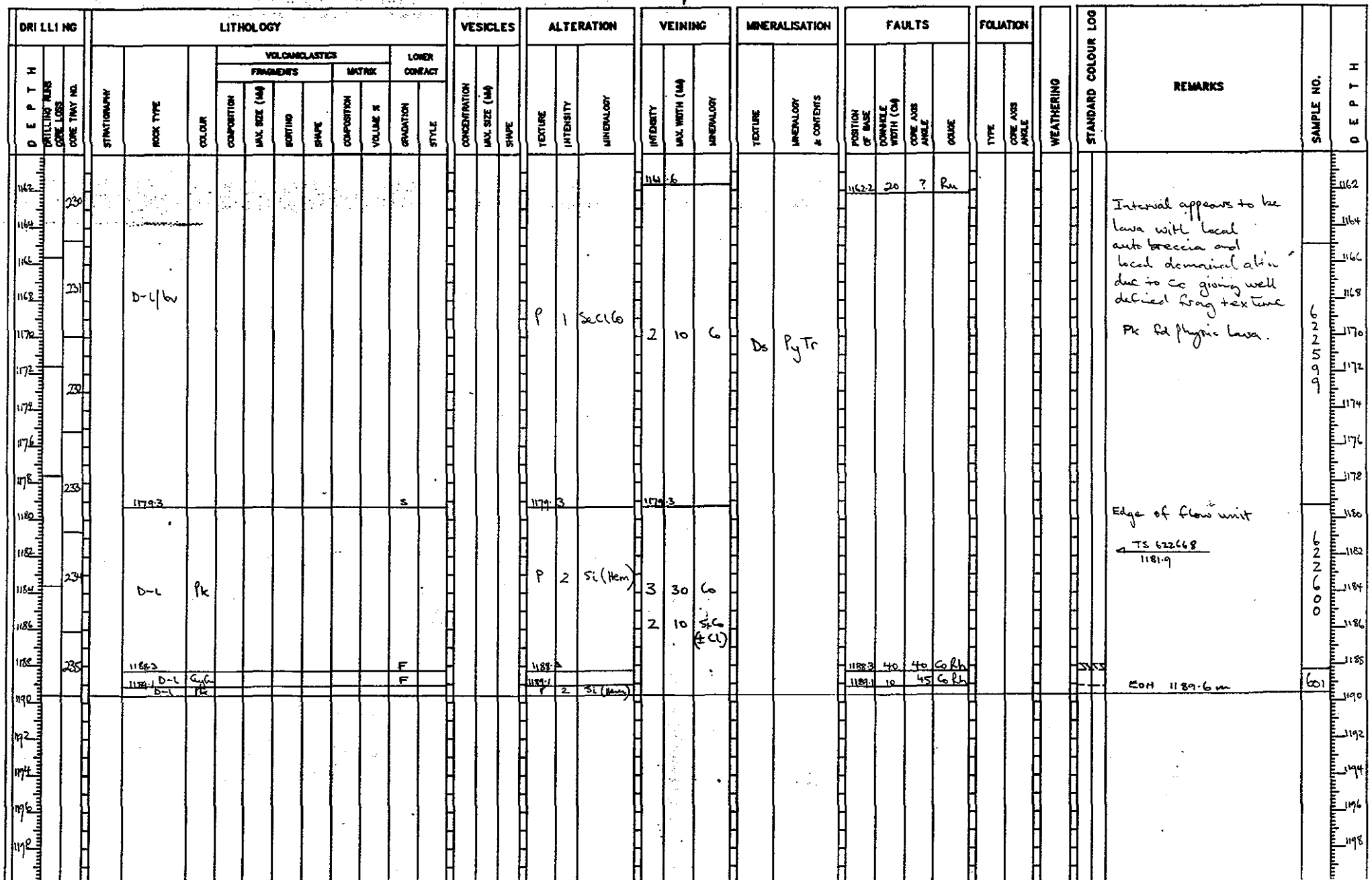
PAGE 30 OF 30

GEO. SR

DATE 24-2-93

5 cm

# DIAMOND DRILL LOG




65534

Aberfoyle Exploration — PETROLOGY GEOCHEMICAL SAMPLE LEDGER

PROJECT: MAC 035

BSS SIEVE SIZE CODE - MESH NUMBER: A 200 B 150 C 100 D 80 E 60 F 40 G 30 H 20 T = TOTAL

SAMPLE TYPE CODE: OXIDIZED PRODUCTS O; FRESH ROCK R; STREAM SEDIMENTS S; WEATHERED BEDROCK W; SURFACE TRANSPORTED T; RESIDUAL SOIL E; MINE DUMP M

CARD PUNCH PRINT: YES / NO — VERIFY: YES / NO

DATE: 6-3-93

SHEET: 1 of 1

| EASTINGS | NORTHINGS | SAMPLE NUMBER | DEPTH In CMS | SIZE FRACTION | Sample Type | METAL VALUES PPM | GEOLOGICAL LOG |
|---|---|---|---|---|---|---|---|
| | | 622650 | 70·4 | | | | |
| | | 622651 | 168·1 | | | | |
| | | 622652 | 239·7 | | | | |
| | | 653 | 260·8 | | | | |
| | | 654 | 376·7 | | | | |
| | | 655 | 426·5 | | | | |
| | | 656 | 521·7 | | | | |
| | | 657 | 632·6 | | | | |
| | | 658 | 697·4 | | | | |
| | | 659 | 757·5 | | | | |
| | | 660 | 785·9 | | | | |
| | | 661 | 881·0 | | | | |
| | | 662 | 109·7 | | | | |
| | | 663 | 915·5 | | | | |
| | | 664 | 980·3 | | | | |
| | | 665 | 1076·8 | | | | |
| | | 666 | 1133·1 | | | | |
| | | 667 | 1155·6 | | | | |
| | | 668 | 1181·9 | | | | |

OPERATOR | COMPUTER | CHECK | PLOTTER | DATE

6559

SAMPLE NUMBER: MAC 35 622650

**SUMMARY: This rock is hydrothermally-altered (chlorite, followed by quartz-albite-Kspar, then calcite) monomict lava breccia dominated by formerly glassy fragments of plagioclase+ sparsely augite-phyric acid andesite.**

HAND SPECIMEN:

This is a dark, strongly altered lava breccia dominated by fragments up to several cm across of sparsely plagioclase-phyric or aphyric andesitic to dacitic lava. Some matrix areas are bleached and probably silicified.

THIN SECTION DESCRIPTION:

This sample is a dacitic to andesitic lava breccia, probably monomict, or nearly so, in which fragments of plagioclase-phyric lava are set in a strongly altered and recrystallized matrix. The largest and least-altered clasts are composed of around 10 modal% of blocky to tabular prisms of strongly sericite-altered albitized plagioclase phenocrysts to about 2mm maximum length and a few chlorite+silica-altered augite(?) phenocrysts set in devitrified and recrystallized glass with a rather small-scale perlitically-cracked texture. Also present are not uncommon small FeTi oxide phenocrysts that have altered to very fine-grained magnetite-leucoxene aggregates spotted with chlorite and sericite. The groundmass of these fragments was perlitically-cracked devitrified glass containing common tiny albite microlites, and which is now quite strongly but patchily chlorite-altered with rather abundant aggregates of magnetite-leucoxene. Some of the smaller fragments have less chloritic groundmasses.

The inter-fragment areas of this sample are extremely heterogeneous in texture and mineralogy, and are due to moderate hydrothermal alteration of what was probably originally a weakly hydrofractured lava breccia. Dominant assemblages in the matrix areas are quite coarse-grained quartz-albite-Kspar intergrowths with interstitial chlorite and abundant late-stage overprinting calcite. Clearly, chlorite alteration preceded the silica-albite-Kspar veining and soaking of the inter-fragment matrix.

This sample is a moderately hydrothermally altered monomict acid andesite lava breccia dominated by chloritized fragments of plagioclase-phyric formerly glassy lava

SAMPLE NUMBER: MAC 35 622651

**SUMMARY: This rock is formerly glassy plagioclase+sparsely augite-phyric acid andesite to dacite lava with moderate hydrothermal alteration dominated by silica-chlorite±pyrite±sphalerite.**

HAND SPECIMEN:

This is a dark green,andesitic lava with common altered plagioclase phenocrysts and a typical mottled texture of devitrified glass. It has an almost 'false brecciated' texture in places.

THIN SECTION DESCRIPTION:

This sample is a texturally very well-preserved plagioclase+augite-phyric andesitic lava with beautifully preserved perlitic cracks in the formerly glassy groundmass. The albitized plagioclase phenocrysts make up around 10 modal% of the rock and are well-formed tabular prisms with strong sericite alteration. Considerably less abundant are small chloritized augite phenocrysts and totally altered former FeTi oxide phenocrysts now composed of messy disaggregated leucoxenitic material.

The groundmass of this sample consists of a very fine-grained quartzo-feldspathic aggregate after devitrified glass, and it shows excellent perlitic cracking, with chlorite defining the former cracks. Patches of more intense chlorite alteration are heterogeneously distributed through the groundmass. Cracks and tension gashes are filled by polycrystalline quartz with subordinate amounts of intergrown chlorite, almost colourless Fe-poor sphalerite and pyrite.

This was a glassy plagioclase+sparsely augite-phyric acid andesite to dacite lava with moderate hydrothermal alteration (silica-chlorite-pyrite-sphalerite).

SAMPLE NUMBER: MAC 35 622652

SUMMARY: This rock is a formerly glassy plagioclase-phyric dacitic lava with a pseudo-spherulitic blebby groundmass texture, and a low-grade burial metamorphic assemblage.

HAND SPECIMEN:

This is a massive plagioclase-phyric andesitic to dacitic lava or shallow intrusive with an unusual rather coarse-grained groundmass texture.

THIN SECTION DESCRIPTION:

This sample is a formerly spherulitic-textured glassy dacitic lava with around 7-10 modal% of albitized plagioclase phenocrysts that are mainly 0.5-1mm long, although not uncommon crystals as large as 3mm are also present. These have a dusty brown colour presumably due to submicroscopic Fe oxide dust, and most have recrystallized internally to several crystallographically discontinuous zones within each crystal. A few very small former augite crystals are pseudomorphed by sericite, rather than chlorite, and small FeTi oxide microphenocrysts are altered to fine aggregates of small sphene granules and sericite, plus minor chlorite.

The very unusual-textured groundmass of this rock has evolved from alteration and recrystallization of an originally glassy texture that at first sight appears to have been spherulitic. However, in the blebs that make up the groundmass show no characteristic radial quartz-albite rosette intergrowths characteristic of spherulites. The groundmass now consists dominantly of rather ovoid to spherical blebs around 1mm average across composed of devitrified glass with abundant unoriented tiny acicular albite microlites surrounding a coarser-grained albite or quartz+albite 'nucleus'. The interstitial areas between the rounded blebs is composed mainly of green chlorite, with trails of tiny leucoxene granules concentrated along the interfaces between the blebs and the chloritic matrix. I even considered that this was a lapilli crystal tuff, but significantly, several long prismatic plagioclase laths extend from one bleb (lapilli?) into an adjacent bleb, effectively ruling out a pyroclastic origin for this rock.

This is a plagioclase-phyric dacitic lava with a formerly glassy groundmass that has devitrified and recrystallized to a pseudo-spherulitic blebby texture.

SAMPLE NUMBER: MAC 35 622653

**SUMMARY: This rock is formerly glassy sparsely plagioclase-phyric dacitic lava breccia in which the original brecciated texture has been enhanced by strong silica-chlorite hydrothermal alteration.**

HAND SPECIMEN:

This is a mid-green-grey altered polymict lava breccia with dark sparsely plagioclase-phyric lava fragments in a lighter, strongly altered matrix.

THIN SECTION DESCRIPTION:

This sample is a very strongly hydrothermally altered formerly glassy dacitic lava with sparse plagioclase phenocrysts. The latter probably make up one to 2 modal% of the rock. These are mainly less than 2mm long and are totally replaced by either dull green chlorite or fine-grained sericite. There were apparently no former mafic phenocrysts in this rock, although the extent of alteration precludes a definite statement to this effect.

The groundmass of the lava fragments was undoubtedly glassy, but has recrystallized during strong hydrothermal alteration to complex and heterogeneous mainly very fine-grained quartzo-feldspathic material spattered with spotty chlorite and containing abundant very fine-grained sericite. Small scattered pyrite grains are not uncommon, but are modally insignificant. The matrix between the lava fragments is exceptionally heterogeneous in grainsize and texture, and varies from quartz-calcite intergrowths to mostly quartz-chlorite intergrowths with overprinting calcite.

This was probably a glassy sparsely plagioclase-phyric dacitic lava breccia in which the original hydrofractured texture has been enhanced by further 'false brecciation' associated with the strong chlorite-silica ±calcite hydrothermal alteration.

SAMPLE NUMBER: MAC 35 622654

SUMMARY: This rock is a low-grade burial metamorphosed augite-phyric basaltic lava breccia or hyaloclastite.

HAND SPECIMEN:

This is a dark green polymict basaltic lava breccia with fragments of lighter coloured lava to several cm long set in a darker matrix.

THIN SECTION DESCRIPTION:

This sample is a lava breccia dominated by augite-phyric basaltic lava fragments in a matrix of more altered and finer-grained polymict basaltic lava breccia. The main basaltic lava fragments are rather vesicular (perhaps 5 modal% of vesicles) and vesicles vary from <<1mm across to almost 1cm across. They are all filled with assemblages of quartz-pumpellyite-epidote±chlorite, and the quartz and pumpellyite always have radiating rosette habits. Perfectly fresh, euhedral augite phenocrysts <1.5mm long dominate the phenocryst assemblage, and the larger phenocrysts show significant compositional zoning. Some clots of augite crystals contain at least twenty phenocrysts, and individual crystals are much less common than crystal clots of two or more crystals. There are a few small altered olivine phenocrysts, and one 2mm-sized totally sericitized former plagioclase phenocryst. The groundmass of this basaltic lava fragment is microvesicular, and vitrophyric textured, with quartz-filled small vesicles making up about 5 modal% of the groundmass, and mainly altered elongate plagioclase microlites set in devitrified glass. The latter is almost isotropic extremely fine-grained quartzo-feldspathic material.

The matrix of this lava breccia is clearly polymict, and is composed a several textural varieties of basaltic lava, although all are augite-phyric with almost trachytic-textured groundmasses. Single crystals of augite are also present, and much of the inter-fragment material appears to have been vesicular and broken-up basaltic glass that has variably altered to fine-grained quartzo-feldspathic material with abundant disseminated granular and vein epidote and chlorite spots and streaks.

This sample is probably a hyaloclastite or subaqueous chill breccia derived from a single eruption of augite-phyric basaltic lava. The apparently diverse lava fragments simply reflect differing groundmass textures and mineralogies, which in turn are related to both the cooling rate (pillow margin, flow interior etc) and degree of alteration. The alteration is related to low-grade regional burial metamorphism.

SAMPLE NUMBER: MAC 35 62655

**SUMMARY: This rock is coarse monomict basaltic lava breccia composed of fragments of augite+sparsely plagioclase-phyric quite vesicular basaltic lava with a weak burial metamorphic overprint.**

HAND SPECIMEN:

This is a very coarse-grained basaltic lava breccia with fragments in excess of 6cm across, composed of augite-phyric basaltic lava with chlorite-filled vesicles, and inter-fragment quartzose patches and bleaching at the margins of some fragments.

THIN SECTION DESCRIPTION:

This sample is a monomict, rather coarse lava breccia derived entirely from what was probably a single eruptive unit of augite+sparsely plagioclase-phyric vesicular basaltic lava. Augite phenocrysts are invariably fresh, and are mainly 0.3-2 mm long and quite euhedral. They make up about 7-10 modal% of the rock. Plagioclase phenocrysts are far less abundant, and are rather rounded, albitized tabular prisms that do not appear to be in equilibrium with the host liquid. They may reflect mixing of this more mafic basalt with a plagioclase-phyric andesitic to dacitic magma. The groundmass of all lava fragments is a similar vitrophyric-textured intergrowth of albite microlites in very fine-grained, almost isotropic quartzo-feldspathic material after devitrified glass. Vesicles are quite abundant and range from rounded to ovoid and mainly 0.5-2mm across, to smaller, more less rounded vesicles in the groundmass. All are filled either by pale green chlorite, quite beautiful radiating pumpellyite, or epidote-quartz intergrowths. Inter-fragmental areas are composed of texturally diverse sugary to coarse-grained quartzo-feldspathic (but quartz-dominated) intergrowths with abundant overprinting patchy to granular epidote.

This is a basaltic lava breccia with a low-grade burial metamorphic degradation assemblage. It differs from the preceding sample only by the presence of the reacted plagioclase phenocrysts

SAMPLE NUMBER: MAC 35 622656

SUMMARY: **This rock is a basaltic lava breccia derived from augite-phyric vesicular basaltic lavas; it has suffered strong epidosite alteration, particularly in the porous matrix.**

HAND SPECIMEN:

This is another basaltic lava breccia composed of bleached (silica-altered?) and unbleached fragments to at least 5cm across of basaltic lava in a darker chlorite-rich matrix that forms only a small proportion of the rock.

THIN SECTION DESCRIPTION:

This sample is a rather altered augite-phyric basaltic lava breccia very similar in most respects to the previous two samples. Fragments to at least several cm across include vesicular augite-phyric basaltic lava with occasional rather reacted plagioclase phenocrysts, identical to those in sample 622655, but heavily riddled with granular epidote-clinozoisite. The groundmass of most fragments is isotropic devitrified glass, lacking the tiny plagioclase microlites present in the groundmass of the previous two samples.

The inter-fragmental matrix of this rock was probably composed of comminuted basaltic glass and occasional augite crystals. However, it has been rather strongly altered, to highly variably-textured quartzo-feldspathic material very strongly (to completely, in places) overprinted by fine-grained yellow epidote aggregates. This epidosite alteration is typically produced in oceanic settings by upwelling, briny fluids that were pumped down in near-ridge axis areas, and, having reacted extensively with basalts, are within a km or two of being discharged at the ocean floor.

SAMPLE NUMBER: MAC 35 622657

**SUMMARY: This rock is a plagioclase+augite-phyric andesitic dyke rock with a weak calcite-sericite-pyrite hydrothermal alteration assemblage.**

HAND SPECIMEN:

This is quite different from the preceding three basaltic lava breccias. It appears to be a massive plagioclase-phyric andesitic lava

THIN SECTION DESCRIPTION:

This sample was a plagioclase+augite-phyric andesitic lava or shallow dyke rock. It consists of around 15 modal% of rather blocky to tabular prisms of albitized plagioclase phenocrysts that commonly occur aggregated in clots. They are fairly heavily overprinted by sericite, and up to about 2mm long. Former augite phenocrysts probably make up a few modal % of this rock and are small prisms now replaced totally by green chlorite. Former FeTi oxide phenocrysts are totally altered to aggregates of fine-grained magnetite and sphene (leucoxene).

The groundmass of this sample has a rather fluidal to trachytic texture defined by long narrow albite microlites and laths that made up almost the entire groundmass before alteration. Interstitial chlorite and tiny Fe oxides granules are common, and calcite is an abundant phase overprinting significant areas of groundmass. A 1-3mm-wide shear zone transects the rock, and is filled by calcite, sericite and abundant small idiomorphic pyrite grains.

After the three basaltic breccia sections from overlying strata in this hole, this sample is quite petrographically distinct. The lath-rich, originally glass-poor groundmass suggests to me that this may be an andesitic dyke rock. It has suffered weak to moderate hydrothermal alteration (calcite-sericite-pyrite) overprinting an original low-grade burial metamorphic assemblage.

SAMPLE NUMBER: MAC 35 622658

SUMMARY: **This rock is a plagioclase+augite-phyric evolved basaltic lava that has suffered strong epidote alteration probably during burial metamorphic degradation.**

HAND SPECIMEN:

This is a rather dull green, epidote-altered intermediate to mafic massive lava with abundant altered plagioclase and mafic phenocrysts

THIN SECTION DESCRIPTION:

This sample is a texturally reasonably well-preserved basaltic lava, although the mineralogical alteration is extreme, with extensive epidote replacement of groundmass and phenocrysts. Due to the strong epidote alteration of both former plagioclase and augite phenocrysts, it is difficult to judge their primary abundances, but probably plagioclase was slightly more abundant than augite (around 12-15 modal% and 5-10 modal%. Some phenocryst are up to 4mm long, although most are 1-2mm long. Augite phenocrysts are altered to epidote plus chlorite, whereas former plagioclase crystals are altered to dominant epidote and minor sericite and chlorite. Not uncommon FeTi oxide phenocrysts are totally replaced by messy leucoxenitic material.

The groundmass of this sample was a vitrophyric intergrowth of albite microlites in glass. The latter has devitrified to exceptionally fine-grained quartzo-feldspathic material spotted with tiny leucoxene granules and chlorite flakes and aggregates. Small veinlets and irregular patches of calcite cut and overprint the groundmass.

This is an evolved plagioclase+augite-phyric basalt that has suffered strong epidote-alteration, although probably not during hydrothermal alteration.

SAMPLE NUMBER: MAC 35 622659

**SUMMARY: This rock is plagioclase+sparsely augite-phyric dacitic to acid andesitic lava from the central portions of a thick cooling unit that has suffered strong carbonate alteration.**

HAND SPECIMEN:

This is a dark green rather chloritic and altered plagioclase-phyric dacitic lava.

THIN SECTION DESCRIPTION:

This sample is a quite strongly hydrothermally-altered plagioclase-phyric dacitic to andesitic lava composed of about 12-15 modal% of rather blocky albitized plagioclase phenocrysts set in a fine- to medium-grained vitrophyric textured groundmass. The plagioclase phenocrysts are up to 5mm across and many are overprinted by very fine-grained sericite and calcite. Thoroughly chloritized former augite prisms make up about 1 modal% of the rock and ar rarely longer than 0.5mm. Former FeTi oxide phenocrysts are uncommon, and have been totally replaced by sericite, chlorite and tiny grains of sphene and magnetite.

The groundmass of this sample consists of an intergrowth of bladed albite laths with interstitial chlorite and tiny leucoxene blebs. This texture was approaching holocrystalline, implying that the sample was well-removed from the glassy margins of these dacitic lava flows. In places, groundmass chlorite is quite abundant, although the rock is not strongly chloritized. Calcite is abundant though, and overprints probably 30-40 modal% of this sample. It occurs as irregular overprinting patches, as well as narrow veins. A single small idiomorphic pyrite grain occurs set in calcite.

This was a dacitic to acid andesitic lava that has suffered strong carbonate alteration.

SAMPLE NUMBER: MAC 35 622660

**SUMMARY: This rock is an unusual lava breccia composed of almost aphyric dacitic to acid andesite formerly glassy lava fragments; it has suffered moderate sericite-calcite hydrothermal overprinting.**

HAND SPECIMEN:

This is a dull green, mottled almost aphyric andesitic to dacitic lava, probably originally glassy, which appears to have suffered either hydrofracturing and healing of the fractures, or 'false brecciation', although fragments are not clearly defined..

THIN SECTION DESCRIPTION:

This sample is a weakly plagioclase-phyric dacitic(?) lava breccia with a most unusual texture, composed of small blebs and fragments, mostly 2-5mm across, of formerly glassy lava, with poorly-defined margins due to strong recrystallization and alteration. Only occasional sudden changes in groundmass texture. Two dominant textural domains are obvious. One is typical of devitrified felsic glass that has recrystallized to a rather coarse-grained quartzo-feldspathic mosaic, overprinted by fine-grained sericite and calcite. The other type, far more abundant, has a considerably finer-grained quartzo-feldspathic intergrowth with occasional small plagioclase (albitized) phenocrysts, and an alteration texture in which narrow chlorite aggregates forms globular or spheroidal structures, almost resembling wall-to-wall vesicles. Sericite overprints these domains as light discontinuous streaks. This is a strange devitrification texture that has probably been enhanced by the moderate hydrothermal alteration suffered by this sample. A 4mm wide veinlet of calcite and strongly strained quartz cuts the sample, and has a rim of calcite. Calcite also occurs as irregular patches replacing significant areas of groundmass.

This rock was probably a dacitic to acid andesitic, almost aphyric glassy lava breccia in which original devitrification textures have been modified by moderate hydrothermal alteration (sericite-calcite).

SAMPLE NUMBER: MAC 35 622661

SUMMARY: This rock is a polymict dacitic lava breccia with weak hydrothermal alteration (sericite-calcite assemblages).

HAND SPECIMEN:

This is a polymict felsic lava breccia with both greenish and cream coloured lava fragments to at least several cm long in a much finer-grained matrix.

THIN SECTION DESCRIPTION:

This sample is a clear polymict felsic lava breccia dominated by glassy lava fragments of dacitic composition, but showing a variety of alteration assemblages. The largest and best preserved lava fragments (cream coloured in hand specimen) are moderately plagioclase-phyric, formerly glassy dacitic lava with 7-10 modal% of albite phenocrysts averaging around 1mm long, with slight sericite speckling. No mafic phenocrysts were present, and the groundmass is highly variable from fragment to fragment, mainly being composed of a quartzo-feldspathic mosaic intergrowths riddled with tiny albite microlites that were set in the original glass. Other lava fragments have fewer plagioclase phenocrysts and abundant very fine-grained chlorite in the groundmass, that was also originally glassy. Small blebs of quartz are set in the chlorite. These more chloritic fragments probably reflect a more mafic precursor, perhaps an acid andesite composition.

The matrix of this lava breccia is highly variable in texture and mineralogy, and was originally composed of glassy chips and finer-grained glassy material. It is now dominated by quartzo-feldspathic intergrowths that vary from very fine-grained and sugary to rather coarser and ragged. Sericite heavily overprints some areas of groundmass, forming a mesh through the altered matrix. Calcite forms discontinuous veinlets and irregular patches overprinting both lava fragments and the matrix.

This was a polymict dacitic lava breccia that shows no sign of reworking by water, and may have formed by mass flows off a dacitic lava dome or plug. It shows weak sericite-calcite hydrothermal alteration.

SAMPLE NUMBER: MAC 35 622662

SUMMARY: This rock is an intensely hydrothermally altered (calcite-chlorite-pyrite) epiclastic sandstone or lithic crystal tuff derived from plagioclase-phyric glassy felsic volcanics.

HAND SPECIMEN:

This is a dark green epiclastic sandstone or lithic tuff with occasional small blebs (to ~2mm across) of dark reddish hematite or Fe-carbonate.

THIN SECTION DESCRIPTION:

This sample is a very strongly altered tuffaceous (epiclastic) sandstone or lithic crystal tuff dominated by broken plagioclase phenocrysts and indistinct clasts of formerly glassy lava. The primary detrital texture is not at all obvious due to the intense sericite-calcite overprint, but the common broken plagioclase crystals, some up to 2mm long, and the rather fine-grained fragmental texture clearly indicates that this is not a lava or lava breccia. The sandstone/tuff was matrix supported, and although it is almost impossible to estimate, I suggest that the detrital plagioclase and lithic clasts probably made up only about 30 modal% of the rock. The remainder was presumably vitric ash and comminuted plagioclase phenocryst debris.

The alteration of this rock is pronounced. Plagioclase was strongly altered to sericite before a more intense alteration, expressed mainly by dense but very fine-grained calcite - (subordinate) chlorite overprinting that has obliterated most of the original texture. Abundant very fine-grained pyrite crystals are disseminated through the calcite-chlorite, but are all altered to translucent red sericite. Chlorite also occurs as small angular patches and fracture fillings, often with stubby crystals of Kspar growing into the chlorite. The reddish patches evident in hand specimen are seen to be large calcite patches riddled with submicroscopic hematite.

This was an epiclastic sandstone or lithic crystal tuff derived from plagioclase-phyric felsic glassy lavas and tuffs. It has suffered intense calcite-chlorite-pyrite hydrothermal alteration.

SAMPLE NUMBER: MAC 35 622663

**SUMMARY: This rock is an almost aphyric, formerly glassy massive dacitic to rhyolitic lava**

**HAND SPECIMEN:**

This is a light brown massive almost aphyric felsic lava with occasional quartz veinlets.

**THIN SECTION DESCRIPTION:**

This sample is a massive, formerly glassy and virtually aphyric dacitic to rhyolitic lava. The glass has devitrified and recrystallized to a rather coarse-grained quartzo-feldspathic mosaic composed of anhedral patchy small (around 0.1-0.2mm) quartz grains intergrown with sericitized feldspar that produces an effect rather like a fine-grained holocrystalline granitic rock. A few 1mm-sized albite phenocrysts are present but are heavily overprinted by calcite and sericite. Fine-grained calcite is common throughout the rock, and the few veinlets that transect this sample are composed of intergrown crystalline calcite and quartz and a few small pyrite crystals.

This is a petrographically simple rock that was originally a massive, very sparsely plagioclase-phyric entirely glassy dacitic to rhyolitic lava.

SAMPLE NUMBER: MAC 35 622664

SUMMARY: **This rock is a weakly plagioclase-phyric monomict dacitic or acid andesite lava breccia with moderate chlorite-silica hydrothermal alteration.**

HAND SPECIMEN:

This is a dark green rather strongly altered fragmental andesitic to dacitic lava breccia with fragments up to several cm long with quite diffuse, poorly-defined margins.

THIN SECTION DESCRIPTION:

The fragmental texture of this sample is much less evident in thin section than in hand specimen. The rock consists of domains of quartzo-feldspathic intergrowths after glass in which chlorite is insignificant, and domains in which chlorite is abundant. These differences don't reflect different original fragment types, but rather result from heterogeneous alteration and recrystallization.

Rather ragged plagioclase (albite) phenocrysts, mainly less than 1mm long and grouped in multi-crystal clots, make up around 3-5 modal% of the rock and are distributed fairly evenly through both the chlorite-rich and chlorite-poor domains. The latter domains are composed of relatively coarse-grained, sugary-textured quartzo-feldspathic mosaic intergrowths with sericite speckling and minor interstitial chlorite. Chlorite-rich domains lack quartzo-feldspathic matrix but carry small albite microlites, indicating slightly slower cooling rates than the quenched glass that formed chlorite-poor areas. Matrix areas between fragments are not obvious, as recrystallization of the glass in the fragments and the matrix has produced similar textured quartzo-feldspathic intergrowths.

This sample was a monomict glassy lava breccia, probably of dacitic to acid andesitic composition, that has suffered weak hydrothermal alteration (silica-chlorite).

SAMPLE NUMBER: MAC 35 622665

SUMMARY: This rock was a moderately plagioclase-phyric dacitic lava with a vitrophyric groundmass, and a chlorite - sericite -silica burial metamorphic alteration assemblage.

HAND SPECIMEN:

This is an almost black plagioclase-phyric massive felsic lava.

THIN SECTION DESCRIPTION:

This sample is a texturally well-preserved moderately plagioclase-phyric dacitic lava with a formerly largely glassy groundmass. Blocky to tabular albitized plagioclase phenocrysts mainly less than 1mm long occur most commonly as clots of subhedral crystals. They are always lightly dusted with ultra fine-grained hematite and much less abundant fine sericite, and make up around 5-8 modal% of the sample. A few small chloritized phenocrysts that were probably augite are also present, but these are modally insignificant. Similarly, small former FeTi oxide phenocrysts are totally altered to messy leucoxene.

The groundmass of this sample was composed of glass charged with small albite microlites. Glass devitrified and then recrystallized to a fairly even-textured, homogeneous quartzo-feldspathic aggregate that is very fine-grained, but characterized by occasional larger angular patches of polycrystalline quartz. Both chlorite and sericite are quite abundantly disseminated throughout the groundmass, although the amount and distribution of chlorite suggest that it is of burial metamorphic origin rather than localized hydrothermal origin. The chlorite-sericite alteration assemblage of this massive dacitic lava contrasts with the calcite-sericite-(coarser grained quartzo-feldspathic intergrowth) of sample 622663, and accounts for the strikingly different colour of these two initially fairly similar dacites.

SAMPLE NUMBER: MAC 35 622666

**SUMMARY: This rock is formerly vitrophyric-textured, moderately plagioclase-phyric dacitic lava with epidote-silica-chlorite low-grade regional metamorphic alteration assemblage. It was originally very similar to sample 622665.**

HAND SPECIMEN:

This is a dark brown massive plagioclase-phyric dacitic lava with quartz veinlets and quartz-filled tension gashes.

THIN SECTION DESCRIPTION:

This sample is a moderately plagioclase-phyric dacitic lava that was originally probably very similar to the preceding sample 622665. It consists of about 5 modal% of subhedral albitized plagioclase phenocrysts with the pinkish colour typical of disseminated hematite dust, that are mainly aggregated in multi-crystal clots of 4 or 5 crystals. Several small cognate inclusions of microgabbro up to 2mm long consist of small tabular plagioclase phenocrysts and much less abundant tiny chloritized augite crystals. These are probably crystal aggregates that formed on the walls of the conduit through which this magma was passing to eruption, and were plucked off by the erupting magma. A few small chloritized augite crystals, and leucoxene-altered FeTi oxides are also present.

The groundmass of this rock was essentially identical to the groundmass of the previous sample. It was a vitrophyric intergrowth of albite laths in glass that has devitrified and then recrystallized to fairly fine-grained quartzo-feldspathic material with occasional spots of coarser-grained anhedral polycrystalline quartz. Unlike 622665. this sample has no sericite in the groundmass, and chlorite is less abundant, but quite common. Instead, clots and small patches of yellow epidote are common throughout the rock, and a single vein of calcite carries spectacular long hematite bladed crystals. Such an abundance of epidote is unusual in metadacites from the Mount Read Volcanics. Epidote is normally restricted to andesitic and more mafic rocks which originally contained plenty of Ca. The act that these two samples (665 and 666) contain more chlorite (665) and more epidote (666) than typical dacites suggests that they may be compositionally transitional to acid andesites. The alteration assemblage is low-grade regional burial metamorphism related.

SAMPLE NUMBER: MAC 35 622667

**SUMMARY: This rock is a formerly glassy and hydrofractured plagioclase-phyric dacitic lava that has been false brecciated during a hydrothermal alteration event that produced chlorite-silica-sericite assemblages,**

HAND SPECIMEN:

This is a massive, almost black massive plagioclase-phyric dacitic lava with pinkish albite phenocrysts.

THIN SECTION DESCRIPTION:

This sample is an finely autobrecciated or false brecciated plagioclase-phyric dacitic lava. Despite the hand specimen showing no sign of brecciation, it is very obvious in hand specimen, as a relatively small-scale jigsaw fit texture with the largest fragments being almost 1cm and the smallest <<<1mm. Blocky to tabular albitized plagioclase phenocrysts are mainly around 1mm long, and are charged with hematite dust, giving them their distinctive pink colour. No former mafic phenocrysts are evident, but not uncommon former FeTi oxide phenocrysts are altered to messy leucoxene aggregates.

The groundmass of this sample was clearly glassy, and it recrystallized to a fairly fine-grained quartzo-feldspathic aggregate that has been subsequently overprinted by quite pervasive silica-chlorite-sericite alteration. The rock was probably hydrofractured but not brecciated, and hydrothermal alteration has enhanced the original incipient brecciation texture to produce a variable jigsaw fit false brecciation texture in which the inter-fragment matrix is paler and cleaner (chlorite-poor) relative to the fragments themselves. The last event in the alteration of this rock was limited calcite veining.

This was a hydrofractured moderately plagioclase-phyric dacitic lava that suffered quite strong chlorite-silica-sericite hydrothermal alteration and false brecciation.

SAMPLE NUMBER: MAC 35 622668

SUMMARY: This is a formerly glassy, weakly hydrothermally-altered (calcite-sericite) massive plagioclase-phyric dacitic lava.

HAND SPECIMEN:

This is a plagioclase-phyric massive dacitic lava with gradational zones of colour change from fresher almost black lava to light brown bleached and silicified lava.

THIN SECTION DESCRIPTION:

This sample is a massive moderately plagioclase-phyric formerly glassy lava. Albitized plagioclase phenocrysts make up around 10 modal% of the rock, and are mainly subhedral tabular crystals that are gathered in multi-crystal clots to about 2mm across. Dusty hematite throughout the plagioclase phenocrysts has preserved ghost compositional zoning in the crystals. A few small totally chloritized augite crystals are also present, and occasional small FeTi oxides are altered to leucoxene.

The groundmass of this sample was largely glassy originally, composed of occasional tiny albite microlites in glass that devitrified an recrystallized to a very fine-grained quartzo-feldspathic material with common tiny chloritic spots and larger anhedral grains of polycrystalline secondary quartz. The gradual change from more pinkish altered lava to almost black less altered lava is shown across the section by a significant decrease in the amount of disseminated secondary calcite and sericite, and an increase in the abundance of fine-grained chlorite in the groundmass. The sample is cut by strained veinlets of calcite and intergrown quartz.

This was a moderately plagioclase-phyric largely glassy dacitic lava that has suffered weak hydrothermal alteration, producing pinkish calcite-sericite alteration in an otherwise almost black dacitic lava.

655295

# ANALABS

A Division of Inchcape Inspection and Testing Services Australia Pty. Ltd. A.C.N. 004 591 564

RECEIVED
7 APR 1993

Phone (004) 316837 | 14 Thirkell St. DODEE TAS 7320 | Fax (004) 318890

## ANALYTICAL REPORT No. 100560.60.09359

THIS REPORT MUST BE READ IN CONJUNCTION WITH THE ACCOMPANYING ANALYTICAL DATA

INVOICE TO:
Aberfoyle Resources Limited
Exploration Division
P.O. Box 952
BURNIE TAS 7320

| ORDER No. | PROJECT |
|---|---|
| 2740 | MAC-35 |

| DATE RECEIVED | RESULTS REQUIRED |
|---|---|
| 09/03/93 | ASAP |

| No. OF PAGES OF RESULTS | DATE REPORTED | No. OF COPIES | TOTAL No. OF SAMPLES |
|---|---|---|---|
| 3 | 06/04/93 | 1 | 19 |

| SAMPLE NUMBERS | SAMPLE DESCRIPTION | ELEMENT/METHOD |
|---|---|---|
| 72650/68 | DC Prep : GP033 - CHROME FREE BOWLS | Cu,Pb,Zn,Ag/GA101<br>Ba,As,Cr,Ir/GX401<br>WHOLE ROCK ANALYSIS/GX408 |

RESULTS TO:
Mr R de Bomford
Aberfoyle Resources Limited
P.O. Box 952
BURNIE TAS 7320

REMARKS

MAC-35 PET.

RESULTS TO:

RESULTS TO:

AUTHORISED OFFICER

655396

# ANALABS

A Division of Inchcape Testing Services (Australia) Pty. Ltd.
A.C.N. 004 591 664

## ANALYTICAL DATA

| SAMPLE PREFIX | REPORT No. | REPORT DATE | CLIENT ORDER No. | PAGE |
|---|---|---|---|---|
| | 100560.60.09359 | 06/04/93 | 2740 | 1 OF 3 |

| TUBE No. | SAMPLE No. | Cu | Pb | Zn | Ag | Ba | As | Cr | Zr | Ti |
|---|---|---|---|---|---|---|---|---|---|---|
| | 622650 | 11 | 29 | 110 | <2 | 474 | 7 | 25 | 179 | 3340 |
| 2 | 622651 | 37 | 2057 | 4059 | <2 | 2005 | <2 | 83 | 155 | 2680 |
| | 622652 | 13 | <5 | 137 | <2 | 550 | 3 | 16 | 175 | 3020 |
| 4 | 622653 | 10 | 46 | 245 | <2 | 401 | 51 | 68 | 161 | 2860 |
| 5 | 622654 | 158 | 152 | 222 | <2 | 3583 | 2 | 307 | 96 | 2840 |
| | 622655 | 97 | 10 | 82 | <2 | 466 | 2 | 311 | 109 | 3210 |
| 7 | 622656 | 96 | 54 | 117 | <2 | 1006 | 3 | 246 | 82 | 2880 |
| | 622657 | 16 | <5 | 77 | <2 | 473 | <2 | 44 | 76 | 2790 |
| 9 | 622658 | 80 | 8 | 130 | <2 | 701 | 2 | 53 | 84 | 2900 |
| 10 | 622659 | 23 | <5 | 62 | <2 | 496 | <2 | 45 | 71 | 2800 |
| 1 | 622660 | 4 | <5 | 36 | <2 | 634 | <2 | 10 | 134 | 2600 |
| 12 | 622661 | 9 | <5 | 57 | <2 | 1692 | 4 | 29 | 240 | 2280 |
| 1 | 622662 | 31 | <5 | 60 | <2 | 576 | 6 | 14 | 53 | 2520 |
| 14 | 622663 | <4 | <5 | 14 | <2 | 575 | <2 | 14 | 217 | 1980 |
| 1 | 622664 | 4 | 10 | 41 | <2 | 412 | <2 | 20 | 206 | 2620 |
| 1 | 622665 | <4 | <5 | 53 | <2 | 308 | <2 | 26 | 206 | 2390 |
| | 622666 | <4 | 5 | 56 | <2 | 876 | 4 | 71 | 191 | 2390 |
| 1 | 622667 | <4 | <5 | 92 | <2 | 621 | <2 | 102 | 210 | 2590 |
| 19 | 622668 | <4 | 6 | 63 | <2 | 1297 | 2 | <5 | 220 | 2080 |
| 2 | | | | | | | | | | |
| 2 | | | | | | | | | | |
| 22 | | | | | | | | | | |
| 2 | DETECTION | 4 | 5 | 4 | 2 | 10 | 2 | 5 | 5 | 60 |
| 24 | UNITS | ppm | ppm | ppm | ppm | ppm | ppm | ppm | ppm | ppm |
| 2 | METHOD | GA101 | GA101 | GA101 | GA101 | GX401 | GX401 | GX401 | GX401 | GX401 |

Results in ppm unless otherwise specified
T = element present; but concentration too low to measure
X = element concentration is below detection limit
– = element not determined

AUTHORISED OFFICER

655297

# ANALABS

A Division of Inchcape Testing Services (Australia) Pty. Ltd.
A.C.N. 004 591 664

## ANALYTICAL DATA

| SAMPLE PREFIX | REPORT No. | REPORT DATE | CLIENT ORDER No. | PAGE |
|---|---|---|---|---|
| | 100560.60.09359 | 06/04/93 | 2740 | 2 OF 3 |

| JBE No. | SAMPLE No. | Al2O3 | SiO2 | TiO2 | Fe2O3 | MnO | CaO | K2O | MgO | P2O5 |
|---|---|---|---|---|---|---|---|---|---|---|
| 1 | 622650 | 16.67 | 59.90 | 0.56 | 7.53 | 0.13 | 1.07 | 1.77 | 4.27 | 0.291 |
| 2 | 622651 | 13.96 | 57.50 | 0.45 | 5.41 | 0.48 | 6.00 | 2.00 | 2.60 | 0.236 |
| 3 | 622652 | 15.42 | 60.40 | 0.50 | 6.47 | 0.22 | 4.17 | 1.37 | 1.77 | 0.263 |
| 4 | 622653 | 15.54 | 57.90 | 0.48 | 6.83 | 0.21 | 4.70 | 3.65 | 2.44 | 0.276 |
| 5 | 622654 | 12.82 | 53.80 | 0.47 | 8.93 | 0.25 | 7.61 | 3.07 | 7.80 | 0.300 |
| 6 | 622655 | 14.01 | 50.90 | 0.54 | 10.08 | 0.16 | 8.76 | 0.54 | 8.32 | 0.300 |
| 7 | 622656 | 14.43 | 53.00 | 0.48 | 9.31 | 0.21 | 8.42 | 1.58 | 7.04 | 0.203 |
| 8 | 622657 | 15.01 | 55.70 | 0.46 | 7.79 | 0.20 | 5.69 | 1.55 | 2.86 | 0.144 |
| 9 | 622658 | 15.82 | 56.80 | 0.48 | 8.60 | 0.19 | 6.91 | 1.33 | 3.60 | 0.157 |
| 10 | 622659 | 14.67 | 50.30 | 0.47 | 7.06 | 0.27 | 9.80 | 1.76 | 2.02 | 0.158 |
| 11 | 622660 | 13.68 | 66.40 | 0.43 | 5.17 | 0.15 | 3.14 | 2.56 | 1.48 | 0.138 |
| 12 | 622661 | 15.40 | 62.60 | 0.38 | 7.11 | 0.14 | 2.49 | 3.30 | 1.28 | 0.081 |
| 13 | 622662 | 14.99 | 49.50 | 0.42 | 8.66 | 0.33 | 8.06 | 2.06 | 3.50 | 0.098 |
| 14 | 622663 | 13.98 | 66.60 | 0.33 | 3.37 | 0.16 | 3.73 | 3.67 | 0.81 | 0.081 |
| 15 | 622664 | 14.69 | 66.50 | 0.44 | 6.39 | 0.09 | 1.09 | 2.09 | 2.07 | 0.110 |
| 16 | 622665 | 14.87 | 68.30 | 0.40 | 5.13 | 0.09 | 0.68 | 1.19 | 2.32 | 0.112 |
| 17 | 622666 | 14.14 | 66.60 | 0.40 | 4.58 | 0.12 | 3.78 | 2.25 | 0.85 | 0.102 |
| 18 | 622667 | 15.83 | 62.60 | 0.43 | 7.52 | 0.13 | 0.83 | 1.99 | 3.48 | 0.113 |
| 19 | 622668 | 14.13 | 67.80 | 0.35 | 4.05 | 0.07 | 2.50 | 4.33 | 0.41 | 0.085 |
| 20 | | | | | | | | | | |
| 21 | | | | | | | | | | |
| 22 | | | | | | | | | | |
| 23 | DETECTION | 0.01 | 0.01 | 0.01 | 0.01 | 0.01 | 0.01 | 0.01 | 0.05 | 0.005 |
| 24 | UNITS | % | % | % | % | % | % | % | % | % |
| 25 | METHOD | OX408 | OX408 | OX408 | OX408 | OX408 | OX408 | OX408 | OX408 | OX408 |

Results in ppm unless otherwise specified
T = element present; but concentration too low to measure
X = element concentration is below detection limit
– = element not determined

AUTHORISED OFFICER

655298

# ANALABS

A Division of Inchcape Testing Services (Australia) Pty. Ltd.
A.C.N. 004 591 664

## ANALYTICAL DATA

| SAMPLE PREFIX | REPORT No. | REPORT DATE | CLIENT ORDER No. | PAGE |
|---|---|---|---|---|
| | 100560.60.09359 | 06/04/93 | 2740 | 3 OF 3 |

| TUBE No. | SAMPLE No. | S | Na2O | LOI | TOTAL | | | | | |
|---|---|---|---|---|---|---|---|---|---|---|
| | 622650 | 0.580 | 3.49 | 4.03 | 100.28 | | | | | |
| 2 | 622651 | 0.890 | 3.35 | 6.70 | 99.58 | | | | | |
| | 622652 | 0.030 | 4.50 | 4.88 | 100.02 | | | | | |
| 4 | 622653 | 0.760 | 0.12 | 7.57 | 100.47 | | | | | |
| | 622654 | 0.040 | 1.52 | 3.13 | 99.72 | | | | | |
| | 622655 | 0.030 | 2.98 | 3.17 | 99.81 | | | | | |
| 7 | 622656 | 0.080 | 2.10 | 3.22 | 100.04 | | | | | |
| | 622657 | 0.140 | 3.34 | 6.83 | 99.70 | | | | | |
| 9 | 622658 | 0.010 | 2.09 | 3.59 | 99.60 | | | | | |
| | 622659 | 0.010 | 3.42 | 9.66 | 99.56 | | | | | |
| | 622660 | 0.020 | 1.45 | 5.08 | 99.68 | | | | | |
| 12 | 622661 | 0.110 | 3.44 | 3.59 | 99.90 | | | | | |
| | 622662 | 0.010 | 2.33 | 10.00 | 99.97 | | | | | |
| 14 | 622663 | 0.070 | 0.89 | 6.03 | 99.74 | | | | | |
| | 622664 | 0.050 | 2.83 | 3.33 | 99.70 | | | | | |
| | 622665 | 0.020 | 4.71 | 2.21 | 100.00 | | | | | |
| | 622666 | 0.010 | 4.69 | 2.55 | 100.07 | | | | | |
| 1 | 622667 | 0.040 | 3.61 | 2.98 | 99.54 | | | | | |
| 19 | 622668 | 0.010 | 3.26 | 2.68 | 99.64 | | | | | |
| 2 | | | | | | | | | | |
| 2 | | | | | | | | | | |
| 22 | | | | | | | | | | |
| 2 | DETECTION | 0.005 | 0.05 | 0.01 | 0.01 | | | | | |
| 24 | UNITS | % | % | % | % | | | | | |
| 2 | METHOD | OX408 | OX408 | OX408 | OX408 | | | | | |

Results in ppm unless otherwise specified
T = element present; but concentration too low to measure
X = element concentration is below detection limit
– = element not determined

AUTHORISED OFFICER

# APPENDIX X

# ABERFOYLE RESOURCES LTD. DRILL LOG

**Area Code** mac
**Prospect** Murchison Zone
**Report Grid** Mack
**Dataset** Geochemical data set

**Holename** DDMA0035
**Stored Grid** Mack

| From | To | Sample | Type | Cu ppm | Pb ppm | Zn ppm | Ag ppm | Au ppm | Ba ppm | As ppm | Cr ppm | Zr ppm | Ti ppm | Ti/Zr |
|---|---|---|---|---|---|---|---|---|---|---|---|---|---|---|
| 2.90 | 9.30 | 622485 | cgri | 42 | 32 | 133 | <2.0 | <0.008 | 732 | 13 | 18 | 204 | 3751 | 18.39 |
| 9.30 | 20.20 | 622486 | cgri | 39 | 35 | 122 | <2.0 | <0.008 | 857 | 8 | 13 | 190 | 3571 | 18.79 |
| 20.20 | 30.10 | 622487 | cgri | 41 | 99 | 159 | <2.0 | <0.008 | 888 | 12 | 18 | 173 | 3247 | 18.77 |
| 30.10 | 40.00 | 622488 | cgri | 55 | 53 | 142 | <2.0 | <0.008 | 739 | 10 | 18 | 176 | 3317 | 18.85 |
| 40.00 | 50.10 | 622489 | cgri | 102 | 65 | 217 | <2.0 | <0.008 | 1247 | 7 | 17 | 175 | 3177 | 18.15 |
| 50.10 | 60.00 | 622490 | cgri | 106 | 63 | 204 | <2.0 | <0.008 | 867 | 4 | 17 | 180 | 3305 | 18.36 |
| 60.00 | 70.00 | 622491 | cgri | 82 | 37 | 221 | <2.0 | <0.008 | 423 | 6 | 15 | 171 | 3200 | 18.71 |
| 70.00 | 80.00 | 622492 | cgri | 93 | 50 | 188 | <2.0 | <0.008 | 406 | 8 | 15 | 177 | 3217 | 18.18 |
| 80.00 | 90.00 | 622493 | cgri | 91 | 96 | 300 | <2.0 | <0.008 | 730 | 7 | 13 | 180 | 3142 | 17.46 |
| 90.00 | 100.00 | 622494 | cgri | 132 | 262 | 412 | <2.0 | <0.008 | 904 | 5 | 22 | 171 | 3026 | 17.70 |
| 100.00 | 110.00 | 622495 | cgri | 116 | 25 | 167 | <2.0 | <0.008 | 758 | 4 | 13 | 157 | 2781 | 17.71 |
| 110.00 | 120.00 | 622496 | cgri | 162 | 38 | 194 | <2.0 | <0.008 | 769 | 11 | 12 | 177 | 3094 | 17.48 |
| 120.00 | 130.00 | 622497 | cgri | 145 | 23 | 157 | <2.0 | <0.008 | 685 | 3 | 15 | 178 | 2972 | 16.70 |
| 130.00 | 140.00 | 622498 | cgri | 151 | 171 | 420 | <2.0 | <0.008 | 1091 | 4 | 17 | 175 | 3021 | 17.26 |
| 140.00 | 154.90 | 622499 | cgri | 105 | 1099 | 2471 | <2.0 | <0.008 | 1191 | <2 | 20 | 166 | 2869 | 17.28 |
| 154.90 | 158.20 | 622500 | cgri | 116 | 791 | 2115 | <2.0 | <0.008 | 1876 | 2 | 16 | 168 | 2872 | 17.10 |
| 158.20 | 170.00 | 622501 | cgri | 124 | 1575 | 2906 | <2.0 | <0.008 | 2571 | <2 | 18 | 167 | 2878 | 17.23 |
| 170.00 | 180.00 | 622502 | cgri | 222 | 1088 | 2255 | <2.0 | <0.008 | 2186 | 12 | 17 | 164 | 2909 | 17.74 |
| 180.00 | 189.50 | 622503 | cgri | 106 | 649 | 1319 | <2.0 | <0.008 | 2144 | 3 | 12 | 179 | 3004 | 16.78 |
| 189.50 | 199.70 | 622504 | cgri | 70 | 609 | 1194 | <2.0 | <0.008 | 1026 | <2 | 26 | 169 | 3024 | 17.89 |
| 199.70 | 211.00 | 622506 | cgri | 84 | 120 | 1257 | <2.0 | <0.008 | 917 | 6 | 16 | 154 | 2762 | 17.94 |
| 211.00 | 222.75 | 622507 | cgri | 93 | 16 | 345 | <2.0 | <0.008 | 698 | 5 | 23 | 167 | 2758 | 16.51 |
| 222.75 | 234.00 | 622508 | cgri | 116 | 61 | 293 | <2.0 | <0.008 | 873 | <2 | 20 | 167 | 2872 | 17.20 |
| 234.00 | 245.00 | 622509 | cgri | 145 | 112 | 282 | <2.0 | <0.008 | 556 | <2 | 26 | 161 | 2826 | 17.55 |
| 245.00 | 256.70 | 622510 | cgri | 92 | 35 | 257 | <2.0 | <0.008 | 797 | 6 | 26 | 173 | 2878 | 16.64 |
| 256.70 | 262.45 | 622511 | cgri | 81 | 37 | 208 | <2.0 | 0.010 | 565 | 44 | 57 | 189 | 3055 | 16.16 |
| 262.45 | 264.20 | 622512 | cgri | 82 | 861 | 4921 | 2.0 | 0.089 | 354 | 505 | 248 | 99 | 2098 | 21.19 |
| 264.20 | 276.00 | 622513 | cgri | 201 | 933 | 1625 | 3.0 | <0.008 | 1139 | 90 | 597 | 135 | 3016 | 22.34 |
| 276.00 | 288.00 | 622514 | cgri | 186 | 108 | 240 | <2.0 | <0.008 | 2167 | 15 | 634 | 142 | 3110 | 21.90 |
| 288.00 | 300.00 | 622515 | cgri | 199 | 187 | 548 | <2.0 | <0.008 | 1036 | 13 | 619 | 142 | 3188 | 22.45 |
| 300.00 | 311.50 | 622516 | cgri | 166 | 85 | 256 | <2.0 | <0.008 | 798 | 6 | 591 | 139 | 3005 | 21.62 |
| 311.50 | 322.00 | 622517 | cgri | 145 | 194 | 473 | <2.0 | <0.008 | 578 | 6 | 604 | 138 | 2964 | 21.48 |
| 322.00 | 337.10 | 622518 | cgri | 135 | 212 | 410 | <2.0 | <0.008 | 1343 | 6 | 651 | 118 | 2715 | 23.01 |
| 337.10 | 341.50 | 622519 | cgri | 123 | 83 | 191 | <2.0 | <0.008 | 1158 | 3 | 647 | 111 | 2471 | 22.26 |
| 341.50 | 344.00 | 622520 | cgri | 161 | 125 | 332 | <2.0 | <0.008 | 1917 | 5 | 964 | 158 | 3337 | 21.12 |
| 344.00 | 354.30 | 622521 | cgri | 110 | 76 | 156 | <2.0 | <0.008 | 776 | 4 | 566 | 104 | 2410 | 23.17 |
| 354.30 | 366.00 | 622522 | cgri | 177 | 189 | 329 | <2.0 | <0.008 | 1154 | 7 | 553 | 119 | 3009 | 25.29 |
| 366.00 | 377.00 | 622523 | cgri | 167 | 117 | 271 | <2.0 | <0.008 | 1469 | 3 | 371 | 99 | 2927 | 29.57 |
| 377.00 | 386.00 | 622524 | cgri | 125 | 72 | 288 | <2.0 | <0.008 | 1013 | 6 | 365 | 96 | 2836 | 29.54 |
| 386.00 | 395.30 | 622525 | cgri | 139 | 52 | 231 | <2.0 | <0.008 | 2521 | <2 | 338 | 86 | 2737 | 31.83 |
| 395.30 | 400.30 | 622526 | cgri | 149 | 25 | 140 | <2.0 | <0.008 | 966 | 2 | 258 | 86 | 2435 | 28.31 |
| 400.30 | 412.00 | 622527 | cgri | 220 | 47 | 236 | <2.0 | <0.008 | 2204 | 3 | 327 | 80 | 2781 | 34.76 |
| 412.00 | 425.00 | 622528 | cgri | 213 | 40 | 199 | <2.0 | <0.008 | 1210 | 2 | 306 | 76 | 2737 | 36.01 |
| 425.00 | 438.00 | 622529 | cgri | 135 | 41 | 140 | <2.0 | 0.010 | 944 | 6 | 321 | 77 | 2988 | 38.81 |
| 438.00 | 450.00 | 622530 | cgri | 193 | 40 | 159 | <2.0 | 0.008 | 1131 | 3 | 317 | 77 | 2699 | 35.05 |
| 450.00 | 461.00 | 622532 | cgri | 205 | 30 | 178 | <2.0 | <0.008 | 1088 | 2 | 396 | 73 | 2687 | 36.81 |
| 461.00 | 473.00 | 622533 | cgri | 243 | 31 | 212 | <2.0 | <0.008 | 1447 | 3 | 359 | 75 | 2500 | 33.33 |
| 473.00 | 484.00 | 622534 | cgri | 307 | 37 | 278 | <2.0 | <0.008 | 747 | 6 | 290 | 76 | 2729 | 35.91 |
| 484.00 | 496.00 | 622535 | cgri | 269 | 45 | 252 | <2.0 | <0.008 | 631 | 4 | 275 | 66 | 2643 | 40.05 |
| 496.00 | 508.00 | 622536 | cgri | 347 | 44 | 320 | <2.0 | <0.008 | 799 | 3 | 269 | 74 | 2727 | 36.85 |
| 508.00 | 520.00 | 622537 | cgri | 325 | 98 | 324 | <2.0 | <0.008 | 577 | <2 | 262 | 66 | 2708 | 41.03 |
| 520.00 | 532.00 | 622538 | cgri | 239 | 62 | 267 | <2.0 | <0.008 | 515 | 2 | 260 | 70 | 2625 | 37.50 |
| 532.00 | 544.00 | 622539 | cgri | 223 | 33 | 260 | <2.0 | <0.008 | 1217 | <2 | 253 | 69 | 2601 | 37.70 |
| 544.00 | 554.00 | 622540 | cgri | 165 | 86 | 538 | 6.0 | <0.008 | 376 | <2 | 262 | 85 | 2688 | 31.62 |
| 554.00 | 566.00 | 622541 | cgri | 135 | 25 | 366 | <2.0 | <0.008 | 841 | 4 | 245 | 66 | 2733 | 41.41 |
| 566.00 | 577.00 | 622542 | cgri | 263 | 38 | 459 | <2.0 | <0.008 | 1269 | 2 | 245 | 72 | 2717 | 37.74 |
| 577.00 | 588.30 | 622543 | cgri | 282 | 32 | 810 | 2.0 | <0.008 | 544 | 4 | 230 | 77 | 2691 | 34.95 |
| 588.30 | 598.00 | 622544 | cgri | 220 | 24 | 449 | <2.0 | <0.008 | 1467 | <2 | 164 | 82 | 2644 | 32.24 |
| 598.00 | 608.20 | 622545 | cgri | 105 | 59 | 469 | <2.0 | <0.008 | 480 | <2 | 171 | 82 | 2701 | 32.94 |
| 608.20 | 620.00 | 622546 | cgri | 90 | 21 | 346 | <2.0 | <0.008 | 427 | <2 | 161 | 82 | 2858 | 34.85 |
| 620.00 | 632.00 | 622547 | cgri | 91 | 19 | 145 | <2.0 | <0.008 | 580 | <2 | 45 | 87 | 2530 | 29.08 |
| 632.00 | 644.00 | 622548 | cgri | 120 | 13 | 144 | <2.0 | <0.008 | 699 | 4 | 51 | 75 | 2760 | 36.80 |
| 644.00 | 656.00 | 622549 | cgri | 94 | 69 | 248 | <2.0 | <0.008 | 815 | <2 | 56 | 81 | 2709 | 33.44 |
| 656.00 | 668.00 | 622550 | cgri | 126 | 47 | 274 | <2.0 | <0.008 | 931 | <2 | 55 | 75 | 2976 | 39.68 |
| 668.00 | 680.00 | 622551 | cgri | 129 | 38 | 308 | <2.0 | <0.008 | 606 | 2 | 55 | 80 | 2856 | 35.70 |
| 680.00 | 692.00 | 622552 | cgri | 152 | 33 | 343 | <2.0 | <0.008 | 1184 | <2 | 50 | 66 | 2856 | 43.27 |
| 692.00 | 704.00 | 622553 | cgri | 96 | 33 | 168 | <2.0 | <0.008 | 781 | 2 | 53 | 68 | 2910 | 42.79 |
| 704.00 | 716.00 | 622554 | cgri | 63 | 20 | 209 | <2.0 | <0.008 | 535 | <2 | 53 | 61 | 2777 | 45.52 |
| 716.00 | 726.00 | 622555 | cgri | 52 | 30 | 189 | <2.0 | <0.008 | 530 | <2 | 55 | 153 | 2867 | 18.74 |
| 726.00 | 736.00 | 622556 | cgri | 54 | 17 | 174 | <2.0 | <0.008 | 441 | <2 | 45 | 172 | 2837 | 16.49 |
| 736.00 | 746.70 | 622557 | cgri | 73 | 30 | 157 | <2.0 | <0.008 | 1766 | <2 | 89 | 89 | 2877 | 32.33 |
| 746.70 | 758.00 | 622558 | cgri | 17 | 5 | 88 | <2.0 | <0.008 | 556 | <2 | 38 | 293 | 2561 | 8.74 |
| 758.00 | 770.00 | 622559 | cgri | 21 | 13 | 72 | <2.0 | <0.008 | 413 | 2 | 44 | 271 | 2570 | 9.48 |
| 770.00 | 778.10 | 622560 | cgri | 29 | 10 | 212 | <2.0 | <0.008 | 508 | 3 | 57 | 307 | 2667 | 8.69 |

# ABERFOYLE RESOURCES LTD. DRILL LOG

**Area Code** mac | **Prospect** Murchison Zone | **Report Grid** Mack | **Dataset** Geochemical data set

**Holename** DDMA0035 | **Stored Grid** Mack

| From | To | Sample | Type | Cu ppm | Pb ppm | Zn ppm | Ag ppm | Au ppm | Ba ppm | As ppm | Cr ppm | Zr ppm | Ti ppm | Ti/Zr |
|---|---|---|---|---|---|---|---|---|---|---|---|---|---|---|
| 778.10 | 788.00 | 622561 | cgri | 26 | 16 | 80 | <2.0 | <0.008 | 541 | 2 | 8 | 248 | 2631 | 10.61 |
| 788.00 | 798.00 | 622562 | cgri | 23 | 38 | 98 | <2.0 | <0.008 | 769 | 4 | 17 | 285 | 2732 | 9.59 |
| 798.00 | 806.90 | 622563 | cgri | 70 | 54 | 467 | <2.0 | <0.008 | 604 | <2 | 81 | 284 | 2692 | 9.48 |
| 806.90 | 818.00 | 622564 | cgri | 32 | 12 | 63 | <2.0 | <0.008 | 506 | <2 | 8 | 210 | 2630 | 12.52 |
| 818.00 | 830.00 | 622565 | cgri | 100 | 29 | 58 | <2.0 | <0.008 | 751 | 2 | 9 | 230 | 2446 | 10.63 |
| 830.00 | 842.00 | 622566 | cgri | 81 | 17 | 98 | <2.0 | <0.008 | 925 | <2 | 13 | 46 | 2143 | 46.59 |
| 842.00 | 856.00 | 622567 | cgri | 21 | 51 | 67 | <2.0 | <0.008 | 735 | <2 | 13 | 214 | 1900 | 8.88 |
| 856.00 | 866.00 | 622568 | cgri | 39 | 24 | 71 | <2.0 | <0.008 | 667 | <2 | 18 | 35 | 1930 | 55.14 |
| 866.00 | 876.00 | 622569 | cgri | 42 | 52 | 103 | <2.0 | <0.008 | 701 | <2 | 24 | 76 | 1905 | 25.07 |
| 876.00 | 886.00 | 622570 | cgri | 78 | 28 | 98 | <2.0 | <0.008 | 1382 | 6 | 18 | 76 | 1871 | 24.62 |
| 886.00 | 895.80 | 622571 | cgri | 34 | 17 | 59 | <2.0 | <0.008 | 652 | 6 | 13 | 62 | 1743 | 28.11 |
| 895.80 | 897.50 | 622572 | cgri | 41 | 6 | 94 | <2.0 | <0.008 | 548 | 3 | 31 | 97 | 2623 | 27.04 |
| 897.50 | 908.90 | 622573 | cgri | 17 | <5 | 59 | <2.0 | <0.008 | 660 | 2 | 8 | 85 | 1642 | 19.32 |
| 908.90 | 913.80 | 622574 | cgri | 31 | 33 | 84 | <2.0 | <0.008 | 586 | <2 | 26 | 112 | 2456 | 21.93 |
| 913.80 | 924.00 | 622575 | cgri | 36 | 32 | 73 | <2.0 | <0.008 | 584 | 4 | 9 | 206 | 1790 | 8.69 |
| 924.00 | 933.20 | 622576 | cgri | 22 | 11 | 41 | <2.0 | <0.008 | 604 | 4 | <5 | 205 | 1640 | 8.00 |
| 933.20 | 937.80 | 622577 | cgri | 30 | 21 | 87 | <2.0 | <0.008 | 372 | 6 | 28 | 44 | 2186 | 49.68 |
| 937.80 | 950.00 | 622578 | cgri | 25 | 25 | 49 | <2.0 | <0.008 | 470 | 9 | 40 | 195 | 2055 | 10.54 |
| 950.00 | 963.70 | 622579 | cgri | 20 | 19 | 38 | <2.0 | <0.008 | 542 | 3 | 15 | 203 | 1871 | 9.22 |
| 963.70 | 975.00 | 622580 | cgri | 13 | 16 | 87 | <2.0 | <0.008 | 349 | 2 | 21 | 191 | 2436 | 12.75 |
| 975.00 | 987.00 | 622581 | cgri | 31 | 6 | 91 | <2.0 | <0.008 | 654 | 2 | 17 | 200 | 2517 | 12.58 |
| 987.00 | 998.00 | 622582 | cgri | 17 | 13 | 70 | <2.0 | <0.008 | 544 | <2 | 17 | 201 | 2478 | 12.33 |
| 998.00 | 1008.00 | 622583 | cgri | 19 | 44 | 71 | <2.0 | <0.008 | 615 | 3 | 18 | 202 | 2389 | 11.83 |
| 1008.00 | 1020.80 | 622584 | cgri | 21 | 23 | 81 | <2.0 | <0.008 | 426 | 3 | 50 | 186 | 2411 | 12.96 |
| 1020.80 | 1031.00 | 622585 | cgri | 23 | 13 | 74 | <2.0 | <0.008 | 710 | <2 | 37 | 182 | 2380 | 13.08 |
| 1031.00 | 1040.50 | 622586 | cgri | 23 | 12 | 70 | <2.0 | <0.008 | 898 | 2 | 29 | 190 | 2380 | 12.53 |
| 1040.50 | 1055.80 | 622587 | cgri | 17 | 17 | 97 | <2.0 | <0.008 | 1084 | <2 | 28 | 168 | 2454 | 14.61 |
| 1055.80 | 1063.20 | 622588 | cgri | 36 | 22 | 90 | <2.0 | <0.008 | 474 | 2 | 58 | 196 | 2414 | 12.32 |
| 1063.20 | 1086.10 | 622589 | cgri | 28 | 35 | 90 | <2.0 | <0.008 | 849 | <2 | 31 | 174 | 2367 | 13.60 |
| 1086.10 | 1088.90 | 622591 | cgri | 88 | 8 | 118 | <2.0 | <0.008 | 1515 | 3 | 35 | 192 | 2500 | 13.02 |
| 1088.90 | 1099.00 | 622592 | cgri | 24 | 29 | 120 | <2.0 | <0.008 | 1192 | 4 | 49 | 191 | 2350 | 12.30 |
| 1099.00 | 1109.50 | 622593 | cgri | 33 | 14 | 103 | <2.0 | <0.008 | 2498 | 5 | 56 | 186 | 2386 | 12.83 |
| 1109.50 | 1112.20 | 622594 | cgri | 76 | 16 | 125 | <2.0 | <0.008 | 2124 | 6 | 63 | 189 | 2410 | 12.75 |
| 1112.20 | 1123.00 | 622595 | cgri | 36 | 21 | 105 | <2.0 | <0.008 | 1015 | <2 | 94 | 176 | 2356 | 13.39 |
| 1123.00 | 1135.30 | 622596 | cgri | 21 | 36 | 101 | <2.0 | <0.008 | 1032 | <2 | 94 | 181 | 2395 | 13.23 |
| 1135.30 | 1150.90 | 622597 | cgri | 121 | 23 | 144 | <2.0 | <0.008 | 1307 | <2 | 153 | 181 | 2526 | 13.96 |
| 1150.90 | 1165.00 | 622598 | cgri | 13 | 29 | 139 | <2.0 | <0.008 | 462 | <2 | 104 | 187 | 2568 | 13.73 |
| 1165.00 | 1179.30 | 622599 | cgri | 10 | 43 | 109 | <2.0 | <0.008 | 513 | <2 | 97 | 179 | 2369 | 13.23 |
| 1179.30 | 1188.30 | 622600 | cgri | 18 | 17 | 63 | <2.0 | <0.008 | 1211 | 2 | 5 | 203 | 2020 | 9.95 |
| 1188.30 | 1189.60 | 622601 | cgri | 98 | 16 | 123 | <2.0 | <0.008 | 943 | 6 | 235 | 130 | 2461 | 18.93 |

# ABERFOYLE RESOURCES LTD. DRILL LOG

**Area Code** mac | **Prospect** Murchison Zone | **Report Grid** Mack | **Dataset** Geochemical data set

**Holename** DDMA0035 | **Stored Grid** Mack

| From | To | SiO2 % | TiO2 % | Al2O3 % | Fe2O3 % | MnO % | MgO % | CaO % | Na2O % | K2O % | P2O5 % | LOI % | TOTAL % |
|---|---|---|---|---|---|---|---|---|---|---|---|---|---|
| 2.90 | 9.30 | 53.20 | 0.63 | 20.87 | 8.00 | 0.29 | 2.15 | 1.73 | 0.66 | 1.47 | 0.40 | 10.41 | 99.87 |
| 9.30 | 20.20 | 58.60 | 0.60 | 17.80 | 7.55 | 0.14 | 2.41 | 2.38 | 2.43 | 1.84 | 0.33 | 5.71 | 99.76 |
| 20.20 | 30.10 | 59.60 | 0.54 | 16.63 | 7.51 | 0.15 | 3.16 | 1.28 | 3.68 | 2.16 | 0.31 | 4.13 | 99.59 |
| 30.10 | 40.00 | 60.60 | 0.55 | 16.50 | 7.41 | 0.16 | 2.47 | 2.72 | 4.69 | 1.15 | 0.30 | 3.10 | 100.01 |
| 40.00 | 50.10 | 58.90 | 0.53 | 16.98 | 7.05 | 0.14 | 2.70 | 3.20 | 3.87 | 1.89 | 0.30 | 3.48 | 99.51 |
| 50.10 | 60.00 | 58.80 | 0.55 | 16.12 | 7.55 | 0.14 | 3.94 | 2.82 | 3.72 | 1.53 | 0.29 | 4.51 | 100.44 |
| 60.00 | 70.00 | 57.30 | 0.53 | 16.19 | 7.34 | 0.15 | 4.04 | 2.99 | 4.26 | 1.12 | 0.29 | 5.27 | 100.02 |
| 70.00 | 80.00 | 56.60 | 0.54 | 15.89 | 7.16 | 0.23 | 4.13 | 3.70 | 3.60 | 1.43 | 0.28 | 5.69 | 99.97 |
| 80.00 | 90.00 | 56.80 | 0.52 | 16.34 | 6.55 | 0.23 | 3.47 | 3.53 | 2.90 | 2.37 | 0.27 | 6.53 | 100.40 |
| 90.00 | 100.00 | 61.00 | 0.50 | 15.56 | 6.30 | 0.18 | 3.67 | 2.81 | 4.32 | 1.22 | 0.25 | 4.00 | 100.46 |
| 100.00 | 110.00 | 55.00 | 0.46 | 14.21 | 6.04 | 0.16 | 3.30 | 7.11 | 3.12 | 1.61 | 0.23 | 7.86 | 99.80 |
| 110.00 | 120.00 | 59.30 | 0.52 | 15.77 | 6.00 | 0.12 | 2.37 | 5.53 | 4.04 | 1.36 | 0.25 | 4.39 | 100.05 |
| 120.00 | 130.00 | 60.10 | 0.50 | 15.19 | 5.91 | 0.13 | 3.04 | 4.57 | 3.59 | 1.57 | 0.25 | 4.62 | 99.98 |
| 130.00 | 140.00 | 61.20 | 0.50 | 15.18 | 5.92 | 0.17 | 2.43 | 4.54 | 3.24 | 1.80 | 0.25 | 4.26 | 99.86 |
| 140.00 | 154.90 | 58.50 | 0.48 | 14.99 | 6.10 | 0.30 | 2.52 | 4.64 | 3.55 | 1.80 | 0.26 | 5.41 | 99.50 |
| 154.90 | 158.20 | 58.60 | 0.48 | 15.20 | 5.98 | 0.33 | 2.02 | 4.48 | 3.86 | 1.98 | 0.25 | 5.60 | 99.64 |
| 158.20 | 170.00 | 59.90 | 0.48 | 15.10 | 5.66 | 0.41 | 2.02 | 4.07 | 3.85 | 2.15 | 0.25 | 4.83 | 99.62 |
| 170.00 | 180.00 | 60.60 | 0.49 | 14.88 | 5.78 | 0.40 | 2.25 | 4.28 | 4.04 | 1.84 | 0.24 | 4.05 | 99.57 |
| 180.00 | 189.50 | 59.70 | 0.50 | 15.46 | 6.00 | 0.27 | 2.02 | 4.64 | 3.77 | 2.06 | 0.25 | 4.42 | 99.65 |
| 189.50 | 199.70 | 59.40 | 0.50 | 15.17 | 6.26 | 0.22 | 2.38 | 4.36 | 2.73 | 2.33 | 0.25 | 5.66 | 99.94 |
| 199.70 | 211.00 | 56.70 | 0.46 | 14.14 | 6.13 | 0.23 | 2.61 | 6.43 | 2.40 | 2.10 | 0.24 | 6.88 | 99.58 |
| 211.00 | 222.75 | 60.90 | 0.46 | 14.95 | 7.80 | 0.21 | 3.50 | 2.18 | 3.17 | 1.62 | 0.24 | 4.38 | 99.67 |
| 222.75 | 234.00 | 60.30 | 0.48 | 14.56 | 5.94 | 0.22 | 2.18 | 5.11 | 3.12 | 1.90 | 0.24 | 5.44 | 99.68 |
| 234.00 | 245.00 | 63.10 | 0.47 | 14.33 | 4.92 | 0.19 | 1.94 | 3.87 | 4.00 | 1.48 | 0.24 | 4.80 | 99.58 |
| 245.00 | 256.70 | 61.10 | 0.48 | 15.05 | 6.39 | 0.22 | 2.42 | 3.58 | 3.25 | 1.90 | 0.25 | 4.75 | 99.60 |
| 256.70 | 262.45 | 56.40 | 0.51 | 16.04 | 6.54 | 0.20 | 2.58 | 4.97 | 1.10 | 3.21 | 0.25 | 7.11 | 99.66 |
| 262.45 | 264.20 | 32.40 | 0.35 | 9.29 | 9.50 | 0.64 | 1.94 | 19.28 | 0.23 | 2.59 | 0.34 | 18.48 | 99.81 |
| 264.20 | 276.00 | 41.30 | 0.50 | 10.31 | 11.58 | 0.40 | 5.04 | 12.45 | 2.26 | 0.99 | 0.54 | 10.26 | 100.35 |
| 276.00 | 288.00 | 43.00 | 0.52 | 11.02 | 8.14 | 0.38 | 6.14 | 16.35 | 2.13 | 1.26 | 0.54 | 8.73 | 99.71 |
| 288.00 | 300.00 | 44.20 | 0.53 | 10.93 | 7.48 | 0.30 | 5.64 | 16.80 | 2.34 | 0.91 | 0.53 | 8.65 | 99.63 |
| 300.00 | 311.50 | 46.40 | 0.50 | 10.87 | 7.47 | 0.27 | 6.31 | 15.46 | 1.71 | 0.90 | 0.50 | 8.75 | 99.54 |
| 311.50 | 322.00 | 44.60 | 0.49 | 11.24 | 8.20 | 0.28 | 7.59 | 13.90 | 1.71 | 0.65 | 0.51 | 10.03 | 99.65 |
| 322.00 | 337.10 | 39.10 | 0.45 | 9.51 | 7.28 | 0.33 | 5.97 | 20.42 | 1.72 | 1.38 | 0.46 | 12.43 | 99.55 |
| 337.10 | 341.50 | 35.40 | 0.41 | 8.67 | 6.25 | 0.28 | 5.01 | 24.72 | 1.25 | 1.38 | 0.42 | 15.67 | 99.69 |
| 341.50 | 344.00 | 51.50 | 0.56 | 12.26 | 8.71 | 0.33 | 6.96 | 10.22 | 1.20 | 2.75 | 0.51 | 4.46 | 99.61 |
| 344.00 | 354.30 | 33.80 | 0.40 | 8.35 | 5.89 | 0.27 | 4.81 | 25.78 | 1.33 | 1.05 | 0.42 | 17.48 | 99.64 |
| 354.30 | 366.00 | 52.10 | 0.50 | 12.70 | 8.93 | 0.28 | 7.41 | 9.78 | 1.83 | 1.40 | 0.37 | 4.23 | 99.65 |
| 366.00 | 377.00 | 51.10 | 0.49 | 12.75 | 9.20 | 0.23 | 9.21 | 7.56 | 2.01 | 1.33 | 0.29 | 5.50 | 99.72 |
| 377.00 | 386.00 | 50.60 | 0.47 | 12.91 | 9.55 | 0.23 | 7.91 | 9.08 | 2.34 | 1.06 | 0.29 | 5.09 | 99.61 |
| 386.00 | 395.30 | 52.40 | 0.46 | 12.88 | 8.87 | 0.20 | 7.58 | 9.04 | 1.97 | 1.79 | 0.29 | 4.15 | 99.65 |
| 395.30 | 400.30 | 45.70 | 0.41 | 10.98 | 7.59 | 0.20 | 6.36 | 15.87 | 2.60 | 0.91 | 0.29 | 9.21 | 100.11 |
| 400.30 | 412.00 | 53.40 | 0.46 | 12.73 | 8.76 | 0.18 | 7.43 | 8.51 | 2.06 | 2.10 | 0.28 | 3.59 | 99.55 |
| 412.00 | 425.00 | 52.20 | 0.46 | 12.97 | 8.95 | 0.17 | 7.56 | 9.68 | 2.39 | 1.43 | 0.29 | 3.55 | 99.67 |
| 425.00 | 438.00 | 52.60 | 0.50 | 13.54 | 9.54 | 0.15 | 7.82 | 8.62 | 2.29 | 1.24 | 0.30 | 3.21 | 99.90 |
| 438.00 | 450.00 | 51.50 | 0.45 | 12.45 | 8.72 | 0.17 | 7.20 | 10.56 | 2.34 | 1.41 | 0.28 | 4.69 | 99.76 |
| 450.00 | 461.00 | 53.60 | 0.45 | 13.10 | 8.99 | 0.18 | 7.47 | 8.89 | 2.44 | 1.42 | 0.25 | 3.01 | 99.80 |
| 461.00 | 473.00 | 51.30 | 0.42 | 12.34 | 8.57 | 0.20 | 7.09 | 10.79 | 2.07 | 1.73 | 0.24 | 4.78 | 99.57 |
| 473.00 | 484.00 | 54.40 | 0.46 | 13.83 | 8.81 | 0.17 | 6.84 | 8.44 | 2.78 | 0.95 | 0.19 | 2.71 | 99.60 |
| 484.00 | 496.00 | 53.20 | 0.44 | 13.93 | 8.78 | 0.18 | 6.93 | 8.51 | 2.43 | 0.72 | 0.19 | 4.20 | 99.62 |
| 496.00 | 508.00 | 53.70 | 0.45 | 14.08 | 8.76 | 0.18 | 6.71 | 9.01 | 2.17 | 1.20 | 0.19 | 3.56 | 100.07 |
| 508.00 | 520.00 | 53.90 | 0.45 | 13.47 | 8.40 | 0.18 | 6.56 | 9.07 | 2.34 | 0.91 | 0.18 | 4.71 | 100.22 |
| 520.00 | 532.00 | 49.50 | 0.44 | 13.13 | 8.36 | 0.24 | 6.97 | 10.98 | 2.19 | 0.78 | 0.18 | 7.25 | 100.07 |
| 532.00 | 544.00 | 49.80 | 0.43 | 13.55 | 8.97 | 0.23 | 7.80 | 9.62 | 2.19 | 0.65 | 0.18 | 6.70 | 100.22 |
| 544.00 | 554.00 | 50.70 | 0.45 | 13.98 | 9.22 | 0.37 | 8.26 | 6.52 | 2.32 | 0.41 | 0.17 | 7.42 | 99.88 |
| 554.00 | 566.00 | 53.20 | 0.46 | 14.26 | 9.31 | 0.51 | 6.51 | 8.26 | 2.30 | 0.82 | 0.17 | 4.47 | 100.24 |
| 566.00 | 577.00 | 52.30 | 0.45 | 14.01 | 9.03 | 0.46 | 6.54 | 8.87 | 2.29 | 0.98 | 0.16 | 4.40 | 99.51 |
| 577.00 | 588.30 | 53.40 | 0.45 | 13.59 | 9.18 | 0.55 | 6.26 | 8.29 | 2.55 | 0.39 | 0.15 | 5.01 | 99.83 |
| 588.30 | 598.00 | 52.40 | 0.44 | 14.86 | 9.58 | 0.53 | 7.10 | 5.76 | 2.22 | 1.18 | 0.13 | 5.94 | 100.18 |
| 598.00 | 608.20 | 50.90 | 0.45 | 14.36 | 11.04 | 0.48 | 6.00 | 5.34 | 1.97 | 0.77 | 0.13 | 7.96 | 99.55 |
| 608.20 | 620.00 | 50.60 | 0.48 | 14.47 | 9.94 | 0.37 | 5.00 | 6.97 | 2.38 | 1.02 | 0.21 | 8.44 | 99.88 |
| 620.00 | 632.00 | 49.60 | 0.42 | 14.09 | 9.57 | 0.35 | 3.54 | 8.69 | 1.30 | 2.06 | 0.14 | 9.72 | 99.57 |
| 632.00 | 644.00 | 51.80 | 0.46 | 14.64 | 7.91 | 0.27 | 2.53 | 9.06 | 3.35 | 1.45 | 0.14 | 8.62 | 100.39 |
| 644.00 | 656.00 | 53.70 | 0.45 | 14.97 | 8.67 | 0.25 | 3.11 | 7.07 | 2.70 | 1.42 | 0.14 | 7.45 | 100.00 |
| 656.00 | 668.00 | 55.20 | 0.50 | 15.69 | 9.33 | 0.27 | 4.03 | 4.27 | 3.41 | 1.18 | 0.15 | 5.41 | 99.53 |
| 668.00 | 680.00 | 55.20 | 0.48 | 15.45 | 7.69 | 0.27 | 3.15 | 7.42 | 3.38 | 1.13 | 0.15 | 5.49 | 99.83 |
| 680.00 | 692.00 | 54.50 | 0.48 | 15.62 | 7.32 | 0.24 | 2.93 | 8.59 | 3.16 | 1.06 | 0.15 | 5.70 | 99.77 |
| 692.00 | 704.00 | 56.00 | 0.49 | 15.59 | 8.17 | 0.20 | 3.51 | 7.78 | 2.07 | 1.39 | 0.15 | 4.96 | 100.27 |
| 704.00 | 716.00 | 53.60 | 0.46 | 15.42 | 8.59 | 0.28 | 4.98 | 6.08 | 2.64 | 1.00 | 0.15 | 6.20 | 99.72 |
| 716.00 | 726.00 | 54.30 | 0.48 | 15.23 | 8.04 | 0.30 | 4.04 | 6.19 | 3.39 | 0.95 | 0.15 | 6.32 | 99.51 |
| 726.00 | 736.00 | 52.90 | 0.47 | 15.18 | 7.94 | 0.26 | 3.36 | 8.79 | 2.97 | 0.96 | 0.15 | 6.63 | 99.61 |
| 736.00 | 746.70 | 51.40 | 0.48 | 14.90 | 7.67 | 0.25 | 3.48 | 9.10 | 2.48 | 1.41 | 0.19 | 8.15 | 99.54 |
| 746.70 | 758.00 | 46.80 | 0.43 | 13.57 | 6.60 | 0.25 | 3.05 | 12.29 | 2.43 | 1.71 | 0.14 | 12.20 | 99.52 |
| 758.00 | 770.00 | 48.40 | 0.43 | 13.77 | 7.59 | 0.26 | 2.26 | 11.49 | 2.98 | 1.61 | 0.15 | 10.89 | 99.91 |
| 770.00 | 778.10 | 49.90 | 0.44 | 14.55 | 13.14 | 0.34 | 4.90 | 5.40 | 2.18 | 1.25 | 0.13 | 8.04 | 100.44 |

# ABERFOYLE RESOURCES LTD. DRILL LOG

**Area Code** mac
**Prospect** Murchison Zone
**Report Grid** Mack
**Dataset** Geochemical data set

**Holename** DDMA0035
**Stored Grid** Mack

| From | To | SiO2 % | TiO2 % | Al2O3 % | Fe2O3 % | MnO % | MgO % | CaO % | Na2O % | K2O % | P2O5 % | LOI % | TOTAL % |
|---|---|---|---|---|---|---|---|---|---|---|---|---|---|
| 778.10 | 788.00 | 63.30 | 0.44 | 14.57 | 6.47 | 0.17 | 1.85 | 3.16 | 2.48 | 2.24 | 0.15 | 4.87 | 99.82 |
| 788.00 | 798.00 | 61.80 | 0.46 | 15.07 | 6.59 | 0.17 | 1.90 | 3.36 | 3.02 | 2.09 | 0.14 | 5.07 | 99.84 |
| 798.00 | 806.90 | 54.70 | 0.45 | 14.65 | 8.41 | 0.29 | 3.61 | 6.10 | 3.55 | 0.99 | 0.14 | 7.42 | 100.34 |
| 806.90 | 818.00 | 66.40 | 0.44 | 14.68 | 4.25 | 0.13 | 1.10 | 2.67 | 4.35 | 1.63 | 0.10 | 3.91 | 99.71 |
| 818.00 | 830.00 | 64.30 | 0.41 | 14.70 | 5.01 | 0.18 | 1.22 | 3.44 | 2.41 | 2.83 | 0.09 | 5.06 | 99.74 |
| 830.00 | 842.00 | 65.50 | 0.36 | 14.36 | 4.35 | 0.16 | 1.04 | 3.48 | 1.12 | 3.61 | 0.08 | 5.39 | 99.58 |
| 842.00 | 856.00 | 68.60 | 0.32 | 14.03 | 3.89 | 0.10 | 0.81 | 2.76 | 2.85 | 2.52 | 0.07 | 4.11 | 100.18 |
| 856.00 | 866.00 | 67.80 | 0.32 | 14.41 | 3.90 | 0.11 | 0.76 | 2.31 | 3.61 | 2.31 | 0.07 | 3.90 | 99.50 |
| 866.00 | 876.00 | 68.40 | 0.32 | 14.00 | 4.08 | 0.12 | 0.69 | 2.12 | 4.29 | 1.90 | 0.07 | 3.46 | 99.57 |
| 876.00 | 886.00 | 68.20 | 0.31 | 13.93 | 4.25 | 0.12 | 0.79 | 2.17 | 3.15 | 3.02 | 0.06 | 3.44 | 99.65 |
| 886.00 | 895.80 | 67.00 | 0.29 | 14.02 | 3.91 | 0.14 | 0.87 | 3.38 | 2.17 | 2.88 | 0.06 | 4.81 | 99.64 |
| 895.80 | 897.50 | 48.90 | 0.44 | 15.76 | 11.01 | 0.29 | 3.17 | 7.13 | 1.49 | 2.18 | 0.11 | 9.52 | 100.21 |
| 897.50 | 908.90 | 66.20 | 0.27 | 13.43 | 5.29 | 0.18 | 1.31 | 3.40 | 0.94 | 3.18 | 0.05 | 5.20 | 99.53 |
| 908.90 | 913.80 | 49.30 | 0.41 | 14.96 | 11.87 | 0.31 | 3.31 | 6.52 | 0.99 | 2.53 | 0.10 | 9.27 | 99.73 |
| 913.80 | 924.00 | 63.80 | 0.30 | 13.66 | 2.60 | 0.21 | 0.83 | 5.80 | 0.87 | 3.82 | 0.07 | 7.52 | 99.60 |
| 924.00 | 933.20 | 61.20 | 0.27 | 13.87 | 3.79 | 0.23 | 1.16 | 6.55 | 0.12 | 4.27 | 0.05 | 8.55 | 100.25 |
| 933.20 | 937.80 | 45.20 | 0.36 | 13.86 | 11.63 | 0.33 | 3.78 | 8.21 | 1.11 | 2.37 | 0.09 | 13.17 | 100.34 |
| 937.80 | 950.00 | 61.90 | 0.34 | 13.41 | 4.60 | 0.19 | 1.59 | 5.93 | 0.76 | 3.46 | 0.10 | 7.66 | 100.19 |
| 950.00 | 963.70 | 63.80 | 0.31 | 13.19 | 2.48 | 0.19 | 0.99 | 6.38 | 0.33 | 4.06 | 0.09 | 7.62 | 99.55 |
| 963.70 | 975.00 | 64.50 | 0.41 | 14.41 | 5.93 | 0.10 | 2.60 | 2.57 | 1.58 | 2.26 | 0.10 | 5.04 | 99.57 |
| 975.00 | 987.00 | 64.60 | 0.42 | 14.96 | 6.42 | 0.09 | 2.59 | 1.53 | 3.10 | 1.98 | 0.11 | 3.99 | 99.91 |
| 987.00 | 998.00 | 65.60 | 0.41 | 14.81 | 6.34 | 0.09 | 2.02 | 1.48 | 2.77 | 2.23 | 0.11 | 3.80 | 99.67 |
| 998.00 | 1008.00 | 65.50 | 0.40 | 14.34 | 5.45 | 0.13 | 1.09 | 2.57 | 2.05 | 2.76 | 0.10 | 5.09 | 99.56 |
| 1008.00 | 1020.80 | 63.60 | 0.40 | 14.36 | 5.98 | 0.14 | 1.26 | 3.20 | 3.32 | 1.50 | 0.10 | 5.64 | 99.59 |
| 1020.80 | 1031.00 | 63.90 | 0.40 | 14.10 | 4.97 | 0.14 | 0.98 | 3.90 | 2.07 | 3.01 | 0.10 | 6.03 | 99.61 |
| 1031.00 | 1040.50 | 64.70 | 0.40 | 13.88 | 3.98 | 0.11 | 0.78 | 4.52 | 4.04 | 2.53 | 0.10 | 4.66 | 99.73 |
| 1040.50 | 1055.80 | 64.70 | 0.41 | 14.39 | 5.36 | 0.10 | 2.07 | 2.55 | 3.53 | 1.87 | 0.13 | 4.41 | 99.55 |
| 1055.80 | 1063.20 | 64.80 | 0.40 | 14.41 | 6.64 | 0.13 | 1.52 | 2.63 | 3.14 | 1.95 | 0.10 | 4.21 | 100.01 |
| 1063.20 | 1086.10 | 65.10 | 0.39 | 13.94 | 4.59 | 0.13 | 1.11 | 4.21 | 3.76 | 2.18 | 0.11 | 4.81 | 100.35 |
| 1086.10 | 1088.90 | 65.70 | 0.42 | 14.30 | 5.42 | 0.12 | 1.45 | 2.27 | 3.44 | 3.06 | 0.10 | 3.27 | 99.68 |
| 1088.90 | 1099.00 | 63.70 | 0.39 | 13.53 | 4.71 | 0.13 | 1.15 | 4.48 | 3.67 | 2.68 | 0.10 | 5.00 | 99.54 |
| 1099.00 | 1109.50 | 65.00 | 0.40 | 14.38 | 5.38 | 0.13 | 1.16 | 2.73 | 3.49 | 3.05 | 0.10 | 3.73 | 99.67 |
| 1109.50 | 1112.20 | 63.60 | 0.40 | 14.52 | 5.96 | 0.16 | 1.74 | 3.59 | 2.46 | 3.40 | 0.10 | 3.56 | 99.63 |
| 1112.20 | 1123.00 | 61.70 | 0.39 | 13.91 | 5.60 | 0.17 | 1.29 | 5.03 | 3.88 | 2.51 | 0.10 | 5.05 | 99.67 |
| 1123.00 | 1135.30 | 63.40 | 0.40 | 13.87 | 4.38 | 0.14 | 0.94 | 5.11 | 4.94 | 2.49 | 0.10 | 4.33 | 100.12 |
| 1135.30 | 1150.90 | 60.70 | 0.42 | 14.30 | 7.22 | 0.15 | 4.19 | 2.57 | 3.43 | 1.43 | 0.13 | 4.97 | 99.59 |
| 1150.90 | 1165.00 | 62.80 | 0.43 | 14.47 | 7.22 | 0.12 | 4.01 | 1.68 | 3.40 | 1.25 | 0.10 | 4.17 | 99.69 |
| 1165.00 | 1179.30 | 61.00 | 0.40 | 13.58 | 7.13 | 0.17 | 2.08 | 4.63 | 2.99 | 1.55 | 0.10 | 5.90 | 99.54 |
| 1179.30 | 1188.30 | 62.70 | 0.34 | 13.07 | 3.23 | 0.13 | 0.35 | 6.77 | 3.03 | 3.75 | 0.09 | 6.12 | 99.59 |
| 1188.30 | 1189.60 | 52.80 | 0.41 | 12.94 | 7.65 | 0.24 | 4.45 | 9.42 | 3.10 | 1.88 | 0.24 | 6.71 | 99.85 |

# ABERFOYLE RESOURCES LTD. DRILL LOG

**Area Code** mac
**Prospect** Murchison Zone
**Report Grid** Mack
**Dataset** Geochemical data set

**Holename** DDMA0035
**Stored Grid** Mack

| From | To | S % | P2O5/Ti | Altn.In |
|---|---|---|---|---|
| 2.90 | 9.30 | 0.03 | 0.63 | 60.23 |
| 9.30 | 20.20 | 0.03 | 0.55 | 46.91 |
| 20.20 | 30.10 | 0.43 | 0.58 | 51.75 |
| 30.10 | 40.00 | 0.38 | 0.55 | 32.82 |
| 40.00 | 50.10 | 0.48 | 0.56 | 39.37 |
| 50.10 | 60.00 | 0.51 | 0.52 | 45.55 |
| 60.00 | 70.00 | 0.56 | 0.54 | 41.58 |
| 70.00 | 80.00 | 0.69 | 0.52 | 43.23 |
| 80.00 | 90.00 | 0.90 | 0.51 | 47.60 |
| 90.00 | 100.00 | 0.66 | 0.49 | 40.68 |
| 100.00 | 110.00 | 0.64 | 0.51 | 32.43 |
| 110.00 | 120.00 | 0.41 | 0.49 | 28.05 |
| 120.00 | 130.00 | 0.49 | 0.50 | 36.10 |
| 130.00 | 140.00 | 0.41 | 0.51 | 35.22 |
| 140.00 | 154.90 | 0.92 | 0.53 | 34.53 |
| 154.90 | 158.20 | 0.88 | 0.52 | 32.41 |
| 158.20 | 170.00 | 0.94 | 0.52 | 34.49 |
| 170.00 | 180.00 | 0.73 | 0.50 | 32.96 |
| 180.00 | 189.50 | 0.52 | 0.50 | 32.67 |
| 189.50 | 199.70 | 0.72 | 0.50 | 39.92 |
| 199.70 | 211.00 | 1.22 | 0.52 | 34.79 |
| 211.00 | 222.75 | 0.26 | 0.53 | 48.90 |
| 222.75 | 234.00 | 0.17 | 0.50 | 33.14 |
| 234.00 | 245.00 | 0.19 | 0.52 | 30.29 |
| 245.00 | 256.70 | 0.20 | 0.51 | 38.74 |
| 256.70 | 262.45 | 0.69 | 0.48 | 48.82 |
| 262.45 | 264.20 | 4.77 | 0.96 | 18.84 |
| 264.20 | 276.00 | 4.70 | 1.07 | 29.07 |
| 276.00 | 288.00 | 1.48 | 1.04 | 28.59 |
| 288.00 | 300.00 | 1.32 | 1.01 | 25.50 |
| 300.00 | 311.50 | 0.44 | 0.99 | 29.57 |
| 311.50 | 322.00 | 0.48 | 1.04 | 34.55 |
| 322.00 | 337.10 | 0.49 | 1.02 | 24.92 |
| 337.10 | 341.50 | 0.21 | 1.03 | 19.75 |
| 341.50 | 344.00 | 0.13 | 0.91 | 45.95 |
| 344.00 | 354.30 | 0.11 | 1.05 | 17.77 |
| 354.30 | 366.00 | 0.09 | 0.74 | 43.14 |
| 366.00 | 377.00 | 0.09 | 0.58 | 52.41 |
| 377.00 | 386.00 | 0.04 | 0.62 | 43.99 |
| 386.00 | 395.30 | 0.02 | 0.63 | 45.98 |
| 395.30 | 400.30 | 0.02 | 0.70 | 28.24 |
| 400.30 | 412.00 | 0.02 | 0.60 | 47.41 |
| 412.00 | 425.00 | 0.03 | 0.63 | 42.69 |
| 425.00 | 438.00 | 0.08 | 0.59 | 45.37 |
| 438.00 | 450.00 | 0.03 | 0.63 | 40.03 |
| 450.00 | 461.00 | 0.01 | 0.55 | 43.97 |
| 461.00 | 473.00 | 0.02 | 0.57 | 40.68 |
| 473.00 | 484.00 | 0.03 | 0.41 | 40.98 |
| 484.00 | 496.00 | 0.08 | 0.43 | 41.15 |
| 496.00 | 508.00 | 0.07 | 0.42 | 41.44 |
| 508.00 | 520.00 | 0.07 | 0.41 | 39.57 |
| 520.00 | 532.00 | 0.07 | 0.42 | 37.05 |
| 532.00 | 544.00 | 0.11 | 0.42 | 41.71 |
| 544.00 | 554.00 | 0.10 | 0.38 | 49.51 |
| 554.00 | 566.00 | 0.02 | 0.36 | 40.97 |
| 566.00 | 577.00 | 0.02 | 0.36 | 40.26 |
| 577.00 | 588.30 | 0.03 | 0.33 | 38.02 |
| 588.30 | 598.00 | 0.02 | 0.30 | 50.92 |
| 598.00 | 608.20 | 0.12 | 0.28 | 48.08 |
| 608.20 | 620.00 | 0.03 | 0.44 | 39.17 |
| 620.00 | 632.00 | 0.09 | 0.34 | 35.92 |
| 632.00 | 644.00 | 0.10 | 0.31 | 24.28 |
| 644.00 | 656.00 | 0.06 | 0.31 | 31.68 |
| 656.00 | 668.00 | 0.06 | 0.30 | 40.42 |
| 668.00 | 680.00 | 0.05 | 0.31 | 28.38 |
| 680.00 | 692.00 | 0.04 | 0.32 | 25.35 |
| 692.00 | 704.00 | 0.02 | 0.30 | 33.22 |
| 704.00 | 716.00 | 0.27 | 0.32 | 40.68 |
| 716.00 | 726.00 | 0.09 | 0.31 | 34.25 |
| 726.00 | 736.00 | 0.02 | 0.32 | 26.87 |
| 736.00 | 746.70 | 0.04 | 0.39 | 29.69 |
| 746.70 | 758.00 | 0.04 | 0.33 | 24.44 |
| 758.00 | 770.00 | 0.10 | 0.35 | 21.10 |
| 770.00 | 778.10 | 0.16 | 0.30 | 44.79 |

# ABERFOYLE RESOURCES LTD. DRILL LOG

**Area Code** mac
**Prospect** Murchison Zone
**Report Grid** Mack
**Dataset** Geochemical data set

**Holename** DDMA0035
**Stored Grid** Mack

| From | To | S % | P205/Ti | Altn.In |
|---|---|---|---|---|
| 778.10 | 788.00 | 0.11 | 0.33 | 42.09 |
| 788.00 | 798.00 | 0.17 | 0.29 | 38.48 |
| 798.00 | 806.90 | 0.07 | 0.31 | 32.28 |
| 806.90 | 818.00 | 0.04 | 0.24 | 28.00 |
| 818.00 | 830.00 | 0.08 | 0.22 | 40.91 |
| 830.00 | 842.00 | 0.12 | 0.23 | 50.27 |
| 842.00 | 856.00 | 0.07 | 0.22 | 37.25 |
| 856.00 | 866.00 | 0.05 | 0.22 | 34.15 |
| 866.00 | 876.00 | 0.10 | 0.21 | 28.78 |
| 876.00 | 886.00 | 0.15 | 0.20 | 41.73 |
| 886.00 | 895.80 | 0.16 | 0.22 | 40.32 |
| 895.80 | 897.50 | 0.18 | 0.24 | 38.30 |
| 897.50 | 908.90 | 0.04 | 0.19 | 50.85 |
| 908.90 | 913.80 | 0.15 | 0.24 | 43.75 |
| 913.80 | 924.00 | 0.14 | 0.23 | 41.08 |
| 924.00 | 933.20 | 0.18 | 0.20 | 44.88 |
| 933.20 | 937.80 | 0.24 | 0.25 | 39.75 |
| 937.80 | 950.00 | 0.28 | 0.29 | 43.02 |
| 950.00 | 963.70 | 0.15 | 0.30 | 42.94 |
| 963.70 | 975.00 | 0.10 | 0.25 | 53.94 |
| 975.00 | 987.00 | 0.10 | 0.25 | 49.67 |
| 987.00 | 998.00 | 0.06 | 0.26 | 50.00 |
| 998.00 | 1008.00 | 0.08 | 0.25 | 45.45 |
| 1008.00 | 1020.80 | 0.03 | 0.25 | 29.74 |
| 1020.80 | 1031.00 | 0.04 | 0.25 | 40.06 |
| 1031.00 | 1040.50 | 0.04 | 0.25 | 27.89 |
| 1040.50 | 1055.80 | 0.05 | 0.31 | 39.32 |
| 1055.80 | 1063.20 | 0.05 | 0.26 | 37.55 |
| 1063.20 | 1086.10 | 0.06 | 0.28 | 29.22 |
| 1086.10 | 1088.90 | 0.13 | 0.25 | 44.13 |
| 1088.90 | 1099.00 | 0.04 | 0.26 | 31.97 |
| 1099.00 | 1109.50 | 0.09 | 0.26 | 40.36 |
| 1109.50 | 1112.20 | 0.10 | 0.26 | 45.93 |
| 1112.20 | 1123.00 | 0.01 | 0.25 | 29.90 |
| 1123.00 | 1135.30 | 0.01 | 0.26 | 25.45 |
| 1135.30 | 1150.90 | 0.06 | 0.31 | 48.36 |
| 1150.90 | 1165.00 | 0.03 | 0.24 | 50.87 |
| 1165.00 | 1179.30 | 0.03 | 0.25 | 32.27 |
| 1179.30 | 1188.30 | 0.03 | 0.25 | 29.50 |
| 1188.30 | 1189.60 | 0.03 | 0.58 | 33.58 |

655406 PAGE 1 OF

CORE GRIND SAMPLING

HOLE No. MAC35

DATE 3-2-93

| No. | SAMPLE NUMBER | INTERVAL | ELEMENTS REQUIRED | ST | SAMPLE NUMBER | INTERVAL | ELEMENTS REQUIRED | ST |
|---|---|---|---|---|---|---|---|---|
| 1 | 622485 | 2.9-9.3 | | | 622517 | 311.5-322 | | |
| 2 | 486 | 9.3-20.2 | | | 518 | 322-337.1 | | |
| 3 | 487 | 20.2-30.1 | | | 519 | 337.1-341.5 | | |
| 4 | 488 | 30.1-40 | | | 520 | 341.5-344 | | |
| 5 | 489 | 40-50.1 | | | 521 | 344-354.3 | | |
| 6 | 490 | 50.1-60 | | | 522 | 354.3-366 | | |
| 7 | 491 | 60-70 | | | 523 | 366-377 | | |
| 8 | 492 | 70-80 | | | 524 | 377-386 | | |
| 9 | 493 | 80-90 | | | 525 | 386-395.3 | | |
| 10 | 494 | 90-100 | | | 526 | 395.3-400.3 | | |
| 11 | 495 | 100-110 | | | 527 | 400.3-412 | | |
| 12 | 496 | 110-120 | | | 528 | 412-425 | | |
| 13 | 497 | 120-130 | | | 529 | 425-438 | | |
| 14 | 498 | 130-140 | | | 530 | 438-450 | | |
| 15 | 499 | 140-154.9 | | | ✱ 531 | STD | | |
| 16 | 500 | 154.9-158.2 | | | 532 | 450-461 | | |
| 17 | 501 | 158.2-170 | | | 533 | 461-473 | | |
| 18 | 502 | 170-180 | | | 534 | 473-484 | | |
| 19 | 503 | 180-189.5 | | | 535 | 484-496 | | |
| 20 | 504 | 189.5-199.7 | | | 536 | 496-508 | | |
| 21 | ✱ 505 | STD | | | 537 | 508-520 | | |
| 22 | 506 | 199.7-211 | | | 538 | 520-532 | | |
| 23 | 507 | 211-222.75 | | | 539 | 532-544 | | |
| 24 | 508 | 222.75-234 | | | 540 | 544-554 | | |
| 25 | 509 | 234-245 | | | 541 | 554-566 | | |
| 26 | 510 | 245-256.7 | | | 542 | 566-577 | | |
| 27 | 511 | 256.7-262.45 | | | 543 | 577-588.3 | | |
| 28 | 512 | 262.45-264.2 | | | 544 | 588.3-598 | | |
| 29 | 513 | 264.2-276 | | | 545 | 598-608.2 | | |
| 30 | 514 | 276-288 | | | 546 | 608.2-620 | | |
| 31 | 515 | 288-300 | | | 547 | 620-632 | | |
| 32 | 516 | 300-311.5 | | | 548 | 632-644 | | |

CORE GRIND SAMPLING

HOLE No. MAC35

DATE

| No. | SAMPLE NUMBER | INTERVAL | ELEMENTS REQUIRED | ST | SAMPLE NUMBER | INTERVAL | ELEMENTS REQUIRED | ST |
|---|---|---|---|---|---|---|---|---|
| 1 | 622549 | 644-656 | | | 622581 | 975-987 | 987 | |
| 2 | 550 | 656-668 | | | 582 | 987-998 | 998 | |
| 3 | 551 | 668-680 | | | 583 | 998-1008 | 1008 | |
| 4 | 552 | 680-692 | | | 584 | 1008-10208 | 1020.8 | |
| 5 | 553 | 692-704 | | | 585 | 1020.8-1031.0 | 1031 | |
| 6 | 554 | 704-716 | | | 586 | 1031.0-1040.5 | | |
| 7 | 555 | 716-726 | | | 587 | 1040.5-1055.8 | | |
| 8 | 556 | 726-736 | | | 588 | 1055.8-1063.2 | | |
| 9 | 557 | 736-7467 | | | 589 | 1063.2-1086.1 | | |
| 10 | 558 | 746.7-758 | | | X 590 | STANDARD | | |
| 11 | 559 | 758-770 | | | 591 | 1086.1-1088.9 | | |
| 12 | 560 | 770-778.1 | | | 592 | 1088.9-1099.0 | | |
| 13 | 561 | 778.1-788 | | | 593 | 1099.0-1109.5 | | |
| 14 | 562 | 788-798 | | | 594 | 1109.5-1112.2 | | |
| 15 | 563 | 798-8069 | | | 595 | 1112.2-1123.0 | | |
| 16 | 564 | 8069-818 | | | 596 | 1123.0-1135.3 | | |
| 17 | 565 | 818-830 | | | 597 | 1135.3-1150.9 | | |
| 18 | 566 | 830-842 | | | 598 | 1150.9-1165.0 | | |
| 19 | 567 | 842-856 | | | 599 | 1165.0-1179.3 | | |
| 20 | 568 | 856-866 | 866 | | 600 | 1179.3-11883 | | |
| 21 | 569 | 866-876 | 876 | | 601 | 1188.3-1189.6 | EOH. | |
| 22 | 570 | 876-886 | 886 | | 602 | | | |
| 23 | 571 | 886-895.8 | | | 603 | | | |
| 24 | 572 | 895.8-897.5 | | | 604 | | | |
| 25 | 573 | 898.5-908.9 | | | 605 | | | |
| 26 | 574 | 908.9-913.8 | | | 606 | | | |
| 27 | 575 | 913.8-924 | 924 | | 607 | | Total 1186.70m. | |
| 28 | 576 | 924-933.2 | 933.2 | | 608 | | | |
| 29 | 577 | 933.2-9378 | 937.8 | | 609 | | | |
| 30 | 578 | 937.8-950 | 950 | | 610 | | | |
| 31 | 579 | 950-9637 | 963.7 | | 611 | | | |
| 32 | 580 | 9637-975 | 975 | | 612 | | | |

655408

# ANALABS

A Division of Inchcape Inspection and Testing Services Australia Pty. Ltd.
A.C.N. 004 591 664

Phone (004) 316837 | 14 Thirkell St. CODEE TAS 7320 | Fax (004) 318890

## ANALYTICAL REPORT No. 100560.60.09379

THIS REPORT MUST BE READ IN CONJUNCTION WITH THE ACCOMPANYING ANALYTICAL DATA

INVOICE TO:
Aberfoyle Resources Limited
Exploration Division
P.O. Box 952
BURNIE TAS 7320

| ORDER No. | PROJECT |
|---|---|
| 2752 | MAC-35 |

| DATE RECEIVED | RESULTS REQUIRED |
|---|---|
| 17/03/93 | ASAP |

| No. OF PAGES OF RESULTS | DATE REPORTED | No. OF COPIES | TOTAL No. OF SAMPLES |
|---|---|---|---|
| 15 | 16/04/93 | 1 | 117 |

| SAMPLE NUMBERS | SAMPLE DESCRIPTION | ELEMENT/METHOD |
|---|---|---|
| A?2485/601 | CG Prep : GP031 CHROME FREE BOWL | Cu,Pb,Zn,Ag/GA101<br>Au,Au(R)/GG309<br>Ba,As,Cr,Zr/GX401<br>Whole Rock Analysis/OX408 |

RESULTS TO
Mr R de Bomford
Aberfoyle Resources Limited
P.O. Box 952
BURNIE TAS 7320

RESULTS TO

RESULTS TO

REMARKS

INSUFFICIENT SAMPLE FOR Au(S) RESULT

MAC-35
GRINDS.

AUTHORISED OFFICER

655409

# ANALABS

A Division of Inchcape Testing Services (Australia) Pty. Ltd.
A.C.N. 004 591 664

## ANALYTICAL DATA

| SAMPLE PREFIX | REPORT No. | REPORT DATE | CLIENT ORDER No. | PAGE |
|---|---|---|---|---|
| | 100560.60.09379 | 16/04/93 | 2752 | 1 OF 15 |

| TUBE No. | SAMPLE No. | Cu | Pb | Zn | Ag | Au | Au(R) | Ba | As | Cr |
|---|---|---|---|---|---|---|---|---|---|---|
| 1 | 622485 | 42 | 32 | 133 | <2 | <0.008 | - | 732 | 13 | 18 |
| 2 | 622486 | 39 | 35 | 122 | <2 | <0.008 | - | 857 | 8 | 13 |
| 3 | 622487 | 41 | 99 | 159 | <2 | <0.008 | - | 888 | 12 | 18 |
| 4 | 622488 | 55 | 53 | 142 | <2 | <0.008 | - | 739 | 10 | 18 |
| 5 | 622489 | 102 | 65 | 217 | <2 | <0.008 | - | 1247 | 7 | 17 |
| 6 | 622490 | 106 | 63 | 204 | <2 | <0.008 | - | 867 | 4 | 17 |
| 7 | 622491 | 82 | 37 | 221 | <2 | <0.008 | - | 423 | 6 | 15 |
| 8 | 622492 | 93 | 50 | 188 | <2 | <0.008 | - | 406 | 8 | 15 |
| 9 | 622493 | 91 | 96 | 300 | <2 | <0.008 | - | 730 | 7 | 13 |
| 10 | 622494 | 132 | 262 | 412 | <2 | <0.008 | - | 904 | 5 | 22 |
| 11 | 622495 | 116 | 25 | 167 | <2 | <0.008 | - | 758 | 4 | 13 |
| 12 | 622496 | 162 | 38 | 194 | <2 | <0.008 | <0.008 | 769 | 11 | 12 |
| 13 | 622497 | 145 | 23 | 157 | <2 | <0.008 | - | 685 | 3 | 15 |
| 14 | 622498 | 151 | 171 | 420 | <2 | <0.008 | - | 1091 | 4 | 17 |
| 15 | 622499 | 105 | 1099 | 2471 | <2 | <0.008 | - | 1191 | <2 | 20 |
| 16 | 622500 | 116 | 791 | 2115 | <2 | <0.008 | - | 1876 | 2 | 16 |
| 17 | 622501 | 124 | 1575 | 2906 | <2 | <0.008 | - | 2571 | <2 | 18 |
| 18 | 622502 | 222 | 1088 | 2255 | <2 | <0.008 | - | 2186 | 12 | 17 |
| 19 | 622503 | 106 | 649 | 1319 | <2 | <0.008 | - | 2144 | 3 | 12 |
| 20 | 622504 | 70 | 609 | 1194 | <2 | <0.008 | - | 1026 | <2 | 26 |
| 21 | 622505 STD. | 126 | 205 | 2236 | <2 | <0.008 | - | 1128 | 15 | 1002 |
| 22 | 622506 | 84 | 120 | 1257 | <2 | <0.008 | <0.008 | 917 | 6 | 16 |
| 23 | 622507 | 93 | 16 | 345 | <2 | <0.008 | - | 698 | 5 | 23 |
| 24 | 622508 | 116 | 61 | 293 | <2 | <0.008 | - | 873 | <2 | 20 |
| 25 | 622509 | 145 | 112 | 282 | <2 | <0.008 | - | 556 | <2 | 26 |

Results in ppm unless otherwise specified
T = element present; but concentration too low to measure
X = element concentration is below detection limit
- = element not determined

AUTHORISED OFFICER

655410

# ANALABS

A Division of Inchcape Testing Services (Australia) Pty. Ltd.
A.C.N. 004 591 664

## ANALYTICAL DATA

| SAMPLE PREFIX | REPORT No. | REPORT DATE | CLIENT ORDER No. | PAGE |
|---|---|---|---|---|
| | 100560.60.09379 | 16/04/93 | 2752 | 2 OF 15 |

| TUBE No. | SAMPLE No. | Cu | Pb | Zn | Ag | Au | Au(R) | Ba | As | Cr |
|---|---|---|---|---|---|---|---|---|---|---|
| 1 | 622510 | 92 | 35 | 257 | <2 | <0.008 | - | 797 | 6 | 26 |
| 2 | 622511 | 81 | 37 | 208 | <2 | 0.010 | - | 565 | 44 | 57 |
| 3 | 622512 | 82 | 861 | 4921 | 2 | 0.089 | - | 354 | 505 | 248 |
| 4 | 622513 | 201 | 933 | 1625 | 3 | <0.008 | - | 1139 | 90 | 597 |
| 5 | 622514 | 186 | 108 | 240 | <2 | <0.008 | - | 2167 | 15 | 634 |
| 6 | 622515 | 199 | 187 | 548 | <2 | <0.008 | - | 1036 | 13 | 619 |
| 7 | 622516 | 166 | 85 | 256 | <2 | <0.008 | - | 798 | 6 | 591 |
| 8 | 622517 | 145 | 194 | 473 | <2 | <0.008 | - | 578 | 6 | 604 |
| 9 | 622518 | 135 | 212 | 410 | <2 | <0.008 | - | 1343 | 6 | 651 |
| 10 | 622519 | 123 | 83 | 191 | <2 | <0.008 | - | 1158 | 3 | 647 |
| 11 | 622520 | 161 | 125 | 332 | <2 | <0.008 | - | 1917 | 5 | 964 |
| 12 | 622521 | 110 | 76 | 156 | <2 | <0.008 | <0.008 | 776 | 4 | 566 |
| 13 | 622522 | 177 | 189 | 329 | <2 | <0.008 | - | 1154 | 7 | 553 |
| 14 | 622523 | 167 | 117 | 271 | <2 | <0.008 | - | 1469 | 3 | 371 |
| 15 | 622524 | 125 | 72 | 288 | <2 | <0.008 | - | 1013 | 6 | 365 |
| 16 | 622525 | 139 | 52 | 231 | <2 | <0.008 | - | 2521 | <2 | 338 |
| 17 | 622526 | 149 | 25 | 140 | <2 | <0.008 | - | 966 | 2 | 258 |
| 18 | 622527 | 220 | 47 | 236 | <2 | <0.008 | - | 2204 | 3 | 327 |
| 19 | 622528 | 213 | 40 | 199 | <2 | <0.008 | - | 1210 | 2 | 306 |
| 20 | 622529 | 135 | 41 | 140 | <2 | 0.010 | - | 944 | 6 | 321 |
| 21 | 622530 | 193 | 40 | 159 | <2 | 0.008 | - | 1131 | 3 | 317 |
| 22 X | 622531 STD | 125 | 201 | 2219 | <2 | 0.008 | 0.009 | 1120 | 16 | 979 |
| 23 | 622532 | 205 | 30 | 178 | <2 | <0.008 | - | 1088 | 2 | 396 |
| 24 | 622533 | 243 | 31 | 212 | <2 | <0.008 | - | 1447 | 3 | 359 |
| 25 | 622534 | 307 | 37 | 278 | <2 | <0.008 | - | 747 | 6 | 290 |

Results in ppm unless otherwise specified
T = element present; but concentration too low to measure
X = element concentration is below detection limit
- = element not determined

AUTHORISED OFFICER

655411

# ANALABS

A Division of Inchcape Testing Services (Australia) Pty. Ltd.
A.C.N. 004 591 664

## ANALYTICAL DATA

| SAMPLE PREFIX | REPORT No. | REPORT DATE | CLIENT ORDER No. | PAGE |
|---|---|---|---|---|
| | 100560.60.09379 | 16/04/93 | 2752 | 3 OF 15 |

| JBE No. | SAMPLE No. | Cu | Pb | Zn | Ag | Au | Au(R) | Ba | As | Cr |
|---|---|---|---|---|---|---|---|---|---|---|
| 1 | 622535 | 269 | 45 | 252 | <2 | <0.008 | - | 631 | 4 | 275 |
| 2 | 622536 | 347 | 44 | 320 | <2 | <0.008 | - | 799 | 3 | 269 |
| 3 | 622537 | 325 | 98 | 324 | <2 | <0.008 | - | 577 | <2 | 262 |
| 4 | 622538 | 239 | 62 | 267 | <2 | <0.008 | - | 515 | 2 | 260 |
| 5 | 622539 | 223 | 33 | 260 | <2 | <0.008 | - | 1217 | <2 | 253 |
| 6 | 622540 | 165 | 86 | 538 | 6 | <0.008 | - | 376 | <2 | 262 |
| 7 | 622541 | 135 | 25 | 366 | <2 | <0.008 | - | 841 | 4 | 245 |
| 8 | 622542 | 263 | 38 | 459 | <2 | <0.008 | - | 1269 | 2 | 245 |
| 9 | 622543 | 282 | 32 | 810 | 2 | <0.008 | - | 544 | 4 | 230 |
| 10 | 622544 | 220 | 24 | 449 | <2 | <0.008 | - | 1467 | <2 | 164 |
| 11 | 622545 | 105 | 59 | 469 | <2 | <0.008 | - | 480 | <2 | 171 |
| 12 | 622546 | 90 | 21 | 346 | <2 | <0.008 | <0.008 | 427 | <2 | 161 |
| 13 | 622547 | 91 | 19 | 145 | <2 | <0.008 | - | 580 | <2 | 45 |
| 14 | 622548 | 120 | 13 | 144 | <2 | <0.008 | - | 699 | 4 | 51 |
| 15 | 622549 | 94 | 69 | 248 | <2 | <0.008 | - | 815 | <2 | 56 |
| 16 | 622550 | 126 | 47 | 274 | <2 | <0.008 | - | 931 | <2 | 55 |
| 17 | 622551 | 129 | 38 | 308 | <2 | <0.008 | - | 606 | 2 | 55 |
| 18 | 622552 | 152 | 33 | 343 | <2 | <0.008 | - | 1184 | <2 | 50 |
| 19 | 622553 | 96 | 33 | 168 | <2 | <0.008 | - | 781 | 2 | 53 |
| 20 | 622554 | 63 | 20 | 209 | <2 | <0.008 | - | 535 | <2 | 53 |
| 21 | 622555 | 52 | 30 | 189 | <2 | <0.008 | - | 530 | <2 | 55 |
| 22 | 622556 | 54 | 17 | 174 | <2 | <0.008 | <0.008 | 441 | <2 | 45 |
| 23 | 622557 | 73 | 30 | 157 | <2 | <0.008 | - | 1766 | <2 | 89 |
| 24 | 622558 | 17 | 5 | 88 | <2 | <0.008 | - | 556 | <2 | 38 |
| 25 | 622559 | 21 | 13 | 72 | <2 | <0.008 | - | 413 | 2 | 44 |

Results in ppm unless otherwise specified
T = element present; but concentration too low to measure
X = element concentration is below detection limit
- = element not determined

AUTHORISED OFFICER

655412

# ANALABS

A Division of Inchcape Testing Services (Australia) Pty. Ltd.
A.C.N. 004 591 664

## ANALYTICAL DATA

| SAMPLE PREFIX | REPORT No. | REPORT DATE | CLIENT ORDER No. | PAGE |
|---|---|---|---|---|
| | 100560.60.09379 | 16/04/93 | 2752 | 4 OF 15 |

| TUBE No. | SAMPLE No. | Cu | Pb | Zn | Ag | Au | Au(R) | Ba | As | Cr |
|---|---|---|---|---|---|---|---|---|---|---|
| 1 | 622560 | 29 | 10 | 212 | <2 | <0.008 | - | 508 | 3 | 57 |
| 2 | 622561 | 26 | 16 | 80 | <2 | <0.008 | - | 541 | 2 | 8 |
| 3 | 622562 | 23 | 38 | 98 | <2 | <0.008 | - | 769 | 4 | 17 |
| 4 | 622563 | 70 | 54 | 467 | <2 | <0.008 | - | 604 | <2 | 81 |
| 5 | 622564 | 32 | 12 | 63 | <2 | <0.008 | - | 506 | <2 | 8 |
| 6 | 622565 | 100 | 29 | 58 | <2 | <0.008 | - | 751 | 2 | 9 |
| 7 | 622566 | 81 | 17 | 98 | <2 | <0.008 | - | 925 | <2 | 13 |
| 8 | 622567 | 21 | 51 | 67 | <2 | <0.008 | - | 735 | <2 | 13 |
| 9 | 622568 | 39 | 24 | 71 | <2 | <0.008 | - | 667 | <2 | 18 |
| 10 | 622569 | 42 | 52 | 103 | <2 | <0.008 | - | 701 | <2 | 24 |
| 11 | 622570 | 78 | 28 | 98 | <2 | <0.008 | - | 1382 | 6 | 18 |
| 12 | 622571 | 34 | 17 | 59 | <2 | <0.008 | <0.008 | 652 | 6 | 13 |
| 13 | 622572 | 41 | 6 | 94 | <2 | <0.008 | - | 548 | 3 | 31 |
| 14 | 622573 | 17 | <5 | 59 | <2 | <0.008 | - | 660 | 2 | 8 |
| 15 | 622574 | 31 | 33 | 84 | <2 | <0.008 | - | 586 | <2 | 26 |
| 16 | 622575 | 36 | 32 | 73 | <2 | <0.008 | - | 584 | 4 | 9 |
| 17 | 622576 | 22 | 11 | 41 | <2 | <0.008 | - | 604 | 4 | <5 |
| 18 | 622577 | 30 | 21 | 87 | <2 | <0.008 | - | 372 | 6 | 28 |
| 19 | 622578 | 25 | 25 | 49 | <2 | <0.008 | - | 470 | 9 | 40 |
| 20 | 622579 | 20 | 19 | 38 | <2 | <0.008 | - | 542 | 3 | 15 |
| 21 | 622580 | 13 | 16 | 87 | <2 | <0.008 | - | 349 | 2 | 21 |
| 22 | 622581 | 31 | 6 | 91 | <2 | <0.008 | <0.008 | 654 | 2 | 17 |
| 23 | 622582 | 17 | 13 | 70 | <2 | <0.008 | - | 544 | <2 | 17 |
| 24 | 622583 | 19 | 44 | 71 | <2 | <0.008 | - | 615 | 3 | 18 |
| 25 | 622584 | 21 | 23 | 81 | <2 | <0.008 | - | 426 | 3 | 50 |

Results in ppm unless otherwise specified
T = element present; but concentration too low to measure
X = element concentration is below detection limit
- = element not determined

AUTHORISED OFFICER

655413

# ANALABS

A Division of Inchcape Testing Services (Australia) Pty. Ltd.
A.C.N. 004 591 664

## ANALYTICAL DATA

| SAMPLE PREFIX | REPORT No. | REPORT DATE | CLIENT ORDER No. | PAGE |
|---|---|---|---|---|
| | 100560.60.09379 | 16/04/93 | 2752 | 5 OF 15 |

| JOBE No. | SAMPLE No. | Cu | Pb | Zn | Ag | Au | Au(R) | Ba | As | Cr |
|---|---|---|---|---|---|---|---|---|---|---|
| 1 | 622585 | 23 | 13 | 74 | <2 | <0.008 | - | 710 | <2 | 37 |
| 2 | 622586 | 23 | 12 | 70 | <2 | <0.008 | - | 898 | 2 | 29 |
| 3 | 622587 | 17 | 17 | 97 | <2 | <0.008 | - | 1084 | <2 | 28 |
| 4 | 622588 | 36 | 22 | 90 | <2 | <0.008 | - | 474 | 2 | 58 |
| 5 | 622589 | 28 | 35 | 90 | <2 | <0.008 | - | 849 | <2 | 31 |
| 6 | 622590 STD | 129 | 203 | 2254 | <2 | 0.009 | - | 1102 | 16 | 899 |
| 7 | 622591 | 88 | 8 | 118 | <2 | <0.008 | - | 1515 | 3 | 35 |
| 8 | 622592 | 24 | 29 | 120 | <2 | <0.008 | - | 1192 | 4 | 49 |
| 9 | 622593 | 33 | 14 | 103 | <2 | <0.008 | - | 2498 | 5 | 56 |
| 10 | 622594 | 76 | 16 | 125 | <2 | <0.008 | - | 2124 | 6 | 63 |
| 11 | 622595 | 36 | 21 | 105 | <2 | <0.008 | - | 1015 | <2 | 94 |
| 12 | 622596 | 21 | 36 | 101 | <2 | <0.008 | <0.008 | 1032 | 2 | 94 |
| 13 | 622597 | 121 | 23 | 144 | <2 | <0.008 | - | 1307 | <2 | 153 |
| 14 | 622598 | 13 | 29 | 139 | <2 | <0.008 | - | 462 | <2 | 104 |
| 15 | 622599 | 10 | 43 | 109 | <2 | <0.008 | - | 513 | <2 | 97 |
| 16 | 622600 | 18 | 17 | 63 | <2 | <0.008 | - | 1211 | 2 | 5 |
| 17 | 622601 | 98 | 16 | 123 | <2 | <0.008 | - | 943 | 6 | 235 |
| 18 | | | | | | | | | | |
| 19 | | | | | | | | | | |
| 20 | | | | | | | | | | |
| 21 | | | | | | | | | | |
| 22 | | | | | | | | | | |
| 23 | DETECTION | 4 | 5 | 4 | 2 | 0.008 | 0.008 | 10 | 2 | 5 |
| 24 | UNITS | ppm | ppm | ppm | ppm | ppm | ppm | ppm | ppm | ppm |
| 25 | METHOD | GA101 | GA101 | GA101 | GA101 | GG309 | GG309 | GX401 | GX401 | GX401 |

Results in ppm unless otherwise specified
T = element present; but concentration too low to measure
X = element concentration is below detection limit
- = element not determined

AUTHORISED OFFICER

655414

# ANALABS

A Division of Inchcape Testing Services (Australia) Pty. Ltd.
A.C.N. 004 591 664

## ANALYTICAL DATA

| SAMPLE PREFIX | REPORT No. | REPORT DATE | CLIENT ORDER No. | PAGE |
|---|---|---|---|---|
| | 100560.60.09379 | 16/04/93 | 2752 | 6 OF 15 |

| JBE No. | SAMPLE No. | Zr | Ti | Al2O3 | SiO2 | TiO2 | Fe2O3 | MnO | CaO | K2O |
|---|---|---|---|---|---|---|---|---|---|---|
| 1 | 622485 | 204 | 3751 | 20.87 | 53.20 | 0.63 | 8.00 | 0.29 | 1.73 | 1.47 |
| 2 | 622486 | 190 | 3571 | 17.80 | 58.60 | 0.60 | 7.55 | 0.14 | 2.38 | 1.84 |
| 3 | 622487 | 173 | 3247 | 16.63 | 59.60 | 0.54 | 7.51 | 0.15 | 1.28 | 2.16 |
| 4 | 622488 | 176 | 3317 | 16.50 | 60.60 | 0.55 | 7.41 | 0.16 | 2.72 | 1.15 |
| 5 | 622489 | 175 | 3177 | 16.98 | 58.90 | 0.53 | 7.05 | 0.14 | 3.20 | 1.89 |
| 6 | 622490 | 180 | 3305 | 16.12 | 58.80 | 0.55 | 7.55 | 0.14 | 2.82 | 1.53 |
| 7 | 622491 | 171 | 3200 | 16.19 | 57.30 | 0.53 | 7.34 | 0.15 | 2.99 | 1.12 |
| 8 | 622492 | 177 | 3217 | 15.89 | 56.60 | 0.54 | 7.16 | 0.23 | 3.70 | 1.43 |
| 9 | 622493 | 180 | 3142 | 16.34 | 56.80 | 0.52 | 6.55 | 0.23 | 3.53 | 2.37 |
| 10 | 622494 | 171 | 3026 | 15.56 | 61.00 | 0.50 | 6.30 | 0.18 | 2.81 | 1.22 |
| 11 | 622495 | 157 | 2781 | 14.21 | 55.00 | 0.46 | 6.04 | 0.16 | 7.11 | 1.61 |
| 12 | 622496 | 177 | 3094 | 15.77 | 59.30 | 0.52 | 6.00 | 0.12 | 5.53 | 1.36 |
| 13 | 622497 | 178 | 2972 | 15.19 | 60.10 | 0.50 | 5.91 | 0.13 | 4.57 | 1.57 |
| 14 | 622498 | 175 | 3021 | 15.18 | 61.20 | 0.50 | 5.92 | 0.17 | 4.54 | 1.80 |
| 15 | 622499 | 166 | 2869 | 14.99 | 58.50 | 0.48 | 6.10 | 0.30 | 4.64 | 1.80 |
| 16 | 622500 | 168 | 2872 | 15.20 | 58.60 | 0.48 | 5.98 | 0.33 | 4.48 | 1.98 |
| 17 | 622501 | 167 | 2878 | 15.10 | 59.90 | 0.48 | 5.66 | 0.41 | 4.07 | 2.15 |
| 18 | 622502 | 164 | 2909 | 14.88 | 60.60 | 0.49 | 5.78 | 0.40 | 4.28 | 1.84 |
| 19 | 622503 | 179 | 3004 | 15.46 | 59.70 | 0.50 | 6.00 | 0.27 | 4.64 | 2.06 |
| 20 | 622504 | 169 | 3024 | 15.17 | 59.40 | 0.50 | 6.26 | 0.22 | 4.36 | 2.33 |
| 21 | 622505 STD | 84 | 2675 | 15.12 | 51.40 | 0.45 | 9.97 | 0.90 | 3.85 | 1.15 |
| 22 | 622506 | 154 | 2762 | 14.14 | 56.70 | 0.46 | 6.13 | 0.23 | 6.43 | 2.10 |
| 23 | 622507 | 167 | 2758 | 14.95 | 60.90 | 0.46 | 7.80 | 0.21 | 2.18 | 1.62 |
| 24 | 622508 | 167 | 2872 | 14.56 | 60.30 | 0.48 | 5.94 | 0.22 | 5.11 | 1.90 |
| 25 | 622509 | 161 | 2826 | 14.33 | 63.10 | 0.47 | 4.92 | 0.19 | 3.87 | 1.48 |

Results in ppm unless otherwise specified
T = element present; but concentration too low to measure
X = element concentration is below detection limit
– = element not determined

AUTHORISED OFFICER

655415

# ANALABS

A Division of Inchcape Testing Services (Australia) Pty. Ltd.
A.C.N. 004 591 664

## ANALYTICAL DATA

| SAMPLE PREFIX | REPORT No. | REPORT DATE | CLIENT ORDER No. | PAGE |
|---|---|---|---|---|
| | 100560.60.09379 | 16/04/93 | 2752 | 7 OF 15 |

| JBE No. | SAMPLE No. | Zr | Ti | Al2O3 | SiO2 | TiO2 | Fe2O3 | MnO | CaO | K2O |
|---|---|---|---|---|---|---|---|---|---|---|
| 1 | 622510 | 173 | 2878 | 15.05 | 61.10 | 0.48 | 6.39 | 0.22 | 3.58 | 1.90 |
| 2 | 622511 | 189 | 3055 | 16.04 | 56.40 | 0.51 | 6.54 | 0.20 | 4.97 | 3.21 |
| 3 | 622512 | 99 | 2098 | 9.29 | 32.40 | 0.35 | 9.50 | 0.64 | 19.28 | 2.59 |
| 4 | 622513 | 135 | 3016 | 10.31 | 41.30 | 0.50 | 11.58 | 0.40 | 12.45 | 0.99 |
| 5 | 622514 | 142 | 3110 | 11.02 | 43.00 | 0.52 | 8.14 | 0.38 | 16.35 | 1.26 |
| 6 | 622515 | 142 | 3188 | 10.93 | 44.20 | 0.53 | 7.48 | 0.30 | 16.80 | 0.91 |
| 7 | 622516 | 139 | 3005 | 10.87 | 46.40 | 0.50 | 7.47 | 0.27 | 15.46 | 0.90 |
| 8 | 622517 | 138 | 2964 | 11.24 | 44.60 | 0.49 | 8.20 | 0.28 | 13.90 | 0.65 |
| 9 | 622518 | 118 | 2715 | 9.51 | 39.10 | 0.45 | 7.28 | 0.33 | 20.42 | 1.38 |
| 10 | 622519 | 111 | 2471 | 8.67 | 35.40 | 0.41 | 6.25 | 0.28 | 24.72 | 1.38 |
| 11 | 622520 | 158 | 3337 | 12.26 | 51.50 | 0.56 | 8.71 | 0.33 | 10.22 | 2.75 |
| 12 | 622521 | 104 | 2410 | 8.35 | 33.80 | 0.40 | 5.89 | 0.27 | 25.78 | 1.05 |
| 13 | 622522 | 119 | 3009 | 12.70 | 52.10 | 0.50 | 8.93 | 0.28 | 9.78 | 1.40 |
| 14 | 622523 | 99 | 2927 | 12.75 | 51.10 | 0.49 | 9.20 | 0.23 | 7.56 | 1.33 |
| 15 | 622524 | 96 | 2836 | 12.91 | 50.60 | 0.47 | 9.55 | 0.23 | 9.08 | 1.06 |
| 16 | 622525 | 86 | 2737 | 12.88 | 52.40 | 0.46 | 8.87 | 0.20 | 9.04 | 1.79 |
| 17 | 622526 | 86 | 2435 | 10.98 | 45.70 | 0.41 | 7.59 | 0.20 | 15.87 | 0.91 |
| 18 | 622527 | 80 | 2781 | 12.73 | 53.40 | 0.46 | 8.76 | 0.18 | 8.51 | 2.10 |
| 19 | 622528 | 76 | 2737 | 12.97 | 52.20 | 0.46 | 8.95 | 0.17 | 9.68 | 1.43 |
| 20 | 622529 | 77 | 2988 | 13.54 | 52.60 | 0.50 | 9.54 | 0.15 | 8.62 | 1.24 |
| 21 | 622530 | 77 | 2699 | 12.45 | 51.50 | 0.45 | 8.72 | 0.17 | 10.56 | 1.41 |
| 22 | 622531 STD | 74 | 2726 | 15.11 | 51.50 | 0.45 | 9.97 | 0.89 | 3.84 | 1.11 |
| 23 | 622532 | 73 | 2687 | 13.10 | 53.60 | 0.45 | 8.99 | 0.18 | 8.89 | 1.42 |
| 24 | 622533 | 75 | 2500 | 12.34 | 51.30 | 0.42 | 8.57 | 0.20 | 10.79 | 1.73 |
| 25 | 622534 | 76 | 2729 | 13.83 | 54.40 | 0.46 | 8.81 | 0.17 | 8.44 | 0.95 |

Results in ppm unless otherwise specified
T = element present; but concentration too low to measure
X = element concentration is below detection limit
– = element not determined

AUTHORISED OFFICER

655416

# ANALABS

A Division of Inchcape Testing Services (Australia) Pty. Ltd.
A.C.N. 004 591 664

## ANALYTICAL DATA

| SAMPLE PREFIX | REPORT No. | REPORT DATE | CLIENT ORDER No. | PAGE |
|---|---|---|---|---|
| | 100560.60.09379 | 16/04/93 | 2752 | 8 OF 15 |

| JBE No. | SAMPLE No. | Zr | Ti | Al2O3 | SiO2 | TiO2 | Fe2O3 | MnO | CaO | K2O |
|---|---|---|---|---|---|---|---|---|---|---|
| 1 | 622535 | 66 | 2643 | 13.93 | 53.20 | 0.44 | 8.78 | 0.18 | 8.51 | 0.72 |
| 2 | 622536 | 74 | 2727 | 14.08 | 53.70 | 0.45 | 8.76 | 0.18 | 9.01 | 1.20 |
| 3 | 622537 | 66 | 2708 | 13.47 | 53.90 | 0.45 | 8.40 | 0.18 | 9.07 | 0.91 |
| 4 | 622538 | 70 | 2625 | 13.13 | 49.50 | 0.44 | 8.36 | 0.24 | 10.98 | 0.78 |
| 5 | 622539 | 69 | 2601 | 13.55 | 49.80 | 0.43 | 8.97 | 0.23 | 9.62 | 0.65 |
| 6 | 622540 | 85 | 2688 | 13.98 | 50.70 | 0.45 | 9.22 | 0.37 | 6.52 | 0.41 |
| 7 | 622541 | 66 | 2733 | 14.26 | 53.20 | 0.46 | 9.31 | 0.51 | 8.26 | 0.82 |
| 8 | 622542 | 72 | 2717 | 14.01 | 52.30 | 0.45 | 9.03 | 0.46 | 8.87 | 0.98 |
| 9 | 622543 | 77 | 2691 | 13.59 | 53.40 | 0.45 | 9.18 | 0.55 | 8.29 | 0.39 |
| 10 | 622544 | 82 | 2644 | 14.86 | 52.40 | 0.44 | 9.58 | 0.53 | 5.76 | 1.18 |
| 11 | 622545 | 82 | 2701 | 14.36 | 50.90 | 0.45 | 11.04 | 0.48 | 5.34 | 0.77 |
| 12 | 622546 | 82 | 2858 | 14.47 | 50.60 | 0.48 | 9.94 | 0.37 | 6.97 | 1.02 |
| 13 | 622547 | 87 | 2530 | 14.09 | 49.60 | 0.42 | 9.57 | 0.35 | 8.69 | 2.06 |
| 14 | 622548 | 75 | 2760 | 14.64 | 51.80 | 0.46 | 7.91 | 0.27 | 9.06 | 1.45 |
| 15 | 622549 | 81 | 2709 | 14.97 | 53.70 | 0.45 | 8.67 | 0.25 | 7.07 | 1.42 |
| 16 | 622550 | 75 | 2976 | 15.69 | 55.20 | 0.50 | 9.33 | 0.27 | 4.27 | 1.18 |
| 17 | 622551 | 80 | 2856 | 15.45 | 55.20 | 0.48 | 7.69 | 0.27 | 7.42 | 1.13 |
| 18 | 622552 | 66 | 2856 | 15.62 | 54.50 | 0.48 | 7.32 | 0.24 | 8.59 | 1.06 |
| 19 | 622553 | 68 | 2910 | 15.59 | 56.00 | 0.49 | 8.17 | 0.20 | 7.78 | 1.39 |
| 20 | 622554 | 61 | 2777 | 15.42 | 53.60 | 0.46 | 8.59 | 0.28 | 6.08 | 1.00 |
| 21 | 622555 | 153 | 2867 | 15.23 | 54.30 | 0.48 | 8.04 | 0.30 | 6.19 | 0.95 |
| 22 | 622556 | 172 | 2837 | 15.18 | 52.90 | 0.47 | 7.94 | 0.26 | 8.79 | 0.96 |
| 23 | 622557 | 89 | 2877 | 14.90 | 51.40 | 0.48 | 7.67 | 0.25 | 9.10 | 1.41 |
| 24 | 622558 | 293 | 2561 | 13.57 | 46.80 | 0.43 | 6.60 | 0.25 | 12.29 | 1.71 |
| 25 | 622559 | 271 | 2570 | 13.77 | 48.40 | 0.43 | 7.59 | 0.26 | 11.49 | 1.61 |

Results in ppm unless otherwise specified
T = element present; but concentration too low to measure
X = element concentration is below detection limit
– = element not determined

AUTHORISED OFFICER

655417

# ANALABS

A Division of Inchcape Testing Services (Australia) Pty. Ltd.
A.C.N. 004 591 664

## ANALYTICAL DATA

| SAMPLE PREFIX | REPORT No. | REPORT DATE | CLIENT ORDER No. | PAGE |
|---|---|---|---|---|
| | 100560.60.09379 | 16/04/93 | 2752 | 9 OF 15 |

| JBE No. | SAMPLE No. | Zr | Ti | Al2O3 | SiO2 | TiO2 | Fe2O3 | MnO | CaO | K2O |
|---|---|---|---|---|---|---|---|---|---|---|
| 1 | 622560 | 307 | 2667 | 14.55 | 49.90 | 0.44 | 13.14 | 0.34 | 5.40 | 1.25 |
| 2 | 622561 | 248 | 2631 | 14.57 | 63.30 | 0.44 | 6.47 | 0.17 | 3.16 | 2.24 |
| 3 | 622562 | 285 | 2732 | 15.07 | 61.80 | 0.46 | 6.59 | 0.17 | 3.36 | 2.09 |
| 4 | 622563 | 284 | 2692 | 14.65 | 54.70 | 0.45 | 8.41 | 0.29 | 6.10 | 0.99 |
| 5 | 622564 | 210 | 2630 | 14.68 | 66.40 | 0.44 | 4.25 | 0.13 | 2.67 | 1.63 |
| 6 | 622565 | 230 | 2446 | 14.70 | 64.30 | 0.41 | 5.01 | 0.18 | 3.44 | 2.83 |
| 7 | 622566 | 46 | 2143 | 14.36 | 65.50 | 0.36 | 4.35 | 0.16 | 3.48 | 3.61 |
| 8 | 622567 | 214 | 1900 | 14.03 | 68.60 | 0.32 | 3.89 | 0.10 | 2.76 | 2.52 |
| 9 | 622568 | 35 | 1930 | 14.41 | 67.80 | 0.32 | 3.90 | 0.11 | 2.31 | 2.31 |
| 10 | 622569 | 76 | 1905 | 14.00 | 68.40 | 0.32 | 4.08 | 0.12 | 2.12 | 1.90 |
| 11 | 622570 | 76 | 1871 | 13.93 | 68.20 | 0.31 | 4.25 | 0.12 | 2.17 | 3.02 |
| 12 | 622571 | 62 | 1743 | 14.02 | 67.00 | 0.29 | 3.91 | 0.14 | 3.38 | 2.88 |
| 13 | 622572 | 97 | 2623 | 15.76 | 48.90 | 0.44 | 11.01 | 0.29 | 7.13 | 2.18 |
| 14 | 622573 | 85 | 1642 | 13.43 | 66.20 | 0.27 | 5.29 | 0.18 | 3.40 | 3.18 |
| 15 | 622574 | 112 | 2456 | 14.96 | 49.30 | 0.41 | 11.87 | 0.31 | 6.52 | 2.53 |
| 16 | 622575 | 206 | 1790 | 13.66 | 63.80 | 0.30 | 2.60 | 0.21 | 5.80 | 3.82 |
| 17 | 622576 | 205 | 1640 | 13.87 | 61.20 | 0.27 | 3.79 | 0.23 | 6.55 | 4.27 |
| 18 | 622577 | 44 | 2186 | 13.86 | 45.20 | 0.36 | 11.63 | 0.33 | 8.21 | 2.37 |
| 19 | 622578 | 195 | 2055 | 13.41 | 61.90 | 0.34 | 4.60 | 0.19 | 5.93 | 3.46 |
| 20 | 622579 | 203 | 1871 | 13.19 | 63.80 | 0.31 | 2.48 | 0.19 | 6.38 | 4.06 |
| 21 | 622580 | 191 | 2436 | 14.41 | 64.50 | 0.41 | 5.93 | 0.10 | 2.57 | 2.26 |
| 22 | 622581 | 200 | 2517 | 14.96 | 64.60 | 0.42 | 6.42 | 0.09 | 1.53 | 1.98 |
| 23 | 622582 | 201 | 2478 | 14.81 | 65.60 | 0.41 | 6.34 | 0.09 | 1.48 | 2.23 |
| 24 | 622583 | 202 | 2389 | 14.34 | 65.50 | 0.40 | 5.45 | 0.13 | 2.57 | 2.76 |
| 25 | 622584 | 186 | 2411 | 14.36 | 63.60 | 0.40 | 5.98 | 0.14 | 3.20 | 1.50 |

Results in ppm unless otherwise specified
T = element present; but concentration too low to measure
X = element concentration is below detection limit
– = element not determined

AUTHORISED OFFICER

655418

# ANALABS

A Division of Inchcape Testing Services (Australia) Pty. Ltd.
A.C.N. 004 591 664

## ANALYTICAL DATA

| SAMPLE PREFIX | REPORT No. | REPORT DATE | CLIENT ORDER No. | PAGE |
|---|---|---|---|---|
| | 100560.60.09379 | 16/04/93 | 2752 | 10 OF 15 |

| JBE No. | SAMPLE No. | Zr | Ti | Al2O3 | SiO2 | TiO2 | Fe2O3 | MnO | CaO | K2O |
|---|---|---|---|---|---|---|---|---|---|---|
| 1 | 622585 | 182 | 2380 | 14.10 | 63.90 | 0.40 | 4.97 | 0.14 | 3.90 | 3.01 |
| 2 | 622586 | 190 | 2380 | 13.88 | 64.70 | 0.40 | 3.98 | 0.11 | 4.52 | 2.53 |
| 3 | 622587 | 168 | 2454 | 14.39 | 64.70 | 0.41 | 5.36 | 0.10 | 2.55 | 1.87 |
| 4 | 622588 | 196 | 2414 | 14.41 | 64.80 | 0.40 | 6.64 | 0.13 | 2.63 | 1.95 |
| 5 | 622589 | 174 | 2367 | 13.94 | 65.10 | 0.39 | 4.59 | 0.13 | 4.21 | 2.18 |
| 6 | 622590 STD | 81 | 2720 | 15.07 | 51.60 | 0.45 | 10.01 | 0.89 | 3.82 | 1.14 |
| 7 | 622591 | 192 | 2500 | 14.30 | 65.70 | 0.42 | 5.42 | 0.12 | 2.27 | 3.06 |
| 8 | 622592 | 191 | 2350 | 13.53 | 63.70 | 0.39 | 4.71 | 0.13 | 4.48 | 2.68 |
| 9 | 622593 | 186 | 2386 | 14.38 | 65.00 | 0.40 | 5.38 | 0.13 | 2.73 | 3.05 |
| 10 | 622594 | 189 | 2410 | 14.52 | 63.60 | 0.40 | 5.96 | 0.16 | 3.59 | 3.40 |
| 11 | 622595 | 176 | 2356 | 13.91 | 61.70 | 0.39 | 5.60 | 0.17 | 5.03 | 2.51 |
| 12 | 622596 | 181 | 2395 | 13.87 | 63.40 | 0.40 | 4.38 | 0.14 | 5.11 | 2.49 |
| 13 | 622597 | 181 | 2526 | 14.30 | 60.70 | 0.42 | 7.22 | 0.15 | 2.57 | 1.43 |
| 14 | 622598 | 187 | 2568 | 14.47 | 62.80 | 0.43 | 7.22 | 0.12 | 1.68 | 1.25 |
| 15 | 622599 | 179 | 2369 | 13.58 | 61.00 | 0.40 | 7.13 | 0.17 | 4.63 | 1.55 |
| 16 | 622600 | 203 | 2020 | 13.07 | 62.70 | 0.34 | 3.23 | 0.13 | 6.77 | 3.75 |
| 17 | 622601 | 130 | 2461 | 12.94 | 52.80 | 0.41 | 7.65 | 0.24 | 9.42 | 1.88 |
| 18 | | | | | | | | | | |
| 19 | | | | | | | | | | |
| 20 | | | | | | | | | | |
| 21 | | | | | | | | | | |
| 22 | | | | | | | | | | |
| 23 | DETECTION | 5 | 100 | 0.01 | 0.01 | 0.01 | 0.01 | 0.01 | 0.01 | 0.01 |
| 24 | UNITS | ppm | ppm | % | % | % | % | % | % | % |
| 25 | METHOD | GX401 | OX408 | OX408 | OX408 | OX408 | OX408 | OX408 | OX408 | OX408 |

Results in ppm unless otherwise specified
T = element present; but concentration too low to measure
X = element concentration is below detection limit
– = element not determined

AUTHORISED OFFICER

655419

# ANALABS

A Division of Inchcape Testing Services (Australia) Pty. Ltd.
A.C.N. 004 591 664

## ANALYTICAL DATA

| SAMPLE PREFIX | REPORT No. | REPORT DATE | CLIENT ORDER No. | PAGE |
|---|---|---|---|---|
| | 100560.60.09379 | 16/04/93 | 2752 | 11 OF 15 |

| JBE No. | SAMPLE No. | MgO | P2O5 | S | Na2O | LOI | TOTAL | | | |
|---|---|---|---|---|---|---|---|---|---|---|
| 1 | 622485 | 2.15 | 0.397 | 0.034 | 0.66 | 10.41 | 99.87 | | | |
| 2 | 622486 | 2.41 | 0.328 | 0.029 | 2.43 | 5.71 | 99.76 | | | |
| 3 | 622487 | 3.16 | 0.312 | 0.427 | 3.68 | 4.13 | 99.59 | | | |
| 4 | 622488 | 2.47 | 0.304 | 0.376 | 4.69 | 3.10 | 100.01 | | | |
| 5 | 622489 | 2.70 | 0.295 | 0.477 | 3.87 | 3.48 | 99.51 | | | |
| 6 | 622490 | 3.94 | 0.288 | 0.508 | 3.72 | 4.51 | 100.44 | | | |
| 7 | 622491 | 4.04 | 0.285 | 0.562 | 4.26 | 5.27 | 100.02 | | | |
| 8 | 622492 | 4.13 | 0.281 | 0.694 | 3.60 | 5.69 | 99.97 | | | |
| 9 | 622493 | 3.47 | 0.267 | 0.896 | 2.90 | 6.53 | 100.40 | | | |
| 10 | 622494 | 3.67 | 0.247 | 0.663 | 4.32 | 4.00 | 100.46 | | | |
| 1 | 622495 | 3.30 | 0.234 | 0.644 | 3.12 | 7.86 | 99.80 | | | |
| 12 | 622496 | 2.37 | 0.253 | 0.406 | 4.04 | 4.39 | 100.05 | | | |
| 13 | 622497 | 3.04 | 0.248 | 0.488 | 3.59 | 4.62 | 99.98 | | | |
| 14 | 622498 | 2.43 | 0.254 | 0.406 | 3.24 | 4.26 | 99.86 | | | |
| 15 | 622499 | 2.52 | 0.256 | 0.919 | 3.55 | 5.41 | 99.50 | | | |
| 16 | 622500 | 2.02 | 0.248 | 0.880 | 3.86 | 5.60 | 99.64 | | | |
| 17 | 622501 | 2.02 | 0.250 | 0.940 | 3.85 | 4.83 | 99.62 | | | |
| 18 | 622502 | 2.25 | 0.244 | 0.728 | 4.04 | 4.05 | 99.57 | | | |
| 19 | 622503 | 2.02 | 0.249 | 0.522 | 3.77 | 4.42 | 99.65 | | | |
| 20 | 622504 | 2.38 | 0.251 | 0.722 | 2.73 | 5.66 | 99.94 | | | |
| 21 | 622505 STD | 7.48 | 0.187 | 0.089 | 3.48 | 5.55 | 99.66 | | | |
| 22 | 622506 | 2.61 | 0.239 | 1.218 | 2.40 | 6.88 | 99.58 | | | |
| 23 | 622507 | 3.50 | 0.244 | 0.256 | 3.17 | 4.38 | 99.67 | | | |
| 24 | 622508 | 2.18 | 0.241 | 0.170 | 3.12 | 5.44 | 99.68 | | | |
| 25 | 622509 | 1.94 | 0.244 | 0.192 | 4.00 | 4.80 | 99.58 | | | |

Results in ppm unless otherwise specified
T = element present; but concentration too low to measure
X = element concentration is below detection limit
– = element not determined

AUTHORISED OFFICER

655420

# ANALABS

A Division of Inchcape Testing Services (Australia) Pty. Ltd.
A.C.N. 004 591 664

## ANALYTICAL DATA

| SAMPLE PREFIX | REPORT No. | REPORT DATE | CLIENT ORDER No. | PAGE |
|---|---|---|---|---|
| | 100560.60.09379 | 16/04/93 | 2752 | 12 OF 15 |

| JBE No. | SAMPLE No. | MgO | P2O5 | S | Na2O | LOI | TOTAL | | | |
|---|---|---|---|---|---|---|---|---|---|---|
| 1 | 622510 | 2.42 | 0.246 | 0.203 | 3.25 | 4.75 | 99.60 | | | |
| 2 | 622511 | 2.58 | 0.247 | 0.688 | 1.10 | 7.11 | 99.66 | | | |
| 3 | 622512 | 1.94 | 0.337 | 4.770 | 0.23 | 18.48 | 99.81 | | | |
| 4 | 622513 | 5.04 | 0.537 | 4.700 | 2.26 | 10.26 | 100.35 | | | |
| 5 | 622514 | 6.14 | 0.542 | 1.478 | 2.13 | 8.73 | 99.71 | | | |
| 6 | 622515 | 5.64 | 0.533 | 1.320 | 2.34 | 8.65 | 99.63 | | | |
| 7 | 622516 | 6.31 | 0.496 | 0.436 | 1.71 | 8.75 | 99.54 | | | |
| 8 | 622517 | 7.59 | 0.508 | 0.482 | 1.71 | 10.03 | 99.65 | | | |
| 9 | 622518 | 5.97 | 0.459 | 0.487 | 1.72 | 12.43 | 99.55 | | | |
| 10 | 622519 | 5.01 | 0.421 | 0.207 | 1.25 | 15.67 | 99.69 | | | |
| 11 | 622520 | 6.96 | 0.511 | 0.131 | 1.20 | 4.46 | 99.61 | | | |
| 12 | 622521 | 4.81 | 0.418 | 0.110 | 1.33 | 17.48 | 99.64 | | | |
| 13 | 622522 | 7.41 | 0.369 | 0.089 | 1.83 | 4.23 | 99.65 | | | |
| 14 | 622523 | 9.21 | 0.285 | 0.091 | 2.01 | 5.50 | 99.72 | | | |
| 15 | 622524 | 7.91 | 0.291 | 0.045 | 2.34 | 5.09 | 99.61 | | | |
| 16 | 622525 | 7.58 | 0.292 | 0.022 | 1.97 | 4.15 | 99.65 | | | |
| 17 | 622526 | 6.36 | 0.285 | 0.023 | 2.60 | 9.21 | 100.11 | | | |
| 18 | 622527 | 7.43 | 0.277 | 0.023 | 2.06 | 3.59 | 99.55 | | | |
| 19 | 622528 | 7.56 | 0.292 | 0.026 | 2.39 | 3.55 | 99.67 | | | |
| 20 | 622529 | 7.82 | 0.295 | 0.084 | 2.29 | 3.21 | 99.90 | | | |
| 21 | 622530 | 7.20 | 0.282 | 0.029 | 2.34 | 4.69 | 99.76 | | | |
| 22 X | 622531 STD | 7.52 | 0.191 | 0.039 | 3.42 | 5.61 | 99.64 | | | |
| 23 | 622532 | 7.47 | 0.248 | 0.014 | 2.44 | 3.01 | 99.80 | | | |
| 24 | 622533 | 7.09 | 0.240 | 0.020 | 2.07 | 4.78 | 99.57 | | | |
| 25 | 622534 | 6.84 | 0.187 | 0.032 | 2.78 | 2.71 | 99.60 | | | |

Results in ppm unless otherwise specified
T = element present; but concentration too low to measure
X = element concentration is below detection limit
– = element not determined

AUTHORISED OFFICER

655421

# ANALABS

A Division of Inchcape Testing Services (Australia) Pty. Ltd.
A.C.N. 004 591 664

## ANALYTICAL DATA

| SAMPLE PREFIX | REPORT No. | REPORT DATE | CLIENT ORDER No. | PAGE |
|---|---|---|---|---|
| | 100560.60.09379 | 16/04/93 | 2752 | 13 OF 15 |

| JBE No. | SAMPLE No. | MgO | P2O5 | S | Na2O | LOI | TOTAL | | | |
|---|---|---|---|---|---|---|---|---|---|---|
| 1 | 622535 | 6.93 | 0.189 | 0.083 | 2.43 | 4.20 | 99.62 | | | |
| 2 | 622536 | 6.71 | 0.188 | 0.074 | 2.17 | 3.56 | 100.07 | | | |
| 3 | 622537 | 6.56 | 0.184 | 0.068 | 2.34 | 4.71 | 100.22 | | | |
| 4 | 622538 | 6.97 | 0.184 | 0.072 | 2.19 | 7.25 | 100.07 | | | |
| 5 | 622539 | 7.80 | 0.180 | 0.111 | 2.19 | 6.70 | 100.22 | | | |
| 6 | 622540 | 8.26 | 0.170 | 0.099 | 2.32 | 7.42 | 99.88 | | | |
| 7 | 622541 | 6.51 | 0.166 | 0.018 | 2.30 | 4.47 | 100.24 | | | |
| 8 | 622542 | 6.54 | 0.160 | 0.021 | 2.29 | 4.40 | 99.51 | | | |
| 9 | 622543 | 6.26 | 0.149 | 0.034 | 2.55 | 5.01 | 99.83 | | | |
| 10 | 622544 | 7.10 | 0.133 | 0.024 | 2.22 | 5.94 | 100.18 | | | |
| 11 | 622545 | 6.00 | 0.127 | 0.124 | 1.97 | 7.96 | 99.55 | | | |
| 12 | 622546 | 5.00 | 0.210 | 0.030 | 2.38 | 8.44 | 99.88 | | | |
| 13 | 622547 | 3.54 | 0.142 | 0.090 | 1.30 | 9.72 | 99.57 | | | |
| 14 | 622548 | 2.53 | 0.144 | 0.096 | 3.35 | 8.62 | 100.39 | | | |
| 15 | 622549 | 3.11 | 0.141 | 0.056 | 2.70 | 7.45 | 100.00 | | | |
| 16 | 622550 | 4.03 | 0.152 | 0.061 | 3.41 | 5.41 | 99.53 | | | |
| 17 | 622551 | 3.15 | 0.147 | 0.052 | 3.38 | 5.49 | 99.83 | | | |
| 18 | 622552 | 2.93 | 0.153 | 0.037 | 3.16 | 5.70 | 99.77 | | | |
| 19 | 622553 | 3.51 | 0.147 | 0.018 | 2.07 | 4.96 | 100.27 | | | |
| 20 | 622554 | 4.98 | 0.146 | 0.273 | 2.64 | 6.20 | 99.72 | | | |
| 21 | 622555 | 4.04 | 0.151 | 0.085 | 3.39 | 6.32 | 99.51 | | | |
| 22 | 622556 | 3.36 | 0.152 | 0.019 | 2.97 | 6.63 | 99.61 | | | |
| 23 | 622557 | 3.48 | 0.185 | 0.044 | 2.48 | 8.15 | 99.54 | | | |
| 24 | 622558 | 3.05 | 0.142 | 0.036 | 2.43 | 12.20 | 99.52 | | | |
| 25 | 622559 | 2.26 | 0.149 | 0.095 | 2.98 | 10.89 | 99.91 | | | |

Results in ppm unless otherwise specified
T = element present; but concentration too low to measure
X = element concentration is below detection limit
– = element not determined

AUTHORISED OFFICER

655422

# ANALABS

A Division of Inchcape Testing Services (Australia) Pty. Ltd.
A.C.N. 004 591 664

## ANALYTICAL DATA

| SAMPLE PREFIX | REPORT No. | REPORT DATE | CLIENT ORDER No. | PAGE |
|---|---|---|---|---|
| | 100560.60.09379 | 16/04/93 | 2752 | 14 OF 15 |

| JBE No. | SAMPLE No. | MgO | P2O5 | S | Na2O | LOI | TOTAL | | | |
|---|---|---|---|---|---|---|---|---|---|---|
| 1 | 622560 | 4.90 | 0.131 | 0.161 | 2.18 | 8.04 | 100.44 | | | |
| 2 | 622561 | 1.85 | 0.146 | 0.114 | 2.48 | 4.87 | 99.82 | | | |
| 3 | 622562 | 1.90 | 0.135 | 0.174 | 3.02 | 5.07 | 99.84 | | | |
| 4 | 622563 | 3.61 | 0.138 | 0.072 | 3.55 | 7.42 | 100.34 | | | |
| 5 | 622564 | 1.10 | 0.104 | 0.045 | 4.35 | 3.91 | 99.71 | | | |
| 6 | 622565 | 1.22 | 0.092 | 0.075 | 2.41 | 5.06 | 99.74 | | | |
| 7 | 622566 | 1.04 | 0.081 | 0.124 | 1.12 | 5.39 | 99.58 | | | |
| 8 | 622567 | 0.81 | 0.069 | 0.066 | 2.85 | 4.11 | 100.18 | | | |
| 9 | 622568 | 0.76 | 0.069 | 0.049 | 3.61 | 3.90 | 99.50 | | | |
| 10 | 622569 | 0.69 | 0.066 | 0.098 | 4.29 | 3.46 | 99.57 | | | |
| 11 | 622570 | 0.79 | 0.063 | 0.152 | 3.15 | 3.44 | 99.65 | | | |
| 12 | 622571 | 0.87 | 0.063 | 0.157 | 2.17 | 4.81 | 99.64 | | | |
| 13 | 622572 | 3.17 | 0.107 | 0.179 | 1.49 | 9.52 | 100.21 | | | |
| 14 | 622573 | 1.31 | 0.052 | 0.045 | 0.94 | 5.20 | 99.53 | | | |
| 15 | 622574 | 3.31 | 0.100 | 0.149 | 0.99 | 9.27 | 99.73 | | | |
| 16 | 622575 | 0.83 | 0.070 | 0.137 | 0.87 | 7.52 | 99.60 | | | |
| 17 | 622576 | 1.16 | 0.053 | 0.176 | 0.12 | 8.55 | 100.25 | | | |
| 18 | 622577 | 3.78 | 0.089 | 0.240 | 1.11 | 13.17 | 100.34 | | | |
| 19 | 622578 | 1.59 | 0.097 | 0.281 | 0.76 | 7.66 | 100.19 | | | |
| 20 | 622579 | 0.99 | 0.093 | 0.154 | 0.33 | 7.62 | 99.55 | | | |
| 21 | 622580 | 2.60 | 0.101 | 0.102 | 1.58 | 5.04 | 99.57 | | | |
| 22 | 622581 | 2.59 | 0.106 | 0.098 | 3.10 | 3.99 | 99.91 | | | |
| 23 | 622582 | 2.02 | 0.106 | 0.062 | 2.77 | 3.80 | 99.67 | | | |
| 24 | 622583 | 1.09 | 0.102 | 0.075 | 2.05 | 5.09 | 99.56 | | | |
| 25 | 622584 | 1.26 | 0.100 | 0.026 | 3.32 | 5.64 | 99.59 | | | |

Results in ppm unless otherwise specified
T = element present; but concentration too low to measure
X = element concentration is below detection limit
-- = element not determined

AUTHORISED OFFICER

655423

# ANALABS

A Division of Inchcape Testing Services (Australia) Pty. Ltd.
A.C.N. 004 591 664

## ANALYTICAL DATA

| SAMPLE PREFIX | REPORT No. | REPORT DATE | CLIENT ORDER No. | PAGE |
|---|---|---|---|---|
| | 100560.60.09379 | 16/04/93 | 2752 | 15 OF 15 |

| JBE No. | SAMPLE No. | MgO | P2O5 | S | Na2O | LOI | TOTAL | | | |
|---|---|---|---|---|---|---|---|---|---|---|
| 1 | 622585 | 0.98 | 0.102 | 0.040 | 2.07 | 6.03 | 99.61 | | | |
| 2 | 622586 | 0.78 | 0.100 | 0.042 | 4.04 | 4.66 | 99.73 | | | |
| 3 | 622587 | 2.07 | 0.126 | 0.055 | 3.53 | 4.41 | 99.55 | | | |
| 4 | 622588 | 1.52 | 0.103 | 0.046 | 3.14 | 4.21 | 100.01 | | | |
| 5 | 622589 | 1.11 | 0.109 | 0.059 | 3.76 | 4.81 | 100.35 | | | |
| 6 | 622590 STD | 7.51 | 0.191 | 0.044 | 3.42 | 5.60 | 99.73 | | | |
| 7 | 622591 | 1.45 | 0.105 | 0.127 | 3.44 | 3.27 | 99.68 | | | |
| 8 | 622592 | 1.15 | 0.100 | 0.038 | 3.67 | 5.00 | 99.54 | | | |
| 9 | 622593 | 1.16 | 0.105 | 0.094 | 3.49 | 3.73 | 99.67 | | | |
| 10 | 622594 | 1.74 | 0.104 | 0.098 | 2.46 | 3.56 | 99.63 | | | |
| 11 | 622595 | 1.29 | 0.097 | 0.014 | 3.88 | 5.05 | 99.67 | | | |
| 12 | 622596 | 0.94 | 0.103 | 0.012 | 4.94 | 4.33 | 100.12 | | | |
| 13 | 622597 | 4.19 | 0.130 | 0.063 | 3.43 | 4.97 | 99.59 | | | |
| 14 | 622598 | 4.01 | 0.104 | 0.032 | 3.40 | 4.17 | 99.69 | | | |
| 15 | 622599 | 2.08 | 0.098 | 0.032 | 2.99 | 5.90 | 99.54 | | | |
| 16 | 622600 | 0.35 | 0.085 | 0.029 | 3.03 | 6.12 | 99.59 | | | |
| 17 | 622601 | 4.45 | 0.238 | 0.029 | 3.10 | 6.71 | 99.85 | | | |
| 18 | | | | | | | | | | |
| 19 | | | | | | | | | | |
| 20 | | | | | | | | | | |
| 21 | | | | | | | | | | |
| 22 | | | | | | | | | | |
| 23 | DETECTION | 0.05 | 0.005 | 0.005 | 0.05 | 0.01 | 0.01 | | | |
| 24 | UNITS | % | % | % | % | % | % | | | |
| 25 | METHOD | OX408 | OX408 | OX408 | OX408 | OX408 | OX408 | | | |

Results in ppm unless otherwise specified
T = element present; but concentration too low to measure
X = element concentration is below detection limit
– = element not determined

AUTHORISED OFFICER

# APPENDIX XI

655425

# Logistics report for an heliborne magnetic and radiometric survey over MacIntosh, Anthony Basin & Lynchford areas Western Tasmania for Aberfoyle Resources Limited

Job No 3-445

May 1993

Geoterrex Pty Ltd
7-9 George Place
Artarmon NSW 2064

## TABLE OF CONTENTS

PAGE

INTRODUCTION ..... 1

1. SURVEY OPERATIONS SUMMARY ..... 2

2. FLIGHT PATH RECOVERY ..... 4

3. EQUIPMENT AND SPECIFICATIONS ..... 5

4. CALIBRATION PROCEDURES AND RESULTS ..... 11

5. DATA PROCESSING ..... 14

6 ITEMS DELIVERED ..... 17

APPENDIX A: SPECTROMETER CALIBRATION DATA

Uranium and Thorium Source Check Data
FIGURE A1 Uranium and Thorium Source Check Spectra
FIGURE A2 Cosmic Background Graphs
FIGURE A3 Height Attenuation Graphs
FIGURE A4 Thorium Peak Resolution Check

APPENDIX B: MAGNETIC DATA TAPE FORMATS

TABLE B1 Located Data Tape Format
TABLE B2 Field Data Tape Format

APPENDIX C: RMS THERMAL PAPER STORAGE INSTRUCTIONS

APPENDIX D: LOCATION MAP

## LIST OF FIGURES

PAGE

FIGURE 1: Sample Analogue Record ..... 10

## LIST OF TABLES

PAGE

TABLE 1: Survey Progress ..... 3

TABLE 2: Altimeter Calibration Results ..... 13

## INTRODUCTION

From 1-25 March 1993, Geoterrex Pty Ltd conducted an heliborne magnetometer and spectrometer survey over three areas on the Franklin and Sophia 1:100,000 sheets in Tasmania (See Appendix D) for Aberfoyle Resources Ltd. This report summarises the logistics, survey parameters, calibration procedures and processing details of the survey.

A total of 1,620 line kilometres were flown over three areas for Aberfoyle Resources:

| | | |
|---|---|---|
| 1) | **Mackintosh:** | 1,087 line kilometres |
| 2) | **Anthony Basin:** | 340 line kilometres |
| 3) | **Lynchford:** | 193 line kilometres |

A line spacing of 100 metres was used. Both magnetic and radiometric data was collected by helicopter. Preliminary in-field processing was undertaken with final processing at Geoterrex's processing centre in Sydney.

The bases of operations were Que River Mine and Queenstown, Tasmania.

655429



## PART 1
## Survey operations summary

| | | |
|---|---|---|
| **Type of survey:** | Magnetic and radiometric | |
| **Base of operations:** | **Area 1:** | Que River Mine |
| | **Area 2/3:** | Queenstown |
| **Aircraft:** | Aerospatiale Squirrel 350B | |
| **Survey Area(s) Name:** | **Area 1:** | Mackintosh |
| | **Area 2:** | Anthony Basin |
| | **Area 3:** | Lynchford |
| **Approximate Survey Size:** | **Area 1:** | 1,087 Line Kilometres |
| | **Area 2:** | 340 Line Kilometres |
| | **Area 3:** | 193 Line Kilometres |
| **Flight Line Direction:** | **Area 1:** | 112° AMG |
| | **Area 2:** | 90° AMG |
| | **Area 3:** | 90° AMG |
| **Line Spacing:** | 100 Metres | |
| **Tie Line Direction:** | Orthogonal to traverse lines | |
| **Tie Line Spacing:** | 1,000 Metres | |
| **Minimum Line Length:** | 3 Kilometres | |
| **Minimum In-fill Line Length:** | 3 Kilometres | |
| **Navigation:** | DGPS | |
| **Nominal sensor terrain clearance:** | 80 metres, above tree canopy | |
| **Nominal aircraft speed:** | 40 metres per second | |

**Field Personnel:**

| | |
|---|---|
| **Pilot:** | D Wood |
| **Navigator:** | J Sparkman |
| **Electronics Technician:** | D Lyus |
| **Project Manager and Data Compiler:** | T Donnollan |

**Table 1: Survey Progress**

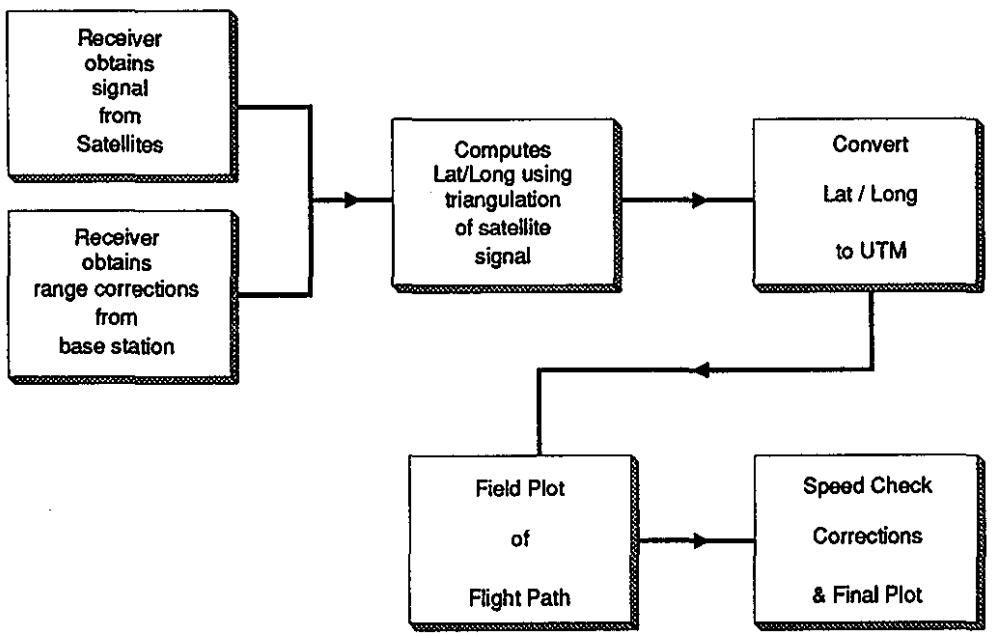
| Date | Flight | Production/ shared days | Progress |
|---|---|---|---|
| 26-28 February | - | - | System installation |
| 1 March | - | x | Move to Que River Mine |
| 2 March | - | - | Weather day |
| 3 March | - | x | Installed DGPS beacon |
| 4 March | 1 | P Area 1 | Tie lines |
| 5 March | 2 | P Area 1 | Traverse lines |
| 6 March | 3 | P Area 1 | Traverse lines |
| 7 March | 4 | P Area 1 | Traverse lines |
| 8 March | 5/6 | x Area 1 | Flight 5 lag test |
| 9-20 March | Flights for another survey | | |
| 21 March | 7 | x Area 2 | |
| 22 March | 8 | x Area 2 | |
| 23 March | - | - | Weather day |
| 24 March | 9 | P Area 2 & 3 | |
| 25 March | 10 | x Area 3 | |

**Total number of days:**

| | |
|---|---|
| **Production (P):** | 5 |
| **Shared (x):** | 6 |
| **TOTAL:** | **11** |

## PART 2
## Flight path recovery

### DGPS Navigation System Procedures




The DGPS receiver mounted in the aircraft determines which satellites are in operation and receives a signal from them. The base station transmits range corrections to the aircraft receiver, which it applies as it uses 3D triangulation of the satellite response to calculate its position in real time as well as providing the pilots with steering information. The DGPS information is stored digitally as Latitudes and Longitudes (Lat / Longs) and later converted to Universal Transverse Mercator (UTM) co-ordinates.

The DGPS data is read into the field computer and plotted on a daily basis to ensure data quality control and to determine any necessary reflights.

## PART 3
## Equipment and specifications

### 3.1) MAGNETOMETER

**Model:** Scintrex cesium vapour optical absorption magnetometer

**Mounting:** Towed Bird

**Sample Interval:** 0.1 seconds

**Sensitivity:** 0.05 nT

**Average noise:** The average noise for the survey data is calculated from the fourth difference monitor using the equation:
(Fourth difference noise envelope)/16 = Average Data Noise

**System parallax:** The system parallax was determined in a test flight (see Section 4 and Appendix A)

### 3.2) GAMMA RAY SPECTROMETER

**Model:** Nuclear Data ADC/ND-560

**Detectors:** 4 Harshaw all viewing 2 pi NaI(Tl) crystals, totalling 16.8 litres.* Crystals, photomultiplier tubes and preamplifiers are all mounted in temperature controlled, insulated compartments.

**Sample Interval:** 1 second

**Number of channels:** 256

**Synchronisation:** The spectrometer sample is allocated to the time recorded at the end of the sample interval.

**Window definitions:**

| | | | |
|---|---|---|---|
| Total Count | - | Channel 68 to 255 | |
| Potassium | - | Channel 116 to 133 | |
| Uranium | - | Channel 141 to 158 | |
| Thorium | - | Channel 206 to 240 | |
| Cosmic | - | Channel 0 | |

**Nominal window MeV Ranges:**

| | | | |
|---|---|---|---|
| Total Count | - | 0.4 to 3.0 MeV | |
| Potassium | - | 1.35 to 1.57 MeV | (K40, 1.46 MeV) |
| Uranium | - | 1.63 to 1.89 MeV | (Bi214, 1.76 MeV) |
| Thorium | - | 2.42 to 2.82 MeV | (Tl208, 2.615 MeV) |
| Cosmic | - | 3.0 - 6.0 MeV | |

* NOTE Due to crystal problems the Macintosh area was flown using a detector crystal volume of 12.6 litres. The other two area were flown with a full crystal volume.

## 3.3) GROUND MAGNETOMETER BASE STATION

**Sensor:** Proton Precession
**Magnetometer:** Geometrics G856
**Sample interval:** 5 seconds
**Sensitivity:** 0.1 nT
**Full scale deflection:** 50 nT

The base station was used to monitor the diurnal field. The sensor was placed in a suitable position which minimises the effects of high magnetic gradients and man-made interference.

## 3.4) ALTIMETERS

### Radar altimeter

**Model:** Sperry Stars AA100 radio altimeter system
**Sample interval:** 1.0 second
**Accuracy:** +/- 1.5% (+/- 1m at 60m)
**Synchronisation:** The average of the output of the altimeter over each second is calculated and assigned to the time recorded at the end of each sample.

### Barometric altimeter

**Model:** Rosemount 840F pressure altimeter
**Sample interval:** 1.0 second
**Sensitivity:** 5 mv per foot

## 3.5) TRACKING CAMERA

**Model:** Sony DXC101P Video Camera with a Panasonic video recovery system

The tracking camera is equipped with a 4 mm wide-angle lens. The video tape is synchronised with the geophysical record by a digital fiducial display that increments every second. These fiducials are recorded on the video tape and displayed on the bottom left of the video screen. Times are recorded from the digital information provided by the MADACS system.

## 3.6) POSITIONING/NAVIGATION SYSTEM

**Model:** 2 Sercel NR103 mobile DGPS receiver and antennae mounted in aircraft and equipped with pilot steering indicator
**Reference station:** 1 Sercel NDS100 portable differential station UHF and DGPS antennae
**Base station:** DGPS base station with lap top data logger

## 3.7) DATA ACQUISITION SYSTEM

**Model:** Geoterrex Pty Ltd MADACS

The MADACS is a computer based software system that is used to control and command the operations of all the ancillary equipment. This includes the magnetometer, spectrometer, *camera, altimeter, tape drive and analogue chart recorder.* The system has the following features.

### Communication system

The MADACS uses a lap top operating as a terminal for operator-system communication. Recorded spectrum are monitored via an oscilloscope trace during acquisition.

### Software system

**Program:** MS8

The key feature of this system is that all data collection, verification, buffering, and recording is software-controlled. Therefore, the acquisition system may be economically altered to fit almost any requirement. Critical parameters are automatically monitored during flight, with visual and aural alarms provided for the operator.

Survey parameters are displayed during flight in their correct physical units, simplifying operator analysis. The survey program operates on a request-response basis, with the system pre-empting the operator and rejecting all illegal responses.

### Tape Drive

**Model:** Kennedy 800

The tape drive has a feature which allows checking of the recording process as many times as the particular application permits.

### Precision Clock

The system is controlled by a precision clock which allows data to be collected at any multiple of 0.1 seconds. Time is digitally recorded as a six-figure number called a "fiducial". A fiducial number equals the real time in tenths of seconds after midnight, for example, 000000 corresponds to midnight and 360000 corresponds to 10.00am. Fiducials are generated on digital tape, video or film and analogue charts at ten second intervals. The fiducial numbers are calculated from the clock time by the computer.

### Computer

**Model:** Interdata 6/16 mini-computer.

Multiple buffers permit recording, processing and acquisition of data to be carried out simultaneously with no dead time. The computer has the following interfaces:

- **Digital Input/Output Bus** This bus is capable of recording from, writing to, testing and controlling 16 external digital devices.
- **ADC / DAC.** This interface is a caesium analogue to digital converter and a digital to analogue converter.
- **Magnetic Tape Controller** This interface/controller is capable of handling four 9-track NRZI tape transports. Tapes are written in an IBM compatible binary format with full parity, cyclic redundancy and longitudinal check characteristics.
- **Magnetometer Interface** This interface converts the signal from the high sensitivity caesium vapour magnetometer into a format acceptable to the MADACS.
- **Camera Controller** The interface allows the MADACS to control and monitor all aspects of the tracking camera's operation and can synchronise timing and navigation data to the video tape.
- **Operator's Console** This interface provides communication between the operator and the system. While on line during survey, all parameters are continuously displayed on the monitor unless the system senses an abnormal condition in which case a diagnostic message and the time sensed are displayed. The message remains until acknowledged by the operator.

### Recorded Digital Data

**Each second:**
Flight number
Time
Radar Altitude
Barometric Altitude
Positioning data
Spectrometer windows
256 channels of radiometric data
Live time

**Each 0.1 seconds:** Total magnetic field

Tape formats are documented in Appendix B.

## 3.8) ANALOGUE CHART RECORDER

**Model:** RMS GR33 Thermal Dot Matrix Printer
**Chart speed:** 10 cm/minute; time increases from left to right
**Chart width:** 30 cm
**Event marks:** 10 second marks are recorded on both sides of the chart with the associated fiducial numbers being printed at the base of the chart.

**Channels recorded & full-scale values:**

| | |
|---|---|
| **Total magnetic field:** | |
| **Fine scale:** | 100 nT |
| **Coarse scale:** | 1000 nT |
| **Magnetic field fourth difference:** | +/-20 nT |
| **Terrain clearance:** | 200 metres |
| **Total Count:** | *2000 counts/sec* |
| **Potassium Count:** | 250 counts/sec |
| **Uranium Count:** | 100 counts/sec |
| **Thorium Count:** | 100 counts/sec |
| **Cosmic Count:** | 500 counts/sec |

All fields increase in value towards the top of the chart.

**Zero Positions:** These zero positions are annotated on the analogue sample. The zero position of each radiometric channel is calibrated automatically at the start of each line. Between lines each trace resides in its mid-range position.

**Synchronisation:** No lags occur between traces, other than that which occurs between *the magnetic field and its fourth difference.*

**Compton Effect Corrections:** The analogue radiometric channels have been Compton corrected using:

| | | |
|---|---|---|
| **Alpha** (Thorium into Uranium) | - | 0.443 |
| **Beta** (Thorium into Potassium) | - | 0.424 |
| **Gamma** (Uranium into Potassium) | - | 0.695 |

The radiometric data recorded on the field tapes has not been corrected.

**Cosmic Background correction:** The analogue radiometric channels have been corrected in real time, for aircraft and cosmic background using the equations set out in *Section 4.*

An annotated sample analogue record is shown in Figure 1.

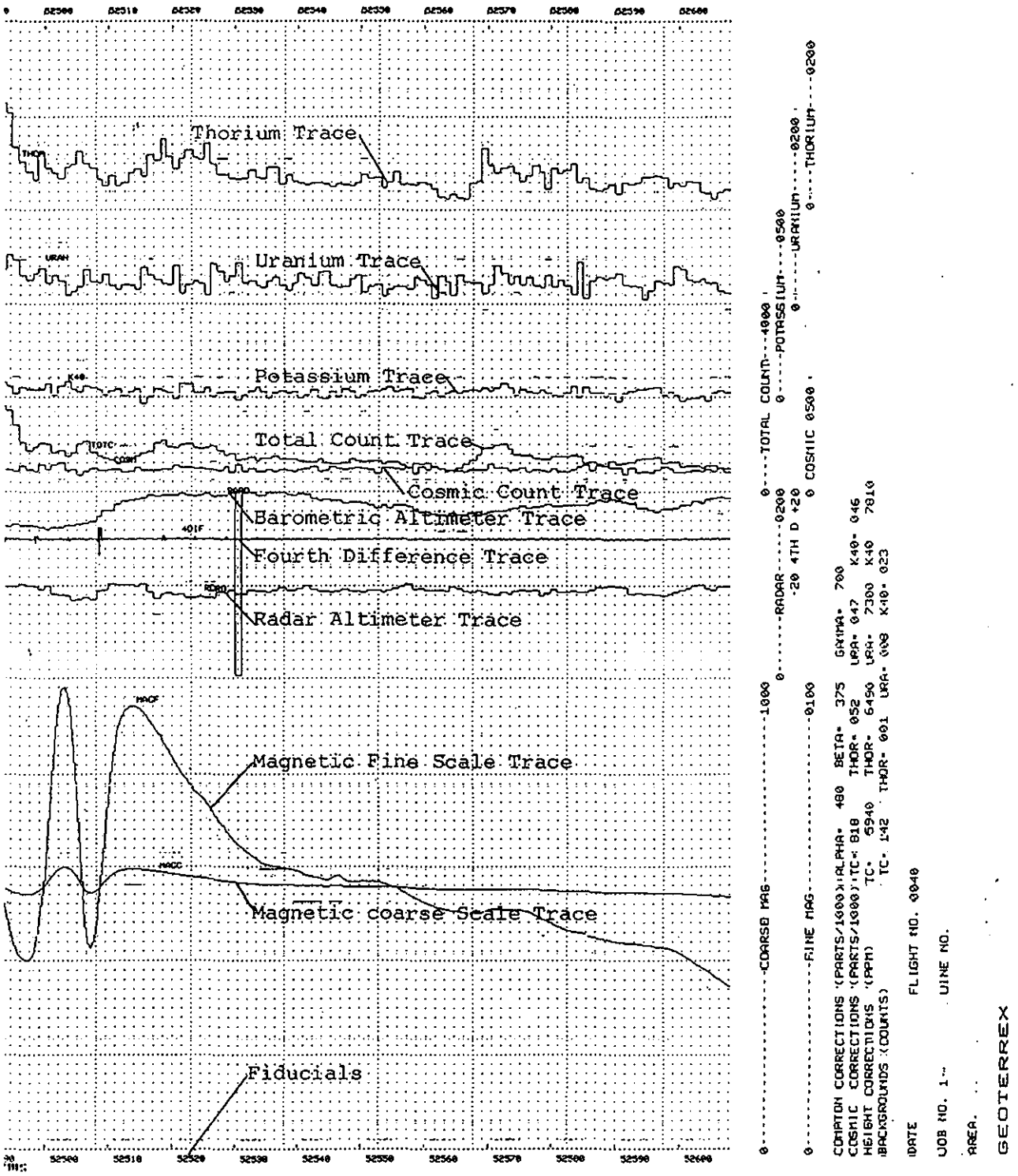



**Figure 1** Sample analogue record

# PART 4
# Calibration procedures and results

## 4.1) MAGNETOMETER

The following calibration tests were carried out on the magnetometer.

**Parallax** (also referred to as 'Lag Test')

This test was carried out on 8 March 1993. The aircraft was flown in opposite directions over a sharp magnetic anomaly with the tracking camera and magnetometer operating. The video system records the fiducial (time and X-Y position) of the body which was the source of the sharp magnetic anomaly. When this was compared to the fiducial (time and X-Y position) of the sharp magnetic anomaly recorded on the digital tape a difference of 1.0 seconds was found. Therefore a parallax correction of this magnitude and sense was applied to the magnetic data only.

## 4.2) SPECTROMETER

The following checks and determinations were carried out for the radiometric data.

### Pre and Post-flight Source Check Procedures

- Pre and post-flight U and Th source checks with samples in a standard position relative to the crystals and the aircraft in a standard parking position - recorded for 100 seconds.
- Pre and post-flight test line recorded at survey altitude.

The results of the pre and post-flight uranium and thorium source checks can be found in Appendix A. A sample of the spectra plotted with each uranium and thorium source check is presented in Appendix A, Figure A1.

### Compton Stripping Coefficients

These coefficients have been recently determined and adjusted from 23 source checks conducted during the survey in June 1992.

| | | | |
|---|---|---|---|
| They are: | **Alpha** | - | 0.421 +/- 0.015 |
| | **Beta** | - | 0.411 +/- 0.024 |
| | **Gamma** | - | 0.678 +/- 0.038 |
| | **Delta** | - | 0.036 +/- 0.017 |

### Background Determination

This test was carried out on 26 March 1993 to determine the relationship between cosmic events (energies greater than 3.0 MeV) and counts recorded in other channels. The test was flown overland with the spectrometer system correctly calibrated as for survey work. Data was recorded at 2000 foot intervals from 2000 feet to 10000 feet ASL.

The best fit linear equations for these tests are:

| | | | |
|---|---|---|---|
| **Th** | background | = | 0.056 x Cosmic + 0.88 |
| **U** | background | = | 0.049 x Cosmic + 5.36 |
| **K** | background | = | 0.052 x Cosmic + 9.26 |
| **TC** | background | = | 0.825 x Cosmic + 84.84 |

| | | | |
|---|---|---|---|
| where: | **cosmic** | = | counts of energies greater than 3.0 MeV stored in channel 0. |
| | **# background** | = | counts to be subtracted from window #. |

Graphs of these equations are presented in Appendix A (Figure A2).

### Height Attenuation Coefficients

Since no height attenuation calibrations were required for the temporary helicopter installation, those used for Geoterrex's permanent fixed wing spectrometer system were used. They were determined using the following procedure:

a) An area with "homogeneous" radioactivity, high count rates and relatively flat terrain was selected.

b) An easily repeatable line was flown over this area at eight different altitudes: 200 feet, 250 feet, 300 feet, 400 feet, 500 feet, 600 feet, 700 feet and 800 feet. The spectrometer was correctly calibrated for this test flight.

c) Sections of each line sharing the most constant terrain clearance and count rate were selected for data processing.

d) The altitude data for each line section was corrected using the altitude calibrations recorded on the same flight, and averaged.

e) The radiometric data for each line section was background corrected using a height correction for alpha. The resultant data was averaged.

f) The resulting count rates in each channel were plotted and attenuation coefficients suitable for an air temperature of 21°C were determined.

Graphs of the results can be found in Appendix A (Figures A3).

| | | |
|---|---|---|
| The coefficients are: | Total count | 0.00630 per metre |
| | Potassium count | 0.00768 per metre |
| | Uranium count | 0.00595 per metre |
| | Thorium count | 0.00643 per metre |

During all spectrometer tests the data used is the window data recorded on field tapes. The widths of these windows are specified in Section 3.2.

### Resolution

The resolution of the spectrometer is defined as the full width of the Thorium peak at its half peak height position, expressed as a percentage of the peak MeV value. The spectrometer resolution was checked before during and after the survey. The results give an average of 5.63%. Appendix A (Figure A4) is a copy of a sample source check.

## 4.3) ALTIMETER

The Sperry radio altimeter is a high quality instrument whose output is factory calibrated. It is fitted with a test function which checks the calibration of a terrain clearance of 100 feet and altitudes which are multiples of 100 feet. Calibration of the recorded terrain clearance, both analogue and digital, with respect to the altimeter reading is carried out using a potentiometer to vary the reading while recording the altimeter's output.

The results of an altimeter calibration carried out in March 1993 are presented in Table 2. A graph of the results is presented in Figure 3. Regression analysis provides a line of best fit for values less than 500' and another for values greater than 500'. These have been included on the graph, and the equations are:

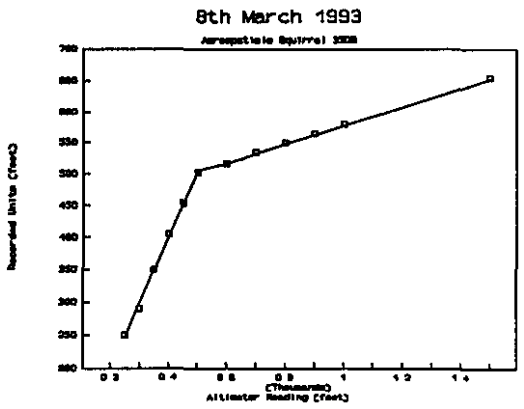
< 500' Recorded Units = 1.04 * Altimeter Reading - 13.4
> 500' Recorded Units = 0.15 * Altimeter Reading + 428

Barometric altitude was also recorded to provide an absolute measure of aircraft altitude rather than aircraft terrain clearance which is measured by the radio altimeter.

**Table 2: Altimeter calibration results**

| **Indicated Alt** (feet) | **Recorded Radar Alt** (feet) |
|---|---|
| 250 | 250 |
| 300 | 290 |
| 350 | 350 |
| 400 | 405 |
| 450 | 455 |
| 500 | 503 |
| 600 | 518 |
| 700 | 535 |
| 800 | 550 |
| 900 | 565 |
| 1000 | 580 |
| 1500 | 655 |

**Figure 3: Altimeter calibrations**



## PART 5
## Data processing

### 5.1) FIELD TAPES

These are recorded in binary format and are compacted and reformatted in binary code. The following information is transferred to a file as the Compacted Field Tape (CFT).

- flight path
- magnetic reading (0.1 nT)
- radiometric data (256 channels)
- radar altimeter (feet)
- barometric altimeter (feet)
- fiducial (time in tenth seconds after midnight)
- DGPS co-ordinates

All channels are checked and edited for single reading spikes and recording gaps, any single reading spikes are removed manually.

### 5.2) DATA TAPES

#### Located Data Tape

A levelled located data tape, containing all traverse line, tie line and calibration line data, was recorded in 9-track ASCII code at a density of 6250 bpi in a format described in Appendix B.

#### Gridded data tape

Gridded data in ER Mapper format with accompanying header files was provided for processed radiometric channels potassium, thorium, uranium and total count and for levelled magnetic data. These files were provided on QIC 150 megabyte cartridge.

### 5.3) FLIGHT PATH

Processing of the flight path consisted of generating a speed report of the DGPS flight path that was checked for erroneous points by comparing the average aircraft speed between adjacent fixes (being real time values in seconds) and the average speed for the entire line. Significant speed changes over short intervals were noted and the DGPS data was checked for errors and corrected where necessary.

The following convention is used for line number: 101/2N

where the number preceding the decimal is the line number (eg. 101)
the number following the decimal is the part number (eg. the line was the second flight along that line)
the letter represents the flight direction (eg flown to the north)

Lines 101 - 152 are traverse lines for Lynchford. Lines 701 - 704 are tie lines for Lynchford
Lines 201 - 292 are traverse lines for Anthony Basin. Lines 711 - 714 are tie lines for Anthony Basin
Lines 301 - 505 are traverse lines for Macintosh. Lines 721 - 732 are tie lines for Macintosh

## 5.4) MAGNETIC DATA

### a) *Corrections*

#### Levelling

The aeromagnetic data is levelled by diurnal subtraction. The base station data is edited and checked for level shifts. This data is then synchronised to the airborne data for subtraction.

#### International Geomagnetic Reference Field

The International Geomagnetic Reference Field known as IGRF (1990) is subtracted from the data and a datum of 2000 nanoteslas is then added to ensure that there are no negative magnetic values before contouring.

### b) Product Specifications

#### Gridding and Contouring

| | | | | |
|---|---|---|---|---|
| **Grid mesh size:** | 25 x 25 metres | | | |
| **Grid filter:** | None | | | |
| **Contour maps:** | Horizontal scale | - | 1:10,000 | |
| | Contour interval | - | **Area 1:** | 2, 20, 200 nT |
| | | | **Area 2:** | 2, 20, 200 nT |
| | | | **Area 3:** | 2, 20, 200 nT |
| **Stacked magnetic profile maps:** | Horizontal scale | - | 1:10,000 | |
| | Vertical scales | - | **Area 1:** | 5,50 nT/cm* |
| | | | **Area 2:** | 50 nT/cm |
| | | | **Area 3:** | 50 nT/cm |

* The three northern sheets plotted with a vertical scale of 5 nT/cm
The three southern sheets plotted with a vertical scale of 50 nT/cm

## 5.5) RADIOMETRIC DATA

### a) Corrections

The radiometric data was corrected for:

#### i) Spectrometer dead time

*"Dead time" is the fraction of 1 second when the spectrometer is* actually counting the energy levels and not registering the incoming counts. A typical "dead time" is 15 msecs in a 1 second sample period.

#### ii) Cosmic effect and aircraft background

Through test flying outlined in Section 4, Geoterrex Pty Ltd has established the coefficients for the linear relationship between the incoming cosmic counts (energies greater than 3 MeV) and their contribution to the background in each window.

### iii) Changes in ambient air temperatures

The effects of changing air temperature are incorporated in the notion of a temperature corrected altitude that will be used in other calculations. The field operator records the outside temperature at regular intervals throughout each flight while at survey altitudes.

### iv) Compton scattering

After testing the Compton stripping coefficients determined from the calibration procedures outlined in Section 4, new values were chosen to minimise over compensation for the actual interchannel relationships on each survey line which were found to be less than the ideal relationship measured on the ground during calibration. The values used were:

| | | |
|---|---|---|
| Alpha | - | 0.421 |
| Beta | - | 0.411 |
| Gamma | - | 0.678 |
| Delta | - | 0.036 |

It should be noted that alpha coefficient is height dependent under the linear relation:

true alpha = ground + 0.02 + 0.00025 x height

### v) Height attenuation

To minimise the possibility of over correcting the data for height variations, an altitude tapering function was applied. The data was attenuated to approximately the mean survey terrain clearance minus one standard deviation (110 metres). Tapering began at 175 metres and finished at 200 metres, so for altitudes greater than 200 metres the data was corrected as if it had been collected at 200 metres.

Attenuation constants:

| | | |
|---|---|---|
| Total count | - | 0.00630 |
| Potassium | - | 0.00768 |
| Uranium | - | 0.00595 |
| Thorium | - | 0.00643 |
| Alpha | - | 0.00076 |

## b) Production specifications

Gridding and contouring

Grid mesh size: 25 x 25 metres
Grid filter: None
Full colour map for each radiometric channel
Map scale: **Area 1:** 25,000
**Area 2:** 25,000
**Area 3:** 10,000

655444



## PART 6
## Items delivered

- Logistics Report

- Final Flight Path Maps on film at 1:10,000 scale
  Final Residual Magnetic Contour Maps on film at 1:10,000 scale
  Final Residual Magnetic Profile Maps on film at 1:10,000 scale
  Laminated radiometric colour maps for each channel at appropriate scale

- Binders containing Analogue Charts
  Diurnal charts

- Located Data Tape
  Gridded Data in ER Mapper Format on QIC 150 Mb cartridge

- Flight Logs and Index
  Mileage listing
  Recovered Line Listing
  Tracking videos

## APPENDIX A: SPECTROMETER CALIBRATION DATA

| Flight | | Pre Flight | | Post Flight | |
|---|---|---|---|---|---|
| | | U Source | Th Source | U Source | TH Source |
| 1 | U count | 8374 | 7295 | 8211 | 6735 |
| | Th count | 412 | 16059 | 304 | 15956 |
| | K count | 6115 | 7144 | 5772 | 7913 |
| | Total count | 89414 | 206206 | 88502 | 206468 |
| 2 | U count | 8715 | 7021 | 8224 | 6723 |
| | Th count | 392 | 16222 | 203 | 15949 |
| | K count | 6124 | 7692 | 6124 | 7861 |
| | Total count | 88942 | 206891 | 89292 | 205350 |
| 3 | U count | 8369 | 7425 | 8477 | 6927 |
| | Th count | 348 | 16070 | 344 | 15927 |
| | K count | 6071 | 7211 | 6278 | 7663 |
| | Total count | 88300 | 205838 | 89090 | 206174 |
| 4 | U count | 8636 | 7187 | 8500 | 7093 |
| | Th count | 486 | 16162 | 450 | 15941 |
| | K count | 6190 | 7408 | 6243 | 7485 |
| | Total count | 89618 | 205940 | 89404 | 206762 |
| 8 | U count | 10755 | 8800 | 10741 | 9248 |
| | Th count | 528 | 20006 | 316 | 19927 |
| | K count | 7755 | 9564 | 7594 | 9197 |
| | Total count | 110265 | 254740 | 111763 | 255522 |
| 9 | U count | 11051 | 9031 | 11008 | 9388 |
| | Th count | 248 | 19905 | 423 | 19227 |
| | K count | 7822 | 9336 | 7593 | 8885 |
| | Total count | 112759 | 254150 | 111954 | 255755 |

FIGURE A1(i) - SAMPLE SOURCE CHECK - URANIUM SOURCE

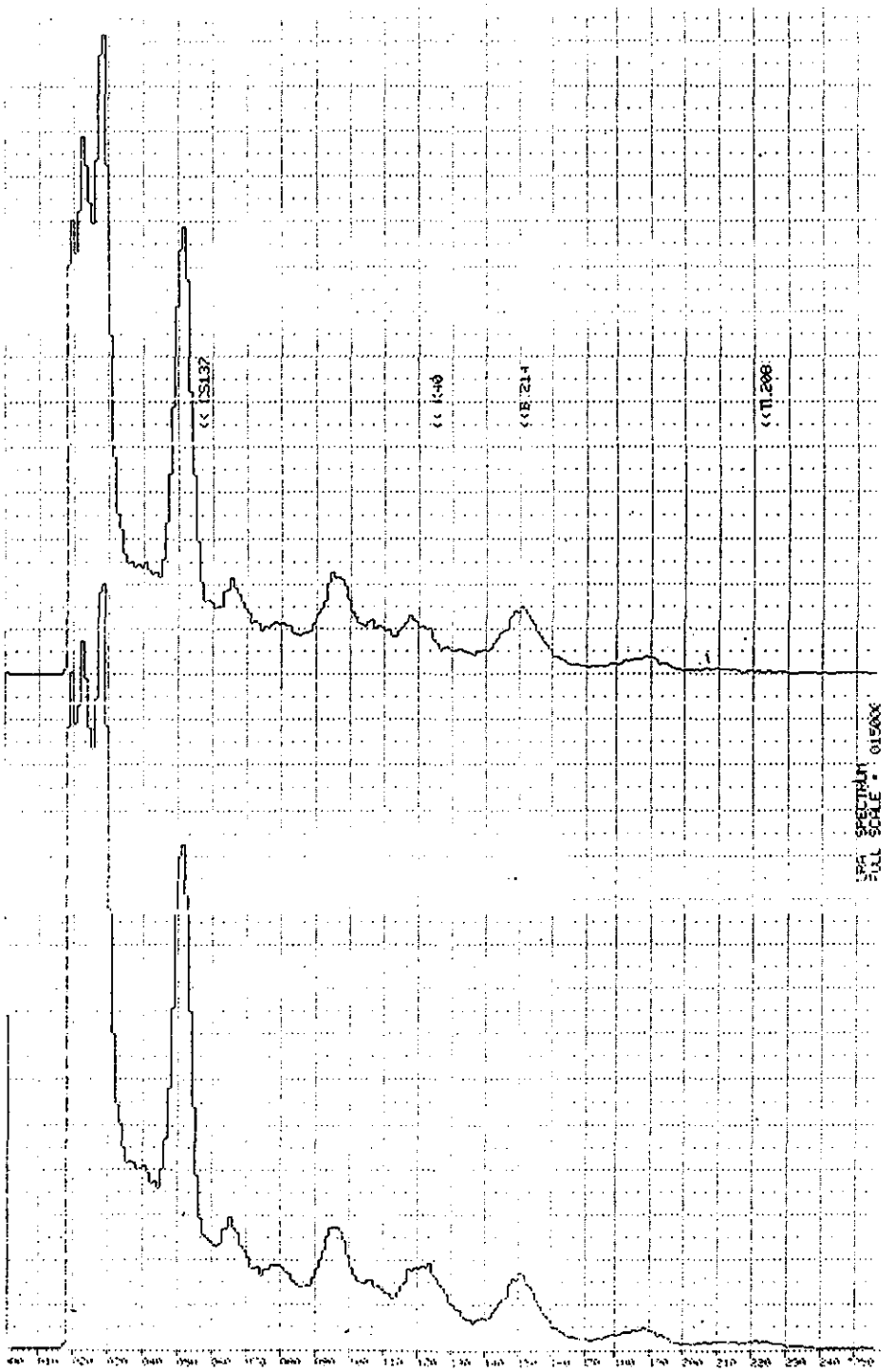
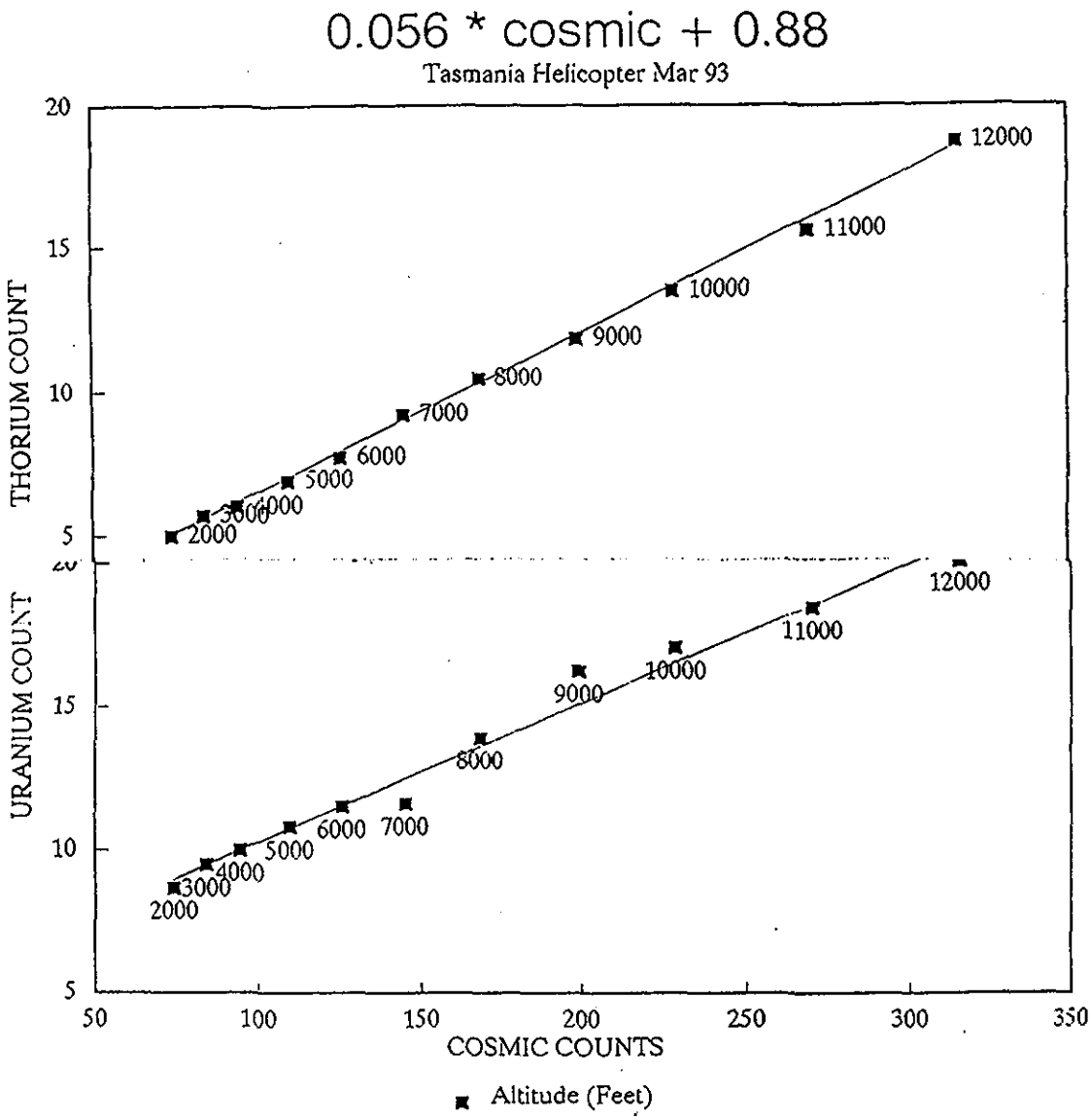


FIGURE A1(ii) - SOURCE CHECK - THORIUM SOURCE



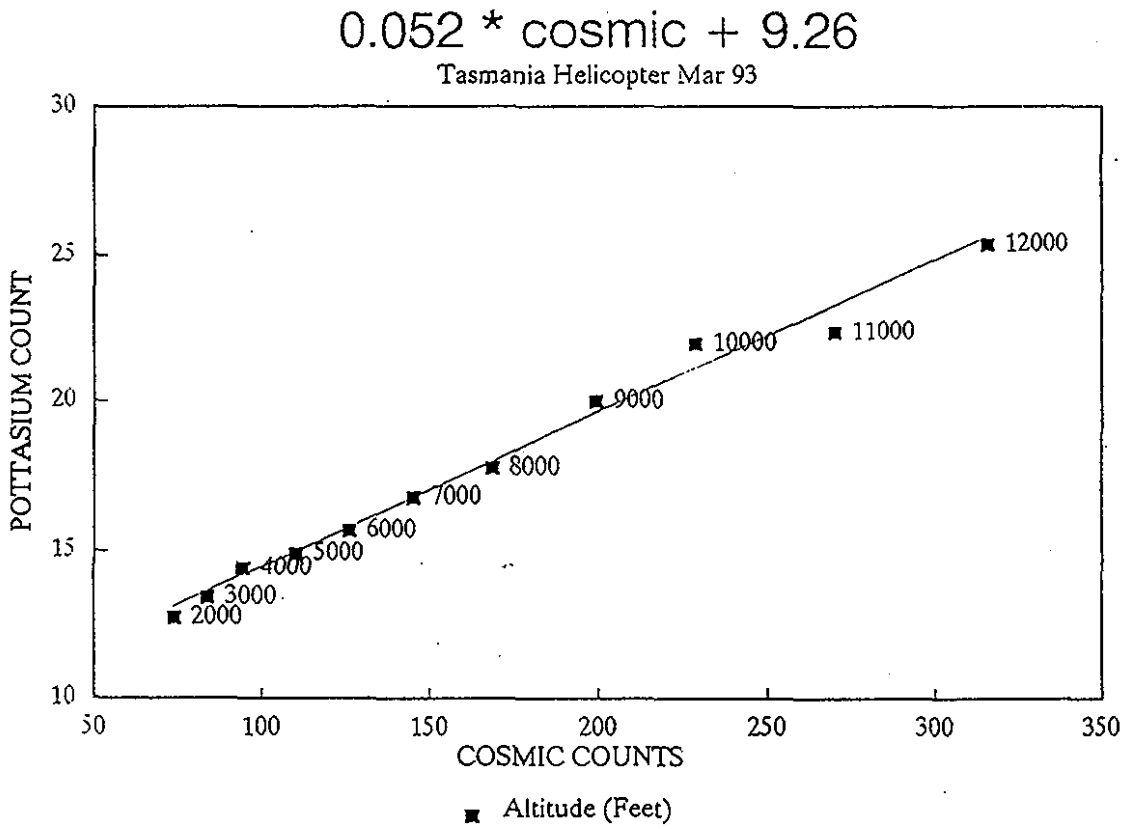
FIGURE A2 COSMIC BACKGROUND TESTS




5 cm

FIGURE A2 COSMIC BACKGROUND TESTS

5 cm



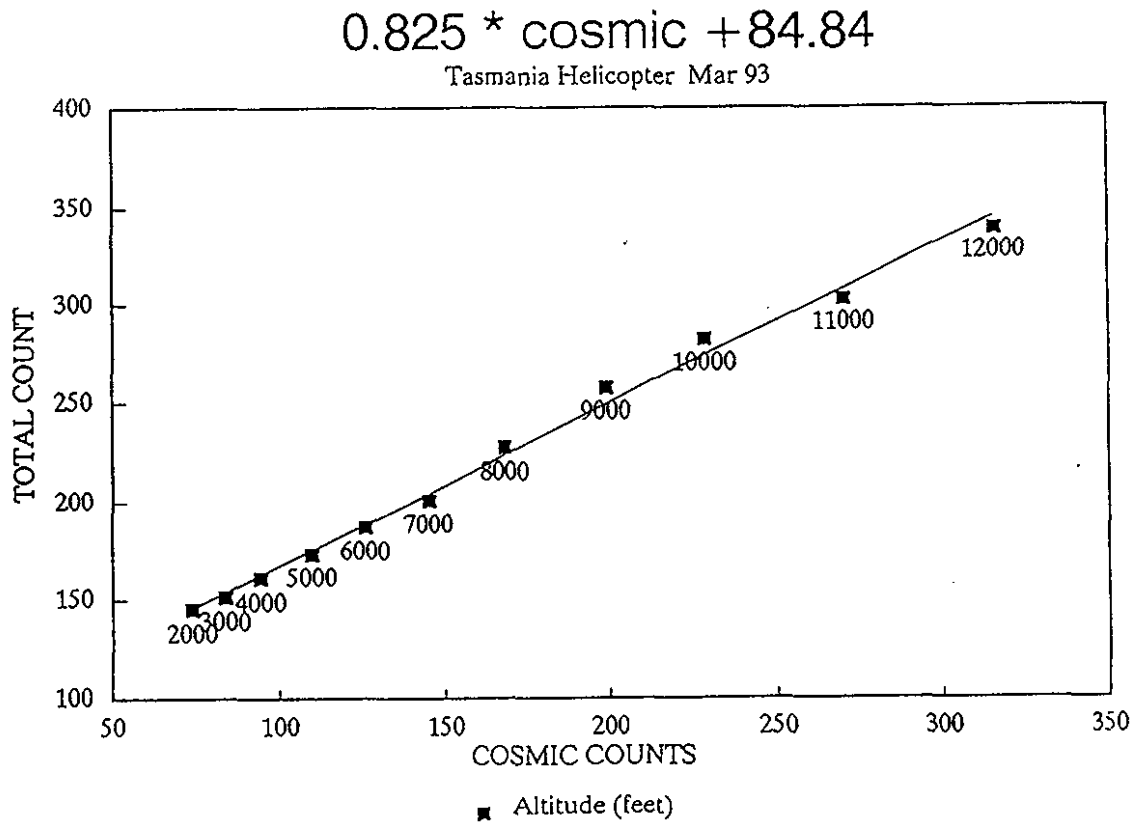
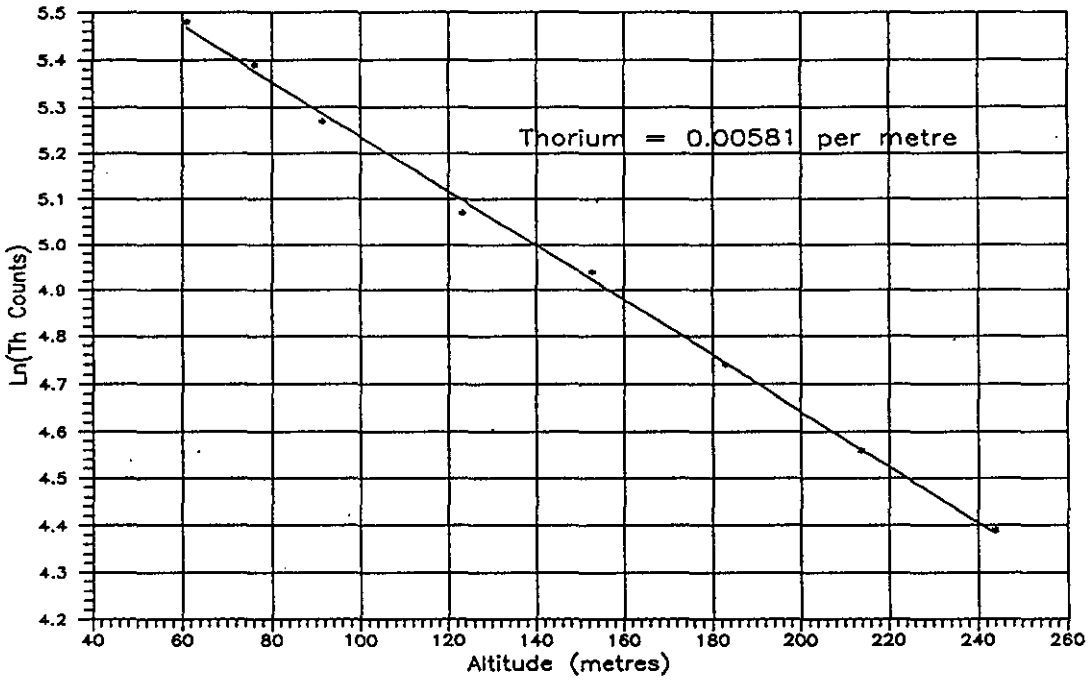
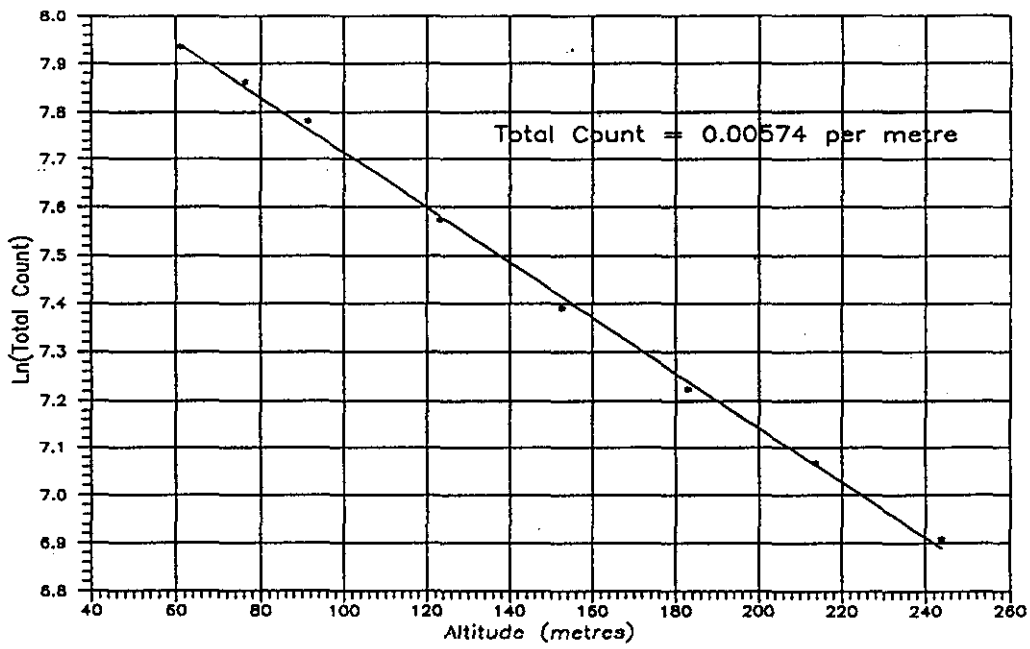



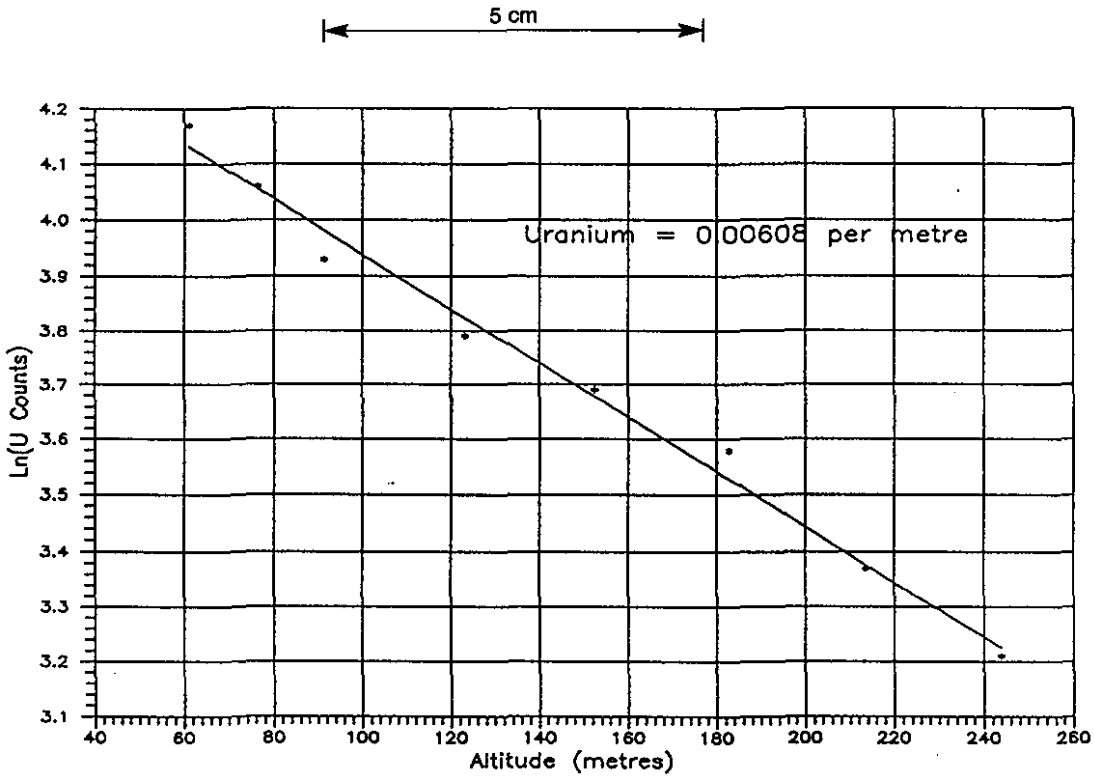
FIGURE A3: HEIGHT ATTENUATION TESTS




5 cm

FIGURE A3: HEIGHT ATTENUATION TESTS



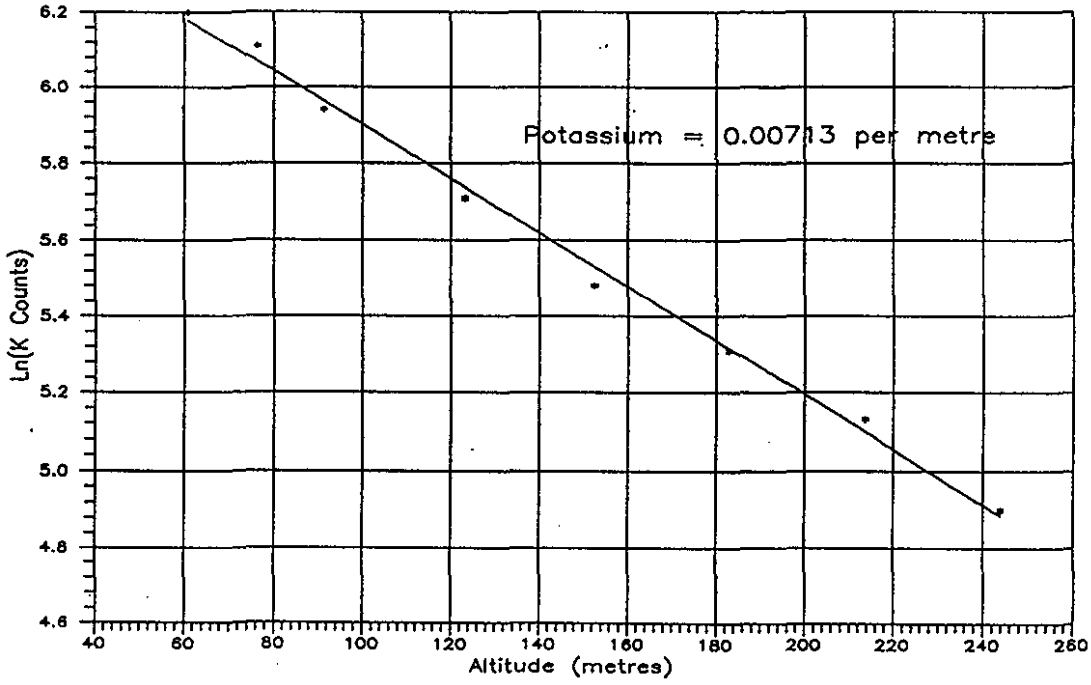
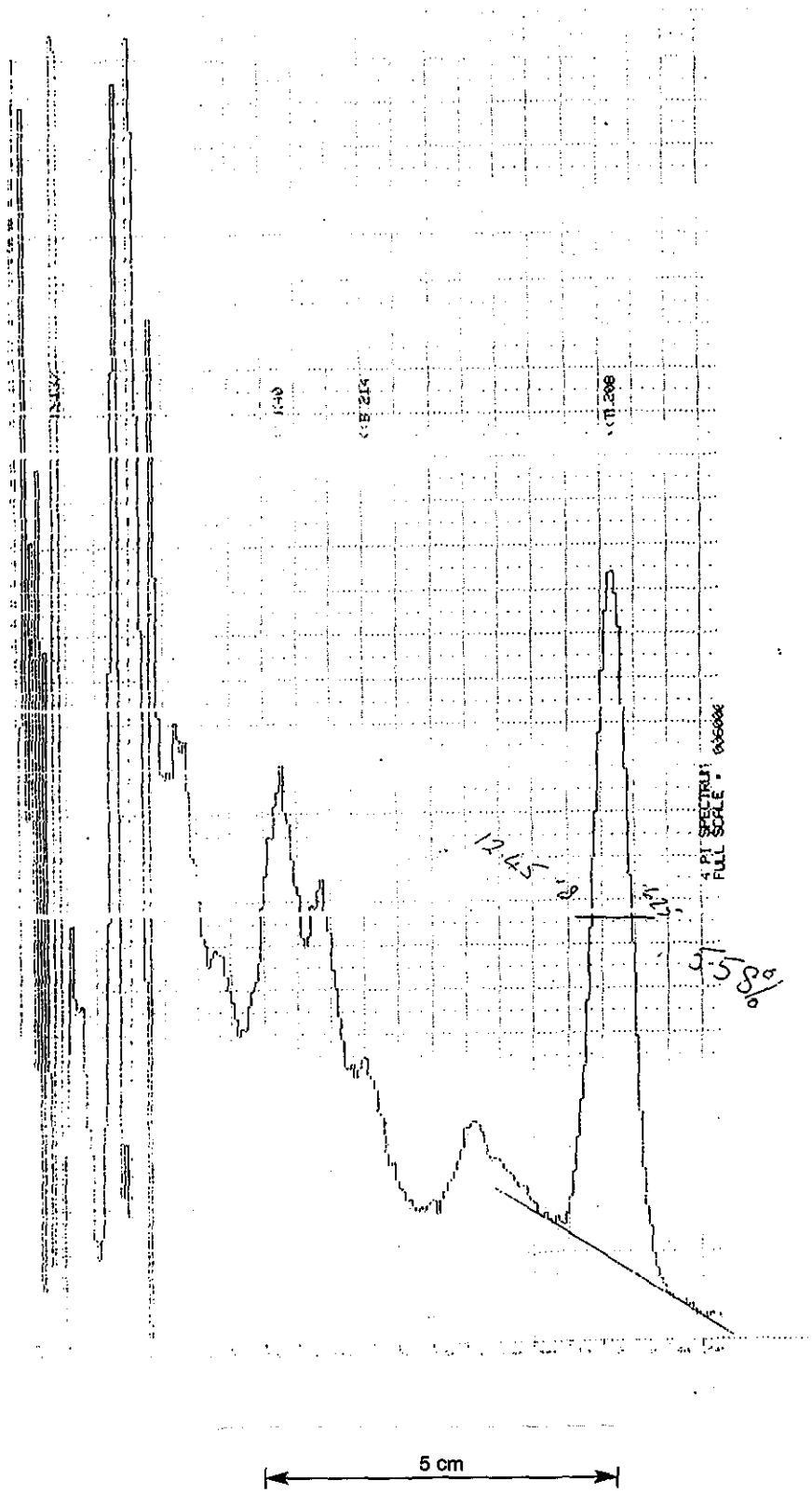



FIGURE A4 (i) - SPECTROMETER RESOLUTION CHECK

March 1993



## APPENDIX B: MAGNETIC DATA TAPE FORMATS

### TABLE B1: LOCATED DATA TAPE FORMAT

| Column | Located Data Tape Format Description |
|---|---|
| 1 - 8 | Flight |
| 9 - 16 | Line |
| 17 - 24 | Fiducial |
| 25 - 32 | Eastings |
| 33 - 40 | Northings |
| 41 - 48 | Date (DDMMYY) |
| 49 - 56 | Levelled Magnetic Value |
| 57 - 64 | Raw Magnetic Value |
| 65 - 72 | Diurnal |
| 73 - 80 | Uncorrected Total Count |
| 81 - 88 | Uncorrected Potassium Count |
| 89 - 96 | Uncorrected Uranium Count |
| 103 - 104 | Uncorrected Thorium Count |
| 105 - 112 | Cosmic Count |
| 113 - 120 | Corrected Total Count |
| 121 - 128 | Corrected Potassium Count |
| 129 - 136 | Corrected Uranium Count |
| 137 - 144 | Corrected Thorium Count |
| 145 - 152 | Radar Altimeter |
| 153 - 160 | GPS ASL |

| | |
|---|---|
| Record Length | 160 Bytes |
| Block Size | 10240 Bytes |
| Density | 6250 Bpi |
| Recording Mode | ASCII |

## APPENDIX C: RMS THERMAL PAPER STORAGE INSTRUCTIONS

### PAPER STORAGE AND HANDLING, RMS 2030 THERMAL PAPER

**STORAGE:**

| | |
|---|---|
| Ambient Temperature: | Less than 25°C |
| Relative Humidity: | Less than 65% |
| Storage Location: | In darkness before and after exposure. |

Under these conditions, the paper should retain its characteristics and the printed images will remain legible for at least 5 years, although in the case of blue image paper, there may be some slight fading.

**TO ELIMINATE PREMATURE PAPER DEVELOPMENT:**

- Colour development begins at temperatures between 70 to 100°C, and reaches saturation density between 80 and 120°C. Premature development of the paper may occur at lower temperatures, and particularly if the humidity is greater than 65%.
  eg. If the paper is stored for 24 hours at a temperature of 60°C, some development may occur. Or if the paper is stored for 24 hours at a temperature of 45°C when the relative humidity is 90%, development may also occur.

- Avoid use of solvent-type adhesives. Adhesives containing volatile organic solvents such as alcohol, ester, ketone, etc causes colour formation and therefore rubber-type adhesives etc should not be used. Starch, PVA and CMC type adhesives are recommended.

- Frictional heat generated by rubbing a finger nail or sharp object over the surface will cause images to develop.

- Thermal paper will develop colour if brought into contact with freshly processed Diazo copying paper.

**TO ELIMINATE PAPER FADING:**

- Thermal paper will turn yellow, and blue printed images will tend to fade if exposed to direct sunlight or to fluorescent lighting for long periods. File exposed paper in the dark immediately after exposure. Do not store paper near windows.

- Prolonged contact with PVC film containing plasticisers such as ester phthalate will reduce the image forming ability of the paper and cause printed images to fade. We recommend that files made of polyethylene, polypropylene, polyester, etc be used.

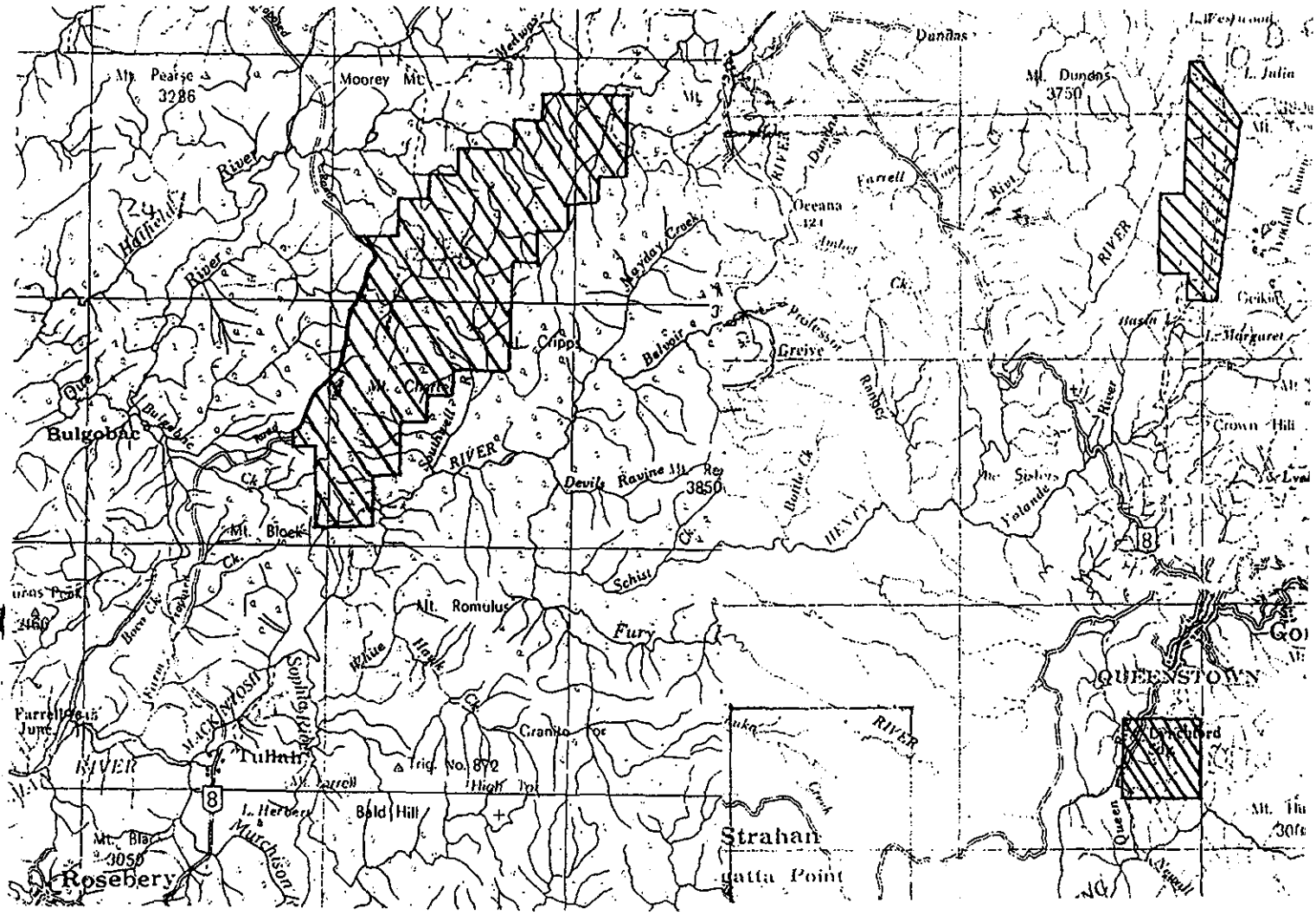
- Self-adhesive cellophane tapes containing an alcohol type plasticiser will cause the image to fade. Double-sided adhesive tape is recommended for use instead of paste.

- Handling thermal paper with dirty or sweaty fingers might cause images to fade.

- Do not store developed paper with the sensitised surfaces touching as images might be transferred from one sheet to another.

## APPENDIX D: LOCATION MAP

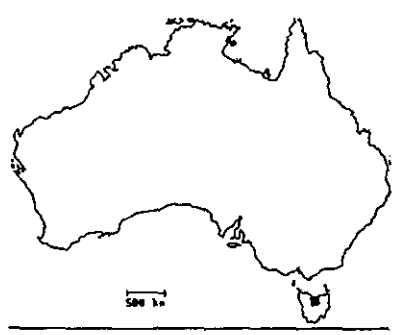
**LOCATION MAP** Scale: 1:250,000




BERNIE 1:250,000

QUEENSTOWN 1:250,000

5 cm



655456

# Aberfoyle Resources Limited

EXPLORATION DIVISION

OPEN FILE

TCR 93-3441

## EXPLORATION LICENCE 106/87

## LAKE MACKINTOSH

## TASMANIA

MICROFILMED
FICHE No. 012721-29B

Progress Report for the Period

April 1992 - April 1993

Volume 3 of 3

PLATES

MINES
FILE EL106/87
15 JUN 1993
DOC. REC.
OFFICE: FOR ACTION: FOR INFO.
See Folios 94-97
REGISTRY DATE

Distribution

| | |
|---|---|
| Aberfoyle - Burnie | (1/3) |
| Aberfoyle - Hawthorn | (2/3) |
| **Division of Mines** | (3/3) |

Internal Report No: Mackintosh 52

2 000 E
4 000 E
6 000 E
8 000 E
12 000 N
10 000 N
8 000 N
6 000 N
4000 N
2 000 N

TAILINGS DAM STRUCTURE
MAC 31
MAC 35
MAC 34 (Abandoned)
MAC 33
MAC 32 (Abandoned)
MURCHISON HIGHWAY STRUCTURE
MT. CHARTER FAULT
AMOEBA ZONE STRUCTURE
MILL SITE STRUCTURE
QUE FAULT
MT. CRIPPS FAULT
BARYTE CREEK STRUCTURE
HENTY FAULT ZONE

0 250 500 750 1000
METRES

5 cm

MINE GRID NORTH
AMG NORTH
22·1°

655457
93-341.

# Aberfoyle Resources Limited
EXPLORATION DIVISION

NORTH WEST TASMANIA

## E.L. 106/87 MACKINTOSH

## INFERRED CAMBRIAN STRUCTURES

| REVISIONS | | | |
|---|---|---|---|
| Init. | Date | Init. | Date |
| | | | |

Location Code :

Scale : 1/10000 | Date : February 1993

Compiled : S.R. / R.C.D.
Drawn :
Traced : J.M.S.
Checked : S.R. / R.C.D.
Plate No : MAC 360

DDH MAC 33 (4534·9N, 3719·7E, 800·7RL)
(proj. 15mN)

DDH MC-1
(proj. 5mN)

DDH MAC 26
(proj. 120mN)

DDH MC-3
(proj. 50mN)

DDH MAC 32 (4876·1N, 4370·5E, 805·6RL)
(proj. 20mS)

800 RL
600
400
200
00

DOLERITE

QUE RIVER SHALE

ANDESITE

ANDESITE

ANDESITE

MT. CHARTER ALTERATION ZONE

DACITE

ALTERATION ZONE

BASALT

ALTERED DACITE

MT. CHARTER EDGE OF

ALTERED DACITE

BASALT

EPICLASTICS

DACITE

MURCHISON HIGHWAY STRUCTURE

BASALT

DACITE

ALTERED DACITE

POLYMICT EPICLASTIC + DACITE + ANDESITE

SILICIC ANDESITE

FOOTWALL ANDESITES

ASH VOLCANICLASTIC

BASALT

BASALT

MICA SANDSTONE

5 cm

93-3441.

Aberfoyle Resources Limited
EXPLORATION DIVISION
655458

| REVISIONS | | | |
|---|---|---|---|
| Init. | Date | Init. | Date |
| | | | |

Location Code :

NORT WEST TASMANIA
MACKINTOSH E.L. 106/87
DDH MAC 32 & DDH MAC 33
(OBLIQUE SECTION 065°G THROUGH 4710N, 4060E)

Scale : 1:1000 | Date : May, 1993

Compiled : SMR
Drawn : SMR
Traced : NB, RJE
Checked :
Plate No : MAC 365

PROSPECT: mac
SECTION definition:
E: .0 735.0
N: .0 .0
RL: -1050.0 .0
Forward extent : 10.0
Backward extent: 10.0
Section Strike: 90.0
Section Length: 735.0
PDF file: shma33a.pdf
PCF file: shma33a.pcf
PLOTfile: mac3dd0a.plt

HOLE LEGEND - RHS:

« HISTOGRAM »
geh SiO2 [%]
Base value: .000
Units per mm: 2.500
Max dist in mm: 40

« HISTOGRAM »
geh Al2O3 [%]
Base value: .000
Units per mm: .750
Max dist in mm: 40

« HISTOGRAM »
geh Fe2O3 [%]
Base value: .000
Units per mm: .500
Max dist in mm: 40

« HISTOGRAM »
geh MnO [%]
Base value: .000
Units per mm: .025
Max dist in mm: 40

« HISTOGRAM »
geh Ba [ppm]
Base value: .000
Units per mm: 80.000
Max dist in mm: 40

« HISTOGRAM »
geh LOI [%]
Base value: .000
Units per mm: .500
Max dist in mm: 40

« HISTOGRAM »
geh Zr [ppm]
Base value: .000
Units per mm: 8.000
Max dist in mm: 40

« HISTOGRAM »
geh TiO2 [%]
Base value: .000
Units per mm: .050
Max dist in mm: 40

« HISTOGRAM »
geh P2O5 [%]
Base value: .000
Units per mm: .013
Max dist in mm: 40

« HISTOGRAM »
geh Cr [ppm]
Base value: .000
Units per mm: 25.000
Max dist in mm: 40

« HISTOGRAM »
geh Ti/Zr
Base value: .000
Units per mm: 1.000
Max dist in mm: 40

« HISTOGRAM »
geh P2O5/TiO2
Base value: .000
Units per mm: .025
Max dist in mm: 40

HOLE LEGEND - LHS:

« ANNOTATION »
geo Rock Type

SiO2 Al2O3 Fe2O3 MnO Ba LOI Zr TiO2 P2O5 Cr Ti/Zr P2O5/TiO2

0d -50d -100d -150d -200d -250d -300d -350d -400d -450d -500d -550d -600d -650d -700d -750d -800d -850d -900d -950d -1000d -1050d

Dol
Sh
Y-lv/bv
Y-lv/av
Y-lv
B-bv/Sh
YB-lv/bv
B-lv/bv
NO CORE
B-lv
B-l
B-l/lv
B-p1
YA-lv
A-l/lv
A-l
A/D-l
A?-l/lv
Y-lv/bv
YB-lv
D-l/lv
D-lv
D-lv/bv
D-l
FP-mlv/clv
B-P1
av/flv
A-av/mlv
av/B-l
Sa
Sa/Sh

TDDMA0033

93-3441.

5 cm

Aberfoyle Resources Limited
EXPLORATION DIVISION
655459

| REVISIONS | | | | Tasmania | Compiled: RdeS |
|---|---|---|---|---|---|
| Init. | Date | Init. | Date | Mackintosh E.L.106/87 | Drawn: |
| | | | | Geochemical Profiles | Traced: |
| | | | | DDH MAC-33 (sheet 1 of 2) | Checked: SMR |
| Location Code: | | | | Scale: 1 : 1000 Date: 21/04/93 | Plate No.: MAC3SSA |

PROSPECT: mac
SECTION definition:
E: 0 725.0
N: 0 .0
RL: -1050.0 .0
Forward extent : 10.0
Backward extent: 10.0
Section Strike: 90.0
Section Length: 725.0
PDF file: shma33b.pdf
PCF file: shma33b.pcf
PLOTfile: mac365b.plt

HOLE LEGEND - RHS:

* HISTOGRAM *
gch Na2O [%]
Base value: .000
Units per mm: .200
Max dist in mm: 40

* HISTOGRAM *
gch MgO [%]
Base value: .000
Units per mm: .350
Max dist in mm: 40

* HISTOGRAM *
gch K2O [%]
Base value: .000
Units per mm: .125
Max dist in mm: 40

* HISTOGRAM *
gch CaO [%]
Base value: .000
Units per mm: .500
Max dist in mm: 40

* HISTOGRAM *
gch Altn.Ind.
Base value: .000
Units per mm: 2.500
Max dist in mm: 40

* HISTOGRAM *
gch S [%]
Base value: .000
Units per mm: .025
Max dist in mm: 40

* HISTOGRAM *
gch Cu [ppm]
Base value: .000
Units per mm: 7.000
Max dist in mm: 40

* HISTOGRAM *
gch Pb [ppm]
Base value: .000
Units per mm: 25.000
Max dist in mm: 40

* HISTOGRAM *
gch Zn [ppm]
Base value: .000
Units per mm: 100.000
Max dist in mm: 40

* HISTOGRAM *
gch Ag [ppm]
Base value: .000
Units per mm: .050
Max dist in mm: 40

* HISTOGRAM *
gch Au [ppm]
Base value: .000
Units per mm: .002
Max dist in mm: 40

* HISTOGRAM *
gch As [ppm]
Base value: .000
Units per mm: .750
Max dist in mm: 40

HOLE LEGEND - LHS:

* ANNOTATION *
geo Rock Type

Na2O | MgO | K2O | CaO | Altn.Ind | S | Cu | Pb | Zn | Ag | Au | As

0d | -50d | -100d | -150d | -200d | -250d | -300d | -350d | -400d | -450d | -500d | -550d | -600d | -650d | -700d | -750d | -800d | -850d | -900d | -950d | -1000d | -1050d

Dol
Sh
BX
Y-lv/bv
Sh
Y-lv/av
Sh
Y-lv
Sh
Dol
Sh
B-bv/Sh
YB-lv/bv
B-lv/bv
NO CORE
B-lv/bv
B-lv/bv
B-lv
B-1
B-lv/bv
B-1
B-lv
B-1/lv
B-lv/bv
B-p1
B-lv/bv
B-1
YA-lv
A-1/lv
A-1
A-1/lv
A-1
A-1v
A-1/lv
A/D-1
A?-1/lv
A/D-1
A-1
Y-lv/bv
YB-lv
D-1/lv
D-lv
D-lv/bv
D-1
D-lv
D-1
D-lv/bv
D-1
B-1
FP-m1v/c1v
B-P1
B-1
A-1v
A-1
A-1/lv
av/f1v
A-av/m1v
av/p1v
B-1
Ss
B-1
Ss/Sh
Ss
Ss/Sh
Ss
DDMAC033
810.7

2.36
1.01
1130
1050
4236
1030
48
32

93-3441.

5 cm

Aberfoyle Resources Limited
EXPLORATION DIVISION
655460

| REVISIONS | | | |
|---|---|---|---|
| Init. | Date | Init. | Date |
| | | | |
| | | | |
| | | | |
| | | | |
| | | | |

Location Code:

Tasmania
Mackintosh E.L.106/87
Geochemical Profiles
DDH MAC-33 (sheet 2 of 2)

Scale: 1 : 1000 Date: 21/04/93

Compiled: RdeB
Drawn:
Traced:
Checked: SMR
Plate No.: MAC365B

3100E 3200E 3300E 3400E 3500E 3600E 3700E

700 RL

600

400

200

00

-200

-400

DDH MAC 035

ANDESITE

QUE RIVER SHALE

ANDESITE

BASALT

DACITE

" MIXED SEQUENCE " EPICLASTICS

DACITE

F

F

F

P622650 P622651 P622652 P622653 P622654 P622655 P622656 P622657 P622658 P622659 P622660 P622661 P622662 P622663 P622664 P622665 P622666 P622667 P622668

T.D. 1185.6 m

5 cm

93-3441.

Aberfoyle Resources Limited
EXPLORATION DIVISION
655461

| REVISIONS | | | |
|---|---|---|---|
| Init. | Date | Init. | Date |
| | | | |

Location Code :

NORTH WEST TASMANIA
MACKINTOSH E.L. 106/87
DDH MAC 035
SECTION 6000N

Scale : 1:1000 | Date : May, 1993

Compiled : SMR
Drawn : SMR
Traced : RJE
Checked :
Plate No : MAC 366

PROSPECT: mac
SECTION definition:
E: .0 1697.5
N: .0 .0
RL: -1570.0 .0
Forward extent : 10.0
Backward extent: 10.0
Section Strike: 90.0
Section Length: 1697.5
PDF file: shmn35b.pdf
PDF file: shmn35b.psf
PLOTvile: mac906b.plt

HOLE LEGEND - RHS

* HISTOGRAM *
geh SiO2 [%]
Show value: .000
Units per mm: 2.500
max dist in mm: 40

* HISTOGRAM *
geh Al2O3 [%]
Show value: .000
Units per mm: .700
max dist in mm: 40

* HISTOGRAM *
geh Fe2O3 [%]
Show value: .000
Units per mm: .500
max dist in mm: 40

* HISTOGRAM *
geh MnO [%]
Show value: .000
Units per mm: .015
max dist in mm: 40

* HISTOGRAM *
geh Ba [ppm]
Show value: .000
Units per mm: 20.000
max dist in mm: 40

* HISTOGRAM *
geh LOI [%]
Show value: .000
Units per mm: .500
max dist in mm: 40

* HISTOGRAM *
geh Zr [ppm]
Show value: .000
Units per mm: 5.000
max dist in mm: 40

* HISTOGRAM *
geh TiO2 [%]
Show value: .000
Units per mm: .030
max dist in mm: 40

* HISTOGRAM *
geh P2O5 [%]
Show value: .000
Units per mm: .010
max dist in mm: 40

* HISTOGRAM *
geh Cr [ppm]
Show value: .000
Units per mm: 25.000
max dist in mm: 40

* HISTOGRAM *
geh Ti/Zr
Show value: .000
Units per mm: 1.500
max dist in mm: 40

* HISTOGRAM *
geh P2O5/TiO2
Show value: .000
Units per mm: .020
max dist in mm: 40

HOLE LEGEND - LHS

* ANNOTATION *
geo Rock Type

SiO2 Al2O3 Fe2O3 MnO Ba LOI Zr TiO2 P2O5 Cr Ti/Zr P2O5/TiO2

0d -50d -100d -150d -200d -250d -300d -350d -400d -450d -500d -550d -600d -650d -700d -750d -800d -850d -900d -950d -1000d -1050d -1100d -1150d -1200d -1250d -1300d -1350d -1400d -1450d -1500d -1550d

FP-bv
FP-flv/mlv
FP-mlv/bv
FP-bv
FP-lv
FP-bv
FP-lv
FP-bv/l
FP-l
FP-mlv
B-bv
B-pl
B-pl/bv
B-bv
B-l/bv
B-lv/l
B-l/bv
B-bv
B-flv/mlv
B-l
B-l/bv
B-l
B-l/bv
B-l
B/D-lv
B-l
D-lv
FP-av
D-l/bv
FP-av
D-l/bv
FP-av?
D-l/mlv
D/FP-mlv
D-l
D-l/lv
D-l
D-l
Y-flv/clv
D-l
D-l/bv
D-l
D-l/bv
D-l
1697.5
DDH40035

0.64
0.84
0.84
0.88
0.81
0.81
1.07
1.04
1.01
1.04
1.08
1.08
1.08

93-3441.

5 cm

Aberfoyle Resources Limited
EXPLORATION DIVISION
655462

| REVISIONS | | | |
|---|---|---|---|
| Init. | Date | Init. | Date |
| | | | |

Tasmania
Mackintosh E.L.106/87
Geochemical Profiles
DDH MAC-35 (sheet 1 of 2)

Location Code:
Scale: 1 : 1500
Date: 21/04/93

Compiled: RdeB
Drawn:
Traced:
Checked: SHR
Plate No.: MAC35BA

PROSPECT: mac
SECTION definition:
E: .0 1087.8
N: .0 .0
RL: -1575.0 .0
Forward extent : 10.0
Backward extent: 10.0
Section Strike: 90.0
Section Length: 1087.8
PDF file: shma35b.pdf
PCF file: shma35b.pcf
PLOTfile: mac366b.plt

HOLE LEGEND - RHB:

« HISTOGRAM »
gch Na2O [%]
Base value: .000
Units per mm: .200
Max dist in mm: 40

« HISTOGRAM »
gch MgO [%]
Base value: .000
Units per mm: .500
Max dist in mm: 40

« HISTOGRAM »
gch K2O [%]
Base value: .000
Units per mm: .125
Max dist in mm: 40

« HISTOGRAM »
gch CaO [%]
Base value: .000
Units per mm: .500
Max dist in mm: 40

« HISTOGRAM »
gch Altn.Ind.
Base value: .000
Units per mm: 2.500
Max dist in mm: 40

« HISTOGRAM »
gch S [%]
Base value: .000
Units per mm: .025
Max dist in mm: 40

« HISTOGRAM »
gch Cu [ppm]
Base value: .000
Units per mm: 7.500
Max dist in mm: 40

« HISTOGRAM »
gch Pb [ppm]
Base value: .000
Units per mm: 25.000
Max dist in mm: 40

« HISTOGRAM »
gch Zn [ppm]
Base value: .000
Units per mm: 12.500
Max dist in mm: 40

« HISTOGRAM »
gch Ag [ppm]
Base value: .000
Units per mm: .250
Max dist in mm: 40

« HISTOGRAM »
gch Au [ppm]
Base value: .000
Units per mm: .062
Max dist in mm: 40

« HISTOGRAM »
gch As [ppm]
Base value: .000
Units per mm: .500
Max dist in mm: 40

HOLE LEGEND - LHB:

« ANNOTATION »
geo Rock Type

Na2O | MgO | K2O | CaO | Altn.Ind | S | Cu | Pb | Zn | Ag | Au | As

0d
-50d
-100d
-150d
-200d
-250d
-300d
-350d
-400d
-450d
-500d
-550d
-600d
-650d
-700d
-750d
-800d
-850d
-900d
-950d
-1000d
-1050d
-1100d
-1150d
-1200d
-1250d
-1300d
-1350d
-1400d
-1450d
-1500d
-1550d

FP-bv
FP-flv/mlv
FP-mlv/bv
FP-bv
FP-lv
FP-bv
FP-l?
FP-bv/l
FP-l
FP-mlv
B-bv
B-pl
B-pl/bv
B-bv
B-l/bv
B-lv/l
B-l/bv
B-bv
B-lv
B-flv/mlv
B-l
B-l/bv
B-l
B-l/bv
B-l
B/D-lv
B-l
D-lv
FP-av
D-l/bv
FP-av
D-l/bv
FP-av?
D-l/mlv
D/FP-mlv
D-l
D-l/lv
D-l
D-l
D-l
Y-flv/clv
D-l
D-l/bv
D-l
D-l/bv
D-l
DDM40035

20.42
24.72
25.78
1.22
4.77
4.7
1.48
1.32
307
347
335
1088
1575
1088
3471
2115
2906
2255
1319
1184
1257
4021
1625
548
538
810
44
506
90

5 cm

93-3441.

Aberfoyle Resources Limited
EXPLORATION DIVISION
655463

| REVISIONS | | | |
|---|---|---|---|
| Init. | Date | Init. | Date |

Tasmania
Mackintosh E.L.105/87
Geochemical Profiles
DDH MAC-35 (sheet 2 of 2)

Location Code:
Scale: 1 : 1500
Date: 22/04/93

Compiled: RDeB
Drawn:
Traced:
Checked: SMR
Plate No.: MAC366B

PROSPECT: mac

SECTION definition:
E: .0 718.0
N: .0 .0
RL: -480.0 .0

Forward azimuth : 50.0
Backward azimuth: 50.0

Section Station 50.0
Section Length: 718.0

PDF file: mac08a.pdf
PCF file: mac08a.pcf
PLOTfile: mac078a.plt

HOLE LEGEND - MAG

MISTOGRAM
mgh SiO2 (%)
Zero value .000
Units per mm 2.750
Max dist in mm 40

MISTOGRAM
mgh Al2O3 (%)
Zero value .000
Units per mm .730
Max dist in mm 40

MISTOGRAM
mgh Fe2O3 (%)
Zero value .000
Units per mm .280
Max dist in mm 40

MISTOGRAM
mgh MnO (%)
Zero value .000
Units per mm .060
Max dist in mm 40

MISTOGRAM
mgh Ba (ppm)
Zero value .000
Units per mm 1280.000
Max dist in mm 40

MISTOGRAM
mgh LOI (%)
Zero value .000
Units per mm .650
Max dist in mm 40

MISTOGRAM
mgh Zr (ppm)
Zero value .000
Units per mm 8.000
Max dist in mm 40

MISTOGRAM
mgh TiO2 (%)
Zero value .000
Units per mm .020
Max dist in mm 40

MISTOGRAM
mgh P2O5 (%)
Zero value .000
Units per mm .010
Max dist in mm 40

MISTOGRAM
mgh Cr (ppm)
Zero value .000
Units per mm 1.000
Max dist in mm 40

MISTOGRAM
mgh Ti/Zr
Zero value .000
Units per mm .150
Max dist in mm 40

MISTOGRAM
mgh P2O5/TiO2
Zero value .000
Units per mm .500
Max dist in mm 40

HOLE LEGEND - LITH

ANNOTATION
gmo Rock Type

SiO2 Al2O3 Fe2O3 MnO Ba LOI Zr TiO2 P2O5 Cr Ti/Zr P2O5/TiO2

0d -50d -100d -150d -200d -250d -300d -350d -400d -450d

598.4

DDMAC032

5 cm

93-3441.

Aberfoyle Resources Limited
EXPLORATION DIVISION
655464

| REVISIONS | | | |
|---|---|---|---|
| Init. | Date | Init. | Date |
| | | | |
| | | | |
| | | | |
| | | | |
| | | | |
| Location Codes | | | |

Tasmania
Mackintosh E.L.106/87
Geochemical Profiles
DDH MAC-32 (sheet 1 of 2)

Scale: 1 : 1000
Date: 26/05/93

Compiled: RdeB
Drawn:
Traced:
Checked: SMR
Plots No.: MAC078A

PROSPECT: mac
SECTION definition:
E: .0 718.0
N: .0 .0
RL: -488.0 .0

Forward extent : 10.0
Backward extent: 10.0

Section Strike: 90.0
Section Length: 718.0

PDF file: shmac3E.pdf
PDF file: shmac3E.pcf
PLOTfile: mac378b.plt

HOLE LEGEND - RHS:

* HISTOGRAM *
gch Na2O (%)
Base value: .000
Units per mm: .010
Max dist in mm: 40

* HISTOGRAM *
gch MgO (%)
Base value: .000
Units per mm: .100
Max dist in mm: 40

* HISTOGRAM *
gch K2O (%)
Base value: .000
Units per mm: .050
Max dist in mm: 40

* HISTOGRAM *
gch CaO (%)
Base value: .000
Units per mm: .010
Max dist in mm: 40

* HISTOGRAM *
gch Alth.Ind.
Base value: .000
Units per mm: 2.500
Max dist in mm: 40

* HISTOGRAM *
gch S (%)
Base value: .000
Units per mm: .050
Max dist in mm: 40

* HISTOGRAM *
gch Cu (ppm)
Base value: .000
Units per mm: 7.000
Max dist in mm: 40

* HISTOGRAM *
gch Pb (ppm)
Base value: .000
Units per mm: 2.500
Max dist in mm: 40

* HISTOGRAM *
gch Zn (ppm)
Base value: .000
Units per mm: 100.000
Max dist in mm: 40

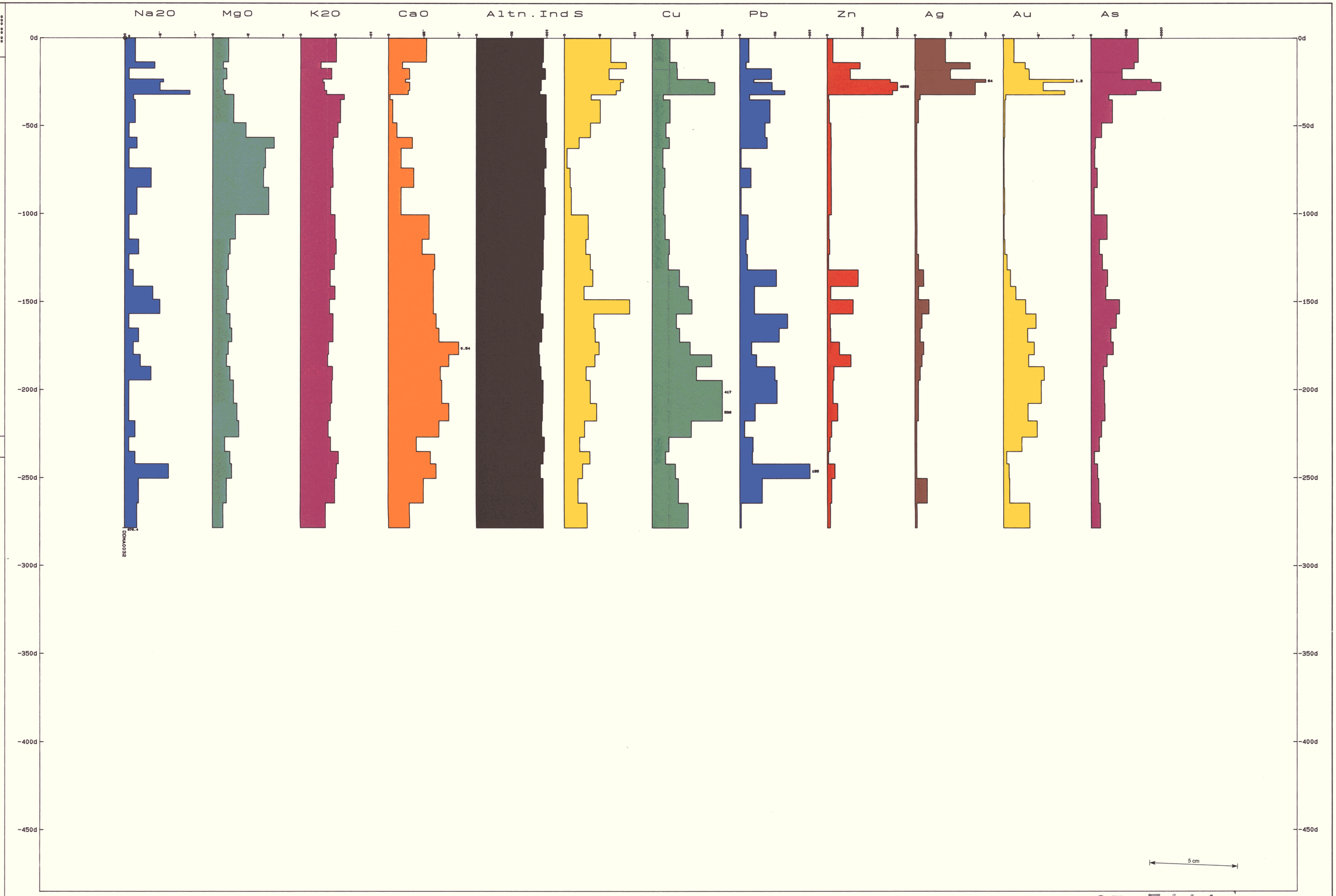
* HISTOGRAM *
gch Ag (ppm)
Base value: .000
Units per mm: 1.000
Max dist in mm: 40

* HISTOGRAM *
gch Au (ppm)
Base value: .000
Units per mm: .025
Max dist in mm: 40

* HISTOGRAM *
gch As (ppm)
Base value: .000
Units per mm: 25.000
Max dist in mm: 40

HOLE LEGEND - LHS:

* ANNOTATION *
geo Rock Type




93-3441.

Aberfoyle Resources Limited
EXPLORATION DIVISION
655465

| REVISIONS | | | |
|---|---|---|---|
| Init. | Date | Init. | Date |
| | | | |
| | | | |
| | | | |
| | | | |
| | | | |

Location Code:

Tasmania
Mackintosh E.L.106/87
Geochemical Profiles
DDH MAC-32 (sheet 2 of 2)

Scale: 1 : 1000 | Date: 26/05/93

Compiled: RdeB
Drawn:
Traced:
Checked: SMR
Plate No.: MAC378B

# MACKINTOSH INTERPRETIVE GEOLOGY

SCALE 1:10000




5 cm

1:10000

0 250 500 750 1000

METRES

MINE GRID NORTH

AMG NORTH

22.1°

TASMANIA

MACKINTOSH E.L.106/87

HELLYER - MT.CHARTER

INTERPRETIVE GEOLOGY

COMPILED : RCD

CHECKED : RCD

PLATE No. : MAC 380

SCALE : 1 : 10000

DATE : MAY 1993

655466

93-3441.